

# **RESEARCH IN PROGRESS**

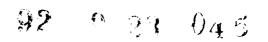


# **U.S.ARMY RESEARCH OFFICE**

PHYSICS, CHEMISTRY, BIOLOGICAL SCIENCES, MATHEMATICS, ENGINEERING SCIENCES, METALLURGY AND MATERIALS SCIENCE, GEOSCIENCES, ELECTRONICS, EUROPEAN RESEARCH PROGRAM

This document has been approved for public release and sale; its distribution is unlimited.

> Department of the Army U.S. Army Materiel Command







# **RESEARCH IN PROGRESS**

**BETWEEN 1 JULY 1990 AND 30 JUNE 1991** 

# **U.S.ARMY RESEARCH OFFICE**

(REPORT EXEMPT FROM REPORTS CONTROL UNDER AR 335-15, PARAGRAPH 5-2b(9))

P.O. Box 12211 Research Triangle Park, N.C. 27709–2211

-

## Foreword

The U.S. Army Research Office, under the U.S. Army Materiel Command (AMC), is responsible for coordinating and supporting research in the physical and engineering sciences, in materials science, geosciences, biology, and mathematics.

This report describes research directly supported by the Army Research Office as well as research supported through this office by the Defense Advanced Research Projects Agency, and several AMC and other Army commands. A separate section is devoted to the research program at the U.S. Army Research, Development and Standardization Group — United Kingdom.

The present volume includes the research program in physics, chemistry, biological sciences, mathematics, engineering sciences, metallurgy and materials science, geosciences, electronics, and the European Research Program. It covers the 12-month period from 1 July 1990 through 30 June 1991.

Additional copies of this report may be requested by writing to this office, attention AMXRO-RT-IP.

## Accession and NTIS CRIVEL DTID TAY Una method I Justification By Distribution / Aveint other is Distribution / Distribution / Aveint other is Specification I A-N

GERALD J. IAFRATE

Director

## DTIC QUALITY INSPECTED 3

# **Table of Contents**

v

Foreword	iii
List of Abbreviations	vii

## **Physics**

Α.	General Physics	1
Β.	Atomic and Molecular Physics	1
С.	Fluid and Plasma Physics	8
D.	Solid State Physics	9
E.	Acoustics, Optics and Cross	
	Disciplinary	18

## Chemistry

Α.	Inorganic, Analytical and	
	Electrochemistry	- 30
Β.	Organic Synthesis and Mechanisms	36
С.	Structural, Surface Chemistry, and	
	Spectroscopy	40
Ð.	Kinetics and Thermodynamics	45
E.	Polymer Chemistry	50

## **Biological Sciences**

Α.	Combat Ration Research	57
Β.	Biodegradation	58
С.	Biotechnology	60
D.	Defense Against Chemical and	
	Biclogical Weapons	64
Ε.	Sensory Factors in Performance	
	Enhancement	67
F.	Optimization of Physical Principles in	
	Biological Systems	68
	Mathematics	

Α.	Applied Analysis and Physical	
	Mathematics	70
<b>B</b> .	Numerical Methods and Scientific	
	Computing	78
С.	Statistics and Probability	83
D.	Systems, Control, Modeling, and	
	Artificial Intelligence	90
Ε.	Logistics and Operational Methods	93
F.	Special Projects	97
	<b>Engineering Sciences</b>	
۸	Solid Mechanics	107

Α.	Solid Mechanics	107
<b>B</b> .	Fluid Dynamics	113
С.	Combustion	119
D.	Structures and Dynamics	125

## **Metallurgy and Materials Science**

Α.	Degradation, Protection, and	
	Reaction	132
Β.	Mechanical Behavior	137
С.	Processing	143
	Physical Behavior	
E.	High Strain Rate Behavior of	
	Materials	160
F.	Miscellaneous	161

## Geosciences

Α.	Geomorphology/Hydrology	164
Β.	Snow, Ice, and Frozen Ground	166
С.	Other (Terrestrial)	167
D.	Propagation	169
Ε.	Atmospheric Remote Sensing	172
F.	Small-Scale Atmospheric Processes	174
G.	Aerosol Research	176

## **Electronics**

Α.	Physical Electronics	178
Β.	Electron Devices	182
С.	Antennas and EM Detection	189
D.	Circuits, Networks, and Related	
	Systems	197
E.	Signal Processing, Communications,	
	and Related Systems	198
F.	External Program	206
G.	Joint Services Electronics Program	207

## **European Research Program**

Α.	Physics and Mathematics	210
B.	Chemistry and Biological Sciences	2!3
C.	Aeronautics and Mechanics	215
D.	Materials Science	216
E.	Environmental Sciences	219
F.	Electronics and Computer Sciences	219

## Indexes

Proposal Numbers	223
Scientific Liaison and Scientific Cognizance	
Representatives	.226
Contractors and Grantees	231
Principal Investigators	237
Subject Index	245

# **Abbreviations**

ACAA	U.S. Army Concepts Analysis Agency
AERO DIR	Aeroflightdynamics Directorate, AVSCOM
AFAL	Air Force Astronautics Laboratory (AFSC)
AFESC	Air Force Engineering and Service Center
AFGL	Air Force Geophysics Laboratory
AFOSR	Air Force Office of Scientific Research
AIRMICS	Army Institute for Research in Management Information and Computer
	Sciences
AMBRDL	U.S. Army Medical Bioengineering Research and Development Laboratory
AMCCOM	U.S. Army Armament, Munitions and Chemical Command
AMRICD	U.S. Army Medical Research Institute of Chemical Defense
AMSAA	U.S. Army Materiel Systems Analysis Activity
AP TEC DIR	Aviation Applied Technology Directorate, AVSCOM
ARDEC	U.S. Army Armament Research, Development and Engineering Center
ARI	U.S. Army Research Institute for the Behavioral and Social Sciences
ARO	U.S. Army Research Office
AROE	U.S. Army Research, Development and Standardization Group (United
	Kingdom)
ASL	U.S. Army Atmospheric Sciences Laboratory
АТНАМА	U.S. Army Toxic and Hazardous Materials Agency
AVRADA	U.S. Army Avionics Research and Development Activity
AVSCOM	U.S. Army Aviation Systems Command
AVSCOM/DERSO	Corpus Christi Army Depot AVSCOM/DERSO
BRADEC	U.S. Army Belvoir Research, Development and Engineering Center
BRL	Ballistic Research Laboratory
BWL	Benet Weapons Laboratories, CCAC, ARDEC
CECOM	U.S. Army Communications-Electronics Command
CERL	Construction Engineering Research Laboratory
CRDEC	U.S. Army Chemical Research, Development and Engineering Center
CRREL	U.S. Army Cold Regions Research and Engineering Laboratory
DARPA	Defense Advanced Research Projects Agency
DPG	U.S. Army Dugway Proving Ground
EOARD	European Office of Aerospace R&D
ETDL	U.S. Army Electronics Technology and Devices Laboratory
ETL	U.S. Army Engineer Topographic Laboratories
HDL	U.S. Army Harry Diamond Laboratories
HEL	U.S. Army Human Engineering Laboratory
LABCOM	U.S. Army Laboratory Command
LAIR	Letterman Army Institute of Research
MICOM	U.S. Army Missile Command
MTL	U.S. Army Materials Technology Laboratories
NRDEC	U.S. Army Natick Research, Development and Engineering Center
NRL	Naval Research Laboratory
NSA/CSS	National Security Agency Central Security Service
NSWC	Naval Surface Weapons Center
NVEOC	U.S. Army Night Vision and Electro-Optics Center
NWC	Naval Air Warfare Center
OASA	(RDA) HQDA, Office of the Assistant Secretary of the Army
ONR	Office of Naval Research
VIIII I	Unite of maral nescales

PM SMOKE Office of Project Manager Smoke/Obscurants	
PROP DIR Propulsion Directorate, AVSCOM	
RIA Rock Island Arsenal, ARRCOM	
SC Scientific Cognizance	
SDC Strategic Defense Command	
SDIO/IST Strategic Defense Initiative Organization, Innovative Science	e and
Technology	
SL Scientific Liaison	
SMO U.S. Army Survivability Management Office	
STRUC DIR Aerostructures Directorate, AVSCOM	
SWC U.S. Army Signals Warfare Center CECOM	
TACOM U.S. Army Tank-Automotive Command	
TECOM U.S. Army Test and Evaluation Command	
TRADOC U.S. Army Training and Doctrine Command	
USAIS U.S. Army Infantry School	
VAL U.S. Army Vulnerability Assessment Laboratory	
WES Waterways Experiment Station	
WRAIR Walter Reed Army Institute of Research	
WSMR White Sands Missile Range	

# **I PHYSICS**

## A. General Physics

#### **B.** Atomic and Molecular Physics

## 25653 COHERENT ANTI-STOKES RAMAN SPECTROSCOPY OF HIGHLY VIBRATIONALLY EXCITED MOLECULES

Eric Mazur Harvard University

#### SC: CRDEC, NVEOC

The thrust of this project has been the study of infrared multiphoton excited (IRMPE) molecules in a free supersonic jet expansion using time-resolved broadband coherent anti-Stokes Raman spectroscopy (CARS). Recent efforts have been concerned with investigating IRMPE in ethylene (C<sub>2</sub>H<sub>4</sub>) and completing work on SF<sub>6</sub>. A new phase in the work began taking shape with new research and design efforts towards the development of a titanium sapphire-based femtosecond laser spectroscopy facility. This laser will make it possible to investigate molecular excitation dynamics on the ultrafast ( $\leq 10^{-13}$  second) time scale, as well as providing a source of extremely intense pulses ( $\geq 10^{12}$ W) for high intensity physics experiments possibly including femtosecond imaging.

#### Reports:

- 1. Collisional and Intramolecular Dynamics of Low Lying Vibrational States of Infrared Multiphoton Excited Molecules, by Eric Mazur et al., MS.
- Multiplex Pure Rotational Coherent Anti-Stokes Raman Spectroscopy in a Molecular Beam, by Nicolaas Bloembergen et al., J Raman Spectrosc 21,819(1990). AD A232 599
- 3. Direct Evidence for  $v_1$ -Mode Excitation in the Infrared Multiphoton Excitation of SO<sub>2</sub>, by Cheng-Zai Lu et al., *Chem Phys Let* 176,355 (1991). AD A234 405

## 26223 THE INTERACTION OF ULTRAVIOLET LASER RADIATION WITH METAL AND SEMICONDUCTOR SURFACES

Richard M. Osgood Columbia University

In the first area of research the initial investigation of photoemission from epitaxial insulator covered surfaces has been completed. The experiments present the first observation of an interesting and surprising new phenomenon, namely, that ultraviolet laser light can be used to photoemit electrons through thick overlayers on silicon surfaces. In particular, when a materials assembly of CaF<sub>2</sub> (or SiO<sub>2</sub>), which is grown on Si (111) surfaces, is illuminated by UV light, electrons are ejected from the interfacial region through the insulator into the vacuum. A careful study of the emission properties of this system has shown that it has a threshold of  $\sim 4.3$  eV corresponding to "internal" photoemission into the CaF<sub>2</sub> conduction band. Electrons in this band then "fall" out of the overlayer surface. The phenomenon has applications for over-coated photo-electrodes for FEL. The investigations in nonlinear photoemission spectroscopy have focused on the use of the spectral shift of photoelectrons from image potential states at the surfaces of transition metals to characterize and monitor changes in surface conditions, such as temperature variation and molecular or atomic adsorption. A typical photoelectron spectrum of a relaxed transition metal surface, excited with near-UV photons, shows a first low energy peak due to one photon emission of thermally excited electrons and, at higher energies, a series of low intensity peaks corresponding to two photon emission with the normally empty image potential states (n = 1, 2, etc.) as intermediate states. These image potential states are localized in vacuum several tens of angstroms from the surface and are, therefore, specifically sensitive to surface conditions. Being free from the interference of other electron surface states, the Cu(100)/near-UV laser excitation system is also a model case for the study

of space-charge modification of photoelectronic spectra: as the laser intensity is raised, the low energy electron emission is increased and leads to a positive shift in the position of the higher energy image potential induced emission. Computerized simulations are being carried out to implement this observation.

Reports:

1. Surface Photochemistry of Divalent Metal Alkyls on SiO<sub>2</sub>, by Ping S. Shaw et al., MS, J Chem Phys.

#### 26257 HIGH POWER SWITCHING AND OTHER HIGH POWER DEVICES

Martin A. Gundersen

University of Southern California

Work has continued on the superemissive cathode. Important results include preliminary measurements of the properties of electron beams produced by this cathode. A study has been made of the superemissive cathode as an electron beam source. The cathode has been demonstrated to be a high current electrode in backlighted thyratron (BLT) and pseudospark switches, which operate in a low pressure glow discharge mode and produce a high current density of  $\geq 10$ kA/cm<sup>2</sup> over an electrode area of  $\sim 1 \text{ cm}^2$ . A temperature rise of the cathode surface caused by ion bombardment during the current build up is responsible for this high electrode emission property. In this work a BLT is operated in the superemissive mode, and a cathode-produced electron beam is extracted through the anode aperture of the BLT and transported to a Faraday cup. Preliminary results include the following: At argon pressure of 55 mTorr and applied voltage of 15 kV, an electron beam of 120 amps maximum current and 120 ns duration was observed 7 cm downstream. An electron energy of less than 4 keV was estimated by a method of magnetic field deflection. The beam energy, as well as the beam current, can be increased by a postaccelerating voltage. Adding differential pumping to reduce the gas pressure in the drift tube to 10 mTorr resulted in an increase in beam current to 260 amps. The superemissive cathode is robust, self-heated, produces very high, uniform current, and operates in a low pressure plasma environment. These data indicate that the electron beam produced by the superemissive cathode should be considered for applications such as accelerators and high power microwave generators.

#### Reports:

No. 1-16 in previous editions.

- Multiple-Gap Back-Lighted Thyratrons for High Power Applications. by T.-Y. Hsu et al., *IEEE Trans on Electron De*vices 38,717(1991). AD A238 125
- Lock-On Effect in Pulsed Power Semiconductor Switches, by M.A. Gundersen et al., MS, Appl Phys Let.
- Avalanche Breakdown Characteristics of AlGaAs/GaAs p-nHeterojunctions for Pulsed Power Applications, by J.H. Hur et al., MS.
- 20. High-Power Multiple-Gap Back-Lighted Thyratrons, by T.-Y. Hsu et al., MS.
- 21. High Speed Static Induction Transistor for Pulsed Power Applications, by P. Hadizad et al., MS.
- 22. GaAs Opto-Thyristor for Pulsed Power Applications, by J.H. Hur et al., MS.
- 23. High Current Operation of the Back Lighted Thyratron Switch, by G. Kirkman-Amemiya and M.A. Gundersen, MS, *IEEE Trans on Electron Devices*.
- 24. High Current Back Lighted Thyratron Switches, by G. Kirkman-Amemiya et al., MS.
- 25. Current Quenching in the Pseudospark, by W. Hartmann et al., Appl Phys Let 58,574(1991). AD A238 126

#### 26462 TWO-PHOTON COOPERATIVE CASCADE SUPERFLUORESCENCE

Sven R. Hartmann Columbia University

An experiment was planned to study two-photon superradiance in cesium vapor in real time. Plans were to optically pump the cesium vapor in order to achieve an isolated group of atoms which was characterized by a narrow inhomogeneously broadened resonance line. The pumping scheme turned out to be impractical. But cesium is heavy and its resonances are relatively low energy. This means that in the absence of any extra narrowing superradiant delays of the order of one nanosecond can be expected, which would be sufficiently long to allow some degree of real time observation. The two-photon superradiance experiment will be performed without first narrowing the cesium resonance. Since it appears that at most a modest narrowing in the range of 3 to 6 is required plans have been made to achieve it by using simple atomic beam techniques. The generation of two photon cascade superfluorescence in cesium vapor requires delivery of a high intensity picosecond pulse at 885 nm which is near the single photon resonance at 852 nm. Unfortunately this is not an efficient dye laser transition as it is rather close to the infrared. Generation of these pulses requires the synchronization of (a) a cw Nd: YAG mode locked laser pump; (b) a sync pumped dye laser; (c) a Nd YAG laser pump; and (d) a 3 stage dye laser amplifier which selects pulses at a 10 Hz

rate for further amplification. Satisfactory performance was obtained at 885 nm by first getting experience with the laser system by working with Rh6G which lases at 650 nm. The Rh6G dye is very efficient. Efficient amplification of the picosecond pulses required upgrading the performance of the Nd:YAG laser pump to improve its spatial and temporal profile. With the experience gained from the Rh6G system it was possible to switch to the redder, less efficient, dyes and after appropriate manipulations obtain satisfactory performance. Plans are being made to observe the two-photon superfluorescence as well as to demonstrate the generation of even parity superposition states by generating second harmonic radiation with the picosecond pulses.

#### 26566 NEW DEVELOPMENTS IN ATOM INTERFEROMETRY

David E. Pritchard Massachusetts Institute of Technology

A major advance was made by the P.I.'s group with the demonstration of the first atom interferometer, a three grating interferometer for sodium atoms. This configuration is much like a Mach-Zender interferometer: the first transmission grating splits the incident atom wave into coherent beams, two of which are diffracted by the second grating so that they recombine at the third. The interferometer, including collimator, is about two meters long, and the two components of the atom wave are separated by 27  $\mu$ m in the middle of the interferometer. The key component of the atom interferometer is the transmission gratings. These consist of a set of slots in a silicon nitride membrane stretched across openings in a silicon wafer. The slots are created by a special reactive ion etch process in which a pattern written by electron beam lithography into PMMA is used as a direct mask for the Si<sub>3</sub>N<sub>4</sub>. The gratings used in the interferometer had a 0.4  $\mu$ m period, but researchers have also made gratings with 0.2 µm period. Atom interferometers should be valuable for three general classes of measurements: inertial effects, fundamental tests, and measurements of atomic and molecular properties. Atom interferometers are particularly sensitive to rotation, having  $\sim 10^{10}$  the sensitivity to rotation of a laser gyro with the same beam geometry. These improvements in atom optics may ultimately permit the construction of gyroscopes good enough to perform tests of relativity.

#### Reports:

1. Research Laboratory of Electronics Progress Report No. 132,

by Jonathan Allen and Daniel Kleppner, TR, Jun 90, 5 pp. AD A224 370  $\,$ 

 Atomic Optics, by David W. Keith and David E. Pritchard, New Frontiers in Quantum Electrodynamics and Quantum Optics, 1990, p467. AD A234-044

## 26709 THE INTERACTIONS OF RADIATION WITH MATTER

Steven T. Manson Georgia State University

The first stage of the work on modeling the secondary electron spectrum resulting from electron and/or ion impact ionization of atoms and molecules over a broad range of incident and secondary energies with relativistic effects included has been completed. The methodology was applied to the simple case of electrons on helium and the resulting comparisons with extant experiments has been excellent. Work on ions has continued. Studies were made of the inner shell properties of atomic ions. The major finding is that all inner shell atomic properties that were examined, x-ray transition energies and rates, photoionization cross sections, and expectation values of various powers of the electron radial coordinates remain constant when outer shell electrons are removed. This behavior has been understood in terms of the spatial extent of the wavefunctions of electrons in different shells. This study has application to any very hot environment. Much has also been done in the area of photoionization. Relativistic studies of resonances in photoabsorption in highly ionized species have been performed; e.g., Mg-like Lr<sup>+91</sup>. Preliminary results of the studies indicate that resonances are far less important for such high Z than for neutral Mg.

#### Reports.

- 1. Photoionization of Rydberg Atoms Very Near Threshold, by C.E. Burkhardt et al., MS. Nucl Inst and Meth.
- Relativistic Model of Secondary-Electron Energy Spectra in Electron-Impact Ionization, by John H. Miller and Steven T. Manson, MS. *Phys Rev.*
- Spectral and Electron-Collision Properties of Atomic Ions. II. Inner-Shell Properties, by Steven T. Manson et al., MS, *Phys. Rev.*
- 4. New Frontiers in X-Ray Photoionization of Ions and Atoms, by Steven T. Manson, MS
- Photoionization of the Excited 6s6p<sup>33</sup>P States of Ytterbium, by Jonathan T. Manson and Steven T. Manson, MS, *Phys Rev.*

#### 26821 ELECTRON-BEAM CONTROLLED SEMICONDUCTOR SWITCHES

Karl H. Schoenbach V.K. Lakdawala Glenn A. Gerdin Old Dominion University

A code was developed which allows one to describe the temporal development of the switch parameters after a pulse excitation with an electron beam. The one-dimensional drift-diffusion model describes the switch as part of a pulsed power circuit. The switch material, which was studied in a first run, is silicon doped, copper compensated GaAs. The use of copper as a dopant induces a pronounced current controlled negative differential conductivity which leads to a bistable behavior of the system. This characteristic feature offers the possibility to design an on-switch which combines a high hold-off voltage and low forward resistance and hence reaches a very favorable efficiency. The electron-beam induced conductance and the recovery behavior of bulk GaAs switches (with ohmic contacts) was compared with pin-diodes made of an identical semiconductor material and with the same dimensions. The conductance of pin-diodes exceeds that of bulk switches by more than an order of magnitude due to the enhanced cathodoluminescence in the heavily doped *p*-layer of the diode. The lock-on effect which was observed in the bulk switch and in the forward biased pin switch at field strengths exceeding 2.8 kV cm, was completely suppressed in the reverse biased pin diode. This result indicates that double injection of carriers through the contacts is at least in part responsible for the lock-on effect.

#### Reports:

- The Recovery Behavior of Semi-Insulating GaAs in Electron-Beam Controlled Switches, by D.C. Stoudt et al., *IEEE Trans* on *Electron Devices* 37,2478(1990) AD A232-441
- The Current-Voltage Characteristics of Semi-Insulating Gallium Arsenide, by R.P. Brinkmann et al., MS, J Appl Phys.
- 3. The Lock-On Effect in Electron-Beam Controlled Gallium Arsenide Switches, by R.P. Brinkmann et al., *IEEE Trans on Electron Devices* 38,701(1991).
- Modeling of Electron-Beam-Controlled Semiconductor Switches, by R.P. Brinkmann, J. Appl. Phys. 68,318(1990) AD A226-568.
- 5. High Power Switching with Electron-Beam Controlled Semiconductors, by R.P. Brinkmann et al., MS
- Switching Properties of Electron-Beam Controlled GaAs Pin-Diodes, by M.K. Kennedy et al., MS.

## 26899 EXCIMER EMISSION FROM ALKALI DIATOMIC AND ALKALINE-EARTH – NOBLE GAS MOLECULES

John P. Huennekens. Lehigh University

#### SL. NVEOC

A paper has been published which reports the observation of several six-wave mixing processes which result in broadly tunable coherent emission in the wavelength range  $1.20-1.45 \ \mu\text{m}$ . These emissions are produced in potassium vapor which is simultaneously pumped by two pulsed dye lasers. One set of processes is produced when the frequency of the first laser is fixed to the potassium  $4S \rightarrow 6S$  two-photon transition frequency, while the frequency of the second laser is tuned. The second set of processes is observed when both lasers are tuned, but with their sum frequency fixed to the  $4S \rightarrow 6S$  two-photon transition. Peak output energies of  $\sim 10$  nJ have been observed.

Reports

- No. 1.3 in previous editions.
- 4 Bound-Free Emission in Alkali Diatomic Molecules, by Mark Francis Masters, PhD Thesis, 1990, 203 pp.

## 26959 DIAGNOSTICS OF DIAMOND FILM DEPOSITION PLASMAS

Kenneth R Stalder Jay B. Jeffries SRI International

SL. ARO

1. The initial experimental laser-based measurements of OH radical in a hot filament reactor were completed. Based on feedback from questions from the diamond research community, a new set of conditions were characterized in the hot filament reactor after the meeting. 2. The results of the arc-jet diagnostics were used as boundary conditions for a more refined modeling calculation. The measured gas temperatures versus position in the jet downstream from the dc-are are significantly lower than most estimates for such a plasma. Modeling results indicate that the methyl radical does not impinge the substrate with a large enough concentration to account for the observed growth rate. In a collaboration with Professor David Goodwin at CalTech, SRI has combined a chemical model with his more complete model of the fluid mechanics of the flow field and boundary laver. Even with this more complete calculation, the predicted

methyl radical concentration is modulial for the observed growth rate. In all the imbulations there is a surprising super-equilibrium of atomic carbon. This large carbon atom concentration leads to speculation about the importance of carbon chemistry at the growing diataond surface. Ongoing experimental effort on the dc arc jet plasma is now aimed at unde danding the mass spectra of atoms, ions and radicals that impinge on the stagnation point where fast diamond growth occurs.

#### Reports

No. 1-2 in previous editions

 Diagnostics of a Diamond Depositing DC Arc Jet Plasma, by George A. Raiche et al., MS

#### 27431 MILLIMETER AND SUBMILLIMETER STUDIES OF NONAMBIENT ENVIRONMENTS

Frank C. De Lucia Duke University

Direct measurements of the gain profile of optically pumped far-infrared lasers show that large shifts in the laser frequency can be caused by the absorption from thermal molecules on the laser transition. The absorption shifting greatly exacerbates pump frequency deviations, resulting in an extreme sensitivity to pump offsets and drifts. This pressure dependent shifting mechanism is not present in transversely pumped lasers, which explains their superior frequency reproducibility compared to longitudinally pumped lasers, and reconciles two apparently conflicting results regarding laser stability.

#### Reports

 Collisional Energy Transfer in Methyl Halides, by Henry Ofin Eventt, III, PhD Thesis, 1990, 220 pp.

#### 27508 FEMTOSECOND LASER STUDIES OF EXCITED STATE DYNAMICS

Peter P. Sorokin IBM Research Center

A paper has been published which presents a simple classical model for understanding time-resolved absorption spectra of molecules that are in the process of dissociating. The model applies to absorption spectra that are obtained by measuring the spectral power density of an ultrafast, continuum probe pulse after transmission through the sample. The authors show that the classical model can yield results in

good agreement with quantum-mechanic wave packet propagation calculations. In a close analogy with collisional line broadening, the time-resolved absorption spectra are shown to have an impact region. near the separated-atom transition frequency and a far-wing region. The impact region is due to radiation emitted after the molecule has separated into atomic fragments, and the far-wing region is due to radiation emitted during the time of strong molecular interaction. The spectrum in the impact region depends upon an effective phase shift for a "partial" collision, which begins at the time that the probe pulse sweeps through the molecular transition frequency. For narrow wave packets, this phase shift can be directly measured, and the molecular transition frequency can be recovered as a function of time. along the path of dissociation. For very broad wavepackets, the time-resolved absorption spectraapproach a statistical limit, in which the absorption line shape becomes an image in frequency space of the probability density in configuration space at the time of excitation by the probe pulse. In all cases, the frequency-integrated absorption is proportional to the net population of molecules that are excited by the probe pulse. In principle, this result can be used to obtain the strength of the transition dipole moment as a function of internuclear separation. Fluorescence induced by a short optical probe pulse, as in the experiments of Zewail and coworkers, is also considered. Eluorescence measurements are shown to be fundamentally different from measurements of the transmitted spectral power density: fluorescence depends upon the net population excited by the probe pulse, whereas the transmitted spectral power density depends upon interference between the incident probe field and the polarization field. Thus these two experimental techniques are sensitive to different aspects of the dissociation process.

#### Reports

- Lime Resolved: Absorption: Spectra: of: Dissociating: Molecules, by R.F. Walkup et al., *Phys. Rev. Lett* 65:2366(1990) AD: X232-478.
- Classical Model of Femtosecond Time Resolved Absorption Spectra of Dissociating Molecules, by R.F. Walkup et al., J. Chem. Phys. 94,3389(1991) AD A238,455
- 3 The Impact Approximation in Transition State Absorption Spectroscopy. On the Possibility of Obtaining Difference Potentials Directly From the Transient Spectra, by R.F. Walkup et al., *Ultratast Phenomena VII*, 1990, p516 AD A232, 262.
- Femtosecond Transition State Absorption Spectroscopy of Br Atoms Produced by Br. Photodissociation: by J.A. Misewich et al., *Frindrics Phonomenic Att.*, 1990, p426 AD X232,263.

#### 27532 OPTICAL FREQUENCY DIVISION USING AN OPTICAL PARAMETRIC OSCILLATOR

Ngai Chuen Wong Massachusetts Institute of Technology

SL: NVEOC SC: ETDL

An optical parametric oscillator (OPO) converts with high efficiency an input pump into two intense, coherent subharmonic outputs whose frequencies are tunable and whose sum frequency equals the input pump frequency. By measuring the output frequency difference relative to a microwave, millimeter wave or even infrared reference source, the output frequencies are precisely determined, and the OPO functions as an optical frequency divider. OPO-dividers can be operated in series or in parallel to measure, compare, and synthesize frequencies from optical to microwave, with high precision and resolution. The initial focus of this research is to demonstrate optical frequency division. A two-element OPO has been constructed. It consists of a mirror and a KTP crystal, one end of which serves as a cavity mirror. The OPO is a doubly-resonant configuration that is resonant in both the signal and idler waves. Fastened to a single mirror mount, the compact structure has good mechanical stability. Stability cw single-mode operation has been obtained from the KTP-OPO near its frequency degeneracy. The OPO is pumped with a krypton ion laser at 530.9 nm with a threshold of 20 mW. Angle tuning of the crystal permits the output frequency separation to be set anywhere within 1 THz of degeneracy. Direct frequency measurements have been made of the subharmonic output difference frequency up to 26 GHz, limited only by the photodetector frequency response and available microwave electronics. Continuous tuning of about 0.5 GHz around the set point is obtained through temperature tuning of the crystal and a piezoelectrically controlled cavity length servo. Success has been achieved in demonstrating a mable optical frequency divider using a KTP-OPO with excellent tuning characteristics; any frequency separation within 1 THz of frequency degeneracy can be obtained by angle and temperature tuning of the crystal.

Reports

#### 27646 A HIGH FLUX RADICAL BEAM FOR DIAMOND GROWTH

J.E. Lawler L.W. Anderson W.N.G. Hitchon University of Wisconsin Madison

The goal of this investigation is to grow diamond film under conditions such that the flux of atoms and molecules to the surface is both known and highly controlled. This will be done using a high flux radical beam system. The radical beam system will be used to do very important, fundamental experiments on the physics and chemistry of diamond film growth. The design of the high flux radical beam system was modified by the addition of a reaction chamber or tube. Both the dwell time and the temperature of gas in the reaction tube are variable and thus will provide a high degree of control over gas phase chemistry. The reaction chamber is between the rf plasma dissociator and the substrate (growth) surface. The plasma does not penetrate to the reaction tube and thus complex and poorly understood plasma chemistry is eliminated. Construction of the high flux radical beam system is nearing completion. Experiments are now underway to identify the best passivation coating for the reaction tube. The passivation coating is necessary to prevent surface chemistry in the reaction tube. Teflon, various silicon rubbers (RTVs), and a coating called "Dreilm" are now being tested.

## 27766 UNCERTAINTY LIMITED ATOMIC POSITION MEASUREMENT USING OPTICAL FIELDS

John E. Thomas. Duke University

A paper was presented which demonstrates ultrahigh resolution atomic position measurements in beams using optical techniques that scale to uncertainty limited precision. Applications include atomic interferometry and minimum uncertainty wave packets. Another paper describes and demonstrates optical techniques for ultrahigh resolution position measurement and localization of moving atoms. The methods can achieve accuracies limited by the Heisenberg uncertainty principle for highly collimated or transversely cooled atomic beams.

Reports.

Demonstration of a Funable Optical Frequency Divider Using a KTP Optical Parametric Oscillator, by N.C. Wong and D. Lee, MS

Precision Position Measurement of Moving Atoms Using Optical Fields, by K.D. Stokes et al., MS, Phys Rev Let.

## 27888 INFRARED/SUBMILLIMETER-WAVE DOUBLE RESONANCE STUDIES OF MOLECULAR COLLISION KINETICS

David D. Skatrud Duke University

A paper on the frequency stability of optically pumped far-infrared (OPFIR) lasers was published in Applied Physics Letters. This work demonstrated that transversely pumped OPFIR lasers are extremely sensitive to offsets in the pump frequency because of a pushing of the gain profile from the sloping background absorption. It was demonstrated that the OPFIR laser frequency could be shifted an order of magnitude more than the effective pump offset at the lasing transition. A paper was presented at the 15th International Conference on Infrared and Millimeter Waves which described the possibility of making a new type of OPFIR laser that would lase on perturbation allowed transitions. The paper compared the operating parameters of standard OPFIR lasers with those the perturbation OPFIR lasers would be expected to have. Of particular importance is the apparent cal ability of operating at higher pressures, which might allow more efficient operation. Gain calculations were performed and the specific example of SO<sub>2</sub> was considered. A new diagnostic cell is being constructed in the laboratory. It will use a specially fabricated dichroic mirror which will transmit the probe beam while reflecting the pump beam. This will provide a better defined and more effective overlap of the infrared and submillimeter doubleresonance signals.

#### Reports:

- 1. Frequency Stability and Reproducibility of Optically Pumped Far Infrared Lasers, by Richard L. Crownover and David D. Skatrud, MS, *Pppl Phys Let*.
- Optically Pumped FIR Perturbation Laser, by David D. Skatrud, MS.

## 28396 THEORETICAL AND EXPERIMENTAL INVESTIGATION OF ELECTRON BEAM ACCELERATION AND SUB-MILLIMETER WAVE GENERATION

N.C. Luhmann, Jr.

D.B. McDermott

University of California, Los Angeles

SL: ETDL SC: NRL

The objective of this research is to conduct basic research on electron beam acceleration and nearmillimeter wave generation in resonant cavities. The approach includes the following tasks: (*a*) gyroresonant acceleration of multi-ampere level electron beams using a 20 MW S-band amplifier driver; (b) use of the high current, high energy electron beams described in (a) to drive MW level high harmonic gyro-devices; (c) development of a 100 kW, 60 GHz gyro-BWO with several percent fast electronic tunability and 30 percent slow magnetic tunability; (d) development of a 200 kW, 28 GHz multicavity gyroklystron amplifier with a gain of 40 dB and investigation of the associated physics issues; (e) optimizing a Bragg resonator and hot-testing it in a 400 kV CARM oscillator and a 100 kV gyro-TWT oscillator operated far above cutoff.

## 28472 CHARACTERIZATION OF SOLID STATE LASER AND NONLINEAR OPTICAL MATERIALS

Richard C. Powell Oklahoma State University

Research will be conducted on the optical properties of materials having applications in solid state laser systems, especially the fundamental physical processes involved in diode laser pumping and frequency agility. Three thrust areas involving different approaches to tunability will be investigated: (a) Studies of bread band vibronic emitters will include laser-induced refractive index changes in Cr3-doped crystals, the spectral dynamics and lasing properties of Cr<sup>3</sup> in new host crystals, and novel lasing materials such as vanadates and organic dyes in sol-gel gases. (b) The spectral dynamics and lasing properties of narrow line emitters such as fluoride and oxide crystals and glasses doped with two or more rare earth ions will be investigated experimentally and with computer models. (c) Nonlinear optical materials including rare earth doped glasses, photorefractive crystals, and liquid crystal polymers will be characterized with laser spectroscopy techniques. The spectroscopy techniques will include four-wave mixing, multiphoton absorption, fluorescence line-narrowing, and subpicosecond time-resolved spectroscopy.

## 28499 ELECTROMAGNETIC PROPAGATION AT ULTRAHIGH INTENSITIES

Charles Rhodes

University of Illinois at Chicago

SC: ASL

A systematic, experimental and theoretical investigation will be made of electromagnetic propagation

under extremely strong-field conditions in the ultraviolet spectra region. The work will concentrate on exploring the possibility of accessing a new quasistable mode of channeled propagation for radiation at intensities of  $\sim 10^{20}$  W/cm<sup>2</sup>. Modes of electromagnetic propagation will be examined both experimentally and theoretically in the strong-field regime with emphasis on: (a) The conditions (e.g., material, density, and intensity) which govern channeled propagation, with particular attention to the regime of intensities  $>10^{18}$  W/cm<sup>2</sup>; (b) the stability and dynamic of formation of the channeled modes; (c) the possibili<sup>\*</sup>y of propagation in over-dense plasma, in particular, media at solid density.

#### 28531 SEMICONDUCTOR FILM CERENKOV LASERS

John E. Walsh Dartmouth College SC: HDL

Investigations will be made of a novel Cerenkov laser which uses a semiconductor-film surface waveguide. The initial work will concentrate on the proof-of-principal demonstration of the semiconductorfilm Cerenkov laser concept. This initial work will use an existing electron beam source and proven resonator design techniques. Next, the following unique features of the SFCL will be investigated: low loss in the desired spectral range; the potential for forming integrated resonators; the high relative indices of refraction; and the ability to bleed charge by their finite dc resistivity. The possibility of integrating a high-brightness cathode technology to produce a compact, tunable source with sufficient spectral purity will also be explored.

## 28561 SEMICONDUCTOR DEPOSITION AND ETCHING INTERACTIONS OF LASER-GENERATED TRANSLATIONALLY HOT ATOMS AND RADICALS

Stephen R. Leone University of Colorado

SC: ETDL. MTL

The objective of the research is to study the interaction of translationally energetic neutral species with semiconductor surfaces. The goal of the work is to attain a detailed understanding of the microscopic mechanisms of semiconductor etching and deposition. A laser vaporization process will be used to produce a beam source of high kinetic energy species that are well characterized in terms of kinetic energies, fragmentation patterns, and internal states. These hot atoms and radicals will be used to study scattering, etching, oxidation, and deposition processes that are important for the basic physics of electronics materials processing. An ultrahigh vacuum apparatus will be used which incorporates x-ray photoelectron spectroscopy, velocity selection of the beam species, and quadrupole mass spectrometric detection of the scattered products. The rates and anisotropy of etching on silicon, gallium arsenide, silicon dioxide, aluminum, and refractory metal silicides will be investigated. Also, the activation barriers of etching will be investigated by varying the kinetic energies and the deposition of thin films of refractory metals and metal fluorides will be explored.

## 28569 VACUUM MICROELECTRONIC DEVICES AND THEIR APPLICATIONS USING COMPOUND SEMICONDUCTOR TECHNOLOGY

Umesh K. Mishra University of California, Santa Barbara

SL: ETDL SC: HDL

An innovative hot electron source will be developed for use in vacuum microelectronic devices. Hot electron emission in a novel planar doped barrier will be investigated in GaAs, AlGaAs, Si, and wide bandgap semiconductors. The initial work will focus on the design, fabrication and testing of the vacuum electronic emitter. The innovative design relies on a drift region of dimension smaller than the mean free path of the electrons. In conjunction with the experimental work, a detailed theoretical study will be performed on the nature and magnitude of the injecting barrier under the constraints of this short drift region. After establishing a preferred vacuum emitter design, efforts will be directed towards the development of the requisite technologies for gate structures and incorporation in transistors and klystrons.

#### C. Fluid and Plasma Physics

## **D.** Solid State Physics

## 25114 INFLUENCE OF DEFECTS IN HgCdTe GROWN BY MOLECULAR BEAM EPITAXY (MBE) ON ELECTRICAL DEVICES

Roger E. DeWarnes

**Rockwell International Corporation** 

A paper has been prepared which presents for the first time, molecular beam epitaxy (MBE) results on the growth of in-situ doped p-on-n heterojunctions on HgCdTe epilayers grown on (211)B GaAs substrates. Long wavelength infrared (LWIR) photodiodes made with these grown junctions are of high performance. The *n*-type MBE HgCdTe/GaAs alloy epilayer in these structures was grown at  $T_s = 185^{\circ}$ C and it was doped with indium (high  $10^{14}$  cm<sup>-3</sup> range) atoms. This epilayer was directly followed by the growth, at  $T_{\rm x} = 165^{\circ}$ C, of an arsenic-doped  $(10^{17} - 10^{18} \text{ cm}^{-3})$ HgTe/CdTe superlattice structure which was necessary to incorporate the arsenic atoms as acceptors. After the structure was grown, a Hg-annealing step was needed to interdiffuse the superlattice and obtain the arsenic-doped p-type HgCdTe layer atop the indium-doped layer. LWIR mesa diodes made with this material have 77 K R<sub>o</sub>A values of  $5 \times 10^3$ , 8.1 and 8.5  $\Omega$ cm<sup>2</sup> for cutoff wavelengths of 8.0, 10.2 and 10.8 µm, respectively; the 77 K quantum efficiency values for these diodes were greater than 55 percent. These recent results represent a significant step toward the demonstration of MBE as a viable growth technique for the in-situ fabrication of large area LWIR focal plane arrays.

#### Reports:

No. 1-2 in previous editions.

 Molecular-Beam Epitaxy in situ Arsenic-Doped p-on-n HgCdTe Heterojunctions, by Jose Arias et al., MS, J Appl Phys.

## 25167 ELEMENTARY EXCITATIONS, OPTICAL AND TRANSPORT PROPERTIES OF ARTIFICIALLY STRUCTURED MATERIALS

John J. Quinn Brown University

#### SL: ETDL SC: HDL

Optical Properties of Donors in a Modulation Doped Superlattice: The numerical calculations of the binding energy of a single donor in the quantum well or in the barrier as a function of  $N_s$ , the concentration of free electrons in the quantum well has been

#### **I** Physics

completed. The spin density functional technique has been used to treat exchange and correlation. The energy of a donor in the center of the quantum well has been determined for both the  $D^0$  (neutral donor) and  $D^{-}$  (negatively charged donor). For a donor in the barrier the energy of the  $D^0$  state has been determined. An investigation is being made of the linear response of a system containing  $N_{I\alpha}$  impurities of type  $\alpha$  and N<sub>s</sub> conduction electrons to an external disturbance with arbitrary space and time dependence. A scheme has been developed for determining the response functions and normal modes of a finite array of layers in terms of simple diagrams and rules for associating with each diagram an analytic contribution to the dispersion relation of the excitation being studied. The method has been applied to plasmons, phonons, magnons and electronic states in a finite array of thin layers.

#### Reports:

No. 1-3 in previous editions.

- 4. Collective Excitations of Electron-Hole Plasma in Semiconductor Superlattices, by X. Xia et al., MS.
- 5. Exchange-Correlation Function for a Spin-Polarized Two-Dimensional Electron Gas, by X. Xia et al., MS, Phys Let.
- Self-Trapped Magnetic Polarons in Two-Dimensional Semimagnetic Semiconductors, by Xiaodong Zhu and J.J. Quinn, MS, Sol St Commun.
- Novel Diagrammatic Method for Analysis of Finite Periodic and Aperiodic Multilayer Structures, by George Vecris and J.J. Quinn, Sol St Commun 76,1071(1990). AD A233 952
- Novel Diagrammatic Method for Analyzing the Surface Electronic Modes of Finite Multilayer Structures, by George Vecris and J.J. Quinn, MS.
- 9. Electronic States and Tunneling in Periodically Modulated Cd<sub>1</sub> xMnxTe Quantum Wires, by P. Hawrylak et al., MS.
- Exact Analytic Dispersion Relations for Dipolar Magnetostatic and Magnetoretarded Modes in Finite Magnetic Superlattices, by George Vecris and J.J. Quinn, *Phys Rev* 43,8303(1991).
- Excitonic Insulator Transition in a GaSb-AlSb-InAs Quantum-Well Structure, by J.J. Quinn and Godfrey Gumbs, Sol St Commun 75,595(1990). AD A233 949

## 25374 MAGNETIC STRUCTURES AND EXCITATIONS IN THIN FILMS AND MULTILAYERS

R.E. Camley Doug L. Mills

University of Colorado at Colorado Springs

SC: ETDL, HDL

An investigation was made of two completely different materials which have promise as signal processing elements in the infrared. In a magnetic field both of these materials can exhibit nonreciprocal reflection

of electromagnetic radiation. Such nonreciprocal properties have been used in microwave devices for delay lines, isolators an circulators. The recent production of ultra-thin magnetic films has produced an interesting and fundamental question. These films are nearly two-dimensional and it is well known that there should be no long-range order in ideal two dimensional films. Nonetheless experimentally these films do exhibit long range order with transition temperatures from the magnetic state to a nonmagnetic state occurring even above room temperature. It has been proposed that magnetic anisotropy allows the magnetic state to exist. This was studied in detail by means of classical Monte Carlo simulations. The Monte Carlo results showed that for a monolayer the transition temperature was in good accord with an approximate formula developed earlier using renormalization group methods. In addition results indicated that for reasonable anisotropy values the change in transition temperature with thickness is quite rapid, with the material reaching a transition temperature which is 90 percent of the bulk value by the time one has only 6 atomic layers.

#### Reports:

No. 1-7 in previous editions.

- Remarks on the Ferromagnetic Resonance Spectrum of Exchange Coupled Ferromagnetic Bilayers, by Kh.M. Pashaev and D.L. Mills, MS, *Phys Rev.*
- Surface Phase Transitions and Spin Wave Modes in Semi-Infinite Magnetic Superlattices with Antiferromagnetic Interfacial Coupling, by J.G. LePage and R.E. Camley, MS, *Phys Rev Let*.
- Nonreciprocal Propagation of Surface Waves in Quasi-Periodic Superlattices, by B.L. Johnson and R.E. Camley, MS, *Phys Rev.*
- Anisotropy Driven Long Range Order in Ultra Thin Ferromagnetic Films, by R.P. Erickson and D.L. Mills, MS, Phys. Rev.
- Bulk and Surface Polaritons in Semi-Infinite Superlattices in a Magnetic Field: Dispersion Relations, Optical Reflection, and ATR, by B.L. Johnson and R.E. Camley, MS, *Phys Rev.*
- Microscopic Theory of Spin Arrangements and Spin Waves in Very Thin Ferromagnetic Films, by R.P. Erickson and D.L. Mills, MS, *Phys Rev.*

#### 25464 DIFFRACTION OF LIGHT FROM RANDOMLY ROUGH SURFACES

Alexei Maradudin Richard Wallis University of California, Irvine

SC: ARO

A paper has appeared in print in which it is shown by numerical simulation calculations that the angular dependence of the intensity of the incoherent component of s-polarized light scattered from a large rms slope random metallic grating displays a welldefined peak in the retroreflection direction, while no such peak is observed in the scattering of s-polarized light from a small rms slope random metallic grating. In another paper the scattering of p- and s-polarized light from random metallic gratings with large rms slopes, characterized by surface profile functions  $\zeta(x_1)$  that are even and odd functions of  $x_1$ , is studied. Such profile functions are no longer stationary stochastic processes. Enhanced backscattering is observed in both polarizations from surfaces of both even and odd symmetry. In a third paper, the results of numerical simulations of the scattering of p- and s-polarized light from random gratings on dielectric and metallic surfaces are presented. In the case of a dielectric surface it is shown that for s-polarization and for not very large angles of incidence the reflectance increases as the rms height of the surface increases due to the higher local angle of incidence that the corrugation produces. At the same time, the Brewster effect disappears due to the roughnessinduced departure of the local angle of incidence from the Brewster angle for a plane surface. The mean transmitted intensity has a maximum at an angle of transmission that is close to the forward direction. Thus, the random roughness of the dielectric surface has the consequence that the incident wave apparently does not "see" the change of refractive index as it crosses the boundary. A fourth paper shows that a planar dielectric/vacuum interface can support a surface electromagnetic wave if the real part of the dielectric constant of the dielectric medium is positive and large compared to unity, while the imaginary part is small but nonzero.

#### Reports:

- 1. Enhanced Backscattering and Transmission of Light From Random Surfaces on Semi-Infinite Substrates and Thin Films, by A.A. Maradudin et al., MS.
- 2. Backscattering Enhancement From a Dielectric Surface, by P. Tran et al., MS, J Opt Soc Am.
- 3. Multiple Light Scattering From Metal and Dielectric Rough Surfaces, by M. Nieto-Vesperinas et al., MS.
- Enhanced Backscattering of Light From a Random Grating, by A.A. Maradudin et al., Ann Phys 203,255(1990). AD A232 296

# 25487 SUBMILLIMETER QUANTUM ELECTRONICS

T.C.L.G. Sollner MIT Lincoln Laboratory SC: ETDL, MICOM In the quasi-optical stabilization of resonant-tunneling diode (RTD) oscillators, improvements in the design of the semi-confocal cavity have decreased the instantaneous linewidth of the 100-GHz RTD oscillator to approximately 10 kHz. Researchers have also demonstrated the guasi-optical stabilization with a 200-GHz RTD oscillator, but linewidth measurements have not been completed. Further characterization of lattice-mismatched InAs/AlSb RTDs has been conducted. Microwave shot-noise measurements on high-current-density, high-speed RTDs have demonstrated shot-noise suppression similar to that measured earlier in low-current-density RTDs. This confirms that the shot-noise suppression is an intrinsic property of double-barrier RTDs. A theoretical analysis, which attributes the cause of the shot-noise suppression to modulation of the transmission function by electrons that are stored in the quantum well, has been completed and agrees with experimental data. Researchers have demonstrated that low-current-density RTDs made from the GaAs/ AlGaAs materials system display a maximum peakto-valley ratio with an Al fraction of about 70 percent. The optimum in Al fraction results from a competition between two excess current mechanisms. At low Al fractions, thermionic emission over the  $\Gamma$ -valley barriers dominates. At higher Al fractions, nonresonant tunneling proceeds via the X-point profile of the double-barrier structure. An RTD has been demonstrated in the GaSb/AlSb materials system. Negative differential resistance (NDR) was observed only at temperatures of 77 K and lower. The absence of NDR at room temperature is caused by mixing between the  $\Gamma$  and L-point conduction-band states in the quantum well. By applying uniaxial pressure, researchers have induced a separation of the two states and improved the peak-to-valley ratio considerably at 77 K.

#### Reports:

No. 1 in previous edition.

- Oscillations Up to 712 GHz in InAs/AISb Resonant-Tunneling Diodes at Room Temperature, by E.R. Brown et al., MS, *Appl Phys Let.*
- 3. Resonant-Tunneling Diode Oscillator Using a Slot-Coupled Quasi-Optical Open Resonator, by K.D. Stephan et al., MS, Electron Let.
- Growth and Characterization of High Current Density, High-Speed InAs/AISb Resonant Tunneling Diodes, by J.R. Soderstrom et al., *Appl Phys Let* 58,275(1991). AD A233 367

## 25697 ANALYTICAL INVESTIGATION OF THE ACCELERATION SENSITIVITY OF ACOUSTIC BULK AND SURFACE WAVE RESONATORS

Harry F. Tiersten

Rensselaer Polytechnic Institute

SL: ETDL

In recent work it was shown that the resultant inplane acceleration sensitivity of contoured quartz resonators vanishes for a perfectly symmetric combined resonator plus support system. This indicates that a biconvex resonator will have lower resultant in-plane acceleration sensitivity than a plano-convex resonator because of its inherent additional symmetry. Since a plano-convex resonator is easier to fabricate, an analysis of the degradation in the inplane acceleration sensitivity that arises from the contour being on one side only is being performed. Under in-plane acceleration the single contour causes a state of flexure to exist in the resonator plate. The flexural biasing deformation is being determined by means of a variational approximation procedure using the variational principle for anisotropic static flexure. The very important shearing stresses and accompanying strains are being determined recursively. The resulting biasing states are being employed in the existing perturbation equation along with the mode shapes of the contoured resonators to calculate the degradation in the in-plane acceleration sensitivity caused by the loss of symmetry of the planoconvex resonator. Currently, the computer programs are being written. Recent work has shown that the normal acceleration sensitivity of contoured quartz resonators vanishes as well as the above mentioned in-plane sensitivity for a perfectly symmetric resonator and support system. It has also been shown that any loss of symmetry in the combined resonator plus support configuration results in a significant degradation in the acceleration sensitivity. Since it is essentially impossible to construct a perfectly symmetric resonator plus support configuration in practice, a stiffened structure is being investigated which reduces the biasing deformation in the active region and provides isolation from the unavoidable variations in the details of the actual mounting devices.

#### Reports:

No. 1-6 in previous editions.

- An Analysis of the Normal Acceleration Sensitivity of Contoured Quartz Resonators with Simple Rectangular Supports, by Y.S. Zhou et al., *Proc of 1989 Ultrasonics Symposium*, 1989, p383. AD A226 425
- 8. On the Normal Acceleration Sensitivity of Contoured Quartz

Resonators with the Mode Shape Displaced with Respect to Rectangular Supports, by Y.S. Zhou and H.F. Tiersten, J Appl Phys 69,2862(1991).

- On the Influence of a Fabrication Imperfection on the Normal Acceleration Sensitivity of Contoured Quartz Resonators with Rectangular Supports, by Y.S. Zhou and H.F. Tiersten, Proc of Forty-Fourth Annual Symposium on Frequency Control, 1990, p452. AD A232 939
- An Analysis of the In-Plane Acceleration Sensitivity of Contoured Quartz Resonators with Rectangular Supports, by H.F. Tiersten and Y.S. Zhou, Proc of Forty-Fourth Annual Symposium on Frequency Control, 1990, p461. AD A232 803

## 25906 ELECTRONIC STRUCTURE OF MICROCLUSTERS AND DEFECT COMPLEXES

Shiv N. Khanna P. Jena B.K. Rao Virginia Commonwealth University

As a continuation of work relating to hydrogen pairing in metals, studies have been completed on the formation and dissociation of hydrogen-pairs interacting with a transition metal atom. The studies involved a detailed theoretical investigation of the Born-Oppenheimer surfaces of NbH<sub>2</sub> and PdH<sub>2</sub> trimers. The work on Nb was motivated by the recent nmr experiments on organometallic molecules containing Nb sites interacting with H<sub>2</sub>. These studies reported the observation of two spin-relaxation times. The theoretical work shows that these spin relaxation times are due to the presence of hydrogen in two different configurations: one in which the H-atoms form a molecular bond and this H<sub>2</sub> is bonded to the metal atoms. In the other, the hydrogen atoms dissociate and form individual bonds with the metal atom. There is a barrier between the two configurations but the system can tunnel through the barrier at high temperatures. The corresponding studies on palladium however reveal no barrier between the two configurations and it should be possible to observe molecular H<sub>2</sub> as well dissociated 2H complexes with palladium even at lower temperatures. To consider the magnetic behavior of transition metal clusters, the magnetization of small ferromagnetic clusters has been studied at finite temperatures using the Ising Model and Monte Carlo techniques. Magnetization of finite clusters is reduced from the bulk value, and increases with the external magnetic field and with the cluster size. The results explain qualitatively the recent observations by W.A. de Heer et al of the reduction with decreasing cluster size of the average magnetic moment in small iron clusters.

Reports: No. 1-2 in previous editions.

- 3. Ferromagnetism in Small Clusters, by J. Merikoski et al., MS. Phys Rev Let
- 4. Electronic Shell Structure and the Crystal Field Splitting in Simple Metal Clusters, by M. Manninen and P. Jena, MS.
- 5. Theory of Hydrogen Pairing in Metals, by S.E. Weber et al., MS.
- Magnetism in Small Vanadium Clusters, by Feng Liu et al., MS, *Phys Rev.*

#### 26015 EL<sup>C</sup>CTRONIC TRANSPORT IN HETEROJUNCTION SUPERLATTICES

D.C. Tsui M. Shayegan

Princeton University

The physical behavior of charge carriers in semiconductors subjected to confining potentials over length scales sufficiently small to produce quantum size effects is of great fundamental interest. Moreover, the effects of confining carriers to systems of reduced dimensionality on their transport and density of states are essential for a number of promising electronic and optoelectronic devices. Advances in various epitaxial growth techniques have made it possible to control the band structure potential in the growth direction on a monolayer scale, permitting the creation of two-dimensional electron gas systems, quantum wells and superlattices, and various resonant tunneling structures. On the other hand, lateral confinement achievable by modern microfabrication techniques is limited to a resolution of  $\sim$ 500 Å; and the confining potentials produced by the standard technique of depositing narrow gates on 2DEG are necessarily weak and smooth, reducing the strength of quantum size effects. Recent work has pursued a novel technique of laterally confining carriers in sharp potentials: the creation of a vertical 2DEG by liquid phase epitaxy (LPE) regrowth on patterned substrates pre-grown by molecular beam epitaxy. In particular, researchers successfully fabricated and measured a vertical resonant tunneling diode, in which the tunneling of two-dimensional electrons through well-resolved one-dimensional quantum wire subbands was observed. The method employed in the creation of a vertical 2DEG involved the regrowth of a modulation-doping n-AlGaAs layer on a vertical interface of a patterned GaAs substrate. Since no 2DEG is produced if the regrowth occurs on an interface that has been contaminated by exposure to air, the patterning of the substrate was performed in-situ in the LPE chamber.

D. Solid State Physics

#### Reports:

- Transport in Transverse Magnetic Fields in Resonant Tunneling Structures, by A. Zasłavsky et al., *Phys Rev* B42,1374 (1990). AD A230 801
- Magnetotunneling in Double-Barrier Heterostructures, by A. Zaslavsky et al., *Phys Rev*B40,9829 (1989). AD A231 296
- Physical Characteristics of Double-Barrier Resonant-Tunneling Structures Below 10 kHz, by Yuan P. Li et al., Phys. RevB41,8388(1990). AD A231 313

## 26195 STUDIES OF PHONONS AND ELECTRONIC EXCITATIONS IN SEMICONDUCTOR HETEROSTRUCTURES

Roberto D. Merlin University of Michigan

Raman studies of wide parabolic quantum wells are aimed to test theoretical results predicting the independence of intersubband transition energy on the electron density. So far, it has not been possible to observe scattering in the geometry required to test these ideas; i.e., the configuration allowing spindensity fluctuations. However, measurements of the spectra of charge-density fluctuations seem to agree rather well with infrared measurements obtained by the group of Professor Drew at the University of Maryland. An interesting development of the work on resonant tunneling is that data have been acquired indicating that tunneling requires alignment of chargedensity excitations. Presently, further measurements are being made to confirm this result. The work on the pressure-dependence of magnon scattering has now moved to the compound Fe<sub>3</sub>BO<sub>6</sub>. The Raman spectrum of this material shows a two-magnon feature close and at an energy lower than that of a phonon of symmetry  $E_{g}$ .

#### Reports:

No. 1-4 in previous editions.

- Low-Density Quantum Plasmas: Semiclassical Screening Oscillations, by D.A. Kessler and R. Merlin, *Phys Rev* B41,10 856. AD A224 211
- 6. Pressure Dependence of Two-Magnon Raman Scattering in NiO, by M.J. Massey et al., MS. Phys Rev.
- 7. Sequential Resonant Tunneling in Superlattices: Light Scattering by Intersubband Transitions, by S.H. Kwok et al., MS.
- 8. Electron-Hole Superconductors, by R. Merlin, MS, Sol St Commun.
- 9. Raman Spectroscopy of Shallow Impurities in Semiconductor Quantum Well Structures, by R. Merlin, MS.
- 10. Effects of Pressure and Isotopic Substitution on the Raman

Spectrum of  $\beta$ -Fe<sub>2</sub>O<sub>3</sub>: Identification of Two-Magnon Scattering, by M.J. Massey et al., *Phys Rev* B41,7822(1990). AD A224 532

#### 26211 SUBPICOSECOND RESOLVED INCIPIENT LASER DAMAGE

W.E. Bron

University of California, Irvine

Investigation into nonequilibrium phonon dynamics in the presence of optically induced incipient laser damage using time-resolved coherent anti-Stokes Raman scattering has progressed in the following areas. A more detailed understanding of the interaction between a hot electron-hole plasma and the LO phonon system in GaP is being investigated. The analysis on data obtained from the electron-hole plasma/LO phonon experiment has continued. A theoretical model to describe the process of electronic cooling and, specifically, the exchange of energy between the collective states of the electronhole system and the LO phonon system has been developed. This model, in conjunction with the experimental results from the electron-hole plasma/LO phonon experiment, will be incorporated in the next phase of the experiment. Specifically, the theoretical model will be used to determine the dynamics of energy transfer between the electronic system and the phonon system under high laser fluences so that the respective roles played by electrons and phonons at the onset of macroscopic damage may be described quantitatively. Pending the completion of the work on the theoretical model, direct measurements of single and multiple pulse incipient laser damage in GaP will be taken. In addition to the above mentioned work, equipment and software development has continued. Single pulse TR-CARS measurements and multibeam absorption monitoring techniques along with the appropriate computer software to control the detecting system have been developed.

## 26442 RADIATIONLESS TRANSITIONS AND EXCITED STATE ABSORPTION IN TUNABLE-LASER MATERIALS

Ralph H. Bartram

University of Connecticut

SC: HDL

A new, more general method was developed for optical lineshape simulation which allows the effects of anharmonicity to be included in the calculation of

nonradiative transition rates. Defect lattice dynamics calculations account for sharply resolved sideband structure of chromium emission spectra in halide elpasolites. Extended vibrational structure of twophoton excitation spectra exhibits different polarization anisotropy for different modes. The pressure dependence of the effective vibration frequency is shown to be related to that of the local compressibility and the linewidth.

Reports:

1. Upconversion by Excited State Absorption of Fb<sup>+</sup> Centers in Alkaline-Earth Fluorides, by J.-M. Spaeth et al., MS, *J Phys. Condens Matter*.

#### 26644 NONLINEAR OPTICAL STUDIES OF RESONANT SYSTEMS

Duncan G. Steel University of Michigan

This program focuses on the study of exciton dynamics, primarily in GaAs heterostructures. The experimental methods are based on the use of nonlinear laser spectroscopy methods developed earlier in this program on simpler systems. Recently, however, efforts have been directed towards an examination of the measurements show behavior which does not seem to be explained by the existing theoretical descriptions. Simultaneous measurements were made of the energy and polarization relaxation rates, corresponding to the longitudinal and transverse rates in simpler systems. Measurements have been based on the use of the stimulated photon echo (SPE). It was earlier shown that at moderate excitation densities, time resolved emission showed both a free polarization decay and a stimulated photon echo. However, at extremely low exciton density, a simple SPE was obtained. Measurements of the longitudinal relaxation time were in reasonable agreement with the earlier measurements, an unambiguous measurement of the dephasing rate was difficult since spectral diffusion contributed to the line shape. While this provided important information, it was not possible to compare the dephasing rate to the longitudinal relaxation rate. Using the SPE, it is possible to make simultaneous measurements. Using this method, both rates were obtained as a function of temperature and excitation wavelength. At low temperature and for lowest energy hhl excitons, researchers found that the dephasing rate is  $\frac{1}{2}$  of the longitudinal rate. However, as the temperature increases or for higher energy excitons, the dephasing rate increased faster than the longitudinal rate. Since, in the standard

#### D. Solid State Physics

picture of relaxation, the dephasing rate is linearly proportional to the excitation rate, the measurements show the presence of an extra dephasing mechanism. In separate measurements, a series of experiments were performed to understand unexpected differences in the cw FWM spectrum and the steady-state differential absorption spectrum. Differential absorption measurements in GaAs/AlGaAs multiple quantum wells based on cw and picosecond lasers show an unexpected spectrum in all samples at very low temperature and low excitation density. The results are not at all predicted by current many body theories and suggest that Coulomb effects in the nonlinear spectrum may dominate phase space filling.

Reports:

No. 1-7 in previous editions.

 High Resolution Nonlinear Laser Spectroscopy Measurements of Exciton Dynamics in GaAs Quantum Well Structures, by Duncan G. Steel et al., MS.

## 26682 A NOVEL APPROACH FOR NEW RADIATION SOURCES BASED ON SOLID STATE PLASMA INSTABILITIES

Pradip Bakshi

K. Kempa

Boston College

A report has been prepared which investigates current driven instabilities of plasma modes in semiconductor heterostructures. Amplification of the plasma modes becomes possible when electrons are driven parallel to the interface by a sufficiently large electric field. Effects of electron-electron and electron-phonon scatterings are included. The report indicates that the idealized, strictly two-dimensional treatment of the charge carriers used in previous studies is an excellent approximation if only one subband is occupied at T=0, and the frequency of the generated oscillation is much less than the intersubband separation. If more subbands are occupied, the threshold drift velocity for this instability can be significantly reduced, making it more practical for device applications. A beam of ballistic electrons moving with a velocity of about twice the Fermi velocity ( $\sim 10^7$  cm/s) with respect to a stationary electron gas has been shown to lead to spontaneous generation of plasmons. A manuscript develops a first principles, self-consistent theory of the far infrared (FIR) electromagnetic response for electrons confined in a quantum dot. For small electron number,  $n_e$ , the FIR absorption spectrum corresponds to that associated with parabolic confinement, i.e., absorption dominated by a single

peak, which occurs at the frequency corresponding to the inter-level separation of the parabolic potential, and is roughly independent of  $n_e$ . For large electron number, an upward shift in the resonance frequency occurs as the electron density probes the increasingly nonparabolic curvature of the dot potential.

Reports:

No. 1-3 in previous editions

- 4. Current Driven Plasma Instability in Quantum Wires, by P. Bakshi et al., Sol St Commun 76,835(1990). AD A238 410
- 5. On the Possibility of Spontaneous Polarization in Quantum Dot Systems, by K. Kempa et al., MS.
- Self-Consistent Far Infrared Response of Quantum Dot Structures, by D.A. Broido et al., *Phys Rev* B42,11 400(1990). AD A238 411
- Spontaneous Generation of Plasmons by Ballistic Electrons, by K. Kempa et al., *Phys Rev* 43,9273(1991). AD A238 174

#### 26827 RELIABILITY OF SOL-GEL DERIVED FERROELECTRIC MEMORIES

Sandwip K Doy

Arizona State University

A simplified process, involving a reduced number of deposition steps of a high molarity (1-1.5 M) polymeric precursor solution at high spinning speeds, was developed for the fabrication of ferroelectric PZT thin films. The reduction in the number of processing steps and time helps in achieving reproducible and reliable films, and is highly desirable for commercial scale integration. The films obtained, with two depositions only, are crack-free and exhibit dense microstructure with an average grain size of  $0.5 \,\mu\text{m}$ , comparable to the films thickness of 0.4-0.5μm. Thin-layer capacitors were fabricated by sputtering an array of circular gold electrodes (1 mm diameter) on the film surface. The electrical properties were determined from the well-saturated P-E hysteresis loop. The average value of  $P_r$  is slightly smaller in the one-layer PZT thin-film than in the two-layer P > T thin-film. The average value of  $E_c$  is higher in the former case (due to its small thickness), despite the fact that it requires a lower voltage to switch it. The dependence of film capacitance on bias voltage. frequency, and oscillation level were plotted and found to be in agreement with results obtained and reported for films made by the conventional multiple deposition method. A fundamental study of the physics and chemistry of the evolution of the micro/nano structure from the thin-film PZT precursor gel, obtained by acid and base catalyzed hydrolysis, is also being carried out. Further studies are still underway, because a more fundamental understanding of the catalyst mechanism will help in tailoring the properties of the end product, as well as aid in deciding the optimum processing conditions.

## 26996 SEARCH FOR FAR INFRARED RADIATION FROM OPTICALLY PUMPED DEFECT MODES

A.J. Sievers

Cornell University

SC: HDL

A recent theoretical and experimental study of the resonant modes associated with KI:Ag<sup>+</sup> has revealed a nearly unstable low temperature defect-host configuration, whose population decreases dramatically with temperature, becoming vanishingly small above 25 K. Surprisingly, the low temperature dynamics appear to be accurately characterized with a temperature independent harmonic model which makes a number of new predictions about the properties of the IR active gap mode. This gap mode, 86.3 cm<sup>-1</sup> at 1.2 K, is nearly coincident with one of the two  $Rb^+$ , 86.32 cm<sup>-1</sup> and 86.93 cm<sup>-1</sup>, produced by the natural isotopic abundance of this unwanted impurity. The Ag<sup>+</sup> gap mode isotope effect, due to the host lattice mass change of <sup>39</sup>K:<sup>41</sup>K with a natural abundance ratio of 93:7, is 1.8 cm<sup>-1</sup>; the shifted line has  $\sim$ 7 percent of the strength of the main line. Uniaxial stress measurements produce resolvable splittings for the Rb<sup>+</sup> modes but not for the Ag<sup>+</sup> mode suggesting a smaller stress coupling coefficients for this latter defect system. Despite the considerable body of work focused on the universal features of glass behavior, substantial differences do exist among glasses. These differences may prove to be as important as the similarities in the quest for an understanding of the glassy state. A dramatic example of the differences among glasses is the three orders of magnitude variation in the relaxation rates of persistent infrared spectral holes (PIRSHs) in various chalcogenide glasses at 1.5 K. The chalcogenides' strong glass-forming tendency over a wide range of compositions and structures, together with the observation of PIRSHs with strongly host-dependent behavior, make these ideal systems for pursuing a systematic study of the effects of glass structure or PIRSH behavior, with implications for the properties of glasses in general.

Reports:

No. 1 in previous edition.

- Effects of Network Topology on Le- Temperature Relaxation in Ge-As-Se Glasses, as Probed by Persistent Infrared Spectral Hole Burning, by S.P. Love et al., *Phys Rev Let* 65,1792(1990). AD A230 693
- 3. Sulfur-Hydrogen Donor Complexes in Silicon, by R.E. Peale et al., MS, *Mat Sci Forum*.

#### 27458 INVESTIGATION OF QUANTUM EFFECTS IN HETEROSTRUCTURES

Leo Esaki Leroy L. Chang IBM Research Center

The application of an electric field breaks the superlattice minibands into Stark ladders and leads to electron localization. The number of the observed ladders is a good measure of the coherence of the electron states. Usi optical spectroscopies on a variety of GaAs-GaAlAs superlattices, the coherence length increases drastically as the superlattice period and the electric fields are decreased, reaching a value well beyond 500 Å. The effect of localization, meanwhile, results in a sharp increase of the exciton binding energy, as the minibands narrow to discrete states, giving rise to a two-dimensional character of the excitons. Intrinsic surfaces states, arising as a result of termination of periodicity at a crystal surface was first proposed by Tamm in 1932. It was never clearly observed because extrinsic effects usually dominate at the surface. In this work, such states were created in a controllable fashion by a terminating layer of AlAs in a GaAs-GaAlAs superlattice. The formation of the "Tamm States" was manifested by excitonic interband transitions in photoluminescence excitation spectra. Critical confirmation was provided by photo current experiments under an electric field, which showed additional transitions and anti-crossing interactions between the Tamm states and the Stark-ladder states associated with the superlattice. The work demonstrated the ability to create and study a prescribed model surface in a controllable way in semiconductors. Chargecarrier spin scattering in CdTe-CdMnTe multiple quantum wells was directly observed through the circular polarization of luminescence in time-resolved experiments in the femtosecond regime. Separate observations of electrons and hole relaxation were also accomplished by varying the applied magnetic field. A new class of III-V based diluted magnetic semiconductors has been successfully synthesized by molecular beam epitaxy.

#### Reports:

1. Observation of "Tamm States" in Superlattices, by H. Ohno-

et al., Phys Rev Let 64,2555(1990). AD A234-148

- 2. Effects of Carrier Mass Differences on the Current-Voltage Characteristics of Resonant Tunneling Structures, by H. Ohno et al., *Appl Phys Let* 56,1793(1990). AD A233 909
- Ultrafast Polarization Spectroscopy of Diluted Magnetic Semiconductor Superlattices, by M.R. Freeman et al., Surface Sci 228,233(1990). AD A233 892
- Magnetic Observations of Carrier Quantization and Dimensional Crossover in Diluted Magnetic Semiconductor Superlattices, by D.D. Awschalom et al., *Surface Sci* 228,220(1990). AD A234 409
- Change in Dimensionality of Superlattice Excitons Induced by an Electric Field, by F. Agullo-Rueda et al., *Phys Rev* B41,1676(1990).
- 6. Spin-Flip Relaxation Time of Conduction Electrons in Cd<sub>1</sub>, Mn,Te Quantum Wells, by G. Bastard and L.L. Chang, *Phys Rev* B41,7899(1990). AD A234 149
- Interactions Between Extended and Localized States in Superlattices, by F. Agullo-Rueda et al., *Phys Rev* B42,1470 (1990). AD A234 260
- Coherence and Localization in Superlattices Under Electric Fields, by F. Agullo-Rueda et al., *Surface Sci* 228,80(1990). AD A234 092
- 9. Temperature Dependence of the Electronic Coherence of GaAs-GaAlAs Superlattices, by E.E. Mendez et al., *Appl Phys Let* 56,2545(1990). AD A233 972
- Femtosecond Spin-Polarization Spectroscopy in Diluted-Magnetic-Semiconductor Quantum Wells, by M.R. Freeman et al., *Phys Rev Let* 64,2430(1990). AD A233 899
- Epitaxy of III-V Diluted Magnetic Semiconductor Materials, by H. Munekata et al., J Vac Sci Tech B8,176(1990). AD A234 241
- Coherence and Localization in Superlattices, by E.E. Mendez, Localization and Confinement of Electrons in Semiconductors, 1990, p224.
- Spin Dynamics and Dimensionality in Diluted Magnetic Semiconductor Quantum Wells, by D.D. Awschal im et al., Proc of 20th Intl Conference on the Physics of Semiconductors, 1990, p1290.

## 27780 EXPERIMENTAL AND THEORETICAL STUDIES OF IONIC MOLECULAR SOLIDS

John R. Hardy Frank G. Ullman University of Netraska

SC: BRL, ETDL

In order to complete earlier work on incommensurate systems, studies have continued on  $Cs_2Znl_4$ . This system has 3–4 closely spaced structural transitions whose exact nature is unclear. In order to elucidate this, extensive Raman measurements have been made over the temperature range of these transitions, and definitive spectra obtained. A number of new features have been observed and are currently under study theoretically. Birefringence measurements have

proved particularly fruitful in determining the behavior at structural transitions. In addition to these studies, collaboration with Drs. Cornelison and Gauss at BRL has produced promising results---in particular they have been able to carry out measurements of microwave loss as a function of temperature (T =300-500 K). These have clearly established a correlation between strong microwave loss and structural phase transitions. Thus, for the first time, one can be sure that the losses they see reflect the dynamic behavior that is found theoretically. In the theory area, there has been major progress. Specifically, it is possible to model realistically the dynamics of a wide range of incommensurate systems with results comparable to the work on K<sub>2</sub>SeO<sub>4</sub>. In these systems, and in the other systems such as nitrates, one can predict structural transition temperatures to better than  $\pm 10$  percent. Researchers are elucidating for the first time the driving mechanisms, and the balance between them, responsible for the wide diversity of behavior seen experimentally. Proceeding from one system to another, confidence is growing that the combined quantum chemistry/molecular dynamics is reliable for many of the different families of ionic molecular solids. These make up most of the rich diversity of inorganic solids, thus giving one a wide range of possible candidate systems to explore.

#### Reports:

- Ab Initio Simulations of Phase Transitions in KNO<sub>3</sub>, by H.M. Lu and J.R. Hardy, *Ferroelectrics* 111,43(1990). AD A230 717
- First-Principles Simulations of Ionic Molecular Solids: The Pase Transitions in K<sub>2</sub>SeO<sub>4</sub>, by H.M. Lu and J.R. Hardy, *Phys Rev Let* 64,661(1990). AD A230-718
- Possible Vibronic Origin of High T<sub>c</sub> Superconductivity: Non-Cuprate High T<sub>c</sub>'s?, by John R. Hardy and John W. Flocken, *Ferroelectrics* 105,3(1990). AD A231-040
- Gyrotropy in Incommensurate Insulating Crystals, by V. Katkanant et al., *Ferroelectrics* 94,349(1989). AD A230 996
- Ab initio Studies of the Phase Transitions in K<sub>2</sub>SeO<sub>4</sub>, by H.M. Lu and J.R. Hardy, *Phys Rev* B42,8339(1990), AD A231 016
- Vibronic Origins of High T<sub>c</sub>, by John Hardy and John Flocken, *Phase Transitions* 22,121(1990). AD A231 017
- A Priori Theory of Incommensurate Behavior in Rb<sub>2</sub>MnCl<sub>4</sub>, by V. Katkanant et al., *Phase Transitions* 15,103(1989).

#### 28336 BLUE SEMICONDUCTOR LASERS BASED ON WIDE-BAND GAP II-VI MATERIALS

J.E. Schetzina North Carolina State University

SC: HDL

The research objective is the fabrication and testing of low-threshold, room temperature, blue-emitting semiconductor lasers. The work will concentrate on ZnSe which has a band gap of 2.3 eV. MBE film growth experiments will be undertaken with the goal of producing a double heterostructure technology for ZnSe. The ternary compounds ZnCdS and ZnSTe will be developed for the barrier layer material for the double heterostructures, since there is no suitable II-VI binary material that is latticematched to ZnSe which could be used as a barrier layer. Characterization of the MBE grown layers will include double-crystal x-ray diffraction experiments of the structural properties and surface studies with a scanning electron microscope. The optical properties will be investigated by means of photoluminescence and electroluminescence measurements. Paaw Hall effect measurements of the electrical properties will be performed. In addition, devices will be fabricated and tested with the goal of developing a blue semiconductor laser.

## 28362 THEORETICAL AND NUMERICAL PREDICTION OF STOPPING PROPERTIES OF COUNTERPART THIN FILMS AND SOLIDS

John R. Sabin University of Florida

SC: BRL

The ultimate objective is to account for the very large "phase effects" that have been experimentally observed in "stopping power" (for example in proton stopping) between the gaseous and solid phases of material. While the atomic and molecular counterparts of this effort are being carried out by another investigator, the complementary objective is to determine stopping power differences between ultra thin films and their parent crystalline solids (dimensionality effects) as these arise from details of the interaction of the incoming flux with the various electronic orbitals of the scattering atoms.

#### Reports:

- The Quadrupole Polarizability and Spectral Moments of the Quadrupole Oscillator Strength Distribution of N<sub>2</sub>, by Jan Geertsen et al., *Mol Phys* 72,1267(1991). AD A238 435
- A Calculation of the Isotropic and Anisotropic Spectral Moments of the Dipole Oscillator Strength Distribution of N<sub>2</sub>, by G.H.E. Diereksen et al., *Intl. J. Quant. Chem.* 39,755(1991), AD A238-685

## 28468 ADDENDUM TO A MICROSCOPIC THEORY OF QUANTUM OPTICS AND NEW PHOTON-LOCKED BISTABLE STATES

Mikael Ciftan L.C. Biedenharn Duke University

Substantial progress was made toward the goal of evaluating and understanding the real-time dynamics of systems in contact with a thermal bath. A microscopic theory of quantum optics developed here has been adapted to the case of the classical and quantum mechanical Heisenberg ferromagnet in both two and three dimensions. At the International Workshop in Condensed Matter Theories in Elba, Italy, the researchers presented initial findings that showed the existence of finite magnetization in two dimensions for the Heisenberg ferromagnet. The attendees remarked that this new approach should be useful for lattice gauge theories as well. In other work, researchers carried out a Monte-Carlo simulation type analysis on the classical Heisenberg ferromagnet and still found the existence of finite magnetization in two dimensions, contrary to the theorem of Wagner and Mermin.

#### 28470 OPTICS WITH SEMICONDUCTORS: ULTRAFAST PHYSICS FOR DEVICES

Philippe Fauchet University of Rochester

The objective of this research is to investigate ultrafast nonlinearities in III-V semiconductors with femtosecond optical pulses and demonstrate waveguide devices that employ these nonlinearities. Femtosecond optical pulses will be used to study the physical origin and time response of nonlinearities in thin films and multiple quantum wells made of GaAs, InP, and related alloys. The real and imaginary parts of the induced susceptibility produced by the real or virtual carriers will be mapped out. Emphasis will be on refractive nonlinearities that have a femtosecond response time, such as the quantum confined AC Stark effect. The experiments will be performed at room temperature and basic devices such as switches and couplers will be demonstrated.

## 28591 ANALYTICAL INVESTIGATIONS OF THE ACCELERATION SENSITIVITY OF ACOUSTIC BULK AND SURFACE WAVE RESONATORS

Harry F. Tiersten Rens elaer Polytechnic Institute SL: ETDL

SLIETUL

The research objective is to determine special configurations that will reduce the acceleration sensitivity of acoustic resonators. The approach will be to use the principal investigator's analytical method of solving a rotationally invariant nonlinear system of electro-elastic equations specifically tailored to piezoelectric resonators in the form of complex geometrical structures that are under simultaneous external stresses and fields. The formalism also includes a variational scheme for the accurate determination of the stress and deformation fields.

## 28652 TOWARDS EXPERIMENTAL VERIFICATION AND DEVICE APPLICATIONS OF CURRENT DRIVEN PLASMA INSTABILITIES

Pradip Bakshi K. Kempa

Boston College

SC: BRL, HDL

The research objective is to carry out specific device configuration and parameter studies on the plasma instability driven solid state MMW/MW amplifier scheme. Attempts will be made to determine the Raman response of current driven plasma instabilities and study methods of radiation coupling, such as a grating, into and out of the solid state plasma holding configurations; include feedback mechanisms to achieve resonator or laser type operation; include effects of inhomogeneity in the device films layers.

#### E. Acoustics, Optics and Cross Disciplinary

## 24749 ELECTRONIC IMAGING

Nicholas George University of Rochester

SC: MICOM

An inversion algorithm has been derived for recovering size information from the optical transform pattern for spherical particles. Comparisons are made with the Shifrin inversion method for two different types of particle size distributions, and the expression is found to perform better when noise is present. Excellent results have been obtained using patterns generated as metallic dots on glass substrates. This research is continuing. In electronic imaging the fidelity of color is of importance. Difficulty in color matching exists both on computer monitors and in the hard copy generated by various printers. One important source of error exists due to the overlapping of consecutive dots. This is a nonlinear error since complex color subtraction is involved. A novel means for correcting this color deviation has been applied to modern error diffusion algorithms. This effort is being continued.

#### Reports

- No. 1.4 in previous editions
- 5 Particle Sizing by Inversion of the Optical Transform Pattern, by Scott D. Coston and Nicholas George, MS, Appl Opt.

## **25349** THE GENERATION OF FEMTOSECOND, HIGH POWER, TUNABLE MID-INFRARED PULSES

John M.J. Madey Duke University

Work has concentrated on simulations that reveal the detailed physics of the electron-photon interaction within the wiggler cavity. In particular work is in progress on simulating very large cavity length detuning where the quadratic phase structure of the light is not preserved. Simulation results continue to be encouraging. Work has been completed on the design and component procurement of the actual experiment, to include both the optical delay line and the data acquisition components. The equipment for the experiment is on hand and the machine parameters necessary for a successful experiment have been well defined.

## 25408 TUNABLE OPTICAL SOURCES AND SYNTHETIC NONLINEAR MATERIALS: GROWTH AND CHARACTERIZATION OF NONLINEAR OPTICAL MATERIALS

Robert L. Byer Robert S. Feigelson Stanford University

SL NVEOC

At low powers researchers have performed single pass second harmonic generation to generate red,

green and blue radiation in periodically poled lithium niobate crystals grown using the laser heated pedestal growth technique. The three doubling crystals were each grown with a different period to optimize performance at a different pump wavelength: 946. 1064, and 1320 nm. First-order quasi-phase-matching requires sign reversals of the effective nonlinear coefficient with a period equal to two coherence lengths. The observed width of the tuning curve is twice what one would expect for a crystal with perfect quasi-phase-matching. This is believed to be due to errors in the domain spacing. Other researchers have performed high efficiency cw resonant harmonic generation with periodically poled lithium niobate crystals at much higher power. These resonant second harmonic generation experiments converted 4.2 watts of 1064 nm Nd:YAG laser output to 1.7 watts of 532 nm radiation for an overall efficiency of 42 percent. The resonant doubling was done in a bow-tie cavity that resonated the fundamental and was frequency locked to the Nd:YAG laser using Pound-Drever locking. No photorefractive damage was observed. Additional efforts have been directed toward operating an infrared lithium niobate parametric oscillator pumped by 7 ns pulses from a lamp pumped Q-switched Nd:YAG laser. This OPO is tunable from 1.4 to 4  $\mu$ m. The signal and idler from the OPO are then difference frequency mixed in silver gallium selenide to generate radiation from 4 to 14  $\mu$ m. The overall efficiency of the source is low and work is in progress to improve the efficiency.

Reports

No. 1.7 in previous editions

 Quasi-Phase Matched Second Harmonic Generation: Tuning and Tolerances, by M.M. Feier et al., MS

#### 25482 OPTICS AND OPTOELECTRONIC SYSTEMS

C.R. Stroud University of Rochester

SC OASA (RDA)

Two optical beams, copropagating in a Kerr medium, interact with each other through cross-phase modulation. Such nonlinear beam coupling leads to a transverse modulation instability that is evident as spatial modulation of the beam profiles. A linearstability analysis in the plane-wave approximation predicts the range of spatial frequencies over which modulation can occur. The case of self-defocusing media is particularly interesting, since modulation instability occurs only when both beams are present

simultaneously. Numerical simulations are used to study how modulation instability can occur for finite-size beams. In particular, the mutual coupling of two copropagating Gaussian beams is studied in detail.

#### Reports:

- Effect of Intrapulse Stimulated Raman Scattering on Soliton-Effect Pulse Compression in Optical Fibers, by Govind P. Agrawal, Opt Let 15,224(1990). AD A220 253
- Observation of the Collapse and Revival of a Rydberg Electronic Wave Packet, by John A. Yeazell et al., *Phys Rev Let* 64,2007(1990). AD A224-778
- Modulation Bandwidth of High-Power Single-Mode Semiconductor Lasers: Effect of Intraband Gain Saturation, by Govind<sup>1</sup>/<sub>4</sub> P. Agrawal, Appl Phys Let 57,1(1990). AD A228 683
- Induced Focusing of Optical Beams in Self-Defocusing Nonlinear Media, by Govind P. Agrawal, *Phys Rev Let* 64,2487(1990), AD A228-639
- Fundamental Limitation on Large-Signal Modulation of Semiconductor Lasers and its Implications for Lightwave Transmission, by G.P. Agrawal. *Electron Let* 26,916(1990).
- Effect of Gain and Index Nonlinearities on Single-Mode Dynamics in Semiconductor Lasers, by Govind P. Agrawał, MS.
- 7 Classical Atoms and Quantum Mechanical Wave Packets, by John A. Yeazell and C.R. Stroud, Jr., MS.
- Effect of Gain Nonlinearities on the Dynamic Response of Single-Mode Semiconductor Lasers, by Govind P. Agrawal, *IEEE Photonics Tech Let* 1,419(1989). AD A220 326
- Transverse Modulation Instability of Copropagating Optical Beams in Nonlinear Kerr Media, by Govind P. Agrawal, J. Opt. Soc. Am B7,1072(1990). AD A228-852

## 25546 EXPERIMENTAL STUDIES OF FUNDAMENTAL PROBLEMS IN QUANTUM OPTICS

Thomas W. Mossberg Michael G. Raymer University of Oregon

Much has been made recently about an unusual and subtle effect that occurs in gain-guided semiconductor lasers. The modes of the structure are nonorthogonal and this leads to correlations between mode amplitudes, and so-called excess noise. It was discovered that this effect is also present in gain-guided amplifiers without resonators, such as Raman or x-ray amplifiers. By measuring the shot-to-shot jitter of the direction of propagation of the generated beam, it is possible to show that the nonorthogonality of the gain-guided modes plays an important role in the spatial structure of the light. It has been demon-

#### E. Acoustics, Optics and Cross Disciplinary

strated that the creation of spatial fringes occurs when two beams of Raman-generated light are superposed. Because the beams are generated from independent groups of molecules, they are statistically independent, and have random, uncorrelated phases and amplitudes. Thus the locations and depth of modulation of the fringes vary on each shot of laser. It has been verified that the statistics of the light is identical to thermal radiation with an effective temperature as high as  $10^{12}$  Kelvin.

#### Reports:

No. 1-6 in previous editions.

- On the Use of Phase-Noisy Laser Fields in the Storage of Optical Pulseshapes in Inhomogeneously Broadened Absorbers, by J.M. Zhang et al., MS, Opt Let.
- Spatial and Temporal Interference in Stimulated Scattering, by M.G. Raymer et al., Acta Physica Polonica A78,193(1990).
- 9. Beam Pointing Fluctuations in Gain-Guided Amplifiers, by S.J. Kuo et al., MS, *Phys Rev Let*.
- Quantum Statistics in Nonlinear Optics, by J. Mostowski and Michael G. Raymer, MS, Contemporary Nonlinear Opts.
- 11. Limits to Wide-Band, Pulsed Squeezing in a Traveling-Wave, Parametric Amplifier with Group-Velocity Dispersion, by M.G. Raymer et al., MS, Opt Let.
- Spatial Interference of Macroscopic Light Fields From Independent Raman Sources, by S.J. Kuo et al., *Phys. Rev* A43,4083(1991). AD A238 619
- The Quantum Spatial Coherence Properties of Stimulated Raman Scattering, by Shihjong Kuo, PhD Thesis, 1991, 99 pp.
- Use of Phase-Noisy Laser Fields in the Storage of Optical Pulse Shapes in Inhomogeneously Broadened Absorbers, by J.M. Zhang et al., Opt Let 16,103(1991). AD A238 290

#### 25631 TUNABLE SOLID STATE LASERS BASED ON MOLECULAR IONS

Alex Lempicki Richard H. Clarke Boston University

## SC: CECOM

The principal investigator has completed work on the various aspects of excited state absorption in bismuth germanate. This is an extremely complicated case because of the pronounced photochromic effects, (dependence of ESA on probe beam intensity). A paper is in print in the *Journal of Luminescence*, 47, 1991. The next case was the rather prototypical  $d^0$  crystal, namely the tungstate CaWO<sub>4</sub>. The luminescence of this crystal has been studied in some detail by others, and this gave clues as to the peculiarities of ESA. First of all there appears to be two contributions to luminescence and by implication to ESA. Apart from the luminescence due to the WO<sub>4</sub> group

there is luminescence due to a Schottky defect, namely WO3. Actually at room temperature the defect process dominates, the WO<sub>4</sub> contribution becoming more important at higher temperatures. The data on the tungstate as well as earlier data on molybdates gives some hope that some generalization can be made concerning the  $d^0$  molecular crystals and the ubiquitous nature of ESA in these materials. It is at present quite tentative but it appears that molecular orbital calculations cannot be taken as a guide for the presence or absence of ESA. The reason is that these calculations do not account for the extreme broadening of the ESA transitions due to the large coupling to the lattice. The nature of the partially forbidden transitions is such that stimulated cross-sections cannot effectively compete with the ESA transitions. The prospects of lasers based on these materials appears therefore to be remote. The important finding is that this could not have been predicted on the basis of known electronic structure calculations. The situation appears to be less critical in glasses because of the shift of ESA spectra towards shorter wavelengths. This creates better conditions for the competition of stimulated emission with ESA. In the region of emission the difference between stimulated and ESA cross-sections is considerably smaller than in crystals, although ESA still appears to win. This indicates that glasses are better candidates for any further development and offer at least some hope that compositions capable of lasing can be found.

## 26088 THE DEVELOPMENT OF AN ALL-SILICON INTEGRATED OPTICAL MODULATOR FOR HIGH-SPEED DATA COMMUNICATIONS AND SENSOR APPLICATIONS

David Bloom Stanford University

#### SL: DARPA SC: MICOM

The development of all-silicon optical modulator has led not only to novel semiconductor devices but has also branched out into other modulator technologies. The bulk e e research into these alternate technologies has focused on the use of electro-optic polymers in high speed modulators and integrated circuit probes. The organic guest/host EO material developed under this contract in 1989 was used for these studies, which included the measurement of the material's electro-optic coefficient out to 20 GHz and the demonstration of the ATR modulator. The frequency response of the Disperse Red 1/PCMA guest/host material was measured and found to be flat up to 20 GHz. At present, a 20 to 40 GHz frequency doubler is being incorporated into the EO sampling system of the Ginzton Ultrafast Electronics Laboratory to allow measurements beyond 20 GHz. Furthermore, experiments designed to measure the permittivity of the organic thin films above 1 GHz were continued. The ring resonator structure was demonstrated for this purpose; however, potentially more straightforward methods are being considered. Utilizing the DRI/PCMA material, a proof-of-principle experiment was carried out for an optical modulator based on the surface plasmon effect. The device is an attenuated total internal reflection modulator (ATR). With a 32 V rms drive, a modulation depth of 30 percent and a 400 kHz bandwidth were observed. A high frequency ATR modulator is being developed. On the other side of the spectrum, a low-power, all-silicon micromachined grating phase modulator (GROD) was designed and fabricated for use with lower frequency signals. The fabrication process for this device is standard technology; and at present, it is being refined. Both the GROD and the ATR are compatible and integrable with other semiconductor devices.

## 26160 RESEARCH STUDIES ON EXTREME ULTRAVIOLET AND SOFT X-RAY LASERS

S.E. Harris J.E. Young

Stanford University

The electromagnetically induced transparency experiments have been completed. A technique was demonstrated by which an optically thick medium may be rendered transparent. The transparency results from a destructive interference of two dressed states which are created by applying a temporally smooth coupling laser between a bound state of an atom and the upper state of the transition which is to be made transparent. The transmittance of an autoionizing (ultraviolet) transition in Sr is changed from exp(-20)without a coupling laser present to exp(-1) in the presence of a coupling laser.

#### Reports:

No. 1-9 in previous editions.

- Nonlinear Generation of 104.8 nm Radiation Within an Absorption Window in Zinc, by K.H. Hahn et al., *Phys Rev Let* 65,2777(1990).
- 11. Lasers Without Inversion: A Closed Lifetime Broadened

System, by A. Imamoglu et al., *Phys Rev Let* 66,1154(1991). AD A238 971

- 116 nm H<sub>2</sub> Laser Pumped by a Laser-Plasma-Excited Electron Source, by S.J. Benerofe et al., MS, Phys Rev Let.
- Annuai Report Research Studies on Extreme Ultraviolet and Soft X-Ray Lasers, by S.E. Harris, TR. Oct 90, 12 pp. AD A231 033
- Interference of Lifetime Broadened Resonances: Nonreciprocal Gain and Loss Profiles, by A. Imamoglu et al., New Frontiers in Quantum Electrodynamics and Quantum Optics, 1990, p223. AD A233 566

## 26264 MASSIVELY PARALLEL OPTICAL-TO-ELECTRONIC DATA TRANSFER

C.M. Verber Georgia Institute of Technology

SL: DARPA

A binary optic random phase plate has been designed and is being fabricated to be used with the data masks in the write system. It was determined that this phase plate was necessary to reduce inter-bit interference during writing of the holograms. This plate will replace the diffuser glass that was previously used for this purpose. The phase plate consists of an array of phase retardation areas randomly distributed into four different quantized levels. The inclusion of such a mask in the system proved to "clean-up" the reconstructed image in computer simulations. A total of 10 data masks for the  $16 \times 16$  bit pages have been designed. They are currently being fabricated. The existing angle-multiplexing write system is being converted to provide both angular and spatial multiplexing of the holograms. When this conversion is complete, this apparatus will be capable of recording the holograms both for the prototype system and for the much denser holographic ROM's. The fiber addressing system for the read-out of the holographic ROM has been designed. Holograms of  $4 \times 4$  arrays have been successfully reconstructed using an optical fiber collimated with GRIN lens. The CMOS chip design and fabrication was completed for the  $(4 \times 4)$  memory array. The finished chip was tested for electrical operation and was successfully incorporated into the complete optical-ROM to electronic-RAM data transferral experiment. Extension to the  $(16 \times 16)$  array was straightforward, but required some modification of the detector geometry and the cell layout to provide for output testing. Circuit analysis of the photodetector scheme has been completed and has been modified to provide for electrical erasing. The new circuit allows for

rapid electrical resetting of the memory array with immediate optical loading of another input matrix.

Reports:

No. 1 in previous edition.

- 2. Computer Modeling of the Effects of Apertures in the Fourier-Transform Plane of Fourier-Transform Imaging Systems by J.T. Gallo et al., MS, *appl Opt.*
- 3. Page-Oriented Holographic Memories: A Reassessment, by C.M. Verber et al., MS, Opt Let.

## 26383 EXPERIMENTAL STUDY OF THE SOLID STATE IR VIBRATIONAL LASER

Albert J. Sievers Cornell University

The frequencies of anharmonic local modes in one, two and three dimensional lattices have been obtained analytically by combining the rotating wave approximation with some of the formalism used previously to characterize defect modes in harmonic crystals. For weak anharmonicity these modes become delocalized, while they take on the vibrational pattern of a small molecule when the anharmonicity becomes large. The first order corrections to the rotating wave approximation are found to be small for any anharmonicity parameter, verifying that this approximate method of analysis can be used to separate the equations of motion. This identification of the weak anharmonicity limit permits researchers for the first time to address the question of the existence of anharmonic local modes in real crystals. With anharmonic parameters similar to those found in alkali halide crystals the energy needed to produce these modes in all three dimensions is estimated. Thermal motion alone does not provide enough amplitude to support these modes in a lattice with the anharmonicity of pure LiF. On the other hand, at some defect sites the requirements could be less severe and anharmonic modes might be generated by a nonthermal process such as an optical excitation of the F center, which introduces an energy equivalent of  $\sim 40$  Debye phonons into the lattice. The large anharmonicities found in solid He and near ferroelectric systems should provide more friendly environments for these modes. Third order nonlinear optical properties of semiconductors have been widely studied at infrared frequencies near and above 1000 cm<sup>-1</sup>. Nonlinear optical techniques have been extended into the far infrared region with the observation of third harmonic generation from free carriers in semiconductors. It has been possible to demonstrate resonant four-wave mixing of two FIR frequencies in *n*-InSb. The dependences of the FWM

signal on magnetic field, carrier concentration, and circular polarization indicate a resonant nonlinear process in which the plasma frequency plays a role different from that predicted by theory.

#### Reports:

No. 1 in previous edition.

- Effects of Network Topology on Low-Temperature Relaxation in Ge-As-Se Glasses, as Probed by Persistent Infrared Spectral Hole Burning, by S.P. Love et al., *Phys Rev Let* 65,1792(1990). AD A230 693
- 3. Four Wave Mixing in the Far Infrared From Free Carriers in *n*-type Indium Antimonide, by R.M. Mart et al., MS.
- Sulfur-Hydrogen Donor Complexes in Silicon, by R.E. Peale et al., Mat Sci Forum 65,151(1990). AD A233-968
- 5. Observation of Coherent Synchrotron Radiation at the Cornell Linac, by E.B. Blum et al., MS, *Nucl Inst and Meth in Phys Res.*
- 6. This number not used.
- Time Resolved Spectroscopy with Fourier Transform Spectrometers: Maintaining the Fellgett Advantage, by J.T. McWhirter and A.J. Sievers, MS. Appl Spectrosc.

#### **26676** PARALLEL READOUT OF OPTICAL DISKS

Demetri Psaltis

California Institute of Technology

Though neural networks have been demonstrated using a variety of optical and electronic technologies, hybrid optoelectronic implementations combine the strength of optics in communications with that of electronics in processing. This research has developed a multilayer feedforward neural network implementation using neurons and synapses fabricated on an integrated circuit. Each synapse contains a photodetector that allows weights governing the connections to be accessed holographically from an optical disk.

#### Reports.

No. 1-9 in previous editions.

- Optical Disk Implementation of Radial Basis Classifiers, by M.A. Neifeld et al., MS.
- Doppler Radar Imaging of Spherical Planetary Surfaces, by R. Scott Hudson and Steven J. Ostro, J Geophys Res 95,10,947(1990), AD A228 901
- Optical Disks in Optical Computing, by M.A. Neifeld et al., MS.
- 13. Handwritten Zip Code Recognition Using an Optical Radial Basis Function Classifier, by M.A. Neifeld et al., MS.

## 26695 FERROELECTRIC LIQUID CRYSTAL OPTICAL INTERCONNECT SWITCHING NETWORKS

Joseph W. Goodman Stanford University Students working on this project have completed their PhD theses. During the course of writing these theses, several problems were attacked for the first time. In one case a new analysis of the effects of crosstalk in switch networks was carried out. This analysis, which derives power penalties as a function of extinction ratio, is the most complete carried out to date in this area. In the other case attention was focused on digital scanner networks, which have many advantages over other network architectures.

Reports:

- No. 1 in previous edition.
- 2. Ferroelectric Liquid Crystal 4×4 Optical Interconnect, by Larry R. McAdams and Joseph W. Goodman, MS.
- 3. Ferroelectric Liquid-Crystal Digital Scanner, by R. McRuer et al., Opt Soc Am 15,1415(1990). AD A234 239
- Liquid Crystal 1×N Optical Switch, by Larry R. McAdams and J.W. Goodman, Opt Let 15,1150(1990). AD A233 804

## 26971 STRUCTURE AND SWITCHING DYNAMICS IN FERROELECTRIC CRYSTAL AND LIQUID CRYSTAL THIN FILMS

Noel A. Clark James Scott University of Colorado

The total internal reflections (TIR) studies of liquid crystal orientation near a rubbed polymer surface have been completed. The results are quite striking, showing that the rubbed polymer surface is highly plastic. Samples are oriented in the nematic and smectic Aphases, where the director aligns along the rubbing direction. This director orientation remains into the smectic C phase, in spite of the director tilt in this phase which would like to rotate the director away from the rubbing orientation. Once a voltage is applied, however, the director reorients to one of the field induced smectic C states, depending on the applied voltage, and stays there. Application of a voltage cycle exhibits a surface hysteresis loop characterized by two surface stabilized states. These experiments enable the surface interactions to be characterized quantitatively for the first time. Another TIR light scattering study of director orientation fluctuations near a LC rubbed polymer interface has been completed.

#### Reports:

 Chevron Layer Structures in Surface Stabilized Ferroelectric Liquid Crystal (SSFLC) Cells Filled with a Material Which Exhibits the Chiral Nematic to Smeetic C\* Phase Transition, by T.P. Ricker et al., MS, *Ferroelectrics*.

#### I Physics

#### 1 Physics

- 2. Thermal Fluctuation Effects in Ferroelectric Liquid Crystal Polarization Reversal: Light Scattering From a Transient Domain Wall Foam, by Joseph E. Maclennan and Noel A. Clark, MS, Phys Rev Let.
- Fluctuation-Quenching of Thermal Focussing in Ba<sub>2</sub>NaNb<sub>5</sub>O<sub>1</sub>, by J.F. Scott and Shou-Jong Sheih, J Phys Condens Matter 2,8553(1990).
- 4. Phase Modulation and Far-Field Spatial Patterns Due to the Transformational Thermal Lens Effect, by Ting Chen et al., *Phys Rev* 43,615(1991). AD A234 236
- 5. Optical Measurements of Diffusivities in Incommensurate Barium Sodium Niobate, by J.F. Scott and W.F. Oliver, MS.
- Proximity Effect for Scrolling Spatial Light Modulator Applications of Surface-Stabilized Ferroelectric Liquid-Crystal Switching, by Robert E. Brooks et al., Appl Phys Let 56,2646(1990). AD A228 064
- Director Orientation in Chevron Surface-Stabilized Ferroelectric Liquid Crystal Cells/Verification of Orientational Binding at the Chevron Interface Using Visible Polarized Light Transmission Spectroscopy, by J.E. Maclennan et al., Liquid Cryst 7,753(1990). AD A228 6
- Surface Electroclinic Effect in Chiral Smectic-A Liquid Crystals by Jinuzhi Xue and Noel A. Clark, *Phys Rev Let* 64,307(1990). AD A227 935
- Anisotropic Thermal-Lens Effect in Ferroelectric Ba<sub>2</sub>NaNb<sub>5</sub>O<sub>1</sub> at T<sub>c</sub>, by J.F. Scott et al., *Phys Rev* B41,9330(1990). AD A227 936
- Director Reorientation Dynamics in Chevron Ferroelectric Liquid Crystal Cells, by J.E. Maclennan et al., Liquid Cryst 7,787(1990). AD A227 888
- 11. Ferroelectric Memories, by James F. Scott and Carlos A. Paz de Araujo, *Science* 246,1400(1989). AD A228 252
- Physical Properties and Alignment of a Polymer Monomer Ferroelectric Liquid Crystal Mixture, by D.S. Parmar et al., MS, J Phys (Paris).
- 13. Molecular Director and Layer Response of Chevron Surface Stabilized Ferroelectric Liquid Crystals to Low Electric Field, by Paula C. Willis et al., MS.
- 14. Optical Symmetry of Ferroelectric Liquid Crystal Cells, by Zhiming Zhuang et al., MS, Jap J Appl Phys.
- 15. Visible Polarized Light Transmission Spectroscopy of the Electro-Optic Switching Behavior Surface of Surface Stabilized Ferroelectric Liquid Crystal Cells, by Zhiming Zhuang et al., MS, Liquid Cryst.

## 26974 NONEQUILIBRIUM SCREENING AND EXCITON DYNAMICS PROBED BY FEMTOSECOND LASER PULSES

Nasser Peyghambarian Stephan Koch University of Arizona

Significant progress was made in both areas of experiment and theory. The theoretical results of the research were published as a paper in *Physical Review Letters*, and the experimental work was accepted as a paper for publication in *Physical* 

#### E. Acoustics, Optics and Cross Disciplinary

Review B. The problem of the dynamics of the exciton under femtosecond laser excitation was solved theoretically for two pumping situations: (a) pumping below the exciton resonance in the transparency region of the semiconductor and (b) resonant pumping. The experimental approach has covered the nonresonant pumping situation so far. The onresonance experiments are currently underway. Femtosecond pump-probe spectroscopy was carried out to study the ultrafast excitonic bleaching recovery in the optical Stark effect of several GaAs-AlGaAs multiple quantum well samples, grown by MBE at room and low temperatures. The experimental results agree well with the theoretical work. Using these results, the concept of adiabatic following in semiconductors has been identified.

Reports:

- No. 1 in previous edition.
- 2. Femtosecond Measurements of Hole-Relaxation in a GaAs-AlAs Type II Structure, by B. Fluegel et al., MS.
- Coupled-Well Superlattices: Transition Crossing and Ferntosecond Dynamics, by G. Khitrova et al., MS.
- 4. Femtosecond Excitonic Bleaching Recovery in the Optical Stark Effect of GaAs-AlGaAs Multiple Quantum Wells and Directional Couplers, by S.G. Lee et al., MS, *Phys Rev.*
- 5. Ultrafast Adiabatic Following in Semiconductors, by R. Binder et al., *Phys Rev Let* 65,899(1990). AD A232 210

#### 27273 RESEARCH IN PHOTOREFRACTIVE CRYSTALS

Amnon Yariv

California Institute of Technology

SC: HDL

Research has involved the growth of photorefractive crystals and the characterization of their properties. A high temperature growth system is used to grow photorefractive  $KTa_{1-x}Nb_xO_3$  (KTN) and  $K_{1-x}Li_xTa_{1-x}Nb_xO_3$ (KLTN) crystals using the top seeded solution growth method. Optical quality crystals are grown with dimensions of up to  $2 \times 2 \times 2$  cm<sup>3</sup>. Efforts have focused on the enhancement of photorefractive properties by the selection of dopants introduced during growth. Photorefractive properties of a number of KTN and KLTN crystals have been investigated.

## 27366 SELECTIVE REACTIVITY, ULTRAFAST ENERGY TRANSFER, AND THE DEVELOPMENT OF CHEMICALLY PUMPED VISIBLE LASERS

James L. Gole

#### Georgia Institute of Technology

A paper has been prepared in which two approaches to visible chemical laser development are outlined.

An extremely efficient near resonant intermolecular energy transfer from selectively formed metastable states of SiO and GeO to sodium atoms is used to form a sodium atom laser amplifier representing an extension of the outlined concept producing the first visible (535 nm) chemical laser amplifier and oscillator based on a thallium atom receptor. The authors outline the thallium laser concept and the development of the sodium based energy transfer system for laser amplification and oscillation in the wavelength ranges 569 and 616 nm. A second approach relies on the high cross section (pumping efficiency) highly selective and exothermic sodium trimer-halogen atom reactions to produce continuous sodium dimer laser amplifiers. Optical gain through simulated emission is demonstrated in regions close to 527 (3.8 percent for individual rovibronic level ( $\alpha = 8 \times 10^{-3}/\text{cm}$ )), 492, and 460 nm ( $\sim$ 2.3 percent for indiv. rovibronic level). Potential extensions to the ultraviolet are noted.

Reports:

- Chemically Driven Pulsed and Continuous Visible Laser Amplifiers and Oscillators, by J.L. Gole et al., MS.
- On the BiF Bond Dissociation Energy and an Evaluation of the BiF Red Emission Band Systems, by T.C. Devore et al., MS. Chem Phys.

### 27418 EFFICIENT NONLINEAR OPTICAL CONVERSION OF CW 1.319 MICRON LASER RADIATION

Robert L. Byer

Stanford University

SL: HDL SC: HDL

The goal of this project is generation of 660 nm radiation by frequency doubling the 1319 nm output of a cw diode-laser-pumped Nd:YAG laser. The multiple approaches that have been pursued on this problem are now starting to yield significant results. The most substantial progress has been with periodically poled lithium niobate. Samples of this material have been grown using the laser-heated-pedestal growth technique. The periodicity of these samples was adjusted for phase-matched second-harmonic generation of blue, green, and red light. The sample with periodicity for green generation has been operated in an external-resonant-cavity harmonic generator and produced 1.77 watts of harmonic output with 67 percent internal conversion efficiency and 42 percent overall conversion efficiency. The periodically poled sample for red generation has also been operated but only in a single-pass configuration at low conversion efficiency. Lithium enriched LiNbO<sub>3</sub> prepared by vapor transport equilibration has been used for the generation of 1.6 watts of 532-nm radiation by external-resonant-cavity harmonic generation. In this case the changes required for 660-nm generation are more difficult. The attempt at discrete-component external-resonant-cavity second-harmonic generation using congruent LiNbO3 was unsuccessful due to problems with multilayer dielectric mirrors and insufficient laser power. In the original efforts with monolithic resonant-cavity harmonic generation with coatings deposited directly on the congruent LiNbO<sub>3</sub> crystal, problems were encountered with coating failure during the thermal cycle. A collaborative effort is being pursued with Hannover Universität in Germany to investigate coatings for this purpose.

## 27425 OPTICAL AND MAGNETIC RESONANCE INVESTIGATIONS IN SINGLE CRYSTAL HOSTS: CANDIDATES FOR TUNABLE SOLID-STATE LASERS

David J. Singel

Harvard University

SL: NVEOC

Crystals were doped with Cr at sufficiently great concentration that electron-pair interactions corrupted the spectra; the spectra of isolated ions could not be distinguished. A more lightly doped crystal was obtained. Intense EPR spectra attributable to  $Cr^{3+}$ at the M1 and M2 octahedral sites of forsterite dominated the spectra. A plethora of additional signals were observed in spectra recorded at high spectrometer gain. Some signals were readily identified as contaminant species such as color centers and  $Mn^{2+}$  ions on the basis of characteristic *epr* spectra. No signals were found that could be attributed to a spin one ion with zero field splittings as small as those previously reported for Cr<sup>4+</sup> in tetrahedral organometallic compounds. A different type of host crystal was obtained which lacks the octahedral sites that successfully compete for the Cr dopant. The goals are to discover and analyze the epr properties of  $Cr^{4}$  in a tetrahedral site of an oxide lattice both as a model to facilitate the search for  $Cr^{4+}$  in other candidate laser materials. Samples of Cr-doped BMAG (Ba<sub>2</sub>MgGe<sub>2</sub>O<sub>7</sub>) were obtained from H. Jensen of the Massachusetts Institute of Technology. Three strong eprabsorptions were identified: Mn<sup>2+</sup> (from its characteristic nuclear hyperfine structure), Fe<sup>3+</sup> at the  $S_4$  (which exhibits an axial *epr* spectrum very similar to  $Fe^{3+}$  in garnet and a signal that was attributed to  $Cr^{4+}$ .

#### 27556 PICOSECOND DEMODULATION AND COHERENT ELECTRON BEAMS

H. Craig Casey Bob D. Guenther Duke University

Research is being performed on the technique of picosecond demodulation. The work seeks to demonstrate the usefulness of picosecond demodulation for the measurement of short optical pulse widths and for the production of microwave radiation.

#### 27586 OPTICAL SIGNAL PROCESSING

Anthony VanderLugt North Carolina State University

SC: CECOM, HDL

Work has continued on demonstrating the feasibility of using acousto-optic channel equalization to significantly reduce multipath distortion in a digital radio. The primary effort was directed toward the experimental verification of the acousto-optic equalizer. A proof-of-principle system was constructed using stock laboratory equipment. Initial tests showed that in-band distortions of up to 25 dB could be equalized. After the optical processor, the residual in-band distortion was less than 3 dB over a 38 MHz bandwidth. This level of optical performance, when coupled with digital equalization, would provide excellent control over the channel distortion. A second generation equalizer, would provide excellent control over the channel distortion. A second generation equalizer was also designed during this time and all components were ordered and received. The new prototype system, which includes the optical equalizer, the optical channel estimator and the electronic channel distortion emulator, will enable full testing of the equalizer. Assembly of the electronic distortion emulator is completed and construction and testing of the optical equalizer has begun. A different form of a quasi-real-time adaptive system is being investigated for signal excision. The experiments involve modulating a baseband pulse to an intermediate frequency, excising various frequency components, demodulating the pulse, and then characterizing the residual distortion on the pulse. These experiments were performed to verify computer simulations. Theoretical analysis were performed comparing detection in the Fourier plane to detection in the image plane. It has been shown that the two detection schemes are equivalent if all the light is collected. However, if a detector is placed in the image plane to collect all the reference beam light, where

the reference beam is much smaller than signal beam, the shot-noise of the photodetector is reduced. These theoretical analyses are confirmed by computer simulations.

Reports:

No. 1-2 in previous editions.

- Generalized Filtering in Acousto-Optic Systems Using Area Modulation, by T.P. Karnowski and A. VanderLugt, MS, *Appl Opt.*
- Multichannel Acousto-Optic Crossbar Switch with Arbitrary Signal Fan-Out, by Dan Owen Harris and A. VanderLugt, MS, Appl Opt.
- Area Modulation Filters in an Interferometric Acousto-Optic Signal Processor, by Thomas Paul Karnowski, MS Thesis, 1990, 137 pp.
- 6. Optimum Sampling of Fresnel Transforms, by A. VanderLugt, *Appl Opt* 29,3352(1990). AD A227 937
- 7. Acousto-Optic Photonic Switching, by Dan Owen Harris, PhD Thesis, 1990, 256 pp.
- Hybrid Acousto-Optic and Digital Equalization for Microwave Digital Radio Channels, by C.S. Anderson and A. VanderLugt. Opt Let 15,1182(1990). AD A231 130
- 9. Multichannel Acousto-Optic Crossbar Switch Experimental Work, by Dan Owen Harris, MS, Appl Opt.
- 10. Multichannel Acousto-Optic Crossbar Switch Theory, by Dan Owen Harris, MS, Appl Opt.
- The Excision of Narrowband Interference From Wideband Signals Using an Open-Loop Adaptive Technique in an Acousto-Optic Signal Processor, by Reeder Noah Ward, MS Thesis, 1991, 105 pp.
- 12. Signal Distortion in an Adaptive Excision System, by Reeder Noah Ward and A. VanderLugt, MS, *Opt Eng.*

## 27591 SCANNING NEAR FIELD OPTICAL MICROSCOPY USING A VIBRATING KNIFE EDGE OR STYLUS

Adrian Korpel

University of Iowa

Recently results were reported on one-dimensional beam profiling with a scanning, vibrating knife edge and its implications for near-field optical microscopy. Results can now be reported on the implementation of this idea in two dimensions. A knife edge corner is made to vibrate in two orthogonal directions with frequencies of 100 Hz and 1100 Hz and amplitudes  $w_1$  and  $w_2$  respectively. A photodiode downstream from the knife edge detects the mixing signal at 100 Hz and records its amplitude, while the vibrating knife edge corner scans out the optical field. A gray scale recording of this amplitude yields an image of the field with (electronically variable) resolution  $w_1 \times w_2$ . A paper is being published which shows images achieved with this mixing technique

and with another more sensitive one that used twodimensional scanning with a one-dimensional vibrating knife edge, combined with computer post-processing. The paper also discusses limits to the electronically variable resolution in the context of signal-to-noise ratio.

#### 27838 OPTICAL LIMITING

E.W. Van Stryland D.J. Hagan M.J. Soileau University of Central Florida

SL: VAL SC: ETDL, SMO

A paper has been prepared which reports a sensitive single beam technique for measuring both the nonlinear refractive index and nonlinear absorption coefficient for a wide variety of materials. The authors describe the experiment and present a a brief analysis including cases where nonlinear refraction is accompanied by nonlinear absorption. In these experiments the transmittance of a sample is measured through a finite aperture in the far-field as the sample is moved along the propagation path (z) of a focused Gaussian beam. The sign and magnitude of the nonlinear refraction are easily deduced from such a transmittance curve (Z-scan). Employing this technique a sensitivity of better than  $\lambda/300$  wavefront distortion has been achieved using picosecond frequency doubled Nd:YAG laser pulses. In cases where nonlinear refraction is accompanied by nonlinear absorption, it is possible to separately evaluate the nonlinear refraction as well as the nonlinear absorption by performing a second Z-scan with the aperture removed. The authors demonstrate this method for a solution of chloro-aluminum-phthalocyanine at 532 nm where excited state absorption is present and the nonlinear refraction is positive.

## 27882 SYNCHROTRON X-RAY DIFFRACTION ANALYSIS OF PHOTOREFRACTIVE CRYSTALS AND THEIR GRATINGS

Mark Cronin-Golomb Tufts University

#### SL: DARPA

Crystals of barium titanate have been examined. The x-ray reflection images showed that the crystals were of very high uniformity, occasionally showing very small angle grain boundaries (few arc second misalignment). However, the surface finish was not

of sufficiently high quality to enable one to see any fine scale structure. The diamond polish commonly used leaves many scratches on the surface. These scratches are highly visible and obscure the underlying volume. Under a microscope, this crystal appears to be scratch free. X-ray images of it will be made. Despite much effort, it has not been possible to make transmission images of barium titanate. The reason is as yet unclear, especially since it was possible produce transmission images of potassium niobate, a closely related crystal. A breadboard apparatus has been designed for real-time imaging of photorefractive grating formation. Visible semiconductor lasers will be used in this setup instead of optical fiber delivered helium neon laser light.

#### 28258 FUSION OF MULTIPLE SENSING MODALITIES FOR MACHINE VISION

J.K. Aggarwal

University of Texas at Austin

SL: NVEOC, WSMR

Work is in progress on (a) investigations of the use of the third camera for stereo analysis, showing that trinocular local matching reduced the percentage of mismatches having large disparity errors by more than half compared to binocular matching, but increased the computational cost of local matching by only about one-fourth; (b) a novel representation of the free space of a mobile robot by distinct, nonoverlapping regions called edge visibility regions, used to capture the geometric relations between features in the world model with respect to their visibility from various positions in the planes in which the robot navigates; (c) a survey of techniques and systems for sensor data fusion for mobile robotics applications, including the feasibility of types of sensors, sensor data fusion techniques for road following and terrain analysis; data fusion techniques for visual, thermal, tactile, and structured-lighting sensors; and several general frameworks for sensor data fusion; (d) a knowledge-based system to interpret laser radar and thermal images in order to detect and recognize man-made objects at kilometer range in outdoor scenes.

#### Reports:

- Matching Aerial Images to 3-D Terrain Maps, by Jeffrey J. Rodriguez and J.K. Aggarwal, *IEEE Trans on Pattern Anal* Mach Intelligence 12,1138(1990). AD A234 261
- Edge Visibility Regions A New Representation of the Environment of a Mobile Robot, by Raj Talluri and J.K. Aggarwal, MVA '90 IAPR Workshop on Machine Vision Applications, 1990, 375. AD A234 386

- 3. Finding Regions of Interest for the Detection of Man-Made Objects in Non-Urban Scenes, by H.Q. Lu and J.K. Aggarwal, TR, Mar 91, 39 pp. AD A238 246
- Multi-Sensor Image Interpretation Using Laser Radar and Thermal Images, by C.C. Chu and J.K. Aggarwal, TR, Mar 91, 22 pp. AD A238 245

## 28271 FAST OPTOELECTRONIC QUANTUM WELL AMPLITUDE MODULATOR DEVICE DEVELOPMENT

Gary L. Duerksen Lawrence C. West AT&T Technology Systems

SL: DARPA

Success was achieved in observing the absorption of 9.6  $\mu$  light by the 1–3 QWEST transition, modulated by an externally applied electrical field. The test sample contained an active region of fifty 180 Å; GaAs quantum wells separated by 150 Å; AlAs barriers, delta-doped at about 10<sup>12</sup> cm<sup>-1</sup> per well, giving an internal field equivalent to an applied field of about +8 V across the wells. The QWEST absorption coefficient was measured by coupling light at Brewster's angle in to the tip surface of the electrode region, making a single traverse of the quantum wells and exiting through the substrate. This geometry afforded a 12 percent coupling to the QWEST dipole and yielded an absorption coefficient of about  $4 \text{ cm}^{-1} \text{ V}^{-2}$ , which corresponds to QWEST absorption of about 50 cm<sup>-1</sup> at +4 V applied bias (to be compared to free-carrier absorption of about 30 cm<sup>-1</sup> for this doping). The measurements were taken at 80 K and low duty cycles in order to minimize what appears to be an enhancement of free-carrier absorption brought about by Joule heating. Additionally, a microwave test facility was constructed for the purpose of microwave modeling of integrated optical elements.

## 28313 DEVELOPMENT OF AN ANALYTICAL PHOTON SCANNING TUNNELING MICROSCOPE

Michael A. Paesler North Carolina State University

SC: ETDL, MTL

The research objective is to develop a photon scanning tunneling microscope and characterize its performance. The following topics will be investigated: (a) develop tip fabrication techniques; (b) measure the spatial resolution and compare with theory; (c) investigate the spectroscopic imaging capability of the microscope; (d) investigate the use of the microscope in internal stress measurement in machined glasses and thin films; and (e) characterize quantum well heterostructures and ferritin proteins.

## 28348 HIGH-POWER CW DIODE-LASER-ARRAY-PUMPED SOLID STATE LASERS AND EFFICIENT NONLINEAR OPTICAL FREQUENCY CONVERSION

Robert L. Byer Stanford University

SL: DARPA

Work is in progress to design, build, study and use in several scientific applications a 100-watt, diffraction limited, diode-laser-pumped Nd:YAG laser. The laser will be designed to operate at 10 percent electrical efficiency and to be scalable to greater than I kilowatt of optical output power. Stable, singleaxial-mode, unidirectional oscillation is to be achieved by injection locking the high power oscillator with a low power stabilized, nonplanar ring oscillator. The output of the high power laser will then be frequency doubled with 80 percent projected conversion efficiency in a resonant harmonic generator to produce green light with the same temporal coherence as the laser. The output will be further doubled to produce 266-nm UV radiation. In addition, the doubled laser will be used to pump optical parametric oscillators whose output can be rapidly frequency tuned and can be used as sources of generation of 2-µm radiation for applications that require eye safety and for nonlinear mid-infrared studies using silver gallium selenide. A paper has been prepared which reports the generation of 3.5 watts of continuous wave 532 nm second harmonic radiation using a LiB<sub>3</sub>O<sub>5</sub> crystal pumped by an 8.5 watt Nd:YAG laser. The generated gre a power represents a 41 percent conversion efficiency. It retains the 15 kHz linewidth of the injection locked pump laser.

#### 28356 RESEARCH IN OPTICAL SCIENCES — JOINT SERVICES OPTICS PROGRAM

Robert R. Shannon Michael A. Cusanovich University of Arizona SL: AFOSR SC: TACOM

A research program will be conducted in classical, physical and quantum optics along with optical mate-

rials. The following topics will be included: (a) applied optics research in x-ray optical elements, diamond films and microlenses; (b) semiconductor optical properties will investigate optical interactions on the surface of nanostructures, development of semiconductor heterostructures for nonlinear optics and optical bistability, femtosecond measurements and theoretical description of semiconductor lasers; (c) quantum optical studies of all optical switches, effects of size on optical properties and atomic interferometry; and (d) modeling of two dimensional infrared focal plane arrays will be developed.

## 28416 ITERATIVE ENCODING METHODS FOR COMPUTER GENERATED HOLOGRAMS

Michael R. Feldman

University of North Carolina at Charlotte

SL: HDL SC: TACOM

A hybrid algorithm has been developed that uses the concept of a rapid Recursive Mean Squared Error (RMSE) function combined with the annealed, multiphase, on-axis capabilities of Iterative Discrete Onaxis (IDO) encoding. High diffraction efficiency and computational speed are obtained through the use of the RMSE algorithm with a constant weighting coefficient in the error function and an iterative initial process for determining phase codes in the output plane. Results for large even spot arrays are presented and comparisons made for diffraction efficiency, spot uniformity and computation speed between original IDO and RMSE based IDO encoding. The IDO method is a computer generated hologram (CGH) encoding algorithm that employs iterative optimization routines such as simulated annealing. The IDO method

has been applied to the optimization of large, two dimensional, even numbered, spot arrays for optical interconnect applications. Even numbered spot arrays have several performance advantages including low sensitivity to fabrication errors, and reduced computational complexity. Binary and multiple phase level CGHs have been designed and fabricated. Intensity and/or phase of the individual output pixels can be controlled. Methods to decrease the computation time have been developed for this application. Diffraction efficiencies of up to 84 percent have been achieved for generating spot arrays with 100 to 1024 points. High efficiency radially symmetric computer generated holograms have been designed and fabricated using an iterative encoding method. Diffraction efficiencies of greater than 80 percent with minimal chromatic aberration have been achieved.

## 28502 AN ADAPTIVE LIQUID CRYSTAL TELEVISION BASED JOINT TRANSFORM CORRELATOR AS APPLIED TO REAL TIME PATTERN RECOGNITION

Francis T.S. Yu

The Pennsylvania State University

SL: MICOM, NVEOC

The research objective is to study an adaptive liquid crystal television based joint transform correlator for real time pattern recognition. The following topics will be explored: (a) evaluation of the phase modulation properties of a liquid crystal TV; (b) investigate the use of an iterative phase correction scheme for a phase only filter; and (c) evaluate the use of phase only circular filters for rotation invariant pattern recognition.

## **II CHEMISTRY**

#### A. Inorganic, Analytical, and Electrochemistry

#### 24411 FUNDAMENTAL PROCESSES OCCURRING AT ELECTRODES

Fred C. Anson California Institute of Technology SC: AROE, BRADEC,

CRDEC

A new model for the behavior of counterions that are strongly and irreversibly bound by Nafion coatings on electrodes was developed and tested experimentally. Its principal assumption involves strong ion-association between the fixed sulfonate sites and normally electroactive counterions to produce ion-pairs that must dissociate before electron-transfer is facile. The research on soluble polyelectrolytes to which electroactive counterions are bound by electrostatic interactions coordination bonds or both has continued. A manuscript describing the results obtained with a polysiloxane polyelectrolyte with two types of binding sites has been accepted by J Phys Chem. A manuscript which summarizes recent results obtained in solutions of polystyrenesulfonate containing electroactive cations such as  $Ru(NH_3)_6^{3+}$ ,  $Co(bpy)_3^{3+}$ (bpy = 2,2'-bipyridine) or Fe<sup>3+</sup> has been submitted to J Phys Chem. The coupling by electron-exchange reactions of the slow diffusion of electroactive ions bound to polyelectrolytes with the faster diffusion of the unbound ions affects the currents measured in solutions containing both types of ions. An analysis of the factors that control the observed currents was carried out.

#### Reports:

No. 1-3 in previous editions.

- Dynamic Consequences of Ionic Permselectivity. Rapid Ejection from Nafion Coatings of Anions Generated Electrochemically from Cationic Precursors, by Ching-Fong Shu and Fred C. Anson. J Am Chem Soc 112,9227(1990). AD A232 486
- Ion Association and Electric Field Effects on Electron Hopping in Redox Polymers. Application to the Os(bpy):<sup>33-23</sup>

Couple in Nation, by Fred C. Anson et al., J Am Chem Soc113,1922(1991). AD A238 408

- Association of Electroactive Counterions with Polyelectrolytes.
   Comparison of Electrostatic and Coordinative Bonding to a Mixed Polycation-Polypyridine, by Junya Kobayashi and Fred C. Anson, J Phys Chem 95,2595(1991). AD A238 509
- Time-Resolved Measurement of Equilibrium Surface Tensions at the Electrified Mercury-Aqueous NaF Interphase by the Method of Wilhelmy, by Donald D. Montgomery and Fred C. Anson, Langmuir 7,1000(1991). AD A238 295
- Association of Electroactive Counterions with Polyelectrolytes.
   Electrochemistry of Cationic Counterions Associated with Poly(Styrenesulfonate), by Rongzhong Jiang and Fred C. Anson, J Phys Chem 95,5701(1991). AD A239 585
- 9. Fundamental Processes Occurring at Electrodes, by Fred C. Anson, FR, Aug 91, 2 pp.

## 25435 BASE CATALYZED NUCLEOPHILIC DISPLACEMENT REACTIONS OF PENTACOVALENT PHOSPHORUS

Robert R. Holmes

University of Massachusetts

SL: CRDEC, NRDEC SC: AMRICD, AROE, CRDEC

Oxidative addition reactions have led to new cyclic pentacoordinate phosphorus compounds that incorporate both hydrogen bonding features and the insertion of the electronegative pentafluorophenyl ligand in azoxy and sulfur-containing derivatives. These substitutional constraints were introduced to ascertain their influence as conformational and structural determinants. In contrasting the action of cyclic adenosine monophosphate (c-AMP) with protein kinases with that of phosphodiesterases, it is important to determine what requirements must be met to cause axial-equatorial ring formation in trigonal bipyramidal geometries to change over to diequatorial ring placement for the trans-annealed phosphorinane ring pentacoordinated reaction intermediates. Hydrogen bonding is present at the active sites referred to and acts to fix substrate geometry in an enzymatic reaction. Experimental results argue against mechanistic proposals in the literature on enzymatic action of c-AMP with protein kinases requiring a preference for diequatorial ring placement in a c-AMP pentacoordinated intermediate. This work supports a greater relief of ring strain encountered in boat and chair conformations that are invariably found for saturated six-membered rings in axial-equatorial sites of a trigonal bipyramid of pentaoxyphosphoranes compared to that encountered for dieguatorial ring placement. In a more general sense both the theoretical and experimental work suggest that enhanced reactivity of cyclic phosphorus compounds should be aided by both ring strain relief and hydrogen bonding of the type revealed here which removes electron density from the phosphorus reaction center. One can expect a large enhancement in reactivity with the proper choice of nucleophile.

#### Reports:

No. 1-4 in previous editions.

- Cyclic Oxyphosphoranes, by K.C. Kumara Swamy et al., MS.
- Conformational Effects of Ring Fusion and Heteroatom Substitution in Six-Membered Rings of Bicyclic Oxyphosphoranes, by Robert R. Holmes et al., MS.
- Influence of Hydrogen Bonding on the Formation of Boat and Chair Conformations of Six-Membered Rings in Spirocyclic Tetraoxyphosphoranes, by R.O. Day et al., MS.
- Boat and Chair Forms for Sulfur-Containing Cyclic Oxyphosphoranes, by Johannes Hans et al., MS.

# 25500 ION MOBILITY SPECTROMETRY / MASS SPECTROMETRY WITH LASER-PRODUCED IONS

David M. Lubman University of Michigan

SL: BRL, NRDEC SC: ARDEC, AROE, CRDEC

Work has proceeded in several directions. One key direction has been the development of an atmospheric pressure ionization/time-of-flight mass spectrometer. This device has been constructed and is now operational. Researchers have been involved in modeling this device on a computer in order to optimize its operation and have written their own software in order to perform this simulation. They have already successfully simulated the pulsed ion injection into the TOE Since the API source produces a continuous ion beam a method is required to produce a start pulse. This is achieved by sweeping the ion beam past an entrance slit into the TOF flight tube. One important observation from the computer model is that this sweep will not be mass dependent so that m/22 should arrive across the slit at the same

time as m/z10,000. The clear advantage of this device is the ability to simultaneously observe an entire spectrum in a single pulse as opposed to scanning mass spectrometers such as quadrupoles. Over 10,000 mass spectra can be obtained and signal averaged each second; thus, the great potential for rapid atmospheric pressure sampling for chemical warfare agents, pesticides, explosives, etc. In addition, the device is relatively simple requiring static DC voltage supplies and a simple flight tube. The device has now started yielding results. Other work has explored high pressure liquid injection of thermally labile molecules into the glow discharge source. Efforts have focused in on trace analysis and detection of organophosphorus pesticides, explosives and various amino acids, neurotransmitters and peptides. A study was made of the ability to inject liquid flow rates up 100 ml/min into the glow discharge and the various parameters required to optimize detection of nonvolatile species. The sensitivity of the technique has been optimized with detection limits in the low picomole regime. In addition, the results obtained for small peptides and drugs have been compared to that obtained by an electrospray ionization source.

Reports:

No. 1-3 in previous editions.

4. The Design of an Atmospheric Pressure Ionization-Time-of-Flight Mass Spectrometer Using a Beam Deflection Method, by Ce Ma et al., MS, *Rev Sci Instr.* 

## 25586 CHARGE TRANSFER PROCESSES IN MULTIPLE SITE CHEMICAL SYSTEMS

Thomas J. Meyer

University of North Carolina at Chapel Hill

SL: NRDEC	SC: AROE, CRDEC, ETDL.
	MTI.

A general procedure has been developed for the attachment of redox or photo-active groups to tin dioxide or glass surfaces. The attachment chemistry involves bond formation between the surfaces and carboxyl groups on the redox or photo-active molecules. Attachment has been verified by electrochemical and photophysical measurements. Solution redox and excited state properties are preserved when appropriate molecules such as derivatives of  $[Ru(bpy)_3]^{2+}$  (bpy is 2.2'-bipyridine) are attached to the surfaces although the excited states are quenched on tin dioxide. Apparent surface coverages of one molecular monolayer have been achieved. The stabilities of the molecular electrode assemblies under different conditions have been investigated and techniques for

preparing complex molecular surfaces with more than one type of molecule attached the same surface have been developed.

Reports.

No. 1-4 in previous editions.

- XPS Sputter Depth Profile Analysis of Spatially Modified Ag Doped Poly-[Fe(4-vinyl-4'-methyl-2,2'-bipyridinyl)<sub>2</sub>(CN<sub>2</sub>]Films, by Susan G. MacKay et al., MS.
- 6. Solvent and Temperature Effects in Mixed-Valence Chemistry, by J.T. Hupp et al., MS.
- X-Ray Photoelectron Spectroscopy Sputter Depth Profile Analysis of Spatially Controlled Microstructures in Conductive Polymer Films, by Susan G. MacKay et al., Anal Chem 63,60(1991). AD A233 975

# 25617 COMBINATION OF ELECTROSPRAY ION SOURCE WITH A HIGH MASS MAGNETIC MASS SPECTROMETER FOR ANALYSIS OF BIOLOGICAL AND CHEMICAL AGENTS

Craig M. Whitehouse John B. Fenn Analytica, Inc.

SC: AROE

Progress was made in improving Electrospray Ion Source (ESPI) performance. Testing has continued using the double pumping stage ESPI source. Bench and instrument testing has concentrated on determining the performance effects when varying parameters in the first three vacuum pumping stages. Information learned from the bench testing resulted in a third redesign and fabrication of the ESPI source. The newer ESPI source was fully bench tested and installed on a JEOL magnetic sector mass spectrometer. This ESPI source allows the installation of different configurations for the second vacuum pumping stage. Vacuum stage porting and line size can be set to achieve conduction from 40 to 200 L/s. Optimization of pressures, gas throughput and electrostatic lens geometries in the first three pumping stages is continuing as indicated by the dramatic improvements in sensitivity, resolution and mass range of the ESPI magnetic sector mass spectrometer combination. With the re-designed ESPI hardware, a degree of performance flexibility has been achieved allowing a broader range of performance testing. Full scan spectra have been obtained for Lysozyme (MW 14,305 amu) with signal to noise over 10:1 using only 50 femtomotes of material. With this improved sensitivity, higher resolution is possible. The measured isotopic distribution is very close to the theoretical prediction. The isotope peak spacing is 0.2 mass units with the +5

#### A. Inorganic, Analytical, and Electrochemistry

peaks falling at 1147 on the m/z scale. The improved resolution has eliminated the peak charge state as an unknown in multiply charged spectra for charge states up to at least +6. Due to the narrow ion energy spread and improved focusing, the sensitivity does not drop off as dramatically as resolution is increased with the ESPI source as compared to more conventional ion sources. The improved resolution of the magnetic sector mass spectrometers as compared to the quadrupole mass spectrometers opens up a number of possibilities in analysis. Higher mass accuracies can be achieved particularly with the higher mass compounds. Mixtures of compounds or multiply charged adduct ion peaks can be more readily identified from the peak separation attainable with the higher resolution. The higher accelerating energy of a magnetic sector mass spectrometer, when compared to quadrupoles, has opened up some important possibilities regarding collisional induced dissociation as well.

# 26145 DERIVATIVES OF BORANES, POSSIBLE METAL BORIDE AND BORON NITRIDE PRECURSORS

Sheldon G. Shore Ohio State University SC: AROE, BRL, MICOM, MTL

Earlier work resulted in two types of simple syntheses of boron nitride. One method involves the reaction of B-trichloroborazine with cesium at about 135°C. The initial product amorphous boron nitride is converted to turbostratic boron nitride at 1100°C. The procedure was fine tuned and the procedure for removing the CsCl by-product of the reaction was improved. Excellent chemical analyses for the product were obtained and the infrared spectra and x-ray powder pattern indicate that a high quality product is obtained. The second procedure for the preparation of boron nitride involves the pyrolysis of the ammoniachloroborane, H<sub>3</sub>NBH<sub>2</sub>Cl. This material seems to be well suited to the formation of thin films of boron nitride. It can be dissolved in an ether solvent and then applied as a solution to the surface of the material to be coated, which is then fired to produce the boron nitride. It was also discovered that a volatile, polymeric boron nitride precursor material with a molecular weight of about 750 is produced from the initial pyrolysis of H<sub>3</sub>NBH<sub>2</sub>Cl. The polymeric material is potentially useful for chemical vapor deposition of boron nitride. Work on the preparation of lanthanide borides through the pyrolyses of lanthanide boride precursors continues, as does work on the preparation and characterization of lanthanide- $B_3H_8$  complexes.

Reports:

No. 1-3 in previous editions.

- Borohydride Complexes of Eu(II) and Yb(II) and Their Conversion to Metal Borides: Structures of (L)<sub>4</sub>Yb[BH<sub>4</sub>]<sub>2</sub> (L = CH<sub>3</sub>CN, C<sub>5</sub>H<sub>5</sub>N), by James P. White III et al., *Inorg Chem* 30,2337(1991). AD A238 169
- 5. Reduction of BH<sub>3</sub>THF by Alkali Metal (K, Rb, Cs) and Ytterbium Mercury Amalgams to Form Salts of [B<sub>3</sub>H<sub>8</sub>] A Simple Procedure for the Synthesis of Tetraborane(10), by Tara G. Hill et al., *Inorg Chem* 30,2952(1991). AD A239 700
- 6. Coordination Complexes of Divalent Lanthanides (Sm(II), Eu(II), Yb(II)) with Decaborates; Evidence for Lanthanide Hydrides En Route to Lanthanide Borides, by James P. White III and Sheldon G. Shore, MS, Inorg Chem.
- 7. The Reaction of Alkali Metals and Trihaloborazines. A New Method to Produce Amorphous Boron Nitride and the Preparation of Boron-Nitrogen, by Shawn Edward Dolan, MS Thesis, 1989, 77 pp.
- Studies on Polyboron Hydride Anions and Amine-Borane, by Philipp M. Niedenzu, PhD Thesis, 1990, 113 pp.
- Synthesis and Characterization of Divalent Lanthanide (Ln<sup>2</sup> = Sm, Eu, Yb) Coordination Complexes with Boron Hydride and Transition Metal Carbonyl Anions; The Formation of Metallic Films and Metal Boride From Complex Precursors, by James White III, PhD Thesis, 1990, 248 pp.

# 26426 ELECTRONICALLY ACTIVE CYCLOCARBORANE-METAL-ARENE ASSEMBLIES

Russell N. Grimes University of Virginia

SC: AROE, MTL

Work has been concerned with preparing and structurally characterizing a number of tetradeckers involving Ni, Co, and Ru as the central metal and a variety of X groups have been employed including acetyl, propargyl, chlorine, and bromine. The original Co-Ni-Co species is a diamagnetic 42-electron complex, but the Co-Co-Co and Co-Ru-Co complexes are 41- and 40-electron systems, respectively, and are paramagnetic. Detailed electrochemical studies have been conducted on these species and will be reported later. Work is in progress on exploring the effects of having more than one electron-withdrawing group on the starting complex, and/or having it on other than he middle boron atom; the objective is to further develop this approach as a useful synthetic tool for the designed synthesis of multidecker sandwiches. In the course of investigating the tetradecker stacking reactions, some novel chemistry and structures have been uncovered whose implications are yet to be fully assessed.

#### Reports:

- Electronic Control of Metallacarborane Stacking Reactions. Directed Synthesis of Cp\*Co(C<sub>2</sub>B<sub>1</sub>)M(C<sub>2</sub>B<sub>1</sub>)CoCp\* Tetradecker Sandwiches, by Kent W. Piepgrass et al., J Am Chem Soc 113,681(1991). AD A238 442
- Unusual Organic Chemistry on a Metallacarborane Substrate: Formation of a B-Vinyl Ester From Acetyl Chloride, by Kent W. Piepgrass et al., J Am Chem Soc 113,680(1991). AD A238 441
- Organotransition-Metal Metallacarboranes. 18. η<sup>6</sup>, η<sup>5</sup>-Benzyltetramethylcyclopentadieneide- as a Bridging Ligand in Multilevel Iron-Cobalt Sandwich Complexes, by James H. Davis, Jr. et el., Inorg Chem 30.1765. AD A238 375
- Organotransition-Metal Metallacarboranes. 19. Indenyliren(II) and -Iron(III) Complexes and Related Species. η<sup>6</sup> → η<sup>5</sup> Haptotropic Rearrangement, Electrochemistry, and Polyhedral Expansion of (Arene)Fe(Et<sub>2</sub>C<sub>2</sub>B<sub>4</sub>H<sub>4</sub>) Clusters, by Achim Fessenbecker et al., J Am Chem Soc 113,3061(1991). AD A238 314

# 26636 DIELECTRICS FOR THE SUPERCAPACITOR

Sergio Petrucci

Polytechnic Institute of New York, Farmingdale

SL: ETDL, MTL SC: AROE, ETDL

Microwave complex permittivities in the frequency range ~0.4 - 90 GHz and far-infrared permittivities at  $\nu = 300 \text{ cm}^{-1}$  (9,000 GHz) and  $\nu = 400 \text{ cm}^{-1}$ (12,000 GHz) for benzonitrile and benzonitrile-CCl<sub>4</sub> mixtures have been documented. In order to characterize the shape of the dielectric relaxation spectrum of liquids and liquid mixtures, it is important to ascertain the value of  $\epsilon_{x}$  (the permittivity at frequencies above the rotational relaxation spectrum) without ambiguities. To this end, the experimental investigation of the far-infrared complex permittivity of benzonitrile and of benzonitrile-CCl4 mixtures at wavenumber of 125 cm<sup>-1</sup> (3750 GHz) was expanded so that a gap of less than two orders of magnitude separates the infrared and microwave data at f = 90 GHz (3 cm<sup>-1</sup>). The data show a monotone decrease from 4.26 at f = 29.85 GHz ( $v = 0.995 \text{ cm}^{-1}$ ) to  $n^2 = 2.33$  at the visible sodium doublet v = 16,969cm<sup>-1</sup> (f = 509 THz). For the far-IR experiments at v = 125 cm<sup>-1</sup> a FTIR spectrometer was used. Air dried over molecular sieves and drierite and filtered for particle size larger than 0.1  $\mu$  was used to purge the instrument and the cell compartment where the cell was thermostated and temperature monitored. The fringe method was used in the wavenumber 150-100

#### **H** Chemistry

cm<sup>-1</sup> to collect the refractive index data. Absorbance v. variable cell thickness was recorded at  $\nu = 125$ cm<sup>-1</sup>, calculating the attenuation coefficient  $\alpha$  (cm<sup>-1</sup>) at this wavenumber. The instrument is computer assisted for spectral digitization graphics and spectral storage.

Reports:

 Infrared and Microwave Dielectric Relaxation of Benzonitrile, Acetonitrile and Their Mixtures with Carbon Tetrachloride at 25°C, by A. Marchetti et al., TR, Jul 90, 43 pp. AD A226 223

# 26748 SINGLE SOURCE PRECURSORS FOR THE OMCVD OF III/V COMPOUND SEMICONDUCTORS

Richard A. Jones John G. Ekerdt University of Texas at Austin

SL: ARO SC: AROE, ETDL, MTi.

Researchers have continued to explore the synthesis, characterization and OMCVD studies of the di- and tri-nuclear class of compounds of general formula  $[R_2M(\mu-ER_2')]_n$  (R = alkyl, aryl, H, etc.; M = Al, Ga, In; E = P, As, Sb; n = 2,3 etc.). Isotope labeling studies are currently in progress and initial results indicate that the dinuclear compound  $[Me_2Ga (\mu-t-BuAs)]_2$  is actually carried to the growing GaAs surface as a monomer. Further progress has been made on the synthesis and characterization of the new class of precursor based on the cubane type of  $M_4E_4$  framework.

#### Reports:

- 1. An Aluminum Phosphorus Cubane. A New Aluminum Phosphide Precursor, by Alan H. Cowley et al., MS.
- III/V Precursors with P-H or As-H Bonds. A Low Temperature Route to Gallium Arsenide and Gallium Phosphide, by Alan H. Cowley et al., Organometal 10,652(1991).

3. Decomposition Pathways of the Novel GaAs Precursors  $[Me_3Ga (\mu-i-Pr_2As)]_3$  and  $[MeGa(\mu-i-Bu_3As)]_2$ , by James E. Miller et al., MS, *Chem Mater* 

- Reaction of (*t*-BuGaCl<sub>2</sub>)<sub>2</sub> with Ar'PHLi (Ar' = 2,4,6-*t*-Bu<sub>3</sub>C<sub>6</sub>H<sub>2</sub>): Preparation of the Chloride-Bridged Dimer (*t*-BuGa(Cl)P(H)Ar')<sub>2</sub>, by Alan H. Cowley et al., *Heteroatom Chem* 2,11(1991).
- X-ray Crystal Structure of the Dimethylgallium Azide Polymer and Its Use as a Gallium Nitride Precursor, by David A. Atwood et al., *J. Organometal Chem.* 394,C6(1990). AD A234-145
- Synthesis and Structure of a Diphosphadigalletane: A Novel Based-Stabilized Ga<sub>2</sub>P<sub>2</sub> Ring System, by Alan H. Cowley et al., Angew Chem 29,1150(1990). AD A233-974
- Growth and Characterization of Gallium Arsenide Using Single-Source Precursors: OMCVD and Bulk Pyrolysis Studies, by James E. Miller et al., *Chem Mater* 2,589(1990), AD A234–144

#### A. Inorganic, Analytical, and Electrochemistry

## 27502 STRUCTURAL AND DYNAMICAL ASPECTS OF ELECTRODEPOSITION

Hector D. Abruna

Cornell University

SL: NVEOC

SC: AROE, ETDL

Continued voltammetric studies on silver ion deposition on well defined Pt(111) electrodes have shown that the mechanism of deposition is dependent on the silver ion concentration in solution. At low concentration ( $< 1 \times 10^{-5}$  M) of silver, the deposition appears to be through island formation which eventually leads to three dimensional clusters. This was quite apparent in that even after the deposition of well over two monolayer equivalents of silver, the voltammetric features associated with hydrogen adsorption/desorption were still present. At high concentration (>1  $\times$  10<sup>-3</sup> M) of silver the deposition is commensurate with the Pt(111) surface as determined from LEED (low energy electron diffraction). It was found that upon deposition of silver the sharp hexagonal pattern, typical of clean and well-ordered Pt(111), remains essentially unchanged except for the fact that the spots get somewhat diffuse. Upon stripping of the silver deposit, the sharp LEED pattern is regenerated. In addition, the electrochemical response prior to and after stripping of the silver deposit is that which is very characteristic of clean and well ordered Pt(111). Moreover, the silver islands formed when deposition is from high concentration of silver ion appear to be larger than those formed at low concentrations. In this study researchers monitored the characteristic  $Cu_{K\alpha}$  and  $I_L$  fluorescence intensities as well as the reflectivity profile across the first order Bragg reflection and under total external reflection. Studies were carried out at applied potential values that corresponded to deposition of fractions of a monolayer up to a complete layer of copper. A preliminary analysis of the data points to some interesting aspects. It was found that at the potential for monolayer deposition the copper fluorescence yield data indicates the presence of a deposited copper layer as well as the presence of copper species in solution in a region very close to the electrode surface. This contribution is much larger than can be accounted for by the bulk concentration of copper and points to a specific interaction with the surface. These copper species, however, could be displaced by rinsing the electrode with clean supporting electrolyte while the electrodeposited copper was unaffected by such a treatment. Furthermore, near edge spectra indicate the presence of metallic copper at potentials where a deposited monolayer is expected and of copper ions at potentials where the deposited copper layer oxidized and stripped off the surface. Researchers have also been able to carry out surface EXAFS experiments on the deposited copper at coverages ranging from fractions up to a full monolayer. The EXAFS measurements reveal changes in the Cu-Cu distances as a function of coverage consistent with ex-situ LEED studies.

## 27600 REACTOR STUDIES OF METAL IONS ASSOCIATED WITH CHROMATOGRAPHIC SILICA

Stanley H. Langer University of Wisconsin-Madison

SC: CRDEC, MTL, NRDEC

Because of promising possibilities for developing robust catalytic systems which may be useful in promoting either oxidations or solvolyses, investigations are continuing on iron/silica and related systems for chromatographic reactor type applications. Work on the development of a statistical moment method based on the overall elution profile for a first order reaction in a chromatographic reactor has proceeded. Applications of <sup>57</sup>Fe Mössbauer spectroscopy to characterize the nature of the metal ions on modified silica are also being studied. Information from the Mössbauer spectra, including the oxidation state and the coordination environment of the iron species on the silica surface, appeared to be useful or supplementing the kinetic and catalytic studies of the probe reaction that are being used. The hydroquinone oxidation reaction is being used to study the oxidative catalytic activity of FeCl<sub>3</sub> adsorbed onto  $SiO_2$  (Fe<sup>3+</sup>SiO<sub>2</sub>) in a batch system to confirm its nature. The presence of Fe<sup>3+</sup>SiO<sub>2</sub> accelerates the reaction in a t-butanol/hexane (8 percent, v/v) mixed solvent. When the solvent is purged with  $N_2$  and the reaction is carried out in a N2-filled glove bag, benzoquinone is detected with a UV-visible spectrometer within a short time after reaction initiation. Eventually almost all the iron is present as  $Fe^{2+}$  and only a trace amount of  $Fe^{3+}$  can be detected.

#### Reports.

- Hydroquinone Oxidation Kinetics in Adsorptive Liquid Chromatographic Bed by Chawn-Ying Jeng and Stanley H. Langer, MS, J Chematography.
- Rate Process Analysis in the Liquid Chromatographic Reactor: An Application of the First Statistical Moment, by Chawn-Ying Jeng and Stanley H. Langer, I&EC Product Res and Dev 30,2489(1991). AD A239 901
- Gas and Liquid Chromatographic Reactors, by J. Coca et al., MS.

4. Reaction Kinetics and Kinetic Processes in Modern Liquid Chromatographic Reactors, by Chawn-Ying Jeng and Stanley H. Langer, MS, J Chromatography.

## 28353 SYNTHESIS OF TUNGSTEN NITRENE COMPLEXES PRECURSORS FOR TUNGSTEN NITRIDE

Lisa McElwee-White Stanford University

#### SC: AROE

The research objective is to prepare stable low valent metal nitrene complexes of the type  $(CO)_5W = NR$  as precursors for the vapor deposition of tungsten nitride. Subsequent decomposition to tungsten carbide is anticipated. Potential routes include: (a) generation of kinetically stabilized nitrene complexes by metathesis of Fischer carbenes, (b) generation of thermodynamically stable complexes by methathesis of Fischer carbenes, or methathesis of Fischer carbenes, or methathesis of Fischer carbenes with heteroatom-substituted azo compounds; (c) preparation of donor-stabilized low valent nitrene complexes, or (d) use of nonmethathesis routes.

# 28402 ENCAPSULATED ALKALINE-EARTH ORGANOMETALLICS AS CONTROLLED SOURCES OF CALCIUM, STRONTIUM, AND BARIUM IONS

Timothy P. Hanusa Vanderbilt University

SC: AROE, MTL

The chief developments centered on the synthesis of new "encapsulated" metallocenes containing highly substituted cyclopentadienyl rings and an evaluation of their air/thermal stability and volatility. The ligands have been synthesized with a phase transfer-catalyzed alkylation method that was previously used to prepare tetraisopropylcyclopentadiene, and from it, the encapsulated metallocenes  $[C_5H(i-Pr)_4]_2M$  ( $M \approx Ca,Ba$ ). Trialkylated rings are generally more accessible than are tetrasubstituted rings.

#### 28469 DECONTAMINATION AND REDOX CATALYSIS

Craig L. Hill Emory University SL: NRDEC SC: AROE, CRDEC, MTL

Polyoxometalates have far more photoredox chemistry under anaerobic conditions that is of potential value in decontaminating toxic materials including cw agents than have semiconductor metal oxides. Under aerobic conditions the most effective catalysts for the photochemical degradation of cw agents are the polyoxometalate decatungstate, W10O324-, and the semiconductor, TiO<sub>2</sub> (anatase). A polyoxotungstate with catalytic activity has been functionalized with aryl phosphonyl groups. This chemistry provides an entry into covalent immobilization of catalytically active polyoxometalates on surfaces and fibers. The first paper on these new classes of polyoxometalates will be submitted shortly. It examines the solution and solid state structures and properties of exemplary complexes in this class. The facile dehalogenation of a range of aliphatic and aromatic halocarbons by the two-electron reduced form of decatungstate,  $W_{10}O_{32}^{6-}$ , has been achieved. Rate structure profiles are consistent with a mechanism for C-X cleavage involving either dissociative electron transfer or halogen atom abstraction.

#### 28486 THE REDOX CHEMISTRY OF SOME PEROXO AND SUPEROXO METAL ION COMPLEXES

Richard C. Thompson University of Missouri at Columbia

SL: NRDEC SC: AROE, CRDEC

The research objective is to investigate the aqueous oxidation-reduction chemistry of peroxo and superoxo complexes of early transition elements and a few actinide elements in their highest oxidation states. Absorption spectroscopy will be employed to establish the concentration of pertinent species, and then equilibrium constants and kinetic parameters determined. Stopped flow techniques will be used when especially fast reactions are involved.

#### **28655 INORGANIC HALOGEN OXIDIZERS**

Karl O. Christe

**Rockwell International Corporation** 

SL: BRADEC, MICOM SC: AROE, CRDEC, MICOM

A three year program will carry out research in high-energy oxidizer chemistry. The main thrust of the program will include the following areas: (a) novel anions at the limits of coordination and oxidation; (b) oxidative oxygenations of energetic materials with  $H_2OF^+$  salts; (c) synthesis and characterization of novel ozonides for singlet delta oxygen gas generators; (d)  $NF_4^-$  chemistry; and, (e) synthesis and characterization of novel biazides. Synthetic techniques appropriate for these compounds, many developed in the P.L's own laboratory, will be utilized to prepare these high-energy compounds. Characterization will utilize the wide range of instrumental and physical techniques available.

# **B.** Organic Synthesis and Mechanisms

**25181 CHEMICAL REACTIVITY AND** 

SELECTIVITY IN ORGANIZED MEDIA

David A. Jaeger University of Wyoming

SC: AROE, CRDEC, MTL, NRDEC

Three diastereomeric, guaternary ammonium surfactants, [3-c-4, c-5-dihexadecyl-r-2-methyl-1, 3-dioxolan-2-vl)propylltrimethylammonium bromide (1a) and its t-4, t-5 (1b) and c-4, t-5(1c) isomers, were prepared and the properties of their vesicles and monolayers compared. The vesicles were characterized by dynamic laser light scattering, differential scanning calorimetry, and [<sup>14</sup>C] sucrose entrapment and release studies. Clear differences among the three systems were found in the latter two studies. The phase transition temperature order for both sonicated and vortexed vesicles was |a>|c>|b|, and for sonicated vesicles the permeability order was |b| > |c| > |a|. The three surfactants also displayed different monolayer characteristics. The degrees of expansion in the surface pressure-area isotherms, the monolayer stability limits, and the propensities of the films to spread from their crystals followed the same order: 1b > 1c > 1a. Overall, the results suggest that in both vesicular and monolayer form 1a has the tightest, and 1b the loosest surfactant packing.

Reports:

No. 1-5 in previous editions.

6. Vesicular and Monolayer Properties of Diastereomeric Surfactants, by David A. Jaeger et al., MS, Langmuir.

#### 25290 SUPER HYDRIDES

Herbert C. Brown Purdue University SC: AROE

A study was made of the kinetic resolution of racemic ketones using  $\beta$ -chlorodiisopinocampheylborane ( $I_{pc2}BCI$ ). Results to date are quite different from those realized 25 years ago in the reduction of 2-alkylcycloalkanones with hindered dialkylboranes, such as  $I_{pc2}BH$  (*J Am Chem Soc* 1966, 88, 2871). This study conducted 25 years ago did not involve kinetic resolution of these racemic ketones. The reagent  $I_{pc2}BH$  undergoes elimination during the reaction forming  $\alpha$ -pinene and  $I_{pc}BH_2$ . Studies are being made of the kinetic resolution with  $I_{pc2}BH$  and  $I_{pc}BH_2$  in order to achieve understanding of the unexpected behavior of the chloroboranes.

Whatever the mechanism for these reactions is, it is clear that the hydride is transferred from the reagent to the carbonyl group in opposite directions in the two cases. The unexpected behavior of the chloroboranes in giving 100 percent *trans* isomer is being looked into more thoroughly to understand this phenomenon, of potential importance in synthetic organic chemistry, especially for steriod chemistry.

#### Reports:

No. 1-2 in previous editions.

- 3. Hydroboration. 85. Synthesis and Hydroboration of (-)-2-Phenylapopinene. Comparison of Mono(2-Phenylapoisopinocampheyl)Borane with Its 2-Methyl and 2-Ethyl Analogues for the Chiral Hydroboration of Representative Alkenes, by Herbert C. Brown et al., J Org Chem 55,1217(1990). AD A225 854
- 4. Selective Reductions. 46. Effect of the Steric Requirement at the 2-Position of Apopinene on Chiral Reductions. B-(Iso-2-Ethylapopinocampheyl)- and B-Iso-2-*n*-Propylapopinocampheyl)-9-Borabicyclo[3.3.1] Nonanes as Improved Reagents for the Chiral Reduction of  $\alpha$ ,  $\beta$ -Acetylenic Ketoanes and  $\alpha$ -Keto Esters, by Herbert C. Brown et al., J Org Chem 55,6328(1990). AD A232 233

## 25411 QUANTITATIVE ASPECTS OF DEPHOSPHORYLATION IN COLLOIDAL SELF ASSEMBLIES

Clifford A. Bunton

University of California, Santa Barbara

SL: CRDEC SC: AROE, CRDEC, LAIR, NRDEC

The effects of a series of cationic micelles ( $C_{16}H_{33}$ NME<sub>3</sub>X, CTAX, X = Cl, Br, Oms) upon reactions of OH<sup>-</sup> with a series of phosphate, phosphinate, thiophosphinate and thione phosphate esters have been analyzed quantitatively by estimating the concentration of OH<sup>-</sup> at the micellar surface by solution of the Poisson-Boltzmann equation in spherical symmetry. Second order rate constants in water vary over a range of  $2 \times 10^4$ , but second order rate constants of reaction in the micellar pseudophase are lower than in water by factors ranging from 0.05 to 0.18 except for reaction of  $pH(i-C_3H_7)PO OC_6H_4NO_2$ where the factor is 0.7 Earlier studies found double rate maxima in reactions of thiophosphinate esters with OH<sup>-</sup> in cationic micelles and ascribed them to formation of reactive complexes of ester and monomeric or submicellar surfactant. Supporting evidence indicates that nonmicellizing hydrophobic ammonium ions, e.g., (CgH<sub>17</sub>)<sub>4</sub>NX speed reactions of OH<sup>-</sup>, and NMR evidence is in hand for interactions between PH<sub>2</sub>PO·SPh and CTAOMS below the cmc. Quantitative analyses of micellar effect have been completed upon oxidations of sulfides by OXONE (HSO<sub>5</sub>)<sup>-</sup> or periodate ion. Second order rate constants are much lower at micellar surfaces than in water. Rates of the nonmicellar reactions are sharply decreased by a decrease of the water content of the solvent. These medium effects are similar to those in alkene bromination by  $Br_3^-$  and may be typical for reactions of anionic electrophiles; the P.I. postulates single electron transfer mechanisms in oxidation and bromination. These results show the desirability of polar aqueous media in oxidations by  $HSO_5^-$ .

#### Reports:

No. 1-6 in previous editions.

- Dephosphorylation by Peroxyanions in Micelles and Microemulsions, by Clifford A. Bunton et al., J Phys Org Chem 3,390(1990).
- 8. Oxidation of Organic Sulfides by Anionic Electrophiles, by Clifford A. Bunton et al., MS.

#### 25669 FUNCTIONAL MICELLES AND VESICLES AS ORGANIC REAGENTS

Robert A. Moss

Rutgers. The State University of New Jersey

SL: CRDEC, NRDEC SC: AMRICD, AROE, CRDEC, LAIR, MTL

Unsaturated oleoyl (cis-2-F, cis-2-NF) and elaidovl (trans-2-F, trans-2-NF) ammonium ion lipids were synthesized (report 15, below). Liposomes were created by sonication of 1:10 functional/nonfunctional lipid blends. These small (300Å liquid crystal phase,  $T_c < 25^{\circ}$ C) liposomes were surface differentiated by exovesicular glutathione in an exovesicular/ endovesicular pH gradient of 8/3.9. At 25°C, the liposomes were quite permeable to  $H^+/OH^-$  ( $t_{10} < 20$  s), and reequilibrated rapidly by lipid flip-flop  $[t_{ij}, (cis-2) < 1 \text{ min};$  $t_{10}$  (trans-2)~4 min.] In contrast, liposomes created from analogous, saturated stearoyl lipids (1:10 3-F/3-NF), where  $T_c = 59^{\circ}$ C, were less permeable to H<sup>+</sup>/OH<sup>-</sup>  $(t_{ib} \sim 21 \text{ min})$ , and less prone to *trans*-bilayer lipid migration after surface differentiation ( $t_{12}$ >30 min at 40°C. The suppressed  $T_c$ , higher permeability, and decreased resistance to trans-bilayer lipid migration found at ambient temperature for the cis-2 or trans-2 liposomes, in comparison to liposomal 3, are consistent with previous reports of looser chain packing in liposomes constructed of unsaturated lipids.

#### Reports:

No. 1-12 in previous editions.

- An Efficient Iodosobenzoate-Functionalized Polymer for the Cleavage of Reactive Phosphates, by Robert A. Moss and Yong-Chan Chung, Langmuir 6,1614(1990). AD A230 808
- Dynamics of Liposomes Constructed From Phytanyl Lipids, by Robert A. Moss and Tsunchisa Fujita, *Tetrahedron Let* 31,7559(1990). AD A233 812
- Effect of Unsaturation on Lipid Dynamics Within Synthetic Lipid Membranes, by Robert A. Moss et al., Langmuir 7,440(1991). AD A238 468

### 25739 NEW MODES OF CATALYSIS AND REACTIVITY

Fredric M. Menger Emory University SL: CRDEC

SC: AROE

The mustard deactivation work has now appeared as a J Am Chem Soc communication. It is felt that the microemulsion technology developed in this work could be useful not only for mustards but also for nerve agents. The advantages (and one disadvantage) of the microemulsion system are: Advantages: (a) mustards are deactivated (i.e., oxidized to harmless sulfoxides) very rapidly (less than 15 seconds), (b) the method is cheap (utilizing only water, hydrocarbon, alcohol, surfactant, and household bleach), (c)the method can deactivate substantial amounts of mustard (i.e., 1.0 ml mustard is destroyed by 15 ml microemulsion), (d) the method is mild (no harsh alkali being used), (e) the method requires no laboratory method (e.g., continual stirring) that would render use in the field impractical, (f) the decontaminating microemulsions can be made nonflammable by using a nonvolatile hydrocarbon. Note that the microemulsions contain water as the main component, and this in itself reduces risk of fire. Disadvantage: The oxidant, household bleach, must be mixed with the microemulsion and used within a couple of days. The microemulsion without the bleach has an infinite shelf-life. Thus, one would have to add a small amount of bleach to the microemulsion prior to use. Although this might be considered an inconvenience, the advantages are so over-riding, that further work with microemulsions would certainly seem warranted.

#### Reports:

- Synthesis of Porous Polystyrene with Chemically Active Surfaces, by F. M. Menger and T. Tsuno, J Am Chem Soc 112,6724(1990). AD A232 165
- Cross-Linked Polystyrene Incorporating Water Pools, by EM. Menger et al., J Am Chem Soc 112, 1263(1990). AD A224 425
- 3. Ion Conductance Along Lipid Monolayers, by F.M. Menger et al., J Am Chem Soc 111,6893(1989). AD A224 426
- Rapid Deactivation of Mustard via Microemulsion Technology, by F.M. Menger and A.R. Elrington, J Am Chem Soc 112,8201(1990). AD A232 541

## 25761 CHEMISTRY OF POLYNITROETHANE DERIVATIVES

Kurt Baum

Fluorochem, Inc.

# SL: ARDEC, BRL, NSWC SC: AFAL, ARDEC, AROE, NWC

Work was continued on the thermolysis of 1,1,2tribromotrinitro-ethane to obtain 1,2-dibromodinitroethylene and 1,1-dibromodinitro-ethylene. Continued attempts to isolate an analytical sample of the latter

#### **B.** Organic Synthesis and Mechanisms

were unsuccessful, although it was characterized as its displacement product with ethylenediamine. Heating 1,1,2-tribromotrinitroethane in benzene gave a 22 percent yield of nitrotribromoethylene. Complex mixtures of products resulted from the reaction of 1,1-dibromo-2,2-dinitroethylene with Zn or Mg in the presence of anthracene. Nitration (100 percent HNO<sub>3</sub>) of trichloroethylene gave a mixture, of which chlorodinitromethane was the major product. Nitration of vinylidene chloride gave complex mixture. Substantial effort during this period was spent completing earlier phases of the work and preparing manuscripts. In addition to the manuscript below on the preparation of 1,1-diiododinitroethylene and its reactions with nucleophiles, a manuscript on nitration of the amine displacement products was prepared, and one on the fluoride reaction of 1,1-diiododinitroethylene to give 1,1,1-trifluoro-2,2-dinitroethane was partially complete.

Reports:

No. 1 in previous edition.

2. Synthesis and Reactions of 1,1-Diiododinitroethylene, by Kurt Baum et al., MS, J Org Chem.

# 26115 CHEMILUMINESCENT SUBSTRATES FOR ACETYLCHOLINESTERASE AND ALKALINE PHOSPHATASE

A. Paul Schaap

Wayne State University SL: CRDEC

SC: AROE, CRDEC, MTL, NRDEC

This research seeks to synthesize phosphate-substituted dioxetanes with potential for use with phosphataselinked immunoassay and DNA probes, as well as dioxetanes with tethered fluorescers which emit in other spectral regions, including the infrared. Chemiluminescent efficiency will be determined, and the effects of structural variations will be determined.

# 26284 NUCLEOPHILIC DECONTAMINATION AGENTS

J. Milton Harris

Samuel P. McManus

University of Alabama-Huntsville

SL: CRDEC, MICOM SC: AROE, CRDEC Ion-Pair Return in Mustard Reactions. Ph-S-CD<sub>2</sub>CH<sub>2</sub>-Cl (1). The availability of this compound has made it possible to follow ion-pair return for a variety of mustard reactions. This information has proven quite useful for better understanding mustard reactions. For example, another group had previously reported that iodide ion in acetone reacted with mustard by a direct displacement SN2 reaction. The evidence for this conclusion was that the reaction exhibited second order kinetics. This conclusion was very surprising. The compound (1) has been used to show that second-order kinetics for the iodide reactions results. not from SN2 attack, but rather from elimination of ion-pair return from the sulfonium ion normally formed by mustards upon solvolysis. Mustard Reactions in Wet Aprotic Solvents. It was previously observed that the reaction of phenolate ion with 2-(thiophenyl) ethyl chloride could be shifted from substitution (SN2) to elimination (E2) by choice of aprotic solvent. In particular it appeared that good hydrogen-bonding solvents (such as dimethylformamide) gave substitution and poor H-bonding solvents (such as dimethylsulfoxide or N-methylpyrrolidone) gave elimination. Since there is interest in using pyrrolidones and decontamination solvents, it was decided to examine mixtures of N-methylpyrrolidone and water. Interestingly, rather large amounts of water did not change the mechanism from elimination. It now appears that each molecule of the pyrrolidone can tie up one molecule of water, and it is necessary to exceed a 1:1 molar ratio of water to pyrrolidone to obtain the substitution reaction.

# 26914 CATALYSTS FOR THE OXIDATION OF THIOETHERS AND AMINES IN MICROEMULSIONS, EMULSIONS AND FILMS

Russell S. Drago University of Florida SL: CRDEC

SC: AROE, CRDEC, MTL, NRDEC

The research has seen several developments in the area of mustard simulant oxidations involving H<sub>2</sub>O<sub>2</sub>. In the area of aqueous systems utilizing  $H_2O_2$ , a binary solvent system consisting of N-cyclohexylpyrrolidinone and H<sub>2</sub>O (50/50) was utilized in the oxidation of the  $H_2O$  insoluble substrate, *n*-butyl sulfide. This system was found to be homogeneous. The uncatalyzed reaction with this solvent system showed only a 15 percent conversion to sulfoxide after one hour of reaction. When the catalyst FeSO<sub>4</sub>·7H<sub>2</sub>O was used, an 11 percent conversion to sulfoxide was seen after one hour. Similar results were observed with the catalyst,  $Co(dmp)Cl_2$  (dmp = 2,9-dimethyl-1,10phenanthroline).  $Mo(O)_2(acac)_2$  (acac = acetylacetonate) showed a 42 percent conversion to sulfoxide with this system. The low conversions seen with these catalysts was thought to possible be due to a competition between the substrate and the N-cyclohexylpyrrolidinone for the oxidant,  $H_2O_2$ , or the metalcatalyzed decomposition of the H<sub>2</sub>O<sub>2</sub>. When followed by NMR, the reaction of N-cyclohexylpyrrolidinone with H<sub>2</sub>O<sub>2</sub> under ambient conditions showed no reaction occurring. This suggests that the metal-catalyzed decomposition of the  $H_2O_2$  may be a problem with the Fe(II) and Co(II) systems. Addition of acetic acid to the above mentioned solvent system led to some very interesting results. When a solvent system consisting of equal volumes of N-cyclohexylpyrrolidinone, H<sub>2</sub>O, and acetic acid was utilized in the uncatalyzed oxidation of *n*-butyl sulfide, both sulfoxide (59 percent) and sulfone (20 percent) were detected at three minutes with the remainder being sulfide. After 30 minutes, the sulfide was converted to sulfoxide (80 percent) and sulfone (20 percent). The Fe(II) catalyzed sulfoxidation in this solvent system led to no improvement. Further work with this system has shown that a reduction in the amount of acetic acid leads to lower conversions. The active oxidant in this system is believed to be peroxyacetic acid. A study of the exact nature of the active oxidant in this homogeneous system is presently being pursued.

Reports:

- 1. The Oxidation of Alkanes by Cobalt(II) Salts of Weakly Coordinating Anions, by Alan S. Goldstein and Russell S. Drago, MS, *Inorg Chem.*
- Homogeneous Metal Catalyzed Oxidations by O<sub>2</sub>, by Russell S. Drago, MS, Angew Chem.

# 27534 PHOTODEGRADATION AND PHOTOPHYSICS OF LASER DYES

Guilford Jones, II

**Boston University** 

SC: AROE, BRL, NRDEC SL: CECOM, MICOM The influence of the solvent medium and polymer and other additives on the photophysical and photochemical properties of laser dyes has been investigated. The coumarin and rhodamine families of dyes have been studied in the initial phases of the work. These hydrophobic molecules or ions are sequestered in microdomains created by the "hypercoiling" of selected polyelectrolytes when the polymers are folded into globular conformations under certain conditions in water. Poly (methacrylic acid) (PMAA) behaves in this fashion for aqueous dilute solutions at pH 3.0. Experiments conducted to date include measurement of fluorescence quantum yields, lifetimes, and anisotropy. These parameters for the dyes under study are highly dependent on solvent polarity and viscosity. The results reveal sharp changes in photophysical properties on binding the coumarins and rhodamines in the PMAA hydrophobic "pockets". Quantum yields and lifetimes of fluorescence are raised signifying a relatively "dry" interior for the polymer globule; polarization measurements further reveal a high local viscosity. The most recent effort involves polymer "hypercoil" binding of the nerocyanine dye, Styrl 7. This dye shows some of

the most dramatic results to date regarding systematic alteration of the Stokes shift of emission and the improvement in quantum efficiency for fluorescence in the 650 nm region. These studies show great promise for the solubilization of laser dyes in water and the protection of these dyes against adventitious quenching and undesirable photodegradation under flash excitation. These investigations are directed to the improvement of performance for dye lasers.

## 27568 THE DEVELOPMENT OF STABLE, HIGH EFFICIENCY LASER DYES

George R. Bird

Rutgers, The State University of New Jersey

SL: CECOM, MICOM SC: AROE, CRDEC, NRDEC

A paper has been prepared which shows that by calculation from transition density theory one can predict that a class of fast emitting excimers could exist. Work in this area has examined the pyrene excimers and first observed a fast excimer under static conditions by applying one full atmosphere of oxygen for selective quenching of monomer and the familiar slow emitting excimer. The fast excimer spectrum was expected to fall at shorter wavelength than the ordinary (slow) excimer emission, and this was observed.

Reports:

A New Fast Emitting Excimer of Pyrene, by Changhe Xiao et al., MS.

## 28013 ARTIFICIAL PHOSPHOESTERASE: METAL ACTIVATION BY STRAIN

Jik Chin

McGill University

SL: AMRICD, NRDEC SC: AROE, CRDEC

New Co(III) and Cu(II) complexes have been synthesized and tested for hydrolyzing phosphate esters. Although Co(III) complexes are ideal for careful mechanistic studies, they are not necessarily good catalysts. Co(III) complexes are generally substitutionally inert making it difficult to obtain any catalytic turnover. Strain effects in substitutionally labile Cu(II) complexes are being investigated. A series of sixmembered ring and five-membered ring complexes were synthesized and their reactivities compared for hydrolyzing phosphate diesters. Significant strain effect was found in Cu(II) complex catalyzed hydrolysis of phosphate diesters.

C. Structural, Surface Chemistry, and Spectroscopy

## C. Structural, Surface Chemistry, and Spectroscopy

## 24413 CARS DIAGNOSTICS FOR SOLID PROPELLANT COMBUSTION INVESTIGATIONS

John H. Stufflebeam Kenneth K. Kuo United Technologies Research Center

SL: AFAL, ARDEC, BRL SC: ARO, AROE, BRL, CRDEC

Nitramine propellants undergo intermediate reactions whose rate is sensitive to the propellant surface temperature. Two major reaction pathways are believed to compete in nitramine combustion, one involves HCN and the other H<sub>2</sub>CO. Utilizing the motorized, servo-controlled propellant combustion vessel, single shot CARS spectra were acquired within 100  $\mu$  of the burning propellant surface where the intermediate reactions occur and clearly showed the products of each of the competing pathways. Work is in progress to delineate the dominant reaction pathway, and to increase the spatial resolution of these surface observations so that quantitative measurements of temperature and species concentration can be made. Similarly, dual broadband CARS spectra have been acquired from the near surface region.

Reports:

No. 1-3 in previous editions.

 CARS Measurements in the Near-Surface Region of Composite Nitramine Combustion, by John H. Stufflebeam, MS.

# 25222 GALLIUM ARSENIDE CLUSTERS AND THEIR INTERFACIAL PHYSICS AND CHEMISTRY

Richard E. Smalley Robert E Curl Frank K. Tittel Rice University

> SC: ARO, AROE, ETDL, HDL, NVEOC

A paper has been prepared in which the electronic structure of small Ga<sub>x</sub>As<sub>y</sub> clusters  $(x + y \le 10)$  are calculated using the local density method. The calculation shows that even-numbered clusters tend to be singlets, as opposed to odd-numbered clusters which are open shell systems. This is in agreement with the experimental observations of even/odd alternations of the electron affinity and ionization potential. In the larger clusters, the atoms prefer an alternating bond arrangement; charge transfers are observed from Ga sites to As sites. This observation is also in

#### Reports:

No. 1 in previous edition.

- 2. Reactions of  $Ga_xAs_x^{(*)}$  Clusters with NH<sub>3</sub>, by L.H. Wang et al., MS.
- 3. Ammonia Chemisorption on Gallium Arsenide Clusters, by Lihong Wang et al., MS. Chem Phys Let.
- 4. Ultraviolet Photoelectron Spectra of Gallium Arsenide Clusters, by C. Jin et al., MS, Chem Phys Let.
- Direct Injection Supersonic Cluster Beam Source for FT-ICR Studies of Clusters, by Shigeo Maruyama et al., MS, *Rev Sci* Instr.
- 6. Efficient Production of  $C_{60}$  (Buckminsterfullerene),  $C_{60}H_{36}$ , and the Solvated Buckide Ion, by R.E. Haufler et al., MS.
- 7. Electronic Structure of Small GaAs Clusters, by L. Lou et al., MS.

### 25605 THE THEORY OF ELECTRON SCATTERING BY ADSORBATES

Horia Metiu

University of California, Santa Barbara

SC: AROE, CRDEC

Electron scattering is being used to study the properties of adsorption-desorption precursor states of molecules on surfaces and electronic excitation caused by electron scattering.

## 26126 APPLICATIONS OF LOW-COORDINATION PHOSPHORUS CHEMISTRY IN THE CHEMICAL MODIFICATION OF SURFACES

Louis D. Quin University of Massachusetts

SC: AROE, CRDEC, MTL

Major emphasis has been given to the extension of surface –OH phosphorylation techniques to new types of solids. In previous work, it was established that two types of chromatographic grade silica gel undergo extensive phosphorylation with EtO-PO<sub>2</sub> generated in the presence of the suspended solid. The product is easily characterized by CP–MAS <sup>31</sup>P NMR spectroscopy; a shift of 8–10 is obtained. It has now been shown that two types of commercial Zeolites can be phosphorylated by these techniques. One of

II Chemistry

these, Zeolite Y, gives an excellent <sup>31</sup>P NMR spectrum with a shift of -13.3, as expected. The other, ZSM-5, gives a poorer quality spectrum, but nevertheless adequate to prove the desired conversion of some OH groups to phosphate groups. These results are of great significance, since chemically modified Zeolites are important in catalysis work. Another solid used in the new work is alumina, and this too has given an excellent spectrum. Again the result could be of relevance in catalysis. Perhaps of even greater significance is the accomplishment of the phosphorylation of OH groups on solid cellulose. The shift in this case (-7.9) is more in the region expected for a sugar pyrophosphate than a simple monophosphate, and more work will be needed to clarify this point. Nevertheless, the result is exciting, since it opens the possibility of using metaphosphate technology for the direct attachment of phosphorus groups on cellulosic fibers and fabrics, thereby endowing them with flame resistance.

#### Reports:

- Studies with Metaphosphoric Acid Derivatives, by Louis D. Quin et al., *Phosphorus, Sulfur and Silicon* 49/50,313(1990). AD A226 337
- 2. Unusual Properties of Phosphorus Functions in the 7-Phosphanorbornene Ring System, by Louis D. Quin, *Reviews on Heteroatom Chemistry Volume 3*, 1990, 39. AD A234 045
- The Mechanism of Fragmentation of Alkyl α(Oxyimino) Benzylphosphonates; Use of Silica Gel as a Novel Hydroxylic Trapping Reactant for an Intermediate Alkyl Metaphosphate, by Louis D. Quin et al., *Tetrahedron Let* 31,44(1990). AD A234 046
- Synthesis of 1,2-Oxaphospholane Oxides by Oxygen Insertion Into the C-P Bond of Phosphetane Oxides, by Jerzy Szewczyk et al., *Phosphorus, Sulfur and Silicon* 54,135(1990).
   AD A234 276

## 26191 NONLINEAR STUDIES OF SURFACES AND INTERFACES OF ADVANCED SEMICONDUCTOR MATERIALS

Geraldine L. Richmond Stephen D. Kevan University of Oregon

SC: AROE, HDL, MTL

The second harmonic (SH) generation experiments conducted on this project have been very productive. The intent has been to understand how the structural and electronic properties of a single crystal metal surface is perturbed by the presence of the electrolyte, overlayer and applied field. The experiments involve measuring the anisotropy in the SH response from Ag(111) in solution as the surface is rotated

azimuthally and comparing the results with identical optical experiments on this metal in UHV where the surface is well defined. The results showed that the surface morphology in solution in the absence of an applied field is comparable to that obtained in UHV after sputtering and annealing. This surface order can then be altered by various electrochemical processes as confirmed by the SH measurements. What was unexpected was that the SH rotational anisotropy obtained from the surface in both environments showed a strong wavelength dependence. In fact, the early studies suggested that one could not only use the technique to monitor surface order in solution, but that by wavelength dependent studies, one could measure the electronic structure of the surface under water. Very little is currently known about the electronic structure of a metal surface in solution, yet it is the electronic properties which govern the surface reactivity and electrochemistry. The studies have confirmed this sensitivity to electronic structure. The experiments have involved monitoring the magnitude and phase of the SH response as the incident wavelength is varied from the infrared region where the metal should be free-electron like, to the visible region where coupling to electronic transitions at the metal surface can occur. What was found is that there are indeed strong resonance effects which have allowed one to "map out" the electronic band structure of the metal under water. These resonance effects involved strong changes in the magnitude and phase of the SH response. These assignments can be confirmed by then performing the experiment in UHV where much is known about the electronic band structure of the metal.

#### Reports:

No. 1-3 in previous editions.

### 26238 THE ACTIVATION OF CHEMICAL BONDS AT SURFACES

John T. Yates

University of Pittsburgh

SL: CRDEC, MTL SC: AROE, CRDEC, NRDEC

The research program has been composed of four broad areas of activity. (a) Organophosphonate Decomposition and Oxidation on Transition Metal Catalysts: A patent has been issued for the use of a Mo catalyst under oxidizing conditions for the destruction of DMMP, a model compound used as a simulant for chemical agents. The patent is based on

#### C. Structural, Surface Chemistry, and Spectroscopy

earlier research here, demonstrating that continuous catalytic activity occurs above about 900 K. In addition, both Ni and Pd have been compared for the the oxidation reaction, with Pd being active at 1075 K. These results, when compared, suggest that the early transition metals may work at lower temperatures than the late transition metals for catalytic oxidation of this class of phosphorus containing compounds. (b) Photoprocesses on Metal Surfaces: The photochemical behavior of chemisorbed O<sub>2</sub> on a Pd(111) surface has been studied using variable energy ultraviolet sources. It has been found in Germany that excitation via the production of a hot electron in the metal occurs. Relatively high photodesorption cross sections are observed, in the  $10^{-18}$ cm<sup>2</sup> range, for photons having about 5 eV energy. Both photodesorption and photodecomposition are observed. In the case of adsorbed dioxygen, an enhancement of the coverage of dissociated O atoms can be achieved by photoexcitation, compared to thermal dissociation processes. (c) Photoprocesses on a Metal Oxide Surface: CO, NO and O<sub>2</sub> photoexcitation have been studied on a thin film of NiO present on a Ni(111) substrate. It has been shown that the electronic excitation of the NiO is responsible for photodesorption of CO and O<sub>2</sub>, and the energy dependence of the desorption cross section has been measured. (d) Thermal Activation and Decomposition of Molecules Using Vibrational Spectroscopies: Three very different chemical systems have been studied using a combination of high resolution electron energy loss spectroscopy and infrared reflection-absorption spectroscopy. In the case of CO on Mo(110), an intermediate species to C-O bond breaking, with a very low C-O stretching frequency, was observed. In the case of ethanol on Ni(111), the production of the ethoxy species could be directly observed, and information about its surface orientation, relative to the parent ethanol, was obtained. The methyl group in the ethoxy lies more closely parallel to the surface than in the ethanol molecule. Evidence for ethanol bonding to the Ni(111) surface through both the O moiety and the H moiety was obtained by means of the observation of a deuterium kinetic isotope effect in ethanol desorption as well as in ethanol decomposition.

#### Reports:

No. 1-9 in previous editions.

<sup>4.</sup> Second Harmonic Generation as an In-Situ Probe of Single Crystal Electrode Surfaces, by G.L. Richmond, MS.

Direct Vibrational Detection of Surface Reaction Channels Leading to CO Dissociation and to Its Inhibition on Mo(110), by J.G. Chen et al., *Chem Phys Let* 177,113(1991). AD A234-096

- Photodesorpton of CO, NO and O<sub>2</sub> From Modified Ni(111) Surfaces, by Jun Yoshinobu et al., *J Vac Sci Tech* A9,1726 (1991).
- Photochemical Studies of Adsorbed Species on Metal Surfaces, by J.T. Yates, Jr. et al., MS.
- Ethanol Decomposition on Ni(111)-Observation of Ethoxy Formation by IRAS and Other Methods, by Jiazhan Xu et al., MS, Surface Sci.
- 14. Ultraviolet Photodesorption of CO From NiO As Measured by Infrared Spectroscopy, by J. Yoshinobu et al., MS. Surface Sci.
- 15. A FT-IRAS Study of Chemisorbed PF<sub>3</sub> on Ni(111): Coverage and Temperature Dependence, by Xingcai Guo et al., MS, *J Chem Phys.*
- A Fourier Transform Infrared Reflection Absorption Spectroscopy Study of Chemisorbed PF<sub>3</sub> on Ni(111): Coverage and Temperature Dependence, by Xingcai Guo et al., J Chem Phys 94,6256(1991). AD A238-372

## 26296 STRUCTURE AND DYNAMICS OF SURFACTANT STABILIZED SYSTEMS

D. Fennell Evans

Stephen Prager

SL: CRDEC

University of Minnesota, Minneapolis

SC: AROE, CRDEC, NRDEC

An investigation is being made of the structure and dynamics of surfactant-stabilized microheterogeneous media such as micelles, microemulsions, and lipid mono- and bilayers. Surfactant-stabilized dispersions will be studied using a variety of physical and chemical techniques. Modern imaging techniques such as cryo-electron microscopy and video-enhanced optical microscopy will play strong roles.

# 26822 PHOSPHORUS-, NITROGEN-, SULFUR-, AND CHLORINE-CONTAINING MOLECULES ON SURFACES

John M. White University of Texas at Austin

SC: AROE, CRDEC

A detailed study has been undertaken of the reaction of phosgene at a Pd(111) surface. Work was completed on the thermal chemistry, which, after low temperature adsorption, is completely reversible; there is no decomposition. Interestingly, the system is very sensitive to ultraviolet light and a study is in progress on the polarization and wavelength response of this system using a pulsed excimer laser. For 6.4 eV photons, there is ready decomposition and, for the most part, it appears to be mediated by substrate absorption. Earlier work, on Pt(111) showed that phosgene was decomposed by direct absorption at 290 nm, but by substrate absorption at 320 nm. Thus, the comparison between platinum and polladium, particularly as a function of wavelength, is turning out to be a very interesting subject. In addition, a major and complete review has been finished on photochemistry at adsorbate-metal interfaces.

Reports:

No. 1-5 in previous editions.

- 6 Donor-Acceptor Interactions Between Molecular Coadsorbates on Ru(001), by Sohail Akhter et al., J Chem Soc Faraday Trans 86,2271(1990), AD A227 399
- Interactions of NH<sub>4</sub>, Coadsorbed with PF<sub>4</sub>, on Ru(001), by Y. Zhou et al., Surface Sci 230,85(1990). AD A226 204
- Decomposition of Methanethiol on Ni(111): A TPD and SSIMS Study, by M.E. Castro and J.M. White, MS, Surface Sci.
- Wavelength Dependent Mechanism of Metal-Adsorbate Photochemistry: Phosgene on Pd(111), by X.-Y. Zhu et al., MS, Surface Sci.
- The Photodissociation of Phosgene on Pd(111) at 193 nm, by C.R. Flores et al., MS, J Phys Chem.
- 11. Kinetics of the Interaction of Azomethane with Low Energy Electrons on Ag(111), by M.E. Castro et al., MS, *Surface Sci.*

## 26887 ENERGETIC SOLIDS DEGRADATION IN HIGH TEMPERATURE WATER

Thomas B. Brill University of Delaware

SC: AROE, BRL

A high temperature, high pressure study of saturated aqueous ammonium nitrate was initiated. Cell pressures were held constant from ambient to 35 MPa while cell temperature ranged from 25 to 430°C. A macro program controlled spectral data collection. Using this macro, one spectrum is collected every 15 seconds. While conducting the heating experiments, a new problem was encountered which was not previously seen in work with the older dispersive Raman instrument. Because the FT-Raman accessory measures energy changes of longer wavelength radiation than the dispersive Raman instrument, the FT instrument is more subject to interference from the black body radiation of heated samples. Although sapphire and aqueous solutions are transparent and considered weak black body radiators, they do emit sufficient radiation above 250°C to drown the weak Raman signal of nitrate ion. Evidence of nitrate decomposition was observed. For reasons discussed above, however, one could not be certain

of the temperature or the rate of decomposition. The sample was pressurized to 400 psi and heated to a maximum temperature of 418°C which was maintained for 5 minutes. The cell was then allowed to cool to 140°C at which time a spectrum was collected. The symmetric nitrate stretch (the only Raman active band seen in solution) was absent. No new bands were observed. In an attempt to determine whether or not ammonium nitrate decomposed slowly in the observed temperature range, a saturated aqueous solution was maintained at 4500 psi and 245°C for 6 hours. No decomposition was observed. To collect accurate data at 250°C, the nitrate peak needs to be significantly more intense than the background black body radiation.

# 27759 PRELIMINARY INVESTIGATIONS OF METAL LIQUID-LIKE FILMS AND COATINGS DERIVED FROM THEM

Michael S. Bradley University of Connecticut

The surface studies of MELLFs coating began with precipitated MELLFs onto silica gel substrates. A paper is in preparation describing the results. A silica gel was immersed in the organic phase, and the aqueous phase was placed on top. Addition of the reductant caused the silver to precipitate to the interface. Black fingers were observed inside the gel as the silver permeated the pores. The MELL which later formed atop the gel was allowed to coat the gel by removal of the solvents. A bright, silver coating was obtained in some cases, a sandpaper like coating in others. Surface studies were undertaken of both types of coating, using SEM and EDAX. SEM showed irregular surface topology, mainly due to the gel and not the coating. When dried slowly, the MELLF evenly coated the gel; rapid drying produced clumps of silver (sandpaper finish). In slowly dried samples, the coating produced in regions where there were surface imperfections in the gel differed greatly from the smoother areas.

# 27770 MODIFICATION OF SEMICONDUCTOR SURFACE PROPERTIES WITH CHEMICALLY BOUND MOLECULAR FILMS

David L. Allara S. Ashok The Pennsylvania State University SC: AROE, CRDEC, ETDL

#### C. Structural, Surface Chemistry, and Spectroscopy

Suitable procedures have been set up for evaluating the electrical properties of chemically modified semiconductor interfaces, measurements have been made on samples prepared by Langmuir-Blodgett processing and researchers have performed initial explorations of chemical routes to functionalize Si and GaAs surfaces with stable organic groups. Useful results have been achieved in all areas.

## 27775 NANO-SCALE METAL OXIDE PARTICLES AS MATERIALS FOR AIR PURIFICATION

Kenneth J. Klabunde

Kansas State University

SL: CRDEC

SC: AROE, BRADEC CRDEC

A modified autoclave hypercritical drying procedure has been used to prepare a hydrated form of MgO from Mg(OCH<sub>3</sub>)<sub>2</sub> in a methanol-toluene solvent mixture. This material was prepared with 1000  $m^2/g$ surface area and 35 Å crystallite size. Heat treatment of this precursor at 500°C under vacuum yielded the dehydrated MgO with 500 m<sup>2</sup>/g surface area and 45 Å crystallite size. Heats of adsorption were measured via a solution calorimeter for a series of heteroatom (oxygen, sulfur, phosphorus) containing organic compounds on thermally activated magnesium oxide (heat treated at 700°C overnight in vacuo followed by cooling to room temperature). Nanoscale particles of MgO were prepared as fine powders of varied surface areas and crystallite sizes. The capacities of these samples for dissociative adsorption of dimethylmethylphosphonate, a chemical agent simulant, were determined using a pulsed microreactor. A series of magnesium oxide samples of varying surface area were prepared and heat treated (thermally activated) at 500 or 700°C. Dimethylmethylphosphonate, trimethylphosphate and triethylphosphate were allowed to adsorb on the MgO samples both in a vacuum environment or in a helium stream. Analyses of the powdered samples were carried out by Ft-IR photoacoustic spectroscopy. These studies revealed that adsorption occurred on all samples in proportion to surface area.

#### Reports:

No. 1 in previous edition.

- 2. A Fourier Transform Infrared Photoacoustic Spectroscopy (FT-IR-PAS) Study of the Adsorption of Organophosphorus Compounds on Heat Treated Magnesium Oxide, by Yong-Xi Li et al., MS, *Langmuir*.
- 3. Nano-Scale Metal Oxide Particles as Chemical Reagents. Heats of Adsorption of Heteroatom Containing Organics on

#### **D.** Kinetics and Thermodynamics

Heat Treated Magnesium Oxide Samples of Varying Surface Areas, by Maher Atteya and J.J. Klabunde, *Chem Mater* 3,182(19910).

- 4. Nano-Scale Metal Oxide Particles as Chemical Reagents. Destructive Adsorption of a Chemical Agent Simulant, Dimethylmethylphosphonate (DMMP) on Heat Treated Magnesium Oxide, by Yong-Xi Li and K.1. Klabunde, MS, Langmuir.
- The Use of Magnesium Oxide as a Model Compound for Decomposing Air Pollutants and Other Chemicals, by Maher Mohammed Obad Atteya, MS Thesis, 1990, 111 pp.
- Molecular Vapor Synthesis: The Use of Titanium Monoxide and Vanadium Monoxide Vapors as Reagents, by Thomas J. Groshens and K.J. Klabunde, *Inorg Chem* 29,2979(1990). AD A232 216

#### 28298 SURFACE MEDIATED PHOTOCATALYSIS

Marye Anne Fox University of Texas at Austin

SC: AROE, CRDEC, MTL. NRDEC

Photocatalytic decomposition of several substituted benzyltrimethylsilanes and stannanes on band-gap irradiated TiO<sub>2</sub> powders suspended in acetonitrile causes deposition of  $-SiR_x$  and  $-SiO_2$  and of  $-SnR_x$ and SnO<sub>2</sub>, respectively, on the photoactive surface. A mechanism consistent with interfacial trapping of a photogenerated electron-hole pair can successfully rationalize the observed kinetics and substituent effects. Research has resumed in characterizing the time-resolved diffuse reflectance spectra of cation radicals generated by pulse radiolysis and laser flash photolysis. The initial targets are photocleavable amines with reasonably low oxidation potentials. A series of diphenyl amines bearing parasubstituted benzyl substituents on nitrogen have been prepared and converted by these techniques to the corresponding cation radicals. Kinetics are currently being monitored. The use of pillared clays as a vehicle for supported TiO<sub>2</sub> clusters has continued, with emphasis on layered double hydroxides and pillared montmorillonites. X-ray diffraction evidence for inclusion of spatially controlled TiO<sub>2</sub> pillars is in hand.

# 28319 TRANSITIONS IN LIQUID CRYSTALS INITIATED WITH CIRCULARLY POLARIZED LIGHT

Gary B. Schuster University of Illinois

SL: MTL

SC: AROE, CRDEC, NRDEC

#### **II Chemistry**

The objective of this research is to accomplish the photoresolution of racemic molecules which are either themselves liquid crystalline, or are immersed in a liquid crystalline medium. Racemic compounds with inherently disymmetric biphenyl-like chromophores, and likely to organize into liquid crystalline states, will be prepared. They will be subjected to circularly polarized light and evidence of photoresolution will be sought.

# 28767 COLLISIONAL AND DISSOCIATIVE PROCESSES INVOLVING OPEN-SHELL MOLECULAR FREE RADICALS

Paul J. Dagdigian Millard H. Alexander The Johns Hopkins University SL: ARDEC

SC: AROE, CRDEC

The research objective is to understand ignition and combustion processes of energetic materials by developing theoretical models for reactive collisions between key radicals thought to be involved in nitramine combustion and carrying out complementary experiments to measure cross sections, energy transfer.

# 29310 DECOMPOSITION PATHWAYS AND MECHANISMS IN THE GAS PHASE AND AT SURFACES

Curt Wittig Hanna Reisler Robert Beaudet University of Southern California

The objective of the research is to understand fundamental processes in energetic materials combustion, perform experiments in molecular excitation by collision of beams with surfaces, interrogate reaction species with laser spectroscopy, prepare clusters, and study photodecomposition processes.

#### **D.** Kinetics and Thermodynamics

# 25523 MECHANISMS OF DECOMPOSITION AND OXIDATION OF BORANE COMPOUNDS

Simon H. Bauer Cornell University

SC: ARDEC, AROE, BRL, MICOM

When B<sub>5</sub>H<sub>9</sub> is injected into a stream of He that is carrying  $O(^{3}P)$  atoms [approximately 100/1], at a total pressure 5-15 Torr, a blue-green flame develops. The major chemiluminescent species is  $BO(A^2II)$ . While its translational and rotational temperatures are  $\approx 350$  K, the vibrational temperature in the A state is high,  $\approx 3800$  K. From among the many products of this reaction, the OH radical can be most easily quantitated by measuring the intensity of its laser induced fluorescence. The central streamline from a flow-tube reactor was extracted into an evacuated plenum via a pinhole. The time-intensity profile was calibrated using C<sub>2</sub>H<sub>6</sub> for the fuel. Check runs were made with  $B_2H_6$ . A multistep mechanism was developed for  $B_5H_9 + O(^{3}P)$  that simulates the shape as well as the magnitude of the OH concentration over a reactor residence time: 0.5-10 ms. Less than a dozen crucial reactions were identified by means of an extended sensitivity analysis. Breakdown schemes for the oxidation of  $B_{2}H_{6}$  and  $B_{5}H_{9}$ have been developed. A heated inlet unit was designed and constructed for the flow tube reactor to inject low vapor pressure boranes (in particular  $B_{10}H_{14}$ ). A new flow tube reactor was designed and constructed. It provides for injection of any reagent directly into the cool flame, at controlled positions. Considerable progress was made in developing the OPMS diagnostic for study of reaction products generated in a flow-tube reactor. Extended test runs, using  $C_{2}H_{6}$  as a fuel, gave measures of stability and reproducibility, based on pen recordings of amplified mass-selected intensity signals, over the mass range 1-50. The small changes in fragmentation patterns of the original species due to the introduction of small levels of  $O(^{3}P)$  proved difficult to quantitate with pen recording of the ion intensities.

#### Reports:

 O<sup>3</sup>P Attack on Boranes II: B<sub>8</sub>H<sub>9</sub>, by H-Z. Cheng and S.H. Bauer, MS.

# 26049 THE DYNAMICS OF MOLECULAR DECOMPOSITION

E Fleming Crim

University of Wisconsin-Madison

#### SC: AROE

A study of nitromethane has been completed. The primary experimental advance has been the development of a heated pulsed molecular beam valve that allows one to study lower vapor pressure compounds than possible previously. This valve was tested by making the first measurements on nitrobenzene, an interesting molecule that could not be studied earlier because of its low vapor pressure. Preliminary measurements show that there are several previously unobserved fragmentation channels, including perhaps one involving an initial isomerization, whose importance changes with excitation wavelength. The most significant development in acquiring and analyzing new data has been with nitroethane (C<sub>2</sub>H<sub>5</sub>NO<sub>2</sub>) photolysis. Several dissociation channels were found, primarily simple C-N bond rupture and NO elimination, which apparently proceed through initial isomerization to the nitrite. The most interesting result, however, is the observation of fragments that indicate the elimination of HONO through a cyclic intermediate. The first measurements using nitropropane clearly produce propene, the predicted product of the HONO elimination in this molecule.

# 26106 CHEMICAL DYNAMICS STUDIES OF UNIMOLECULAR REACTIONS IN ENERGETIC MATERIALS

Donald L. Thompson

Oklahoma State University

SL: A	RDEC.	BRL
-------	-------	-----

SC: AMCCOM, AROE, BRADEC, MICOM

The collisional excitation and relaxation of *para*difluorobenzene (*p*-DFB) molecule by light atoms have been studied by a wave-packet scattering method. In the P.1.'s model, the light atom is represented by a two-dimensional wave-packet and the vibrations of *p*-DFB molecule are treated classically. Evidence was found that excitation of the v<sub>30</sub> mode, which is the mode with lowest vibrational frequency and involves an out-of plane motion of the fluorine atoms, is more easily excited or relaxed in the collisions. This is in agreement with the experimental and other theoretical results. This study shows that this combined trajectory/wave packet approach can be used to treat intermolecular energy transfer in collisions of atoms with polyatomic molecules.

#### Reports:

No. 1-8 in previous editions.

- 9. Theoretical Studies of Mode Specificity in Polyatomic Molecules, by Huadong Gai, PhD Thesis, 1984, 121 pp.
- Molecular Dynamics Simulation of Conformational Changes in Gas-Phase RDX, by Eric P. Wallis and Donald L. Thompson, MS, J Phys Chem.
- Mode Specificity in Intramolecular Conversions, by Donald L. Thompson, MS.
- Comparisons of Statistical and Nonstatistical Behavior for Bond-Fission Reactions in 1.2-Diffuoroethane, Disilane, and the 2-Chloroethyl Radical, by Thomas D. Sewell et al., MS, J Chem Phys.

## 26256 KINETICS AND DYNAMICS OF REACTING SYSTEMS

Sidney Redner Boston University

SC: AROE, CRDEC, MTL, NRDEC

The primary advance has been the elucidation of the spatial organization in two-species annihilation. A new length scale has been found which characterizes the width of the "gap" between unlike pairs. In terms of this length, the behavior of the distribution function was quantified for nearest-neighbor distances of same-species particles. In catalysis kinetics, various aspects of the statistical properties of the clusters that form on the surface were determined as a function of time. The "coarsening" of the clusters resembles spinodal decomposition, except that the total number of clusters exhibits nonmonotonic behavior. Finally, extreme value statistics were applied to calculate the distribution for the distance between the closest particle in a system of Brownian particles and an absorbing trap.

#### Reports:

No. 1-8 in previous editions.

- 9. Nearest-Neighbor Distances of Diffusing Particles From a Single Trap, by S. Redner and D. ben-Avraham, MS.
- A Nonequilibrium Tricritical Point in the Monomer Dimer Catalysis Model, by D. Considine et al., MS.
- 11. Spatial Organization in Two-Species Annihilation, by E Leyvraz and S. Redner, MS, *Phys Rev Let*.
- 12. Statistical Properties of Aggregation with Injection, by Hideki Takayasu et al., MS, J Stat Phys.
- Kinetics in Models of Heterogeneous Catalysis, by David Considine, PhD Thesis, 1991, 123 pp.

## 27025 ULTRAFAST RESPONSE OF ENERGETIC SOLIDS TO LIGHT, HEAT AND SHOCK PULSES

Dana D. Dłott University of Illinois

A molecular dynamics simulation of crystalline naphthalene was used to study nanometer scale thermal transport in solids. One molecule in a cluster of 75 is heated to a large initial temperature and then allowed to cool. Stochastic boundary conditions which preserve the time averaged volume of the cluster are used. The excess translational and librational energy of the hot molecule is lost within one ps. The excess vibrational energy is lost on the 100 ps time scale. Translational and librational energy propagates rapidly throughout the cluster at velocities which are

#### **II Chemistry**

comparable to the speed of sound. Despite the far slower rate of vibrational energy loss from the hot molecule, the growth of vibrational energy occurs uniformly on the other molecules in the cluster. Therefore intermolecular vibrational energy transfer occurs primarily via an indirect mechanism. Vibrational excitations are first converted into translational and librational excitations, which propagate throughout the cluster and then excite vibrations on distant molecules via multiphonon up pumping. Examination of the molecular neighbors shows that intermolecular transfer of mechanical energy can be anisotropic, since the hot molecule can only transfer energy where it contacts atoms on adjacent molecules. Energy transfer along the band c-crystallographic axes is more efficient than along the a-axis. The most efficient energy transfer is in the direction of two of the four nearest neighbors. Transient hot spots are produced on these neighboring molecules. A new time-resolved coherent Raman technique (three-color ps CARS) which uses a backscattering geometry and three colors obtained from three different lasers was demonstrated. The advantage of this technique over conventional two-color ps CARS is that it is insensitive to sample morphology. It is used to study time-dependent vibrational dephasing from opaque, polycrystalline solids at low temperature. A quantitative treatment of the limiting apparatus timeresponse where each pulse has a different duration, and where there is arrival-time jitter between the pulses is derived. New measurements of vibrational dynamics in low temperature carbon disulfide indicate that polycrystalline samples are more homogeneous, on a microscopic level, than the large single crystals used in previous work. Raman line broadening in a sample of naphthalene in which strain is induced intentionally by grinding and compression was also investigated.

#### Reports:

No. 1 in previous edition.

- 2. Low Temperature Vibrational Relaxation of High Explosives, by Sheah Chen et al., MS, J Chem Phys.
- 3. Time-Resolved Three-Color Coherent Raman Scattering Applied to Polycrystalline and Opaque Solids, by Xiaoning Wen et al., J Opt Soc Am 8,813(1991). AD A238 349
- Theory of Ultrahot Molecular Solids: Vibrational Cooling and Shock-Induced Multiphonon Up Pumping in Crystalline Naphthalene, by Hackjin Kim and Dana D. Dlott, J Chem Phys 93,1695(1990). AD A228 633

## 27505 THE REMOVAL OF HETEROATOMS FROM ORGANIC COMPOUNDS BY SUPERCRITICAL WATER

Thomas Houser Western Michigan University

SC: AROE, ATHAMA, CRDEC

Since the chlorohexane (CH)-supercritical water (SW) reaction products were being distorted by stainless steel reactor walls, attempts to reduce the wall reaction were made by plating the reactor first with gold, second with copper and third with chromium; each coating had an underlayer of nickel. The integrity of each coating was not maintained at reaction conditions resulting in flaking or peeling and subsequent wall reactions. The study of the CH-SW reaction has been postponed until a reactor can be made from Inconel 600 which has been obtained. A few new experiments were run with p-nitrotoluene in SW at 400°C. The volatile products were the same as last time and the char/tar (non volatile products) amounted to about 30 percent of the reacted material. However, the material balances for these experiments have not been satisfactory and work is continuing to improve this and to determine conditions at which the char/tar yields would be reduced. Some initial experiments were run to examine the reactions of ethyl benzilate (EB) and trihexyl amine with SW at 400°C with one EB run at 540°C. The EB was essentially completely reacted at the mildest condition, 0.5 hr and 400°C. At both temperatures the most abundant product was diphenylmethane followed by lesser amounts of benzophenone, diphenyl carbinol, benzene, toluene, ethylbenzene, phenol and products with molecular weights above 260.

#### Reports:

 Reactions of Organic Compounds with Supercritical Water Involving Chemical Oxidation, by T.J. Houser and C.C. Tsao, MS.

## 27603 THIN FILM LASER PYROLYSIS OF NITRAMINE PROPELLANTS

Charles A Wight University of Utab

SL: ARDEC, BRL SC: AFAL, AROE

A line-tunable pulsed  $CO_2$  laser has been installed and is used for pyrolysis of thin film nitramine propellant samples. A few experiments have been conducted with the laser at reduced pulse energy. Samples of semicrystalline RDX have formed by vapor deposition onto a room temperature substrate under vacuum conditions. These samples were cooled to 77 K and were subjected to low-fluence photolysis with the CO<sub>2</sub> laser with no apparent effect, as observed visually and by FTIR spectroscopy. Higher fluence pulses were obtained by focusing the beam with a concave mirror, though this technique necessarily involves a smaller working area of the sample. This approach does produce measurable changes in both the optical properties and the FTIR spectra of the films. Preliminary analysis indicates that most of these changes are associated with an increase in the degree of crystallinity of the propellant. That is, rapid heating by the laser induces a disorder  $\rightarrow$  order transition in the film. The next step will be to explore this effect at different CO<sub>2</sub> laser wavelengths to see if such changes can be facilitated or perhaps even reversed, and whether tuning the laser to specific absorption bands in the 10 micron region can induce decomposition of the material.

# 27887 INSENSITIVE ENERGETIC MATERIALS: THE IMPORTANCE OF PHYSICAL PROPERTIES AND MOLECULAR STRUCTURE

**Richard Behrens** 

Sandia National Laboratories

SL: ARDEC SC: AROE, CRDEC

The products formed in the thermal decomposition of HMX have been traced using mixtures of different isotopically labeled analogues of HMX. The isotopic analogues of HMX used in the experiments include:  $^{2}$ H,  $^{13}$ C,  $^{15}$ NO<sub>2</sub>,  $^{15}$ N<sub>ring</sub>, and  $^{18}$ O. The fraction of isotopic scrambling and the extent of the deuterium kinetic isotope effect (DKIE) are reported for the different thermal decomposition products. Isotopic scrambling is not observed for the N-N bond in N<sub>2</sub>O and the C-H bonds in CH<sub>2</sub>O. Only one of the C-N bonds in N-methyl-formamide undergoes isotopic scrambling. The lack of complete isotopic scrambling of the N-NO bond in 1-nitroso-3,5,7-trinitro-1.3.5.7-tetrazocine is shown to imply that some HMX decomposition occurs in the lattice. The behavior of the DKIE in different mixtures of isotopic analogues of HMX suggests that water probably acts as a catalyst in the decomposition. The results demonstrate that decomposition of HMX in the condensed phase has several reaction branches.

Reports.

<sup>1.</sup> Thermal Decomposition of Energetic Materials: Temporal Behaviors of the Rates of Formation of the Gaseous Pyrolysis Products from Condensed-Phase Decomposition of Octahydro-

1,3,5,7-Tetranitro-1,2,5,7-Tetrazocine, by Richard Behrens, Jr., J Phys Chem 94,6706(1990). AD A231 091

# 28103 CONDENSED AND GAS PHASE DIAGNOSTICS OF NITRAMINE PROPELLANT COMBUSTION

Charles E. Kolb Aerodyne Research, Inc.

SL: BRL

SC: AROE, CRDEC

Plans have been made to break the experiment into components and test them individually before attempting the first full experiments. One question that needs to be answered before the study of burning propellants is what rapid heating does to fiber transmission. As a test source of heat, plans have been made to use a  $CO_2$  laser. The test apparatus has now been assembled.

# 28371 DESTRUCTION OF HAZARDOUS CHEMICALS BY OXIDATION IN SUPERCRITICAL WATER: A THEORETICAL AND COMPUTATIONAL TREATMENT

Jefferson W. Tester

Massachusetts Institute of Technology

SL: AFESC	SC: AROE, ATHAMA CRDEC,
	NRDEC

Oxidation in supercritical water has been shown to be an efficient way of treating aqueous organic wastes. In addition to the near complete destruction of the organic matter, the process also provides a means for the separation of salts from the aqueous waste stream. Salts are contained in some industrial aqueous wastes, and are also formed during the oxidation and subsequent neutralization of certain organic waste compounds, such as methylene chloride. Due to their low solubility in supercritical water, most salts rapidly precipitate from the waste stream. Knowledge of nucleation and crystal growth rates of salts in supercritical water is essential for efficient salt separator design in the SCWO waste treatment process. An experimental and theoretical program is currently underway to obtain a fundamental understanding of these phenomena. Experimental techniques have been developed and tested for examining phase behavior and precipitation in saltwater systems near and above the critical point of pure water (374°C and 221 bar). An optically accessible cell has been designed and constructed for supercritical water studies up to 600°C and 400 bar. Methods for observing phase transformations and locating phase boundaries under isobaric conditions have been tested on the NaCl-H<sub>2</sub>O system at a pressure of 250 bar. A flow system has been incorporated into the cell for studying the rapid precipitation of salts from supercritical water, and initial experiments on this phenomenon have been conducted.

# 28555 A MOLECULAR DYNAMICS SIMULATOR FOR OPTIMAL CONTROL OF MOLECULAR MOTION

Herschel Rabitz

Princeton University

SC: AROE

Nonlinear mechanical force fields: Following the original work on harmonic bonds, it was possible to design a series of variable pitch, backwound, mechanical springs capable of simulating the repulsive part and a portion of the long range attractive region of intramolecular bonds. The optimal control formulation was applied to this nonlinear regime and laboratory demonstrations were performed. It was found that the inclusion of nonlinear effects in the design process is essential for obtaining successful results. The one limitation of these mechanical type springs was their inability to handle the truly long range portion of potentials and hence dissociation. Research with magnetic bonds will alleviate this difficulty. Magnetic simulation of intramolecular bonds: By the the use of carefully designed permanent ceramic magnets, it was possible to theoretically establish that simulated atoms carrying these magnets would very accurately describe the structure of true interatomic potentials including the repulsive, long range attractive and dissociative properties. Using a one dimensional air track, these magnetic potential field capabilities were verified. Currently, the optimal design machinery is being applied to simulate full dissociative motion. Applications will be considered for linear and planer polyatomic molecules.

# 28565 EXCITED ELECTRONIC STATES OF ENERGETIC MATERIALS STRUCTURE, DYNAMICS, REACTIVITY

Elliot R. Bernstein Colorado State University SL: ARDEC

SC: AROE, BRL, MICOM

The research objective is to explore excited states of nitramines and their clusters to provide information of ignition and decomposition of energetic materials. Two photon absorption will be used to generate highly excited vibronic states. Resulting species will be detected using resonantly enhanced multiphoton ionization.

# 28700 STATE RESOLVED DIFFERENTIAL CROSS SECTIONS FOR REACTIONS IMPORTANT TO THE DECOMPOSITION OF ENERGETIC M \TERIALS

Paul L. Houston Cornell University

SL: ARDEC, BRL SC: AROE, CRDEC

The research objective is to characterize the reactions of hydrogen atoms with species important in energetic material reactions. A new spectroscopy developed by the P.I. will be exploited: a crossed beam reaction occurs, the products are ionized and recoil along the trajectory caused by the reaction, the spatial distribution of ions is projected onto a two dimensional detector screen using a pulsed electric field. This technique permits a determination of the three dimensional velocity distribution of state selected reaction products.

# E. Polymer Chemistry

## 25104 OXYGEN PERMSELECTIVE METAL-MACROCYCLE CONTAINING PLASMA POLYMER MEMBRANES

Alvin L. Crumbliss Nicholas Morosoff Duke University

SL: CRDEC SC: AROE, CRDEC

The overall goal has been to prepare and characterize oxygen permselective membranes using new plasma polymer thin films containing metal chelates. The membrane design is such that permselectivity is expected to occur due to facilitated transport of  $O_2$ through the membrane as a result of each metal site's ability to selectively and reversibly coordinate  $O_2$ . Due to the important role of facilitated transport in these membranes, some of the efforts were directed towards evaluating the ability of the plasma polymer thin films to reversibly bind  $O_2$ . Other experiments are designed to measure permeabilities and  $O_2/N_2$  separation ratios for the plasma polymer thin films deposited on Silastic<sup>R</sup> and aluminum oxide membranes. Work has continued with CoTPP and CoSalen containing plasma polymer films. Experiments were designed to prepare plasma polymer thin films containing the "picket fence" porphyrin, CoTpivPP, and the use of electrochemical measurements to detect O<sub>2</sub> interactions with CoTPP in the plasma polymer film. A summary of accomplishments is as follows: (a) CoTPP/trans-2-butene plasma polymer films have been deposited onto Silastic<sup>R</sup> substrates for permeability measurements. Permeabilities between 10<sup>-1</sup> and 10<sup>2</sup> barriers have been achieved for the plasma polymer layer. (b) CoTPP/trans-2-butene plasma polymer films on Silastic<sup>R</sup> have modest separation values ( $O_2N_2 = 2.6$  at 46 torr). Upon exposure to 1-MeIm vapor separation factors have increased to as high as 9.6 at 164 torr. (c) CoSalen/cyclooctene plasma polymer films (700 Å; thick) deposited on Silastic exhibited a very high separation factor  $(O_2N_2 = 28.4 \text{ at } 8.5 \text{ torr}).$ 

Reports:

 Preparation of Plasma Polymers Containing Ligated Transition Metals, by N.C. Moroscoff et al., MS, *Polymeric Mater Sci and Eng.*

# 25229 POLYMER-POLYMER INTERFACES IN BLENDS AND COMPOSITES

Donald R. Paul University of Texas at Austin

SL: MTL SC: AROE, CRDEC, MTL

The toughening of nylon 6 using triblock copolymers of the type SEBS and a maleic anhydride functionalized version SEBS/g-MA was examined and compared with a conventional maleated ethylene/propylene elastomer. The changes in rheology, adhesion, crystallinity, morphology, and mechanical behavior associated with the reaction of the anhydride with the nylon 6 were documented. The toughening of nylon 6,6 using triblock copolymers of the type SEBS and a maleic anhydride functionalized version SEBS-g-MA was examined and compared with the behavior reported for nylon 6. Nylon 6,6 can be made super-tough by blending with SEBS-g-MA, and addition of SEBs merely reduced toughness.

#### Reports:

No. 1-20 in previous editions.

- Toughening of SAN Copolymers by an SAN Emulsion Grafted Rubber, by Hyungsu Kim et al., *Polymer* 31,869(1990). AD A224-213
- 22. Terminal Anhydride Functionalization of Polystyrene, by Inha

Park et al., J. Polym Sci. Polym Chem. 29,1329(1991). AD A239-897

- 23. Effect of Acrylonitrile Content on the Toughness of ABS Materials, by Hyungsu Kim et al., *Polymer* 32,1447(1991).
- 24. The Role of Inherent Ductility in Rubber Toughening of Brittle Polymers, by Hyungsu Kim et al., MS, Polymer.
- 25. Prediction of Polymer-Polymer Miscibility with a Group Contribution Method, by J.W. Barlow et al., Contemporary Topics in Polymer Science, Vol 6, Multiphase Macromol Systs, AD A224 210
- 26. Rubber Toughening of Polyamides with Functionalized Block Copolymers: Part I: Nylon 6. by A.J. Oshinski et al., MS, *Polymer*.
- 27. Rubber Toughening of Polyamides with Functionalized Block Copolymers: Part II: Nylon 6.6, by A.J. Oshinski et al., MS. *Polymer*.
- Gas Transport Properties of Liquid Crystalline Poly(Ethylene Terephthalate-Co-P-Oxybenzoate), by D.H. Weinkauf and D.R. Paul, J Polym Sci Polym Phys 29,329(1991). AD A234-147
- Strategies for Compatibilization of Polymer Blends, by D.R. Paul, Mechanical Behaviour of Materials-VI, Vol 3, Pergamon Press, 1991. AD A239 898
- Phase Homogenization of Mixtures of Poly(M-Xylene Adipamide) and Nylon 6 by Interchange Reactions, by Y. Takeda and D.R. Paul, MS, *Polymer*.
- 31. Adhesion of Styrenic Triblock Copolymers to Miscible Blends of Polystyrene and a Phenylene Ether Copolymer, by Inha Park et al., *Polymer* 31,2311(1990). AD A234 146

### 25286 SYNTHESIS AND CHARACTERIZATION OF NEW POLYPHOSPHAZENES

Patty Wisian-Neilson Robert H. Neilson Southern Methodist University

SE: BRADEC, NRDEC SC: AROE, CRDEC, NRDEC

Polyphosphazenes with simple alkyl and aryl substituents directly attached to the backbone by P–C linkages can be prepared by the condensation polymerization of N-silylphosphoramine precursors. These simple polymers can then be converted to a variety of functionalized polyphosphazenes by derivatization reactions. In a paper, the synthesis and characterization of some derivatives of poly(methylphenylphosphazen). [Me(Ph)P=N]<sub>n</sub>, and the copolymer, [Me(Ph)P=N]<sub>n</sub>, are discussed. These polymers include grafted copolymers, water soluble carboxylated polymers, and polymers with silyl, vinyl, alcohol, ester, ferrocene, phosphine, thiophene, and/or fluoroalkyl groups.

#### 26072 DETECTION AND/OR DOSIMETRY IN POLYMERIC MATERIALS

Harry L. Frisch Walter Gibson State University of New York at Albany

SE: DARPA SC: CRDEC, MTL, NRDEC

#### **II Chemistry**

Research has proceeded along two fronts. First, researchers have examined the sorption of tri-nbutylphosphate (TBP) by commercial polystyrene films utilizing P-31 nmr spectroscopy. Under static (nonspinning) conditions, evidence is found for two TBP species having different molecular mobilities. The observed signal consists of a superposition of sharp (species with relatively high mobility) and very broad (low mobility) resonances. The magicangle spinning results lend themselves to a similar interpretation; while both mobile and immobile species contribute to the isotropic peak intensity, only immobile species with larger chemical shift anisotropies give rise to the spinning sideband intensity. A typical spinning sideband array is depicted for tri-i-noctylphosphine oxide. In summary, the above results are consistent with a dual-mode sorption of the TBP by the PS. More specifically, some of the penetrant molecules are in regions of the film where the backbone micro-brownian motion is completely frozen out. Qualitative simulation of the powder patterns with one broad and one narrow component indicates that the broad signal can not be modeled as arising from only one type of "immobile" species. Rather, this suggests that the broad resonance likely arises from molecules whose relative lack of mobility spans a comparatively large range.

#### Reports:

No. 1-4 in previous editions.

- Evidence for Steric *Trans* Influences and Effects in Perfluoroisopropyl Cobaloximes. Molecular Structure of *trans-Bis* (Dimethylglyoximato) (Triphenylphosphine ( (F-Isopropyl) Cobalt (III), by Paul J. Toscano et al., MS, *Organometal*.
- Synthesis, Characterization, and Stereochemical Preferences of Cobalt(III) Ternary Amino Acid Complexes Containing N-((2-Pyridy1)methy1)-2-2((2-Aminoethy1)Thio)Acetamide, a Stereospecific Linear NSNN Tetradentate Ligand, by Paul J. Toscano et al., *Polyhedron* 10,977(1991).
- Novel Square Pyramidal Copper(II) Complexes of the Stereospecific Linear NSNN Tetradentate Ligand, N-[(2-Pyridyl) Methyl]-2-[Aminoethyl)Thio]Acetamide (pygeH). The Crystal Structures of [Cu)pyge)X], (X = Br, N<sub>3</sub>), by Paul J. Toscano et al., *Polyhedron* 9,2375(1990). AD A233 882
- The Enantioselective Fluoroacetamide Acetal Claisen Rearrangements of N-Fluoroacetyl (2R,5R)-2,5-Dimethylpyrrolidine, by John T. Welch et al., MS.
- Dual-Mode Sorption of Tri-n-butyl Phosphate in Polystyrene Studied via High-Resolution Solid-State <sup>31</sup>P NMR Spectroscopy, by Paul J. Toscano and Harry L. Frisch, J Polym Sci Polym Chem A29,1219(1991).
- The Stereoselective Construction of (Z)-3-Aryl-2-Fluoroalkenoates, by John T. Welch and Randal W. Herbert, J Org Chem 55,4782(1990), AD A228 223
- 11 Regioselective Aza-Cope Rearrangement of α-Halogenated and Nonhalogenated Imines, by John T. Welch et al., J Org Chem 55,4981(1990) AD A228-518

- 12. Inverse Solution for Some Travelling-Wave Reaction-Diffusion Problems, by C. Borzi et al., MS, J Phys.
- 13. Sorption of Small Molecules in Polymeric Media Studied via High-Resolution Solid-State NMR Spectroscopy, by Paul J. Toscano and Harry L. Frisch, MS.
- 14. Diffusion from Sessile Droplets Through Membranes, by G.O. Williams and H.L. T.tsch, MS.
- Diffusion Through Foams and Fractal-Like Cellular Solids, by J.C. Kimball and H.L. Firsch, *Phys Rev* A43,1840(1991). AD A233 895

## 26441 CHAIN PROPAGATION/STEP PROPAGATION POLYMERIZATION CHEMISTRY

Ken B. Wagener University of Florida

SC: ARDEC, AROE, BRADEC, CRDEC, MTL, NRDEC

Microphase separation in a series of triblock poly-(pivalolactone-block-oxyethylene-block-pivalolactone) oligomers, represented by  $(PVL)_m - (OE)_{24} - (PVL)_m$ , where m = 5, 7, 9, 12, 16, and 24, was investigated by differential scanning calorimetry. With the poly (pivalolactone) hard-segment length maintained at 24 repeat units, a very distinct transition from phase mixed to essentially complete microphase separation occurs when m is increased from 9 to 12. Complete microphase separation occurs for m = 16. Defect-free poly(oxyethylene-block-pivalolactone) telechelomers, represent by  $(OE)_{34}$ - $(PVL)_m$ , where m = 5, 12, and 16, were synthesized by sequential anionic ringopening polymerization of ethylene oxide and pivalolactone with hydroxypivalic acid. These telechelomers exhibited excellent microphase separation, allowing both the hard and soft segments to crystallize. Essentially complete microphase separation occurs for m = 12and 16, and the sample with m=5 showed some microphase mixing in the hard phase. Step polymerization of the  $(OE)_{34}$ - $(PVL)_m$  telechelomers was achieved by alanine-mediated melt esterification with a titanium tetrabutoxide added in catalytic amounts, producing low molecular weight segmented copolymers, represented by  $[(OE)_{34}-(PVL)_m]_p$ .

Reports:

No. 1-2 in previous editions.

- Chain Propagation/Step Propagation Polymerization. Synthesis of Defect-Free Telechelomers, by K.B. Wagener and J.C. Matayabas, Jr., MS.
- 4 Quantitative Study of Microphase Separation. Pivalolactoneblock-Oxyethylene Oligomers: Effect of Hard-Segment Length, by K.B. Wagener and J.C. Matayabas, Jr., MS, *Polymer Preprints*.

#### 26839 COLLOIDAL CATALYSTS IN WATER

Warren T. Ford

Oklahoma State University

SC: AROE, CRDEC, MTL

Research efforts have indicated that 0.01-0.41 mg/mL of cationic latex particles and  $0.40-5.0 \times 10^{-5}$  MIBA catalyze hydrolysis of p-nitrophenyl diphenyl phosphate at 25°C and pH 8.0 with a pseudo first-order rate constants of up to  $0.064 \text{ s}^{-1}$ , which corresponds with a shortest half-life of 12 seconds. The highest second-order rate constant under these conditions exceeds by a factor of about 2 the maximum value reported by Moss for IBA in CATCI micelles, the previous fastest medium for IBA-catalyzed hydrolysis of phosphate esters. The most active latexes are 150 nm diameter particles swollen 2.4-10 times their dry volume in water. Less swollen latexes form much less active catalysts. The particles have been characterized by ion exchange analysis, dynamic light scattering, and transmission electron microscopy. Research is in progress to analyze the contributions of intrinsic activity inside the particles and of concentration of reactants and catalyst in the particle phase to the high activity. Preliminary estimates are that the major reason for high activity is simply a concentration effect, as in micellar catalysis. These colloidal ion exchange resins could be precipitated to obtain an easily packaged and transported catalyst, and redispersed quickly into water for use in the field. Previous work resulted in a colloidal catalytic method for the epoxidation of styrene to styrene oxide by sodium hypochlorite in water at room temperature catalyzed by meso-tetrakis (2,6-dichloro-3-sulfonatophenyl) porphinatomanganese (III) bound to quaternary ammonium ion exchange latexes. Hydrophilic latexes were active only for styrenes, whereas more lipophilic latexes were active also for aliphatic alkenes. Research now indicates that with the same latex-bound porphyrin catalysts potassium monoperoxysulfate (oxone) is more reactive than NaOCl. Moreover, the activity in the absence of the porphyrin, in the absence of latex, and in the absence of phase transfer catalysts is only slightly less than that of the more complex colloidal systems. At initial pH 6.8 and 25°C oxone selectively epoxidizes cyclooctene, whereas at lower pH it produces mostly cyclooctanediol. Similar results were found with other alkenes. The most important results from this research are that oxone can be used for selective oxidations of alkenes in mixtures of water and organic reactant with no organic solvent, surfactant, PTC, or latex.

#### E. Polymer Chemistry

#### Reports:

No. 1-3 in previous editions.

- Epoxidation of Styrene with Aqueous Hypochlorite Catalyzed by a Manganese(III) Porphyrin Bound to Colloidal Anion Exchange Particles, by Hayrettin Turk and Warren T. Ford, J Org Chem 56, 1253(1991). AD A238-328
- Analysis of Surface Modified Colloidal Silicas, by Rickey D. Badley et al., Chemically Modified Oxide Surfaces, 1990, 295. AD A226 245
- 6. Epoxidation of Cyclooctene with Aqueous Hydrogen Peroxide Catalyzed by Molybdate Bound to Colloidal Polymers, by Sanjay Srinivasan and Warren T. Ford, MS. J Org Chem.
- Rapid Hydrolysis of *p*-Nitrophenyl Diphenyl Phosphate Catalyzed by o-lodosobenzoate in Cationic Latexes, by Warren T. Ford and Hui Yu, *Langmuir* 7,615(1991). AD A238-378
- Hydrolysis of p-Nitrophenyldiphenyl Phosphate Catalyzed by IBA in Cationic Latexes, by Warren T. Ford and Hui Yu, TR.
- Oxidation of Alkenes with Aqueous Potassium Peroxymonosulfate and No Organic Solvent, by Weiming Zhu and Warren T. Ford, MS. J Org Chem.

# 27054 FUNDAMENTAL STUDIES OF POLYPHOSPHAZENE AND POLYSILOXANE POLYELECTROLYTES FOR ELECTROCHEMICAL DEVICES

Duward F. Shriver Mark A. Ratner Northwestern University

SL: ETDL	SC: AROE, ETDL, MTL,	
	NRDEC	

The simple polymer/salt complex polymer electrolytes exhibit unmistakable signs of ion clustering; these include peaks in the infrared spectrum, salt formation at higher temperatures, reduced equivalent conductivity and diffraction peaks from clusters. In the polyelectrolytes, the distribution of charges of one sign along the backbone militates against the formation of actual clusters of ions, and should result in higher conductivity if the mobility can be provided. Conversely, however, the mobile ions can act effectively as crosslinkers, and thereby reduce chain flexibility, ion mobility, free volume and conductivity. In an attempt to understand mechanistically how ionic interactions can change conductivity in polyelectrolytes, simulation efforts have been initiated on both polyelectrolytes and complex polymer electrolytes. A model is being used in which charges are localized on sites and the jump time for charges is determined both by the local ion concentration and by the chain mobility. While these simulations have just begun, it is clear that some important mechanistic understandings will result from this research. For example, by encapsulation of charge in a cryptand

#### **II Chemistry**

ligand, it should be possible to reduce the coulomb trapping and thereby increase conduction. The relative efficiency of such a scheme will drop off with increase in charge density, since then the local effective potential will have more minima and, therefore, lower barriers. Computations testing this and other possible schemes for increasing ionic conduction are now in full swing.

Reports:

- Influence of Macrocyclic Ligands on Ion Transport in Solid Polyelectrolytes, by K. Chen et al., MS, Mat Res Soc Symp Proc.
- Characterization of Polyiodide-Polymer Complexes by Resonance Raman Spectroscopy, by Maria Forsyth et al., Solid State Ionics II. Proc of Materials Research Society Symp, Vol 210, 1991, 215. AD A238 201
- 3. MD Studies of Transport in Polymer-Salt Complexes: A Progress Report, by M. Forsyth et al., Solid State Ionics II, Proc Materials Research Society Symp Vol 210, 1991, 203.
- 4. Influence of Macrocyclic Ligands on Ion Transport in Solid Polyelectrolytes, by K. Chen et al., Solid State Ionics II, Proc Materials Research Society Symp Vol 210, 1991, 211. AD A238 371

# 27440 SYNTHESIS AND POLYMERIZATION OF AZAETHYLENES AND AZA-1,3-DIENES, NEW REACTIVE MONOMERS

Henry K. Hall, Jr. University of Arizona

The most promising monomer in the N-acceptor imine series was the N-cyano-2-phenylazaethylene Ph-CH = N-CN, but only low molecular weight oligomers could be obtained. In recent work, similar monomers have been synthesized with either electron-donating or electron-accepting substituents in the para position. The p-methoxyphenyl and p-cyanophenyl derivatives have been synthesized by the same method as described before, namely reaction of the aromatic aldehyde with bis(trimethylsilyl) carbodiimide, using TiCl<sub>4</sub> as catalyst. The yields still have to be optimized in this synthesis. Work is continuing on the 1-aza-butadienes with a cyano-substituent on the nitrogen position. Direct reaction of methacrolein with the silylated carbodiimide in the presence of 0.5 equivalents of TiCl<sub>4</sub> leads to the desired N-cyano azabutadiene. The monomer has not been isolated yet, but was identified in solution by NMR spectroscopy. This direct synthesis method will now also be applied to the synthesis of N-phenyl-azabutadiene, which was previously synthesized by the reverse Diels-Alder reaction, and to other related monomers. Recently

it was found that trimethylsilyl triflate can be used as the acid catalyst in these imine-forming reactions instead of  $TiCl_4$ . Better yields are obtained in the synthesis of N-cyano-2-phenylazaethylene and the work-up of the reactions is much easier because all the side products are volatile.

Reports:

- Synthesis and Polymerization Studies of New Azaethylene Monomers Carrying Electron-Acceptor Groups on Nitrogen, by Jin-Bong Kim et al., *Macromol* 23,21(1990). AD A228 900
- Synthesis and Reactions of Highly Electrophilic Imines Containing the N-Cyano Group, by Merrikh Ramezanian et al., J Org Chem 55,1768(1990). AD A228 068
- Exploratory Studies on the Polymerization of C = N Monomers, by H.K. Hall, Jr., Polymer Preprints 32,318(1991).

## 27445 PREPARATION AND STUDIES OF URAZOLE-CONTAINING POLYMERS

Mark A. Bausch

Southern Illinois University at Carbondale

SC: AROE, CRDEC.

NRDEC

Equilibrium acidity constants have been determined for several 1,2,4-triazolidine-3,5-dione substituted urazoles, and other related acids, in both dimethyl sulfoxide (DMSO) and aqueous solution. In DMSO, urazole has  $pK_a$  of 13.1. In water, urazole has a  $pK_a$ of 5.8. In general, N-methyl and N-phenyl substituents are found to acidify the urazole moiety, in both DMSO and water. The acidifying effects of these substituents are attenuated by a factor of 3.3 in water. The solvent effects are ascribed to the aqueous stabilization of urazole anions via hydrogen bonding interactions, and the aqueous-promoted relief of one pair-lone pair electronic interactions that manifest themselves upon deprotonation of a hydrazyl proton. Deprotonation of 4-substituted and 1,4-substituted urazoles, 4.4-dimethylpyrazolidine-3,5-dione, and diacetylhydrazine results in shifts in the positions of the carbonyl resonances that range from 5 ppm upfield to 3 ppm downfield. Deprotonation of species containing both imide and hydrazyl protons results in shifts in the carbonyl carbon resonances consistent with hydrazyl proton removal. Comparison of DMSO-phase  $pK_a$ 's for acetamide (25.5), diacetylhydrazine (16.7), 4,4-dimethylpyrazolidine-3, 5-dione (13.5), and urazole (13.1) suggest that the remarkable acidity of the hydrazyl proton in urazole and substituted urazoles is due mainly to its cyclic diacylhydrazide structure.

Reports:

- Dimethyl Sulfoxide Phase N-H Equilibrium Acidities for Urazole and Substituted Urazoles: For Urazole and I-Substituted Urazoles, Which Proton is More Acidic?, by M.J. Bausch et al., MS, J Org Chem.
- Dimethyl Sulfoxide Phase Anodic Oxidation of the Monoanion Derived from 4-Phenylurazole: Implications of the Acidic Nature of the 4-Phenylurazolyl Radical, by M.J. Bausch et al., MS, J Org Chem.
- 3. Dimethyl Sulfoxide Phase Urazole, Hydantoin, and Succinimide N-H Homolytic Bond Strengths: In Urazole, Which N-H Bond is Stronger, by M.J. Bausch et al., MS, *J Phys Org Chem.*
- Potentiometric and Spectroscopic Investigations of the Aqueous Phase Acid-Base Chemistry of Urazole and Substituted Urazoles, by Mark Bausch et al., MS, J Phys Org Chem.
- 5. Proton Transfer Chemistry of Urazoles and Related Imides, Amides, and Diacylhydrazides, by M.J. Bausch et al., MS, J Org Chem.

# 27808 COPOLYMERS AND BLENDS WITH ENHANCED POLYMER FILM DIELECTRIC PROPERTIES

John R. Reynolds

University of Texas at Arlington

SL: BRL, ETDL SC: AROE, MTL

The initial synthetic work directed towards producing polymer films with elevated dielectric permittivities has centered on poly(fluoroacrylonitrile). Synthesis of the monomer 2-fluoro-2-propenenitrile, commonly called 2-fluoroacrylonitrile (FAN), has been accomplished. The intermediates, and the final product in the six step synthesis, have been characterized by Fourier Transform-Infrared spectroscopy along with <sup>1</sup>H, <sup>13</sup>C and <sup>19</sup>F nuclear magnetic resonance spectroscopy. The overall yield from commercially available starting materials is about 30 percent. From the intermediates in the synthesis of FAN, several other monomers will be prepared and used to generate other polymers, which are expected to have controllable dielectric properties based on copolymer composition. Two free radical polymerization methods were used to polymerize FAN. The first method involved a redox initiation which did not produce a substantial yield of polymer. The second method has utilized the bulk polymerization of FAN using azobisisobutyronitrile as an initiator and has been quite successful. Blends of the fluorinated copolymer poly(trifluoroethylene-co-vinylidene fluoride) ( $VF_3$ - $VF_2$ ). having a composition of 36/64 mol percent, and poly(methyl methacrylate) were prepared in weight fraction ranging from 0 to 1 of VF<sub>3</sub>-VF<sub>2</sub>. Solutions of these blends in DMF were precipitated into a solution of methanol/ $H_2O$  and films pressed from these precipitates at 180°C were optically clear throughout the entire composition range. Differential scanning calorimetry revealed single glass transition temperatures for the blends that were intermediate to those of the two constituent polymers as expected for a miscible polymer system.

# 28053 SOLUBILIZATION OF HYDROPHOBIC SUBSTANCES INTO BLOCK COPOLYMER MICELLES IN AQUEOUS MEDIA AND THEIR RELEASE

Petr Munk Stephen E. Webber University of Texas at Austin

SC: AROE, CRDEC, MTL

Experimental work was initiated on the use of fluorescence methods to characterize the exchange of aromatic molecules between micelles composed of poly(styrene)-poly(methacrylic acid). It has been found that these techniques work very well and researchers are able to monitor the kinetics of the take-up and release with very high accuracy. It has been found that the rate of equilibration for hydrophobic adsorbates (which almost certainly reside in the polystyrene core) is very slow, requiring almost a week in some cases. The addition of a small amount of good solvent for the polystyrene core to the aqueous solution greatly enhances the rate of these processes. The very efficient system has been developed for carrying out the requisite anionic polymerizations, permitting a wide range of block polymer preparations. This will allow one to determine the effect of block length and overall molecular weight on the properties of these micelles. It has been possible to prepare these block polymers with a short sequence of naphthalene chromophores at the poly(styrene) terminus for A-B systems. These will be used to monitor the rate of adsorbate exchange, similarly to the earlier experiments in which both adsorbates were small molecules. In addition time-dependent depolarization studies have been initiated in which the rate of chromophore rotation can be estimated. It will be interesting to compare small molecule probes with the polymer-bound probes, like the naphthalene system already synthesized.

#### Reports:

 Fluorescence Studies of Amphiphilic Poly(Methacrylic Acid)-Block-Polystyrene-Block-Poly(Methacrylic Acid) Micelles, by T. Cao et al., MS.

## 28153 MACROMOLECULAR CHARACTERIZATION AND SOLUTION BEHAVIOR OF POLYMER ADDITIVES

Benjamin Chu

State University of New York at Stony Brook

SL: MTL SC: AROE, BRADEC, CRDEC

A magnet enhanced falling needle/sphere rheometer equipped with a precision optical monitor and signal feedback system has been developed. The instrument which utilized the basic features of a magnetic sphere/ needle rheometer could be controlled using a PC/AT (286) computer. The important advantages of this instrument over existing falling needle/sphere viscometers are as follows: (a) an extremely large viscosity range from the usual solvent viscosity (say,  $\sim 1.0$  cP) to that of polymer melts (say,  $10^{10}$  cP) is available with an experimental precision of <1 percent; (b) the measurement time could be reduced by about 4 orders of magnitude, e.g., from hours to seconds for a high viscosity fluid; (c) one single needle/sphere could cover a few orders of the viscosity range and two needles with appropriate densities could cover the whole viscosity range (1 cP  $\leq \eta \leq$  $10^{10}$  cP); (d) only a small amount (~4 mL) of sample is needed; (e) the sample chamber can be sealed hermetically and is suitable for toxic fluids; (f) the instrument permits measurements of the shear rate dependence of viscosity using a single needle/sphere; (g) for non-Newtonian fluids, the viscoelastic behavior could be measured. A set of viscosity standards was used to calibrate the device. Linear calibration curves of viscosity against the reciprocal of the falling needle velocity under both natural gravity field and fixed artificial magnetic field were obtained. A flow curve was determined for a random copolymer solution using a single needle but varying the magnetic field, showing the applicability of the device for measuring the rheological properties of polymer solutions and melts.

# 28314 SYNTHESIS, STRUCTURE AND PROPERTIES OF SEGMENTED POLYMERS CONTAINING MESOGENS

William J. MacKnight

University of Massachusetts

SL: MTL, NRDEC SC: AROE, CRDEC

A series of polyurethanes derived from bis-4,4'hydroxyhexyloxybiphenyl and diisocyanates, e.g., toluene diisocyanate, will be synthesized and characterized in detail regarding the kinetics of mesophase

formation and thermodynamic stability. The studies of the segmented polyurethanes will include synthesis, characterization, structural, mechanical and thermal properties, and morphology. A new calorimetric technique will assess the thermodynamics of deformation. Processing conditions tc produce maximum orientation of the mesophase in both films and fibers will be be determined. Appropriate spectroscopic techniques will be used for molecular characterization, deformation response, and nonlinear optical properties.

## 28373 REACTIVE POLYMERS: MAIN-CHAIN COORDINATION POLYMERS FOR AIR SEPARATION

G. Ronald Husk Rey T. Chern North Carolina State University

SC: AROE, NRDEC

Some laboratory work was accomplished. Preparation of cobalt monomer was successful. Initial studies were made in attempting to prepare copolymers from terephthaloyl dichloride, phenophthalein and the cobalt monomer.

## 28631 WELL-DEFINED POLYPHOSPHAZENES BY ANIONIC POLYMERIZATION OF PHOSPORANIMINES

Krzysztof Matyjaszewski Carnegie-Mellon University

SL: MTL, NRDEC SC: ARDEC, AROE, BRADEC, CRDEC

The research objective is to perform detailed mechanistic and kinetic studies of the anionic polymeriza-

#### E. Polymer Chemistry

tion and copolymerization of various phosphoranimines and to prepare new and well-defined phosphazenes. New polyphosphazenes will be synthesized particularly those utilizing anionic catalyzed polymerization of N-silylphosphoranimines with fluoride ion. Synthetic techniques combined with spectroscopic methodology will be combined to determine a detailed kinetic picture of the reaction. Various initiation systems and reaction conditions will be used in order to optimize the polymerization process, improve control of molecular weights and polydispersities.

## 28711 THE SYNTHESIS AND STRUCTURE OF POLYPHOSPHAZENES

H.R. Allcock

The Pennsylvania State University

SL: ARDEC, NRDEC SC: AROE, BRADEC

The objective of the research is the synthesis of new and useful high polymers that contain inorganic elements in the skeleton and organic or organometallic units as side groups. These polymers will be polyphosphazenes, including poly (phospazophospi-azenes), poly (carbophosphazenes), poly (thiophosphazenes) and poly (elementophosphazenes). Synthetic methods will be developed for placing elements other than phosphorus and nitrogen in the backbone of the polymer, vis, C, S, Se, transition metals, etc. In addition, new substituent side chains will be introduced to tailor the properties of the polymers. All polymers will be fully characterized.

Reports:

 The Syntheses and Molecular Structures of Cyclic and Short-Chain Linear Phosphazenes Bearing the o-Dichlorophenoxy and o-Dimethylphenoxy Side Groups, by Harry R. Allcock et al., MS.

# **III BIOLOGICAL SCIENCES**

# A. Combat Ration Research

## 27494 FOOD RELATED STUDIES

Myron Solberg Jozef L. Kokini Rutgers, The State University of New Jersey SL: NRDEC

A porous glass optical humidity probe was designed and fabricated. It will incorporate the new high temperature indicator compound (for measurement  $\geq$  300°C) and a rugged porous cover for protection from contaminants in a commercial environment. Two other optically-based moisture probes use a fluorescent Aluminum-Morin complex on polymer film and an inorganic cobalt-based complex on polymer film. Both of these have potential for the most rapid response of any of the new sensors but are likely to be limited to under 200°C environments. The design of an automated data acquisition and analysis module that can be used with any of the optical moisture sensors is complete. Piezoelectric material tests are continuing to extend moisture sensitivity beyond 200°C. Electronic circuit and mechanical design are underway. For rheological measurement, slit rheometer testing is continuing to examine wall "slip" of the dough materials. An automated control scheme was designed for twin screw extrusion. In numerical simulation the numerical predictions have been found to agree closely with the experimental data on pressure and temperature lending strong support to both the FEM and FDM models. The coupling of the FEM and FDM models has shown that a twin screw extruder can be satisfactorily modeled. With appropriate inputs of rheology, thermal properties, and kinetics, the numerical scheme can be used to predict the temperature, velocity and pressure in single screw extruders and in twin screw extruders. The work is being extended to simulate the ZSK-30 extruder and a variety of food materials.

# 28022 MECHANISMS OF RESISTANCE IN MICROBIAL SPORES

Philipp Gerhardt Robert E. Marquis Michigan State University

A paper has been prepared for publication in which thermograms of exosporum-less model spores showed irreversible endothermic peaks at 56, 99, 110°C, and an irreversible exothermic peak at 115°C. An endothermic peak at 90°C that was identified as DNA in germinated spores and vegetative cells was not shown in dormant spores. Thermograms of heat-activated spores did not show the 56°C peak, and those of coat-divested spores did not show the 110°C peak. Thus, the large endothermic peak at 99°C apparently represented the rate-limiting critical target in heat inactivation of the native dormant spores. In another paper, the effects of mineralization and thermal adaptation on another exosporum-less model spore were analyzed by differential scanning calorimetry. Mineralization by ion exchange of native spores to H, Na, and Ca forms and thermal adaptation by sporulation at different temperatures altered relative sporal heat resistances with a hierarchy of Ca>native>Na>H and 42>35>30>20°C, respectively. Three main endothermic peaks in the thermograms were shown to represent the heat activation process, the inactivation of the spore, and the denaturing of the spore coat. A direct relationship was found between the temperature of the thermal death peak and the resistance; i.e., increased sporal resistance to heat resulted in a shift of the thermal death peak to a higher temperature.

# 28691 GENETICS AND MECHANISM OF CHEMICAL MARKER FORMATION AND WATER-ACTIVATED HEAT GENERATION

Kenneth Kustin Brandeis University SL: NRDEC

#### **III Biological Sciences**

The effort on part of the research project has been to establish a working mechanism for formation of a chemical species, called a chemical "marker" or "monitor", not present in significant amounts in plant food prior to a septic thermal processing, to use this mechanism to model marker accumulation in plant foods, and to compare the kinetics of chemical marker formation with the kinetics of microbial destruction. A mechanism consistent with chromatographic and mass spectrometric analyses of heated samples of plant foodstuffs is the transformation of fructose into 5-(hydroxymethyl)-2-furaldehyde (HMF). The reaction is sequential formation of a series of intermediate precursors of HMF that are formed in the first 10 minutes of processing at temperatures in the range 80-140°C. The individual steps consist of fructose cyclization and water loss leading to the formation of a long lived intermediate of molecular mass 144 dalton. The kinetics of formation of this compound (M-1), is rigorously first-order with the following Arrhenius parameters: activation energy 2.37  $\times$  10<sup>4</sup> cal mol<sup>-1</sup> and pre-exponential factor  $2.11 \times 10^{11}$  min<sup>-1</sup> (the rate constant for M-1 accumulation at 120°C is  $1.7 \times 10^{-2}$ ). Calculations of M-1 formation compared with destruction of Clostridium botulinum indicate that this marker should be useful in determining the thermal history of aseptically processed foods.

# **B. Biodegradation**

## 25493 CONTROL OF BIODEGRADATION IN BACTERIA

L. Nicholas Ornston Yale University

#### SC: CRDEC

Interest has focused upon regulation of genes for the  $\beta$ -ketoadipate pathway in *Acinetobacter calcoaceticus*. Previous work has shown how structural genes for the catechol pathway are governed by repression exerted by catM in *A. calcoaceticus*. This finding is of particular interest because homologous cat structural genes are transcriptionally activated under control of catR in *Pseudomonas putida*. The catM repressor and catR activator respond to the same inducer and prove to be closely homologous in amino acid sequence. Thus relatively recent evolutionary divergence delineated the seemingly opposite physiological functions of repression and activation in the respec-

#### **B.** Biodegradation

tive cat regions of A. calcoaceticus and P. putida. The ben and cat genes are clustered closely together in the A. calcoaceticus chromosome. Both ben and cat genes participate in utilization of benzoate, but the two sets of genes are under separate transcriptional control. The genetic basis for selection of continued clustering of the separately transcribed genes is unknown, but could be explored by engineering recombinants in which the cat genes have been transposed from their normal chromosomal cluster to another. Regulation and stability of the cat genes could be examined after their transposition to a new chromosomal locus. The procedures allow selection of mutant strains in which a functional pobA gene is not expressed. Many mutations inactivating pobA expression lie outside this structural gene and fall within a DNA sequence that is designated pobR. This gene, divergently transcribed from pobA, appears to activate its transcription. A cloned DNA fragment containing both pobA and pobR expresses p-hydroxybenzoate hydroxylase inducibly in Escherichia coli. Thus the presence of the pobR activator and the inducer, p-hydroxybenzoate, seems to be sufficient to elicit pobA expression.

#### Reports:

No. 1-5 in previous editions.

- 6. Past and Future Evolution of Oxygenases, by L. Nicholas Ornston, MS.
- Selection of Acinetobacter calcoaceticus Mutants Deficient in p-Hydroxybenzoate Hydroxylase Gene in pobA, a Member of a Supraoperonic Cluster, by Gail B. Hartnett et al., J Bacteriology 172,6160(1990). AD A233 813
- Recovery of DNA From the Acinetobacter calcoaceticus Chromosome by Gap Repair, by Leslie A. Gregg-Jolly and L. Nicholas Ornston, J Bacteriology 172,6169(1990). AD A234 402
- Evolution of Genes for the β-Ketoadipate Pathway in Acinetobacter calcoaceticus, by L. Nicholas Ornston and Ellen L. Neidle, MS.
- Characterization of Acinetobacter calcoaceticus catM, a Repressor Gene Homologous in Sequence to Transcriptional Activator Genes, by Ellen L. Neidle et al., J Bacteriology 171,5410(1989). AD A225 867
- Subtle Selection and Novel Mutation During Evolutionary Divergence of the β-Ketoadipate Pathway, by L. Nicholas Ornston et al., *Pseudomonas: Biotransformations, Patho*genesis, and Evolving Biotechnology, 1990, 207. AD A226 079
- DNA Sequences of Genes Encoding Acinetobacter calcoaceticus Protocatechnuate 3.4-Dioxygenase: Evidence Indicating Shuffling of Genes and of DNA Sequences Within Genes During Their Evolutionary Divergence, by Christopher Hartnett et al., J Bacteriology 172,956(1990). AD A225 868

## 26576 MOLECULAR BIOLOGY OF ANAEROBIC AROMATIC BIODEGRADATION

Caroline S. Harwood University of Iowa

SL: NRDEC

SC: WRAIR

Work is in progress to characterize a series of Rhodopseudomonas palustris mutants that were previously generated by an indirect transposon mutagenesis procedure. These mutants were grouped into five classes based on growth on 4-hydroxybenzoate, benzoate, and proposed intermediates in the benzoate biodegradation pathway. The mutants were also screened for production of benzoate and 4-hydroxybenzoate-CoA ligase protein. A 3.2 fragment of R. palustris DNA was identified which complements the mutants in classes I-IV. A 3.2 kb DNA fragment would be expected to encode three or four proteins at most, and its small size is difficult to reconcile with the apparent diversity of mutants that it is able to complement. The most straightforward explanation is that mutations in just one or a few genes can give rise to the phenotypes presented in the table. If this is the case, then it is surprising that these are the only classes of mutants that have been isolated, because it would seem that at least six or seven genes would be needed to encode the required enzymes for benzoate and 4-hydroxybenzoate degradation. One explanation might be that many of the steps of benzoate and 4-hydroxybenzoate degradation can be catalyzed by more than one enzyme and that there are only a few R. palustrisgenes which specify a unique enzyme or regulatory protein. Only these unique genes would give a mutant phenotype when disrupted. This would also explain why all the mutants the P.I. has obtained are "leaky" with respect to growth on benzoate and proposed benzoate pathway intermediates. If this explanation is correct then one should be able to obtain double mutants that are totally blocked in growth on benzoate.

Reports:

 Benzoate-CoA Ligase From Rhodopseudomonas palustris, by Jane Gibson et al., Methods in Enzymology 188,154(1990), AD A232 218

## 26750 LIMITING FACTORS. ENHANCEMENT AND KINETICS OF BIODEGRADATION

Martin Alexander Cornell University

SC: CRDEC, CRREL

Studies have continued on the mechanism of bacterial degradation of organic compounds present in a nonaqueous phase liquid. Tests with growing and stationary-phase cells in the presence and absence of heptamethylnonane indicated that biodegradation did not involve the microbial formation of surfactants that solubilized hexadecane. Further studies have been conducted on how microorganisms utilized sorbed organic compounds. Methods have been developed to enrich for such microorganisms. An investigation was also conducted to determine the effect of low concentrations of surfactants on the desorption and biodegradation of sorbed phenanthrene and biphenyl in Lima silt loam and Edwards muck. The sorption of the arematic compounds was almost complete in both soils. The data show that surfactants at low concentrations promote the mineralization of aromatic compounds sorbed to soils without a detectable influence on solubilization.

#### Reports:

No. 1-4 in previous editions.

- Biodegradation of Sorbed Chemicals in Sediments and Model Systems, by Rochelle Araujo, PhD Thesis, 1990, 206 pp.
- 6. Effect of Diffusion on the Kinetics of Biodegradation: Experimental Results with Synthetic Aggregates, by Kate M. Scow and Martin Alexander, MS, Soil Sci Soc Am J.
- Biodegradation by an Arthrobacter Species of Hydrocarbons Partitioned into an Organic Solvent, by Rebecca A. Efroymson and Martin Alexander, Appl and Environ Microbiol 57,1441 (1991). AD A238 829
- 8. Sorption and Microbial Degradation of Organic Compounds in Model Systems, by Rochelle Araujo et al., MS, *Appl and Environ Microbiol*.
- Influence of Calcium, Iron, and pH on Phosphate Availability for Microbial Mineralization of Organic Chemicals, by B.K. Robertson and Martin Alexander, MS, Appl and Environ Microbiol.

## 27314 MICROBIAL DEGRADATION OF POLY-B-ESTERS: A MECHANISTIC STUDY

Richard A. Gross Shan S. Wong University of Lowell SL: NRDEC

#### SC: CRREL, NRL

The initial work thus far has focused on the purification and characterization of different exoenzymes which show high specificity for the depolymerization of bacterial polyesters. This should provide fundamental information into the diversity of polyester degradation mechanisms operative in nature, structural relations between these exoenzymes, and an

#### **III Biological Sciences**

understanding of the enzyme structural features which lead to substrate specificity. To date, an extracellular poly(\(\beta\)-hydroxyalkanoate) depolymerase enzyme has been isolated from the culture medium of Penicillium funiculosum (ATCC 9644). Growth of the micro-organism on  $poly(\beta-hydroxybutyrate)$ as the sole carbon source led to the production of the depolymerase. The enzyme was purified using a hydrophobic Norleucine Sepharose column to homogeneity. Studies on a range of different substrates to establish the specificity of this enzyme are currently in progress. From a comparison of the fungal exoenzyme from P. funiculosum with the two other poly( $\beta$ -hydroxybutyrate) depolymerase enzyme systems of bacterial origin which have thus far been investigated, important differences in both the structure and mechanism of enzymatic catalysis were observed. Further comparative studies which are planned will provide fundamental information into the various mechanisms existing in nature for the degradability of polyesters.

# C. Biotechnology

24435 CHEMICAL FUNCTION OF SUBSTITUTED AMINO ACIDS IN GLYCERALDEHYDE-3-PHOSPHATE DEHYDROGENASE

Ralph M. Hecht University of Houston

SC: CRDEC, WRAIR

The NAD<sup>+</sup> - agarose purified T. aquaticus enzyme from the E. coli host exhibits extreme thermostability. For example, the thermophilic GAPDH from B. stearothermophilus is totally inactivated after 10 minutes while the cloned T. aquaticus GAPDH is stable for 1 to 2 hours at 90°C. Attempts to crystallize the T. aquaticus GAPDH have not yet been successful. A recent publication has indicated that the strain the researchers are using produces an inactive E. coli GAPDH that copurifies with a recombinantly expressed GAPDH from chicken. Perhaps the presence of this truncated form is responsible for their inability to obtain a 100 percent homogeneous preparation with respect to the T. aquaticus GAPDH. A new strain which is lacking the host contaminant has been ordered. Upon receipt of this strain researchers will set another transformation up to obtain a better system for the expression and purification of the GAPDH.

polymerase chain reaction. This method generates site-directed mutants in the initiation signal and tests their function entirely in vitro, thus eliminating the need to generate mutations in living cells, which

# must subsequently be grown, characterized phenotypically, and used as a source of nucleic acids for confirmation of the mutant sequence.

24931 TRANSLATIONAL REGULATION OF

Experiments have continued to optimize translation

initiation signals for expression of heterologous genes

in Saccharomyces cerevisiae. A new and rapid method

has been developed for testing translation initiation

signal function in vitro based on the use of the

**CLONED GENES** 

University of Medicine & Dentistry of New Jersey

Michael J. Leibowitz

SC: CRDEC, NRDEC

#### Reports:

No. 1 in previous edition.

- 2. Coupling of Killer Virus Transcription with Translation in Yeast Cell-Free Extracts, by Francis P. Barbone and Michael J. Leibowitz, MS.
- The Leader Sequence of Tobacco Mosaic Virus as a Translational Enhancer in Yeast, by Chong-Kiong Ho, MS Thesis, 1990, 102 pp.
- In Vitro Translation of Messenger RNA of the Killer Virus of Saccharomyces cerevisiae, by Francis Paul Barbone, PhD Thesis, 1991, 183 pp.
- 5. Virus-Host Interactions in Killer Virus of Yeast, by Lee Ann Weinstein, PhD Thesis, 1991, 155 pp.

## 25126 PLASMID STABILIZATION TO INSURE GENE EXPRESSION

Arnold L. Demain

Massachusetts Institute of Technology

A genomic library of Clostridium thermocellum DNA in a  $\lambda$ gt11 phage vector was constructed. Genes coding for subunits of the sub-cellulosome fraction (which is composed of six main protein subunits, named J1 to J6) were screened by an immunological reaction. Four of the genes (encoding J2, J4, J5 and J6) from the recombinant lambda phages were cloned on vectors pBR325 and pUC8 to form recombinant plasmids which were transformed into E. coli. Two of the four genes, coding for subunits J2 and J5, were found to be identical by Southern blot hybridization and restriction mapping. Each recombinant protein was prepared by ion-exchange column chromatography from heat-treated crude E. coli cell-free extract. Recombinant proteins, J2, J5 and J6 showed CMCase activity; J2 and J5 were also able to hydrolyze PNP cellobioside and xylan. Recombinant protein J4 did not show any enzymatic activities. It has also been possible to clone the gene (or part of the gene) encoding protein  $S_L$ . By using a combination of ion exchange and hydrophobic interaction chromatography, it was possible to isolate endoglucanase  $S_S$ without the use of denaturants. This endoglucanase was identified as the cellulosomal subunit  $S_S$  by the use of specific antibodies.

#### Reports:

No. 1-2 in previous editions.

- Inhibition of Growth of Bacillus subtilis by Recombinant Plasmid pCED3, by Y. Shoham et al., MS, Appl and Environ Microbiol.
- A Sub-cellulosome Preparation with High Cellulase Activity from *Clostridium thermocellum*, by T. Kobayashi et al., *Appl* and Environ Microbiol 56,3040(1990). AD A238 419
- Kinetics of Loss of a Recombinant Plasmid in *Bacillus* subtilis, by Yuval Shoham and Arnold L. Demain, *Biotech* and Bioeng 37,927(1991). AD A238 420
- Effects of the β-Lactamase Gene and Orientation of the Kanamycin-Resistance Gene in Plasmid PCED3 on the Growth of *Bacillus subtilis*, by Y. Shoham and A.L. Demain, MS.
- 7. Purification and Characterization of the Key Endoglucanase (Ss) From *Clostridium thermocellum*, by U. Fauth et al., MS, *Biochem J.*

#### 25731 CONFORMATION OF MEMBRANE PROTEINS: BACTERIORHODOPSIN

Gerald D. Fasman Brandeis University

SC: CRDEC

The growth of the Halobacterium halobium was further improved and the present yield is about 150 mg per 10 liter culture. The purity of the purple membrane (PM) samples were checked by using the following analytical methods: sodium dodecyl sulfate polvacrylamide gel electrophoresis; ultraviolet (UV) and visible (Vis) spectroscopy; circular dichroism spectroscopy. The polyethylene glycol derivative (PEG-BR) of PM reacted with 2-Omethoxypolyethylene glycol-4,6-dichloro-S-triazene. was also examined by the above methodologies: The UV and Vis spectrum are identical to the unreacted PM, thus indicating that the modification did not alter the conformation of the PM. The circular dichroism spectra of the PM and PEG-BR were also identical, giving further evidence that their conformations were identical. Four different reagents, activated PEGs, were investigated to get a maximum yield of the product, PEG-BR. They

#### **III Biological Sciences**

were: 2-O-methoxypolyethylene glycol-4,6-dichloro-S-triazene (1); 2,4-bis-O-methoxypolyethylene glycol-6-chloro-S-triazene (2): 2-O-methoxypolyethylene glycol-succinimidyl succinate (3); and methoxypolyethylene glycol tresvlate (4). The yields of product and side reactions were estimated by a gel scan of the SDS-PAGE gels. The most reactive reagent, giving the highest yield, was (1), which vielded 43 percent of the desired PEG-BR, 31 percent unreacted PM, 26 percent of a dimer. Work is in progress on the isolation of the desired PEG-BR product. The denaturation and renaturation of PM by various solvents was studied. The most effective reagent was found to be tetramethyl urea (TMU). By the use of UV-spectrophotometry, one can observe the change of the absorption peak at 560 nm (native) to 380 nm (unfolded). An interesting intermediate was discovered with absorption maximum at 490 nm. Reaction rates were studied for a mixture of 35 percent TMU, 65 percent H<sub>2</sub>O. Dilution of the denatured PM in 35 percent TMU caused refolding of PM to its native state.

#### 27488 SYNTHETIC HELIZYME ENZYMES

John M. Stewart University of Colorado at Denver SC: NRDEC

Work is progressing well on studies on helizyme. Chymohelizyme 1 (CHZ-1): Detailed kinetics studies with various substrates are being done as well as various physical studies that have demonstrated the remarkable stability of CHZ-1 to various conditions of salt concentration, temperature and pH. Chymohelizyme 1A (CHZ-1A): Initial studies with CHZ-1 suggested that increased stability of the active site might be achieved by increasing the hydrophobicity in that area. Consequently, an analog (CHZ-1A) was synthesized in which the N-terminal acetyl group on the histidine chain was replaced by tert-butylacetyl. The resulting CHZ-1A showed approximately 5 times the catalytic activity of CHZ-1. Following the above results, work is in progress on resynthesizing CHZ-1 by a route that will leave two of the four peptide chains blocked with independently removable blocking groups so that a range of acylating groups may be selectively placed on these chains. This will allow detailed studies of stability and mechanism. Chymohelizyme-2 (CHZ-2): This variant, currently being synthesized, contains: (a) cysteine residues on two chains to

#### **III Biological Sciences**

form disulfide crosslinks for greater stability, (b) a C-terminal modification to allow selective covalent attachment to an insoluble support and (c) an appropriately placed glutamine residue to allow crosslinking between chains by transglutaminase. Helicholinesterase (HCASE): By computer graphics the substrate binding pocket of CHZ-1 was modified to accommodate acetyl choline in the substrate site.

## 27890 TOXIN MEDIATED TRANSFER AND EXPRESSION OF GENES IN NERVE CELLS

Gregory P. Mueller Uniformed Services of the Health Sciences

SC: CRDEC

Much of the effort has focused on the synthesis and chemical characterization of DNA carrier conjugates. The objective of these experiments is to determine optimal coupling reactions for covalent attachment of receptor ligands to polylysine. These conjugates will then serve as vehicles for targeting foreign gene expression in vivo. Optimal conditions for conjugate synthesis and gene transfer will be determined in vitro using cells that readily internalize receptors and express foreign DNA. These conditions will then be applied to the investigation of tetanus toxin C-fragment as a neuron-specific targeting agent. A preliminary experiment was conducted in an effort to quickly demonstrate ligand targeting and expression of foreign DNA in cells of neuronal origin. Using one set of conditions researchers evaluated the ability of a lectin-polylysine conjugate to mediate uptake and expression of RSV- $\beta$ -GAL in PC12 cells. The results of this experiment were negative. This requires a systematic, step-bystep approach to the problem.

## 27956 BACTERIAL SPORE ULTRAVIOLET LIGHT RESISTANCE AND REGULATION OF THE ACTIVITY OF A SPORE PROTEASE

Peter Setlow

Connecticut University Health Center

SL: NRDEC

The major progress has been in studies of  $\alpha/\beta$ -type SASP-DNA binding, including both parameters of this binding and the effects of such binding. Studies of SASP-DNA interaction by both filter-binding and

## C. Biotechnology

topological assays have shown that SASP binds cooperatively to DNA, with saturation achieved at a 3-to-1 mass ratio, similar to what is observed in vivo. This binding takes place to many different plasmid and chromosomal DNAs, does not require a divalent cation is unaffected by ionic strength up to ~0.4, and has at least one slow step  $(t_{1/2} \sim 15-30 \text{ min at})$ 30°) in the binding. Binding of SASP to relaxed closed-circular plasmid DNA, followed by treatment with topoisomerase and then deproteinizing and analysis of topoisomer distribution indicates that SASP binding introduces  $\sim 1$  negative supercoil per 150 nt. This value is similar to that seen upon SASP binding in vivo, and is consistent with the change in DNA from the  $B \rightarrow A$  conformation. Current studies of SASP-DNA interaction are examining the ability of SASP-DNA binding to confer DNAse resistance. Initial studies have indicated that DNAse resistant regions are found at low SASP-DNA ratios, with essentially the entire molecule protected at high ratios. Identification of the DNA regions protected at low SASP-DNA ratios indicate these are GC rich, possibly with moderate dG:dC regions. This makes sense because the latter should be in the A conformation, and these studies are being extended further by examining SASP binding to both single and double stranded synthetic polymers. This work should give good information on the DNA specificity of SASP binding. One of the most gratifying results recently has been the demonstration that SASP binding changes the photochemistry of DNA in vitro from cell type to spore type. This can be achieved in dilute aqueous solution, and indicates that SASP binding alone is sufficient to account for spore DNA photochemistry in vivo, and thus spore UV resistance.

#### Reports:

- Cloning, Nucleotide Sequence, and Regulation of the Bacillus subtilis gpr Gene, Which Codes for the Protease That Initiates Degradation of Small, Acid-Soluble Proteins During Spore Germination, by Michael D. Sussman and Peter Setlow, J Bacteriology 173,291(1991). AD A232 607
- Binding of DNA in Vitro by a Small, Acid-Soluble Spore Protein from *Bacillus subtilis* and the Effect of This Binding on DNA Topology by Wayne L. Nicholson et al., *J Bacteriology* 172,6900(1990). AD A234 245
- Cloning and Nucleotide Sequence of Three Genes Coding for Small, Acid-Soluble Proteins of *Clostridium perfringens* Spores, by Rosa Martha Cabrera-Martinex and Peter Setlow, *FEMS Microbiol Let* 77,127(1991). AD A234-140
- Synthesis of a Bacillus subtilis Small, Acid-Soluble Spore Protein in Escherichia coli Causes Cell DNA to Assume Some Characteristics of Spore DNA, by Barbara Setlow et al., J Bacteriology 173,1642(1991). AD A238-368

## 28011 INVESTIGATION OF PPESSURE REGULATION IN ENZYMES

Alan J. Russell University of Pittsburgh

SC: CRDEC

Chromosomal DNA was isolated from Methanococcus jannaschii cell paste. Using this preparation, a genomic library has been constructed. The chromosomal DNA was ligated into pUC19 and transformed into E. coli (DH5). The library is being screened for the F420 unreactive hydrogenase, glyceraldehyde-3phosphate dehydrogenase, alcohol dehydrogenase, and a protease. In order to search for the hydrogenase, the two hydrogenases have been purified from Methanococcus jannaschii. The protein had never been purified to better than 25 percent purity as *n* easured by silver-staining and gel electrophoresis It has been possible to obtain a concentrated sample of the F420 unreactive hydrogenase with about 80 percent electrophoretic purity. This sample is being used to obtain an N-terminus sequence which will then be used to design a degenerative oligonucleotide probe with which the library can be screened. The first attempt at peptide sequencing showed that the N-terminus was blocked.

## 28043 BIOCATALYTIC PROCESSING OF POLYMERS IN SUPERCRITICAL FLUIDS

Alan J. Russell Eric J. Beckman University of Pittsburgh

SL: CRDEC, NRDEC SC: AROE, CRDEC

The experimental system was designed and constructed. An additional cell is currently in production. This cell will enable basic studies on the phase behavior of acrylates to be performed. The solubility and basic phase behavior of methyl-, ethyl-, and propylmethacrylate in supercritical carbon dioxide has been investigated. There is no elevation in the critical temperature for 3 percent acrylate solutions, and thus the reactor can be run at high concentrations of acrylate. This will enable a determination of the Km for enzymatic reactions in supercritical fluids. Quantitative analysis of acrylates from supercritical fluid mixtures was performed in a gas chromatograph. The sampling technique is experimentally difficult but it was possible to optimize the system such that standard curves could be made for MMA, a A, and PMA. Finally, it has been demonstrated that subtilisin is remarkably active in supercritical carbon dioxide: there is an accumulation of 5  $\mu$ M of PMA in a

reaction between EMA and propanol after only one hour. The enzyme appears to be stable over a 10-hour period.

# 28090 STRUCTURE-FUNCTION ASPECTS OF MEMBRANE ASSOCIATED PROCARYOTIC DNA REPLICATION

William Firshein Wesleyan University

SC: NRDEC, WRAIR

A Bacillus subtilis membrane-associated protein that binds specifically to the origin of replication, including a putative initiation site, may act as an inhibitor of initiation of DNA replication. This protein, originally estimated to be 64 kdaltons (kDa), had a slightly lower molecular weight during different stages of the life cycle as determined by SDS polyacrylamide gel electrophoresis. The size difference may be due to processing that results in modification of the protein. The protein can be extracted from both cytosol and membrane fractions and the levels in these fractions vary during the developmental cycle of B. subtilis. A complex pattern of expression was revealed in which significant levels were detected in spores; levels decreased dramatically during germination and increased after the first round of DNA replication. The decrease during germination was due to protease activity. During vegetative growth the protein levels increased until stationary phase, after which there was another decrease during sporulation. The decrease during sporulation may be due partially to sequestering of the protein into forespores, since as the 64 kDa protein decreased in the mother cell, it increased in the forespores. However, protease activity was also involved in the decrease in the mother cell. The changes in expression of this protein are consistent with its role as a repressor of initiation of DNA replication. Additional studies including sequence and restriction analysis, Southern hybridization, and further antibody analysis show that this protein is not related to a subunit of the pyruvate dehvdrogenase complex.

# 28361 ELECTROPORATION OF BACTERIA AND YEASΓ. AN EXPERIMENTAL STUDY OF MOLECULAR TRANSPORT

James C. Weaver Arnold L. Demain Massachasetts Institute of Technology

SC. CRDEC, NRDEC

#### **III Biological Sciences**

An investigation is being made of increased molecular transport into microbial cells using applied electrical fields. Research seeks to determine quantitatively how molecular transport can be significantly altered, and to elucidate the basic mechanisms involved. Using both bacteria and yeast, the cells are exposed briefly to strong electric fields to determine uptake of fluorescent molecules. Release of molecules from cells by electroporation will also be studied. Survival of the cells will be checked by conventional methods and by a new microplating method which the P.I. developed.

### 28457 SPIDER SILK STRUCTURE AND MECHANISMS OF FUNCTION

Randolph V. Lewis University of Wyoming

SL: NRDEC SC: CRDEC

Efforts have been devoted to cloning and sequencing a partial clone for a second silk protein. This protein has several important differences from the first one. There is a poly-Ala region in both but the second has a series of proline-containing repeats which must exist in  $\beta$ -turn confirmation. This severely restricts the possible structures for this protein. A peptide based on this repeat has been synthesized and studies are being made of its biophysical properties. Several possible clones have been identified for protein(s) from minor ampullate and cocoon silk but they were all very small inserts. Work is in progress on creating new cDNA libraries which should produce larger DNA and will ligate more efficiently. Bacterial synthesis of the the silk protein has been greatly increased by using a different vector. The silk protein becomes insoluble at high production levels which makes it easy to obtain. The silk is connected to the maltose binding protein and purified by affinity chromatography. The extra protein is cleaved off by Factor X. This has been accomplished in small quantities and the protein produced is now being analyzed to insure it is the proper sequence.

## 28669 CLONING OF cDNA FOR TWO GLUTAMATE RECEPTOR PROTEINS

Elias K. Michaelis Mary Michaelis University of Kansas

Studies will be made to characterize the primary structure and functional role played by two previously

isolated proteins associated with the glutamate excitatory amino acid neuronal receptor system. Immunochemical tools already developed will be used in cloning and DNA sequencing for two proteins, from which structure will be deduced; proteins will be expressed as gene product in cells transfected with vectors carrying cDNA; functional characteristics of each expressed protein will be characterized using ligand binding and ion channel activity studies.

## D. Defense Against Chemical and Biological Weapons

# 25476 THE RAPID DETECTION OF BACTERIA AND OTHER MICROORGANISMS: APPLICATION OF UV RESONANCE RAMAN SPECTROSCOPY

Wilfred H. Nelson University of Rhode Island

SL: CRDEC, WRAIR SC: CRDEC

Resonance Raman studies of bacteria and bacterial taxonomic markers have been extended to the 200 nm and 257 nm excitation regions. In addition the P.I. will report his first high quality spectra obtained using the newly constructed UV micro-Raman systems. Excitation of bacteria at 218 nm produced some real surprises. While the spectra excited at 218 nm strongly resemble the 222 nm-excited ones, they have much stronger nucleic acid peaks relative to protein peaks. The nucleic acid peaks at least in part appear to be due to ribosomal RNA since the ratio of protein to nucleic acid peak intensities showed a modest but very noticeable dependence upon cultural conditions. This is most noticeable when comparing the relative heights of the peaks near 1550 cm<sup>-1</sup> attributed to trp with those near 1580  $\text{cm}^{-1}$  which are attributed to A + G. The trp 1550 cm<sup>-1</sup> peak is relatively stronger in the stationary phase cultures with the 1580 cm<sup>-1</sup> peak increasing in magnitude in the log phase cultures. While preliminary data suggest that it may be possible to obtain nucleic acid base pair ratios from the 218 nm spectra, it is not likely that those spectra can be used directly for fingerprinting. A wavelength, 222 nm, was found which provides spectra which are independent of cultural conditions. This independence of cultural conditions appears to be associated with the presence of the sharp, intense protein trp absorption maximum near 222 nm which interferes with expected strong scattering from rRNA.

#### Reports:

No. 1-8 in previous editions.

 Ultraviolet Resonance Raman Spectroscopic Studies of Bacteria and Bacterial Spores, by Ebrahim Ghiamati, PhD Thesis, 1990, 206 pp.

# 25663 IDENTIFICATION OF CHEMICAL MARKERS FOR MICROORGANISMS BY PYROLYSIS GC-MS

Stephen L. Morgan Alvin Fox University of South Carolina

SL: CRDEC SC: CRDEC, NRDEC

This research seeks to identify the relevant biological fingerprints generated by pyrolysis that are capable of differentiating or characterizing important biological threats. The investigators will use a selected group of microorganisms, cell fractions, and model compounds, and will subject them to analytical pyrolysis followed by high resolution capillary gas chromatography-mass spectrometry to obtain information on relevant chemical markers for target agent identification.

## 25702 GLUTAMATE/NMDA RECEPTOR ION-CHANNEL PURIFICATION, MOLECULAR STUDIES AND RECONSTITUTION INTO STABLE MATRICES

Elias K. Michaelis Mary Michaelis Theodore Kuwana University of Kansas

SL: AMRICD, CRDEC SC: AMRICD, CRDEC

Two proteins have been isolated. They appear to be part of the glutamate/NMDA receptor-ion channel complex, a glutamate binding protein of 70 kDa and a CPP binding protein of 58 kDa protein, and the papers describing this work were both published in the Journal of Biological Chemistry. Colleagues at DuPont used antibodies (Ab's) raised at the University of Kansas against the 70 kDa protein to screen brain cDNA expression libraries and identified five clones which expressed glutamate binding protein. These clones were transferred to the P.L.'s laboratories and researchers have continued to characterize the fusion proteins and to sequence the cDNA for the most reactive protein. A paper describing the immunochemical characterization of polyclonal Ab's raised against the 70 kDa protein has recently been published in the Journal of Biological Chemistry.

This paper contains a description of the efficient immunopurification of the 70 kDa protein and immunoextraction of glutamate binding activity from solubilized synaptic membranes by the Ab's. Another paper describes the use of the Ab's to determine the distribution of the glutamate binding protein in the brain. The primary neuronal culture systems derived from neonatal rat brain have been developed so that one can compare the ion fluxes activated by glutamate analogs in the reconstituted systems with similarly induced ion fluxes in intact neurons and neuronal cell lines.

# 25752 ROLE OF AXON-SCHWANN CELL INTERACTIONS IN NERVOUS SYSTEM IONIC HOMEOSTASIS

Edward M. Lieberman East Carolina University

SC: AMRICD, CRDEC

The membrane potential of cultured rat sciatic nerve Schwann cells was determined with conventional microelectrode and voltage-sensitive fluorescent dye, Di-S-C<sub>3</sub>, optical techniques. The value for membrane potential obtained with microelectrodes was  $-42.1\pm4.7$  mV (n=8). Using optically-determined fluorescent intensity changes caused by changes in external potassium ion concentration, in the presence or absence of valinomycin (null point method), the membrane potential was estimated at  $-45.7\pm6.2$  mV (n=7) and with a gramicidin and valinomycin double ionophore method,  $-52.2\pm9.1$  (n=4). The membrane potential of Schwann cells was found to be potassium sensitive at and above the physiological range of  $[K^+]$  at 27.5 mV / 10X  $\Delta[K^+]$ , which is approximately half the Nernstian value. This result suggests that other ion permeabilities strongly influence the resting membrane potential of cultured Schwann cells. Since Na<sup>+</sup> had little effect on the membrane potential, it is concluded that Cl<sup>-</sup>; is a likely candidate for the other permeant ionic species. The optical method has been shown to be a useful tool for the systematic study of the membrane potential of Schwann cells in culture and for the characterization of its ionic basis and regulation.

Reports:

- 1. Axon-Glia Interactions in the Crayfish: Glial Cell Oxygen Consumption is Tightly Coupled to Axon Metabolism, by P.T. Hargittai and E.M. Lieberman, MS.
- Effect of Extracellular Potassium on Ouabain-Sensitive Consumption of High-Energy Phosphate by Crayfish Giant Axons: A Study of the Energy Requirement for Transport in the

#### **III Biological Sciences**

#### D. Defense Against Chemical and Biological Weapons

Steady State, by Edward M. Lieberman et al., J Neurochem 55,155(1990). AD A228 238

 High Potassium Selective Permeability and Extracellular Ion Regulation in the Glial Perineurium (Blood-Brain Barrier) of the Crayfish, by P.T. Hargittai et al., *Neurosci* 38,163(1990). AD A233 898

## 26232 EXPRESSION CLONING OF THE HIGH AFFINITY CHOLINE TRANSPORTER

Cameron B. Gundersen

University of California, Los Angeles

SC: CRDEC

Choline Transporter: Homology screening of cDNA libraries using probes based on the cDNA for the yeast choline transporter failed to identify any viable clones. An alternative strategy is being used that relies on the possibility that yeast will express functional transporters after transfection with Torpedo cDNA. Using yeasts that are mutant for choline transport, researchers plan to screen colonies that grow successfully on media that contain low levels of choline. While cDNAs from higher eukaryotes have been expressed functionally in yeast, this technology is not yet fully developed.

#### Reports:

- Mercuric Ions are Potent Noncompetitive Antagonists of Human Brain Kainate Receptors Expressed in *Xenopus* Oocytes, by Joy A. Umbach and Cameron B. Gundersen, *Mol Pharm* 36,582(1989). AD A226 239
- α-Latrotoxin Triggers an Increase of Ionized Calcium in *Xenopus* Oocytes injected with Rat Brain mRNA, by Joy A. Umbach et al., *Mol Brain Res* 8,31(1990).

### 26582 ELECTROSTATIC CONTROL OF ACETYLCHOLINESTERASE REACTIVITY

Harvey A. Berman

State University of New York at Buffalo

Research in the laboratory concerns catalysis by acetylcholinesterase (AchE) and agents that alter catalysis and gene expression of the enzyme in muscle and neuron. The laboratory has been concerned with examining inhibition, reactivation, and aging of AchE from Torpedo with respect to a number of structurally-related *n*-alkyl-, branchedalkyl-, and phenylphosphonates. While all *n*-alkylphosphonates are potent inhibitors of AchE, they differ in their bimolecular rates of inhibition, with short chain agents ( $C_1$ ,  $C_2$ , and  $C_3$ ) inhibiting with rates in the range  $10^8$  M<sup>-1</sup>, and longer chain agents ( $C_4$ ,  $C_5$ , and  $C_6$ ) inhibiting with rates  $10^6$  M<sup>-3</sup>. The covalent alkylphosphono-AchE conjugates differ in their capacities to undergo reactivation and aging. Capacity for reactivation and aging is not related in any simple way to *n*-alkyl chain length. Some agents (C<sub>1</sub>-phosphonofluoridates; C<sub>3</sub>- and C<sub>5</sub>-phosphonyl thiocholines) form conjugates that undergo only incomplete reactivation (40-75 percent relative to 100 percent of the initial enzyme specific activity). Still other agents (C<sub>4</sub>-, iso-C<sub>3</sub>-, and phenyl-phosphonofluoridates and iso-C<sub>3</sub>-phosphonyl thiocholines) form conjugates that undergo essentially no reactivation (<25 percent relative to initial enzyme specific activity). Quite surprisingly, the capacity for reactivation depends on whether the initial agent was an alkylphosphofluoridate or an alkylphosphonyl thiocholine. For example, the conjugate formed from  $C_3$ -phosphonyl thiocholine undergoes reactivation in the presence of HI-6 to 75 percent of the initial enzyme specific activity in an exponential manner consistent with a single rate constant. However, under identical conditions the conjugate formed from C<sub>3</sub>-phosphonofluoridate undergoes reactivation to 58 percent of the initial enzyme specific activity in a biphasic manner consistent with 2 independent rate constants. As discerned by decidium association, however, those conjugates that undergo no reactivation also appear to undergo no apparent aging either. Hence, the poor capacity for reactivation is not linked to onset of aging.

#### Reports:

- Ligand Exclusion on Acetylcholinesterase, by Harvey Alan Berman and Kathryn Leonard, *Biochem* 29,10640(1990). AD A232 018
- Dihydropyridine Receptor Regulation of Acetylcholinesterase Biosynthesis, by M.M. Decker and H.A. Berman, J Biol Chem 265.11796(1990). AD A232 231
- Denervation-Induced Alterations of Acetylcholinesterase in Denervated and Nondenervated Muscle, by M.M. Decker and H.A. Berman, *Exptl Neurology* 109,247(1990). AD A232 011

# 27468 THE GENETIC AND BIOCHEMICAL MANIPULATION OF A BROAD– SPECTRUM ORGANOPHOSPHATE DEGRADING SYSTEM

James R. Wild

Texas A&M University

SL: NRDEC SC: CRDEC

The organophosphorus acid hydrolases represent a distinct class of enzymes that catalyze the hydrolysis of a variety of organophosphate substrates, including many insecticides and their structural analogues. The plasmid-borne opd gene of *Pseudomonas diminuta* 

### E. Sensory Factors in Performance Enhancement

# strain MG specifies an organophosphorus acid hydrolase, a phosphotriesterase, that has been well characterized and can hydrolyze a broad spectrum of insect and mammalian neurotoxins. The in situ functioning of this enzyme in the metabolism of organophosphates has been analyzed directly in insects by transferring the opd gene into embryos of Drosophila melanogaster by P element mediated transformation. The chromosomal locations of this stably inherited transgenic locus differed from strain to strain and demonstrated various expressivity on the whole-insect basis. Transcriptional induction of opd in one of these strains under control of the Drosophila heat shock promoter, hsp 70, resulted in the synthesis of stable active enzyme that accumulated to high levels with repeated induction. The heat shock-induced synthesis of organophosphorus acid hydrolases intransgenic flies conferred enhanced resistance to toxic paralysis by the organophosphate insecticide paraoxon.

#### Reports:

- The Genetic and Biochemical Manipulation of a Broad-Spectrum Organophosphate Degrading System, by James R. Wild and Frank M. Raushel, TR, Jan 91, 7 pp. AD A234 110
- Detoxification of Organophosphate Pesticides Using a Nylon Based Immobilized Phosphotriesterase from *Pseudomonas diminuta*, by Steven R. Caldwell and Frank M. Raushel, *Bio/Tech and Bio/Eng* 37,103(1991). AD A238 500
- Transfer and Expression of an Organophosphate Insecticide-Degrading Gene from *Pseudomonas* in *Drosophila melanogaster*, by J.P. Phillips et al., *Proc Natl Acad Sci* 87,8155(1990), AD A238-510

## 27916 ENZYME DECONTAMINATION OF O-P TOXINS

Michael Syvanen University of California, Davis

SL: CRDEC, NRDEC SC: CRDEC

A paper has been prepared which reports the cloning and sequencing of a glutathione S-transferase (GST) gene from the housefly *Musca domestica*. A cDNA  $\lambda$ gt11 library was prepared from the organophosphate insecticide-resistant housefly strain CornelI-R — a variant which has elevated glutathione S-transferase activity. The  $\lambda$  phage GST clone was identified on the basis of its ability to cross-hybridize to a GST DNA probe from *Drosophila melanogaster*. Based on amino acid homology to other GSTs and expression of Gstase activity in *Escherichia coli*, the *Musca* GST gene belongs to the GST gene family. Although organophosphate resistance in CornelI-R is largely due to one of the glutathione S-transferases, MdGST-1

#### **III Biological Sciences**

is probably not the enzyme responsible for resistance. The mutation which controls resistance to organophosphate insecticides in Cornell-R is highly unstable and researchers isolated spontaneous variants to both insecticide sensitivity and to even higher levels of resistance. This provided an isogenic set of three strains. It was found that MdGST-1 transcript levels as measured by Northern assays are higher in all three Cornell-R strains relative to the sensitive wild-type, but that the sensitive Cornell-R strain has more MdGST-1 transcript than does the highly resistant Cornell-R strain. These data as well as Southern analysis of genomic DNA allow the following conclusions: (a) there are multiple GST genes in Musca domestica; (b) the natural variant Cornell-R over-produces excess transcript from two and probably more of these genes; and (c) the unstable mutations in Cornell R influences the levels of multiple GSTases.

# 28479 SPECIFIC PATHOGEN DETECTION IN 2.5M GUSCN

David Gillespie Hahnemann University

SL: CRDEC. WRAIR SC: CRDEC

The research objective is to study the specificity of molecular hybridization of oligonucleotide probes in a DNA probe system configured as a pathogen detection system with potential for field use. Determine ability of oligonucleotide probes to discriminate pathogen sequences; systematically study the specificity of molecular hybridization in concentrated guanidine thiocyanate, between target nucleic acids and specifically mutated oligonucleotide probes.

## E. Sensory Factors in Performance Enhancement

# 25521 BRAIN MECHANISMS UNDERLYING INDIVIDUAL DIFFERENCES IN REACTION TO STRESS: AN ANIMAL MODEL

Jerome Siegel

University of Delaware

SC: AFOSR

Data have been collected on the effects of AP-5, a specific NMDA receptor antagonist, and CNQX, a specific non-NMDA receptor antagonist, on VEPS in albino rats using the cortical cup preparation. The

#### **III Biological Sciences**

results from this experiment complement the data collected using kynurenic acid, a non-specific EAA receptor antagonist. CNQX significantly decreases the amplitudes of ipsilateral N<sub>1</sub> and N<sub>2</sub> ( $p \le 0.05$ ) in a dose dependent manner, while AP-5 had no significant effect. This agrees with studies using microiontophoresis that suggest non-NMDA receptors are responsible for voltage dependent conductance changes across the post-synaptic membrane, while NMDA receptors are responsible for initiating biochemical changes within the post-synaptic cells. Finally, a paper on the differential effects of chloral hydrate anesthesia on EEG power spectrum and VEPS of Wistar albino rats v. Westenberg Long-Evans albino and hooded rats was revised and resubmitted to Pharmacology, Biochemistry and Behavior.

# F. Optimization of Physical Principles in Biological Systems

## 26099 EFFECT OF CYTOSKELETAL REAGENTS ON STRETCH ACTIVATED ION CHANNELS

Frederick Sachs State University of New York at Buffalo

The greatest success has been in demonstrating that mechanical forces can induce calcium fluxes in intact heart cells. Using fluorescent calcium indicators the P.I. has been able to visualize the flux resulting from prodding and pulling on cells and he has even visualized the flux from what he believes to be single SA channels. This material is in a manuscript submitted to Science. Studies of the mechanosensitive channels in heart cells have revealed five types: two nonselective cation channels and three K selective, one of which is an inward rectifier. All are stretch activated. Removing the extracellular ions greatly reduces the open channel noise of the these channels. This may be helpful in understanding the origin of the noise that is so characteristic of SA channels. SA channels have been found in a new renin secreting cell line developed at Roswell Park Memorial Institute. These channels would explain the mechanosensitive release of renin in juxtaglomerlular cells of the kidney. The cells which were extremely difficult to patch could be made readily accessible by treatment with a xyloside that inhibits synthesis of the extracellular matrix. The procedure has worked on two cell lines thus far and promises to be a general tool to allow patching cells that are otherwise difficult or impossible.

Reports:

No. 1 in previous edition.

- 2. A Fast and Robust Algorithm for Alignment of Tomographic Projections, by Zhongqi Jing and Frederick Sachs, MS.
- 3. Mechanical Transduction by Membrane Ion Channels: A Mini Review, by Frederick Sachs, MS.
- Alignment of Tomographic Projections Using an Incomplete Set of Fiducial Markers, by Zhongqi Jing and Frederick Sachs, Ultramicroscopy 35,37(1991). AD A238 536
- 5. Inhibiting Synthesis of Extracellular Matrix Improves Patch Clamp Seal Formation, by Y.C. Izu and F. Sachs, MS, *European J Physiology*.

## 26385 CELLULAR LOCALIZATION OF INFRARED SOURCES

Guenter Albrecht-Buehle Northwestern University, Chicago

Previous work led to the description of the actinedge bundle (AEB), a "cable" like structure lining the webbed edges of well spread 3T3 fibroblasts [Zand and Albrecht-Buehler, (1989) Cell Motil. Cvtoskel. 13:195-215]. It was suggested that AEBs, along with their cell-substratum adhesions, resist the retractile force of cortical tension and prevent the collapse of cytoplasm towards the nucleus. A paper has been prepared which reports the stages of AEB disassembly and formation induced by the following micromanipulations: (a) when long processes of single 3T3 cells were detached at their distal adhesions, their AEBs disassembled within 2 minutes. Similarly, when detached processes were bent at angles of  $\leq 90$ , they moved until they projected orthogonally to the cell edge, and formed webbed edges within 10 minutes. Newly formed AEBs were found lining the nascent webbed edges; (b) when the webbed edge of a 3T3 cell was scored with a micro-needle, the sides of the score retracted and the severed AEB appeared to disassemble down to its terminal adhesion points. The retraction stopped after 20-40 seconds and the cells formed a webbed edge with large curvature that was lined by a new AEB. Over a period of 20-80 minutes, the new web decreased in length and depth, until it regained its approximate original shape. It is proposed that AEBs are formed by a bootstrapping process between tension in the cytoplasm and microfilament bundling. Once AEBs are formed, this tension is necessary to maintain them, and upon its release they disassemble.

Reports:

- 1. Speculation About the Function and Formation of Centrioles and Bassal Bodies, by Guenter Albrecht-Buehler, MS.
- 2. The Iris Diaphragm Model of Centriole and Basal Body

Formation, by Guenter Albrecht-Buehler, Cell Motility and Cytoskeleton 17,197(1990). AD A232 049

3. Do Actin Edge-Bundles Form Along the Webbed Edges of Fibroblasts by a Boot-Strapping Process?, by Martin S. Zand and Guenter Albrecht-Buehler, MS.

## 26767 PRIMARY EVENTS IN OLFACTORY RECEPTION

Robert R.H. Anholt Duke University Medical Center

SC: CRDEC, NRDEC

Studies have continued on olfactomedin, a recently discovered novel olfactory protein. Olfactomedin is a 57 kD glycoprotein, which is expressed exclusively in olfactory tissue. Previously, it was shown that olfactomedin occurs in its native form as a 120 kD dimer in which two monomers are linked together via intermolecular disulfide bonds. Olfactomedin also contains N-acetylglucosamine and B-D-galactoside sugar residues which account to a large extent for its immunogenicity. A polyclonal rabbit antiserum was used to verify the unique presence of olfactomedin in olfactory tissue. Immonohistochemical studies were performed both at the light microscopic and electron microscopic level to visualize olfactomedin in olfactory neuroepithelium. The data from these studies indicate that olfactomedin is produced by olfactory glands and sustentacular cells and deposited at the mucociliary surface of the olfactory neuroepithelium. The immunohistochemical patterns of staining and the recovery of olfactomedin in preparations of olfactory cilia suggest that it may bind to the dendritic cilia of olfactory receptor cells. The hypothesis that soluble proteins may mediate odorant recognition and facilitate transduction finds analogies in the immune system. Both the olfactory system and the immune system are devoted to molecular recognition. the former phylogenetically preceding the latter. Based on its dimeric disulfide-linked structure and the presence of intramolecular disulfide bonds that stabilize its conformation, it is conceivable that olfactomedin may resemble an ancestral immunoglobulin-like protein. Consolidation of this hypothesis has to await molecular cloning of DNA encoding olfactomedin and the elucidation of its primary structure.

#### Reports:

## 27634 FUNCTIONAL RECONSTITUTION OF OLFACTORY RECEPTOR FOR ANALYTICAL APPLICATION

Vitali Vodyanoy Auburn University SL: AMRICD

SC: CRDEC

The effect of fatty acid desaturation on the surface properties of lung surfactant were studied on a Wilhelmy surface balance by using two preparations of lamellar body (LB) material with markedly different fatty acid profiles: (a) lamellar bodies from adult rabbit lung tissue, and (b) lamellar bodies from fetal rabbit lung tissue maintained in organ culture for 7 days. The fetal lung preparation contains an unusually high level of 16:1 fatty acid (principally palmitoleic acid) at position sn-2 of phosphatidylcholine. Surface pressure - surface area isotherms were obtained for both preparations and compared to isotherms of monolayers of dipalmitoylphosphatidylcholine. In addition, the elasticity of the lamellar body preparations were analyzed as a function of surface pressure, temperature, and rate of compression, both in the presence and absence of Ca2+ plus Mg2+. At slow rates of compression, it was found that fetal LB films have lower elasticity and better respreading ability compared to the adult LB films, which can be explained by the high concentration of unsaturated palmitoleic acid in the fetal preparation. A dynamic component of elasticity was observed at high rates of compression only if  $Ca^{2+}$  and  $Mg^{2+}$  were present in the subphase. The analysis of the free energies, enthalpies, and entropies of compression suggests that films with low concentrations of unsaturated fatty acids are likely to undergo irreversible collapse, but films with excess unsaturated fatty acids accommodate the overcompression with a reversible loss of molecules from the surface.

# Reports:

No. 1-2 in previous editions.

- Surface Properties of Two Rabbit Lung Lamellar Body Preparations with Markedly Different Fatty Acid Profiles, by Vitaly Vodyanoy et al., *Biochim Biophys Acta* 1047,284(1990). AD A232–300
- Cyclic AMP-Sensitive Ion Channels in Olfactory Receptor Cells, by Vitaly Vodyanoy, *Chem Senses* 16,175(1991). AD A238-379

Olfactomedin: Purification, Characterization and Localization of a Novel Olfactory Glycoprotein, by David A. Snyder et al., MS, *Biochem.*

# **IV MATHEMATICS**

## A. Applied Analysis and Physical Mathematics

# 24166 INTERDISCIPLINARY STUDY IN PHYSICAL MATHEMATICS

M. Howard Lee Robert L. Anderson Ray A. Kunze University of Georgia

SL: CRDEC SC: MICOM

Periodic banded linear systems of equations typically arise from discretizing second- or higher-order differential equations with periodic boundary conditions. A paper has been prepared in which a parallel-vector algorithm is introduced to solve such systems. Implementation of the new algorithm is carried out on an Intel iPSC/2 hypercube with vector processor boards attached to each node processor. Comparisons of the execution times of the new method with its sequential counterpart for solving different sizes of periodic tridiagonal systems are obtained. The time evolution of a spin in the spin- $\frac{1}{2}$  van der Walls model has been obtained by solving the Heisenberg equation of motion exactly. Using this solution, the researchers have obtained the long time behavior of the autocorrelation function of a spin. A study has been made of the origin of dimensional independence in the classical susceptibility. This study has led to an expression for the finite-temperature susceptibility of a free electron gas. At finite temperatures the singularity of the susceptibility is no longer at twice the Fermi wave vector. It becomes instead a function of the chemical potential. Thus, anomalies associated with  $2k_F$  occur at different values depending on the temperature and dimensions.

Reports:

No. 1.30 in previou editions.

31. Finite Dimensional Integrable Hamiltonian Systems in Loop Algebras, by M.R. Adams et al., MS.

- 32. A Parallel Algorithm for Solving Higher KdV Equations on a Hypercube, by Thiab R. Taha, Proc of 5th Distributed Memory Computing Conference, 1990, 564.
- Solution of Periodic Tridiagonal Linear Systems on a Hypercube, by Thiab R. Taha, Proc of 5th Distributed Memory Computing Conf, 1990. 346. AD A231 979
- Time-Dependent Behavior of Classical Spin Chains at Infinite Temperature, by R.W. Gerling and D.P. Landau, *Phys Rev* B42,8214(1990). AD A232 189
- 35. Slow Decay in a Spin Model, by Raf Dekeyser and M.H. Lee, MS.
- 36. The Classical Susceptibility and the Temperature-Dependent Susceptibility of a Free Electron Gas, by N, MS, J Math Phys.
- 37. A Parallel-Vector Algorithm for Solving Periodic Banded Linear Systems of Equations, by Thiab R. Taha, MS.

# 25069 TECHNIQUES IN LINEAR AND NONLINEAR PARTIAL DIFFERENTIAL EQUATIONS

Louis Nirenberg

New York University Courant Institute of Mathematics

SL: NVEOC SC: NRDEC

Work has continued on semilinear equations in cylinders, on equations related to combustion theory. Work has started on the problem of characterizing and studying principal eigenvalues—corresponding to positive eigenfunctions for the Dirichlet problem for arbitrary bounded open sets. No regularity is assumed about the boundary. Work has continued on free boundary problems. Work has also continued on the hydrodynamic scaling limit of the Ginzburg-Landau models. This involves derivation of macroscopic equations for conserved quantities of microscopic dynamics. One hopes to study the deeper question such as finding the next order connection to the macroscopic equations.

# 25396 ADIABATIC SHEAR BANDS IN SIMPLE 25428 TRANSITIONS AND DEFECTS IN AND DIPOLAR VISCOPLASTIC MATERIALS

Romesh C. Batra University of Missouri at Rolla

SL: BRL SC: BWL. MTL

Studies have ascertained the effect of thermal conductivity on the initiation and growth of shear bands in a structural steel by analyzing the development of shear bands in a thermally softening viscoplastic block undergoing overall adiabatic simple shearing deformations. The thickness of the block is assumed to vary smoothly, with the thickness at the specimen center being five percent smaller than that at the outer edges. Three constitutive relations, namely, the Litonski law, the Bodner-Partom law, and the Johnson-Cook law, have been used to represent the viscoplastic response of the material. The values of the material parameters used are such that each constitutive relation gives essentially the same stress-strain curve as that observed by Marchand and Duffy for a HY-100 steel deformed in torsion at a strain-rate of 3300 s <sup>- 1</sup>.

#### Reports:

No. 1-16 in previous editions.

- 17. Dynamic Shear Band Development in a Thermally Softening Bimetallic Body Containing Two Voids, by R.C. Batra and Z.G. Zhu, Acta Mech 86,31(1991). AD A234 400
- 18. Analysis of Shear Banding in Plane Strain Compression of a Bimetallic Thermally Softening Viscoplastic Body Containing an Elliptical Void, by Z.G. Zhu and R.C. Batra, Thermal Effects on Structures and Materials, 1990, 77. AD A230 716
- 19. Dynamic Adiabatic Shear Band Development in a Bimetallic Body Containing a Void, by R.C. Batra and Z.G. Zhu, Intl J Sol and Struct 27,1829(1991). AD A238-173
- 20. Dynamic Shear Band Development in Plane Strain Compression of a Bimetallic Body, by R.C. Batra and Z.G. Zhu, Trans of Eighth Army Conf on Appl Math and Computing. ARO Rpt 91-1, 1991, 127. AD A238 673
- 21. Modelling of Shear Bands in a HY-100 Structural Steel, by R.C. Batra and C.H. Kim, MS.
- 22. Effect of Thermal Conductivity on the Initiation, Growth and Band Width of Adiabatic Shear Bands, by R. C. Batra and C. H. Kim, Intl J Eng Sci 29,949(1991).
- 23. An Approximate Linear Stability Analysis of Simple Shearing Deformations of a Dipolar Viscoplastic Material, by Xiang-Tong Zhang and R.C. Batra, MS, J Math and Phys.
- 24. Effect of Initial Temperature on the Initiation and Growth of Shear Bands in a Plain Carbon Steel, by C.H. Kim and R.C Batra, MS, Intl J Non-Linear Mech

#### **IV Mathematics**

# ORDERED MATERIALS: NONLINEAR THEORY, COMPUTATION, AND EXPERIMENT

Jerald L. Ericksen Robert Hardt University of Minnesota, Minneapolis SL: BRL

SC: ETDL. MTL

Consideration is being given to electrical properties, and elastic properties of mixtures of components with very different electrical or elastic properties. These investigations lead to bounds for the effective moduli for mixtures made of cells of very high or very low conductivity inserted in a conducting matrix, and for the overall elastic properties of materials with holes. For some random systems in which the particle sizes are 20 percent away from the touching size, these new bounds determine the effective properties with an uncertainty of 5 percent. These constitute the first rigorous and accurate estimates for effective moduli of strongly heterogeneous mixtures, which had been previously treated by numerical calculations for somewhat restrictive geometries, such as periodic arrays of spheres. In an investigation of the optical properties of diffraction gratings, a new method for solving a class of PDE's of mathematical physics was introduced. The method was subsequently applied to the problem of determining the diffraction of light by an interface between two dielectrics. This method is based on computing the solution to a PDE by variations of the boundary of the domain where the solution is sought. The basic result here, which was conjectured to be false by some authors, is that the solution of, say, Maxwell's equations associated to diffraction problems, is an analytic function with respect to variations of the boundaries. This method was numerically implemented, and gave excellent results for the kinds of commercial gratings used in applications. In other work, the asymptotic behavior of a new type of aerosol arising in photographic applications was studied. The mathematical model, which leads to a nonlinear Boltzman-like differential equation, can be described as follows. Consider spherical particles of volume x having "paint" on a fraction y of their surface area. The particles are assumed to be homogeneously distributed at each time t, so that one can introduce the density number n(x, y, t). When collision between two particles occurs, the particles will coalesce if and only if they happen to touch each other. at impact, at points which do not belong to the

painted portions of their surfaces. Introducing a dynamics for this model, the investigators studied the evolution of n(x,y,t) and, in particular, the asymptotic behavior of the mass xn(x,y,t)dx as  $t \rightarrow \infty$ . It was found that, for large times, the system reaches a stationary state with all particles painted. Furthermore, the stationary state was shown to depend continuously with respect to variations of the initial conditions.

Reports:

 Transitions and Defects in Ordered Materials: Nonlinear Theory, Computation and Experiment, by Richard D. James and Oscar Bruno, FR, Sep 91, 3 pp.

# 25782 NONLINEAR WAVES, DYNAMICAL SYSTEMS AND OTHER APPLIED MATHEMATICS PROGRAMS

Avner Friedman

Willard Miller, Jr. University of Minnesota, Minneapolis

SL: AVSCOM SC: BRL, BWL, MTL

The existence of solutions for the Riemann problem of a mixed type system was established by a vanishing similarity viscosity approach. The solutions are also admissible by the traveling wave criterion derived from the most common form of viscosity. The assumption needed includes the constitutive function of van der Waals fluids.

#### Reports:

No. 1-6 in previous editions.

- 7. Time Series, Statistics, and Information, by Emanuel Parzen, MS.
- 8. Navier-Stokes Equations in Thin 3D Domains: Global Regularity of Solutions I, by Genevieve Raugel and George R. Sell, MS.
- 9. Perturbations of Attractors of Differential Equations, by Victor A. Pliss and George R. Sell, MS.
- Hypergeometric Expansions of Heun Polynomials, by E.G. Kalnins and W. Miller, Jr., MS.
- 11. Ghost Tori for Monotone Maps, by Christophe Gole, MS,
- 12. Ghost Circles for Twist Maps, by Christophe Gole, MS,
- 13. Hopf Bifurcation on a Square Lattice, by Mary Silber and Edgar Knobloch, MS.
- Robust Stabilization of Systems Governed by Singular Integro-Differential Equations, by Hitay Ozbayand Janos Turi, MS.
- 15. On the Existence of Smooth Breathers for Nonlinear Wave Equations, by M. W. Smiley, MS.
- Global Attractions and Approximate Inertial Manifolds for Abstract Dissipative Equations, by M.W. Smiley, MS
- 17. Determining Nodes, Finite Difference Schemes and Inertial Manifolds, by Ciprian Foias and Edriss S. Titi, MS.

## A. Applied Analysis and Physical Mathematics

- 18. Markov Partitions for Expanding Maps of the Circle, by Matthew Stafford, MS.
- 19. Reproduction Numbers and the Stability of Equilibria of S1 Models for Heterogeneous Populations, by Carl P. Simon and John A. Jacquez, MS.
- AIDS: The Epidemiological Significance of Two Different Mean Rates of Partner Change, by John A. Jacquez and Carl P. Simon, MS.
- 21. Simultaneous Binary Collisions in the Collinear N-Body Problem, by Mohamed Sami Elbialy, MS.
- 22. Continuation to Gradient Flows, by James F. Reineck, MS.
- 23. Global Analysis of the Phase Portrait for the Kuramoto-Sivashinsky Equation, by Ju.S. II'yashenko, MS.
- 24. Simplified Equations for Low Mach Number Combustion with Strong Heat Release, by Andrew Majda and Kevin Lamb, MS.
- 25. Monotone Maps of  $T(n) \times R(n)$  and Their Periodic Orbits, by Christophe Gole, MS.

# 25874 NONLINEAR PROBLEMS AND NUMERICAL METHODS IN DIFFERENTIAL EQUATIONS AND APPLIED PHENOMENA

H.B. Keller

California Institute of Technology

SC: BRL, ETL

The research objective is to investigate various nonlinear problems related to stability and diffusion processes, turbulence modeling, biochemical systems, membrane and shell buckling, steady viscous flow, bifurcation theory and multigrid methods. Research will proceed by studying specific problems of interest; analytical methods, such as singular perturbation theory, bifurcation theory, numerical analysis, path or continuation methods, as well as computational methods, will be used.

# 26113 MATHEMATICAL ANALYSIS OF STRONG FLUID MECHANICAL EFFECTS AT HIGH MACH NUMBER IN REACTIVE AND NONREACTIVE FLOW

Andrew J. Majda Princeton University

SL: BRL, CRDEC SC: ARO

Research efforts have resulted in (a) achieved understanding of the transition to instability for unstable one-dimensional detonations; and (b) development of the first rigorous model with exact renormalization for turbulent transport. This model can be used to

check the wide variety of renormalization theories for eddy diffusivity.

#### Reports:

No. 1-11 in previous editions.

- 12. Nonlinear Development of Low Frequency One-Dimensional Instabilities for Reacting Shock Waves, by A. Bourlioux et al., MS.
- 13. Simplified Equations for Low Mach Number Combustion with Strong Heat Release, by Andrew Majda and Kevin Lamb, MS.
- 14. Asymptotic Analysis of Reacting Materials with Saturated Explosion, I. Low-Frequency Waves, by Robert F. Almgren et al., MS.
- 15. Asymptotic Analysis of Reacting Materials with Saturated Explosion, II. High-Frequency Waves, by Robert F. Almgren et al., MS.
- 16. Vorticity, Turbulence, and Acoustics in Fluid Flow, by Andrew J. Majda, MS, SIAM Rev.
- 17. Homogenization and Renormalization of Multiple-Scattering Expansions for Green Functions in Turbulent Transport, by Marco Avellaneda and A.J. Majda, MS.
- The Interaction of Nonlinear Analysis and Modern Applied Mathematics, by A.J. Majda, MS.

## 26218 SYSTEMS OF EVOLUTION EQUATIONS IN THERMOMECHANICAL PROCESSES

A.E. Tzavaras

University of Wisconsin-Madison

A study is being made of the adiabatic plastic shearing of an infinite plate subjected to prescribed tractions or steady shearing at the boundaries. The following objectives have been set: (a) to analyze completely a simple model, intended as a paradigm for understanding the instability scenario, (b) to define mathematically what is meant by a shear band, (c) to understand the dissipative effect of strain rate sensitivity on inelastic deformations occurring under strain softening conditions. These questions were pursued in the context of an isothermal model. A constitutive law, appropriate for a material exhibiting strain softening and strain-rate sensitivity was employed. In this model thermal effects are only implicitly taken into account, as being the cause of strain softening. The model consists of a system of nonlinear partial differential equations, belonging to what is formally classified as hyperbolic-parabolic systems. Nevertheless, strain softening causes some associated linearized problems to be parabolic regularizations of elliptic systems. This is thought of as the underlying cause of instability. Using techniques of nonlinear analysis, sufficient conditions were identified both for stable as well as unstable response in the cases

that the shearing deformation is caused by prescribed tractions or prescribed velocities. Also the possibility of response leading to spatially nonuniform structures, like shear bands, has been demonstrated. This analysis demonstrates a simple strain-softening, strainrate dependent constitutive relation as capturing the essential response expected in shear strain localization at high speed deformations.

Reports:

No. 1-3 in previous editions.

4. Strain Softening in Viscoelasticity of the Rate Type, by A.E. Tzavaras, J Integral Eq and Appl 3,195(1991). AD A238 620

## 26272 OSCILLATIONS AND CONCENTRATIONS IN COMPRESSIBLE AND INCOMPRESSIBLE FLUIDS

Phillip Colella

University of California, Berkeley

The research objective consists of mathematical analysis of static structure and dynamic behavior of oscillations and concentrations in compressible and incompressible fluids and solids. Functional analysis approach will be used to solve the pertinent nonlinear partial differential equations.

# 26463 MATHEMATICAL PROBLEMS IN MICROMECHANICS AND COMPOSITE MATERIALS

Robert V. Kohn Marco Avellaneda Graeme Milton New York University Courset Institute of Mat

New York University Courant Institute of Mathematics

Papers have been prepared on (a) studies of coherent, energy-minimizing mixtures of two linearly elastic phases with identical elastic moduli. A formula is derived for the "relaxed" energy of the system, and energy minimizing microstructures are investigated. The analysis provides a link between the work of Khachaturyan and Roitburd in the metallurgical literature, and that of Ball, James, Pipkin, Lurie, and Cherkaev in the recent mathematical literature: (b) studies of the asymptotic behavior of solutions of  $u_t - \Delta u = u^p$  as they blow up. This is done by using a sort of center manifold analysis for the equation in similarity variables. This leads to refined asymptotics for u in a backward space-time parabola; (c) the relaxation of a multiwell energy of the form W = $min_i |\lambda u - a^i|^2$ . It shows how the relaxed energy

QW can be expressed in terms of certain "tensors of geometric parameters." These tensors must lie within a certain convex set; this fact yields a new lower bound on QW. For the special case of three wells and two space dimensions, the authors compute the extreme points of this convex set. Other papers study the propagation of initial oscillations in solutions of one-dimensional inviscid gas dynamics equations. A system of homogenized equations is derived. Its behavior is compared with that of numerical solutions, to verify that it correctly captures the average behavior. The validity of the averaged equations is proved with mathematical rigor in some circumstances. Another paper studies the large time behavior of solutions of scalar conservation laws in one and to space dimensions. A suitable condition of nonlinearity assures that the solution must converge to a constant. This result is then applied to the initial-value problem for scalar conservation laws with oscillatory initial data.

#### Reports:

No. 1-13 in previous editions.

- Bubbly Flow and Its Relation to Conduction in Composites, by Peter Smereka and Graeme W. Milton, MS, J Fluid Mech.
- Enhanced Diffusivity and Intercell Transition Layers in 2D Models of Passive Advection, by Marco Avellaneda, MS, *Phys Rev Let.*
- Homogenization and Renormalization of Multiple-Scattering Expansions for Green Functions in Turbulent Transport, by Marco Avellaneda and Andrew J. Majda, MS.
- L(p)-Bounds on Singular Integrals in Homogenization, by M. Aveilaneda and Fang Hua Lin, MS, Commun Pure Appl Math.
- Variational Constraints for Electrical Impedance Tomography, by James G. Berryman and Robert V. Kohn, MS, *Phys Rev Let*.
- Composite Materials and Structural Optimization, by Robert V. Kohn, MS.
- The Initial-Value Problem for Measure-Valued Solutions of a Canonical 2 × 2 System with Linearly Degenerate Fields, by Weinan E. and Robert V. Kohn, MS, Common Pure Appl Math.
- Propagation of Oscillations in the Solutions of 1-D Compressible Fluid Equations, by Weinan E. MS, Commun in Partial Diff Eq.
- 22. The Field Equation Recursion Method, by Graeme W. Milton, MS.
- Inverse Transport Problems for Composite Media, by Ross C. McPhedran and Graeme W. Milton, MS.
- Numerical Study of Oscillatory Solutions of the Gas Dynamics Equations, by E. Weinan and Huanan Yang, MS. Studies in Appl Math.
- Homogenization of Scalar Conservation Laws with Oscillatory Forcing Terms, by E. Weinan, MS, SIAM J Appl Math.
- 26. Large Time Behavior and Homogenization of Solutions of

#### A. Applied Analysis and Physical Mathematics

Two-Dimensional Conservation Laws, by Bjorn Engquist and E. Weinan, MS, Commun Pure Appl Math.

- 27. Homogenization of Linear and Nonlinear Transport Equations, by E. Weinan, MS. Commun Pure Appl Math.
- Controllabilite Exacte, Homogeneisation et Localisation d'ondes Dans Un Milieu Non-Homogene, by Marco Avellaneda et al., MS.
- 29. The Relaxation of a Double-Well Energy, by Robert V. Kohn, MS.
- 30. Geometric Parameters and the Relaxation of Multiwell Energies, by N.B. Firoozye and R.V. Kohn, MS.
- 31. Diffusion and Geometric Effects in Passive Advection by Random Arrays of Vortices, by M. Avellaneda et al., MS, *Phys Fluids*.
- 32. Refined Asymptotics for the Blowup of  $ut \Delta \tau = u(p)$ , by Stathis Filippas and R.V. Kohn, MS. Commun Pure Appl Math.

## 26909 STRESS SENSITIVITY OF DIELECTRIC RESONATORS

Peter C.Y. Lee Princeton University

SL: ETDL

The research on the stress sensitivity of the dielectric resonators has been progressing very well. A system of two-dimensional governing equations for guided EM waves in dielectric plates surrounded by free space is derived and is shown to give accurate predictions for the dispersion relations. These newly derived two-dimensional equations are presently being employed for the study of guided EM waves in strip dielectric resonators with rectangular cross-sections for which the continuity conditions of E and H fields must be satisfied on two pairs of lateral faces of the strip resonators.

#### Reports:

 A Variational Principle for the Equations of Piezoelectromagnetism in Elastic Dielectric Crystals, by P.C.Y. Lee, MS, *J Appl Phys.*

# 27403 DYNAMICAL SYSTEMS AND NONLINEAR PARTIAL DIFFERENTIAL EQUATIONS

C.M. Dafermos

Brown University SL: CRDEC

#### SC: MICOM

A paper has been prepared which presents a study of the limiting behavior of solutions to appropriately rescaled versions of the Allen-Cahn equation, a model for phase transition in polycrystalline material. Researchers have rigorously establish the existence in the limit of a phase-antiphase interface evolving according to mean curvature motion. This assertion is valid for all positive time, the motion interpreted in the generalized sense of Evans-Spruck and Chen-Giga-Goto after the onset of geometric singularities. Another paper considers the resolvent equations for a scalar, one-dimensional conservation law and its approximations by MUSCL method second-order, TVD, finite-differences approximations. Proof was obtained for the convergence towards the entropic weak solution in the case of strictly convex flux. The proof relies upon the theory of viscosity solutions.

#### Reports:

No. 1 in previous edition.

- Uniqueness and Singularities of Cylindrically Symmetric Surfaces Moving by Mean Curvature, by H.M. Soner and P.E. Souganidis, MS.
- 3. Phase Transitions and Generalized Motion by Mean Curvature, by L.C. Evans et al., MS.

## 27433 NUMERICAL METHODS FOR SINGULAR INTEGRAL EQUATIONS

Ram P. Srivastav

State University of New York at Stony Brook

#### SL: CRDEC SC: MICOM, MTL

The study of Cauchy singular integral equations was continued. The following has been accomplished: A procedure for the numerical solution of CSIE's using arbitrary quadrature and collocation nodes has been developed and preliminary results were presented at the Conference of Army Mathematicians at Cornell University in June 1990. Earlier partial success was reported in determining the singular behavior of CSIE's numerically. For the constant coefficient, one can compute the weight-function with an adaptation of Stenger's quadrature formula. The approach seems to work also for systems of equations with constant coefficients. Approximation of singular functions by rational functions is an important tool for the solution of many problems of physical interest. Singularities most frequently encountered are logarithmic or power law singularities. Suitable formulae for numerical integration give a rational function approximation with high degree of accuracy, without sophisticated analytical tools.

#### Reports:

- On Solving Cauchy Singular Integral Equations by Using General Quadrature-Collocation Nodes, by R.P. Srivastav and Fenggang Zhang, Comp Math with Appl 21,59(1991). AD A238 765
- 2. On a Hyperbolic Tangent Quadrature Rule for Solving Singular Integral Equations with Hadamard Finite Part Integrals, by Fenggang Zhang, MS, *Comp Math with Appl.*

- 3. Numerical Methods for Solving Singular Integral Equations
- with O-Index, by R.P. Srivastav and Fenggang Zhang, MS.
  4. The Minimum Norm Least Squares Solution of the Cauchy Singular Integral Equation, by R.P. Srivastav and Fenggang Zhang, MS, Math of Computation.

## 27557 NONLINEAR MATHEMATICS APPLIED TO THE SCIENCE OF MATERIALS

Morton E. Gurtin William O. Williams Carnegie-Mellon University

The study of a crystal shrinking or growing in a melt gives rise to equations relating the normal velocity of the motion to the curvature of the crystal boundary. Often these equations are anisotropic, indicating the preferred directions of the crystal structure. In the isotropic case this equation is called the mean curvature flow or the curve shortening equation, and has been studied by differential geometric tools. In particular, it is known that there are no classical solutions to these equations. A paper develops a weak theory for the "generalized mean curvature' equation using the newly developed theory of viscosity solutions. The approach is closely related to that of Osher and Sethian. Chen. Giga and Goto, and Evans and Spruck, who view the boundary of the crystal as the level set of a solution to a nonlinear parabolic equation. The main results are the existence of a solution. large time asymptotics of this solution, and its connection to the level set solution of Osher and Sethian, Chen, Giga and Goto, and Evans and Spruck. In general there is no uniqueness even for classical solutions, but the authors prove a uniqueness result under restrictive assumptions. They also construct a class of explicit solutions which are dilations of Wullf crystals.

# 27580 ANALYTICAL THEORY OF CONTINUED FRACTIONS AND TIME EVOLUTION IN MANY-BODY SYSTEMS

M. Howard Lee University of Georgia

The research objective is to investigate problems associated with nonequilibrium state (diffusion, relaxation, etc.,) in multibody dynamical system and methods of solution for such problems. The theory of continued fractions will be used in solving the relevant time evolution problems.

## 27641 SOME PROBLEMS IN NONLINEAR ANALYSIS

Paul H. Rabinowitz University of Wisconsin-Madison

A paper has been prepared which develops a new variational method to prove the existence of infinitely many homoclinic solutions for a class of Hamiltonian systems. It is to some extent a variational analogue of classical symbolic dynamics arguments to find homoclinics.

#### Reports:

1. Homoclinic Orbits for Second Order Hamiltonian Systems Possessing Superquadratic Potentials, by V.C. Zelati and P.H. Rabinowitz, MS.

## 27869 VISCOSITY SOLUTIONS OF FULLY NONLINEAR EQUATIONS

Michael G. Crandall University of California, Santa Barbara

An investigation is being made of problems involving fully nonlinear differential equations of first order in infinite dimensions and of second order in finite and infinite dimensions. The method of viscosity solutions incorporating variational inequalities and boundary controls is used.

# 28514 STABILITY AND THERMAL INFLUENCES IN NONLINEAR CONTINUUM MECHANICS AND MATERIALS SCIENCE

Morton E. Gurtin Carnegie-Mellon University

SC: MTL

The research objective is to study the nonequilibrium thermodynamics of multiphase continua. The methods of nonlinear continuum mechanics and the fundamental laws of thermodynamics and techniques for free boundary problems will be used.

## 28548 NONLINEAR WAVES IN MECHANICS AND GAS DYNAMICS

Tai-Ping Liu Stanford University

The research objective is to study nonlinear differential equations in mechanics and gas dynamics characterized by compressibility, and with convection sources due to reactions and geometry, dissipation and delay. A quite general, uniform and refreshing

## A. Applied Analysis and Physical Mathematics

approach evolved from such methods as wave tracing, characteristic energy and nonlinear superposition through time-asymptotic expansions developed by the P.I. in the recent past will be used.

# 28606 THE STROH FORMALISM FOR ANISOTROPIC ELASTICITY WITH APPLICATIONS TO COMPOSITE MATERIALS

T.C.T. Ting

University of Illinois at Chicago

The objective of the research is to investigate new approaches for anisotropic elasticity with special emphasis on singularities at the interface of composite materials. The approach will be to explore the Stroh formalism based on stress functions and the theory of complex variables.

## 28702 SYSTEMS OF HYPERBOLIC PARTIAL DIFFERENTIAL EQUATIONS

Michael Shearer

North Carolina State University

The research objective is to study nonlinear partial differential equations of hyperbolic type with specific emphasis on dynamics for elastoplastic materials and on various conservation laws. The principal investigator will extend his previous results in basic understanding of hyperbolic PDE's and Riemann problems to the more difficult and realistic situations cited above, and will seek correlations to analytical and numerical solutions.

## 28797 THREE PROBLEMS IN FLUID DYNAMICS

Daniel D. Joseph Matthew Tirrell University of Minnesota, St. Paul SL: CRDEC

The objective of the research is to study the dynamics of spinning viscous fluids, to obtain correct hydrodynamic forces on particles in viscous fluids based on Navier-Stokes equations and to identify correct physical mechanisms to regularize ill-posed problem in two phase flows. The methods of Hadamard for ill-posed problems, intensive computational modeling and other techniques developed successfully by P.L. will be used for the work.

# 28803 ANALYTICAL STUDIES OF NONLINEAR PARTIAL DIFFERENTIAL EQUATIONS OF INTEREST IN NONLINEAR OPTICS

M.J. Potasek Columbia University

A study was made of optical switching in various nonlinear devices using nonlinear partial differential equations. Interest in optical switching is growing in Importance. Of particular interest are solitons and solitary waves because of their high fidelity. Furthermore the recent development of femtosecond light sources in the visible and infrared spectral regions makes possible the exploration of new phenomena on ultrashort time scales. Therefore researchers have been investigating nonlinear optical phenomena. In particular, success has been achieved at applying analytical techniques, such as the inverse scattering transform method to obtain new solitons solutions in complex partial differential equations. For example, a new result was obtained for phase-shifted induced gain switching. Exact coupled equations were derived and then IST was used to obtain exact solutions. Besides obtaining a new class of exact soliton solutions, the results have significant practical applications. An appropriate gain factor can actually reduce the device length required. This finding could have significant application by reducing the device length. The overall device length is one of the important parameters for applications. Furthermore, exact coupled equations were derived for femtosecond all-optical switching and, again using IST, exact solutions were obtained. Then applying a realistic model experimental parameters can be described for their observation. These results are new and particularly significant because they represent the first results for ultrashort all optical switching which definitively expands soliton switching to the femtosecond time domain in a rigorous manner.

Keports.

 Obtaining Coupled Integrable Equations for Nonlinear Directional Couplers, by M.J. Potasek et al., MS, *Phys.Let*.

## 28957 CONSERVATION LAWS FOR ELASTIC SYSTEMS WITH DISSIPATION

George Herrmann Stanford University

SL. ARO

The objective of the research is to derive conservation laws for viscoelastic solids using a novel methodology of invariants and to explore the connection of the conservation laws and the material forces acting on surfaces of discontinuity, such as defects. A combination of variational methods and a systematic and algorithmic implementation of invariant conditions will be used to derive the stated objectives.

# 28969 DISPERSIVE REGULARIZATION OF SHOCKS

S. Venakides

Duke University

SL: BWL

The research objective is to study the generation and propagation of dispersive waves in the presence of nonlinearity: nonlinear hyperbolic equations perturbed by small-coefficient dispersive terms. The principal investigator will apply some highly analytical, new and innovative approaches, such as the modulation theory, the Lax-Levermore procedure and some novel asymptotic techniques to gain basic understanding of the generation and propagation of dispersive waves.

## 28980 MATHEMATICAL ANALYSIS OF REACTIVE MULTIPHASE FLOWS

Pedro Embid

University of New Mexico

SL: BRL

The research objective is to study transition to detonation and structure of detonation waves in reactive multiphase flow. Asymptotic, numerical and analytical methods combined will be used in this work.

## 28986 SOME PROBLEMS IN THE MECHANICS OF SOLIDS WITH PHASE MIXTURES

Roger Fosdick

University of Minnesota, Minneapolis

SL. BRL

The research objective is to advance the understanding of the relationship between constitutive theory in continuum physics and observed material behavior by way of several important technological problems, such as the minimization problems involving coarsemixture structures, alloy concentrations, interfaces, swelling and collapses of materials. A combination or mathematical analysis and computational methods will be used. The common thread and guiding physical ideas are the coexistent phases and phase mixtures and materials stability.

## B. Numerical Methods and Scientific Computing

# 26391 ITERATIVE METHODS FOR LARGE SPARSE LINEAR SYSTEMS ARISING FROM PARTIAL DIFFERENTIAL EQUATIONS

Howard C. Elman University of Maryland

SL: BRL

SC: AVSCOM

A study of the parallel implementation of the hpversion of the finite element method on a shared memory computer has been completed. This study examines the behavior of two-dimensional elliptic solvers on the eight processor Alliant FX/8 computer. The methodology used includes local elimination of high order basis functions with support internal to elements, combined with preconditioned conjugate gradient solution of unknown on element interfaces. Results indicate that the fully parallel parallel computations (local assembly and elimination) dominate the computational cost, and that the global, i.e., less highly parallel, operations, such as preconditioners. present a small percentage of overall costs. New results include a clear picture of the effects of cache memory, showing that care must be taken in matching problem sizes with memory resources to achieve full efficiency; and a predictive model of the effects of synchronization of local operations.

#### Reports:

No. 1-4 in previous editions.

- Parallel Implementation of the *hp*-Version of the Einite Element Method on a Shared-Memory Architecture, by J. Babushka et al., MS, *SIAM J. Sci Stat Comput.*
- Parallel Sparse Cholesky Factorization on a Shared Memory Multiprocessor, by G. Zhang and H.C. Elman, MS. Parallel Comp.

## 26616 FRONT TRACKING AND THE INTERACTION OF NONLINEAR WAVES

James Glimm

State University of New York at Stony Brook

SL BRI SC BWI

The main focus is shock wave interactions, chaotic fluid mixing, parallel methods for front tracking, and three dimensional front tracking. Work is in progress to develop a robust front tracking method for the long time simulation of large amplitude shock accelerated interfaces. An analysis of the shock retractions that occur while the shock is passing through

#### **B.** Numerical Methods and Scientific Computing

the interface is needed due to the sensitivity of the unstable interface to perturbations in the flow. In collaboration with Ralph Menikoff of the Los Alamos National Laboratory, and Prof. L.F. Henderson of the Institute of Space and Astronautical Science in Japan, the wave refractions of a shock at a material has been classified into four broad classes, depending on whether the reflected wave is a shock or rarefaction wave, and on whether the acoustic impedance increases or decreases across the fluid interface. These four cases are distinguished by the different irregular wave patterns that are produced for sufficiently large angles between the incoming shock and the material interface. This analytic theory is being implemented into the front tracking hydrodynamics code. This has now been accomplished in two of these cases. Progress in the application of parallel MIMD methods to front tracking is proceeding at a good rate. The implementation is now 90 percent complete and mainly only debugging issues remain to be resolved before a working code is produced. The strategy here is to use a domain decomposition method to partition the computational domain of the problem into individual sections that can be farmed out to distinct processors in a distributed memory parallel computer. Since the equations of compressible unsteady fluid flow are hyperbolic, the need for communication between the different processors is reduced to the boundary information near the edges of the decomposition cells. The main technical difficulty is the communication between different processors of the complicated data structures and state information in the different cells. This requires the mapping of memory addresses from one processor to another. Tracked fronts are communicated by clipping a section of the tracked waves near the cell boundaries and transmitting these clipped sections to adjacent cells. State information is similarly communicated for states near a decom position cell boundary.

#### Reports

No. 1.6 in previous editions.

- 7 Chaotic Mixing as a Renormalization Group Fixed Point, by James G. Glimm, MS, *Phys Rev Let*
- 8 Parallel Computations Using Interface Methods for Ehud Dynamics in Three Dimensions, by Yuetan Deng and James Glimm, MS
- Nonlinear and Stochastic Phenomena. The Grand Challenge for Partial Differential Equations, by James Glimm, MS, *SIAM Rev.*
- Hurd Dynamics Using Interface Methods on Parallel Processors, by Yuetan Deng and James Gluum, MS

# 26871 HIGHLY-ACCURATE ADAPTIVE FINITE ELEMENT SCHEMES FOR NONLINEAR HYPERBOLIC PROBLEMS

J. Tinsley Oden

University of Texas at Austin

SL: BRL

A new class of numerical schemes for high-order approximation has been developed which is nonoscillatory, produces shock resolution, can ultimately be fully adaptive and promises to be applicable to a wide class of important applications. The technique generalizes the ideas of Cockburn and Shu for onedimensional scaler conservation laws and is based on the use of high-order Runge-Kutta methods and discontinuous Galerkin methods. These RKDG techniques are built around a special maximum principle in which a projection is defined which limits oscillations in the neighborhood of shocks to terms of order  $h^2$ , h being the mesh size. The fact that high-order oscillations are allowed in the vicinity of the shocks is the key to extending TVB schemes to multidimensional problems. Several working codes have been developed, both for one-dimensional problems, for two-dimensional scaler problems and more recently for two-dimensional hyperbolic systems. Applications to the Euler equations of gas dynamics have been developed and consideration of applications of first order systems for stress wave propagation are under study

## 27690 MULTIVARIATE SPLINE APPROXIMATION

Carl de Boor Amos Ron University of Wisconsin Madison

SL: BRL

The book on box splines is closer to completion. A manuscript concerning the linear independence of integer translates of exponential box splines with rational directions has been submitted. It is a reflection on earlier work by Sivakumar. This has its origin in the unhappy fact that, in general, the integer translates of a box spline M fail to be linearly independent, and this makes it harder to construct good approximation schemes with it. Linear independence can be achieved by considering only the translates M with j in some appropriate sublattice of the full integer lattice. This is equivalent to considering box splines with rational directions. Another manuscript supplies a surprisingly simple characterization of the space of polynomials contained in the

### **IV Mathematics**

span S(M) of integer translates of a box spline M with arbitrary directions. This space is important since it characterizes how well one can approximate from S(M) and provides the ready means for the construction of approximants giving that rate of approximation. The joint paper of de Boor and Jia (report 2 below) picks up on earlier work of de Boor and Hollig concerning upper bounds on how well one can approximate from spaces of smooth bivariate piecewise polynomials.

Reports.

- 1. The Least Solution for the Polynomial Interpolation Problem, by Carl de Boor and Amos Ron, MS.
- A Sharp Upper Bound on the Approximation Order of Smooth Bivariate pp Functions, by C. de Boor and R.Q. Jia, MS, *J Approx Theory*.

# 27786 A NUMERICAL SOLVER FOR INITIAL AND BOUNDARY VALUE PROBLEMS IN DIFFERENTIAL-ALGEBRAIC SYSTEMS

Stephen L. Campbell Kenneth D. Clark North Carolina State University

SL: TACOM

Differential algebraic equations (DAEs) are systems of differential and algebraic equations which have not been reworked into an explicit format. Many engineering problems are initially modeled as DAEs. This project is to develop numerical methods for working directly with the original implicit equations. One current thrust of the research is to develop the theoretical basis of the general method. This has proven to be highly nontrivial. One issue currently being resolved is that alterations of the numerical iteration in order to speed up the computation, such as less frequent Jacobian updating, can actually alter the equations characterizing the limit of the iteration. Thus each numerical modification must be accompanied with a corresponding theoretical analysis. Quite recently, studies have shown that nonlinear index three Hessenberg systems can be solved by this method. This result is important since many mechanics and control problems have this form. A second thrust of the research has been to develop numerical methods and guidelines for their use. A research assistant is currently developing a software package that will carry out the entire general procedure for both integrating DAEs and for finding initial conditions. The user will need only to write down the equations and specified desired quantities. The software will then symbolically differentiate the equations several times, generate Jacobians of the

corresponding derivative arrays, generate FORTRAN code for these arrays and Jacobians, and finally carry out the numerical calculations in FORTRAN. One advantage of this software is that the symbolic part will need to be done only once. Design and model parameters can then be varied in the numerical routines. The first goal is to get a working prototype. Then extensive testing and analysis will be needed to speed up execution and make the code robust. The symbolic portion of the prototype code is already written and is being tested.

#### Reports:

No. 1 in previous edition.

- Descriptor Systems in the 90's, by Stephen L. Campbell, Proc of 1990 Conference on Decision and Control, 1990, 442. AD A232 796
- Least Squares Completions of Nonlinear Higher Index DAE Control Problems, by Stephen L. Campbell, MS.
- Duality, Observability, and Controllability for Linear Time Varying Descriptor Systems, by Stephen L. Campbell et al., MS, Circuit Sys Signal Proc.
- 5. 2-D (Differential-Delay) Implicit Systems, by Stephen L. Campbell, MS.
- Least Squares Completions of Nonlinear Index Three Hessenberg DAEs, by Stephen L. Campbell, MS.
- 7. Decomposition of Hessenberg DAE Systems to State Space Form, by Kenneth D. Clark, MS, Linear Alg and its Appl.

## 28007 LINEAR ALGEBRAIC COMPUTATION ON DISTRIBUTED MEMORY PARALLEL MACHINES

Stanley C. Eisenstat Yale University

SC: TACOM

The first phase of the project has focused on the symmetric tridiagonal eigenvalue problem. A new arrowhead divide-and-conquer method has been derived that seems to be equal or superior to Cuppen's method in terms of sequential speed and parallelizability, and that better explains the phenomenon of deflation. Moreover, using the fast multipole method, the new method can be used to compute only the eigenvalues in  $O(N\log_2 N)$  time, where N is the size of the matrix. All other known methods have complexity at least  $O(N^2)$ .

## 28025 FINITE DIFFERENCE METHODS FOR INCOMPRESSIBLE VISCOUS FLOW IN SCIENTIFIC COMPUTING

John C. Strikwerda University of Wisconsin Mathematics Research Center

SL. ARO, WES SC. ARO, AVSCOM, BRL, BWL

#### **B.** Numerical Methods and Scientific Computing

Work is in progress on developing fast solvers for the Stokes and Navier-Stokes equations. The pressure equation method for the Stokes equations on simple domain shapes converges in number of grid points, which is optimal. The method is based on the multigrid algorithm. Current work is being done to extend the method to the Navier-Stokes equations and to employ the method with domain decomposition. Fourth-order accurate methods for the Stokes and Navier-Stokes equations on rectangular domains have recently been developed and tested. In using domain decomposition, the higher order accurate methods can lead to great efficiency by requiring fewer grid point in rectangular domains. It remains to be seen whether the domains with coarser grids and higher-order accurate schemes will combine well with the standard second-order accurate methods of neighboring domains.

# 28034 A STRUCTURED PROGRAMMING APPROACH TO LARGE-SCALE BATTLEFIELD SIMULATION

Patrick J. Burns

Colorado State University

Large scale computerized battlefield simulations have been in existence for a long period of time. CEM VI (Concepts Evaluation Model VI) was first developed in 1968. Since then, it has evolved through several different authors and types of Fortran implementations. The last critical update occurred in 1983 with the introduction of attrition using calibrated parameters (ATCAL) algorithm. CEM VI is a discrete event simulation. As such, it is subject to random and a priori unknown branching. Thus, data are not contiguous in memory, and the data structure evolves with the simulation. The algorithm, as formulated, was not amenable to vectorizing on the new Cray architectures. A typical CEM VI simulation, executed in the scalar CPU, typically consumes several to 10 hours of Cray 2 CPU time. To ameliorate this situation, a strategy was developed whereby the kernel of CEM VI (ATCAL) could be vectorized. After careful investigation it was determined that data motion was the key in realizing the potential for vectorizing the ATCAL algorithm. Three different strategies were investigated, with execution rates determined for each method. Taking advantage of the Cray gather/ scatter hardware was determined the most feasible of the strategies investigated. After implementing the strategy in ATCAL, a speedup of 8.09 was obtained. With the implementation of the vectorized ATCAL algorithm into the CEM VI code, one should expect considerable improvements in overall CPU run times. With increased performance, this will enable the Army to run more cases, and the cases each can be of greater fidelity. This may be particularly germane now that the development of a stochastic version of CEM VI is underway.

## 28071 ALGORITHMIC ISSUES IN HIGH-PERFORMANCE COMPUTING

Jeffrey Vitter Brown University

SC: TACOM

Researchers have recently presented an optimal deterministic sorting algorithm. The algorithm is an interesting variant of merge sort. In each merge pass, a priority scheme guarantees that each record ends up sufficiently close to its correct position, so that another pass of column sort can complete the merging. Other researchers have developed optimal algorithms for prefetching that are novel in that they use data compression techniques that are both theoretically optimal and good in practice. The motivation is the intuition that in order to compress data, you have to be able to predict future data well, and thus good data compressors should be able to predict well for purposes of prefetching. They show for powerful models such as Markov sources and mth order Markov sources that the page fault rates incurred by their prefetching algorithms are optimal for almost all sequences of page accesses. Parallel algorithms have been developed for several graph and geometric problems, including transitive closure and topological sorting in planar st-graphs, preprocessing planar subdivisions for point location queries, and construction of visibility representations and drawings of planar graphs. Most of these algorithms achieve optimal running time. A new data structure was devised for point location in a convex cell complex. The technique combines space-sweep, dynamic planar point location, and persistent data structures.

## 28143 RESEARCH IN GRAPH ALGORITHMS AND COMBINATORIAL OPTIMIZATION

Serge A. Plotkin Stanford University

SC: ACAA

The research objective is to investigate core issues arising in the development of efficient algorithms for

## **IV Mathematics**

graph algorithms and in particular algorithms for combinatorial optimization. The research will involve investigations in several related areas: development of deterministic parallel algorithms for basic combinatorial optimization problems such as network flow problems; locality in the context of distributed computation in which the objective is to design polylogarithmic complexity distributed algorithms for set partitioning problems such as the Maximal Independent Set problem; design of efficient sequential combinatorial optimization algorithms for problems which do not have efficient parallel algorithms.

# 28192 PARALLELISM DETECTION AND SCHEDULING STRATEGIES FOR RELIABLE AND EFFICIENT EXECUTION ON MULTICOMPUTERS

Dharma P. Agrawal North Carolina State University

SL: SDC SC: ETDL

Work is in progress on exploring the concept of a static dynamic scheduling technique for both shared and private memory multiprocessors, and applying it to Palm, a parallelism enhancement environment. The purely static scheduling scheme suffers from the limitation of inaccurate compile time estimates of the task timings, whereas the purely dynamic scheme has the large runtime overhead of task arbitration. The key idea is to create scalable parallel tasks within a basic block of the given program, and to allocate processors to each thread of execution at run time. The static dynamic scheduler, which is a part of the environment, estimates the processor requirements of basic blocks of a given program statically and allocates the processors partially at compile time and partially at run time, to obtain a good tradeoff between speedup and utilization. The initial experiments carried out using this method on Urban Airshed Fortran Code of the US Environmental Protection Agency yielded an improvement of 4-7 times over the speedup obtained using the existing Automatic Parallelizer on Alliant FX-40. It has also been possible to demonstrate implications of static-dynamic scheduler for a private memory machine like Intel iPSC/2.

## 28320 FINITE ELEMENT TECHNOLOGY FOR PENETRATION PROBLEMS

Ted Belytschko Northwestern University SL: BRL

Work is continuing on three efforts: (a) the pinball contact-impact algorithm; (b) the development of improved three-dimensional one-point quadrature elements; (c) study of explicit methods on partitioned memory parallel computers. In the work on the pinball algorithm, researchers are developing multipinball extensions for treating elements which erode and single-surface slidelines. The motivation for this development is that when erosion occurs, if the pinballs are the same size as the elements, it is very difficult to eject them from the contact region. By subdividing a pinball into 9 to 16 smaller pinballs, it becomes possible to reasonably simulate actual behavior at the interface. The three-dimensional element is being examined from the viewpoints of convergence and improved hourglass mode control. Preliminary work has shown that the centroidal integration which is used in DYNA3D does not give the correct volume and does not pass the patch test. Hence it is unlikely that the element converges when its shape is irregular. Work is progressing on the implementation of explicit finite element methods on the connection machine. The two-dimensional pinball algorithm has now been implemented and is being tested. In addition, a viscoplastic material law has been implemented in the connection machine version and will now be used to study large scale problems of scientific interest, the generation of shear bands and fracture at a crack tip.

# 28377 MODIFIED EIGENVALUE PROBLEMS, WITH APPLICATION TO STRUCTURAL DYNAMIC RE-ANALYSIS ON PARALLEL COMPUTERS

Gene H. Golub K.H. Law Stanford University

SC: AERO DIR. BRL

The objective of this research is to investigate efficient solution methods for solving generalized eigenvalue problems with application to recomputing a few of the natural frequencies and modes of large scale structures when small changes in design have been made. The focus will be on parallel algorithms for MIMD architectures. The research involves (a)parallel implementation of efficient solution procedures for solving modified systems of linear equations, (b) evaluating the applicability of subspace iteration and the Lanczos methods for dynamic reanalysis, and (c) studying the feasibility of low rank modification methods for computing some but not all of the eigenvalues. All of these activities are consid-

#### **B.** Numerical Methods and Scientific Computing

ered in the context of parallel MIMD message passing and shared memory computing environments.

# 28535 NUMERICAL ANALYSIS AND COMPUTATION OF NONLINEAR PARTIAL DIFFERENTIAL EQUATIONS FROM APPLIED MATHEMATICS

Donald A French University of Cincinnati

SC: BRL, BWL

Progress has been made on space-time finite element methods. Here one used finite elements to discretize a domain that includes the time dimension. The key advantage is the flexibility to refine the mesh around a singularity that moves in time as well as space. Hughes and Hulbert give a clever scheme of this type for elastodynamics problems. Their method has discretizations of the time and space derivatives plus several extra terms that give added stability which they exploit to prove a convergence theorem. They require the width of the time slabs to be of the same order as the mesh elements within the slab. A similar scheme was developed here. It has the same convergence rate in the linear case, has no extra stabilizing terms, and does not have any conditions on the width of the time slab. Numerical tests show this method is as accurate as the method of Hughes and Hulbert.

Reports:

 Approximation of an Elliptic Control Problem by the Finite Element Method, by Donald A. French and J. Thomas King, MS, Numer Functional Anal and Optimiztin.

## 28701 NEW METHODS FOR NONLINEAR Optimization

Robert B. Schnabel University of Colorado

The research objective is to develop limited memory, tensor, and new trust region methods for large, possibly sparse, nonlinearly unconstrained and constrained optimization problems, including bound constraints, equality and inequality constraints.

# 28716 MULTIDIMENSIONAL HIGH ORDER NON-OSCILLATORY NUMERICAL METHODS FOR DISCONTINUOUS PROBLEMS IN PARALLEL STRUCTURE

Chi-Wang Shu Brown University SL ASL

SC: BRL, WES

## C. Statistics and Probability

The research objective is to investigate the theoretical and computational aspects of high order nonoscillatory finite difference, finite elements, and spectral methods for multidimensional problems in nonlinear PDE's with discontinuous or nonsmooth solutions. Attempts will be made to study the Navier-Stokes equations with high Reynolds numbers and Euler equations of gas dynamics, Hamilton-Jacobi type equations in control and optimization, and semiconductor device models using numerical codes which the investigator will develop for parallel and/or vector machines to solve 2–D and 3–D problems in general geometries. These codes will also be used to study compressible turbulence

# 28735 MASSIVELY PARALLEL ITERATIVE METHODS: MULTISCALE PRECONDITIONERS AND IMPLICIT METHODS

Tony EC. Chan University of California, Los Angeles

## SL: ASL, BRL SC: WES

The objective of the research is to develop iterative methods for solving large systems of equations, resulting from discretization of elliptic and 3--D computational fluid dynamics models, which are especially suitable for massively parallel computer architectures. Investigate parallel preconditioners for accelerating convergence of the methods.

## 28799 THE QUANTUM HYDRODYNAMIC MODEL FOR SEMICONDUCTOR DEVICES

Carl L. Gardner Duke University

SL: ARO

Research will be concerned with steady state numerical simulations and analysis of 1–D quantum semiconductor device models, including resonant tunneling diodes, transistors, and superlattice devices. Special emphasis will be on analyzing nonlinear waves supported by QHD equations.

## 28908 HIGH-LEVEL PARALLEL PROGRAMMING TOOLS FOR FINITE ELEMENT ANALYSIS

Paul Wang Kent State University SC T M OM **IV Mathematics** 

The research objective is to investigate the automatic generation of parallel programs for finite element analysis through symbolic computation.

# 28916 NONLINEAR AND STOCHASTIC NUMERICAL METHODS AND THEIR APPLICATIONS

R. Catlisch

University of California, Los Angeles

The research objective is to develop and analyze nonlinear numerical methods, such as shock capturing methods, vortex methods, fast iterative and multipole methods, numerical homogenization. Also investigate stochastic numerical methods such as the random vortex method, Monte Carlo and direct simulation methods for plasma physics and transport problems, and quasi-random methods.

## **C.** Statistics and Probability

# 24557 THE CONTINUATION OF RESEARCH IN LOGISTICS READINESS, RELIABILITY AND QUALITY CONTROL

N.D. Singpurwalla George Washington University

SL: USAIS SC: AMSAA, MTL

The research objective is to conduct research in several areas relating to reliability, quality control, and logistics. Approaches and techniques from life testing methodology. Bayesian statistics, expert systems, quality control procedures and principals, Kalman filtering techniques and other tools will be utilized.

# 25347 DISTRIBUTIONS OF MEASURES OF VISIBILITY IN RANDOM FIELDS OF OBSTRUCTING ELEMENTS

Shelemyahu Zacks

State University of New York at Binghamton SC: AMSAA, BRL, WSMR

DC: AMOLAY DIGH, WOMK

An algorithm was developed for the determination of the distribution of the length of a shadow cast by obscuring elements, which constitutes a random Poisson field. For the first time an explicit algorithm for determining such distributions is available. This allows one to compute survival of moving targets, in

cases where complete visibility is required to hit the target. The above algorithm was applied to determine the distribution of the number of shadows on a line segment. Presently, work is in progress on the Hunter-Escort problem. In this problem, the Hunter may be hit by the Escort, and therefore the Hunter tries to evade the escort by employing regions which are invisible to the Escort.

#### Reports:

No. 1 in previous edition.

2. The Distribution of the Size and Number of Shadows Cast on a Line Segment in a Poisson Random Field, by S. Zacks and Gang Li, TR, Feb 91, 11 pp. AD A233 697

# 25706 EFFICIENT ALGORITHMS FOR EVALUATION OF PLANAR NETWORK RELIABILITY

#### A. Satyanarayana

Stevens Institute of Technology

The central problem in the research was the computational complexity of the all terminal reliability problem for planar networks. The approach was to study important subclasses of the planar networks in the hope of finding a polynomial time algorithm for the entire class. In a recent work, D. Vertigan showed that the problem is NP-hard, so there is little hope that an efficient polynomial algorithm will ever be found for planar networks. However, this only makes more important the discovery of significant subclasses of planar networks for which efficient algorithms can be found and the work is continuing in this direction. Specifically, a linear time algorithm was found for the class of cube-free graphs and for the class of planar Y- $\Delta$  graphs.

#### Reports:

- K-Sparse Graphs with Applications to Graph Colorings and Network Reliability, by Mohamed Khalifat, PhD Thesis, 1990, 119 pp.
- A Linear-Time Algorithm to Compute the Reliability of Planar Cube-Free Networks, by Themistocles Politof and A. Satyanarayana, *iEEE Trans on Reliability* 39,556(1990). AD A232 047

# **25819** TOPICS IN THE SEQUENTIAL DESIGN OF EXPERIMENTS

Michael B. Woodroofe University of Michigan

#### SC: WSMR

After several false starts, efforts have finally produced an understanding of conditions under which

## C. Statistics and Probability

very weak expansions may be used to produce numerically accurate corrections to confidence intervals after sequential testing: The stopping boundaries must be reasonably smooth. Then the simple procedure outlined in the proposal produces remarkably accurate corrections to confidence intervals. It does not appear to work well when the stopping region has sharp corners. The details have been worked out for the case of a smoothly truncated sequential probability ratio test. The more challenging case of repeated significance tests remains. A paper on the sequential probability ratio test was completed.

Reports:

No. 1-5 in previous editions.

- 6. Nonparametric Bayes Estimation of a Distribution Function with Truncated Data, by Mauro Gasparini, MS, Ann Stat.
- 7. A Martingale Proof of Normality for Wei's Biased Coin Design, by Jeffrey Eisele and Michael Woodroofe, MS, Ann Stat.
- 8. A Local Limit Theorem for Perturbed Random Walks, by Mei Wang, MS, Stat & Camp: Prob Let.

# 25836 ORDER STATISTICS AND NONPARAMETRIC STATISTICS

Herbert A. David Iowa State University of Science and Technology

#### SC: BRL, MTL

Ranking by row-sum scores in the case of balanced paired-comparison experiments was generalized to unbalanced experiments in David (1987). Statistical properties of the proposed scores and associated tests of significance are developed in Andrews and David (1990), where extensions to unbalanced ranked data are also treated. A brief account of this work is given in a paper and a possible generalization is introduced and examined. The simple methods here advanced make no assumptions on the pair wise preference probabilities. A secondary aim of the paper is to provide a review of competing methods also involving no such assumptions as well as of related methods requiring only mild assumptions.

#### Reports:

No. 1-7 in previous editions.

- Nonparametric Methods of Ranking From Paired Comparisons, by H.A. David and D.M. Andrews, MS.
- Comparing Two Groups of Ranked Objects by Pairwise Matching, by Jingyu Liu and H.A. David, MS, J Appl Prob.

## 26108 SOME PROBLEMS IN DENSITY ESTIMATION, MODELING AND TIME SERIES

James R. Thompson Rice University

SL: BRL

#### SC: ETL

Researchers have continued their collaboration on business related applications of the simulation based parameter estimation algorithm, SIMEST, of the P.I. Marketing data on microcomputer related products has proved a fruitful information source. Work has been done on computationally efficient iterative algorithms for estimating the parameters of an autoregressive process and on multivariate density estimation. The P.I. has continued his work in model building. His fourth book, Nonparametric Function Estimation, Modeling, and Simulation, recently published with SIAM, shows how modeling and simulation naturally follow the exploratory nonparametric function estimation step. He is currently working on a new book in process control and productivity.

## 26144 MULTIDIMENSIONAL SIGNALS, DATA, AND PROCESSES

Jean Walrand

University of California, Berkeley

The issue of call acceptance in virtual circuit ATM networks is complex because of the bursty nature of the traffic. The goal here is to design a call setup and routing algorithm that guarantees and preserves statistical bounds on the fraction of calls lost and/or probability of buffer overflow. The method proposed for call acceptance and routing does not require parameters describing the statistics of the traffic. During call setup, each switch delivers to the router estimates of the probability of buffer overflow if the new call were added to one of its outgoing links. The algorithm then routes the call by using these estimated probabilities as the link metric. If the estimated probability of buffer overflow on a link of the optimal route is greater than a threshold, the call is refused. The problem for each buffer is, therefore, to estimate what this loss probability becomes if the new call is added to its input. These estimates are obtained by monitoring what is currently in the buffer and extrapolating. Arguments are made for the validity of the extrapolation method for two models of the call processes: batch Poisson and Markov modulated Poisson. Also, simulations were performed using Markov modulated Poisson sources to verify the algorithm.

# 26394 TIME SERIES ANALYSIS AND MULTIVARIATE ANALYSIS

Theodore Anderson Stanford University

SC: AMSAA, BRL, ETL,

WSMR

The principal investigator with Raul P. Mentz has been studying iterative methods for estimating the parameters of a Gaussian moving average process of order 1. These procedures yield the exact maximum likelihood estimates. Efficient calculation is based on the calculation of quadratic forms of relevant matrices in the time domain and the traces of related matrices in the frequency domain. The principal investigator has been studying goodness of fit tests for normalized spectral distributions. The difference between the sample and process spectral distributions is asymptotic equivalent to the sum of a Brownian bridge and a normal variate times a certain function. Asymptotic distributions of some goodness of fit criteria were characterized. A very general asymptotic distribution for autocorrelation was derived.

Reports.

No. 1-2 in previous editions.

- Theory and Applications of Elliptically Contoured and Related Distributions, by T.W. Anderson and Kai-Tai Fang, TR, Sep 90, 28 pp. AD A230 672
- Iterative Procedures for Exact Maximum Likelihood Estimation in the First-Order Gaussian Moving Average Model, by T.W. Anderson and R.P. Mentz, TR, Nov 90, 57 pp. AD A230 812
- 5. The Asymptotic Distributions of Autoregressive Coefficients, by T.W. Anderson, TR, Apr 91, 21 pp. AD A238 538

# 26649 SOJOURNS, EXTREMES AND SELF-INTERSECTIONS OF STOCHASTIC PROCESSES

Simeon Berman

New York University Courant Institute of Mathematics

Let p(x) and q(y) be density functions on the real line, and form the convolution  $(p^*q)(x)$ . The problem considered in a paper is the determination of the asymptotic form of  $(p^*q)(x)$  for  $x \rightarrow \infty$  or  $x \rightarrow b$ , where *b* is the least upper bound of the support of  $(p^*q)$ , on the basis of the asymptotic forms of p(x) and q(x), for  $x \rightarrow \infty$  or  $x \rightarrow b$ . In particular, the focus is on the case where *p* and *q* are different orders of magnitude for large *x*. Three cases are considered: (*a*) p(x) and q(y)have support unbounded above, (*b*) p(x) has support unbounded above, and q(y) has support bounded above, and (*c*) p(x) and q(y) have support bounded above.

Reports:

No. 1-4 in previous editions.

- The Tail of the Convolution of Densities and its Application to a Model of HIV-Latency Time, by Simeon M. Berman, MS, Ann Prob.
- Self-Intersections and Local Nondeterminism of Gaussian Processes, by Simeon M. Berman, Ann Prob 19,160(1991).
   AD A238 813

## 26746 RANK TRANSFORMATION TEST FOR BIB DESIGNS

W.J. Conover

Texas Tech University

SC: BRL

The first objective of the research was completed. That is, the theory of rank transformations was extended to the balanced incomplete block design to show that if the data in a balanced incomplete block design are replaced by ranks, in an overall ranking over all blocks and treatments, and if the usual analysis of variance F statistic is then calculated on those ranks, then the asymptotic null distribution of F, under the null distribution of no treatment effects. has (under some very general conditions on the block effects) an asymptotic chi-square distribution divided by its degrees of freedom. This is the same asymptotic distribution the F statistic has under the usual parametric assumptions of normality and additivity of block effects, with no treatment effects. The completion of this objective was crucial to the success of the rest of the project. The derivations have been examined thoroughly to make sure that there are no flaws in them, and it is believed that they are solid. Programs for computer simulation were written in order to attain the second objective in the project, which is to compare the exact null distribution of the F statistic on ranks with the Fdistribution with t-1 and N-T-B-1 degrees of freedom, which is the exact null distribution of the Fstatistic under the classical assumptions of normality and additivity of block effects. The results of the simulation show that the classical F distribution provides a reasonable approximation in nearly all cases examined, but that for some balanced incomplete block designs exact tables are still necessary.

## 26993 MODELING PROBABILISTIC AND LOGICAL RELATIONS WITH BELIEF FUNCTIONS

Arthur P. Dempster Harvard University

SL: BRL

## C. Statistics and Probability

The research objective is to develop belief function models and associated algorithms for application to reliability, probability risk assessment, statistical inference and Gaussian linear network analyses. A coordinated investigation will be made of modeling probabilistic and logical relations with belief functions on commonly encountered models.

## 26997 INTRODUCTION TO MODERN ANALYSIS OF VARIANCE

J.W. Tukey

Princeton University

SC: ACAA, BRL, WSMR

The research objective is the development and extension of methods of analyzing data for modern analysis of variance including robust techniques, and limited randomization of experiments.

# 27381 COMPETITIVE TRADEOFF MODELING: METHODOLOGY, COMPUTATION, AND TESTING

Stephen M. Robinson

University of Wisconsin-Madison

The major activities of this research project were: (a) informing senior Army leadership of the capabilities of scenario analysis methodology and of current research and implementation efforts, (b) in cooperation with the TRADOC Analysis Command, enhancing the brigade force structure model previously developed as a test bed for this methodology, and (c) devising and implementing techniques for decomposing the large structured deterministic problems produced by scenario analysis, in order to permit numerical solution of more detailed and useful models.

## 27574 FUNCTIONAL STATISTICAL DATA ANALYSIS AND MODELING

Emanuel Parzen Texas A&M University

SC: BRL, WRAIR

The goal of developing unified approaches to statistical data analysis has achieved a significant advance which hopefully can be developed in detail in the coming year under the title "Change Analysis. Functional Statistical Analysis, and Dynamic Statistics."

#### C. Statistics and Probability

The problem of detecting and estimating change points (when a change occurs in normal means, Bernoulli probabilities, or nonparametric probability distributions) has an extensive but disorganized literature. It is regarded as a hard problem not studied by most statisticians. Attempts will be made to organize and extend known theory by using a density estimation approach rather than classical hypothesis testing approaches. All nuances of this work find application in the change problem. Therefore research on change analysis will accomplish two goals: (a) contribute to the solution of the important change problem; and (b) by applying previous research, demonstrate and popularize its usefulness to applied statisticians.

### Reports:

- Unification of Statistical Methods for Continuous and Discrete Data, by Emanuel Parzen, TR, May 90, 27 pp. AD A224 307
- Goodness of Fit Tests and Entropy, by Emanuel Parzen, TR, May 90, 13 pp. AD A224 860
- 3. Time Series, Statistics, and Information, by Emanuel Parzen, TR, Jun 90, 34 pp. AD A224 317
- 4. Comparison Change Analysis, by Emanuel Parzen, TR, Feb 91, 22 pp. AD A233 690

## 27790 OBJECT ORIENTED SEGMENTATION OF IMAGES

Jayant Shah

Northeastern University

One of the basic problems in computer vision is the problem of segmenting an image into meaningful regions. A new global model was formulated which integrates three sequential steps for segmenting an image, namely, noise filtering, local edge-detection and integration of local edges into object boundaries. The model overcomes some of the difficulties inherent in earlier global models, particularly their tendency to oversegment, and the lack of practical numerical algorithms for implementing them. The new model consists of two coupled elliptic functionals, one for smoothing out the noise, and the other for boundary detection. The latter is obtained by regularizing the usual pointwise thresholding employed for boundary detection. The first variation of these functionals leads to a coupled system of diffusion equations which are implemented by a simple finite difference scheme. The scheme may easily be converted into a parallel algorithm.

## 27862 TOPICS IN STATISTICAL ESTIMATION AND CONTROL

Herbert Robbins

Rutgers, The State University of New Jersey

When an individual is assigned to one of two treatments A, B on the basis of whether a pre-treatment observation  $X \le a$  or  $X \ge a$ , it is not obvious how to evaluate the effects of the two treatments on each of the two subpopulations ( $X \le a$ ) and ( $X \ge a$ ), since treatment B will not have been used on the first of these nor treatment A on the second. Under certain hypotheses, it has been shown that this can be done when the effects of the treatments are normal, binomial, or Poisson. This work is being extended to the nonparametric case when two pre-treatment observations X and X' are available for each individual. Suppose that the errors produced by various "bugs" in a computer program form independent Poisson processes with a finite total intensity. The program is tested and a bug is detected as soon as it produces an error. Can a stopping rule be found such that, with a pre-assigned confidence level, the total error intensity of the undetected bugs at the end be as small as desired? This and several other problems can be formulated in a change point model, and progress has been made in the investigation of this group of problems. In a paper, "A change point problem and some applications," the authors study three types of stopping rules, based on individual waiting times, sums of waiting times, and delayed sums of waiting times. Various inequalities and approximations are obtained for the operating characteristics of the stopping rules.

## 27868 PROBLEMS IN RELIABILITY, STATISTICS AND PROBABILITY

Jayaram Sethuraman Florida State University

SC: NVEOC

A technical report has been prepared in which an alternative concept of the role of a module, that is a part of a system, is introduced. The role of a module is defined to be the probability that the module has failed at the time of the failure of the system. The role of a module is studied under various system structures. Applications of these results to optimal allocations of modules are presented. Renyi gave a definition of a maximal correlation coefficient of bivariate distribution in 1959. Another technical re-

port gives the asymptotic distribution of the sample maximal correlation coefficient based on a sample from a discrete bivariate distribution when the marginals are independent. This result can also give the asymptotic distribution of the Fisher maximal linear correlation between two sets of random vectors which are independent.

#### Reports:

- A Study of the Role of Modules in the Failure of Systems, by Emad El-Neweihi and Jayaram Sethuraman, TR, Jul 90, 14 pp. AD A225 811
- The Asymptotic Distribution of the Renyi Maximal Correlation, by Jayaram Sethuraman, TR. Oct 90, 7 pp. AD A228 148
- On the Analysis of Grouped Survival Data Using Cumulative Occurrence/Exposure Rates, by Ian W. McKeague and Mei-Jie Zhang, TR, Mar 91, 25 pp. AD A238 219
- Singularities in Gaussian Random Fields, by T.V. Kurien and Jayaram Sethuraman, TR, Nov 90, 13 pp. AD A238 220
- A Mixed Limit Theorem for Stable Random Fields, by T.V. Kurien and J. Sethuraman, TR, Sep 90, 11 pp. AD A238 222
- Estimating and Modeling Gene Flow for a Spatially Distributed Species, by T. Burr and T.V. Kurien, TR. Jan 91, 21 pp. AD A238 221
- 7. A Constructive Definition of Dirichlet Priors, by Jayaram Sethuraman, TR, May 91, 12 pp. AD A238 689

## 27993 FAILURE DATA ANALYSIS BASED ON ENGINEERING AND GEOMETRIC PRINCIPLES

Richard E. Barlow University of California, Berkeley

Using the principle of indifference conditional on sums of transformed lifetimes researchers have obtained a class of life distributions, which is called generalized gamma. If the transform derivative is logconcave then the conditional joint density of original lifetimes is Schur-concave. Using the principle of indifference conditional on sums of lifetime maintenance costs one obtains a class of life distributions, which is called generalized Weibull. If the lifetime cost function is convex as a function of lifetime. then the conditional joint survival distribution of lifetimes is Schur-concave. Schur-concave joint survival probabilities constitute the class of life distributions which model aging. Very recently research has shown that such joint survival distributions which are continuous can be characterized as convex combinations of logarithmically-concave joint survival probabilities. In particular, assuming only that units are exchangeable with respect to lifetimes, it was shown that continuous Schur-concave joint survival distributions are convex combinations of so-called generalized Weibull distributions.

## 28309 VISUALIZATION METHODS FOR EXPLORATION OF HIGH DIMENSIONAL DATA

Edward J. Wegman George Mason University

Research has resulted in a class of nonparametric density estimators on a low dimensional space. The support of these estimators is defined by the convex hull of the set of observations. A random sample from the set of observations is used to tessellate the interior of the convex hull. The attribution of empirical probability mass to the tiles resulting from the tessellation produces a density estimate. With a set of appropriate linear constraints on the attribution of mass, the estimator is shown to be a conditional maximum likelihood estimator. Repeating this procedure, and averaging these density estimates within tiles, produces a bootstrap-like estimate of the density function. The results of this resampling and density estimation process may be presented in graphic form.

## 28679 BOOTSTRAP AND RECURSIVE PARTITIONING METHODS

Wei-Yin Loh

University of Wisconsin-Madison

SL: USAIS SC: BRL, WRAIR

The research objective is to improve methods for the selection of statistical procedures and to develop methods for classification and smooth function estimation. Resampling methods will be used for the selection problem and recursive partitioning methods for the classification and estimation problems.

### Reports:

- 1. Identification of Active Contrasts in Unreplicated Factorial Experiments, by Wei-Yin Loh, MS, Comp Stat and Data Anal.
- Tests of Fit for Regression Models, by Wei-Yin Loh and Bin Yu, MS, J Am Stat Assn.

## 28715 STOCHASTIC CONTROL AND TOPICS IN APPLIED PROBABILITY

Ioannis Karatzas Columbia University SL: NVEOC

### C. Statistics and Probability

The research objective is to investigate Gittins' index processes and the dynamic allocation problem, the stochastic control problem with partial observations of the predicted miss type and a singular stochastic control problem. The approach will use results from the theory of optimal stopping for processes with one and multidimensional time, and the notion of optional increasing paths for the dynamic allocation problem. The optimization problems utilize results on Brownian local time, time-changes, martingale problems, the theory of Markovian resolvents and semigroups, and stochastic calculus of variations.

# 28718 PERFORMANCE AND ROBUSTNESS OF SELF-TUNING AND ADAPTATION ALGORITHMS FOR IDENTIFICATION, CONTROL AND FILTERING

P.R. Kumar

University of Illinois

SC: AMSAA, TACOM

The research objective is the further development of a unified mathematical theory for the performance and robustness of self-tuning and adaptation algorithms for identification, control and filtering of discrete time linear systems of unknown order having colored noise. The research focuses on the design of algorithms which adapt not only to the system model, but also to stochastic disturbances, and then tune the system accordingly.

# 28722 OPTIMAL UNIVERSAL CODING AND DENSITY ESTIMATION

Bin Yu

University of Wisconsin Madison

SL: BRL

The research objective is the development of a mathematical theory for second order optimal universal coding. Attempts will be made to investigate the universal coding problem or, equivalently, the statistical estimation problem in terms of accumulated prediction error, taking into account both uniform quantization and dependence, and to study second order optimality in rate distortion theory and for the algorithm context.

#### Reports

- 1. Edgeworth Expansions for a Test of Fit in Regression Models, by Bin Yu, MS
- 2 Tests of Fit for Regression Models, by Wei-Yin Loh and Bin Yu, MS

- 3. On Optimal Rate Universal D-Semifaithful Coding, by Bin Yu and T.P. Speed, MS, *IEEE Trans on Info Theory*.
- Density Estimation in L<sup>4</sup> Norm for Dependent Data with Applications to Gibbs Sampler, by Bin Yu, MS, Ann Stat.

## 28743 DIFFERENTIAL GEOMETRICAL METHODS IN TIME SERIES

Nalini Ravishanker University of Connecticut

SC: BRL

The research objective is the characterization of time series models by differential geometric methods. Researchers will utilize geometric properties such as the Riemannian metric tensor, the  $\alpha$ -connections,  $\alpha$ -Riemann Christoffel curvature and statistical curvature. Relative curvature will measure severity of model nonlinearity; when nonlinearity is severe, high order correction terms will be derived. Numerous other problems will be investigated based on the geometry of various time series models.

## 28982 PROBABILITY AND STATISTICS APPLIED TO THE THEORY OF ALGORITHMS

J Michael Steele University of Pennsylvania

SC: TRADOC

The research objective is to attack a general series of problems in the probabilistic analysis of algorithms. These problems range from developing a central limit theory and a theory of large deviations for an important class of network optimization problems for multidimensional random samples to the study of empirical processes of lines. This research starts from recent work on the probabilistic theory of the traveling salesman problem, the application of the Efron-Stein inequality to the theory of algorithms, two sample matching problems, the conditioning technique of random cost linear programs, and Gibbs measures on combinatorial objects.

## 29016 STOCHASTIC ANALYSIS AND ITS APPLICATIONS

Stamatis Cambanis	
G. Kalljanpur	
M.R. Leadbetter	
University of North Carolina at	Chapel Hill
SE INVEOC	SC: MICOM

Research will be conducted on fundamental mathematical issues in stochastic analysis. Specific prob-

lems will be investigated in the areas of stochastic partial differential equations with applications to physics, nonlinear filtering and signal detection for random fields, additive stochastic set functions, and central limit theory for strongly mixing random measures and fields. The research utilizes the theories of Ito, Malliavin, Stratonovich, the general theory of stochastic processes and previous research of the principal investigators.

# D. Systems, Control, Modeling, and Artificial Intelligence

## 25264 KNOWLEDGE-BASED SYSTEMS FOR FAULT-TOLERANT CONTROL

Robert F. Stengel Princeton University

## SL: AVSCOM SC: ARDEC, TACOM

Principal objectives were to conduct an extensive analysis of robust-control solutions offered for the 1990 American Control Conference Benchmark Problem and to further explore concepts for control system synthesis. Ten controllers designed by several researchers have been compared, and the results of the stochastic-robustness analysis will be presented at the 1991 American Control Conference. Continued attention was directed at the use of artificial neural networks in system identification for adaptive control. The network's function is to present force and moment coefficients as highly coupled nonlinear functions of the state and control. An approach is being developed that allows online learning to be conducted. An extended Kalman filter estimates time histories of both the state vector and a vector of forces and moments. Together with control settings, the state estimate forms the input (feature) vector of the neural network, while the vector of forces and moments is the desired output required for training. Work continued on the implementation and testing of the feedforward network. Another objective is to incorporate "machine intelligence" in computer-aided control system design (CACSD). As such, the methods developed look toward the "next great leap" beyond existing, commercially available CACSD tools, A comprehensive computer program for designing and analyzing multidisciplinary flight control systems has been chosen as a focal point. The flight CAD program will contain a variety of modeling, synthesis, simulation and evaluation alternatives. The program will be organized around a desktop metaphor that takes advantage of unique capabilities of the NeXT Computer. For the first demonstration of capabilities, a direct digital synthesis technique will be employed; it will produce a proportional-integralfilter controller with scheduled linear-quadratic-Gaussian gains. Tight following of commands will be assured by a forward-loop command generator tracker, and the controller with be sufficiently robust to account for specified levels of parameter uncertainty, the use of artificial neural networks for efficient gain scheduling also will be examined. A principal feature of the control design package will be the enhanced ability to iterate and search during the modeling, design, and analysis process.

## Reports:

No. 1-2 in previous editions.

- Intelligent Failure-Tolerant Control, by Robert E Stengel, IEEE Control Systems P14, Jun (1991). AD A238-581
- 4. Stochastic Performance Robustness of Aircraft Control Systems, by Laura Ryan Ray and Robert E Stengel, MS.
- 5. Systematic Methods for Knowledge Acquisition and Expert System Development, by Brenda L. Belkin and Robert E Stengel, MS.
- Computer-Aided-Analysis of Linear Control System Robustness, by Laura Ryan Ray and Robert F. Stengel, MS.
- Computer-Aided Design of Flight Control Systems, by Robert E. Stengel and Subrata Sircar, *Proc. of 1991 AIAA Guidance*, *Navigation, and Control Conference*, Am Inst of Aeronautics, 1991, 7 pp.
- Rule-Based Guidance for Vehicle Highway Driving in the Presence of Uncertainty, by Axel Niehaus and Robert E Stengel, MS.
- A System Identification Model for Adaptive Nonlinear Control, by Dennis J. Linse and Robert E Stengel, MS.
- Robustness of Solutions to a Benchmark Control Problem, by Robert E. Stengel and Christopher I. Marrison, MS
- Optimal Aircraft Performance During Microburst Encounter, by Mark L. Psiaki and Robert F. Stengel, J Guidance 14,440(1991), AD A238 524
- Knowledge Based System Applications for Guidance and Control, by Brenda L. Belkin and RoSert F. Stengel, AGARD Conference Proceedings No 474, AD A238 715

## 25859 RESEARCH IN APPLIED MATHEMATICS RELATED TO IDENTIFICATION OF NOISY SYSTEMS

R.E. Kalman

University of Florida

SC: AMSAA, AVSCOM, TACOM

The research objective is to develop data-interactive prejudice-free methods to solve noisy identification problems, such as system identification from noisy time series. Algebraic rather than statistical proce-

dures will be developed using realization theory employing, for instance, Hankel matrices.

## 26656 INTELLIGENT DECISION STRATEGIES AND SOME APPLICATIONS

Rangasami L. Kashyap Purdue University

A new method was found for analyzing a natural 3 dimensional scene which combines both shape from shading ideas and random field modeling of images via a fractional model. This procedure was used to develop a classification procedure for classifying textures. The recognition procedure has some interesting invariant properties. Results reported earlier on segmentation boundaries can now be improved by using prior knowledge of the patterns expressed in terms of a procedure or rules. It has been shown that there is a considerable improvement in the quality of segmentation by using these rules. Work has continued on the development of algorithms for combining several evidences about a hypothesis where each evidence is expressed as a numerical interval of the probability of the hypothesis being correct.

#### Reports:

No. 1-3 in previous editions.

- 4. Composite Edge Detection with Random Field Models, by Kie Bum Eom and Rangasami L. Kashyap, *IEEE Trans on Systs, Man. & Cybernetics* 20,81(1990). AD A224 313
- Geometric Reasoning for Recognition of Three-Dimensional Object Features, by M. Marefat and R.L. Kashyap, *IEEE Trans on Pattern Anal Mach Intelligence* 12,949(1990). AD A232 259
- Modeling, Estimation, and Pattern Analysis of Random Texture on 3–D Surfaces, by Yoonsik Choe and R.L. Kashyap, TR, Jan 91, 175 pp. AD A231 849

## 26674 P.D.E., DIFFERENTIAL GEOMETRIC AND ALGEBRAIC METHODS IN NONLINEAR FILTERING

Stephen Yau

University of Illinois at Chicago

SC: AMSAA

Ever since the technique of the Kalman-Bucy filter was popularized, there has been an intense interest in finding new classes of finite dimensional recursive filters. In the late seventies, the concept of the estimation algebra of a filtering system was introduced. It has proven to be an invaluable tool in the study of nonlinear filtering problems. A paper has been prepared in which a simple algebraic necessary and sufficient condition is established for estimation algebra of a special class of filtering systems to be finite-dimensional. Also presented is a rigorous proof of the Wei-Norman program which allows one to construct finite-dimensional recursive filters from finite dimensional estimation algebras.

Reports:

No. 1–3 in previous editions.

4. Structure and Classification Theorems of Finite Dimensional Exact Estimation Algebras, by Rui-Tao Dong et al., MS, *SIAM J Control and Optmztn.* 

# 26736 STUDIES IN ESTIMATION THEORY. APPLICATIONS AND IMPLEMENTATIONS

Thomas Kailath

Stanford University

SL: ARDEC

Work on displacement structure is being continued by developing a whole new approach to this class of problems, based on a state-space formulation. This has allowed for a more generalized displacement structure corresponding to equations of the form  $\Omega R \Delta^* - F R A^* = G J B^*$ . This approach leads to a unified algorithm for the factorization of matrices with Toeplitz-like or Hankel-like structures. These recursive algorithms are being extended to deal with structured matrices that are not necessarily strongly regular. Special cases of the recursive algorithm are closely connected to the theory of Reproducing Kernal Hilbert Spaces, as recently developed by deBranges, Dvm and Alpay.

Reports:

- No. 1 in previous edition.
- Fast Algorithms for Structured Matrices with Arbitrary Rank Profile, by Debajyoti Pal, PhD Thesis, 1990, 211 pp.
- On Gaussian Feedback Capacity, by Amir Dembo, IEEE Trans on Info Theory 35,1072(1989), AD A219-141
- Simple Proof of the Concavity of the Entropy Power with Respect to Added Gaussian Noise, by Amir Dembo, *IEEE Trans on Info Theory* 35,887(1989).
- Some New Algorithms for Reconfiguring VLSI/WSI Arrays, by Theodora Varvarigou et al., 1990 Proc Intl Conf on Wafer Scale Integration, 1990, 229. AD A226 095
- 6. Approximate AR Modeling: An Alternative to Regularization via Schur Algorithm for Matrices with Arbitrary Rank Profile, by Debajyoti Pal and Thomas Kailath, MS.
- 7. A Generalization of the Schur-Cohn Test: The Singular Cases, by Debajyoti Pal and Thomas Kailath, MS.
- FAST ESPRIT Application of Fast Signal Subspace Decomposition in Array Processing, by Guanghan Xu et al., MS.
- 9. Parallel Implementation and Performance Analysis of Subband

Signal Subspace Algorithms, by Seth D. Silverstein et al., MS.

- 10. Fast Signal Subspace Decomposition Without Eigendecomposition, by Guanghan Xu and Thomas Kailath, MS.
- 11. Obtaining Schedules for Digital Systems, by H.V. Jagadish and T. Kailath, MS. IEEE Trans on Acoust, Speech, and Signal Proc.
- 12. A Simple and Effective Algorithm for Estimating Time Delay of Communication Signals, by Guanghan Xu and Thomas Kailath, MS
- 13. A Fast Algorithm for Signal Subspace Decomposition and Its Performance Analysis, by Guanghan Xu and Thomas Kailath. Proc 1991 Intl Conf on Acoustics, Speech and Signal Processing. IEEE, 1991, 3069
- 14. Parallel Implementation and Performance Analysis of Beamspace ESPRIT, by Guanghan Xu et al., Proc 1991 Intl Conf on Acoustics. Speech and Signal Processing, IEEE, 1991, 1497.
- 15. On the Ptak-Young Generalization of the Schur-Cohn Theorem, by Reuven Ackner and Thomas Kailath, MS, IEEE Trans on Auto Control
- 16. The Nevanlinna Algorithm for Scalar Meromorphic Functions, by Reuven Ackner et al., MS, Math Control Signals Systems.
- 17. The Schur Algorithm for Scalar Meromorphic Functions, by Reuven Ackner et al., MS, IEEE Trans on Circuits and Systs.
- 18. This number not used.
- 19. Fast Decomposition of the Principal Eigenspace via Exploitation of Eigenvalue Multiplicity, by Guanghan Xu and Thomas Kailath, MS, SIAM J Matrix Anal Appl.
- 20. Reconfiguring Processor Arrays Using Multiple-Track Models, by Theodora A. Varvarigou et al., MS, IEEE Trans on Comp
- 21. State-Space Approach to Factorization of Lossless Transfer Functions and Structured Matrices, by H. Lev-Ari and T. Kailath, MS, Linear Alg and its Appl.
- 22. Fast Signal-Subspace Decomposition --- Part I: Ideal Covariance Matrices, by Guanghan Xu and Thomas Kailath, MS, IEEE Trans on Acoust, Speech, and Signal Proc.
- 23. Fast Signal-Subspace Decomposition Part II: Sample Covariance Matrices, by Guanghan Xu and Thomas Kailath, MS. IEEE Trans on Acoust, Speech, and Signal Proc.
- 24. Onsager Machlup Functionals and Maximum a Posteriori Estimation for a Class of Non Gaussian Random Fields, by Amir Dembo and Ofer Zeitouni, MS, J Multivariate Anal.
- 25. Fast Algorithms for Computing the Principal Singular Values and Vectors, by Guanghan Xu and Thomas Kailath, MS.

## 27044 THE DESIGN AND ANALYSIS OF **ROBUST FEEDBACK SYSTEMS**

Pramod P. Khargonekar University of Michigan

#### SL: ARDEC SC: AMSAA

Researchers have worked on robust and  $H^{x}$  control theory and obtained some significant results. Efforts so far have been focused on the  $H_2H^{\times}$  problem which presents the problem of optimal nominal performance subject to a robust stability constraint, extensions of the recent state-space H<sup>x</sup> control theory, and on the problem of identification in H<sup>\*</sup>. Solution to the robust performance problem --- guaranteed performance in the face of plant uncertainty — has been the goal of robust multivariable control theory over the last decade. Despite much progress in this area, the robust performance problem has turned out to be very difficult still awaiting a complete analytical solution. Consequently, it is important to consider simpler related problems which may yield insights into solving the robust performance problem.

Reports:

No. 1-10 in previous editions.

- 11. H<sub>2</sub> Optimal Control for Sampled-Data Systems, by Pramod P. Khargonekar and N. Sivashankar, MS, Systs and Control Let.
- 12. Robust Stability and Performance Analysis of Sampled-Data Systems, by N. Sivashankar and Parmod P.P. Khargonekar, MS, IEEE Trans on Auto Control.
- 13.  $L_x$ -Induced Norm of Sampled-Data Systems, by N. Sivashankar and Parmod P. Khargonekar, MS.
- 14. A Class of Algorithms for Identification in H\*, by Guoxiang Gu and Pramod P. Khargonekar, MS.
- 15. Decentralized Control and Periodic Feedback, by Pramod P. Khargonekar and A. Bulent Ozguler, MS.
- 16. Decentralized Simultaneous Stabilization and Reliable Control Using Periodic Feedback, by Konur A. Unyelioglu et al., MS, Systs and Control Let.
- 17. A Class of Algorithms for Identification in Hx: Continuous-Time Case, by Huseyin Akcav et al., MS. IEEE Trans on Auto Control.

# **27365** AN INTERPOLATION THEORETIC APPROACH TO THE ROBUST CONTROL OF DISTRIBUTED AND NONLINEAR **SYSTEMS**

Allen Tannenbaum

University of Minnesota, Minneapolis SL: ARDEC

SC: AMSAA

Work has been concerned with a broad research program for the study of the robust control of systems using functional analysis and interpolation theory. In particular, a new interpolation method was developed which is not norm-based which has arisen out of research into the robust design of systems with structured uncertainty. This new type of interpolation scheme should lead to important new directions in operator theory as well. Extensive research was performed on the use operator theoretic methods in H<sup>\*</sup> optimization theory. This involves an interesting class of operators called skew Toeplitz, which

## E. Logistics and Operational Methods

seem ideally suited for studying  $H^{x}$  design problems, especially for distributed systems. These methods are quite powerful since they allow one to do design just using the input/output operators. This has led to an explicit solution of the four block problem for large class of multivariable distributed systems. (This is the most general Hx; optimization problem.) This method has been applied to certain problems in aircraft control. H<sup>\*</sup> techniques have now also been implemented for sampled-data systems using a lifting approach. A large portion of the research effort was also devoted to nonlinear systems. This has led to an iterative competent lifting theorem which gives an explicit design procedure for nonlinear systems and captures the H<sup>x</sup> control problem in the nonlinear framework.

#### Reports:

- 1. Causality in Competent Lifting Theory, by Cipcian Foias and Allen Tannenbaum, MS, J Am Math Soc.
- 2. Abstract Model and Controller Design for an Unstable Aircraft, by Dale Enns et al., MS. J Guidance Control Dynamics.
- 3. Mixed Sensitivity Optimization for a Class of Unstable Infinite Dimensional Systems, by Hitay Ozbay et al., MS, SIAM J Control and Optimztn.

## 28511 ROBUST HYBRID STATE-SPACE SELF-TUNING CONTROL USING DUAL-RATE SAMPLING

L.S. Shieh

C.K. Koc University of Houston

SL: ARDEC

A paper has been prepared which presents a multistage design scheme for determining an optimal control moment gyro momentum management and attitude control system for the Space Station Freedom. First, the space station equations of motion are linearized and then block decomposed into two block decoupled subsystems using the matrix sign algorithm. Next, a sequential design procedure is utilized for designing a linear quadratic regulator for each subsystem, which optimally places the eigenvalues of the closed-loop subsystem in the region of an open sector, bounded by a line included at  $\pm x2k$  (for k=2 or 3) from the negative real axis and the left hand side of a line parallel to the imaginary axis in the s plane. Simulation results are presented to compare the resultant designs. Another paper considers the problem of optimal regulator design of linear multivariable systems with prescribed pole locations and/or poles corresponding to specified relative sta-

## **IV Mathematics**

bility A sequential method based on the frequencydomain optimality condition is proposed for achieving the desired pole assignment and determination of the corresponding quadratic performance index. This design method enables the retention of some stable open-loop poles and the associated eigenvectors in the closed-loop system. An illustrative example is provided to demonstrate the effectiveness of the proposed method.

## 28835 RAPID PROTOTYPING OF NONLINEAR CONTROLLER DESIGNS

Shankar Sastry Andrew Packard University of California, Berkeley

SL: AERO DIR, ARDEC

The research objective is to investigate the robustness of nonlinear and adaptive control schemes for electromechanical systems with emphasis on rapid prototyping, design and implementation of algorithms for nonlinear problems. A study will be made of the robustness of linearization of nonlinear regulators and approximate linearization of nonholonomically constrained systems. The techniques will involve a fusion of methods from nonlinear control, classical mechanics along with advanced graphics simulations.

## E. Logistics and Operational Methods

## 23908 SIGNAL PROCESSING ALGORITHMS FOR HETEROGENEOUS ARCHITECTURES

M.J. Irwin

R.M. Owens

The Pennsylvania State University

SC: ARO, ETDL

Work is in progress to complete a hardware prototype of the Arithmetic Cube II. Initial versions of the full custom CMOS chips used in the cube have been designed, fabricated, and tested. Final versions have been designed and await fabrication. While the National Science Foundation is funding the actual construction of the Arithmetic Cube II, algorithm development for the cube has been done with ARO support. Since the cube is not yet available, a simulator has been used for algorithm development. This simulator uses a VHDL description of the Cube. Since the cub is synthesized from this same VHDL description, the simulator accurately reflects the Cube

at the bit level. Algorithms have been developed for linear transformations like the discrete Fourier transform and different cyclic convolutions. In the area of very fine grained architectures, the investigation has continued into a new two-dimensional shared logic architecture. Like other existing shared logic architectures, each processor in the new architecture is a content addressable memory (CAM). While it is generally recognized that CAM based architectures are suitable for applications requiring pattern matching, it is often overlooked that CAM based architectures can also be suitable for applications requiring arithmetic operations. In this situation each CAM cell functions as a arithmetic processor. Since each CAM cell is relatively small, many CAM cells can be implemented on a single chip. This results in a chip which contains thousands of SIMD arithmetic processors. An initial version of one CAM cell has been designed. A full version of the CAM architecture is in design. In the area of image recognition algorithms have been developed. They are based on the concepts of local-distance diagrams, dynamic programming, and the minimum principle. The first algorithm is used to find the minimum distance between two areas. The second algorithm is used to find the minimum distance between a line and an area.

Reports:

No. 1-12 in previous editions,

 Being Stingy with Multipliers, by Robert Michael Owens and Mary Jane Irwin, *IEEE Trans on Comp* 39,809(1990). AD A228 059

## 25324 NEURAL NET ARCHITECTURE FOR COMPUTING STRUCTURE FROM MOTION

Josef Skrzypek University of California, Los Angeles SL: ETDL SC: BRL

Simulating neural models requires the ability to analyze and process architectures of varying complexity. Structured neural nets are characterized by highly regular structures processing simple yet massively parallel data, while other neural models deal with abstract data processed by irregular architectures. SFINX offers a simulation environment for modeling a wide spectrum of neural architectures with both regular and irregular connectivity patterns. SFINX is not based on a specific neural paradigm; it supports a variety of computational models ranging from simple convolution filters such as Difference of Gaussians receptive fields used in image processing to learning paradigms such as Backward Error Propagation.

Reports:

No. 1-5 in previous editions.

- Categorizing Visual Stimuli: Specification of a Neural Network Architecture, by Josef Skrzypek and Valter Rodrigues, MS.
- 7. Peripheral-Motion-Triggered Attention, by Josef Skrzypek and Michael Stiber, MS.
- Dynamics of Clustering Multiple Back Propagation Networks, by William P. Lincoln and Josef Skrzypek, MS.
- A Tool for Simulating Neural Models, by Edmond Mesrobian and Josef Skrzypek, MS.

## 25514 COMPUTATIONAL TECHNIQUES FOR PROBABILISTIC INFERENCE

Edward H. Shortliffe Greg Cooper Stanford University

#### SL: SWC SC: AIRMICS

The acquisition and application of probabilistic models may be facilitated significantly by having a system that can explain belief-network inference. For example, an expert can use automatic explanations of test-case results as feedback during the beliefnetwork acquisition process. An explanation system also could provide additional insight about inference results to the end user of a probabilistic expert system. Currently, experiments are being conducted with methods that evaluate the influence of the structure of a belief network on the propagation of evidence. Structural information is used to explain why the probabilistic-inference results follow from the evidence in test cases. Such explanations can guide the process of editing and refining belief-network structures and probabilities.

Reports:

No. 1–14 in previous editions.

- A Randomized Approximation Analysis of Logic Sampling, by R. Martin Chavez and Gregory E Cooper, Proc of Conf on Uncertainty in Artificial Intelligence, 1990, 130. AD A226 226
- Ideal Reformulation of Belief Networks, by John S. Breese and Eric H. Horvitz, Proc of Conf on Uncertainty in Artificial Intelligence, 1990, 64, AD A225 900
- A Combination of Cutset Conditioning with Clique-Tree Propagation in the Pathfinder System, by H.J. Suermondt et al., *Proc of Conf on Uncertainty in Artificial Intelligence*, 1990, 273. AD A226 081
- An Empirical Analysis of Likelihood-Weighting Simulation on a Large, Multiply Connected Belief Network, by Michael Slowe and Gregory Cocpet. Proc. of Conf. on Uncertainty on Artificial Intelligence, 1990, 498. AD A226 241

#### E. Logistics and Operational Methods

- Kutato: An Entropy-Driven System for Construction of Probabilistic Expert Systems from Databases, by Edward Herskovits and Gregory Cooper, Proc of Conf on Artificial Intelligence, 1990, 54. AD A225 944
- 20. A Probabilistic Reformulation of the Quick Medical Reference System, by Michael Shwe et al., MS.
- 21. A Probabilistic Reformulation of QMR, by Michael Shwe, MS Thesis, 1990, 45 pp.
- A Bayesian Method for the Induction of Probabilistic Networks from Data, by Gregory E Cooper and Edward Herskovits, MS.
- Architectures and Approximation Algorithms for Probabilistic Expert Systems, by Ramon Martin Chavez, PhD Thesis, 1990, 203 pp.
- 24. A Combination of Exact Algorithms for Inference on Bayesian Belief Networks, by H.J. Suermondt and G.F. Cooper, MS, *Intl J Approx Reasoning*.
- 25. Computation and Action Under Bounded Resources, by Eric Joel Horvitz, PhD Thesis, 1990, 281 pp.
- KNET: Integrating Hypermedia and Normative Bayesian Modeling, by R. Martin Chavez and Gregory E. Cooper, Uncertainty in Artificial Intelligence 4, 1990, 339. AD A232 565

## 25662 REAL-TIME IMAGE PROCESSING ARCHITECTURES FOR PERCEPTUAL GROUPING, DEPTH SEGREGATION, AND OBJECT RECOGNITION

Stephen Grossberg Boston University

SL: ETDL, MICOM,	SC: CRDEC
NVEOC	

The most important new results concern further progress towards understanding biological motion perception and its relationship to form perception. Researchers have discovered new computational principles and are rapidly developing a neural network theory that is providing a unified explanation of many heretofore unexplained perceptual and neurobiological data. This theory embodies novel nonlinear dynamical systems, new ideas about geometry and statistical decision theory, and new concepts about rapidly resettable, yet coherent, parallel computation.

#### Reports:

No. 1-7 in previous editions.

 Cortical Dynamics of Visual Motion Perception: Short-Range and Long-Range Apparent Motion, by Stephen Grossberg and Michael E. Rudd, MS.

# 26438 INVESTIGATIONS OF LOGIC OF RETROSPECTION AND RELATED MODES OF REASONING WITH APPLICATIONS

#### Wiktor Marek

University of Kentucky

SL: BRL

SC: CECOM

#### **IV Mathematics**

Investigations of properties of formalisms for nonmonotonic and commonsense reasoning were continued. Main topics of the research were: Modal nonmonotonic logics: Characterizations of nonmonotonic consequence operator for various modal logics were investigated. Algorithms were designed for computing nonmonotonic consequences and studied complexity. Complexity issues in nonmonotonic reasoning: The complexity of computing intersection of autoepistemic expansions of modal theories was studied. In a separate project descriptions of classes of stable models of logic programs are being considered. Ground modal nonmonotonic logics: A variant of modal nonmonotonic logic is being investigated in which "negation as failure to prove" is restricted to modal-free formulas.

#### Reports:

No. 1-2 in previous editions.

- 3. A Theory of Nonmonotonic Rule Systems I, by W. Marek et al., *Ann Math and Artificial Intelligence* 1,241(1990). AD A232 184
- 4. A Theory of Nonmonotonic Rule Systems II, by W. Marek et al., MS, Ann Math and Artificial Intelligence.
- Modal Nonmonotonic Logic with Restricted Application of the Negation as Failure to Prove Rule, by Mirosław Truszczynski, MS.
- Modal Nonmonotonic Logics: Ranges, Characterization, Computation, by Wiktor Marek et al., MS.
- 7. Disjunctive Defaults, by Michael Gelfond et al., MS.
- 8. Pure Logic of Necessitation, by M.C. Fitting et al., MS.
- 9. Modal Interpretations of Default Logic, by Moroslaw Truszczynski, MS.

# 26487 AN INFORMATION THEORETIC APPROACH TO RULE BASED EXPERT SYSTEMS

Rodney M. Goodman

California Institute of Technology

SL: ARI SC: AIRMICS, SWC

The field being developed is the application of information and communications theory techniques to the design and analysis of real time rule-based expert systems. A novel information theoretic approach to the design of rule-based expert systems has been developed in which one can automatically extract an explicit model of the data in the form of rules, automatically load the model into an expert system shell, or onto the weights and nodes of a neural network, and then run the network to perform fast real-time probabilistic inference on unseen data. Work is in progress in developing an information theoretic approach to the following areas: (a) automatic derivation of generalized rule graphs from real world example data; (b) handling uncertain information and how uncertainty propagates through inference (uncertainty calculus); (c) knowledge representation from example data; (d) controlling and guiding the inference process; (e) fast parallel execution using neural networks.

Reports:

No. 1-5 in previous editions.

- 6. Decision Tree Design Using Information Theory, by Rodney M. Goodman and Padhraic Smyth, MS.
- An Information Theoretic Approach to Rule Induction from Databases, by Padhraic Smyth and Rodney M. Goodman, MS.
- The Information Content of a Probabilistic Rule, by Padhraic Smyth and R.M. Goodman, MS, *IEEE Trans on Info Theory*.
- 9. Rule Induction Using Information Theory, by Padhraic Smyth and R.M. Goodman, MS.
- A Polynomial Time Algorithm for Finding Bayesian Probabilities from Marginal Constraints, by John W. Miller and R.M. Goodman, MS.
- 11. Rule Based Networks for Classification and Probability Estimation, by R.M. Goodman and John Miller, MS.
- 12. Automated Knowledge Acquisition From Network Management Databases, by R.M. Goodman and H. Latin, MS.
- 13. Texture Classification Using Information theory, by Rodney M. Goodman and H.K. Greenspan, MS.
- 14. Incremental Learning with Rule-Based Neural Networks, by C.M. Higgins and R.M. Goodman, MS.
- 15. Texture Analysis via Unsupervised and Supervised Learning, by H. Greenspan et al., MS.
- Fuzzy Control Using Rule-Based Neural Networks, by Rodney M. Goodman and Charles M. Higgins, MS.
- A Combined Neural Network and Rule Based Framework for Pattern Recognition, by Rodney M. Goodman and H.K. Greenspan, MS.
- Rule-Based Neural Networks for Classification and Probability Estimation, by Rodney M. Goodman et al., MS, Neural Computation.
- 19. Incremental Rule-Based Learning, by Rodney M. Goodman and C.M. Higgins, MS.

## 26779 ARTIFICIAL INTELLIGENCE CENTER OF EXCELLENCE

Aravind K. Joshi Norman I. Badler Ruzena Bajcsy University of Pennsylvania

SL: MICOM

An AI Center has been established to integrate and coordinate various research efforts in AI in which the University has excellent strengths. The key thrusts are in the following areas: (a) natural language processing: language and speech; (b) machine perception and robotics: exploration and perceptual development; (c) task oriented computer animation; (d) programming structures for databases and knowledge bases; and (e) parallel processing in Artificial Intelligence.

Reports:

No. 1-11 in previous editions.

- Machine Systems for Exploration and Manipulation a Conceptual Framework and Method of Evaluation, by Ruzena Bajcsy et al., TR, Jan 89, 30 pp. AD A225 896
- The Relevance of Connectionism to AI: A Representation and Reasoning Perspective, by Lokendra Shastri, TR, Jan 89, 35 pp. AD A225 898
- 14. A Connectionist System for Rule Based Reasoning with Multi-Place Predicates and Variables, by Lokendra Shastri and Venkat Ajjanagadde, TR, Jan 89, 31 pp. AD A225 897
- 15. Qualitative Simulation of Ordinary and Intermittent Mechanisms, by Pearl Pu, PhD Thesis, Jan 89, 176 pp.

# 27567 MOTION PLANNING AND SENSORY PROCESSING IN A DYNAMIC ENVIRONMENT

Ren C. Luo

David W. Histop

North Carolina State University

The research as been extended in both the motion planning and sensory processing realms. The implementation of the MARGE Mobile Autonomous Robot for Guidance experiments has progressed to a degree where experimentation is possible. The vehicle is now able to navigate through dead-reckoning and a global data base. The vehicle has been tested in the laboratory for accuracy and compensation of vehicle limitations through software and sensory feedback. The path planning subsystem is also operational, providing efficient paths given the geometric representation of the work environment. The image processing system. consisting of 3 boards arrived in November 1990. The system is comprised of a frame acquisition board, a frame buffer, and an image processing board. The boards were installed and tested on the host computer. The MARGE vision system is not functional. The hardware modifications using a structure for allowing flexible camera adjustment are underway.

# 27892 CONTINUATION OF THE POSTGRES PROJECT

Michael Stonebraker University of California, Berkeley SL: SWC, TRADOC SC: SWC

## E Special Projects

The research objective is the implementation of a rule management system that allows POSTGRES (a next generation database management system developed in part under an ARO contract) to handle the special rules of relational database systems. Query modification algorithms and special syntax will be added to support the multiple views of data contained in a database. These query modifications which themselves are a collection of rules would allow for query rewrite which would facilitate the processing of conventional relational views.

## 28131 HUMAN BODY MODELING AND SIMULATION

Norman I. Badler University of Pennsylvania

SL: HEL, NRDEC

Jack is a workstation-based system for the definition, manipulation, animation, and human factors performance analysis of simulated human figures. Built on a powerful representation for articulated figures, Jack offers the interactive user a simple, intuitive, and yet extremely capable interface into any 3-D articulated world. Jack incorporates sophisticated systems for anthropometric human figure generation, multiple limb positioning under constraints, view assessment, and strength model-based performance simulation of human figures. Geometric workplace models may be easily imported into Jack. Various body geometries may be used, from simple polyhedral volumes to contour-scanned real figures. High quality graphics of environments and clothed figures are easily obtained. A biomechanically correct, 17 segment vertebral spine and torso geometry was designed and integrated into Jack. Both polyhedral bodies and biostereometric (high resolution) bodies may be manipulated with natural torso bending and motion ranges. The flexible spine is the most significant enhancement to body modeling to date and places Jack far beyond any other commercial or proprietary human modeling system of similar intent or scope. The flexible spine was combined with the reach and constraint mechanism in Jack to permit a number of very natural-looking behaviors including pelvis rotation, stepping, and weight shifting. Critical to the success of these interactive manipulations is the treatment of the figure's center of mass as just another end effector to be manipulated by kinematics or inverse kinematics. A fully articulated hand was added to jack and implemented an automatic hand grasp, 3 grip types, rather arbitrary grasped object

## **IV Mathematics**

geometry, and contact based on collision detection. The hand is positioned to the major axis of the target object by Jack's inverse kinematics procedure using a palm to object position and orientation constraint. The actual grip is determined by moving the fingers until object contact is achieved. No consideration of friction is included, however.

# 28328 AUTOMATICALLY COMBINING CHANGES TO SOFTWARE SYSTEMS

Valdis Berzins Naval Postgraduate School

SL: CECOM

The research objective is to develop means to support automatic enhancements to software systems. The operation of combining changes will be formalized using embedded lattices with Boolean algebras. The problem of inconsistencies in large software systems will be addressed by automatically, with provable correctness, combining changes or versions of systems in a mathematically provable correct way.

# 28950 ACCELERATING THE TRANSFER OF TECHNOLOGY FOR IMPLEMENTING DOMAIN SPECIFIC SOFTWARE ARCHITECTURE

Vincent P. Heuring University of Colorado

The objective of the research is to demonstrate the ELI System (an environment for automatic development of application specific software) for Domain Specific Architectures. Several Army applications/ sites are now being considered as means to move this work from the university to the Army R&D community.

## **F. Special Projects**

# 23306 CENTER OF EXCELLENCE IN THE MATHEMATICAL SCIENCES

Anil Nerode Philip J. Holmes James T. Jenkins Cornell University

SC: OASA (RDA)

S. Vavasis has solved a long-standing, open question concerning complexity of general quadratic programming. J. Bramble et al., have now made preliminary

computational tests on their Domain Decomposition Methods for problems with partial refinements and related problems, which have shown the methods to be highly effective. R. Durrett has made significant advances in cellular automata. His result on multicolor particle systems with large threshold was singledout, where the main result states that when the threshold is less than range/2k, k = number of colors, then for large r there is a very random stationary distribution. This and other results were discussed in his ICM invited talk in Tokyo. R. Zippel has given a polynomial time solution for determining when rational f(x) can be written g(h(x)), in all characteristics. M. Stillman has developed a fast algorithm for computing Hilbert functions. J. Guckenheimer has used symbolic and numerical methods (with Isabel Labouriau) to give a systematic analysis of bifurcations and phase portraits for the four dimensional Hodgkin-Huxley equations, which are the basis of most work on electrically active biological membranes. In perturbation methods for convex polyhedra, Kahn has shown that there exists a family of perturbations rich enough to "correct" small errors due to roundoff in intersecting a convex polyhedron with a plane. A. Nerode and A. and V. Yakhnis have developed a potentially very powerful mathematical too' for concurrent program development and verification, to a point where it can be tried out on practical problems. A. Nerode, J. Remmel, and W. Marek have established firm foundations and many theorems for most of the area called nonmonotonic logics, of potential use in many areas of robot planning, default and diagnosis for computers.

#### Reports:

No. 1-419 in previous editions

- 420. Source Apportionment with One Source Unknown, by Karen Bandeen-Roche and David Ruppert, MS.
- 421. Constructive Concurrent Dynamic Logic I, by A. Nerode and D. Wijesekera, MS.
- 422. Exact Mean Integrated Squared Error, by J.S. Marron and M.P. Wand, MS.
- 423. Constructive Modal Logics L by D. Wijesekera, MS.
- 424. Determining Nodes, Finite Difference Schemes and Inertial Manifolds, by Ciprian Foias and Edriss S. Titi, *Nonlinearity* 4,135(1991), AD A233-590
- 425. Hidden Mixtures and Bayesian Sampling, by Christian Robert, MS.
- 426. A Paradox in Decision-Theoretic Interval Estimation, by George Casella et al., MS.
- 427. On the Dynamics of Rotating Elastic Beams, by A.M. Bloch and E.S. Titi, MS.
- 428. Realizability and Kripke Forcing, by James Lipton, MS, Ann Math and Artificial Intelligence.
- 429. Nonlinear Voter Models, by J.T. Cox and R. Durrett, MS

- 430. Stochastic Models of Growth and Competition, by Richard Durrett, MS.
- 431. Capture-Recapture Models and Bayesian Sampling, by Edward I. George and Christian P. Robert, MS.
- 432. Facts About the Normal Density, by B. Aldershof et al., MS.
- 433. The Volume of Duals and Sections of Polytopes, by P. Filliman, MS.
- 434. An Application of the Very Weak Bernoulli Condition for Amenable Groups, by Scot Adams and Jeffrey E. Steif, MS.
- 435. Global Properties of the Set of Tatonnement Stable Equilibria, by John D. Herman and Peter J. Jahn, MS.
- 436. Small Perturbations of Stressed Graphs, by Peter J. Kahn, MS.
- 437. Lambda Calculi Constructive Logics, by Anil Nerode and Pierogiorgio Odifreddi, MS.
- 438. Approximate Inertial Manifolds for Parabolic Evolutionary Equations via Yosida Approximations, by Mario Taboada, MS.
- 439. Triple Multiplicities for sl(R + 1) and Spectrum of the Exterior Algebra of Adjoint Representation, by A.D. Berenstein and A.V. Zelevinsky, MS.
- 440. Some Stability Results for Perturbed Semilinear Parabolic Equations, by Mario Taboada and Yungcheng You, MS.
- 441. Global Existence, Regularity, and Boundedness for the Kuramoto-Sivashinsky Equation in Thin 2D Domains, by George R. Sell and Mario Taboada, MS.
- 442. Infinity-Groupoids and Homotopy Types, by M.M. Kapranov and V.A. Voevodsky, MS.
- 443. On the Dynamics of Fine Structure, by J.M. Ball et al., MS.
- 444. Generalized Euler Integrals and A-Hypergeometric Functions, by I.M. Gelfand et al., MS.
- 445. A Characterization of A-Discriminantal Hypersurfaces in Terms of the Logarithmic Gauss Map, by M.M. Kapranov, MS.
- 446. Homoclinic Orbits for Eventually Autonomous Planar Flows, by P.J. Holmes and C.A. Stuart, MS.
- 447. Large Rotatory Oscillations of Transversely Isotropic Rods: Spatio-Temporal Symmetry-Breaking Bifurcation, by Timothy J. Healey, MS.
- 448. Domain Decomposition Methods for Nonselfadjoint Operators, by Zbigniew Leyk, MS.
- 449. Constructive Kripke Semantics and Realizability, by James Lipton, MS.
- 450. Rigidity and the Alexandrov-Fenchel Inequality, by P. Filliman, MS.
- 451. On the Estimation of the Exceedance Probability of a High Level, by Vincent Dijk and Laurens de Haan, MS.
- 452. A Survey of Matrix Computations, by Charles VanLoan, MS.
- 453. On a Criterion for Approximating Time-Periodic Solutions to the Navier-Stokes Equations, by Edriss Saleh Titi, C.R. Acad Sci Paris 312,41(1991). AD A234 088
- 454. Transfinite P-Adic Puiseau Expansions of Algebraic Numbers, by M.M. Kapranov, MS.
- 455. Stochastic Growth Models: Bounds on Critical Values, by R. Durrett, MS, J Appl Prob.

**F.** Special Projects

- 456. Computer Simulations of Rapid Granular Shear Flows Between Parallel Bumpy Boundaries, by M.Y. Louge et al., *Phys Fluids* A2,1042(1990). AD A230 768
- 457. Concurrent Programs as Strategies in Games, by Anil Nerode et al., MS.
- 458. Higher Order Hydrodynamic Equations for a System of Independent Random Walks, by R. Dobrushin and E. Sokolovskii, MS.
- 459. On the Number of Determining Nodes for the 2-D Navier-Stokes Equations, by Don A. Jones and Edriss S. Titi, MS, *J Math Anal and Appl.*
- 460. LRU is Better Than FIFO Under the Independent Reference Model, by J. van den Berg and A. Gandolfi, MS, *J Appl Prob.*
- 461. Multigrid Algorithms for Feynman Integrals, by Dov Bai, MS.
- 462. Reaction-Diffusion Systems Modeling Pattern Formation in the Couette Flow Reactor, by J. Elezgaray and A. Arneodo, MS, J Chem Phys.
- 463. Improving Known Solutions is Hard, by Desh Ranjan et al., MS.
- 464. Cascades of Homoclinic Orbits to, and Chaos Near, a Hamiltonian Saddle-Center, by Alexander Mielke et al., MS.
- 465. Beyond Hyperbolicity: Expansion Properties of One Dimensional Mappings, by John Guckenheimer and Stewart Johnson, MS.
- 466. Symmetry Properties of Confined Convective States, by John Guckenheimer, MS.
- 467. Resonant Surface Waves in a Square Container, by Dieter Armbruster et al., MS.
- 468. Bifurcation of the Hodgkin and Huxley Equations: A New Twist, by John Guckenheimer and I.S. Labouriau, MS.
- 469. Chow Polytopes and General Resultants, by M.M. Kapranov et al., MS.
- 470. Global Convergence of Damped Newton's Method for Nonsmooth Equations, via the Path Search, by Daniel Ralph, MS.
- 471. Bifurcation Into Gaps in the Essential Spectrum, II, by T. Kupper and C.A. Stuart, MS.
- 472. Duality and Minors of Secondary Polyhedra, by L.J. Billera et al., MS, *J Combinatorial Theory*.
- 473. Local Dissipativity and Attractors for the Kuramoto-Sivashinsky Equation in Thin 2D Domains, by George R. Sell and Mario Taboada, MS.
- 474. Unique Solvability of Nonlinear Volterra Equations in Weighted Spaces, by Peter Rejto and Mario Taboada, MS.
- 475. Invariant Manifolds for Retarded Semilinear Wave Equations, by Mario Taboada and Yuncheng You, MS.
- 476. Predator-Prey Systems, by R. Durrett, MS.
- 477. How Complicated is the Set of Stable Models of a Recursive Logic Program?, by W. Marek et al., MS.
- 478. Solvability of Nonlinear Equations in Spectral Gaps of the Linearization, by H.-P. Heinz and C.A. Stuart, MS.
- Hidden Symmetry of Fully Nonlinear Boundary Conditions in Elliptic Equations: Global Bifurcation and Nodal Structure, by T.J. Healey, MS.
- 480. Face Numbers of PL-Spheres, by P. Filliman, MS.

- 481. Global Attractor. Inertial Manifolds and Stabilization of Nonlinear Damped Beam Equations, by Mario Taboada and Yuncheng You, MS.
- 482. Computational Efficiency and Approximate Inertial Manifolds for a Benar! Convection System, by Michael D. Graham et al., MS, *Physica*.
- 483. Quotients of Toric Varieties, by M.M. Kapranov et al., MS.
- 484. On a Modified Coupling Procedure for Exterior Boundary Value Problems, by Gabriel N. Gatica, MS.
- 485. Dissipativity of Numerical Schemes, by C. Foias et al., MS.
- 486. Anisotropic Elasticity for Random Arrays of Identical Spheres, by James T. Jenkins, MS.
- 487. On the Coupled BEM and FEM for a Nonlinear Exterior Dirichlet Problem, by Gabriel N. Gatica and George C. Hsiao, MS.
- 488. On the Combinatorics of Permutation Polytopes, by Shmuel Onn, MS.
- 489. Extremes of Moving Averages of Random Variables with Finite Endpoint, by Richard A. Davis and Sidney I. Resnick, *Ann Prob* 19,312(1991). AD A238 504
- 490. Inelastic Microstructure in Rapid Granular Flows of Smooth Disks, by Mark A. Hopkins and Michel Y. Louge, *Phys Fluids* A3,47(1991). AD A238 579
- 491. On the Linear Instability of the Hall-Stewartson Vortex, by S.N. Brown et al., *Theoretical and Computational Fluid Dynamics*, 1990, 27. AD A238 580
- 492. On Superconvergence up to Boundaries in Finite Element Methods: A Counterexample, by Lars B. Wahlbin, MS.
- 493. Combinatorial Stratification of Complex Arrangements, by Anders Bjorner and Gunter M. Ziegler, MS.
- 494. A Garding's Inequality for Variational Problems with Constraints, by Gabriel N. Gatica and George C. Hsiao, MS.
- 495. On a Conjecture of Baues in the Theory of Loop Spaces, by L.J. Billera et al., MS.
- 496. On a Nonlinear Moments Problem, by Mario Taboada, MS.
- 497. Asymptotic Behavior of Brownian Tourists, by R.T. Durrett and L.C.G. Rogers, MS, Probab Th Rel Fields.
- 498. A New Proof of Robinson's Homeomorphism Theorem for Pl-Normal Maps, by Daniel Ralph, MS.
- 499. Interpolation and Hyperinterpolation, by Ian H. Sloan, MS.
- 500. Basic Linear Algebra Functions for C Language Usage (C-BLAF), by Zbigniew Leyk, MS.
- 501. Extensional Flow of a Suspension of Fibers in a Dilute Polymer Solution, by O.G. Harlen and D.L. Koch, MS, *Phys Fluids*.
- 502. Hyperdeterminants, by I.M. Gelfand et al., MS.
- 503. A Globally Convergent Method for Lp Problems, by Yuying Li, MS.
- 504. Polynomial-Time Abelian Groups, by Douglas Cenzer and Jeffrey Remmel, MS. Ann Pure and Appl Logic.
- 505. Hook-Schur Function Analogues of Littlewood's Identities and Their Bijective Proofs, by J.B. Remmel and M. Yang, MS, European J Combinatorics.
- 506. Superattractive Fixed Points in *C(n)*, by John H. Hubbard and Peter Papadopol, MS.
- 507. Infinite Quantum Group Symmetry of Fields in Massive 2D Quantum Field Theory, by Andre LeClair and EA. Smirnov, MS. Intl J Modern Phys.

- 508. Sparse Elimination Theory, by Bernd Sturmfels, MS
- 509. Preservation of Nodal Structure on Global Bifurcating Solution Branches of Elliptic Equations with Symmetry, by Timothy J. Healey and Hansjorg Kielhofer, MS, J Diff Eq.
- 510. Recursively Presented Games and Strategies, by Douglas Cenzer and Jeffrey Remmel, MS, J Math Social Sci.

## 26063 ADAPTIVE INFORMATION PROCESSING AND GLOBAL OPTIMIZATION

### P.R. Kumar

University of Illinois

A rather complete theory of adaptation for parallel model schemes has been developed. This theory encompasses the well studied but previously open problems of adaptive IIR filtering and output error identification. Adaptive feedforward control was covered as well as adaptive active noise canceling. For adaptive IIR filtering and output error identification, it was possible to develop the full asymptotic theory, and similarly also for adaptive feedforward control and active noise canceling. In fact the adaptive active noise canceling scheme which uses two microphones is so promising that the university is filing for a patent. A general convergence theory was developed for extended least squares based schemes. These results treat the behavior of general control designs operating in colored noise environments. Previously fairly comprehensive results were obtained for the white noise environment. It has also been possible to obtain what are perhaps the best results on robustness of continuous time adaptive controllers. More than a decade ago, it was shown that projection of parameter estimates yields robustness with respect to bounded disturbances. However, the problem of robustness with respect to unmodeled dynamics was much more difficult. Hence over the last decade, several additional and cumbersome fixes were suggested. However, it has been shown here that projection gives robust performances as well as robust stability with respect to unmodeled dynamics in addition to bounded disturbances. This is perhaps the simplest robust adaptive controller possible.

#### Reports:

No. 1-11 in previous editions.

- 12. On Dynamic Scheduling of Manufacturing Systems, by Steve Lu and P.R. Kumar, MS.
- The Convergence of Output Error Identification and Adaptive IIR Filtering Algorithms in the Presence of Colored Noise, by Wei Ren and P.R. Kumar. Proc of 29th Conf on Decision and Control, 1990, 3534.
- Convergence of Least-Squares Parameter Estimate Based Adaptive Control Schemes, by P.R. Kumar, Proc of 11th IFAC World Congress, 1990, 87.

- The Convergence of Output Error Recursions in Infinite Order Moving Average Noise, by Wei Ren and P.R. Kumar, MS.
- 16 Direct Stochastic Adaptive Minimum Variance Control with Non-Interlaced Algorithms, by Wei Ren and P.R. Kumar, MS.
- 17. A Robust Adaptive Controller for Continuous Time Systems, by Sanjeev M. Naik and P.R. Kumar, MS.
- Recent Results on Least Squares Based Adaptive Control of Linear Stochastic Systems in White Noise, by Wei Ren and P.R. Kumar, MS.
- Robust Continuous Time Adaptive Control by Parameter Projection, by S.M. Naik et al., MS.
- Stochastic Adaptive System Theory: Recent Advances and a Reappraisal, by W. Ren and P.R. Kumar, MS.
- 21. Learning and Estimating Classes of Sets Over Classes of Probabilities, by Kevin Buescher and P.R. Kumar, MS.
- 22. Robust Adaptive Control of Continuous Time Systems by Parameter Projection, by Sanjeev Naik and P.R. Kumar, MS.
- 23. The Convergence of Stochastic Adaptive Controllers, by Wei Ren and P.R. Kumar, MS.
- 24. Robust Continuous Time Adaptive Control by Parameter Projection, by Sanjeev Naik et al., MS, *IEEE Trans on Auto Control*.
- 25. Stochastic Parallel Model Adaptation: Theory and Applications to Active Noise Canceling, Feedforward Control, IIR Filtering and Identification, by Wei Ren and P.R. Kumar, MS, IEEE Trans on Auto Control.
- 26. Interlacing is not Necessary for Adaptive Control, by Wei Ren and P.R. Kumar, MS.
- 27. Robustness of ELS-Based Adaptive Control, by Sanjeev M. Naik and P.R. Kumar, MS, *IEEE Trans on Auto Control*.
- 28. Simulation of Discrete Time Systems Using ISIM, by R. Ravikanth, MS Thesis, 1991, 43 pp.

## 26792 SIGNAL DETECTION AND ESTIMATION

C.R. Rao

The Pennsylvania State University

An important recent contribution is the study of asymptotic properties of maximum likelihood estimates of the unknown signal parameters in the superimposed exponential model. It is shown that the m.l.e.'s of these parameters attain the Cramer-Rao lower bound for the asymptotic covariance matrix. Test criteria similar to multivariate analysis of variance and covariance were developed under the M-theory for the standard multivariate linear mode. A new line of research was initiated on the study of weighted sums of random variables which arises in practical work. The strong law of large numbers, law of iterated logarithms and convergence rates were established for weighted sums of random variables. Analysis of nonlinear time series was developed through the estimation of bispectrum. This is useful

in estimating the parameters of signals in the presence of noise and for discriminating deterministic nonlinear models and chaotic models.

Reports.

No. 1-2 in previous editions.

- 3. Asymptotic Properties of the Complex Valued Non-Linear Regression Model, by Debasis Kundu, MS.
- Rao's Score Test of Goodness of Fit and Independence, by K.V. Mardia, MS.
- 5. Edgeworth Expansions for EIV, by Gutti Jogesh Babu and Z.D. Bai, MS.
- 6. Estimating the Parameters of Exponential Signals, by Debasis Kundu, MS.
- Tracking the Directions of Arrivals of Signals From Moving Targets Part 1: A Review and Some Improved Algorithms, by Z.D. Bai et al., MS.
- Edgeworth Expansions of a Function of Sample Means Under Minimal Moment Conditions and Partial Cramer's Condition, by Gutti Jogesh Babu and Z.D. Bai, MS.
- 9. On Rates of Convergence of Efficient Detection Coheria in Signal Processing When the Noise Covariance Matrix is Arbitrary, by Kwok-Wai Tam and Yehua Wu, MS
- On Modified LVLP Method for Estimating Superimposed Exponential Signals, by C. Radhakrishna Rao and Nandini Kannan, MS.
- 11. On the Estimation of Skewness of a Statistic Using the Jackknife and the Bootstrap, by Dongsheng Tu and Lu Zhang, MS.
- Asymptotic Expansions for the Standardized and Studentized Estimates in the Growth Curve Model, by Yasunori Fujikoshi, MS.
- 13. Almost Sure Behaviour for F-Valued Random Fields, by Li Deli et al., MS.
- The Exact Bispectra for Bilinear Realizable Processes with Hermite Degree 2, by Gyorgy Terdik and Laurie Meaux, MS.
- An Elementary Proof for an Extended Version of the Choquet-Deny Theorem, by C. Radhakrishna Rao and D.N. Shanbhag, MS.
- On Realization and Identification of Stochastic Bilinear Systems, by Gyorgy Terdik, MS.
- A Comparison of Some Jackknife and Bootstrap Procedures in Estimating Sampling Distributions of Studentized Statistics and Constructing Confidence Intervals, by Lu Zhang and Dongsheng Tu, MS.
- Linear Representation of M-Estimates in Linear Models, by C. Radhakrishna Rao and L.C. Zhao, MS.

## 26802 PFRFORMANCE ANALYSIS OF SUBSPACE BASED METHODS

Bhaskar D. Rao

University of California, San Diego

The main goal of this research is to obtain a thorough understanding of the performance of the high resolution subspace based methods like MUSIC (Multiple Signal Classification) and ESPRIT (Estimation

#### **IV Mathematics**

of Signal Parameters via Rotational Invariant Techniques) for the problem of resolving closely spaced sources from measurements obtained using a sensor array. A statistical analysis of the effect of spatial smoothing is fairly complicated, and for this purpose a novel approach was developed. The approach consists of considering the effect of errors in the covariance estimate on the space spanned by the signal and noise eigenvectors. This is in contrast to previous work that looked at the effect of errors on the individual eigenvectors of the subspaces. Directly considering the errors in the subspaces has a number of advantages. The approach is more general in that various assumptions made in the previous work can be relaxed, e.g., statistics of the signal amplitudes, distinct nature of the signal eigenvalues, etc. Furthermore, compared to the previous approaches, this approach provides one with the ability to deal with the more complicated problem of spatial smoothing elegantly, resulting in tractable expressions. Expressions for the mean squared error in the direction of arrival estimates obtained using MUSIC, the Minimum-Norm method, and State Space Methods/ESPRIT have been derived. Based on these expressions various important properties were derived. It was shown that the forward backward approach is more desirable than using a forward only. This result has been known to the signal processing community, but a rigorous proof of this has not been available, and is provided in this work. It was shown that the time series frequency estimation problem can also be treated in the same framework, and the results obtained are more accurate than previously available results.

#### Reports:

- State Space Methods/ESPRIT and Spatial Smoothing: A Statistical Analysis <sup>1</sup> <sup>(h)</sup>askar D. Rao and K.V.S. Hari, MS, *IEEE Trans on Acoust, Speech, and Signal Proc.*
- 2. Effect of Spatial Smoothing on State Space Methods: ESPRIT, by Bhaskar D. Rao and K.V.S. Hari, MS.
- Effect of Spatial Smoothing on the Performance of Music and the Minimum-Norm Method, by Bhaskar D. Rao and K.V.S. Hari, *IEEE Proc* 137,449(1990). AD A233-589
- 4. Analysis of Subspace Based DOA Estimation Methods, by Bhaskar D. Rao and K.V.S. Hari, MS.
- Spacial Smoothing and MUSIC. Further Results, by Bhaskar D. Rao and K.V.S. Hari, MS.
- Performance Analysis of Subspace Based Methods for Direction of Arrival (DOA) Estimation, by Hari V.S. Kuchibhotla, PhD Thesis, 1990, 172 pp.
- 7. Analysis of Roundoff Noise in Floating Point Digital Filters, by B.D. Rao, MS.
- 8. On Spatial Smoothing and Weighted Subspace Methods, by B.D. Rao and K.V.S. Hari, MS
- 9. A Systematic Approach for the Analysis of Roundoff Noise In Floating Point Digital Filters, by B.D. Rao, MS.

 Weighted State Space Methods ESPRIT and Spatial Smoothing, by B.D. Rao and K.V.S. Hari, MS.

# 26811 A MULTILEVEL-MULTIRESOLUTION METHOD FOR IMAGE PROCESSING, A BAYESIAN FRAMEWORK FOR RECONSTRUCTING AND REPRESENTING SHAPES IN ROBOT VISION AND SPEECH RECOGNITION

Basilis Gidas Brown University

Remote Sensing Application: A coheront statistical framework has been developed for estimating 3-D shapes and surface composition from a single noisy image. The method has been tested with video data acquired under uncontrolled illumination. Tomography: An open problem in tomography has been the incorporation into the algorithms of blur due to scintillation cameras. A two-stage EM algorithm has been developed for 3-D emission tomography to account for camera degradation. A publication introduces a multiresolution method, via multigrid ideas. for Maximum Likelihood and back-proj ction estimation in tomography. The method should have applications to other image processing tasks. Parameter Estimation for MRF: The problems of image processing and speech recognition lead to estimation problems which generalize those of time series analysis. In the past studies were made of consistency and large "size" beha for of ML and other estimators. Recently an efficient estimation technique was developed for Markov Random Fields based on the microcanonical ens able and molecular dynamics. This method provides also a new estimation procedure for traditional problems in statistics. Code Theory for Gibbs Fields: The theory of Large Deviations for Markov Random Fields was used to show that the number of bits per symbol for Ziv-Lengel cours is given by the maximum entropy of all Gibbs fields with the same potential. The methodology provided also a strong version of the Shannon-McMillan theorem for Gibbs random fields.

## 26930 SVD-BASED SIGNAL PROCESSING ALGORITHMS

Franklin T. Luk Cornell University

Research interests have been broadened to include real-time control. It was discovered that an important problem in control, namely, linear prediction, can be solved via the singular value decomposition (SVD) of a product of three matrices. A new algorithm was developed for this product SVD problem, and it was proved that the method will always compute an accurate decomposition in that all relevant residual elements will be small. The feasibility of solving the linear prediction problem in real time was initiated by implementing the product SVD algorithm on a systolic machine.

## 26932 PARALLEL STRUCTURED OPTIMIZATION ALGORITHMS FOR INVERSE PROBLEMS

John E. Dennis

Rice University

Progress has been made on two fronts. Researchers have been working with visitors to the NSF Center for Research on Parallel Computation on interior point method: for linear programming. They have found a method with the best known iteration complexity as well as the best known asymptotic rate of convergence. There are several other reports in preparation on interior point methods as well. A graduate student and researchers are working in the NSF center on a generalization of the Brown-Brent methods for large scale problems. These methods can be thought of as between traditional SQP and GRG approaches. The work is motivated by parameter ID and control for systems governed by differential equations.

#### Reports:

- A View of Unconstrained Optimization, by J.E. Dennis Jr. and R.B. Schnabel, *Handbooks in OR&MS*, Vol 1, 1929. AD A238-373
- 2. On the Convergence of the Multi-Directional Search Algorithm, by Virginia Torczon, MS.
- Direct Search Methods on Parallel Machines, by J.E. Dennis and V. Torczon, MS.
- 4 A Curvilinear Search Using Tridiagonal Secant Updates for Unconstrained Optimization, by J.E. Dennis Jr. et al., MS.
- 5. An SQP Augmented Lagrangian BFGS Algorithm for Constrained Optimication, by R.H. Byrd et al., MS.
- Multi-Directional Search: A Direct Search Algorithm for Patallel Machines, by Virginia J. Torczon. PhD Thesis, 1989, 85 pp.
- A Robust Trust Region Algorithm for Nonlinear Programming, by Karen Anne Williamson, PhD Thesis, 1990, 91 pp.
- An Optimal Basis Identification Technique for Interior-Point Linear Programming Algorithms, by R.A. Tapia and Yin Zhang, MS
- 9. On the Superlinear Convergence of Inc. (or Point Algorithms for a General Class of Problems, by Y. Zhang et al., MS.

### F. Special Projects

- A Global Convergence Theory for the Celis-Dennis-Tapia Trust Region Algorithm for Constrained Optimization, by Mahmound E. Alem, MS.
- Convergence Rates for the Variable, the Multiplier, and the Pair in SQP Methods, by Jershan Chiang and Richard Tapia, MS.
- A Quadratically Convergent Polynomial Primal-Dual Interior-Point Algorithm for Linear Programming, by Yin Zhang and R.A. Tapia, MS.
- A Unified Approach to Global Convergence of Trust-Region Methods for Nonsmooth Optimization, by J.E. Dennis et al., MS.

# 26945 PARALLEL ALGORITHMS AND COMPOSITE TASKING IN SENSOR ARRAY SIGNAL PROCESSING

Allan O. Steinhardt Adam W. Bojanczyk Cornell University

The hyperbolic singular value decomposition (HSVD) is a new canonic matrix decomposition. This matrix factorization was developed in order to retain the benefits of the SVD (numerical stability, detection of fuzzy rank) in certain signal processing problems where the conventional SVD cannot be applied. The purpose of this hyperbolic decomposition is to find the eigenstructure of a matrix formed from the difference of two covariance matrices. Such a task arises in certain methods of bearing estimation in colored noise, as well as high resolution spectral estimation of nonstationary data using a sliding rectangular window. Algorithms were for computing the HSVD for the case when the difference of two covariance matrices is full rank. The hyperbolic SVD algorithms are the first dedicated algorithms for this task. They give better numerical results than stable competing methods which all involve explicit outer product formation. One of the algorithms is also easily computed in parallel using a linear systolic array. The problem of computing the singular value decomposition of a product of matrices occurs in many applications. The singular value decomposition of a product of matrices can be computed by the Jacobi method. It is important not to form the explicit product of the matrices as this obliterates the smallest singular values. A new way is proposed for implementing the Jacobi method without explicitly forming the product of the matrices involved. The algorithm can achieve the best possible numerical accuracy in a given finite precision arithmetic.

#### Reports

 The Hyperbolic Singular Value Decomposition, by Adam W. Bojanczyk et al., MS

- 2. An Accurate Product SVD Algorithm, by Adam W. Bojanczyk et al., MS.
- 3. The Hyperbolic Singular Value Decomposition and Applications, by Ruth Onn et al., MS.
- Stability Analysis of a Householder-Based Algorithm for Downdating the Cholesky Factorization, by Adam W. Bojanczyk and Allan O. Steinhardt, MS.

### 27282 PARALLEL SCIENTIFIC COMPUTATION

Joseph E. Flaherty Mark H. Holmes Robert E. O'Malley Rensselaer Polytechnic Institute

The objectives of this research are to (a) design and develop parallel languages and compilers, and matrix algorithms exploiting parallel architectures, (b) investigate automatic load balancing in heterogeneous computing environments, and (c) develop and analyze parallel adaptive methods for solving nonlinear partial differential equations.

### 27392 ADVANCED PARALLEL SYSTEMS

John R. Rice

Purdue University

The research objective is to investigate methodologies for exploiting massively parallel systems in the solution of computation intensive problems such as nonlinear elliptic PDEs. Investigate the development of user interfaces which remove the task of parallelization of problems and distribution of computational workload from the user and which place this burden on an automated software system. This is a twophase study. (a) Algorithm infrastructure: Study various methods which arise in the applications, e.g., discretization methods, domain decomposition, pipelined iterative methods, etc., and determine how to best implement these techniques on various architectures such as hypercube or shared memory machines. (b) Problem solving environments user interfaces: Investigate and develop methodologies for controlling distributed computations in highly heterogeneous computing environments with respect to both hardware and software systems.

# 27524 MATHEMATICAL METHODS AND ALGOPITHMS FOR REAL-TIME APPLICATIONS

Charles K. Chui Texas A&M University

The integral wavelet transform (IWT) distinguishes itself from any window Fourier transform for time-

#### **IV Mathematics**

frequency and phase-space analysis in that it has the zoom-in and zoom-out capability. When a basic wavelet which generates an orthonormal basis of  $L^2$ (IR) is used as the wavelet window function, the infinite wavelet series recovers the original function from its IWT information. In general, even if a basic wavelet only generates an unconditional basis for every orthogonal scale-subspace, its dual basis can be used for the same purpose. This more general approach allows greater flexibility for introducing new basic wavelets with more desirable features such as "linear phases" and readiness for implementation of orthogonal wavelet decompositions. The pair of two-scale formulas and the two suguences in the decomposition formula in this general setting can be "interchanged" to yield the desired dual basis. An important consequence is that polynomial B-splines and compactly supported basic wavelets can be used directly without orthonormalization to facilitate various applications of spline approximations and wavelet decompositions. One such application is real-time digital signal processing.

### Reports:

- 1. A Cardinal Spline Approach to Wavelets, by C.K. Chui and J.Z. Wang, MS. Proc Am Math Soc.
- On Compactly Supported Spline Wavelets and a Duality Principle, by C.K. Chui and J.Z. Wang, MS, *Trans Am Math Soc.*
- 3. Real-Time Signal Analysis with Quasi-Interpolatory Splines and Wavelets, by A.K. Chan and C.K. Chui, MS.
- 4. An Overview of Wavelets, by C.K. Chui, Approximation Theory and Functional Analysis, 1991, 47. AD A233 910
- 5. Wavelets and Spline Interpolation, by Charles K. Chui, MS.
- 6. On Cardinal-Spline Wavelets, by C.K. Chui, MS.
- 7. Polynomial Expansions for Cardinal Interpolants and Orthonormal Wavelets, by C.K. Chui et al., MS.

#### 27620 HIGH RESOLUTION SIGNAL PROCESSING

Donald W. Tufts University of Rhode Island

A Fourier analysis method using an iterative Arithmetic Fourier Transform (AFT) was discovered. It overcame the difficulty of dense, Farey-fraction sampling which is inherent in the original AFT algorithm. This disadvantage of the AFT is turned into an advantage and dense frequency-domain samples are obtained without any additional interpolation or zero-padding. The implementation of the iterative computations is designed to preserve the advantage of the AFT for VLSI implementation by using a permuted difference coefficient structure. This iterative AFT is intended for cases in which (a) the function to be analyzed can only be sampled uniformly and at a rate close to the Nyquist rate or (b) dense frequency domain samples are needed. The AFT is a novel algorithm for accurate high speed Fourier analysis and synthesis. The arithmetic computations in the AFT can be performed in parallel. Except for a small number of scalings in one stage of the computation, only multiplications by 0, +1 and -1 are required. The AFT has been proposed for computation of the Discrete Cosine Transform (DCT). Recently, a new approach to iterative realization of the AFT has also been proposed. It removes the requirement for the Farey-fraction sampling in the original AFT which is a disadvantage for image processing applications. The iterative AFT can be modified to compute the 1-D or 2-D DCT. The computational structure of the resulting iterative arithmetic DCT (ADCT) has been shown. This algorithm iteratively calculates the successive approximations to a dense transform-domain vector.

#### Reports:

- The Effects of Perturbations of Matrix-Based Signal Processing, by Donald W. Tufts, MS.
- 2. Iterative Realization of the Arithmetic Fourier Transform, by Donald W. Tufts and Haiguang Chen, MS. *IEEE Trans on Acoust. Speech. and Signal Proc.*
- 3. Computation of the 2-D Discrete Cosine Transform Using the 2-D AFT and the 2-D Iterative AFT, by Donald W. Tufts et al., MS, *IEEE Trans on Video Imaging*.
- 4. Computation of the Discrete Cosine Transform Using the Iterative Arithmetic Fourier Transform, by Haiguang Chen et al., MS, J Visual Commun and Image Representation.
- One-Dimensional and Two-Dimensional Discrete Cosine Transforms Using the Iterative Arithmetic Fourier Transform, by Haiguang Chen and D.W. Tufts, MS.

# 27817 SINGULAR VALUE DECOMPOSITIONS: GENERALIZATIONS, ALGORITHMS AND APPLICATIONS

Gene H. Golub Stanford University

The progress of VLSI and wafer-scale technology has led to the development of high-performance digital signal processing systems. Reliability of such systems is obviously a critical issue. Algorithmbased fault tolerance has been proposed to meet this need, since the most common practice of triplicating hardware is often too expensive and too bulky for real time signal processing. The weighted checksum scheme provides a low-cost error protection for basic matrix operations. Very general sequences of poly-

### E. Special Projects

nomials can be used to generate the checksum, so as to reduce the chance of numerical overflows. In addition, the Lanczos process can be applied in the error correction step, so as to save on the amount of work. The singular value decomposition (SVD) is commonly used in the solution of unconstrained linear least squares problems, matrix rank estimation, and canonical correlation analysis. In applications such as information retrieval, seismic reflection tomography, and real-time signal processing, the solution to these problems is needed in the shortest possible time. Given the growing availability of multiprocessor computer systems, there has been great interest in the development of efficient implementations of the singular value decomposition. In applications such as information retrieval and seismic tomography, the data matrix whose SVD is sought is usually large and sparse. A procedure has been devised for determining a few of the extremal singular values and corresponding left and right singular vectors of a large sparse matrix. The method by Golub and Kent which uses the method of modified moments for estimating the eigenvalues of operators used in iterative methods for the solution of linear systems of equations is appropriately modified in order to generate a sequence of bidiagonal matrices whose singular values approximate those of the original sparse matrix. The potential asynchronous computation of the bidiagonal matrices using modified moments with the iterations of an adapted Chebyshev semi-iterative method is an attractive feature for parallel computers.

#### Reports:

- 1. Nonsymmetric Lanczos and Finding Orthogonal Polynomials Associated with Indefinite Weights, by Daniel L. Boley et al., MS.
- 2. Adaptive Lanczos Methods for Recursive Condition Estimation, by William R. Ferng et al., MS.
- 3. The Nonsymmetric Lanczos Algorithm and Controllability, by Daniel Boley and Gene Golub, MS.
- 4. Jacobi Matrices for Sums of Weight Functions, by Sylvan Elhay et al., MS.
- 5. Line Iterative Methods for Cyclically Reduced Discrete Convection-Diffusion Problems, by Howard C. Elman and G.H. Golub, MS.
- 6. OR-Like Algorithms for Arrow Matrices, by Peter Arbenz and G.H. Golub, MS.

# 28060 ALGORITHMS AND ARCHITECTURES FOR HIGH SPEED SIGNAL PROCESSING

Thomas Kailath Stanford University

#### **IV Mathematics**

Work has been concerned with investigating issues related to the more general field of parallel computation than the previous focus on Regular Iterative Algorithms (RIAs) and their parallel implementations. In some ways, however, the current topics have evolved naturally from the interest in RIAs, and efficient VLSI implementations of such algorithms. In one of the research efforts, work has concentrated on the problem of scheduling tasks on multiprocessor architectures, especially when there is a delay involved in inter-processor communication. In another effort, an investigation is being made of the computational power of neural networks, which are increasingly being studied in the context of massively parallel computation.

# Reports:

- Rate Distortion Functions for Self-Similar Sets, by Tsutomu Kawabata and Amir Dembo, MS, *IEEE Trans on Info Theory*.
- 2. How to Play Bowling in Parallel on the Grid?, by Jehoshua Bruck and V.P. Roychowdhury, MS, J Algorithms.
- 3. A Polynomial Time Algorithm for Reconfiguring Multiple-Track Models, by T.A. Varvarigou et al., MS, *IEEE Trans on Comp.*
- 4. New Algorithms for Reconfiguring VLSI/WSI Arrays, by T.A. Varvarigou et al., MS.
- 5. Reconfiguring Processor Arrays Using Multiple-Track Models, by T.A. Varvarigou et al., MS, *IEEE Trans on Comp.*
- 6. A Geometric Approach to Threshold Circuit Complexity, by Vwani Roychowdhury et al., MS, SIAM J Discrete Math.
- 7. Fast Algorithms for Structured Matrices with Arbitrary Rank Profile, by Debajuoti Pal, PhD Thesis, 1990, 211 pp.

### 28408 DESIGN AND ANALYSIS OF SCALABLE PARALLEL ALGORITHMS

Vipin Kumar

University of Minnesota, Minneapolis

The research is continuing on the development of parallel algorithms and data structures for a variety of numeric and nonnumeric problems. Emphasis is being placed on the analysis of the parallel formulations so that the performance and scalability of these algorithms can be predicted on different kinds of large-scale parallel architectures. The intention is to find what important practical problems can be solved cost-effectively on large-scale parallel processors, and what architectural features are most critical in obtaining good performance. Research has determined best scalable parallel formulations of algorithms such as sorting, shortest path for a variety of practically feasible architectures such as mesh and hypercubes. Under certain situations, parallel formulations of some important search algorithms can provide superlinear speedup.

# 28476 SIGNAL PROCESSING FOR HIGH-RESOLUTION IMAGE FORMATION

A.S. Karalamangala University of Illinois

The research objective is to investigate some related problems in high-resolution image formation. Specifically, consider minimax-error construction of an image from noisy linear measurements and reliable convex constraints, estimation of parameters of a noncausal rational model for a random field from random field observations, and phase recovery from magnitude measurements. Study Hx optimal reconstructions that minimize the worst case reconstruction error when there is some additive noise in the measurement data. Develop spectrum estimation algorithms that work directly with the random field samples, avoiding the covariance estimation step altogether. Formulate phase retrieval problem as a problem of recovering a member of a given convex set in a Hilbert space from measurements of the modulus of a finite number of linear functionals.

### 28809 SIMULATION METHODOLOGY

Donald L. Iglehart Peter W Glynn Stanford University

The research objective is to develop probabilistic and statistical methodology for improving the efficiency, and reducing the run-time of computer simulations and for analyzing the output of these simulations. The research will extend the mathematical foundation of the areas of importance sampling for rare events, output analysis, variance reduction techniques and stochastic optimization.

# 28994 CENTER OF EXCELLENCE IN MATHEMATICAL SCIENCES

Morton E. Gurtin David Kinderlehrer Luc Tartar Carnegie-Mellon University

The research objective is to develop a unified and highly visible interdisciplinary research activity with focus on nonlinear analysis and its applications. Specific areas include research on calculus of variation, nonlinear partial differential equations and continuum mechanics with emphasis on mathematics of advanced materials.

# 29031 CENTER OF EXCELLENCE IN MATHEMATICAL SCIENCES

Anil Nerode Cornell University

The objective of this research is to develop an interdisciplinary and interactive research program ir. mathematical sciences with focus on (a) symbolic methods in algorithmic mathematics covering topics such as computational algebra and geometry.and applied logic, (b) stochastic analysis with emphasis on interacting particle systems and applications, mathematical physics, stochastic PDE's, measure-valued diffusions and diffusions on manifolds, and (c) nonlinear analysis with emphasis on nonlinear wave analysis, high resolution flow simulation, numerical analysis and dynamical systems.

### 29053 LARGE DEVIATION LIMIT THEOREMS, WITH APPLICATIONS

N.R. Chaganty

Old Dominion University

The objective of this research is to investigate strong large deviation theorems, strong moderate deviation theorems and large deviation local limit theorems for arbitrary and dependent sequences of random vectors. Applications of the large deviation limit theorems will be made to importance sampling for Monte-Carlo simulations and to obtaining bounds on the Bahadur efficiency of various test statistics.

# 29190 DISCRETE EVENT DYNAMIC SYSTEMS MODELING AND OPTIMIZATION WITH APPLICATIONS TO C<sup>3</sup>I PROBLEMS

Yu-Chi Ho Harvard University

The objective of this research is to develop high level mathematical modeling and performance optimization techniques for general discrete event dynamic systems, with emphasis on simulation of battle management systems. A high level automata/ language model of DEDS will be developed to assess system performance. Seek combination of techniques from generalized Semi-Markov Process and mini-max algebra to develop a unified approach to DEDS.

# **V** ENGINEERING SCIENCES

# A. Solid Mechanics

# 25345 THREE-DIMENSIONAL ELASTIC STRESS ANALYSIS IN MATERIALS WITH MANY INHOMOGENEITIES

Mark Kachanov Tufts University

#### SL: MTL SC: ARDEC, BRL

The work on the relationship between the effective elastic constants of a brittle microcracking solid and its progression towards fracture continued. (The existence of such a relationship is the main assumption of many damage models; it is also a fundamental issue from the point of view of various NDE techniques). The P.I. argues that no such correlation exists, except for the cases when microcracking follows a deterministic reproducible path (as may be the case in certain laminated composites, under certain loading conditions). The work on crack interactions in anisotropic matrices (relevant for multiple cracking in composites) continued. Various aspects of the impact of the matrix anisotropy on crack interactions have been investigated (impact on the stress intensity factors, on the effective elastic moduli, on the mechanics of crack-microcrack interactions). A simple model for the effective elastic properties of a cracked medium for arbitrary crack orientation statistics was constructed (the existing models for the effective moduli deal only with either random orientation statistics or with one system of parallel cracks). Work on a higher order model for crack interaction was started. Preliminary results show a substantial improvement of accuracy at close spacings between cracks, particularly under the conditions of mixed mode interactions.

#### Reports:

No. 1-5 in previous editions.

 On Interaction of Cracks in Anisotropic Matrix and Related Problems, by C. Mauge and M. Kachanov, *Microcracking-Induced Damage in Composites*, AMD-Vol 111, MD-Vol 22, 1990, 95. AD A232 676

- On the Relationship Between Fracturing of a Microcracking Solid and Its Effective Elastic Constants, by Mark Kachanov, *Toughening Mechanisms in Quasi-Brittle Materials*, 1991, 373. AD A238 648
- Three-Dimensional Interactions of a Crack Front with Arrays of Penny-Shape Microcracks, by J.-P. Laures and M. Kachanov, *Intl J Fracture* 48,255(1991). AD A238 526

# 25400 INELASTIC DEFORMATION AND FAILURE ANALYSIS OF FILAMENT-WOUND COMPOSITE STRUCTURES

Gerald A. Wempner Wan-Lee Yin Georgia Institute of Technology

SL: BRL

SC: ARDEC, BWL, MTL

Major research effort was directed toward the analysis of two important failure mechanisms: (a) delamination fracture caused by edge effects and interlaminar stresses and (b) interfacial fracture induced by debonding between fibers and the resin material. The first problem was studied by a stress-function based variational formulation where each unidirectionally wound lamina is modeled as a homogeneous anisotropic continuum. Lekhnitskii's stress functions in the successive thin layers are approximated by polynomial functions of the thickness coordinate. The complementary energy principle yields a system of differential equations governing the coefficients of the polynomials. The equations and the edge conditions define an eigenvalue problem whose solutions determine the interlaminar stresses. The results for a filament-wound tube show large mode 3 interlaminar shear stress near a free edge or opening when the external loading on the tube produces a significant circumferential strain. The situation may lead to the initiation of delamination fracture from the edge. A micromechanical model with various debonding lengths between a stiff fiber and the resin material was used to investigate the initiation and progress of debonding failure when two adjacent fibers undergo a relative

displacement in the x- or y-direction (which results in a far-field shear strain  $\gamma$  or a y-direction extensional strain  $\epsilon_{\gamma}$  in the resin material). The two problems are solved by the boundary-element method. The interfacial stresses ahead of the debonding crack are obtained. One component of the stress has a rapid oscillatory behavior near the crack tip, as may be expected for the solutions of interface crack problems between dissimilar materials.

#### Reports:

No. 1-2 in previous editions.

- 3. Thermal Stresses and Free-Edge Effects in Laminated Beams: A Variational Approach Using Stress Functions, by Wan-Lee Yin, MS, J Electron Packaging.
- Free-Edge Effects in Laminates Under Extension, Bending and Twisting, Part 1: A Stress Function Approach, by W.-L. Yin, MS.
- Refined Buckling and Postbuckling Analysis of Two-Dimensional Delaminations, by W.-L. Yin and K.C. Jane, MS. Intl J Sol and Struct.

### **25459** PLASTIC, FINITE–STRAIN–INDUCED ANISOTROPY IN DUCTILE MATERIALS

Erastus H. Lee Erchard Krempl Ting-Leung Sham Rensselaer Polytechnic Institute

SL: BRL, MTL SC: ARDEC, BRL

Measurements of the evolution of yield loci in tensionshear stress space, generated by nonproportional straining experiments in combined tensile-straining and twisting of thin tube specimens, have produced a series of combined isotropic-kinematic hardening yield loci from which hardening laws can be deduced. These involve the evolution of the isotropic hardening modulus as well as the back stress which incorporates the anisotropic component of the hardening. The combined isotropic-kinematic hardening law has been found to express the behavior of the material over a wide range of strain-increment directions and hence to permit stress analysis of problems involving nonproportional stressing or straining. Yield surfaces or yield loci provide one of the basic internal state variables needed to express the plastic constitutive relations for ductile metals. The combined isotropickinematic hardening, the radii of the yield loci express the isotropic hardening which can be represented by a plastic hardening modulus function as for isotropic hardening. The back stress is given by the center of the yield circle and its evolution provides both a hardening modulus type variable based on the magnitude of this stress and a plastic-spin type variable expressed by the rotation of the back stress. The plastic spin can be large, even in the presence of small material rotations, since the center of the yield locus rotates around the stress origin associated with the generation of impediments to continuing dislocation mobility caused by the prior plastic flow. In the plasticity literature this is commonly referred to as the influence of variation of the substructure.

Reports:

No. 1-6 in previous editions.

 Some Basic Aspects of Elastic-Plastic Theory Involving Finite Strain, by Erastus H. Lee, MS.

# 25594 LASER SPECKLE TECHNIQUE FOR THE DETERMINATION OF MATERIAL RESPONSE UNDER HIGH STRAIN RATE, HIGH TEMPERATURE AND FATIGUE

Fu-Pen Chiang State University of New York at Stony Brook

SL: MTL SC: STRUC DIR

There are three major thrusts of research under the current program. One is the continued development of computer aided speckle interferometry. The aim is to fully automate the technique of laser speckle photography. This approach completely eliminates the need for photographic wet process. Speckle patterns generated from a specimen surface before and after deformation are digitized using a CCD (Charge Coupled Device) camera or a digital video camera into gray levels. They are Fourier transformed, filtered and inverse transformed to yield the displacement information through the concept of Young's fringes used in the conventional approach. Now a new approach has been tried using differential phase information and neighbor prediction. This approach yields full field displacement and strain information much faster. The second major thrust of the research is the development of scattered laser speckle pattern as a direct measure of fatigue damage and plastic strain. This approach eliminates the need for double exposure and the requirement of an initial speckle pattern with which to compare the subsequent ones. The third major thrust of the research is on the investigation of the fundamental mechanism of surface roughness due to plastic deformation. This study is essential in order to place the application projects on a sound physical basis. Among the four materials plastic deformation roughens surfaces resulting from slip bands within individual grains and relative rotation and sliding between and among neighboring grains studied. The low frequency component of a

#### **A.** Solid Mechanics

surface profile contributes dominantly to both the vertical surface roughness parameter and the horizontal surface roughness parameter, and the relative rotation between grains increases linearly to the amount of plastic deformation in terms of effective strain. While the surface vertical surface roughness parameter in terms of RMS roughness is mainly due to grain rotation, the horizontal surface roughness parameter in terms of correlation length is proportional to average grain size and becomes saturated at a certain plastic deformation.

#### Reports:

No. 1-9 in previous editions.

- 10. Determination of Elastic-Plastic Boundary by Speckle Pattern Correlation, by EP. Chiang et al., MS.
- 11. Estimation of Plastic Strain by Fractal, by Y.Z. Dai and E.P. Chiang, MS.
- Application of Laser Speckle Interferometry to Measuring Dynamic Strain, by James Francis Emslie, MS Thesis, 1990, 81 pp.
- 13. Computer Aided Speckle Interferometry (CASI), by D.J. Chen and F.P. Chiang, MS.
- 14. Investigation of Optimal Sampling Resolution in Digital Laser Speckle Correlation, by D.J. Chen and E.P. Chiang, MS, *Exptl Mech*.
- 15. Laser Speckle Interferometry Applied to Measuring Strain at High Temperatures, High Heating Rates and Dynamic Loading Conditions, by J.E. Emslie et al., MS.
- 16. Application of Scattering Theory to Plastic Strain Estimation, by Y.Z. Dai and E.P. Chiang, MS.

#### 26057 MICROMECHANICS OF DEFECTS

Toshio Mura

Northwestern University

An analysis is in progress on the inverse problem in which residual surface displacements are used to evaluate nonelastic deformation in a domain, which is called the damage domain, of a solid. The problem is taken as an example to elucidate the nonlinearity of a class of inverse problems. The problem can be formulated as a system of multidimensional Fredholm integral equations of the first kind. It is a complicated nonlinear problem since both damage domain (which appears as the domain of integration in the integral equation) and the nonelastic strains are unknown. The surface data are not sufficient to determine the shape of the damage domain and the exact distribution of the nonelastic strains. However, these data can be used to obtain some important characteristic quantities associated with the nonelastic deformation of the solid, such as elastic energy, stresses in certain region of the solid or the fracture

toughness enhancement due to localized nonelastic deformation.

Reports:

No. 1-12 in previous editions.

- Crack Branching Behavior in Stress Corrosion Cracking of High Strength Steel, by Y. Hirose and T. Mura, Eng Fracture Mech 34,729(1989), AD A226 362
- Nonlinearity of Inverse Problems, by T. Mura and Z. Gao, Trans of the Seventh Army Conf on Appl Math and Computing, ARO Report 90-1, 1990, 117. AD A226 408

### 26443 STUDIES IN PENETRATION MECHANICS

Romesh C. Batra

University of Missouri at Rolla

SL: BRL SC: ARDEC

A paper has been prepared in which the coupled nonlinear partial differential equations governing the thermomechanical and axisymmetric deformations of a cylindrical rod penetrating into a thick target, also made of a rigid/viscoplastic material, are solved by the finite element method. It is assumed that the deformations of the target and the penetrator as seen by an observer situated at the stagnation point and moving with it are independent of time. Both the rod and the target material are assumed to exhibit strainrate hardening and thermal softening, and the contact between the penetrator and the target at the common interface is smooth. An effort has been made to assess the effect of the strain-rate hardening and thermal softening on the deformations of the target and the penetrator. It is found that the axial resisting force experienced by the penetrator, the shape and location of the free surface of the deformed penetrator and the target/penetrator interface, and normal tractions on this common interface depend rather strongly upon the speed of the stagnation point, and hence on the speed of the striking rod. Results presented graphically include the distribution of the velocity field, the temperature change, the hydrostatic pressure, and the second invariant of the strain-rate tensor. In an attempt to help establish desirable testing regimes for determining constitutive relations appropriate for penetration problems, histories were also found for the effective stress, hydrostatic pressure, temperature, and the second invariant of the strain-rate tensor experienced by four penetrator and two target particles.

#### Reports.

No. 1-4 in previous editions.

 Steady State Axisymmetric Deformations of a Thermoviscoplastic Rod Penetrating a Thick Thermoviscoplastic Target, by R.C. Batra and T. Gobinath, *Intl J Impact Eng* 11,1(1991). AD A238 351

- Computations of Boundary Tractions in Finite Element Solution of an Axisymmetric Quasi-nonlinear Problem, by R. Jayachandran and R. C. Batra, Proc of Intl Conf on Computational Engineering Science, ICES Pub, 1991, p414.
- Effect of Viscoplastic Flow Rules and Transverse Isotropy on Steady State Penetration of Thick Targets, by Aslam Adam, MS Thesis, 1990, 68 pp.
- A Steady State Axisymmetric Penetration Problem for Rigid-Perfectly Plastic Materials, by T. Gobinath and R.C. Batra, MS, Intl J Eng Sci.
- 9. Effect of Viscoplastic Flow Rules on Steady State Penetration of Thermoviscoplastic Targets, by R.C. Batra and Aslam Adam, MS. Intl J Eng Sci.
- Steady State Penetration of Transversely Isotropic Rigid-Perfectly Plastic Targets, by R.C. Batra and Aslam Adam, MS, Comp & Struct.
- 11. Steady State Penetration of Elastic Perfectly Plastic Targets, by R. Jayachandran and R.C. Batra, MS, Acta Mech.

# 26908 WAVE PROPAGATION AND DYNAMIC RESPONSE OF LAMINATED STRUCTURES

R.K. Kapania J.N. Reddy

Virginia Polytechnic Institute and State University

SL: AP TEC DIR SC: AERO DIR, BRL, STRUC DIR

The nonlinear dynamic equations of the first-order shear deformation theory and the third-order shear deformation plate theory of Reddy were reformulated into equations describing the interior and edge-zone problems of rectangular plates. Viscous damping terms were also included. It was shown that, for certain boundary conditions, the number of governing equations can be reduced to three, as in the classical plate theory. Two problems related to static largedeflection and dynamic small-deflection of rectangular plates were considered. Numerical results demonstrate the effects of nonlinearity, shear deformation, rotatory inertia, damping, and sonic boom type loadings.

# 27315 DURABILITY PREDICTIONS FOR ADHESIVELY BONDED JOINTS IN HUMID CONDITIONS

Gregory J. Rodin Kenneth M. Liechti University of Texas at Austin

SL: BRADEC, MTL SC: ARDEC

The research effort was directed towards investigations of diffusion kinetics in the neat adhesive and its stress/strain characteristics. A literature review of various models of viscoplastic behavior of polymers was also conducted. The diffusion kinetics were examined by mass gain measurements on neat films of cured adhesive 3-H. It was found that the use of glycerol solutions in water to control humidity caused the specimens to become coated with glycerol which in turn affected the diffusion characteristics. Direct control of temperature and humidity was therefore provided by a temperature/humidity cabinet and consistent water uptake measurements have been made at a number of temperature and humidity levels. Two additional temperature/humidity cabinets are being fabricated. Costs have been minimized by providing central computer control for three cabinets. The three units will allow conditioning and testing of specimens to be conducted in parallel. A series of constant strain rate and creep tests to failure have been conducted on the neat tensile coupons of adhesive 3-H. The specimens were conditioned at various temperatures and humidities prior to testing. The experiments have been plagued by a large degree of scatter even after satisfactory improvements in specimen gripping were made. When the specimens were examined under crossed polars, the birefringence patterns revealed multiple shear banding along the gage length of the specimen which would explain the large scatter in strains to failure. Consideration is being given to measuring the local rather than the overall strain in the specimens. Alternate specimen geometries which are less susceptible to shear banding are also being considered.

# 27409 THEORETICAL. EXPERIMENTAL AND COMPUTATIONAL STUDIES IN PLASTICITY

Elias C. Aifantis

Michigan Technological University

SL: BWL, MTL SC: ARDEC, BRL

Progress has been made towards establishing and setting up the relevant experimental procedures and equipment: developing constitutive relations for large plastic deformations; and numerically investigating anisotropy and shear banding. In particular, the following has been established: (*a*) the method of photoelasticity has been utilized to examine inhomogeneous plastic flow including evaluation of yield surfaces and localized shear banding. The method has been employed in investigation the shear banding phenomenon in hot rolled 1018 steel and cold rolled 1018 steel at high strains, yielding approximate measurements for the band width. A number of photoelastic

### A. Solid Mechanics

coatings with different thicknesses, adhesives and elongations have been examined. Analysis for yield surface measurements has also been conducted using thin walled cylinders with marginal success; (b) the theoretical work has involved the development of a framework for describing plastic deformation with emphasis on predicting anisotropy, noncoaxiality and their implication to the phenomena of axial effects in torsion and shear banding at finite strains. To this end, models based on dislocation slip are being developed; (c) the numerical work includes the evaluation of the aforementioned models in predicting shear banding and axial effects in torsion; and their implication to specific problems such as high ballistic penetration and the manufacturing processes of deep drawing and metal cutting; (d) some progress has also been made towards an understanding of the relationship between micro and and macro instabilities during finite plastic deformation and rotations.

# 27538 CONTINUUM MECHANICAL MODELING OF SOLID UNDERGOING A PHASE TRANSFORMATION

Rohan Abeyarathe Massachusetts Institute of Technology

### SC: BRL. MTL

Thermomechanical effect: Historically, phase transformations in solids were first observed to occur as a result of heat treatment, and this is the setting of many metallurgical studies. Many of the recent modeling efforts at the continuum level, however, have been concerned with purely mechanical aspects of this phenomenon, and so effectively have been restricted to isothermal situations. Work is in progress on extending the continuum modeling of the mechanical response of such materials to general thermomechanical situations. The model is based on constructing an appropriate Helmholtz free-energy potential from which the theory then stems. Researchers have constructed a model for such a free-energy function and are looking at (a) the isothermal mechanical response of the material at different temperatures, and (b) the thermal response of the material at different (constant) stress levels. Preliminary indications suggest that the model can predict behavior similar to those observed in experiments on shape memory materials. Surface structure: The continuum-level modeling of stress-induced phase transformations has involved three basic ingredients: (a) a free energy function characterizing the bulk response of the two different phases, (b) a kinetic law describing the rate at which material transforms from one of these phases to the other, and (c) a nucleation criterion which signals the onset of the transformation. One facet of the theory that is conspicuously missing here is a model for the interfacial free energy of the boundary between the two phases. Efforts are being made to construct this model.

# 28222 PROCESS DEFECTS IN COMPOSITES

D. Krajcinovic

M.P. Mignolet

Arizona State University

SL: BWL, STRUC DIR

The research effort was directed towards the development of a rational analytical model for physicochemical processes characterizing polymerization, and the investigation of possible mechanisms leading to the clustering of fibers during the early stages of the curing process. The first task involves considerations of two models of equilibrium gelation: (a) Flory-Stockmayer mean field theory of random formation of bonds on an infinite Cayley tree, or Bethe lattice, and (b) bond percolation model of cluster formation as a description of a polycondensation process. At the moment, it seems that the second class of models has certain advantages. In particular, it allows for spatially cyclical structures, preserves physical tength scales and provides for statistical estimates of defect dimensions. Additionally, switching to bond-site percolation models it becomes possible to consider initial distribution of initiators, trapped solvents. At the same time studies are being made of at least three different kinetic rate equations in an attempt to derive the expressions for the time rate of change of the viscosity, elastic moduli and strength as a function of temperature, pressure in the autoclave and the type of the chemical reaction. The principal concern is, at the moment, to establish a rational physicochemical basis for the future micro- and macro-mechanical models in tune with the current developments in polymer sciences. In particular, the current emphasis is to relate the so-called cure degree, used in phenomenological models, to actual physical and chemical processes taking place during the cure process.

# 28253 EFFECT OF NOSE SHAPE AND MASS OF THE IMPACTOR ON IMPACT DAMAGE OF LAMINATED COMPOSITE SHELLS

Fu-Kuo Chang Stanford University SC: BWL, MTL

The research objective is to study impact damage in thin to thick shells fabricated from fiber reinforced polymer based matrix composites subjected to low velocity impact under different types of impactors and determine the effect of the impactor's mass and nose shape on impact damage in laminated composites as a function of ply orientation, thickness, and laminate curvature.

# 28283 CONSIDERATION OF MICROSTRUCTURAL CHANGES IN THE STUDY OF ADIABATIC SHEAR BANDS

Romesh C. Batra University of Missouri at Rolla

SL: BRL SC: BWL

A paper is being published on a study of the development of shear bands in a viscoplastic hollow circular cylinder containing two elliptical voids on a radial line and located symmetrically about the center. The material of the cylinder is assumed to exhibit strain- and strain-rate hardening and thermal softening. The impact loading on the inner surface of the cylinder is simulated by applying a known radial velocity to particles on the inner surface; the outer surface of the cylinder is taken to be traction free. Both of these surfaces are taken to be perfectly insulated. It is found that shear bands initiate from void tips closer to the inner surface sooner than those form the other void tips. The effect of strain-hardening is to delay the initiation of shear bands.

### 28307 HIGH VELOCITY IMPACT OF COMPOSITE LAMINATES

C.T. Sun

Purdue University SL: BWL

### SC: BRL, STRUC DIR

The research objective is to conduct theoretical and experimental studies to contribute to the understanding of the key elements in high velocity impact of composite laminates and to model the penetration, perforation, and delamination processes during impact. Static perforation tests will be performed to obtain a perforation force-displacement relation needed for the development of an analytical model. A finite element analysis will be applied to the individual layers in thin laminates, but a theory of homogeneous media with equivalent elastic constants will be used for thick laminates. An analysis of shock wave propagation will be conducted in the target laminated plate that is modeled by the Mindlin plate theory that accounts for transverse shear deformation, and ray theory will be used to study the growth or decay of the shock wave. A series of ballistic impact experiments will be performed to establish penetration depth for a given impact velocity, the ballistic limit of the laminate, and delamination inflicted by the impact. Experimental measurements will be compared with analytical predictions to validate the analytical models.

# 28317 LARGE DEFORMATION ANALYSIS OF NONLINEAR HOMOGENEOUS AND HETEROGENEOUS MEDIA USING AN ARBITRARY LAGRANGIAN-EULERIAN FINITE ELEMENT METHOD

S. Ghosh

University of Alabama-Tuscaloosa

SC: BRL, BWL, MTL

An implicit Arbitrary Lagrangian Eulerian large deformation finite model is being enhanced with adaptive mesh movement capability. Incremental and accumulated forms of interpolation error in the effective plastic strain and domain boundary error due to stretching, have so far been the criteria for monitoring the adapted mesh movement. In particular, a generalized error indicator with both sources of error have been combined into a single expression to yield an effective error. Presently, the principal investigator is involved in making a comparative analysis of the various models available in this area by testing them with his large deformation FEM codes to evaluate their characteristics. At the initial stages of this work, a viscoplastically regularized elastic-plastic model seems to naturally introduce a length scale that sets the width of the shear bands. However, a substantial amount of dynamic analysis needs to be done before this can be confirmed. Significant progress has been achieved in the area of research, where a new finite element formulation has been developed for composites with the second phase, randomly dispersed in a matrix. The analysis involves the introduction of an unique mesh by Dirichlet tessellation of the domain, thus accounting for the randomness in location, shape and size of the second phase. The resulting mesh consists of Voronoi polygons, which serve as elements in the finite element analysis of composites. A hybrid assumed stress formulation has been invoked in order to accommodate elements with varying number of nodes. An element based local coordinate system has been used to provide

### **B.** Fluid Dynamics

invariance properties to the element stiffness matrix and load vector. The second phase material has been modeled by decomposition of the nonhomogeneous part and a deviation part and the introduction of a transformation strain, as in the self-consistent methods. Only linear elastic materials have been considered so far.

# **B.** Fluid Dynamics

# 25461 ROTORCRAFT CENTER OF EXCELLENCE

Daniel P. Schrage Georgia Institute of Technology

> SL: AERO DIR, SC: OASA (RDA) AP TEC DIR, AVSCOM, STRUC DIR

The following research tasks are being studied; studies in three-dimensional viscous aerodynamics, aerodynamic interactions, blade tip aerodynamics, unsteady aerodynamics for rotor aeroelasticity, vibration and trim of elastic rotor blades with dynamic stall, unsteady aerodynamic testing of model rotors, nonlinear beam theory, rotorcraft vibrations and structural dynamics, damage resistance in rotorcraft structures, and modern and active control research for rotorcraft applications.

#### Reports:

No. 1-35 in previous editions.

- Tripping of Thin-Walled Plating Stiffeners in Axial Compression, by D. A. Danielson et al., *Thin-Walled Structures* 10,121(1990). AD A226 348
- 37. The Interaction Between a Vortex-Dominated Wake and a Separated Flowfield, by N.M. Komerath et al., MS.
- 38. Results From a Time-Stepping Computation of Rotorcraft Aerodynamic Interactions, by O. Schreiber and N.M. Komerath, MS, Comp and Fluids.
- 39. A Three-Dimensional Navier-Stokes/Full-Potential Coupled Analysis for Viscous Transonic Flow, by L.N. Sankar et al., MS.

# 25467 ROTORCRAFT CENTERS OF EXCELLENCE

Alfred Gessow University of Maryland

> SL: AERO DIR, SC: OASA (RDA) AP TEC DIR, AVSCOM, STRUC DIR

Research is being conducted in the following areas: dynamics, flight dynamics, aerodynamics, composite

#### **V Engineering Sciences**

structures. The dynamics studies include theoretical and experimental analysis of tailored composite beams under static and dynamic environments, aeromechanical stability test of a bearingless rotor, dynamics of helicopters with dissimilar blades and damping estimation from rotor stability data. Flight dynamics studies include stability and control. Helicopter maneuverability aerodynamic studies include experimental and theoretical investigation of rotor/body/ lifting surface interactional aerodynamics, rotor wake studies in hover and forward flight using wide-field shadowgraphy, experiments on unsteady circulation control, rotor/wind-tunnel wall interference effects and modeling of unsteady aerodynamics and dynamic stall. Composite structure studies include delamination suppression via structural tailoring, crashworthiness of composite structures and multiaxial loads, manufacture of foam-core composite box beams, strength of parallel discontinuities, finite element modeling of composite rotor blades, strength of tapered composite structures and active vibration control of rotorcraft structures.

### Reports:

No. 1-25 in previous editions.

- Bearingless Rotor Aeromechanical Stability Measurements and Correlations Using Nonlinear Aerodynamics, by James M. Wang and Inderjit Chopra, MS.
- 27. Measurements of a Rotor Flowfield and the Effects on a Fuselage in Forward Flight, by J.G. Leishman and Nai-pei Bi, MS.
- 28. Crashworthiness of Truncated Composite Cones Under Side Loads, by David C. Fleming and Anthony J. Vissini, MS.
- 29. Analysis of Unsteady Pressures Induced on a Body in the Vicinity of a Rotor, by Nai-pei Bi and J.G. Leishman, MS.
- 30. A Study of Rotor Wake Development and Wake/Body Interactions in Hover, by A. Bagai et al., MS.
- 31. Vibration Control of Composite Beams Through Strain Actuation and H-Infinite Control Theory, by Gregory Stephen Agnes, MS Thesis, 1991, 91 pp.
- 32. Contributions to the Experimental Investigation of Rotor/ Body Aerodynamic Interactions, by Nai-pei Bi, PhD Thesis, 1991, 331 pp.
- 33. Effects of Ply Drop Sequence on the Delamination Strength of Tapered Composite Structures, by Anthony Botting, MS Thesis, 1991, 111 pp.

# 25623 FREE–WAKE COMPUTATION OF HELICOPTER ROTOR FLOW FIELDS FOR GENERAL FLIGHT REGIMES

John Steinhoff

Flow Analysis Incorporated

SL: AERO DIR SC

SC: OASA (RDA)

Researchers completed development of a preliminary version of the HELIX II forward flight computer code. This involved implementing a time-dependent version of the marker-based Vortex Embedding Method for treating the rotor wake. This basic method is used in the HELIX I hover code and has been validated by extensive free-wake studies. This markerbased method should be accurate everywhere except in those regions where the wake impinges on the helicopter body or on a blade. With the method, the wake is accurately computed with no numerical diffusion as it convects through the flow field. At the same time, compressibility effects, including transonic flow with shocks, are also accurately treated. Preliminary results have been obtained in applying the new Vortex Capturing Method for a single rotor which sheds a concentrated tip vortex which convects with the flow. A HELIX I hover solution was used as an initial velocity field. The flow was then numerically convected using a time-accurate fixedgrid Euler finite-difference scheme as it evolved from this initial state such that the vortex convected through an azimuth of 50 degrees.

### 26595 BOUNDARY LAYERS INDUCED BY THREE-DIMENSIONAL VORTEX LOOPS

A.T. Conlisk Ohio State University

SL: AERO DIR

In the present work the interaction of a three dimensional vortex filament with a cylinder is considered. The problem is a simplified model of the interaction between a tip-vortex shed from a helicopter rotor and the fuselage. The Biot-Savart law is employed to describe the flow induced by the vortex and the flow is assumed to be inviscid and irrotational outside the core of the vortex. The motion of the filament indicates that a strong interaction between the vortex and the cylinder will take place as the vortex approaches the cylinder. The numerical calculations indicate that a large adverse pressure gradient develops under the vortex on the wall causing a rapid drop in the pressure there; large variations in the curvature of the vortex are not observed. The present results are compared with recent experimental measurements and the numerical results for both the motion of the filament and the pressure distribution are in broad agreement. The nature of the initial stages of the breakdown of local axisymmetry of the core of the vortex filament is suggested based on both the numerical and experimental results.

Reports:

 The Unsteady Interaction of a 3-Dimensional Vortex Filament with a Cylinder, by H. Affes and A.T. Conlisk, MS.

# 26631 AN OSCILLATING THREE-DIMENSIONAL WING EXPERIMENT

Franklin O. Carta Peter E. Lorber United Technologies Research Center

SL: AERO DIR.	SC: AERO DIR, AFOSR,
STRUC DIR	PROP DIR

This experiment explores the transient compressible aerodynamic response of a three-dimensional wing undergoing unsteady pitching motions to high angles of attack. The experiment obtained basic information applicable to both helicopter rotors during high speed forward flight and to fixed wing aircraft undergoing large amplitude unsteady maneuvers. It expanded upon the results for a similar two-dimensional wing obtained in 1986 under AFOSR sponsorship. A further objective was to also obtain information on incipient torsional stall flutter by studying small amplitude (0.5-2.0) oscillations near static stall. This information is being used to uncover new fluid dynamic phenomena, to clarify the understanding of previously known phenomena, and to provide a data set for validation of current and future computational methods. The wind tunnel test was successfully completed. Data for the unswept configuration were acquired. The  $\lambda = 15^{\circ}$  configuration was tested next. Data were acquired for 33 constant pitch rate ramps, 65 large amplitude sinusoids, 21 small amplitude sinusoids, and 87 steady-state conditions. The independent variables were Mach number, pitch rate or reduced frequency, mean angle of attack, and oscillation amplitude. Finally,  $\lambda = 30^{\circ}$  data were acquired for an additional 43 ramps, 105 large amplitude sinusoids, 140 small amplitude sinusoids, and 91 steady-state conditions, for a total of 934 test points. Two papers describing the primary features observed during initial examination of the data were prepared.

#### Reports.

 Incipient Torsional Stall Flutter Aerodynamic Experiments on a Swept Three-Dimensional Wing, by Peter E. Lorber and Franklin O. Carta, AIAA 91, AIAA-91-0935, 1991, 1692, AD A238-764

 Dynamic Stall Experiments on a Swept Three-Dimensional Wing in Compressible Flow, by Peter E Lorber et al., AIAA 91, AIAA-91-1795, 1991. AD A238 3611

# 26863 THEORETICAL STUDY AND TURBULENT MIXING BETWEEN HYPERSONIC STREAMS

David C. Wilcox DCW Industries, Inc.

#### SL: BRL

The principal investigators have done testing of compressibility modification for both the k- $\omega$  and multiscale models and have found that initial assessment was incorrect in one important aspect. On the one hand, using the k- $\omega$  model, the modification permits accurate prediction of the compressible mixing layer without causing a loss of accuracy for boundary layer predictions but not for shock-separated flows. On the other hand, using the multiscale model, the principal investigators are now able to make accurate predictions for the compressible mixing layer, the compressible flat-plate boundary layer and shockseparated flows. This is convincing evidence that the k- $\omega$  model's use of the Boussinesq approximation is unsuitable for separated flows.

#### Reports

No. 1.3 in previous editions

 Theoretical Study of Turbulent Mixing Between Hypersonic Streams, by David C. Wilcox, MS

# 27062 COMPUTATIONAL FLUID DYNAMICS RESEARCH ON DYNAMICALLY ADAPTIVE MESH METHODS FOR TRANSONIC FLOWS

Richard G. Hindman Iowa State University of Science and Technology

SC: BRL

The efforts to date promise to bring what has been a great amount of effort on various phases of the overall task into focus and integrate all of the knowledge gained in dynamically adaptive mesh generation into a final product. Information has been generated which guides the researcher regarding when adaptive meshes are useful and when they just produce excess baggage. The various methods of coupling the mesh dynamics and the flow dynamics are still being explored. The strong coupling procedure is the most elegant, and the most rigorous. It produces the best results in the cases studied so far. However, it is also the most expensive. The expense may turn out to be prohibitive in multiple aimensions. The mesh adaptation procedures explored in this research are ideally suited for use it problems with moving and deforming boundaries.

Reports:

- A Quantitative Study of the Meaning of "A Good Grid", by R.G. Hindman et al., MS, J Comp Phys.
- Annual Report Progress on Dynamically Adaptive Grid Methodologies Applied to Unsteady Fluid Flow Problems, by R.G. Hindman and Brad Beck, TR, Nov 90, 24 pp

### 27515 RAPIAL INFLOW TURBINE

Widen Tabakoff Awalet Hamed

University of Cincinnati

SC: TACOM

Laser Doppler velocity measurements were conducted to determine the detailed flow field in a radial inflow turbine nozzle without rotor. The flow velocities were measured at the nozzles upstream, inside and downstream of the nozzle blades. The flow field inside the nozzle blade passages was found to be strongly influenced by the upstrea. scroll geometry. Significant end wall cross flows and flow mixing were observed. The turbine test rig was modified by introducing a corresponding radial rotor to study the influence on the flow behavior in the nozzle (guide vanes). TSI rotary encoder equipment was added which indicate the rotor position with respect to the intervide vanes (IGV) at a given time and software for use in the new LDV measurements with the rotor. The rotary encoder requires pulse signal from the turbine rotor to indicate the starting position (lock cn). Unsteady LDV measurements of the flow at the mid span plane of the turbine IGV were performed. Two hundred data were taken for each rotor blade position at a given IGV location. This requires 8,000 velocity measurements for each IGV measuring location. Results were obtained for three different rotor positions for the mean velocity, flow angles and turbulence contours in the measuring plane.

# 27558 FLUID DYNAMIC MECHANISMS AND INTERACTIONS WITHIN SEPARATED FLOWS

J. Craig Dutton

A.L. Addy

University of Illinois

SL. BRL

An experimental investigation has been conducted to study the effects of a base cavity on the near-wake flowfield of a slender, two-dimensional body in the subsonic speed range. Three base configurations were

investigated and compared: a blunt base, a shallow rectangular cavity base of depth equal to one-half the base height, and a deep rectangular cavity base of depth equal to one base height. Each configuration was studied at three freestream Mach numbers, ranging from the low to high subsonic range. Schlieren photographs revealed that the basic qualitative structure of the vortex street was unmodified by the presence of a base cavity. However, the vortex street was weakened by the base cavity, apparently due to enhanced fluid mixing occurring at the entrance of the cavity. The weaker vortex street yielded higher pressures in the near-wake for the cavity bases, increases in the base pressure coefficients on the order of 10-14 percent, and increases in the shedding frequencies on the order of 4-6 percent relative to the blunt-based configuration. The majority of the observed changes occurred in going from the blunt base to the shallow cavity base. An experimental investigation of the complex interaction region generated by the separation of two supersonic streams past a finite-thickness base has been conducted in a two-dimensional wind tunnel. The data were obtained using schlieren photography, pressure measurements, and two-component LDV measurements. The shear laver mixing regions are characterized by initially constant pressure mixing, by an evolution of velocity profiles from truncated boundary layer shapes to wake-like profiles farther downstream, and by relatively high levels of turbulence. The separated flow region is characterized by large reverse flow velocities and strong interactions with the low velocity regions of both sheet layers. Turbulence intensities and kinematic Reynolds stresses are strongly affected by the separation process at the base and increase greatly in the latter portions of the two shear layers and in the recompression region. Recovery of the mean velocity field in the redeveloping wake occurs quickly, while the turbulence field remains perturbed to the furthest streamwise location investigated.

### Reports

- 1 Experimental Investigation of an Embedded Separated Flow Region Between Two Supersonic Streams, by V.A. Amatucci et al., 3/AA/90, 4/AA/90, 0.07, 1990, AD A226 339.
- 2 The Two-Stream, Supersonic, Near-Wake Flowfield Behind a Finite-Thickness Base Part I. General Features and Trends, by V.A. Amatucci et al., MS, AIAA J.
- Effects of Base Cavity on Subsonic Near-Wake Flow, by R W Kruiswyk and J C. Dutton, 474.4 J 28, 1885(1990) AD A232, 339.

### 27625 COLLABORATIVE TESTING OF TURBULENCE MODELS

Peter Bradshaw

Stanford University

Progress has been very slow because modelers have mostly failed to keep to the requested deadlines. fhis is partly because many of them have had to make minor or major changes in their models to produce reasonable agreement with data, even with the correlations of skin-friction data for flat-plate boundary layers at various Mach numbers used as initial "entry" test cases. This has made it impossible to distribute full sets of test results to the collaborators for comments on the timetable originally laid down. However a great deal of useful information has been accumulated and redistributed. A notable feature is the wide range of empirical constants used. or predicted, for the "law of the wall," which is supposed to be universal. This simply indicates inadequate communication between modelers and experimenters, because the community should be able to achieve a consensus: the present project is an ideal vehicle for such communication. Also notable, in view of the funding agencies' interest in compressible flow, is the large scatter in predictions at high Mach numbers. The present position is that a quasifinal set of results for the "entry" test cases and the first set of real test cases will be distributed shortly, together with a second major set of test cases. The second set will include three-dimensional and unsteady flows, with several test cases at supersonic or hypersonic Mach numbers. However, the figures in the cited reference show that some of the models which nominally function at high Mach numbers actually produce results which are far from the consensus data correlation.

Reports.

1. Collaborative Testing of Turbulence Models, by P. Bradshaw et al., AIAA 97, AIAA-97-0275, 1991, AD A232 881

# 27627 UNSTEADY FLOW PHENOMENA IN DISCRETE PASSAGE DIFFUSERS FOR CENTRIFUGAL COMPRESSORS

Edward M. Greitzer

Mass, husetts Institute of Technology

SC: PROP DIR, TACOM

A new graduate student has started work on this research project. He has familiarized himself with the data acquisition system and the hardware aspects of the design of the centrifugal diffuser research rig.

### **B.** Fluid Dynamics

He has now run the rig and acquired initial diffuser pressure rise characteristics. Additional Kulites have been ordered to enable more detailed resolution of the unsteady flow field. The goal with this instrumentation is to obtain improved definition of the onset of stall in the radial diffuser at off-design operation. The experimental rig has been dismantled for installing the necessary transducers for steady state performance of two diffuser configurations and for detection of the existence of diffuser stall precursor.

# 27752 STUDIES ON DYNAMIC STALL PHENOMENON IN THREE-DIMENSIONAL FLOWS

G.R. Srinivasan JA! Associates

SL: AERO DIR, STRUC DIR

Progress is being made on two related problems of dynamic stall phenomenon. Most of the computations on the dynamic stall phenomenon are limited to two-dimensional flows and have addressed the deep stall regime consisting of massive separation made ip of large scale vortex structure of the order of the chord of the airfoil. Although these studies have used a variety of turbulence models to model the viscous separated flow, their findings have been largely similar showing very little influence for the eddy viscosity model used. In contrast, there have been very limited studies on modeling light stall regime of the dynamic stall largely because of the difficulty in modeling the separation and the dynamic stall vortex and the sensitivity to the turbulence model used. The present investigation is concerned about modeling the vorticity dynamics, viz., the physical mechanism of transport of vorticity from the viscous boundary layer in to the most inviscid vortex structure. This means understanding the physical mechanism of the separation and formation of dynamic stall vortex in light stall regime of oscillating wing or airfoil is of primary concern in this investigation. Towards this end, studies have begun to model light stall regime of an oscillating airfoil with a Navier-Stokes code using three turbulence models, viz., Cebeci-Smith, Baldwin-Lomax, and Johnson-King nonequilibrium models. The above to calence models have been incorporated into a two-dimensional Navier-Stokes code. Currently, the airfoil has been taken through one cycle of oscillatory motion using Baldwin-Lomax turbulence model. The results do not properly model the lift hysteresis as shown by the experimental data. Each calculation has to be carried out for a least

two-cycles of the airfoil motion. The oscillating wing calculations will start after the airfoil studies. *Reports*:

- Flowfield of a Lifting Hovering Rotor—A Navier-Stokes Simulation, by G.R. Srinivasan et al., Proc 15th European Rotorcraft Symp, NASA Technical Memorandum 102862, 1990. AD A231 336
- 2. Flowfield Analysis of Modern Helicopter Rotors in Hover by Navier-Stokes Method, by G.R. Srinivasan et al., MS.
- 3. Navier-Stokes Solutions of a Helicopter Rotor in Hover and Forward Flight, by G.R. Srinivasan, MS.

# 27894 COMPRESSIBILITY EFFECTS ON AND CONTROL OF DYNAMIC STALL OF OSCILLATING AIRFOILS

M.S. Chandrasekhara M.F. Platzer

Naval Postgraduate School

SL: AERO DIR SC: AERO DIR

The major thrust was on obtaining conditionally sampled LDV measurements. The flow velocities were mapped in the range  $-0.25 \le \frac{1}{c} \le 0.75$ ,  $0 \le 2\frac{1}{6} \le 0.67$  for  $\alpha = 10^{\circ} - 10^{\circ}$  sin  $\omega t$  at M = 0.3and k = 0.05. These are being analyzed. Additional data processing software was developed to incorporate the changes necessitated by the computer upgrade at NASA/FML and also to present the data suitably. The most significant result is the measurement of large, time averaged streamwise velocities of 1.6  $U_{x}$  near the leading edge region, a slight distance ( $\sim 2$  mm) above the airfoil upper surface. Schemes are being devised to allow an even closer approach to the surface. Additional experiments were also carried out just to explore the leading edge region at a very fine resolution (1.25 mm) at M = 0.3and 0.4, at 2 degrees amplitude. In addition, some very high quality real-time interferograms were obtained for a broad matrix of experimental conditions. The most striking result of the interferometry study is the inferred pressure distribution in the leading edge region for  $0 \le \frac{1}{2} \le 0.004$ . Such a detailed unsteady pressure measurement in the region is impossible by any other presently available techniques.

#### Reports:

- 1. Comparison of Pitch Rate History Effects on Dynamic Stall, by M.S. Chandrasekhara et al., MS.
- 2. Impact of Compressibility on Boundary Layer Behavior on Dynamically Stalling Airfoils, by L.W. Carr et al., MS.
- 3. A Study of Dynamic Stall Using Real-Time Interferometry, by L.W. Carr et al., AIAA 90, AIAA-91-0007, 1991, AD A232 449

### 28002 FAR-FIELD ROTOR NOISE

Valana L. Wells Arizona State University

SL: AERO DIR SC: STRUC DIR

The aerodynamic analysis of the rotor blade using a fully viscous, three-dimensional methodology has progressed well, in fact, beyond the point necessary for the acoustic study. The developed code solves the three-dimensional Reynolds-averaged Navier-Stokes equations in steady or unsteady regimes. After a fairly extensive verification phase, the code has been adapted for evaluating the flow over the BERP planform. The code incorporates the ability to prescribe virtually any velocity to the grid so that it can accommodate feathering and flapping motions as well as forward flight. Results up to this point include those for a rectangular blade in hover and forward flight at zero angle of attack. Results for the BERP blade include rectilinear flight at high angle of attack and low Mach number, hover at subsonic and transonic tip Mach number and at zero and 10 degrees pitch angle, and forward flight at 10 degrees pitch. A case incorporating forward flight at a nominal pitch of 10 degrees but with prescribed feathering and flapping motion is currently running.

# 28159 INTERACTIONS OF SPANWISE AND CHORDWISE VORTICITY ASSOCIATED WITH THREE-DIMENSIONAL DYNAMIC STALL OVER AN OSCILLATING WING

B.R. Ramaprian

Washington State University

#### SL: AERO DIR SC: AERO DIR

Experiments are being performed in a wind tunnel on a NACA 0015 wing of aspect ratio 2. The wing is oscillated sinusoidally in pitch about its quarterchord axis at a frequency of 1 Hz and an amplitude of 5 degrees around a mean angle of incidence of 10 degrees. Phase-locked measurements of the three components of velocity and the six components of turbulent stresses within the wing-tip vortex are being measured using a 3-component laser Doppler velocimeter. Measurements have been completed at two longitudinal locations downstream of the trailing edge of the wing. These correspond to one and 3 chord lengths respectively. Measurements will be obtained at other locations, including the very near field of the wing wake. A second wing model instrumented for obtaining surface pressure measurements has been designed and is being fabricated in the shop.

**B.** Fluid Dynamics

# 28215 VORTICAL FLOWS OVER AXISYMMETRIC SLENDER BODY CONFIGURATIONS WITH APPENDAGES

Mukand Acharya

H. Nagib

Illinois Institute of Technology

Work focused on the design and fabrication of windtunnel models and model positioning systems, as well as the assembly of experimental equipment including flow-visualization systems and pressuremeasurement systems. Work is also in progress to develop the required software for model positioning in the wind tunnel, as well as for automated data acquisition.

### 28249 WING-BODY JUNCTURE FLOW

Richard J. Bodonyi Ohio State University

SL: PROP DIR SC: BRL

Efforts have been concentrated towards a careful derivation of the governing equations, based on the work of Smith and Gajjar. It was felt that review was necessary since the possibility was raised that the problem as formulated by Smith and Gajjar is incomplete, at least for the "slender two-dimensional wing" case. After careful analysis, it has been concluded that the original formulation was correct. The linearized solutions of Smith and Gaijar were also verified since they will ultimately be useful in testing the accuracy of the finite-difference solutions of the full nonlinear problem. Also, a computer code appropriate for the solution of these equations which is based on the method used by Bodonvi and Duck for three-dimensional external flows with viscousinviscid interaction is under development. At the present time, the computer code is working reasonably well in this development stage.

# 28252 FUNDAMENTAL CAUSE OF ASYMMETRIC SEPARATED FLOWS

Frank Marconi

Grumman Aerospace Corporation

SC: BRL

The research objective is to study the fundamental cause of asymmetric vortex flows on projectiles at angle of attack. Modern computational fluid dynamics techniques to solve the conical Navier-Stokes and Euler equations will be coupled with traditional stability analysis methods to investigate the onset of asymmetric vortex shedding.

# 28293 UNSTEADINESS OF SHOCK-INDUCED TURBULENT BOUNDARY LAYER SEPARATION—AN INHERENT FEATURE OF TURBULENT FLOW OR SOLELY A WIND TUNNEL PHENOMENON

David S. Dolling Richard Gramann University of Texas at Austin

SC: BRL

In earlier work, it was observed that in unsteady shock wave boundary layer interaction specific motions of the separation shock correlated with specific "pressure signatures" in the incoming boundary layer. The objective of the current work is to determine whether these signatures are generated by turbulent structures or by some other source. Three sets of experiments have been carried out to date. The results of the first experiments show that the characteristic pressure signature corresponding to a turnaround can be detected at the furthest upstream station. The signature clarity decreases with distance, suggesting that there is not a specific structure over the upstream transducer for each turn-around detected on the downstream transducer. The implication is that the structures responsible "evolve" and that new structures are being "born" downstream of the upstream transducer. Thus, since some of the structures corresponding to turn-around do not pass over the upstream locations, the ensemble-averages at the upstream stations have a "weaker" signature. This provides concrete evidence that the signature associated with the turn-arounds results from turbulent phenomena that evolve and have a certain lifetime; it is not a wave propagating downstream with little change in amplitude. A more sophisticated analysis, now underway, will focus on individual events rather than ensemble-averages. By examining each of the turn-arounds individually and determining whether or not a particular structure passed over the upstream transducers, information on individual structures and their lifetime can be determined. With respect to the second experiment, no results are available yet. With respect to the third experiment, the undisturbed boundary layer studies, the largescale structure lifetime is at least  $22\delta_0$  and the span-wise scale is at least  $2\delta_0$ . The phrase "at least" is used because the conclusions are drawn from cross-correlations and because the measurements are made at the wall. Flowfield data will probably generate somewhat larger values.

# C. Combustion

# 24487 STUDIES OF ELECTRON-MOLECULE COLLISION PROCESSES IN PLUMES AND FLOW FIELDS

Vincent McKoy California Institute of Technology

SL: MICOM, SDIO/IST

The research objective is to obtain quantitative estimates of the cross sections for low energy electronmolecule collision processes. Cross sections for rotational, vibrational, and electronic excitation as well as dissociative recombination and dissociative attachment will be calculated for electron collisions with molecules of interest to rocket exhaust plume signature prediction. Calculations will be done using the P.I.'s multichannel formulation for computing the outcome of inelastic, electron-molecule collisions.

# 25190 AUTOIGNITION AND COMBUSTION IN DIESEL ENGINES UNDER COLD STARTING CONDITIONS

N.A. Henein

Wayne State University

SL: TACOM SC: BRADEC, CRDEC, TACOM

The autoignition and combustion in diesel engines under cold starting conditions has been investigated both theoretically and experimentally. The theoretical work consisted of a detailed analysis of the autoignition reactions by using the chain reactions developed in the Shell Model. It has been found that the coefficients need to be calibrated in order to simulate the experimental data obtained on the LABECO-TACOM engine at different ambient temperatures. Recent work indicated that the change in the calibration coefficients could be correlated to the inlet air temperature or any other operating parameter. The experimental work is conducted on the LABECO-TACOM single cylinder direct injection water cooled diesel engine. The engine is located in the cold room where the ambient air temperature can be controlled, by a microprocessor, from normal room temperature to 40°C. Two types of tests have been conducted by using diesel fuel. The first set of tests was under steady state conditions in order to

determine the effect ambient temperature on the ignition delay. The next set of tests was conducted to simulate the cold starting condition. The engine was motored at a steady speed without fuel injection. Then fuel was injected and detailed cylinder gas pressure traces were obtained for 70 successive cycles. The transient behavior of the engine was analyzed by calculating the rate of heat release and the cumulative heat release. In some runs the engine fired, accelerated and then misfired.

# 25245 ADVANCED CONCEPTS FOR CONTROLLED COMBUSTION IN DIESEL ENGINES

A.K. Oppenheim R.F. Sawyer A.C. Fernandez-Pello University of California, Berkeley

SL: PROP DIR, TACOM

Work has concentrated upon the studies of the mechanism of Pulsed Jct Combustion (PJC) systems, the essential control element that is of equal interest to both the non-premixed charge diesel combustion as well as to premixed stratified-charge engines. For this purpose experiments were carried out using a constant volume test chamber with ample optical accessibility, using combustion-driven PJC generators. Nonetheless, a U.S. Patent on Pulsed Jet Combustion for Non-Premixed Charge Engines, of particular relevance to direct injection diesel engines, has been issued by the U.S. Patent Office. The results of the test performed here to reveal the mechanism of a variety of multistream PJC systems are to be presented.

Reports:

No. 1-3 in previous editions.

- 4. Performance of Multiple Stream Pulsed Jet Combustion Systems, by J.A. Maxson et al., MS.
- 5. Turbulent Combustion in Contrast to Flames, by A.K. Oppenheim, MS.
- 6. Mechanics of Turbulent Flow in Combustors for Premixed Gases, by A.K. Oppenheim, MS.

# 25794 THEORY OF COMBUSTION OF LIQUID PROPELLANTS BASED ON HYDROXYLAMMONIUM NITRATE

Forman A. Williams University of California, San Diego

The research on HAN deflagration assumed condensedphase chemistry to control the deflagration velocity, addressed steady, planar, isobaric deflagration neglecting multiphase flow effects, employed one-step, Arrhenius chemistry and approximated the specific heats of all liquid species as being equal. Activation-energy asymptotics were applied, under these simplifying assumptions, for large values of the Zel'dovich number, to derive an expression for the deflagration velocity. These studies thus indicated that the adopted mechanism is consistent with available information. The studies of RDX deflagration continue to focus on identifying the most reasonable reduced chemicalkinetic mechanism. Entirely satisfactory reductions of kinetic mechanisms still have not been obtained. However, it has become clear that uniniolecular RDX decomposition cannot be the sole initiating step. There must be significant bimolecular contributions of some kind if the observed pressure dependence of the deflagration rate is to be predicted correctly. The work has not yet identified which bimolecular steps are likely to be most important. The studies are continuing towards adoption of a preferred reduced mechanism capable of producing agreement with observed deflagration velocities while maintaining consistency with known rates of elementary steps.

Reports:

1. Effects of Two-Phase Flow in a Model for Nitramine Deflagration, by S.C. Li et al., *Combust and Flame* 80,329(1990). AD A233 018

# 26403 PREDETONATIVE COMPRESSION OF PROPELLANTS

Neale Messina

Princeton Combustion Research Laboratory, Inc.

SL: ARDEC SC: BRL, MICOM

Experimental research on dynamic mechanical properties of propellants for both uniaxial and biaxial loading is being conducted utilizing the PCRL Ballistic Compressor, as a dynamic pressure generating system, and a specially-designed mechanical properties test chamber. Uniaxial Compressive Loading: Materials evaluated to date under uniaxial compressive loading are: gun propellants JA-2, M-30, M-9, XM43, and XM39; rocket propellant AP/HTPB/Al; and RTV rubber, all in the form of solid right circular cylinder grains. The tests were conducted over the range of conditioning temperatures from  $-40^{\circ}$ C up to 65°C. Biaxial Compressive Loading: The approach is to utilize the PCRL Ballistic Compressor dynamic pressure generating system with specially designed mechanical properties test chamber capable of withstanding maximum working pressure of 30 ksi, to simultaneously apply both a

### C. Combustion

time-varying confining pressure and axial load to the propellant grain.

### Reports:

1. The Ballistic Compressor: A New Test Method for Propellant Mechanical Properties Characterization Under Dynamic Loading, by N.A. Messina et al., MS.

### 26456 STUDY OF STREAMWISE VORTICITY STIRRED COMBUSTION

John McVey

A. Vranos

United Technologies Research Center

SL: PROP DIR

The objective of the effort is to establish the effect of large-scale, intense, streaming vortices on the gas turbine engine combustion process. Previously conducted efforts showed, using direct-flame photography, that the rate of propagation of confined, atmospheric-pressure, turbulent, high-speed diffusion flames could be significantly influenced by the introduction of streamwise vorticity in the approach flow. The current effort is directed at obtaining quantitative information on improvements in volumetric heat release that can be achieved using this technique in high-pressure flows. An assessment of the characteristics of the vortex arrays generated by different vortex generator surfaces is being conducted. Efforts are underway in a parallel effort to complete the design of an elevated-pressure combustion apparatus in which the combustion characteristics of a sected combustion configurations will be established. The rectangular-cross section apparatus incorporates windows that are approximately 12.5 cm wide and 38 cm long situated on the upper- and two side-walls of the test section. The windows are double-paned. That is, two quartz windows, separated by a gap through which air will flow, constitute each of the walls and upper surface. Heated air at a pressure of 7 atm will be delivered to the gap as well as to the interior of the test section, thereby minimizing the pressure load across the interior window pane. The outer window will be approximately 1.9 cm thick to support the pressure loading. The design is currently being analyzed and details of the design are being prepared.

### 26720 DROP WEIGHT IMPACT INITIATION OF ENERGETIC MATERIALS

A.M. Mellor Vanderbilt University

SL: ARDEC

SC: BRL, MICOM

#### **V Engineering Sciences**

An ongoing analysis using DYNA2D examined the elastic wave propagation in the drop weight for various drop weight geometries without a sample, and showed that the period of large oscillations in the experimental acceleration data corresponds to twice the elastic wave transit time for one length of the drop weight. New sample material properties (Young's modulus, E = 20,000 psi, hardening modulus, E = 19,000 psi), which should represent the propellant response to a high rate compression better than the old properties (E = 10,000 psi,  $E_t = 1000$ psi), were used. However, numerical problems, particularly hourglassing at the sample edge, once again arose prior to a typical reaction time. Accelerometer output data for tests conducted in 1989 were digitized. A computer program was written to calculate several previously undetermined parameters, e.g., sample thickness at reaction time, and sample kinetic energy. Initial calculations of sample thickness occasionally indicate values of less than zero. This implies that the anvil strain must be significant, thus allowing the bottom of the sample to be displaced. The program also uses an analytic method to estimate the sum of the change in drop weight kinetic energy and the drop weight elastic energy as a function of time using the accelerometer data. Preliminary results show that the previous data may overestimate the work done on the sample prior to ignition by as much as 25 percent. New experimental data obtained will be analyzed with this computer program. Analytical modeling of the wave propagation through the sample, drop weight, and anvil has also begun. High rate compression and tension data for the nine research propellants have been obtained. As suspected, the compression moduli, particularly at cold temperature, are much higher than the tensile moduli. All of the moduli are low compared to actual fielded propellants since the solids loading is also low. Differences in the moduli between the propellants can be attributed to the formulation differences.

Reports:

No. 1~3 in previous editions.

4. The Critical Impact Initiation Energy Test, by P.J. Baker et al., MS.

# 26769 DIAGNOSTIC TECHNIQUES FOR COMBUSTION ENGINES

Naeim A. Henein Karur R. Padmanabhan Wayne State University

SL: TACOM

SC: CRDEC

Many diagnostic techniques for the detection of malfunctions in diesel engines have been investigated. The work consists of theoretical and experimental parts. The theoretical work included the analysis of all possible diagnostic concepts and methodologies related to the different systems of the engine. Also, a detailed computer program was developed to calculate the instantaneous frictional torque of the engine and the rate of heat release at any crank angle degree during the cycle. The experimental work is being conducted on a Cummins 6 CTA 8.3 diesel engine.

# 26797 MECHANISM OF INTERMITTENT ATOMIZATION

S.P. Lin

Clarkson University

SC: BRL, TACOM

A new phenomenon of successive branching of a liquid jet induced by pulsating the jet was discovered. It was found that an intact jet can be made to bifurcate successively into a two-, three-, and multiplepronged jet by oscillating the nozzle along its axis at successively higher frequency. This phenomenon shall have a profound impact on combustion. A theoretical analysis of this phenomenon is currently being carried out. An intact liquid jet emanating from a nozzle is subjected to a periodic external forcing in the axial direction. It is discovered that the jet may be induced to atomize in a widely separated frequency bands. Droplets of different uniform diameters can be produced in different frequency bands. This new phenomenon may be exploited for programmed fuel injections.

#### Reports:

- Instability of a Viscous Liquid Jet Surrounded by a Viscous Gas in a Vertical Pipe, by S.P. Lin and E.A. Ibrahim, J Fluid Mech 218,641(1990). AD A231 981
- 2. Breakup of a Liquid Jet in a Swirling Gas, by Z.W. Lian and S.P. Lin, *Phys Fluids* A2,2134(1990). AD A233 022

# 27018 MULTIPLE DROP-CONTAINING TURBULENT EDDIES EFFECTS ON EVAPORATION, IGNITION AND COMBUSTION OF CLUSTERS OF DROPS

J. Bellan

Jet Propulsion Laboratory California Institute of Technology

SC: PROP DIR, TACOM

The model has progressed to the next level of sophistication where instead of one-dimensional it is now quasi-two-dimensional. The reason for this is the fact that in a one-dimensional model there is no way to get heat transferred from the high temperature boundary to ignite the fuel except by counter-flow convection. This picture would be realistic for clusters of drops on the centerline of the spray, but would not be realistic for clusters of drops located in the shear layer, such as the model describes. These clusters of drops obtain the heat necessary for evaporation from the adjacent, outer gas flow through entrainment of this gas in the shear layer vortices. To describe this new, more realistic physics the equations are now written for a new configuration. These new equations have now been coded for the steadystate case and the code has been debugged. The reasons that a steady state situation is studied first are the following: (a) it represents the simple case where the same average cluster is continuously injected and the injection rate is constant and (b) it provides a good code check before the unsteady case is treated.

Reports:

 A Model for the Evaporation of Clusters of Drops Embedded in Jet Vortices: I. Steady Injection of Identical Clusters, by J. Bellan and K. Harstad, MS.

# 27417 HIGH PRESSURE PREIGNITION CHEMISTRY OF HYDROCARBONS AND HYDROCARBON MIXTURES

Nicholas P Cernansky David L. Miller Drexel University SL: PROP DIR

R SC: BRADEC, TACOM

The research program to investigate the high pressure oxidation and ignition characteristics of hydrocarbon fuels has continued. Efforts were directed at continuing propane oxidation studies on the pressurized flow reactor, continuing static reactor studies for pentane oxidation, continuing atmospheric pressure flow reactor studies investigating the correlation between low temperature CO formation and octane number, and the installation of new Fourier Transform Infrared spectroscopy equipment to be used for the development of in situ measurement capabilities.

#### Reports:

- Investigating the Relationship Between Octane Number and Low Temperature Reactivity for Primary Reference Fuel Blends, by A.V. Gupta et al., MS.
- Effects of Pressure on Hydrocarbon Oxidation Chemistry, by David N. Koert, PhD Thesis, 1990, 404 pp.

### 27455 THE STRUCTURE OF LAMINAR FLAMES OF CH<sub>4</sub>/NO<sub>2</sub>, CH<sub>2</sub>/ONO<sub>2</sub>, AND HCN/NO<sub>2</sub>

K. Seshadri

University of California, San Diego

SL: BRL SC: ARDEC, MICOM

The principal objective of this research is to develop fundamentally sound models to describe the structure of diffusion flames and premixed flames burning CH<sub>4</sub>/NO<sub>2</sub>, CH<sub>2</sub>O/NO<sub>2</sub>, and HCN/NO<sub>2</sub>. It appears that the structure of CH<sub>4</sub>/NO<sub>2</sub> diffusion flames is fundamentally different from the structure of most hydrocarbon/air flames. The chemical reaction in CH<sub>4</sub>/NO<sub>2</sub> diffusion flames appears to proceed in three distinct layers. In the "fuel consumption layer" CH<sub>4</sub> reacts with radicals to form H<sub>2</sub>, and CO, and in the "NO<sub>2</sub> consumption layer", which is distinct from the fuel consumption layer, NO<sub>2</sub> is attacked by radicals to form NO, and O<sub>2</sub>. The "product formation layer" is located between these layers and in this layer the products CO<sub>2</sub>, H<sub>2</sub>O, and N<sub>2</sub> are formed. Using these results of the numerical calculations the chemical kinetic mechanism was reduced to six overall reactions, using a systematic reduction procedure, wherein the concentration of a number of intermediate species were assumed to be in a dynamic steady state.

### 27469 BOOST-PHASE DISCRIMINATION RESEARCH

David M. Cooper George S. Deiwert NASA Ames Research Center

SC: ARO, MICOM

Efforts have continued to investigate low density effects on flows at hypersonic speeds. Previous work involving compressed flow through a hypersonic shock wave has been updated and accepted for publication in the AIAA Journal of Thermophysics and Heat Transfer. This work showed that the Burnett equations produce simulations of shock wave structure that are significantly more accurate than the Navier-Stokes equations and will therefore form a necessary basis for the representation of nonequilibrium chemical reactions. Accurate prediction of chemistry will be necessary for the estimation of radiation signatures arising from hypersonic shock waves. This work is now being extended to the expanding region behind a vehicle, to both the base flow and to the more highly expended portions of the plume. Comparisons are being made to Navier-Stokes calculations and will be summarized in a paper that is in preparation. The Burnett terms are also being investigated in conjunction with thermochemical modeling in order to understand the radiation signature of the BSUV experiment. Other research efforts have been concerned with computing radiative intensity factors, transport properties, and reaction rates of air species that contribute to the radiation signatures of hard bodies and exhaust plumes.

# 27480 HIGH-ALTITUDE HYPERSONIC FLOWFIELD RADIATION

Robert W. MacCormack D.R. Chapman Stanford University

The new augmented Burnett equations have been developed and tested for 1D- and 2D-planar flows. This equation set has proven to be analytically stable (linearized stability analysis) and also computationally stable (numerical computations at high altitudes). The augmented equations exhibit the same degree of accuracy as the conventional Burnett equations in those cases at lower altitudes where solutions to the latter set can be obtained. The simplified Burnett equations have been programmed for axially symmetric flow and solutions obtained for the temperature and density distributions around blunt-nose shapes at various altitudes, low and high. This new code is currently in process of being coupled to the NEQAIR code for radiation, although at this writing numerical solutions have not yet been obtained for coupled codes. The main conclusion of this work is that the combined effect of rotational nonequilibrium and of Burnett terms on radiation can be large at high altitudes. This is due to the extreme sensitivity of radiation to flow field temperature. Although one must wait for results from the coupled NEQAIR code to be certain, it is possible that a significant part, if not the major part, of the observed discrepancy at high altitudes between rocket flight measurements of radiation and Candler-Park computational results, may be attributed to the omission of rotational relaxation effects combined with the use of Navier-Stokes equations instead of the more realistic Burnett equations.

#### Reports:

No. 1 in previous edition.

Stabilization of the Burnett Equations and Application to High-Altitude Hypersonic Flows, by X. Zhong et al., AIAA-91-0770, 1991. AD A231 082

### 27565 IGNITION STUDIES IN NONPREMIXED HYDROCARBON/AIR COMBUSTION

Chung K. Law Princeton University

SC: BRADEC, TACOM

This investigation explores the nature of the ignition "kernel" in nonpremixed hydrocarbon/air combustion: its spatial extent, its structure and chemical composition, and its sensitivity to variables such as temperature, pressure, and aerodynamic straining. The study is composed of two parallel investigations, one experimental and one numerical. Work has concentrated on H<sub>2</sub> air ignition because of the relative simplicity and accuracy of current reaction mechanisms used to describe the combustion process. After an experimental methodology has been developed for H<sub>2</sub>/air combustion, the study will be extended to the ignition of more complex hydrocarbons.

# 27864 KINETICS AND ENERGY TRANSFER IN NONEQUILIBRIUM FLUID FLOWS

D.R. Crosley

G.P. Smith

D.J. Eckstrom

SRI International

Analysis was concluded of the quenching data for the  $A^2\Sigma^+$ . v' = 0 level of nitric oxide in the shock tube. These measurements were made using the time decay of User-induced fluorescence (LIF) at two different pressures of NO. The temperature was 3500 K as determined from the shock speed. The quenching cross section (2- $\sigma$  error) is 59±20 Å<sup>2</sup>, slightly larger than the previously determined value of  $37\pm 8$  Å<sup>2</sup> at room temperature. Preliminary measurements indicate that, at this high temperature, N<sub>2</sub> quenches NO with cross section of 1.7  $Å^2$ . At room temperature, the value is very small, <0.01 Å<sup>2</sup>, and quenching of NO by  $N_2$  is generally ignored. This result shows it contributes significantly at high temperatures, and must be accounted for in emission or LIF measurements in flames and heated air. The experiment investigating the final state of quenching of  $A^2\Sigma^+$  NO has commenced. The object of this experiment is to learn the final distribution over vibrational levels of NO which has been collisionally transferred to the ground  $X^2\Pi$  state, a question having important implications for the application of microscopic reversibility for collisional excitation. In the experiment, a powerful laser at 226 nm pumps NO at a pressure of 4.4 Torr to the v' = 0 level of the A state. The excited NO is rapidly quenched by collisions with ground

state NO molecules. After a time delay of  $1-10 \ \mu$ s, a second tunable laser is fired. This probes the vibrational level distribution in the ground state NO via LIF in the  $B^2-X^2$  transition. In this initial experiment, v(X) = 7 was detected pumping the (0.7) band at 305 nm. Individual rotational lines near the band head could be easily resolved. Little change in signal level was seen over this delay range, indicating that v = 7 is formed directly in the quenching collision. In this self-quenching case, it could be NO removed from the A state, or ground state NO excited by the quenching collision. In either case, v = 7 represents a large jump in vibrational energy. Separating the two would be easy using <sup>15</sup>NO.

Reports:

- 1. Emission Spectra and LIF Decay Lifetimes of NO in Shock Tubes, by Ulrich E. Meier et al., MS.
- 2. Laser-Induced Fluorescence Decay Lifetimes of Shock-Heated NO ( $A^2\Sigma^+$ ), by Ulrich E. Meier et al., MS.

# 28250 DEVELOPMENT AND APPLICATION OF FLUORESCENT DIAGNOSTICS TO FUNDAMENTAL DROPLET AND SPRAY PROBLEMS

Lynn A. Melton

SL: CRDEC

University of Texas at Dallas

SC: BRL, PROP DIR, TACOM

The research objective is to develop and apply laserinduced fluorescent diagnostic techniques to measurements of droplet and spray heating and vaporization. Techniques of exciplex fluorescence visualization of liquids will be extended to provide fluorescent imaging of the local fuel/oxygen equivalence ratio. This will be accomplished through determination of both the fluorescence intensity and decay rate, obtained via a unique, gated detection system. Exciplex systems will be investigated to determine approaches to measurement of local mixing in turbulent, shear flows and to measurement of liquid and vapor fractions during droplet oxidation by N<sub>2</sub>O. Exciplex techniques will be investigated for the determination of dissolved oxygen in hydrocarbon liquids. Exciplex and normal fluorescence emissions from droplets and sprays will be used to determine internal flow fields in droplets and sprays at sub and supercritical pressures and temperatures.

# 28310 A THERMOCHEMICAL TRANSPORT MODEL FOR ANALYSIS OF HOT-SPOT FORMATION IN ENERGETIC MATERIALS

P. Barry Butler University of Iowa

SL: BRL

SC: AMCCOM

#### **D**. Structures and Dynamics

This research program addresses the issue of inadvertent ignition and detonation of condensed-phase, energetic materials. Specifically, the work focuses on hot spot formation and growth to detonation in heterogeneous, high-energy propellants and explosives which are subjected to stress-time profiles that are sustained shock, short duration pulse shock and ramp-like shock. To analyze the potential for hot spot formation under these conditions, a viscoplastic pore collapse model has been developed to model the dynamic behavior of a material void after it has been subjected to a specified stress-time profile. The model takes into account the effects of condensedphase material viscosity, yield strength, and pore gas pressure on the time-evolving pore deformation and heating. In addition to treating pore dynamics, energy balances for the condensed-phase material and pore gas are introduced in order to track temporal variations of interface and gas temperatures. Important thermal processes such as viscoplastic heating, finite-rate chemical effects in the gas phase, surface reaction, phase change, and heat exchange between the pore gas and surrounding material are included in the model. The results of this research effort will serve as a mechanism for evaluating the influence of propellant physical and chemical properties on the potential for hot spot formation and growth to detonation. The present hot spot model is based on a micromechanics approach to hot spot formation, and one goal of the research is to ultimately incorporate the micromechanics model into an existing macroscopic hydrocode.

# 28316 TWO-COLOR INFRARED DIGITAL IMAGING FOR DETERMINATION OF IN-CYCLINDER TEMPERATURE AND SPECIES DURING COMPRESSION AND COMBUSTION PERIODS OF A DIESEL ENGINE

Kyung Tai Rhee

Rutgers. The State University of New Jersey

SL: TACOM SC: BRADEC, PROP DIR

The objective of the research is to determine instantaneous spatial distributions of temperature and species, in-cylinder, during diesel engine ignition and combustion. A high speed, two color measurement system will be developed for near-instantaneous imaging of radiation from in-cylinder combustion processes. Data will be analyzed to give spatial distributions of species, initially water vapor, and temperature.

# 28427 THE EFFECT OF TURBULENCE ON VAPORIZATION AND MIXING IN FUEL SPRAYS

D.A. Santavicca

The Pennsylvania State University

SL: TACOM SC: BRADEC

Attempts will be made to determine the effects of swirl and turbulence on vaporization and mixing in fuel sprays. A steady droplet spray, radially uniform in drop density, temperature, size and velocity distributions, will be introduced into a high pressure, high temperature, turbulent flow reactor under conditions which simulate those in diesel engines. Measurements will be made of drop size-velocity and sizetemperature correlations of the evaporating spray and of temperature, pressure, mean and turbulent velocity components, length scales and turbulence energy spectrum.

### 28912 STAR 63: MULTILASER TRANSMISSION EXPERIMENT

K.S. Beale

Arnold Engineering and Development Center

SC: SDIO/IST

The objective of the research is to determine rocket exhaust plume temperatures and radiative characteristics. Ultraviolet and infrared spectral data, taken during the test firing of two STAR-63 solid propellant rocket motors in 1990, will be analyzed. Gas phase temperature will be determined from the observed aluminum chloride molecular absorption. This will be compared to temperature determined from the particulate continuum radiation. Temporal and spectral dependence of plume IR emission will be analyzed to determine the contribution of multiply scattered radiation to the total near-field radiation.

### **D.** Structures and Dynamics

# 24362 DYNAMIC PLASTIC INSTABILITIES IN NONLINEAR INELASTIC RESPONSE TO PULSE LOADING

P.S. Symonds Herbert Kolsky Brown University

SL: ARDEC, BWL SC: BRL, MTL

Calculations were continued on the two-degree of freedom (2DoF) beam model and a quasi-static test

procedure is proposed which provides sufficient conditions for the sign of the final displacement in a pulse-loaded beam or other fixed edge structure. The 2DoF beam model has response defined by two displacements and four strains (in two Shanley deformable cells treated as sandwich beam sections). Researchers have assumed the loading to be a short pulse of fixed duration, so that the force during the pulse is the single load parameter. The ends are attached to fixed pins. The response behavior of interest takes place long after the application of the pulse. When the plastic strains have reached terminal values the system is one of coupled autonomous Duffing equations. This system can exhibit chaotic behavior, with qualitatively different character depending upon the four plastic strain magnitudes, parameters in the equations. The quasi-static test consists of loading the specimen over a full displacement cycle. Concurrent calculations of the total work are made. On the basis of reasonable approximations, the latter permit identification of the extreme displacements that would occur at the ends of the first and second swings of the free dynamic motion following the first peak displacement: the signs of these displacements provide sufficient conditions for the final midpoint displacement to be positive or negative, respectively.

#### Reports:

No. 1-8 in previous editions.

- 9. Chaotic Responses of a Fixed Ended Elastic-Plastic Beam Model to Short Pulse Loading I. Response Characteristics; Sensitivity to Parameters, by J.-Y. Lee et al., MS, J Appl Mech.
- Chaotic Responses of a Fixed Ended Elastic-Plastic Beam Model to Short Pulse Loading II. Energy Approach: Role of Damping and Plastic Strains, by J.-Y. Lee et al., MS. J Appl Mech.
- Some Experimental Observations of Anomalous Response of Fully Clamped Beams, by H.Kolsky et al., MS. Intl J Impact Eng.

# 25327 STABILITY OF ELASTICALLY TAILORED ROTOR SYSTEMS

D.H. Hodges L.W. Rehfield Georgia Institute of Technology

A paper has been prepared in which two new elastic coupling mechanisms that occur in thin-walled composite tubular beams, bending-transverse shear and extension-transverse shear, are presented and evaluated. The evaluation is conducted for two limiting types of construction, one designed for classical bending-twist coupling and the other for extensiontwist coupling. The new couplings naturally occur in a parasitic manner. They cause the beams to respond as if they are much more flexible for certain modes of deformation. The magnitude of the effects produced are enormous. The effectively increased flexibilities may hinder or limit the use of elastic co<sup>11</sup> ling for structural tailoring

# 25409 PARAMETER IDENTIFICATION AND ADAPTIVE CONTROL OF COOPERATIVE ROBOTS

Devandra P. Garg Duke University

Excellent progress continues to be made in the areas of analysis, experiments, and dissemination of research results. In the area of analysis, a transformation matrix was developed relating the two IBM 7540 robot locations. This matrix, in conjunction with the calibration matrix developed earlier to map the image coordinates of an IRI D256 vision processor, provides the corresponding object coordinates in the work envelopes of the two cooperating manipulators. A supervisory computer commands the two robot controllers to generate appropriate instructions for the manipulator end effectors to follow a prescribed trajectory. The experimental work includes the integration of Adept vision system, force/torque sensor, and the motion control system in the existing robotic work cell. With this addition, the control of first two joint actuators on each robot, force/torque sensor, and vision system have been located on the same bus leading to an efficient and speedy exchange of data. In addition, a provision has been made to operate the robots in two alternate control configurations-the original IBM supplied mode and the Adept control mode.

#### Reports:

No. 1-2 in previous editions.

- 3. This number not used.
- 4. Nonlinear Dynamic Analysis and Control of Scara Robots, by Devendra P. Garg et al., MS.
- Adaptive Identification and Control of Robotic Manipulators, by Devendra P. Garg et al., MS.
- 6. This number not used.
- Camera-Robot Transform for Vision-Guided Tracking in a Manufacturing Work Cell, by Abhijit Nagchaudhuri et al., MS, J Intelligent and Robotic Systs.

### 25462 ROTARY WING TECHNOLOGY CENTER

Robert G. Loewy Russell J. Diefendorf Rensselaer Polytechnic Institute

SL: AERO DIR, SC: OASA (RDA) AP TEC DIR, AVSCOM, STRUC DIR

Research is being conducted in the following areas: Crash worthiness of rotorcraft, analysis and design of composite fuselage frames, effects of hygrothermal environment and microcracking on tension-torsion coupled composite rotor blades, optimization and experimental studies of composite drive shafts, helicopter maneuver rotor loads, development of a finite element based modal analysis, rotor blade optimization, computer-aided conceptual design of rotorcraft, blade vortex interaction, and effect of rotor shaft flexibility on ground/air resonance.

# 25630 LARGE-AMPLITUDE FORCED RESPONSE OF DYNAMIC SYSTEMS

Ali H. Nayfeh

Virginia Polytechnic Institute and State University

SL: AP TEC DIR SC: AERO DIR, TACOM

A published paper presents a study of the planar dynamic response of a flexible L-shaped beam-mass structure with a two-to-one internal resonance to a primary resonance. The structure is subjected to low excitation levels and the resulting nonlinear motions are examined. The Lagrangian for weakly nonlinear motions of the undamped structure is formulated and time averaged over the period of the primary oscillation, leading to an autonomous system of equations governing the amplitudes and phases of the modes involved in the internal resonance. Later, modal damping is assumed and modal-damping coefficients, determined from experiments, are included in the analytical model. The locations of the saddle-node and Hopf bifurcations predicted by the analysis are in good agreement, respectively, with the jumps and transitions from periodic to quasi-periodic motions observed in the experiments. The current study is relevant to the dynamics and modeling of other structural systems as well. Another paper discusses a study of the three-dimensional autonomous system treated by Rand. The method of multiple scales is used to obtain an asymptotic expansion for the amplitude and frequency of the limit cycle near the Hopf bifurcation of the system. The resulting analytical approximation is valid only in a small range near the Hopf bifurcation point.

No. 1-6 in previous editions.

Reports

- Motion Near a HOPF Bifurcation of a Three-Dimensional System, by A.H. Nayfeh and B. Balachandran, *Mech Res Commun* 17, 191(1990).
- Nonlinear Motions of Beam-Mass Structure, by B. Balachandran and A.H. Nayfeh, *Nonlinear Dynamics* 1,39(1990). AD A232 675
- Three-Dimensional Nonlinear Vibrations of Composite Beams—

   Equations of Motion, by Perng-Jin E Pai and Ali H. Nayfeh, MS, Nonlinear Dynamics.
- Three-Dimensional Nonlinear Vibrations of Composite Beams--II. Flapwise Excitations, by Perngjin E Pai and Ali H. Nayfeh, MS, Nonlinear Dynamics.
- Three-Dimensional Nonlinear Vibrations of Composite Beams— III. Chordwise Excitations, by Perngjin F. Pai and Ali H. Nayfeh, MS, Nonlinear Dynamics.
- Observations of Modal Interactions in Resonantly Forced Beam-Mass Structures, by B. Balachandran and A.H. Nayfeh, MS, Nonlinear Dynamics.
- Cyclic Motion Near a Hopf Bifurcation of a Four-Dimensional System, by B. Balachandran and A.H. Nayfeh, MS, *Nonlinear Dynamics*.
- 14. On Methods for Continuous Systems with Quadratic and Cubic Nonlinearities, by A.H. Mayfeh et al., MS.
- 15. Linear Free Vibrations of Cross-Ply Laminated Plates Using the State-Space Concept, by Ali H. Nayfeh and Jafar Hadian, MS.
- 16. Dynamic Characteristics of Slewing Metallic and Composite Beams, by Perngjin F. Pai and Ali H. Nayfeh, MS.
- 17. Buckling of Shear-Deformable Cross-Ply Laminated Plates Using the State-Space Concept, by Jafar Hadian and Ali H. Nayfeh, MS.

# 25771 DYNAMIC INSTABILITY AND TRANSIENT VIBRATIONS IN GAS-PROPELLED GUNS

Iradj Tadjbakhsh

Rensselaer Polytechnic Institute

The main task during the third year of the present contract is the refinement of the model for transient vibrations and dynamic instability in flexible guns that were developed during the first two years. Refinements include the effect on vibrations of the guns when projectiles are spin-stabilized and the effect of variations in the pressure of propellant gases. These effects were not included in the model that was developed and presented at the Sixth Army Symposium on Gun Dynamics. Work in the area of optimal control of vibrations of continuous systems is in progress. This work has already resulted in two publications that were reported previously and dealt with control of vibrations of conservative and selfadjoint systems. Work is underway on extending the method to cover damped and possibly nonself-adjoint systems.

#### Reports:

No. 1-3 in previous editions

- A New Approach to Microbuckling of Fibrous Composites, by Dimitris C. Lagoudas et al., MS, J Appl Mech.
- Optimal Control of Beams with Dynamic Loading and Buckling, by Yuan-An Su and Iradj G. Tadjbakhsh, J Appl Mech Paper No. 91-APM-5, (1991).
- 6. Transient Vibrations and Instability in Flexible Guns---I. Formulations, by Yuan-An Su and Iradj G. Tadjbakhsh, MS, J Impact Eng.
- Transient Vibrations and Instability in Flexible Guns--II. Response Characteristics, by Yuan-An Su and Iradj G. Tadjbakhsh, MS, J Impact Eng.
- Vibrations and Instability of Thick Cylindrical Shells with Moving Internal Pressure and Projectile, by Yuan-An Su, PhD Thesis, 1990, 99 pp.

# 26061 A NEW TREATMENT OF PERIODIC SYSTEMS WITH APPLICATIONS TO HELICOPTER ROTOR BLADE DYNAMICS

Subhash C. Sinha

Auburn University

SL: AERO DIR, SC: AP TEC DIR STRUC DIR

A proposed technique for determining the stability of multidimensional linear periodic systems has been extended to the case when the mass matrices appearing in the equations of motion also vary periodically with time. Two possible formulations of the solution technique were investigated. The "State-Space Formulation" is suitable for a set of first order equations while the "Direct Formulation" can be applied directly to a system of second order equations. The modified new technique was applied to study the flap-lag stability behavior of a multibladed helicopter in forward flight. In particular, the following problems were investigated: (a) generate stability boundaries as a function of flap and lead-lag frequency in forward flight; (b) investigate numerical efficiencies for three, four and five bladed rotors using multiblade coordinate transformations, and (c) examine the influence of parameter changes on the numerical efficiency and accuracy. In addition to the above numerical investigations, an attempt was also made to show that the proposed technique can also be applied to obtain approximate analytical solutions, at least for small systems. The technique has been implemented through MACSYMA to find an approximate analytical solution of the Mathieu equation.

#### Reports:

- 2. Dynamic Analysis of Anisotropic Rotor-Bearing Systems via Chebyshev Polynomials, by Tsan-Kai Chen, MS Thesis, 1990, 91 pp.
- An Efficient Computational Scheme for the Dynamic Analysis of Anisotropic Rotor-Bearing Systems, by S.C. Sinha et al., Intl Cong on Recent Dev in Air- and Structure Borne Sound and Vibrtn, 1990, 909. AD A225 901
- 4. Analysis of Dynamic Systems with Periodically Varying Parameters via Chebyshev Polynomials, by S.C. Sinha et al., MS, J Vibrtn and Acoust.
- 5. A New Approach in the Analysis of Systems with Periodic Coefficients with Applications in kotorcraft Dynamics, by Der-Ho Wu, MS, *J Am Helicopter Soc.*
- Analysis of Dynamic Systems with Periodically Varying Parameters via Chebyshev Polynomials, by S.C. Sinha et al., MS.
- 7. An Approximate Analytical Solution for Systems with Periodic Coefficients via Symbolic Computation, by S.C. Sinha and Vikas Juncja, Proc of 32nd Structures, Structural Dynamics and Materials Conference, 1991, 790.

# 26934 DYNAMICS OF DEFORMABLE MULTIBODY SYSTEMS USING RECURSIVE PROJECTION METHODS

A.A. Shabana

University of Illinois at Chicago

SL: AERO DIR, TACOM SC: STRUC DIR

The kinematic and dynamic equations based on the recursive projection methods were developed for open loop kinematic chains that consist of interconnected deformable bodies. This formulation has been implemented on the digital computer and the developed computer program was tested using simple examples. Initial results show that the use of the absolute and joint variables is more efficient than the use of the augmented formulation that employs the absolute coordinates and Newton-Raphson algorithms, even in the case of mechanical systems with relatively small number of degrees of freedom. The computational efficiency gained by using the absolute and joint variables and the resulting large system of loosely coupled equations is lost, however, when projection methods are applied to mechanical systems with relatively small number of degrees of freedom. Current research efforts are now directed at analyzing relatively large scale mechanical systems and examining the computational advantage of using projection methods.

#### Reports:

 Nonlinear Finite Element Formulation for the Large Displacement Analysis of Plates, by Bilin Chang and A.A. Shabana, J Appl Mech 57,707(1990). AD A232-626

An Efficient Computational Scheme for the Analysis of Periodic Systems, by S.C. Sinha and Der-Ho Wu, MS. J Sound and Vibrtn.

# 26995 THE FURTHER DEVELOPMENT AND REFINEMENT OF AN EXPERT-SYSTEMS APPROACH TO THE CREATIVE DESIGN OF MECHANISMS AND MECHANICAL SYSTEMS

E Freudenstein D. Hoeltzel M. Shoham Columbia University

SL: ARDEC, TACOM

A two-tier pattern matching scheme has been developed which presents a designer with a mechanism structure having a prescribed coupler curve pattern from a database of dimensionally parameterized mechanisms. The database for the prototype system includes one hundred and eighty four-bar mechanisms, and sixty six-bar mechanisms. Image: A digital video camera serves as the means for entering the image of a desired coupler curve, i.e., the target curve, and also to expand the database. This target curve is compared with curves in the library of mechanisms using a two-tier pattern matching algorithm. In the first tier, the entire database is scanned for a match of the invariants of the moments of the coupler curves, and the system calculates numerical certainty factors which quantify the degree of matching. Second tier matching employs the Fourier and Mellin Transforms as a basis for a more refined comparison of the twenty best matching curves from tier one, and presents a list of candidate mechanism structures possessing coupler curves which approximate that of the target curve. This methodology represents an extension of the P.L's previous work, called pattern matching synthesis, for automating the process of creative mechanism synthesis using backward reasoning.

#### Reports:

1. Stable Grasping with a Multi-Fingered Hand, by Moshe Shoham and Fuhua Jen, MS.

### 27075 SYNTHESIS AND SIMULATION OF ROBOTIC SYSTEMS

Bahram Ravani

University of California, Davis

SL: BWL, TACOM SC: ARDEC

This research program is concerned with the development of methods for design synthesis as well as CAD cased high performance dynamic simulation of mechanical systems such as robot manipulators. There has been two basic developments during this last reporting period. One involved technology transfer to an Army laboratory and the other has resulted in

### **V Engineering Sciences**

three technical publications. The first development has involved completing the documentation and software packaging of the computer program "OptAct" for optimal sizing of actuators for robotic and other equipment and transferring a copy of the program to Benet Weapons Laboratory. The development of a rational method for sizing and design of actuators has been of interest to Dr. John Vasilakis' group at the US Army Benet Weapons laboratory. The theoretical basis for this technique was published. The computer implementation has now been completed and a copy with documentation has been transferred to Benet Laboratory for their use. The program would allow the user select and optimally size a servo-controlled actuator for any articulated mechanical system from a payload specification. The program considers all the dynamics of the system and provides near optimal choices for the actuator. The program can be used to fine tune the design and the selection of actuators used in robotic system and other equipment such as Army's automatic ammunition loading systems. The second development involves preliminary results in applications of Clifford Algebra to dynamic analysis and CAD based simulation of robotic systems. Work is completed on the development of a technique that can obtain locations of objects from noisy images or field data by a simple averaging linear computation. The results have been applied to CAD based simulation of robotic systems but also have applications in image processing and target localization in smart weapons systems.

# 27300 MODAL INTERACTIONS AND COMPLEX RESPONSES IN NONLINEAR MULTIDEGREE-OF-FREEDOM MECHANICAL SYSTEMS

A. BajajP. DaviesPurdue University

The primary focus of the research is on the multimode dynamics of weakly nonlinear multidegree-of-freedom as well as continuous structural and mechanical systems. This is motivated by the recognition that for improved design, performance, and control of mechanical systems, it is necessary to understand the conditions and design parameters that can lead to complex, large amplitude response. Potential applications include the vibrations of thin panel structures in rotocraft fuselages, slender rotor blades, and rob\_sic manipulators. Three different models of physical systems are being studied. These include: 1.

Resonant motions and mode coupling in thin rectangular panels, 2. An autoparametric 2 degree-offreedom pendulum vibration absorber, and 3. The orthogonal double pendulum. The first one is an example of systems with cubic geometric nonlinearities, whereas the latter two systems possess important quadratic and cubic inertial nonlinearities. In each of these systems, resonant coupled-mode motions have been studied and the combination of parameters leading to single-mode and coupled-mode responses have been identified. Chaotic amplitude modulated motions have been observed in every one of these systems and the mechanisms for their creation and destruction are now being investigated. A rig has been designed and built to experimentally investigate the resonant response of thin rectangular panels with constant in-plane loading. The rig can accommodate panels with different aspect ratios, thereby allowing for several different mode-couplings to be investigated. Noncontacting electromagnetic exciters and transducers have been ordered and the stage is set to begin some exploratory experiments.

# 27510 CLOSED LOOP VIBRATIONAL CONTROL: THEORY AND APPLICATIONS

Semyon M. Meerkov Pierre T. Kabamaba University of Michigan

The goal of the project is the development of a control theory for dynamical systems with control inputs acting as amplitudes for periodic average zero functions. Such systems describe, for instance, helicopters with HHC control and chemical reactors under periodic operation. The following results have been obtained: (a) It has been shown that a linear dynamical system is closed loop vibrationally stabilizable by a state space feedback if it is controllable and its trace is negative. (b) An analogous property has been shown to exist for the output feedback. In addition, it has been shown that the separation principle holds for the closed loop vibrationally controlled systems utilizing the observer-controller configuration. (c) Due to structural constraints (such as the trace invariance), closed loop vibrational control cannot ensure any desired pole locations in the open left half of the complex plane. The locations that can indeed be attained have been characterized. (d) Disturbance rejection capabilities of closed loop vibrational control have been investigated. It has been shown that, in addition to modifications in the system's matrix, closed loop vibrational control leads

to a modification of the system's control vector (somewhat akin the feedforward control). This additional capability allows for more efficient disturbance rejection capabilities as compared with the usual feedback. (*e*) Since the system control vector can be modified, a question arises: which locations of zeros are optimal from the point of view of the disturbance rejections properties? Answering this question, it has been shown that the locations of zeros optimal in H<sub>2</sub> sense, i.e., from L<sub>2</sub> disturbance to L $\propto$  output, are guaranteed by the system's control vector which is collinear with the eigenvector of the observability Grammian corresponding to its smallest eigenvalue.

Reports:

- 1. Hs-Optimal Zeros, by P.T. Kabamaba et al., MS
- Closed Loop Vibrational Control: State and Output Feedback Stabilizability, by P.T. Kabamaba, TR, Jun 91, 13 pp. AD A238 217

# 28123 HIGH- AND LOW-FREQUENCY DYNAMICS OF ISOLATED BLADES AND ROTORS WITH DYNAMIC STALL AND WAKE

G.H. Gaonkar

Florida Atlantic University

SL: AERO DIR SC: AP TEC DIR

The effects of dynamic stall lift, dynamic stall drag and dynamic stall pitching-moment on the aeroelastic stability of an isolated hingeless rotor blade are being investigated. The study includes bending and torsional flexibility under highly stalled conditions in forward flight in untrimmed conditions. The aerodynamic description is based on the ONERA dynamic stall models of lift, drag and pitching moment. In hover, the predictions are verified by correlating the measured lead-lag mode damping levels of a soft-intorsion model rotor. The measurements were made at the U.S. Army Aeroflightdynamics Directorate, Ames Research Center. The nonlinear equations of blade motion and stall dynamics are perturbed about a periodic orbit and the damping is evaluated by Floquet eigen analysis. In hover, the substall drag effects provide predictions which are closer to the measurements than the predictions from linear aerodyno nics. Inclusion of unsteady effects brings further improvement in the correlation. In forward flight, the damping predictions are qualitatively different for stiff in-torsion and soft-in-torsion configurations. The correct representation of aerodynamic pitching moment becomes increa ingly crucial at high-speed/high-thrust conditions.

# 28155 NUMERICAL ANALYSIS OF THIRD AND HIGHER HARMONIC OVERTONES OF THICKNESS-SHEAR VIBRATIONS IN SC-CUT QUARTZ RESONATORS

Yook-Kong Yong

Rutgers, The State University of New Jersey

SL: ETDL

The first phase of the project involving literature review of laver-wise plate theories and their numerical solutions is essentially completed. It has been concluded that for the numerical analysis of third harmonic overtone of thickness-shear vibrations in SC-cut quartz resonators the layer-wise plate theories are not as accurate and efficient as the Lee-Nikodem plate theory. The Lee-Nikodem plate theory is similar to Mindlin's plate theory with the exception that the displacements are expanded through the plate thickness using trigonometric functions instead of polynomial functions. The layer-wise plate theories are very useful for laminated plates and for low frequency vibrations. For the high frequency vibrations of the third harmonic overtone of thicknessshear mode, the layer-wise plate theories require at least seventeen degrees of freedom per node of finite element, while the Lee-Nikodem plate theory requires at most twelve degrees of freedom per node. Hence, in terms of storage requirements and numerical implementation, the latter plate theory is chosen. The one disadvantage of the Lee-Nikodem theory is the difficulty in taking into account the stiffness properties of the electrode layers. Currently, only the mass effect of the electrode layers is considered. The electrode stiffness is not critical in the quartz resonator. Among workers in piezoelectric resonators, the electrode layer, besides being an electric conductor, is generally assumed to have no stiffness and contribute only mass effects.

## 28350 ADAPTIVE CONTROL OF NONLINEAR FLEXIBLE SYSTEMS

Robert L. Kosut Integrated Systems Inc

The research objective is to establish theoretical foundations, performance limitations, and engineering design guidelines for the application of adaptive control to nonlinear flexible systems.

# 28399 SEVERE EDGE EFFECTS AND SIMPLE COMPLEMENTARY INTERIOR SOLUTIONS FOR ANISOTROPIC AND COMPOSITE STRUCTURES

C.O. Horgan J.G. Simmonds L.R. Quarles University of Virginia

SC: BRL

A detailed analysis has been made of a transversely isotropic semi-infinite strip in plane strain, free of traction on its faces and at infinity, and subject to edge loads or displacements that produce stresses and displacements that decay in the axial direction. The governing equations are reduced to a single fourth-order partial differential equation for the dimensionless Airy stress function. If the strip is weak in shear, an asymptotic analysis reveals interesting boundary layer phenomena. The effect of nonlinearity on the decay of end effects has been examined within the context of a theory of plane strain for isotropic materials. The model takes material nonlinearity into account while restricting attention to small displacement gradients. An estimate for the decay of Saint-Venant end effects is obtained for a rectangular region subjected to end loads only. The results predict a progressively slower decay of end effects with increasing load level. Thus, a wide boundary-layer phenomenon is also obtained in this problem, but now due to nonlinearity. Such effects are ever more important to understand in view of the current demands on the U.S. Army to improve the performance of materials and structures.

Reports:

- Asymptotic Analysis of an End-Loaded. Transversely Isotropic, Elastic, Semi-Infinite Strip Weak in Shear, by C.O. Horgan and J.G. Simmonds, *Intl J Sol and Struct* 27,1895 (1991). AD A238 195
- 2. A Saint-Venant Principle for a Theory of Nonlinear Plane Eiasticity, by C.O. Horgan and L.E. Payne, MS, *Quart Appl Math.*

### 28651 INCIPIENT SEPARATION IN SUBSONIC PITCHING AIRFOILS

Doyle Knight

Rutgers. The State University of New Jersey

SL: AERO DIR SC: AERO DIR, STRUC DIR

The research objective is to provide improved understanding of incipient separation in subsonic pitching airfoils. Unstructured adaptive grid techniques will be coupled with a flux-split discretization technique to solve the two-dimensional compressible Navier-Stokes equations numerically.

# **VI METALLURGY AND MATERIALS SCIENCE**

### A. Degradation, Protection, and Reaction

# 21545 POSITRON ANNIHILATION STUDIES OF HYDROGEN TRAPPING BY INTERSTITIALS

James T. Waber Northwestern University

SL: CERL, ETDL

The objective of the research is to determine the interactions of hydrogen with a number of interesting materials systems/phenomena. These include minor dopant/hydrogen effects on deformation and positron trapping sites of iron, nickel, and chromium single crystals, the influence of palladium plating and oxide films on hydrogen pickup into the bulk of crystals and to confirm the diffusion and trapping of deuterium by dislocations. The approach will involve: (a) Positron annihilation studies of defect trapping lifetimes for iron, nickel, and chromium single crystals that have been deformed so as to have specific defect configurations, (b) positron annihilation studies of palladium plating and oxide coatings, (c) transmission electron microscopy characterization of samples examined with positron techniques, (d) positron annihilation studies of deuterium charged samples analogous to hydrogen experiments above, and (e) theoretical calculation relating to above solid state phonomena.

# 24845 SURFACE STRUCTURES AND SURFACE PROCESSES OF CERAMICS WITH ATOMIC RESOLUTION—A STUDY BY SCANNING TUNNELING MICROSCOPY

I.S.T. Tsong William Petuskey Arizona State University

SL: CERL, ETDL

Efforts have continued on imaging silicon carbide surfaces with the ultrahigh vacuum (UHV) scanning

tunneling microscope (STM). The samples include cubic  $\beta$ -SiC (111) and hexagonal  $\alpha$ -SiC (0001) surfaces, both of which are grown by chemical vapor deposition (CVD) on  $\alpha$ SiC{0001} substrates. The experiments were carried out using samples grown on Si-terminated  $\alpha$ -SiC (0001) surfaces. All samples were annealed in situ at temperatures between 1150 and 1200°C in UHV to eliminate the oxide layer prior to tunneling. STM experiments have been initiated to observe strains on an atomic scale when an external tensile stress is applied to the sample. The sample is a  $\alpha$ -SiC (0001) single crystal substrate. The sample is in the form of a long thin wafer, 25 mm long and 2 mm wide. One end of the sample is rigidly clamped, while the other end is bent slightly by a mechanical UHV linear feed-through. At this point, the experiment has not been entirely successful. This is not due to the design of the experiment, but to the problems associated with the sample, whose CVDgrown surface is not smooth enough to allow atomresolved imaging. The experiments will be repeated with new samples.

Reports:

No. 1-7 in previous editions.

- Studies of β-SiC (001) and (111) Surfaces by Scanning Tunneling Microscopy, by C.S. Chang et al., MS, J Vac Sci Tech.
- Thermochemistry of Ceramic-Metal Reactions in Ti-Si-N and Ti-Si-C Systems at High Temperatures and Pressures, by Sankar Sambasivan, PhD Thesis, 1990, 136 pp.
- Scanning Tunneling Microscopy and Spectroscopy of Cubic β-SiC(111) Surfaces, by C.S. Chang et al., MS, Surface Sci.

# 25199 NONDESTRUCTIVE ANALYSIS FOR HYDROGEN CONCENTRATIONS IN MATERIALS

Walter Meyer William H. Miller Syracuse University SL: CERL SC: MTL, TACOM

The objective of the research is to detect hydrogen at a concentration of one weight part per million (a concentration of approximately  $4.7 \times 10^{17}$  atoms of H cm<sup>-3</sup>) in bulk samples of high strength steel. A further objective is to develop a technique that is applicable to bulk samples displaying the engineering properties of the host material. Laboratory work has concentrated on increasing the sensitivity of both  $v^{10}$  notched and iron filter techniques for nondestructively measuring the hydrogen content.

### Reports:

No. 1 in previous edition.

 Workshop On Surface Science and Technology, by Walter Meyer and William H. Miller, TR, Nov 90, 19 pp.

### 25760 MODIFIED EPOXY ADHESIVES AND PRIMERS

Andrew Garton University of Connecticut

SL: BRADEC, MTL, SC: ARDEC STRUC DIR

The work on epoxy additives is now approaching its conclusion. The characterization of the epoxy/ VCDHAA system, in terms of both physical and chemical properties, has allowed researchers to identify the desired molecular characteristics of "fortifiers." This hypothesis is now being tested with pure materials of the desired structures which can be purchased from chemical supply houses. The envelope of adhesive joint performance has been explored, and the benefits of fortifier addition determined. The greatest property improvements for torsional and lap-shear joints are obtained in low temperature cured systems and under conditions of high humidity. The polyimide work is further from completion, but additives have been identified which can increase modulus and strength of three linear polyimides. Efforts are now concentrated on the development of additives sufficiently thermally stable to survive under polyimide cure and service conditions.

#### Reports.

No. 1-4 in previous editions.

 The Production of Modulus Gradients at Interfaces, by Andrew Garton et al., Mat Res Soc Symp Proc 170,291(1990). AD A232 791

### 25833 LARGE SCALE SURFACE MODIFICATION BY HIGH CURRENT ION IMPLANTATION

SC: AVSCOM/DERSO, TACOM

Ian G. Brown

Lawrence Berkeley Laboratory

SL: MTL

VI Metallurgy and Materials Science

The Mevva V ion source that was developed early under this contract has continued to operate flawlessly. This high current (over 1 ampere peak pulse ion beam current), broad beam (10 cm diameter beam extractor), multicathode (cathode assembly holds 18 separate cathodes) ion source has been completely successful. For pulsed Mevva operation, the Mevva V source embodiment thus represents the culmination of the P.I.'s ion source research and development program. Some experiments were carried out on the removal of macroparticle contamination (microsized solid cathode debris) from the pre-extraction plasma beam using a small, bent magnetic solenoid ("magnetic duct"), through which the plasma is ducted but the macroparticles not. Initial results look very encouraging. This work is continuing. The ion source test stand has been progressively improved in various ways so that it constitutes a fairly complete "Mevva ion implantation facility." The facility has operated reliably over long periods, and certainly it is now well-established that the Mevva V metal ion implanter is a dependable and user-friendly tool for carrying out high dose metal ion implantation. An anomalously deep ion penetration, of order microns as opposed to a classical range of hundreds of Angstroms, has recently been observed by several workers to occur under conditions of very high dose implantation and high substrate temperature. Together with Dr. Peter Evans, of the Australian Nuclear Science and Technology Organization, preliminary search for this effect is being made. Together with Dr. D. Rueck of GSI, Germany, they have initiated a program that has been initiated to investigate the tribology of implanted hard steels and ceramics. Some Pt and Pd implants into steels, over a range of doses and combinations, were done as part of a collaboration with the Army MTL, Watertown. The experiment is an investigation of improvement in hydrogen embrittlement in steels by noble metal implantation. As a collaboration with the University of Rhode Island Au and Ti have been implanted into steel to investigate the effect on corrosion resistance. Results of testing are coming out now, and the results look very good.

#### Reports:

- 1. Metal Vapor Vacuum Arc Ion Sources, by I.G. Brown et al., MS.
- 2. Vacuum Arc Ion Charge State Distributions, by I.G. Brown and X. Godechot, MS.
- Broad-Beam, High Current, Metal Ion Implantation Facility, by I.G. Brown et al., MS.
- Beam Intensity Eluctuation Characteristics of the Metal Vapor Vacuum Arc Ion Source, by I.G. Brown et al., Nucl Inst and Meth A295,12(1990). AD A232 358

# 26400 IN SITU SURFACE STUDIES OF CONVERSION COATINGS AND PASSIVE FILMS ON STEEL AND ALUMINUM BASED METAL MATRIX COMPOSITES USING INFRARED TUNNELING AND IMPEDANCE SPECTROSCOPIES

Henry W. White

University of Missouri at Columbia

SC: ARDEC, TACOM

Zn:Ph coatings on Steel - Analysis of early samples with Raman spectroscopy had shown no support for Sugama's three layer model of the Zn:Ph coated surface, as evidenced by spectra taken at various depths by removal of surface material. Subsequent samples prepared with pure iron substrates showed clear presence of species other than Zn:Ph. However, these other species are not in a simple layered structure; they are more island-like. Work is in progress to identify these species by collecting reference spectra for likely candidates. Micro-Raman spectra have been obtained on individual surface crystallites. A vast majority of the crystallites on the surface are Zn<sub>3</sub>(PO<sub>4</sub>)<sub>2</sub> ·2H<sub>2</sub>O. Other crystallites include (a) some that are clear, with CH stretch modes, which may be poly(acrylic acid), and (b) some that are transparent, but brown tinted, that are probably an Fe compound-but not Fe<sub>2</sub>O<sub>3</sub> or Fe<sub>3</sub>O<sub>4</sub>, more likely a hydrated iron oxide. As an effort to determine mechanisms associated with film growth, Raman spectra have been obtained at various early stages of growth by removing the substrates from the bath during initial film formation. The spectra indicate that  $Zn_3(PO_4)_2 \cdot 2H_2O$  forms within a few minutes, and that it is the first detectable film. Ce coatings on Aluminum — Raman spectra on a series of Al samples coated with various protective films showed distinctive features peculiar to the chemical composition of the treatment bath. The conclusion is that anions of the modification solution are being incorporated in the protective film. The baths contained mixtures of rare earth chlorides and nitrates with various treatment times and temperatures. Earlier Raman spectra were obtained on samples of 6061-T6 soaked in various rare earth chloride solutions in an attempt to identify the characteristics signatures of the rare earth and chloride ion in the protective film. STM of Solid  $C_{60}/C_{70}$  — Researchers have measured and reported direct imaging of C<sub>60</sub> molecules in sub-micrometer sized particles of fullerite using STM. The images reveal spherical molecules, spaced about 1 nm apart, stacked in close-packed arrays. The results give a direct demonstration of the highly

symmetric structure of these clusters. Such molecules and clusters are thought to play an important role in soot formation, and may have applications in catalysis, lubrication or transport of caged atoms. Atomic Force Microscopy — A new AFM design which utilizes the high sensitivity of a tunnel junction has been developed by P. Bryant and coworkers at UMKC. It has been successfully applied to physical and biological samples, including protein chains.

# 26427 PROCESS PARAMETER/GROWTH ENVIRONMENT/FILM PROPERTY RELATIONSHIPS FOR REACTIVE SPUTTER DEPOSITED METAL OXIDE, NITRIDE, AND OXYNITRIDE FILMS

Carolyn R. Aita

University of Wisconsin - Milwaukee

SL: MTL	SC: ARO, BRADEC, NVEOC,
	TACOM

Reactive sputter deposition was used to grow a phase-separated 0.40 Au/0.56 Au<sub>2</sub>O<sub>3</sub>/0.04 Au-hydroxide cermet film and x-ray photoelectron spectroscopy was used to examine the Au 4f and O 1s core electron binding energy of each phase. The valence bandstructure of Au<sub>2</sub>O<sub>3</sub> was reported for the first time, and consists of an O 2p electron-derived peak centered at 5.5 eV and a density of states that approaches zero at the Fermi energy, characteristic of a semiconductor. The results were compared to other third long period conducting and semiconducting oxides.

# 26449 INHIBITION OF CORROSION BY ELECTRODEPOSITED CONDUCTIVE– POLYMER FILMS

Dale P. Barkey

University of New Hampshire

SL: MTL SC: ARDEC, BRADEC, PROP DIR

A series of experiments was completed. (a) Electropolymerized poly(3-methyl thiophene) films can be firmly bonded to polished type 430 stainless steel substrates that have been pretreated by anodic phosphating; (b) the films galvanically fix the substrate, including uncoated portions, at a passive potential, and prevent loss of material in 1 N sulfuric acid solution; (c) the redox capacity and stability of the films depend on the transport and reaction conditions used in film preparation. Electrochemical investigations of film properties as they depend on electropolymerization conditions are largely complete. Still in progress is a study of the macromorphology of polymer films grown under controlled kinetic and transport conditions. These films can, in principle, protect 430 stainless steel in an acid environment in which it otherwise corrodes rapidly. The films, however, are not effective in protecting C1010 mild steel.

#### Reports:

No. 1 in previous edition.

2. Electrochemically Prepared Poly(3-Methylthiophene) Films for Passivation of 430 Stainless Steel, by S. Ren and D. Barkey, MS, J Electrochem Soc.

## 26667 ADHESION AND POLYMER-MODIFIED PRECOATINGS

Toshifumi Sugama

Brookhaven National Laboratory

SL: ETDL, TACOM SC: ARDEC, BRADEC, PROP DIR, RIA

Polyimide (PI) resins which are produced in an in-situ imidization condensation reaction of polyamic acid (PAA) precursors were evaluated for use as binders in high-temperature performance lightweight cement-filled material systems. Unfortunately, the presence of partially hydrated cement in the system led to strength retrogression at room temperature. Significant mechanical failure was observed upon exposure of the specimens to steam at 150°C. This was found to be due mainly to alkali catalyzed hydrolysis of the functionaries of unreacted PAA adjacent to the cement surfaces and the imide rings of PI matrices. The formation of Ca-complexed carboxylate salts derived from the hydrolysis resulted in chain scission of the polymer, thereby decreasing the mechanical strength, and making the composites unsuitable for use in aqueous environments.

#### Reports

No. 4-3 in previous editions.

- 4. Polyacid-Zinc Phosphate Anhydride Conversion Coatings, by T. Sugama, MS.
- 5. Pyrogenic Polygermanosiloxane Coatings for Aluminum Substrates, by T. Sugama et al., MS, J Non-Cryst Sol.
- 6. Interfaces of Polyphenylene Sulfide-to-Metal Joints, by T. Sugama and N. R. Carciello, MS, J Adheston and Adhesives.
- 7. Advanced Poly(Acrylic)Acid-Modified Zinc Phosphate Conversion Coatings: Use of Cobalt and Nickel Cations, by T. Sugama and R. Broyer, MS, Surface and Coatings Tech
- 8. Chemical Degradations of Pyrogenic Polytitanosiloxane Coatings, by T. Sugama and C. Taylor, Mater Let 11,187(1991).

#### VI Metallurgy and Materials Science

- 9. Characteristics of Transition Metal-Adsorbed Anhydrous Zinc Phosphate Coatings as Corrosion Barriers for Steels, by Toshifumi Sugama and Jin Pak, Mater and Manufacturing Proc 6,227(1991).
- 10. Influence of the High Temperature Treatment of Zinc Phosphate Conversion Coatings on the Corrosion Protection of Steel, by T. Sugama et al., J Mater Sci 26,1045(1991). AD A238 508
- 11. The Corrosion Protection of Steel and Bond Durability at Polyphenylene Sulfide-to-Anhydrous Zinc Phosphate Interfaces, by T. Sugama and N.R. Carciello, MS, J Appl Polymer Sci

### 26678 CORROSION INHIBITION BY PLASMA ION IMPLANTATION

J. Reece Roth

Raymond A. Buchanan University of Tennessee, Knoxville SL: MTL

#### SC: BRADEC

The major thrust of the laboratory work consisted of operating the microwave plasma facility with a plasma present, at power levels up to 800 watts. It was possible to generate a steady-state nitrogen plasma at pressures from 8 to 50 millitorr. The plasma appeared uniform along the axis and radius to visual inspection. This was clearly an important milestone toward the goal of a large-volume, steady-state plasma for plasma ion implantation. Ion-beam-implantation corrosion studies were continued in collaboration with Oak Ridge National Laboratory, the Corpus Christi Army Depot and the Army Materials Technology Laboratory. The purpose of the work is to define the implantation elements, energies, and fluences required to significantly improve the resistance of aluminum and aluminum alloys to chloride-induced pitting corrosion. In these studies, the ion-beamimplantation processing is being performed at Oak Ridge National Laboratory, the electrochemical corrosion characterizations at The University of Tennessee, and the salt-fog corrosion characterizations at the Corpus Christi Army Depot. Commercially pure aluminum and wrought aluminum alloy 2014 were ion beam implanted with N. Cr. Ti, and Si at various energies and fluences. The corrosion properties of the implanted commercially-pure Al specimens were evaluated by cyclic anodic-polarization testing in deaerated 1 w/o NaCl solution. The corrosion properties of the implanted 2014 Al alloy specimens were evaluated by both cyclic-anodic-polarization and saltfog testing. For commercially-pure Al N implanted at 20 keV and  $3 \times 10^{17}$  ions cm<sup>-2</sup> proved to be the most beneficial, followed by Cr implanted at 35 keV

and  $5 \times 10^{16}$  ions cm<sup>-2</sup>. However, for the 2014 alloy, Cr implanted at 150 keV and  $3 \times 10^{17}$  ions cm<sup>-2</sup> appeared to be the most beneficial.

Reports:

No. 1 in previous edition.

- 2. A Microwave Generated Plasma for Plasma Ion Implantation Studies, by Philip F. Keebler and J. Rece Roth, MS.
- 3. A Large-Volume, Unmagnetized, Microwave Generated Plasma for Industrial Plasma Engineering Applications, by P.F. Keebler et al., MS.
- 4. Ion Implantation for Corrosion Inhibition of Aluminum Alloys in Saline Media, by J.M. Williams et al., MS, Nucl Inst and Meth.

# 26806 ION BEAM MODIFICATION OF CERAMICS: MECHANICAL PROPERTIES AND STRUCTURE

James W. Mayer Cornell University

SC: ARDEC, MTL

Work has concentrated on the microstructure of ceramics so as to relate structure to hardness and to other mechanical properties. After directly looking at the structure of zirconia, the material which has been the focus of the mechanical testing, it was found that the zirconia did not amorphize completely, if at all, Also, evidence was found that solid xenon forms in the zirconia, as it did in magnesia, indicating that the pressure is high within the crystal after implantation. Channeling and transmission electron microscopy techniques were used to examine the microstructure of single crystal Y<sub>2</sub>O<sub>3</sub> stabilized cubic zirconia after implantation with 240 KeV Xe. These measurements were related to previous Knoop indentation hardness measurements which showed increases in hardness for low dose and decreases in hardness for high doses. In the hardening regime, below a dose of  $7.5 \times 10^{15}$  Xe cm<sup>-2</sup>, point defects and dislocations were visible in the TEM micrographs. Channeling showed an increase in damage with dose. For doses between  $7.5 \times 10^{15}$  Xe cm<sup>-2</sup> and  $3 \times 10^{16}$  Xe cm<sup>-2</sup> the hardness fell, the amount of damage measured with channeling saturated, and a pattern of streaking appeared in the diffraction pattern. In this dose range the xenon continued to accumulate in the lattice although the damage began to saturate. For high doses, greater than  $3 \times 10^{16}$  Xe cm<sup>-2</sup> new diffraction spots were visible which were attributed to solid Xe formed due to the high pressure in the lattice after implantation. A diffuse ring from fluid Xe trapped in the lattice was apparent as well. While the lattice appeared damaged at these high doses, both

channeling and TEM showed that a significant amount of oriented single crystalline zirconia remained even to doses of  $1 \times 10^{17}$  Xe cm<sup>-2</sup>. Some recrystallized zirconia was present as well. This shows that amorphization was not the dominant cause of the softening at high doses. However, the compressible Xe precipitates may have played a role.

Reports:

No. 1 in previous edition.

2. Hardness, Friction, and Structure of Ion Beam Modified Titanium Alloys, Magnesia, and Zirconia, by Elizabeth Lee Fleischer, PhD Thesis, 1991, 188 pp.

# 27037 MOLECULAR DYNAMICS OF PHYSICAL AGING PROCESSES IN POLYMER GLASSES, EXPERIMENT AND THEORY

John D. McGervey

SL: MTL

Case-Western Reserve University

SC: ARDEC, MTL, PROP DIR

Positron Annihilation Lifetime (PAL) spectroscopy was used to characterize changes in free volume of amorphous bisphenol A polycarbonate (PC) under applied tensile strains. The intensity of orthopositronium (o-Ps) annihilation, I<sub>3</sub>, appears to be proportional to the number of trapping sites ("holes") and the o-Ps lifetime,  $\tau_3$ , is a measure of hole size. The behavior of  $I_3$  and  $\tau_3$  under strain-free conditions is consistent with literature data. Under applied strains, PAL data indicate an increase in free volume, mainly due to an increase in average hole size, up to a level of 3.5-4.0 percent strain, beyond which no further change occurs. These observations are consistent with the known phenomenon of strain-induced rejuvenation in the mechanical properties of PC. PAL analysis during physical aging of "old" polycarbonate under constant tensile strain shows that deformation reactivates the aging process; after the initial increase, free volume decreases continuously to levels lower than those in the material prior to deformation. The free volume decrease during isothermal aging in both unstrained and strained PC is deduced from a decrease in the o-Ps intensity.

# 27552 FORMATION OF TRANSITION ELEMENT NITRIDE COATINGS ON STEELS USING ELEVATED-TEMPERATURE PLASMA SOURCE ION BEAM ENHANCED DEPOSITION

John R. Conrad Richard A. Dodd Frank J. Worzala University of Wisconsin – Madison

SL: MTL

SC: ARDEC, TACOM

### **B.** Mechanical Behavior

The variation in hardness of 52100 bearing steel upon tempering in the temperature range 250-650°C for time periods 1 and 3 hours has been evaluated. The objective of this study was to enable the prediction temperature from hardness changes which occur during implantation or deposition during PSII processing. Three types of hardness measurements were made, each serving a different purpose. Ion beam enhanced deposition has been used to successfully form wear resistant titanium nitride coatings on 52100 bearing steel and commercial superalloy inconel 718. The procedure involved sputter depositing a 300Å titanium layer using a dc sputter cathode biased at -600 V in an argon plasma while the target was pulse-biased at 35 kV. TAMIX (Transport and Mixing from Ion Irradiation), developed at UW-Madison is a Monte Carlo program to simulate the interactions of energetic ions with a solid surface. This program predicts the atomic concentration of the implanted elements during and after ion implantation. Sputtering coefficients and surface recession due to sputtering are also computed. This code is used primarily to test different implantation parameters before they are run.

#### Reports:

1. Ion Beam Assisted Coating and Surface Modification with Plasma Source Ion Implantation, by J.R. Conrad et al., *J Vac Sci Tech* A8,3146(1990). AD A231 978

# 28369 REAL TIME X-RAY SCATTERING STUDY OF PROCESSING OF HIGH PERFORMANCE THERMOPLASTICS

Peggy Cebe

Massachusetts Institute of Technology

SL: MTL, NRDEC SC: AROE, BRADEC, TACOM

The objective of the research is to utilize synchrotron x-ray diffraction techniques for in-situ characterization of the processing of high performance thermoplastic polymers. The approach will consist of the following: (a) characterize crystallinity and subcrystallinity of thermoplastic polymers by x-ray diffraction under model processing conditions, (b) mechanical properties will be measured concurrently so that structure as determined in (a) can be correlated with properties.

# 28509 GROWTH AND CHARACTERIZATION OF REFRACTORY METAL MULTILAYERS: POTENTIAL ULTRA-HIGH STRENGTH-HIGH TEMPERATURE SURFACE COATINGS

John C. Bilello Steven M. Yalisove University of Michigan SC: BWL, MTL VI Metallurgy and Materials Science

The objective of the research is to investigate, characterize, and optimize the mechanical and physical properties of metal multilayer composites. The laminate composites fabricated by thin film techniques will have alternating high and low elastic modulus materials. The approach will consist of: (a) control and optimization of growth conditions to assure high quality stress free films; (b) measure the residual stress and otherwise characterize the materials fabricated through x-ray techniques, Rutherford backscattering, electron microscopy, LEED and Auger techniques; (c) determine the relationship of film thickness, quality and microstructure to the mechanical properties of the multilayer condensates formed.

# **B. Mechanical Behavior**

# 24583 STRESS STATE EFFECTS ON STRENGTH AND FRACTURE OF PARTIALLY-STABILIZED ZIRCONIA

Dinesh K. Shetty Anil V. Virkar University of Utah

SL: BRL

SC: BRADEC, TACOM

Significant research results obtained were as follows: Effect of confining hydrostatic pressure on the transformation yield stress of Ce-TZP in uniaxial compression was investigated at Southwest Research Institute. The data support a linear increase in transformation yield stress according to the equation:  $\sigma_v^{\ p}$ =  $\sigma_v^c$  +  $\alpha^c p$  where  $\sigma_v^p$  is the compression yield stress under a confining pressure, p,  $\sigma_x^c$  is the transformation yield stress in uniaxial compression and  $\alpha^{c}$  is the pressure sensitivity of the yield stress. The theoretical analysis of stress-state effect based on Eshelby's inclusion theory was extended to treat transformation yielding under hydrostatic pressure by modifying the interaction energy by the dilatation strain energy,  $p\Delta$ . The crack-growth-resistance behavior of Ce-TZP ceramics will be analyzed in terms of transformation zone shielding models taking into account the actual shapes of transformation zones at crack tips. An important question to be addressed here is whether the insensitivity of the R-curves of Ce-TZPs to the zone size can be explained in terms of the shielding theory.

#### Reports:

No. 1-5 in previous editions.

6. Fatigue Crack Propagation in Ceria-Partially-Stabilized Zirconia (Cc-TZP)-Alumina Composites, by Jing-Fong Tsai et al., J Am Ceram Soc 73,2992(1990). AD A230 961

#### VI Metallurgy and Materials Science

- Stress-State Effects on Transformation Yield Stress and Fracture Toughness of Zirconia Ceramics, by Cheng-Sheng Yu, PhD Thesis, 1991, 194 pp.
- Role of Autocatalytic Transformation in Zone Shape and Toughening of Ceria-Tetragonal-Zirconia-Alumina (Ce-TZP/ Al<sub>2</sub>O<sub>3</sub>) Composites, by Jing-Fong Tsai et al., J Am Ceram Soc 74,678(1991). AD A238 525

### 24981 THERMAL WAVE IMAGING AND CHARACTERIZATION OF SOLIDS

Robert L. Thomas Lawrence D. Favro Pao-Kuang Kuo Wayne State University

SL: TACOM SC: ETDL

The development of synchronous IR video thermal wave imaging and NDE applications of these techniques has progressed well. The IR camera purchased earlier on a cost-sharing basis with Army and WSU funds is producing excellent results in imaging a variety of sub-surface defects of industrial and military interest. Some of these results have been presented in various publications. Another IR project, that of developing a version of an IR "flying-spot" thermal wave camera, is also progressing well. Preliminary results have been achieved from this system. Excellent progress has been made with the mirage-effect work, also. Work has concentrated on detailed numerical fits between experiment and theory, using a multiparameter, nonlinear, least-squares fitting routine developed here. The results are excellent, both for pure materials and for coatings.

#### Reports:

No. 1-4 in previous editions.

- A Novel "Flying-Spot" Infrared Camera for Imaging Very Fast Thermal-Wave Phenomena, by Y.Q. Wang et al., *Photoacoustic and Photothermal Phenomena II*, 1990, p24. AD A224 369
- Real-Time Thermal-Wave Imaging of Plasma-Sprayed Coatings and Adhesive Bonds Using a Box-Car Video Technique, by T. Ahmed et al., *Photoacoustic and Photothermal Phenomena II*, 1990, p30. AD A224 316
- Thermal Wave Measurement of Diamond Films, by P.K. Kuo et al., *Photoacoustic and Photothermal Phenomena II*, 1990, p124. AD A224 315
- Real-Time Asynchronous/Synchronous Lock-In Thermal-Wave Imaging with an IR Video Camera, by L.D. Favro et al., *Photoacoustic and Photothermal Phenomena II*, p490. AD A224 590
- 9. Noise Suppression in IR Thermal-Wave Video Images by Real-Time Processing in Synchronism with Active Stimula-

tion of the Target, by L. D. Favro et al., SPIE Proc 1313,302(1990). AD A228 319

- Thermal Wave and Raman Characterization of Diamond Films, by R.W. Pryor et al., *Review of Progress in Quantitative Nondestructive Evaluation*, Vol 9, 1990, p1123. AD A228 320
- Flying Laser Spot Thermal Wave IR Imaging of Horizontal and Vertical Cracks, by Y.Q. Wang et al., *Review of Progress* in Quantitative Nondestructive Evaluation Vol 9, 1990, p511. AD A228 321
- In-Situ Characterization of Thin Polycrystalline Diamond Film Quality by Thermal Wave and Raman Techniques, by R.W. Pryor et al., *Mat Res Soc Symp Proc*162,273(2990). AD A231 084
- Thermal Diffusivity of Isotopically Enriched <sup>12</sup>C Diamond, by T.R. Anthony et al., *Phys Rev* B42,1104(1990). AD A231 051
- Infrared Thermal-Wave Studies of Coatings and Composites, by L.D. Favro et al., SPIE Proc 290,1467(1991). AD A234 708

# 25193 HIERARCHICAL STRUCTURE IN POLYMERIC SOLIDS AND ITS INFLUENCE ON PROPERTIES

Eric Baer

Case-Western Reserve University

SL: MTL SC: AROE

A study of the relationships between the morphology of fibers spun from blends of a thermotropic liquid crystalline polymer and PET and the mechanical properties in tension has led to the following conclusions: (a) Discontinuous fibrous LCP domains were found in the blend fibers with 35 and 60 percent by weight LCP. When the LCP content was higher, 85 and 96 percent, the fibrous LCP phase was continuous. The basic structural entity of the LCP domains was the 0.5 micron fibril. (b) The transition from discontinuous to continuous LCP fibrils was accompanied by an increase in modulus and a change in the fracture mode from brittle fracture when the LCP fibrils were discontinuous to delamination fracture when the LCP was continuous. (c) Analytic models for short aligned fibers were applicable when the LCP fibrils were discontinuous, while modulus and strength of blend fibers with continuous LCP fibrils were described by the rule of mixtures.

#### Reports:

No. 1-4 in previous editions.

5. Morphology and Mechanical Properties of Blend Fibers From a Liquid Crystalline Polymer and Poly(Ethylene Terephthalate), by J.X. Li et al., MS.

# 25390 MICROMECHANISMS OF DEFORMATION AND FRACTURE IN ALUMINUM BASED MMC'S—INTERFACE EFFECTS

John J. Lewandowski

Case-Western Reserve University

SL: ARDEC SC: MICOM

Work has continued to focus on determining the effects of microstructural changes on the resulting fracture toughness of metal matrix composites. In previous work, investigations were made of the effects of systematic changes in reinforcement size, volume fraction, matrix alloy type, and matrix aging condition on the resulting fracture toughness. Attempts are now being made to increase the fracture toughness of these composites via a laminate approach. It has been well demonstrated that the introduction of ceramic reinforcements may significantly decrease the fracture toughness of aluminum alloys while increasing the strength and stiffness. Most recent work here has focused on attempting to increase the fracture toughness of composites by laminating monolithic aluminum alloys to the composite. Preliminary results have been quite impressive. It has been demonstrated that a composite laminate consisting of a 2XXX (Al-Mg-Cu) aluminum alloy reinforced with 20 volume percent SiC particulates bonded to a monolithic 2XXX alloy exhibits increases in both the fracture initiation and growth toughness. While the above work focuses on toughness, tests have been made on laminated specimens under conditions of bending, where the monolithic alloy is subjected to tension while the composite is tested in compression. Such a design permits the high ductility of the monolithic alloy and the high ductility of the monolithic alloys and the high compressive strength of the composite to be exploited. Again, the results have indicated significant effects of the thickness of the monolithic alloy on the resulting bend ductility of the composite laminate.

#### Reports:

No. 1-3 in previous editions.

- Microstructural Effects on the Toughness of Aluminum Alloy Based Metal-Matrix Composites, by M. Manoharan and J.J. Lewandowski, 7 pp., Fundamental Relationships Between Microstructure and Mechanical Properties of Metal-Matrix Composites, P.I. Liaw, ed., Minerals, Metals & Mater Soc, 1990.
- Combined Mode I Mode III Fracture Toughness of a Particulate Reinforced Metal-Matrix Composite, by M. Manoharan an I.J.J. Lewandowski, MS, J Composite Mater.
- Laminated Composites with Improved Toughness, by M. Manoharan et al., Scripta Met 14, 1515(1990), AD A226 080

#### **VI Metallurgy and Materials Science**

- Effect of Reinforcement Size and Matrix Microstructure on the Fracture Properties of an Aluminum Metal-Matrix Composite, by M. Manoharan and J.J. Lewandowski, MS, Acta Met.
- 8. Laminated Composites with Improved Bend Ductility and Toughness, by L. Yost Ellis and J.J. Lewandowski, MS. J. Mater Sci Let.

# 25397 NONDESTRUCTIVE CHARACTERIZATION OF TWO-PHASE METAL-MATRIX MATERIALS

Kamel Salama

University of Houston

SC: MICOM, MTL

A study was made of the effect of the volume content of reinforcement in metal-matrix composites on two nonlinear elastic quantities, namely the acoustoelastic constant and the acoustic nonlinearity parameter. The results of this study show that the acoustoelastic constants and the acoustic nonlinearity parameter are influenced by the amount of reinforcement in metal-matrix composites. Therefore, they are promising candidates to characterize the mechanical behavior of MMCs nondestructively. Also, the two quantities clearly indicate a decreasing elastic nonlinearity of the composite with the increasing content of SiC. The nonlinearity parameter changes linearly as a function of second phase content. The absolute values of the calculated as well as the directly measured acoustic nonlinearity parameter are in good agreement within the accuracy of the measurements. This shows that both techniques, measurements of absolute amplitudes using the capacitive gap receiver and measurements of the acoustoelastic effect, are suitable methods for the determination of the nonlinearity parameter. The direct measurement of the nonlinearity parameter using the capacitive gap receiver requires a careful preparation of the specimen surfaces. The measurement of the acoustoelastic effect is restricted to simple specimen geometries since it requires the application of external stresses. The selection between the two methods depends on the geometry condition of the sample.

## 25424 FRACTURE BEHAVIOR OF IONOMERS AND IONOMERIC BLENDS

Masanori Hara

John A. Sauer Rutgers, The State University of New Jersey

SL: MTL SC: STRUC DIR, TACOM

Previously it was found from tensile testing of bulk samples of PS ionomer/PS blends (Na salt) that toughness of glassy polymers can be significantly enhanced by the formation of a rigid second phase made mainly of ionomers. Studies have been made of the effect of ion content and counterion on deformation/fracture behavior of the blends in order to find optimum conditions for improvement of mechanical properties, such as toughness, by modifications of ionomer structure. TEM observation of thin films have shown that an increase in ionic interactions, by increase of either ion content or valency of the counterions (from Na<sup>+</sup> to Ca<sup>++</sup>), leads to formation of larger ionomer-rich second phase particles.

#### Reports:

No. 1-7 in previous editions.

- Effect of Sample History on Ionic Aggregate Structures of Sulfonated Polystyrene Ionomers, by M. Hara et al., *Polymer* 32,1380(1991).
- 9. Deformation and Fracture of Sulfonated Polystyrene Ionomer/ Polystyrene Blends: Effect of Ion Content, by M. Bellinger et al., MS, *Polymer Preprints*.
- 10. Deformation and Fracture Behavior of Polystyrene Ionomer and Ionomer Blends, by M. Hara et al., MS.
- 11. Blends of Sulphonated Polystyrene and Polystyrene: Morphology and Deformation Modes, by M. Hara et al., MS.
- 12. Deformation/Fracture Behavior of Ionomer Blends, by M. Hara et al., Proc of 8th Intl Conf on Deformation, Yield and Fracture of Polymers. AD A238 327
- 13. Deformation Modes and Morphology in PS/Sulphonated PS Ionomer Blends, by M. Hara et al., *Prepr. IUPAC International Symposium, Polymer 91*, 1991, p222. AD A238 326

## 26164 COMPUTATIONAL MODELING OF DYNAMIC FAILURE MECHANISMS IN ARMOR/ANTI-ARMOR MATERIALS

Robert D. Caligiuri Leonard E. Schwer Failure Analysis Associates

SL: BRL. MTL

A review was made of dynamic properties and penetration mechanisms of tungsten and depleted uranium (DU) penetrators. Penetration mechanisms were of particular interest, as it is felt that the differences in these mechanisms may be the reason why DU and W penetrators perform differently. Conclusions, based on available data, include: DU and W alloys respond differently to high rate loading conditions, both in terms of mechanical properties and failure (penetration) mechanisms. Under tensile loading, DU alloys exhibit a higher ultimate tensile strength and a higher strain to failure than W alloys. Under shear loading, DU and W alloys exhibit similar strengths, but DU exhibits a higher strain to failure. Against steel targets, both DU and W penetrator tips undergo ductile flow. However, subsequent penetration results in bulged tip sharpening by shearing. This sharpening occurs more readily in DU than W. Against ceramic composite targets, W alloys penetrate by erosion/ localized plastic deformation. The ballistic performance of DU and W alloys against monolithic steel targets is similar — at best a 5 to 10 percent difference. Current improvements in mechanical properties of DU and W alloys give at best a 5 to 10 percent improvement in ballistic performance. Against oblique spaced arrays, DU alloys significantly outperform W alloys. An increase in ductility/toughness in either alloy can result in a substantial improvement in ballistic performance. Based on preliminary finding, it appears that the best way to improve the ballistic performance of W alloy penetrators against oblique spaced arrays is to improve their resistance to fracture during penetration. Based on preliminary findings, it may also be ultimately possible to achieve a sharp tip during penetration in W alloys by proper microstructural control.

## 26167 ENHANCED COMPUTATIONAL /MODELING CAPABILITIES FOR DYNAMIC MATERIAL BEHAVIOR

James Lankford, Jr. Charles E. Anderson Kwai S. Chan Southwest Research Institute

SL: BRL, MTL

The research effort has been curtailed due to budgetary limitations. However, remaining FY 1990 resources were used to write a paper describing measurements of intense (0.5), but high localized matrix strains, and the observation of apparent compressive, adiabatic shear bands (and associated fracture) in certain tungsten heavy alloys. Other work on the influence of microstructure on dynamic tensile behavior in tungsten heavy alloys was presented at Explomet 90 (August 1990, San Diego).

Reports:

 Microstructural Dependence of High Strain Rate Deformation and Damage Development in Tungsten Heavy Alloys, by J. Lankford et al., MS.

## 26673 INTEGRATED SYNTHESIS AND POST-PROCESSING OF SiC AND AIN

Angus I. Kingon

North Carolina State University

SL: PROP DIR SC: BKL, MTL, TACOM

## **B.** Mechanical Behavior

A new technique has been developed to condense nanoparticles of SiC and other nonoxide materials in a nonthermal microwave plasma. The experimental rationale and approach was described. It utilizes silane and acetylene precursors in an Ar diluent, with the synthesis carried out in a microwave plasma at pressure of  $\sim 1$  torr. The plasma conditions have been characterized as have the effect of important parameters (gas ratios, flow rates and pressure) on the product nanoparticles. The resultant nanoparticles have been characterized ex-situ by TEM, Auger, and XPS spectroscopy. SiC particles collected are  $\sim$ 5 nm in size, with 3C and hexagonal and rhombohedral modifications. Silicon nitride has also been synthesized similarly by using silane and nitrogen as the precursor gases. Implications of the new technique are discussed.

#### Reports:

- Integrated Synthesis and Post-Processing of Silicon Carbide and Aluminum Nitride, by A.I. Kingon et al., TR. 4 pp. AD A230 810
- 2. Crystalline Napparticles of Si by Nonthermal Microwave Plasma, by A.K. Singh and A.I. Kingon, MS. J Mater Sci.
- 3. Non-Thermal Synthesis of SiC and Si<sub>3</sub>N<sub>4</sub> Ultrafine Particles, by A.K. Singh and A.I. Kingon, MS, *J Mater Sci.*
- 4. Synthesis of SiC Clusters in a Nonthermal Microwave Plasma, by A.K. Singh and A.I. Kingon, MS.

# 26747 NANOGRAIN SUPERPLASTIC PROCESSING OF CERAMICS

Rishi Raj

Cornell University

SC: BWL, ETDL, MTL

Superplastic experiments were carried out in tension on small specimens having a cross section of  $50 \times 1.1$  $\mu$ m, and a gage length of 4 mm. The specimens, in the form of fibers, were prepared by lithography from thin films that were obtained by physical vapor deposition. Experiments with ZrO<sub>2</sub>-3.5 mol percent  $Y_2O_3$  exhibited a threshold stress for superplastic flow. While the measurements of the average flow stress were in agreement with data from bulk materials, the stress-strain curves obtained from the microspecimens were serrated, which researchers attributed to discrete grain sliding events. The serrations are believed to occur in the microfiber specimens because the gage section contained relatively few grains. A new approach for conceptualizing superplastic flow in ultrafine grained ceramics was proposed.

**VI Metallurgy and Materials Science** 

Reports:

1. Microtensile Superplasticity in Ceramic Fibers, by R. Lappalainen and R. Raj, MS.

# 26825 A STUDY INTO THE EFFECTS OF ELECTRIC FIELDS AND CURRENTS ON THE AGING AND HARDENING OF STEELS

Hans Conrad

North Carolina State University

SL: ARDEC SC: BWL, MTL

The influence of an externally applied electric field on the quench aging of a low carbon (0.04 w/o C) steel sheet was investigated. The specimens were placed in solution in a vacuum for 90 min at 728°C and quenched in an ice-water bath at 2°C. The quenched specimens had a mean linear intercept grain size of 13 µm. Following quenching, the specimens were aged for various times at 56 to 100°C (± 2°C) with, and without, an electric field (produced by a voltage of 6.7 kV), and for both polarities of the field. Typical aging results were shown in a plot of the increase in Vickers hardness (50 g load) v aging time at 56°C. The time to reach the maximum change in hardness increased in the order: (a) V = 0, (b) V = 6.7 kV and (c) V = +6.7 kV, i.e., the electric field retarded the aging reaction, the effect being larger when the specimen was connected to the positive terminal of the power supply compared to the negative terminal. This retarding effect of the electric field occurred at all aging temperatures, the effect however being smaller as the aging temperature was increased. Also, the peak hardness was decreased by the electric field. A semi-log plot was made of the time at which the maximum increase in hardness occurred v the reciprocal of the absolute temperature. The data points lie reasonably well on straight lines whose slopes increase in the same order as the time to attain the maximum increase in hardness. Also, the present results for V = 0 are in reasonable accord with the quench aging data from Davenport and Bain (Trans ASM 23 (Dec 1935) 1047). Worthy of note is that the hardness measurements were made on the side of the sheet opposite that where an electric field is established. Thus, the influence of the electric field extended into the sheet specimen to a depth nearly that of the thickness of the sheet; i.e.,  $\sim 40 \ \mu m$ .

#### Reports

No. 1-8 in previous editions

 Effects of Electric Current and External Electric Field on the Mechanical Properties of Metals-Electroplasticity, by H. Conradet al., MS

- Constitutive Laws Pertaining to Electroplasticity in Metals, by H. Conrad et al., Constitutive Laws of Plastic Deformation and Fracture, p305. AD A227 938
- 11. Effect of Electric Field on Cavitation in Superplastic 7475 Al, by H. Conrad et al., MS. *Mater Sci and Eng.*
- Effects of Electric Fields and Currents on Microstructure, Properties and Processing of Metals and Alloys, by Hans Conrad and Arnold F. Sprecher, TR, Jul 90, 16 pp. AD A228 647
- Electroplasticity The Effect of Electricity on the Mechanical Properties of Metals, by H. Conrad et al., *JOM* 42,28(1990). AD A233-897
- 14. Influence of an Electric Charge During Quench Aging of a Low-Carbon Steel, by Hao An Lu and Hans Conrad. MS. Appl Phys Let.

## 27163 TOUGHENING MECHANISMS IN ULTRAHIGH-STRENGTH STEELS

Gregory B. Olson Northwestern University

SL: BWL, MTL SC: MTL

M<sub>2</sub>C carbide precipitation was investigated in martensitic Co-Ni steels, including the commercial AF1410 steel and a series of higher-strength model alloys. Results of TEM and x-ray diffraction were combined with results of collaborative SANS and APFIM studies to determine phase fractions, compositions, and lattice parameters throughout precipitation, including estimation of carbide initial critical nucleus properties. The composition dependence of the M<sub>2</sub>C lattice parameters was modeled to predict the composition-dependent transformation eigenstrains for coherent precipitation: this was input into collaborative numerical calculations of both the coherent carbide elastic self energy and the dislocation interaction energy during heterogeneous precipitation. The observed overall precipitation behavior is consistent with theoretically-predicted behavior at high supersaturations where nucleation and coarsening compete such that the average particle size remains close to the critical size as supersaturation drops. However, the coarsening in this system follows a  $t^{i_x}$  rate law consistent with heterogeneous precipitation on dislocations. Initial precipitation appears to be coherent, the carbides tending toward a rod shape with major axis oriented along the minimum principal strain direction. At initial nucleation, particles are Fe-rich and C-deficient, diminishing the transformation eigenstrains to a near invariant-line strain condition. The observed relation between carbide volume fraction and the shape-dependent capillarity parameter implies a coherency loss transition in AF1410 reached at 8 h tempering at 510°C.

Reports.

1. Overview: Science of Steel, by G.B. Olson, MS.

# 27407 THE ROLE OF SECOND PHASE PARTICLES IN THE DESIGN OF ULTRAHIGH STRENGTH STEELS OF IMPROVED TOUGHNESS

Warren M. Garrison, Jr. Carnegie-Mellon University

SL: BWL, MTL SC: MTL, STRUC DIR

This research seeks to improve the fracture toughness of ultrahigh strength steels and to identify and model the mechanisms involved in the sharp crack upper shelf fracture of these materials. An investigation will be made of the nature of the  $Ti_2CS$  inclusion/ matrix interface and the composition, spacing and shape of the inclusions in heats of ferrous alloys including Hy180 steel, prepared with controlled chemistry and under conditions of melting and subsequent heat treatments. The chemistry and processing parameters will be optimized to achieve improved fracture toughness combined with high strength. The influence of microstructure on the various aspects of the fracture process will be studied.

# 28480 MEASUREMENT OF INTERFACE STRENGTH, INTRINSIC TOUGHNESS AND THEIR DEPENDENCE ON INTERFACIAL SEGREGANTS

Vijay Gupta

Dartmouth College

SC: ARDEC, CERL

The objective of the research is to develop and implement a laser spallation technique to investigate the mechanical properties of selected interface systems. The determination of interfacial strengths using laser Doppler interferometry in laser spallation experiments will be made on selected interface systems. The systems of interest will include the interfaces between fibers and the diffusion barrier coatings in composite materials, between ceramics and metals in multilayer devices, and between wear- and corrosionresistant coatings and their underlying substrates. The results of these measurements will be used to relate interfacial strength with intrinsic toughness. TEM and Rutherford backscattering techniques will be combined with the laser spallation experiments to investigate the effects of embrittling and ductilizing segregants on interfacial strength.

# **28549** LASER-INDUCED CONTROLLED FLAW TESTING IN CERAMICS

Y.T. Chou M.P. Harmer J. Huennekens Lehigh University

SC: ARDEC, AROE

The research objective is to investigate the mechanisms and kinetics of the initiation and growth of internal cracks in ceramic materials. The study will consist of the following: (a) The mechanism of laser-induced crack (LIC) generation will be analyzed theoretically using thermal mechanics in order to establish a reliable procedure for initiating controllable internal cracks. (b) Single crystals of MgO, Al<sub>2</sub>O<sub>3</sub>, ZrO<sub>2</sub>, and partially stabilized PZT will be irradiated by a laser pulse to produce a single system of internal cracks in a contamination-free environment. Fracture properties will be determined through tensile tests and the results compared with those obtained by single-edge-notch bending tests. (c) These single crystal specimens will also be exposed to different gaseous environments following LIC generation to study environmental effects on crack growth under sustained loading.

## 28608 SMART MATERIALS/STRUCTURES TECHNICAL ANALYSIS

Phillip Parrish BDM Corp.

SC: AROE

The objective of the research is to conduct a technical analysis of concepts in Smart Materials and Structures. The approach will involve, but would not necessarily be limited to the following: (a) selection of a small number of DoD systems where incorporation of intelligent control through structures and/or materials has high potential payoff, (b) identification of appropriate Smart Materials/Structures concepts, relevant environmental and hardening issues, and system integration concerns, (c) determination of additional components which must be developed in order to produce smart prototypes, (d) establishment of manufacturing techniques and facilities for prototype production.

## 28761 SUPERFLASTIC CERAMICS

Oleg D. Sherby Stanford University SC: ARDEC, AROE, BRL The research objective is to study the mechanism of superplasticity in fine-grain ceramic materials and the related structure-property relationships. Superplastic properties in tension and in compression will be studied for two alloy compositions. One will be based on Fe<sub>3</sub>C and the other on Fe<sub>3</sub>AlC<sub>x</sub>. The alloys will be processed by powder and ingot metallurgy routes with the appropriate thermomechanical processing to develop a stable fine-grain two phase alloy. The tensile and compressive deformation behavior in these alloys will be measured and the associated microstructure determined by SEM, TEM, x-ray, and optical microscopy.

## C. Processing

## 25202 PROCESSING AND PROPERTIES OF SILICON CARBIDE REINFORCED REACTION BONDED SILICON NITRIDE COMPOSITES

John S. Haggerty Yet-Ming Chiang Massachusetts Institute of Technology

SC: BRADEC, MICOM, PROP DIR

Work has focused on making RBSN matrix composites based on particulate and whisker reinforcements. Samples have been characterized to provide a basis for interpreting mechanical property measurements. Parameters that were studied include percent reaction (weight gain and XRD),  $\alpha/\beta$  ratio, porosity, and specific surface area. The strength, toughness and R-Curve behavior of unreinforced RBSN and RBSN containing either whisker or particulate SiC reinforcements were studied. Strengths were measured both in three-point bending (approximately  $1.5 \times 2 \times 10.4$  mm bend bars) and by the ball-on-ring technique (approximately 11 mm dia.  $\times$  1.4 mm thick discs). Toughness was characterized by fractography, the indentation cracklength method indentation-strength and by a coupled indentation crack-length/strength method. The last is attributed to a recently developed technique by Krause (J Am Ceram Soc 71[5]338-43 (1988)), and its advantage is that it is capable of measuring and characterizing the material R-Curve.

## 25373 A FUNDAMENTAL INVESTIGATION INTO THE JOINING OF ADVANCED LIGHT MATERIALS

W. A. Baeslack, III L. Adler Ohio State University SL: MTL, TACOM

SC: CERL

The microstructures of inertia-friction weldments in a rapidly solidified powder metallurgy Al-8.7Fe-2.8Mo-1V alloy were characterized using light and transmission electron microscopy. Extensive plastic deformation at the weld interface during the welding process was shown to fracture and disperse relatively coarse, spherical dispersoids present in the original base-metal microstructure, thereby resulting in a refined dispersoid size in this region. These fine dispersoids promoted an increase in hardness at the weld interface as compared to the unaffected base metal. Local regions of nonuniform interface deformation at the weld outer periphery resulted in a heterogeneous microstructure comprised of adjacent regions of high and low dispersoid density. The dispersoid-lean regions were characterized by appreciably coarsened alpha grains and a hardness well below that of the base metal. The greater extent of dispersoid-lean regions in welds produced with low axial force promoted preferential weld interface failure during three-point bend testing, while the near absence of these regions in welds produced with high attial force promoted failure in the unaffected base metal remote from the weld.

#### Reports.

No. 1-4 in previous editions.

- Characterization of Inertia-Friction Welds in a High-Temperature RS/Pm AI-8.5Fe-1.7Si-1.3V Alloy (AA 8009), by H.H. Koo et al., MS
- Solid-Phase Welding of a Rapidly-Solidified Dispersion-Strengthened AI-Fe-V-Si Alloy-EVS1212, by H.H. Koo et al., MS
- Characterization of Inertia-Friction Welds Between a Rapidly-Solidified AI-Fe-Mo-V Alloy and IM 2024 T351, by H.H. Koo et al., MS, J Mater Sci
- Friction Welding of a Rapidly-Solidified Al-Fe-V-Si Alloy, by H.H. Koo and W.A. Baeslack III, MS. Welding J.
- Structure, Properties and Fracture of a Linear Friction Weld in Rapidly-Soliditied Al-Fe-V-St Alloy 8009, by H.H. Koo and W.A. Baeslack III, MS.

## **25526** NANOPHASE CERAMICS

Robert S. Averback T. A. Parthasarathy University of Illinois

SC: MTL

Superplastic deformation: Many earlier measurements were refined and submitted for publication. One of the most significant of the results is the enormous potential found for superplastic deformation of nanophase materials. Continuation of that work is leading to a better understanding of the constitutive

relations governing superplastic deformation in these materials. TEM studies: Efforts were made to better characterize the microstructure of the samples by conventional and high resolution TEM. This work is just in its initial stages, and methods have been developed for preparing samples. Specimens of TiO<sub>2</sub> were examined in the off-stoichiometric and fully oxidized states. Of primary concern is whether the boundaries contain amorphous phases. To date researchers have not found indication for this. Control of grain growth: Efforts were initiated to control grain growth during sintering and/or superplastic forming. Two approaches are being attempted, impurity doping and additions of second phase inclusions. Nanophase ZrO<sub>2</sub>: Correct procedures have been found to routinely synthesize nanophase ZrO<sub>2</sub>. The "as compacted" and sintered material are both monoclinic even though the grain sizes are 15 to 100 nm. The stability of ultrafine grained ZrO<sub>2</sub> is controversial. For example, sol gel techniques do not yield the monoclinic phase directly, probably due to surface contamination of the particles. This question of phase stability in  $ZrO_2$  will be explored in the future.

#### Reports:

No. 1-3 in previous editions.

- Grain Growth in Nanocrystalline TiO<sub>2</sub> and Its Relation to Vickers Hardness and Fracture Toughness, by H.J. Hofler and R.S. Averback, *Scripta Met* 24,2401(1990). AD A232 474
- Low Temperature Sintering and Deformation of Nanocrystalline TiO<sub>2</sub>, by H. Hahn et al., MS, *Mat Res Soc Symp Proc.*
- 6. Sintering and Grain Growth in Nanocrystalline Ceramics, by R.S. Averback et al., MS, Acta Metall Mater.
- 7. Temperature Dependence of the Hardness of Nanocrystalline TiO<sub>2</sub>, by M. Guermazi et al., MS, J Am Ceram Soc.

## 26021 ADVANCED ARMOR MATERIALS DEVELOPMENT TiB<sub>2</sub>Al<sub>2</sub>O<sub>3</sub>

Kathryn V. Logan Georgia Institute of Technology

SL: BRL, MTL SC: BRL, MTL

Initial ballistic testing has been completed. Test results show improved ballistic performance in TiB<sub>2</sub>  $Al_2O_3$  samples which had greater TiB<sub>2</sub> dispersion in the  $Al_2O_3$  matrix. Additional material refinement should further increase ballistic performance.

## 26068 DEVELOPMENT OF ALUMINUM NITRIDE: A NEW LOW COST CERAMIC ARMOR

William Rafaniello The Dow Chemical Co

SE: BRL MTI SC BRL

#### C. Processing

The primary focus of this contract was to develop a low-cost process for densifying large aluminum nitride armor tiles with improved ballistic performance. The program goals were to produce tiles at least 4-inches dia.  $\times$  2-inches thick using low-cost ceramic processing and to establish sintered aluminum nitride as a viable armor material. Phase I has been completed with the establishment of a ballistic baseline for the five hot-pressed powders. Dynamic compressive strengths for the 20 + sintered compositions have been added to the extensive database already established for these materials. However, LRP ballistic performance has not vet been determined for several sintered AIN compositions which have been prepared for testing. Meanwhile, examination of the SiC/AIN composite system for enhanced ballistic performance, has been started.

#### Reports:

No. 1 in previous edition.

2. Processing of Aluminum Nitride Ceramics, by E.P. Skeele and W. Rafaniello, MS.

# 26123 A FUNDAMENTAL UNDERSTANDING OF THE EFFECTS OF CERAMIC PROCESSING ON PRODUCT MICROSTRUCTURE

G.G. Long

National Institute of Standards and Technology

SL: MTL SC: MTL, PROP DIR, TACOM

High resolution small-angle x-ray scattering measurements have been carried out on final stage sintering of doped and undoped alumina. Earlier neutron results on these systems were confirmed and extended to densities greater than 99 percent of theoretical. Analysis of this data, which includes deriving pore size distributions, indicates that the median size of the remaining pores and the width of their distribution both increases as density increases. Electronmicrographs of these samples support these results, and indicate, in addition, that the grain sizes also increase as density increases. Comparison of the evolution of the pore size distribution in the final stage sintering of doped and undoped alumina indicates that, at a given density, the pore distribution in the undoped is broader than in the doped material. The series of unseeded and  $\alpha$ -alumina-seeded gets were characterized by high temperature x-ray diffraction, and their behavior as they were converted to corundum was compared to that of materials generated from boehmite precursors. The addition of  $\alpha$ -alumina seed particles to the boehmite gel reduces its transition temperature to corundum by about 125°C.

#### VI Metallurgy and Materials Science

However, the addition of such seeds to the hydrous vitreous alumina precursors lowers its transition temperature by nearly 75°C to a temperature even lower than that measured for seeded boehmite. These results indicate that the hydrous vitreous alumina precursors offer a new route to a fine grained alumina. Gravimetric data on the boehmite and hydrous vitreous alumina precursors suggest that the material obtained from gels with pH>0.7 contains a significant fraction of boehmite. Below pH~0.7 there is no clear evidence of bayerite, gibbsite or other known aluminum trihydroxides. These materials are most likely hydroxides or oxides of aluminum which chemically incorporate water, and possibly alcohol, into structures.

Reports:

No. 1 in previous edition.

- 2. Characterization of the Densification of Alumina by Multiple Small-Angle Neutron Scattering, by S. Krueger et al., MS. *Acta Cryst.*
- 3. The Effect of Green Density and the Role of Magnesium xide Additive on the Densification of Alumina Measured by Small-Angle Neutron Scattering, by Gabrielle G. Long et al., *J Am Ceram Soc* 74,1578(1991).
- Evolution of the Pore Size Distribution in Final State Sintering of Alumina Measured by Small-Angle X-Ray Scattering, by Susan Krueger et al., MS, J Am Ceram Soc.
- Small-Angle Neutron Scattering Characterization of Processing/ Microstructure Relationships in the Sintering of Crystalline and Glassy Ceramics, by G.G. Long et al., MS, J Mater Res.

# 26392 PRODUCTION AND EVALUATION OF DENSE CERAMIC COMPOUNDS BY COMBUSTION SYNTHESIS AND DYNAMIC COMPACTION

Marc A. Meyers University of California, San Diego

SL: BRL, MTL SC: BRL. MTL

The activities on titanium carbide continued with successful production of 4-inch disks. Thirteen compaction experiments were conducted. The material was characterized by optical, scanning and transmission electron microscopy. The involvement of Dr. G.T. Gray III and of Professor K.S. Vecchio were instrumental in obtaining TEM of the SHS product; the microstructure was compared to that of hotpressed product provided by CERCOM. The microhardness of SHS TiC is comparable to that of hot-pressed TiC (CERCOM). The titanium diboride experiments were initiated and a series of six experiments were performed at increasing DYNAPAK impact velocities. This series was conducted after the reaction was observed in the reaction chamber, with

its rate controlled by the addition of different amounts of inert titanium diboride powder. Three-inch disks of titanium diboride were produced. The DYNAPAK continues to be modified to better suit the experimental requirements specific to the research projec' The maximum pressure was increased from 2,000 to 3,000 psi. A rapid extraction was added by means of a pressure accumulator. A new furnace (maximum operating temperature: 1,800°C) was acquired and is being modified. It will replace the 1,100°C furnace being currently used. It is expected that reduced temperature gradients will improve the integrity of the compacts by eliminating thermal cracking.

#### Reports:

- The Prospects for Superplasticity at High Strain Rates: Preliminary Considerations and an Example, by A.H. Chokshi and M. A. Meyers, *Scripta Met* 24,605(1990).
- Production of Dense Titanium Carbide by Combining Reaction Synthesis with Dynamic Compaction, by Jerry Christopher LaSalvia, MS Thesis, 1990, 146 pp.

## 26439 MECHANICAL BEHAVIOR AND PROCESSING OF ALUMINUM METAL MATRIX COMPOSITES

E.J. Lavernia

E A. Mohamed University of California, Irvine

SL: MTL SC: ARDEC, BRADEC, PROP DIR

Rapid solidification/spray atomization and deposition studies have been performed on four aluminum lithium alloy compositions. Various processing parameters have been used and then evaluated in an attempt to characterize the microstructure. Within the deposit, porosity levels vary from about 3 to 15 percent, depending in part on the gas type and on the amount of liquid phase present within the atomized droplet upon impact to the deposition substrate. The amount of entrapped gas is low: 71 ppm of oxygen and 10 ppm of nitrogen. Studies on powder size and mass distributions indicate that there is a higher mass concentration of droplets in the center of the spray, relative to that measured in the periphery. In addition, the results suggest that the coarser droplets tend to populate the center of the spray; these facts, coupled with the correspondingly high droplet velocity profiled from earlier studies result in the coarse grain sizes and higher deposit density characteristically found in the center. Because of the changing metal flow rates during deposition and the changing thermal/solidification profile of the growing deposit,

densities and grain sizes vary spatially throughout the deposit. The average grain size varied from about 9 to 67  $\mu$ m, depending on the system and its processing variables. Room temperature mechanical performance varied with processing conditions and thermomechanical treatment; ultimate strengths approaching 500 MPa and ductilities exceeding 43 percent have been obtained, indicating there is a great deal of potential for the alloys investigated. This observation should provide the incentive to better optimize the processing and thermomechanical parameters relative to future studies.

#### Reports:

No. 1-16 in previous editions.

- The Spray Atomization and Deposition of Weldalite 049, by J.M. Marinkovich et al., J Minerals, Metals & Mater Soc 41,36(1989). AD A219 037
- The Effects of Solidification Phenomena on the Distribution of Ceramic Reinforcements During Spray Atomization and Deposition, by Manoj Gupta et al., Metal & Ceramic Matrix Composites: Processing, Modeling & Mech Behavior, 1990, p91. AD A224 430
- Review Strength, Deformation, Fracture Behaviour and Ductility of Aluminum-Lithium Alloys, by E.J. Lavernia, J Mater Sci 25,1137(1990). AD A225 150
- 20. Processing of Two Al-LiX-Zr (X = Cu,Mg and Ge) Alloys Using Spray Atomization and Deposition, by M. Gupta et al., Advances in Powder Metallurgy, Volumes 1-3, 1989, p139. AD A219 721
- 21. Spray Atomization and Deposition Processing of Particle Reinforced Metal Matrix Composites, by E.J. Lavernia, MS.
- Spray Atomization and Deposition Processing of 6061 Al SiC<sub>p</sub> Metal Matrix Composites, by I. A. Ibrahim et al., MS.
- 23. Economic Feasibility of Producing Metal Matrix Composites by Spray Atomization and Deposition, by Jeffrey E. Jacob et al., MS.
- Heat Transfer Mechanisms and Their Effect on Microstructure During Spray Atomization and Co-Deposition of Metal Matrix Composites, by M. Gupta et al., MS.
- 25. This number not used.
- Influence of Oxides on the Properties of P/M Al-Li-Cu Alloys, by E.J. Lavernia et al., Intl J Powder Met 26,321(1990). AD A232 433
- 27. The Influence of Spray Atomization and Deposition Processing on the Microstructure of an Aluminum-Copper-Lithium Alloy, by T.S. Srivatsan et al., MS.
- High Temperature Creep of Silicon Carbide Particulate Reinforced Aluminum, by Kyung-Tae Park et al., Acta Metall Mater 38,2149(1990). AD A232 360
- 29. Particulate Reinforced Metal Matrix Composites---A Review, by I.A. Ibrahim et al., *J Mater Sci* 26,1137(1991).
- Spray Atomization and Deposition Processing of Aluminum Lithium Alloys with Elemental Additions of Cu,Mg,Mn,Zr,Ag and Ti, by Jean Marie Marinkovich, MS Thesis, 1990, 141 pp.
- Precipitation and Excess Solid Solubility in Mg-Al-Zr and Mg-Zn-Zr Processed by Spray Atomization and Deposition, by E.J. Lavernia et al., *Mater Sci and Eng* A132,119(1991).

C. Processing

#### VI Metallurgy and Materials Science

- 32. Rapid Solidification Processing with Specific Application to Aluminum Alloys, by E.J. Lavernia et al., MS.
- Manufacture of Particulate Reinforced Metal Matrix Composites Using Spray Atomization and Deposition, by E.J. Lavernia, Society of Manufacturing Engineers Technical Paper EM90-439, 1990. AD A232 327
- 34. Spray Atomization and Deposition Processing of Particulate Reinforced Metal Matrix Composites, by E.J. Lavernia, MS.

## 26485 TO STUDY AND EVALUATE SPECIAL REACTIVE ARMOR CONCEPTS

Louis Zernow

Zernow Technical Services, Inc.

## SL: BRL, MTL SC: BRL

A subcontract begun on 2 July 1990 has the objective of studying the shock response and consequent temperature inhomogeneities in selected materials. The polymer sample assembly is shocked by impacting it with a 20 mm gun-fired projectile, in an evacuated chamber. The light emitted and transmitted through the translucent sample, as the shock progresses through the sample, is being examined with a high speed image converter camera and is also being analyzed by a spectrometer. Temperature inhomogeneities and an estimate of the associated peak temperatures are being sought as a guide to the nature of the thermal decomposition of the sample. Initial experiments have been concerned with selection of the impact velocity and adjustment of the light outputs to match the recording equipment capabilities.

## 26571 IN-PROCESS CURE MONITORING OF COMPOSITES VIA FIBER-OPTIC FLUORESCENCE

C.S.P. Sung University of Connecticut SL: MTL

## SC: ARDEC, BRADEC, STRUC DIR

An analysis was made of the kinetics parameters for thermal imidization of polyamic acid made from 1.5 diaminonaphthalene and a nonconjugated anhydride. In dilute solution, the dissociation rate was about three times greater than that of imidization with activation energies of about 15 Kcal/Mole. In solid state reactions, much less dissociation was observed. Activation energies of about 24 Kcal/ mole were observed for imidization whose rate is slightly faster than those in dilute solution. An investigation was made of the possibility of using intrinsic fluorescence due to the curing agent itself during cure. A common curing agent for high temperature epoxy matrix resins, diamino diphenyl sulfone shows a progressive red shift of about 20 nm when it is reacted with epoxide both in UV absorption and fluorescence spectra, due to the conversion of primary amines to secondary and finally to tertiary amines. The excitation spectra exhibits a easily measurable peak shift, which has also been observed by fiber-optic fluorimeter.

#### Reports:

 Network Structure in Diamine-Cured Tetrafunctional Epoxy by UV-Visible and Fluorescence Spectroscopy, by Eumi Pyun and Chong Sook Paik Sung, *Macromol* 24,855(1991). AD A238 450

## 26579 USE OF BLOCK COPOLYMER AS POLYMER BLEND COMPATIBILIZER

R.J. Roe

University of Cincinnati

SC: ARDEC, NRDEC

Block copolymer is often added to incompatible polymer blends to reduce the phase-separated domain sizes and to improve the adhesion between the phases. The domain size reduction probably arises as a result of the lowered interfacial tension due to accumulation of the block copolymer there, but experimental evidence on the detailed mechanism has been lacking, especially on the question of whether this is an equilibrium or kinetic effect. Experimental results show that the added block copolymer retards Ostwald ripening of phase-separated domains, thus producing smaller average domain sizes when a fixed time period is allowed for the domain growth. The Ostwald ripening process has been studied, by direct optical microscopic observations and by light scattering, with a blend of low molecular weight polystyrene and polybutadiene to which styrene-butadiene block copolymer has been added. The dependence of the retardation effect on the amount and molecular weight of the block copolymer has been studied.

# Reports:

No. 1 in previous edition.

 Effect of Added Block Copolymer on Phase-Separation Kinetics of Polymer Blend. 2. Optical Microscopic Observations, by Dong-Won Park and Ryong-Joon Roe, MS, Macromol.

# **26591** SUPERCRITICAL FLUID EXTRACTION: A NEW PROCESS FOR PRODUCING HIGH-PERFORMANCE, LOW-COST CARBON FIBERS

Mark C. Thies Michael J. Drews Joseph C. Mullins Clemson University

SL: CRDEC, NRDEC SC: ARDEC, BRADEC, CRDEC

The objective of this research program is to investigate a supercritical fluid extraction process for producing a superior mesophase pitch from which carbon fibers can be made. A continuous-flow apparatus has been constructed and is being used to fractionate petroleum pitch with supercritical toluene. Analytical methods are being used to characterize the resulting fractions and quantify the effects of the extraction process. A thermodynamic model of the process is being developed and will guide the selection of optimum operating conditions. Finally, pitch fractions with suitable properties will be spun into carbon fibers and their physical properties will be evaluated.

#### Reports:

No. 1-2 in previous editions.

 An Equilibrium View Cell for Measuring Phase Equilibria at Elevated Temperatures and Pressures, by J.R. Roebers and M.C. Thies, *I&EC Res* 29,2568(1990). AD A238 409

## 26617 MARTENSITIC TRANSFORMATIONS IN IRON ALLOYS

C.M. Wayman

University of Illinois

SL: BRL SC: ARDEC, BRADEC, BWL, MTL, TACOM

Previous work has shown that Fe-Ni-Mn alloys (without cobalt and molybdenum) undergo an appreciable maraging response. However, excessive manganese (more than five percent) presents an embrittlement problem. Thus, the focus of recent work has been on lower-Mn alloys while keeping the Ni-content at 20 percent. The age-hardening characteristics of Fe-20a/ oNi-1.27a/oMn (alloy A-O) and Fe-20a/oNi-3.23a/ oMn (alloy B-O) maraging alloys have been studied in detail using analytical electron microscopy and computer simulation of selected-area diffraction patterns (SADPs). Only alloy B O showed substantial maraging response and the activation energy of 24.3 kcal mol<sup>-1</sup> obtained suggests the nucleation and growth of precipitates along dislocations. An ordered f.c.t.  $\phi$ -NiMn precipitate was identified in overaged samples and confirmed by energy-dispersive x-ray analysis and computer simulation of SADPs. The shape of precipitates depends on the aging temperature. Lower temperature aging resulted in rod-shaped precipitates, while disc-shaped precipitates appeared at higher temperatures. Rod-shaped Widmanstatten austenite, having the Kurdyumov-Sachs orientation relationship with the matrix, appeared simultaneously within the lath martensite.

## 26728 THE PYRO-METALLURGICAL, PHYSICAL, AND MECHANICAL BEHAVIOR OF WELDMENTS

David L. Olson Robert H. Frost Colorado School of Mines

SL: MTL, TACOM SC: ARDEC, BRADEC, CERL

Research to understand the weld metal chemical composition created during direct current arc welding process has continued with special interest devoted to the role of electrochemical reactions. Both the slag and the plasma can serve as an electrolyte. The effect of electrochemical reactions on the transfer of sulfur during direct current arc welding is being investigated. Stationary gas tungsten arc welding is being performed on the low carbon microalloyed steel rounds as a function of time, current, and polarity. Helium gas containing various concentrations of sulfur dioxide gas provides the sulfur source. The extent of sulfur transfer was shown to be altered by electrochemical phenomena. However, difficulties arose in obtaining systematic data when direct current electrode positive polarity was employed, due to melting of the tungsten electrode during welding. Therefore, a gas tungsten arc welding system with a water cooled tungsten electrode is under construction, and good results are expected. The influence of zirconium and boron on the microstructure of low carbon steel weld deposits is being investigated. The specific combination of zirconium (0.02-0.05 w/o) and boron (40-60 ppm) additions in the weld suppresses the formation of grain boundary ferrite at the prior austenite grain boundary, and promotes the intragranular formation of acicular ferrite, as does the combination of titanium and boron additions. Acicular ferrite microstructures promote an excellent combination of strength and toughness for microalloyed HSLA steels which are to be used in lower temperature service. By substituting zirconium for titanium in titaniumboron additions it is possible to evaluate suggested

models for the nucleation and growth of acicular ferrite. Preliminary results show that acicular ferrite formation is controlled by the size distribution of nonmetallic inclusions, rather than by the degree of crystallographic mismatch between nonmetallic inclusions and resulting ferrite.

## Reports:

No. 1-4 in previous editions.

- A Consideration of the Processing Variables and Solidification Kinetics for Optimization of Titanium and Zirconium Additions in Relationship to Weldability, by Matthew J. Dvornak, PhD Thesis, 1990, 233 pp.
- Effects of Grain Refinement on Aluminum Weldability, by M.J. Dvornak et al., Weldability of Materials, 1990, p289, AD A232 264
- Effect of Electrochemical Reactions on Submerged Arc Weld Metal Compositions, by J.H. Kim et al., Welding Res Sup Dec 90, p448s. AD A239 893
- Effects of Welding Flux Additions on 4340 Steel Weld Metal Composition, by P. A. Burck et al., Welding Res News Mar 90, p115-s. AD A225 875
- The Fundamentals of Welding Consumables, by D.L. Olson, Recent Trends in Welding Science and Technology TWR '89, 1990, p553. AD A226 256
- 10. Functional Forms of Equations to Predict Steel Weld Metal Properties, by S. Ibarra et al., Proc of 9th Intl Conf of Offshore Mechanics & Arctic Engineering, 1990, p517. AD A225 852
- A Consideration of the Processing Variables and Solidification Kinetics for Optimization of Titanium and Zirconium Additions in Relationship to Weldability, by Matthew J. Dvornak, PhD Thesis, 1990, 233 pp.
- The Influence of Boron and Titanium on Low-Carbon Steel Weld Metal, by D.W. Oh et al., Welding Res Sup Apr 90, p151-8. AD A232 265
- Present Consumable Technology Advances Into the 21st Century. by D.L. Olson and T.A. Siewert, Welding J Nov 90, p 37. AD A232 203
- Effect of Shielding Gas Oxygen Activity on Weld Metal Microstructure of GMA Welded Microalloyed HSLA Steel, by R.E. Francis et al., Welding Res Sup Nov 90, p 408-s. AD A232 202

## 26751 SUPERPLASTICITY IN FINE-GRAINED CERAMIC COMPOSITES

## T.G. Nieh

Lockheed Missiles & Space Co., Inc.

SC: BRADEC, PROP DIR

A paper has been prepared in which the microstructures and high-temperature deformation characteristics of fine-grained, yttria-stabilized, zirconia composites, including  $AI_2O_3$  particle-reinforced and SiC whisker-reinforced ZrO<sub>2</sub>, are described. Tensile tests were carried out at temperatures between 1000 and

#### **VI Metallurgy and Materials Science**

1650°C over the strain rate range from  $2.7 \times 10^{-5}$  to  $2 \times 10^{-3}$  s<sup>-1</sup>. Tensile elongation as a function of temperature, strain rate, and grain size is also presented. The Al<sub>2</sub>O<sub>3</sub> particle-reinforced ZrO<sub>2</sub> was found to be superplastic, but SiC whisker-reinforced ZrO<sub>2</sub> was not. These properties have been correlated with microstructure of the composites. The mechanisms which lead to superplasticity in Al<sub>2</sub>O<sub>3</sub> particle-reinforced ZrO<sub>2</sub> are discussed. Superplasticity in ceramics and ceramic composites is reviewed. Deformation characteristics, and in particular the strain rate sensitivities in these materials, are discussed in another manuscript. From the strain rate sensitivity and grain size dependence, deformation mechanisms in these superplastic materials have been addressed. It appears that grain boundary sliding is the predominant deformation mechanism. Constitutive equations governing the superplastic flow in superplastic ceramics and ceramic composites are presented. Microstructural features in these materials, e.g., grain size and morphology, and glassy phases at grain boundaries, are described. Microstructure stability, and particularly, concurrent grain growth during superplastic deformation and its effect on superplastic elongation, is discussed. In this review, the superplastic properties and microstructures of some other advanced materials, e.g., intermetallics, metal-matrix composites, and mechanically alloyed alloys, are also briefly reviewed and compared with those of superplastic ceramics.

Reports:

- Recent Advances in Superplastic Ceramics and Ceramic Composites, by T.G. Nieh and F. Wakai, MS.
- 2. Superplasticity in Fine-Grained YTZ Composites, by T.G. Nich, MS.

## 26882 ENABLING TECHNOLOGIES FOR ECONOMICAL MANUFACTURING OF COMPOSITES

Alan K. Miller Curtis W. Frank George S. Springer Stanford University

> SC: BRADEC, MTL, NRDEC

Experimental tests of coil geometry continued. In these tests, a short pulse of 450 kHz induction power is applied to a specially-designed coil held adjacent to the test specimen. Temperature at the critical location on the top surface of the specimen is measured using a thin copper-constantan thermocouple,

with the thermocouple leads being aligned for minimal interference from the magnetic field of the induction coil. Tests on a pre-existing set of test specimens demonstrated that the measured temperature response correlates with the size of the gap between the prepreg and the laminate, and that quite small gaps can be resolved. Modeling and analysis indicated that the response appears to be controlled by variations in the transient conduction of heat from the underlying laminate to the top prepreg ply where the temperature is monitored. For composites manufacturing, even if the gap size is zero it is also important to be able to sense regions of lack of ply-to-ply autohesion. These are so-called "kissing unbonds", or KUB's. Accordingly, a new set of test specimens was fabricated in which the gap size was zero but intentional KUB's were present.

#### Reports:

- A Technique for Measuring the Mechanical Properties of Thick Composite Laminates, by Peter R. Ciriscioli et al., MS. J Composite Mater.
- An Expert System for Controlling Autoclave Temperature, by Peter R. Ciriscioli et al., Proc of 35th Intl SAMPE Symposium, 1990, p1507. AD A226 457

## 26891 PERFORMANCE PREDICTIONS FOR COMPOSITE MATERIALS

H. Reiss W.M. Gelbart

University of California, Los Angeles

SC: BRADEC, HDL, MTL

Multiple scattering blurs the distinction between different material systems beyond a certain distance from the observation point, thereby rendering most random systems cloudy in appearance and opaque in the sense of structure delineation. However, based on a theoretical analysis, researchers showed that, due to the phase coherent nature of wave propagation through random media, some remnant information is still present which can be used to detect and locate new growing cracks. This offers the possibility to extend acoustic nondestructive evaluation techniques in the realm of highly heterogeneous media, such as composites or concrete analyzed by high frequency sound waves.

#### Reports:

 Acoustic Nondestructive Evaluation of Heterogeneous Materials in the Multiple Scattering Regime, by Shechao Feng and Didier Somette, MS. J Acoust Soc Am. 2. Statistical Thermodynamic Approach to Fracture, by Robin L. Blumberg Selinger et al., MS, *Phys Rev Let.* 

## 27373 POLYMER GELS AS PRECURSORS TO HIGH-PERFORMANCE MATERIALS

James E. Mark University of Cincinnati

SL: NRDEC

SC: BRADEC, MTL

The basic apparatus to be used in characterizing the gelation process in ceramic precursor systems has now been constructed. It has been tested on several polymer samples that undergo gelation by simple crystallization to form thermoreversible gels. Data of good precision and good reproducibility have now been obtained. Reliable and useful data are now being obtained on the systems of direct interest with regard to the new sol-gel approach to high-performance ceramics. The specific reaction being investigated is the hydrolysis of tetraethoxysilane (tetraethylorthosilicate) to give silica-type materials. A variety of catalysts, catalyst concentrations, temperatures, and miscibility-promoting additives are being used. Plots of the modulus of the gel against time show an induction period during which the hydrolysis, condensation, and branching are occurring. Once sufficient branching has occurred for gelation, the modulus begins to develop, increasing in an S-shaped manner, and then finally leveling off at its equilibrium value. The kinetic data thus obtained are being correlated with the hydrolysis reaction conditions and various mechanical properties, and will be also be correlated with structural information obtained from electron microscopy and scattering measurements. Small-angle scattering measurements using either neutrons or x-rays are being carried out at the Oak Ridge National Laboratories. Of particular interest in this regard are the inorganic-organic composites obtained by bonding polymer chains into the ceramiclike phases. The microscopy and scattering data are being interpreted to provide information on particle sizes, particle size distribution, degrees of agglomeration, and degrees of phase interpenetration in the case of bicontinuous systems.

## Reports:

<sup>1.</sup> Some Novel Polysiloxane Elastomers and Inorganic-Organic Composites, by J.E. Mark, MS.

<sup>2.</sup> Polymer Distribution in Silica Aerogels Impregnated with Siloxanes by <sup>1</sup>H Imaging, by Leoncio Garrido et al., MS, *Polymer*.

## 27472 SOLIDIFICATION STRUCTURE SYNTHESIS IN UNDERCOOLED LIQUIDS

John H. Perepezko

University of Wisconsin -	- Madison
SL: MTL	SC: ARDEC, PROP DIR

One of the central objectives of the current program is the identification and control of the thermodynamic and kinetic factors governing the synthesis of solidification structure in undercooled liquids. In much of the previous work on crystallization in undercooled alloys, it has been established that the main factor limiting the amount of undercooling and solidification structure options is the action of the most potent heterogeneous nucleation site. As a result one of the thrusts of the research has concentrated on heterogeneous nucleation studies in well-characterized systems and under well-defined conditions. An example of this type of study is the current examination of grain refinement and microstructural modification in Al alloys. With the droplet emulsion technique samples have been produced in which both effective and ineffective inoculant particles are segregated to individual droplets. A high sensitivity DTA capability which can monitor the behavior of about 50 droplets and a microstructural morphology analysis on quenched samples have been used to identify the minor fraction of inoculant particles which are actually the active nucleants. In other work on the undercooling and solidification behavior in Al-Y alloys the control of thermodynamic and kinetic factors has been used to obtain several novel microstructures. Supersaturated Al solid solutions have been produced from undercooled alloys containing up to 5 w/o Y. Thermal analysis measurements indicate that the metastable solid solutions decompose at about 240°C to yield a high density of Al<sub>3</sub>Y dispersoids. In the most recent work alloys with compositions between Al-40 w/o Y have been undercooled to yield solidification structures consisting almost entirely of the Al<sub>2</sub>Y, an intermetallic Laves phase compound. X-ray diffraction analysis reveals that the lattice parameter of the cubic Al<sub>2</sub>Y phase decreased linearly with increasing Y content. This indicates that the supersaturation of Al<sub>2</sub>Y with Al is substitutional in in nature. It should be noted that this level of supersaturation is extraordinary since Al<sub>2</sub>Y is essentially a line compound at equilibrium. Thermal analysis runs demonstrate that the supersaturated Al<sub>2</sub>Y solutions are stable up to about 400°C which is also remarkable for an Al-base alloy. Ongoing studies are directed at a microstructural analysis of the solid state decomposition reactions with TEM methods.

Reports:

- Solidification of Undercooled Sn-Sb Peritectic Alloys: Part II. Heterogeneous Nucleation, by W.P. Allen and J.H. Perepezko, *Met Trans* 22A,765(1991). AD A238 369
- Solidification of Undercooled Sn-Sb Peritectic Alloys: Part I. Microstructural Evolution, by W.P. Allen and J.H. Perepezko, *Met Trans* 22A,753(1991). AD A238 578
- Evaluation of Al-Ti-Si Alloys as Grain Refining Agents, by M.K. Hoffmeyer and J.H. Perepezki, *Light Metals*, 1991, p1105. AD A238 122

## 27579 HIGH PERFORMANCE HEAVY ALLOYS BY ALLOYING AND PROCESS CONTROL

Randall M. German

Rensselaer Polytechnic Institute

SL: MTL SC: BRL

Alloying additions to the W-Ni-Fe systems through powder mixing have proven beneficial, resulting in an increase in both ultimate and yield strengths of these composites. The decrease in ductility associated with these additions is not very critical for most applications associated with the heavy alloy system. Among the additives used in this case (rhenium, tantalum, molybdenum), rhenium is the most potent strengthener, but molybdenum additions are superior as far as cost and mechanical properties are concerned. Alloying with molybdenum results in a decrease in the sintered grain size through limiting the solubility of tungsten in the solid solution matrix. Hence grain refinement is achieved by retarding the solution-reprecipitation stage of liquid phase sintering. Along with grain refinement, the solubility of molybdenum in the matrix as well as in the tungsten grains contributes to solid solution strengthening. However, the distribution of molybdenum in the heavy alloy system is not uniform when powder mixing is used. Hence a homogeneous molybdenum coating on the tungsten grains is desirable. This coating will further decrease the solubility of tungsten in the matrix which in turn alters grain coarsening. Various alloying techniques such as electroless plating and milling with different routes are being investigated. For this purpose, characterization techniques such as electron microscopy, electron microprobe, and energy dispersive spectroscopy are being utilized to investigate the distribution of molybdenum in the heavy alloy system. Metallographic techniques and mechanical universal instruments are also used to evaluate the mechanical properties of these composites.

Reports:

 Sintering Time Influence on the Microstructure and Mechanical Properties of Tungsten Heavy Alloys, by R.M. German et al., MS, *Met Trans.*

- 2. Grain Growth in Liquid Phase Sintered W-Mo-Ni-Fe Alloys, by P.B. Kemp and R.M. German, MS, J Less-Common Metals.
- 3. Properties of High Density Tungsten-Rhenium Alloys by Liquid Phase Sintering, by R.M. German and A. Bose, MS.
- 4. Tungsten and Tungsten Alloys by Powder Metallurgy A Status Review, by A. Belhadjhamida and R.M. German, MS.

# 28005 MATERIALS PROCESSING AND MICROSTRUCTURE CONTROL IN HIGH TEMPERATURE ORDERED INTERMETALLICS

John H. Perepezko

University of Wisconsin - Madison

SL: ARDEC, MTL SC: AROE, PROP DIR, TACOM

In the Ti-Al-Nb system new information on the phase stability at elevated temperature has been applied for the design of a specific multiphase microstructure which represents essentially an in-situ composite. The microstructure design is based upon the previous observation that a single grain of a high temperature phase, i.e., B2 structure, forms a unidirectional  $(\alpha_2 + \gamma)$  lath microstructure upon decomposition during cooling. A high temperature anneal is used to promote rapid grain growth so that under directional cooling a gradient will yield large grains or single crystals. Recent experiments have confirmed this design with large grains centimeters in size, that contain the unidirectional  $(\alpha_2 + \gamma)$  lath structure, forming during gradient cooling from 1500°C. Even larger grains have been produced by a single crystal growth from the melt technique, but this approach also yields an as cast solute segregation profile. Based upon this initial success current efforts are directed towards optimizing the directional growth treatment and a transformation kinetics analysis. It is expected that samples suitable for mechanical property tests will be available soon. In the Nb-Cr system the microstructural development in alloys bordering the NbCr<sub>2</sub> Laves phase composition has been evaluated following solidification processing. At high undercooling a metastable supersaturated BCC phase is produced for all compositions along with suppression of the NbCr<sub>2</sub> phase. Ternary additions of Ti are soluble in NbCr<sub>2</sub> along the pseudobinary NbCr<sub>2</sub>-TiCr<sub>2</sub> section for C15 Laves phase structures and completely miscible in BCC solutions. Further, relatively modest additions of Ti of a few percent promote the development of supersaturated BCC solutions during the freezing of undercooled liquids. The microstructural options involving two phase BCC +

NbCr<sub>2</sub> structures that have been developed through solidification processing, solid state transformations and alloying have been shown to reduce the generally brittle behavior of the as-cast structures.

# 28067 SYNTHESIS AND STRUCTURAL PROPERTIES OF NEW METALLIC PHASES EXHIBITING NONCRYSTALLOGRAPHIC SYMMETRIES

S. Joseph Poon Gary J. Shiflet University of Virginia

SL: MTL

SC: ETDL, PROP DIR

As a continuation of work on aluminum glasses, efforts are being made to determine which mechanical properties of the new materials can be enhanced. This is carried out by varying the chemical compositions of the alloys and also by controlling the microstructures of the samples. Partially crystallized aluminum-glass samples containing Al noncrystallites are obtained by either quenching or isothermal annealing just below the crystallization temperature. An increase of about  $\frac{1}{3}$  in fracture tensile strength in the Al<sub>90</sub>Fe<sub>5</sub>Gd<sub>5</sub> alloy is observed. The partially crystall red metallic glasses reveal similar fracture behavior to the pure metallic glass. Further studies will be carried out to study the interaction of slip bands with the Al particles in the glassy matrix. The other class of unusual-symmetry materials being studied is the decagonal AlCu-Co quasi-crystal. The studies of stability and atomic-scale structure of decagonal phases are both interesting and fundamental. The key questions to be answered are: Are the decagonal phases thermodynamically stable? Is the Penrose tiling picture realized in the decagonal crystal? A study was made of the stability of the decagonal (d) phase in melt-spun Al<sub>65</sub>Cu<sub>15</sub>Co<sub>20</sub> ribbons, through thermal annealing, electron beam irradiation and recovery experiments using x-ray and HREM measurements. It was found that the *d*-phase is stable from  $\sim$  940°C to at least 550°C. The HREM pictures can be analyzed in terms of tiles selected from the Penrose pattern sets P1 and P3. The observed structures can be described by a random tiling model based on Penrose tiles from set P1 and P3, which is different from conventional random binary tiling. The role of frozen-in phason disorder is found to be important in the stability of the decagonal phase.

# 28368 PRODUCTION AND EVALUATION OF DENSE CERAMIC COMPOUNDS BY COMBUSTION SYNTHESIS AND DYNAMIC COMPACTION

Marc Andre Meyers University of California, San Diego SL: BRL SC: BRL, MTL

Considerable progress was made both with the titanium carbide and diboride compactions. Characterization of TiC produced by SHS and conventional hot pressing by transmission electron microscopy was performed. Quasi-static and dynamic testing of the TiC specimens was also performed. The specimens exhibited a compression strength above 1500 MPa. The addition of controlled amounts of nickel to TiC yielded a decrease in cracking. Systematic experiments are planned.

## 28409 CONCURRENT ENGINEERING FOR COMPOSITE MATERIALS

John Henshaw Dick Wilkins University of Delaware

SL: CRDEC, MTL

SC: CRDEC, MTL, TACOM

The Total Quality Design methodology, established under a previous contract, was further developed and its application demonstrated through its use in composites and RTM in particular. Special emphasis was placed on the integration of the phases of design and manufacturing, through the coupled aspects of materials, processes, and configuration. Conceptual modifications were made to the TQD methodology so as to enable the inclusion of cost metrics, and through the concept of deselection as a rapid discrimination 'ool. Experiments were conducted using this methodology in conjunction with the Taguchi method to show its capabilities in technology development. The TQD methodology is shown to be a facilitation process that enables the efficient development of the product realization process in a critical advanced technology. The RTM process was chosen to demonstrate the use and further development of this methodology as it presents an ideal complex technology. incorporation issues of flow and structure, thus resenting an interwoven set of decisions that need to be taken very early in the conceptual stage of design. The use of TQD allows concurrent engineering principles to be easily and efficiently applied to this technology.

# 28639 MECHANICAL ALLOYING PROCESSING AND APPLICATION TO DEVELOPMENT OF STRUCTURAL MATERIALS

Thomas H. Courtney University of Virginia

SL: ARDEC, MTL

SC: AROE, BWL, PROP DIR

The technical objective of the research involves developing a fundamental understanding of the mechanical alloying (MA) process and its utilization as a precursor for multiphase materials with enhanced properties. The approach will include: (a) MA kinetic studies on alloying insoluble metals (or metals having limited mutual solid solubility) possessing different mechanical characteristics. (b) Investigations into the rate of mechanical alloying based on MA machine characteristics; e.g., the Spex mill v an attritor. (c) Theoretical modeling of the densification behavior of mechanically alloyed powders vis HIPing. (d) Development of amorphous Ni-W alloy powders via MA and the evaluation of properties derived from consolidated alloys of such systems.

# 28883 THERMOPLASTIC AND THERMOSETTING HIGH GLASS TRANSITION TEMPERATURE MATRIX RESINS: SYNTHESIS AND CHARACTERIZATION

James E. McGrath

Virginia Polytechnic Institute and State University

SL: BRADEC, MTL, SC: AROE, MTL NRDEC

The objective of the research will involve the synthesis of new and modified high glass transition temperature thermally and oxidatively stable thermoplastics and thermosets that have potential for utilization in the 600–700°F range. The approach will include (*a*) synthesis of very high glass transition temperature soluble but curable polyimides; (*b*) synthesis of thermoplastic polybenzoxazoles utilizing "3F" monomeric systems; (*c*) synthesis of "reactive" thermosetting maleimide, nadimide, and benzocyclobutene functional poly(arylene ethers), and (*d*) molecular, thermal and mechanical characterization of the new and modified materials to demonstrate fundamental properties.

# 28900 INTELLIGENT SYNTHETIC POLYMERS: A BLEND OF POLYMER SYNTHESIS AND BIOTECHNOLOGY

Paul Calvert University of Arizona SL: NRDEC

SC: AROE, MTL, STRUC DIR

The objective of the research is to synthesize block copolymers having structures similar to globular proteins, to study the relationship between structure and conformation, and to use this information to design polymers which mimic biological membrane channels. Procedures will be established for synthesizing polymers of controlled structure using (a) group transfer polymerization to produce defined helices of acrylic polymers or (b) coupling methacrylate polymers to polypeptide helices by reacting the chloride end group of polymethacrylic acid with the N-terminus of the polypeptide. Molecular modeling and nmr studies will be conducted to calculate steric hindrance and to determine chain conformation and microstructure. Suitable block copolymers will be incorporated into lipid membranes to study transport through such membranes. The results will be used to synthesize membrane channels which are specific for particular chemical species.

## **D.** Physical Behavior

## 22459 NEW APPROACH TO CHEMICALLY INDUCED SILICON OXIDATION

Ralph J. Jaccodine Donald Young Lehigh University SL: ETDL

SC: AROE

The work on the addition of small amounts of impurity to SiO<sub>2</sub> as a means of improving properties has continued with several near term goals. The focus has been in continuing the work on the electrical implications of this process as well as the physical effects brought about by this impurity addition. It has already been shown in the past that fluorine induces large effects on physical properties such as the growth rate and defect injection. One important effort is to quantify the role of fluorine on interface strain and also the strain gradient which is proposed as one of the causes for interface trap generation. It has been demonstrated that fluorine incorporation results in marked oxide stress relaxation. Specifically, it has been observed that there is a rapid stress decrease with increasing NF<sub>3</sub> concentration values up to a point - about 100 ppm - followed by a flattening out of the stress values beyond that point. This stress release implies a decrease in the strain gradient and is thus consistent with a fluorine-induced suppression of interface trap generation according to the bond strain gradient model. The rapid stress

release corresponds to the rapid enhancement in the oxidation rate observed over the same range of  $NF_3$  concentration values. Moreover, the stress release saturation for higher  $NF_3$  concentrations corresponds to the observed saturation of the oxidation kinetics enhancement in that same  $NF_3$  concentration range. SIMS profiling results indicate that these saturation trends correspond to a saturation in the amount of fluorine incorporated in the oxide which indicates that the solid solubility limit of fluorine in the oxide has been reached.

## 23577 DEVELOPMENT OF HIGH EFFICIENCY NONLINEAR OPTICAL MATERIALS

R.S. Feigelson Stanford University

SC: MTL

Program objectives relating to barium borate were two-fold: (a) learning how to grow large, high optical quality crystals by the top-seeded solution growth (TSSG) method at reasonable growth rates; and (b) developing an alternative growth method which will overcome some of the difficulties intrinsic to the TSSG method. Initial work involved studies of potentially suitable solvents which concluded with a decision to use Na<sub>2</sub>O for crystal growth studies. Well over two dozen crystals were grown by the TSSG method. Many were >5 cm in diameter and some as thick as 15 mm. Growth experiments still take upwards of a month because cooling rates have to be held in the 1-2°C/day range to limit the density of inclusions and achieve useful optical quality. Melt viscosity which appears to be in the 100 cp range is still assumed to be partly responsible for this limitation. Most growth experiments were carried out using c-axis seeds in steep temperature gradient furnaces. Growth in the c-direction yields the familiar shallow lens-shaped crystals shown in the BaB<sub>2</sub>O<sub>4</sub> literature. It proved difficult to grow these crystals thicker than  $\sim 15$  mm without suffering interface breakdown. All crystals grown from Na<sub>2</sub>O solutions had varying densities of scattering centers, which is the major problem with BaB<sub>2</sub>O<sub>4</sub>. SEM dispersive analysis carried out on anhydrously polished  $\beta$ -BaB<sub>2</sub>O<sub>4</sub> samples from a number of different boules has confirmed that sodium is a major constituent of the inclusions. A gradually escalating program to explore the growth of lithium borate (LiB<sub>3</sub>O<sub>5</sub>) from solution finally yielded significant positive results. A long term study is currently underway on AgGaSe<sub>2</sub> to elucidate the nature of the optical scattering defects in as-grown crystals.

## 25251 HIGH RESOLUTION STUDY OF DOMAIN WALL-DEFECT INTERACTIONS

Robert C. O'Handley Massachusetts Institute of Technology

SL: ETDL

Work on the SEMPA system has reached the stage where researchers are in a position to begin designing in more detail the most fruitful experiment to probe domain wall-defect interactions. Work is in progress on accumulating a series of prototypical materials characteristic of "good" and "bad" behavior related to single-domain (effectively grain-boundary pinning) or multidomain magnetization reversal. Some of these (FeNdB and FeCr) have already been prepared and characterized by SEM.

## 26287 DEVELOPMENT OF STABLE METALLIZATION SYSTEMS

Marc-A. Nicolet

California Institute of Technology

SL: ETDL SC: ETDL, HDL

Efforts are being made to demonstrate the effectiveness of Ta-Si-N diffusion barriers in examples that are close to real applications as can be done in an academic surrounding. For this purpose, resources were combined with those of two commercial semiconductor device manufacturers. In collaboration with a small manufacturer of discrete devices in La Mirada. CA, it has been shown that an amorphous Ta-Si-N diffusion barrier maintains the electrical characteristics of a Schottky diode with an Al metallization for temperature exposures above the melting point of Al (20 min at 700°C). An additional twist to this experiment was that an amorphous W-Si-N contacting layer was inserted between the diffusion barrier and the *n*-type Si. The presence of W in the contacting layer raises the electron barrier height significantly (to about 630 meV). A corollary of this successful demonstration is that one can now conceive of building stacks of Schottky barriers to produce high voltage rectifiers by a very simple manufacturing process. In collaboration with a large manufacturer of integrated circuits, it was demonstrated that the same Ta-Si-N barrier successfully protects shallow (300 nm deep) Si  $n^+p$  junctions from any deleterious effects by an overlying Cu film for heat treatments as high as 900°C for 30 min. This accomplishment constitutes a major step towards an acceptable Cu metallization technology. Both results are described in papers submitted to IEEE Electron Device Letters.

They demonstrate that Ta-Si-N is by far the best diffusion barrier on record in terms of the thermal stability in Si/Al and Si/Cu metallization.

Reports:

No. 1-5 in previous editions.

- 6. Amorphous Ternary Thin-Film Alloys as Diffusion Barriers in Silicon Metallizations, by E. Kolawa et al., MS.
- 7. Diffusion Barriers in Semiconductor Contact Metallizations, by M-A. Nicolet, MS.
- Thermal Oxidation of Reactively Sputtered Amorphous W<sub>80</sub>N<sub>20</sub> Films, by Quat T. Vu et al., *J Appl Phys* 68,6420(1990). AD A232 167
- Sputtered Ta-Si-N Diffusion Barriers in Cu Metallizations for Si, by E. Kolawa et al., *IEEE Electron Device Let* 12,321(1991). AD A239 583
- Silicon Schottky Barriers and pn Junctions with Highly Stable Aluminum Contact Metallization, by L.E. Halperin et al., *IEEE Electron Device Let* 12,309(1991). AD A239 584
- Amorphous Ternary Ta-Si-N Diffusion Barrier Between Si and Au, by P.J. Pokela et al., J Electrochem Soc 138,2125 (1991). AD A240 279
- 12. Characterization of the Al/Ta-Si-N/Au Metallization, by P.J. Pokela et al., MS, *Thin Sol Films*.
- Thermal Stability and the Failure Mechanism of the Al/W<sub>76</sub> N<sub>24</sub>Au Metallization, by P.J. Pokela et al., MS, *Thin Sol Films*.
- Tantalum Based Diffusion Barriers in Si/Cu VLSI Metallizations, by E. Kolawa et al., MS, J Appl Phys.
- 15. Diffusion of <sup>195</sup>Au in Amorphous W-N Diffusion Barriers, by W. Dorner and H. Mehrer, MS, *Mater Sci and Eng.*
- Arsenic Loss During Palladium Reaction with Bulk and Thin Film Gallium Arsenide, by K. Morishita et al., *Thin Sol Films* 196,85(1991). AD A234 042
- 17. Thermal Oxidation of Amorphous Termary  $Ta_{36}Si_{14}N_{50}$  Thin Films, by P.J. Pokela et al., MS.
- Amorphous Ta-Si-N Diffusion Barriers in Si/Al and Si/Cu Metallizations, by E. Kolawa et al., MS.
- Performance of W<sub>100-x</sub>N<sub>x</sub> Diffusion Barriers Between [Si] and Cu, by P.J. Pokela et al., MS.
- 20. Epitaxial Growth of GaAs by Solid-Phase Transport, by J.S. Chen et al., MS, Appl Phys Let.
- 21. Reliability of High Temperature Metallizations with Amorphous Ternary Diffusion Barriers, by E. Kolawa et al., MS.
- 22. Stress and Resistivity in Reactively Sputtered Amorphous Metallic Ta-Si-N Films, by C.-K. Kwok et al., MS.
- 23. A Comparison Between CVD and Sputtered Tin Diffusion Barriers in Cu and Al Metallizations for Si, by J.S. Reidet al., MS.
- 24. Interfacial Reactions of Ag Thin Films on (001) GaAs, by J.S. Chen et al., MS.
- Tantalum-Based Encapsulants for Thermal Annealing of GaAs, by J.M. Molarius et al., *J Electrochem Soc* 138,834(1991). AD A238 200

## 26601 DIAMOND EPITAXY AND DIAMOND-LIKE COATINGS BY LASER ASSISTED AND ELECTRON BEAM ENHANCED TECHNIQUES

J. Narayan

J. Krishnaswamy

North Carolina State University SC: MICOM, MTL, NVEOC.

TACOM

Work has concentrated on processing and characterization of diamond like carbon (DLC) films in terms of mechanical properties, electrical properties and thermal stability measurements. In addition, in the CVD diamond program, deposition on a variety of substrates was carried out including tungsten carbide, stainless (tool) steel, copper, alumina and quartz. The DLC films were deposited at various substrate temperatures. Resistivity as a function of temperature was measured. The measurements showed two regimes when plotted as a function of inverse temperature. These were a linear region at high temperatures and a curvilinear region at low temperatures with a sharp transition in between. The transition temperature moved towards higher values with increasing  $T_{sub}$ , eventually resulting in a plateau in the resistivity for  $T_{sub} = 500^{\circ}$ C. The activation energy obtained from the plots in the low temperature regime (at T = 100 K) indicated a linear decrease. The low activation energy and the increase in transition temperature are typical of heavily defect/impurity doped crystalline semiconductors. The variation of resistivity of the amorphous DLC films can be ascribed to increasing defect/impurity concentration in the films.

## 26729 SUPERLATTICE DISORDERING AND DIFFUSION MECHANISMS IN GaAs

Teh Y. Tan Ulrich M. Gosele Raphael Tsu Duke University

SC: ETDL, HDL

The diffusion of the substitutional Cr atoms,  $Cr_s$ , in GaAs results from the rapid migration of the interstitial atoms,  $Cr_i$ , and their subsequent changeover to occupy Ga sites, a typical substitutional-interstitial diffusion (SID) process. There are two possible ways for the  $Cr_i - Cr_s$  change-over to occur: the kick-out mechanism in which Ga self-interstitials are involved, and the dissociative mechanism in which Ga vacan-

cies are involved. The Cr<sub>s</sub> in-diffusion profiles are of characteristic shapes indicating the dominance of the kick-out mechanism, while the Cr<sub>s</sub> out-diffusion profiles are error-function shaped, indicating the dominance of the dissociative mechanism. In this study, an integrated SID mechanism, which takes into account both the kick-out and dissociative mechanisms, is used to analyze Cr diffusion results. Going beyond just qualitative consistency, the Cr in- and out-diffusion features in GaAs are explained on a quantitative basis. It is confirmed that the kick-out mechanism dominates Cr in-diffusion while the dissociative mechanism dominates Cr out-diffusion. Parameters used to fit existing experimental results provided quantitative information on the Ga self-interstitial contribution to the Ga self-diffusion coefficient. The values obtained are consistent with those obtained from a study of Zn diffusion in GaAs, and with available experimentally determined Al-Ga interdiffusion coefficients.

#### Reports:

No. 1-4 in previous editions.

- 5. Point Defects, Diffusion Mechanisms, and Superlattice Disordering in GaAs-Based Materials, by T.Y. Tan et al., MS.
- 6. Physical Modeling of Zinc and Beryllium Diffusion in Gallium Arsenide, by S. Yu et al., MS.

## 26883 POLING OF THIN POLYMER FILMS IN ELECTRO-OPTIC APPLICATIONS

Gerald Fuller Stanford University

SC: MICOM, NVEOC

Samples ranging in chromophore concentration from 10 to 100 percent, and of two different spacer lengths, have been investigated. The contribution of the spacer length can be seen most clearly in the lack of the initial fast transients from the response waveforms for the samples having 3-carbon spacers. In these cases, the coupling between the pendant side groups and the polymer backbone has been strengthened, thereby reducing or eliminating the independent side group motion. The effect of NLO chromophore concentration may be seen from the behavior of the samples which range in concentration from 30 to 100 percent monomer substitution. As the concentration increases, the response times likewise increase, and the orientation process progressively approaches the dynamic behavior of the main polymer chains.

# 27548 RELIABILITY AND REPRODUCIBILITY ACHIEVED VIA GRAIN BOUNDARY ENGINEERING OF HIGH PERFORMANCE ELECTRONIC CERAMICS

Vasantha Amarakoon Robert Condrate Robert Snyder Alfred University

SL: ETDL

SC: MTL

Lithium zinc ferrite powders of composition Li<sub>0.3</sub>Zn<sub>0.4</sub>Mn<sub>0.05</sub>Fe<sub>2.25</sub>O<sub>4</sub> were prepared by solid-state synthesis. Liquid-phase borosilicate sintering additives were applied to the ferrite particle surfaces at room temperature via a sol-gel coating technique. Calcined and comminuted ferrite powder was dispersed in methanol with predetermined quantities of tetraethyl orthosilicate and triethyl borate. Hydrofluoric acid was used to catalyze the sol-gel reactions. Amorphous coatings of 10-20 nm thickness were observed on the particle surfaces using diffuse reflectance FTIR spectroscopy. Lithium zinc ferrites Li<sub>0.3</sub>Zn<sub>0.4</sub>Mn<sub>0.05</sub>Fe<sub>2.25</sub>O<sub>4</sub> of 97 percent theoretical density were prepared with alkoxide derived borosilicate sintering additive. A sol-gel technique was used to incorporate the borosilicate phase into the ferrites prior to sintering. The effect of borosilicate composition and additive quantity on microstructural development and densification were reported. D.C. resistivity, dynamic hysteresis, and microwave property data were gathered in terms of processing parameters and resultant microstructures. SEM and TEM analysis of the sintered ferrites indicated liquid phase coalescence and intergranular liquid phase inclusions in some cases. Samples prepared with lower B:Si ratio additive compositions yielded ferrites with properties comparable with industrial samples prepared with Bi<sub>2</sub>O<sub>3</sub>.

# 27605 IONIZED-CLUSTER-BEAM/PARTIALLY-IONIZED-BEAM DEPOSITION OF ELECTRO-OPTICAL AND NONLINEAR OPTICAL ORGANIC MATERIALS AND DEVICE DEVELOPMENT

Toh-Ming Lu Nickolas P. Vlannes John F. McDonald Rensselaer Polytechnic Institute SL: NVEOC SC: ETDL

Progress has been made on partially ionized beam vacuum deposition of thin films of 2-methyl-4-nitroaniline (MNA) and other nonlinear optical (NLO)

materials. Previous efforts to grow MNA at room temperature failed to give reproducible control over film microstructure and orientation, because of the high deposition rate needed to achieve sticking. Accordingly, a substrate cooling unit was installed, and the deposition rate lowered. The vacuum was improved to the low  $10^{-6}$  torr range by using a liquid nitrogen cold trap. Finally, the ionization efficiency of the source was enhanced by a change in filament geometry and power supplies. Films were then grown on a variety of substrates, including Si, Cu. Ag, glass, and SiO<sub>2</sub>. Cooperation with G. Enek led to the growth of prototype poled polymer NLO films. Specifically, N,N-di(2-hydroxyethyl-p-nitroaniline) and p-diisocyanobenzene were codeposited by conventional vapor deposition onto Si and glass substrates. Importantly, the vapor-deposited films show indications of being much denser than melt or solventgrown samples, and evidence no microporosity or pinholes commonly found in spun-on films. In conjunction with the high degree of hydrogen bonding known to pertain in this material, this may improve their resistance to relaxation (undesirable randomization of aligned chromophore moieties after the poling field is removed). Although the present indication (by nuclear magnetic resonance) is that polymerization did not occur thermally on the substrate, experiments are under way involving simultaneous curing and poling of the NLO chromophoics. Polymerization is known to occur thermally during curing of melt-grown polymers, resulting in a backbone-pendant type NLO polyurethane with excellent relaxation resistance. Polymerization by ultraviolet light during film growth is also being pursued.

Reports:

## 27764 FUNDAMENTAL AND APPLIED ASPECTS OF DEFECT ENGINEERING IN GaAs

Jacek Lagowski University of South Florida

SL: ETDL SC: HDL

An experimental facility for "defect engineering study" has been set up. The electronic defect characterization techniques include: fully computerized photoluminescence mapping system; computerized Hall effect system; computerized minority carrier diffusion length and lifetime mapping system; DLTS and photo-DLTS; and FTIR system. The most ini-

<sup>1.</sup> Photonic Multichip Packaging (PMP) Using Electro-Optic Organic Materials and Devices, by John F. McDonald et al., MS.

port result, which may have significant impact on defect monitoring on IC fabrication lines, is the discovery of noncontact deep level transient spectroscopy based on surface photovoltage. The principles of the approach have been derived on a theoretical basis and they are currently being tested in a series of experiments on GaAs and silicon. Using the characterization lab it was possible to obtain for the first time wafer scale maps of the photoluminescence and minority carrier lifetime using independent techniques. This approach should overcome limitations of photoluminescence mapping alone which contains uncertainties due to spatial variations of the nonradiative lifetime. This work will be continued with emphasis on the behavior of stoichiometry-controlled antisite defects. In collaboration with Carnegie Mellon University, deep level defects have been studied in oxygen doped GaAs crystals. The investigation resulted in a positive identification of the DLTS signature of the oxygen-arsenic vacancy defect through correlation with FTIR measurements of LVM line previously correlated with oxygen using the oxygen isotope (<sup>18</sup>O) doped GaAs crystals. The energy level 0.55 eV below the conduction band was identified as due to the "two electron state" of the defect with negative U characteristics.

## 27794 MAGNETIC HARDENING STUDIES AND NOVEL TECHNIQUES FOR PREPARATION OF HIGH PERFORMANCE MAGNETS

George C. Hadjipanayis University of Delaware

SC: ETDL

The effect of carbon, oxygen and nitrogen on the microstructure of Nd-Fe-B magnets has been examined in three sintered magnets containing different amounts of the above elements. Carbon was introduced during the melting process while oxygen and nitrogen were introduced during powder processing. All samples had a coercivity greater than 10 kOe. Scanning electron microscopy data showed that the low oxygen and nitrogen magnet has mainly the  $\alpha$ -Nd phase as a primary Nd-rich phase at the grain boundaries. When oxygen is high, the  $\alpha$ -Nd phase disappears and instead the light gray Nd-oxide appears as a primary Nd-rich phase. When both oxygen and nitrogen contents are high, a Nd-oxide appears as a primary Nd-rich phase instead of  $\alpha$ -Nd or light gray Nd-oxide. The phase change at grain boundaries may be responsible for the corrosion rate of Nd-Fe-B magnets. TEM data reveal that the Nd-oxides inside

the samples are mainly fcc Nd<sub>2</sub>O<sub>3</sub>. The important effect of carbon when combined with an appropriate oxygen content is proved to help segregate inclusions in triple conjunctions and to clean and stabilize the grain boundaries. Ternary compounds of R<sub>2</sub>Fe<sub>17</sub>N<sub>3</sub> (R = Nd, Sm) have been prepared by heat treating tine powders of R<sub>2</sub>Fe<sub>17</sub> alloys in N<sub>2</sub> gas. The Sm Fenitrides were found to retain the Th<sub>2</sub>Zn<sub>17</sub> structure of the original alloys but the increased lattice constants (a and c). The Curie temperature increases strongly with x up to 475°C. In  $Sm_2Fe_{17}N_x$ , the introduction of interstitial nitrogen atoms also leads to an easy axis anisotropy. However, Nd<sub>2</sub>Fe<sub>17</sub>N, still has an easy-plane anisotropy. A coercive field of 6 kOe has been obtained in Sm-Fe-N powders. A systematic investigation of the magnetic and structural properties of as-cast Sm<sub>2</sub>Fe<sub>17</sub>C, compounds with  $0 \le x \le 1.5$ has been made with x-ray diffraction, thermomagnetic analysis and SQUID magnetometry. Crystal structure studies have shown that the ternary carbides form a rhombohedral Th<sub>2</sub>Zn<sub>17</sub> type structure.

## 27846 INDIUM-VACANCY COMPLEXES IN MERCURY CADMIUM TELLURIDE

M.L. Swanson

University of North Carolina at Chapel Hill

SL: NVEOC

A series of experiments were performed in II-VI compounds, using the perturbed angular correlation (PAC) method. This method permits the environment of a radioactive probe nucleus to be studied on an atomic scale, by measuring the electric field gradient (efg) at its nucleus. The efg is determined via the nuclear procession caused by the hyperfine interaction between the probe in nucleus and the local electric field gradient. Results were obtained for  $Cd_{0.96}Zn_{0.04}Te$ .  $Cd_{0.8}Mn_{0.2}Te$  and  $Hg_{0.79}Cd_{0.21}Te$ (MCT) samples. The radioactive In was diffused into bulk samples in evacuated quartz capsules or in capsules containing Cd or Hg. Clear PAC signals were observed after annealing in vacuum. In the case of MCT, quenching from temperatures of 350-400°C caused the production of two dominant PAC signals. having characteristic frequencies 83 MHz and 91 MHz, and asymmetry parameters of 0.08, indicating almost axially symmetric efg's. These signals are attributed to a defect complex consisting of a Hg vacancy trapped by an In atom on a Hg or Cd site. The two slightly different frequencies could be caused by ordering in the lattice. This hypothesis will be tested by measurements on MCT compounds with

#### D. Physical Behavior

different stoichiometries. The PAC signals vanished on annealing in a saturated Hg atmosphere, thus supporting the idea that vacancies are part of the observed complex. This identification of In-vacancy complexes in MCT is the first atomic-scale characterization of point defects in MCT. The interaction of these defects with impurities can now be studied, in order to assess the influence of various impurities on electrical properties. In addition, the PAC data can provide basic information about mobilities of vacancies, self-interstitials and impurities in MCT. Preliminary data indicate a migration energy of 0.6 eV for vacancies.

#### Reports:

- Perturbed Angular Correlation Observation of Vacancy-Indium Atom Defect Complexes in (Hg.Cd)Te, by W.C. Hughes et al., MS.
- Indium-Eg Vacancy Interactions in Hg<sub>1</sub>, Cd<sub>1</sub>Te Measured by Perturbed Angular Correlation, by W.C. Hughes et al., MS, Appl Phys Let.
- 3. PAC and XPS Studies of II-VI Compounds, by M.L. Swanson et al., MS, *Thin Sol Films*.

## 28109 INTRINSIC BISTABLE PHOTONIC MATERIALS BY COPPER COLLOID FORMATION IN SILICA

Robert H. Magruder, III Vanderbilt University

SL: CECOM SC: ETDL

Measurements have been made of the nonlinear index of refraction in fused silica implanted with Pb and Cu ions, using the 100-ps pulses from a cw, model locked, trequency-doubled Nd: YAG laser (532 nm). The nonlinear index is extracted from the far-field radial intensity profile of the beam passing through the sample. The nonlinear refractive index for both materials is very large compared to the nonlinear index for CS<sub>2</sub>, the most commonly used calibration standard. Infrared reflectance spectra of the samples show significant differences between the mode of incorporation of the Cu and Pb in the glass substrate: Whereas the Cu appears in colloids of 2.5 nm diameter, the Pb is incorporated in a Pb-O-Si glassy phase, possibly in small clusters as well. The optical spectra of Bi implanted high purity silica samples subsequently irradiated with 5.0 eV KrF laser light. were found to depend on total implanted dose and on 5 eV photon flux. The effects of 5 eV photons on optical absorption is attributed to changes in the electronic states of Bi-SiO aggregates. It is suggested that these changes are due to increasing number of Bi ions in the aggregates with increasing dose.

## 28141 UNCOMPENSATED GARNETS: A MAGNETIC SEMICONDUCTOR

Philip E. Wigen Ohio State University

SL: MTL SC: ETDL

The objective of this research is to develop a fundamental understanding of the complex dependence between the magnetic, optical and electrical properties of uncompensated, magnetic semiconductor garnets. The magnetic behavior of the films will be determined using vibrating-sample magnetometry and ferro-magnetic resonance, the electrical behavior by measuring film resistivity, and optical properties by monitoring photo-induced absorption/transmission by the films.

# 28146 STUDIES DIRECTED TOWARD NEW AND IMPROVED PERMANENT MAGNET MATERIALS

W.E. Wallace Carnegie--Mellon University

SL: ETDL

Nitrogenation of Y<sub>2</sub>Fe<sub>17</sub>, Gd<sub>2</sub>Fe<sub>17</sub> and Sm<sub>2</sub>(Fe<sub>1-x</sub>  $(Co_y)_{17}$  systems has been investigated in the temperature range from 573 to 873 K. The optimum nitrogen absorbed in the R<sub>2</sub>Fe<sub>17</sub> system is around 2.5 to 2.7 atoms per formula unit. Lattice parameters and volume expansion coefficients all increase with increasing nitrogen content. The  $Sm_2(Co_1Fe_{1-x})_{17}$  (x=0, 0.25 and 0.5) and their nitrides have been made by the thermal chemistry method. The x-ray diffraction patterns were obtained for the parent compounds and their nitrides on random and magnetically aligned powders. Both the hosts and the nitrides exhibit the same rhombohedral Th<sub>2</sub>Zn<sub>17</sub> structure except lattice expansion. The pressure-composition-isotherms measurements were performed. It appears that the Sievert's Law may hold for nitrogen in the R-T systems. Both PrTiFe<sub>11</sub> and NdTiFe<sub>11</sub> alloys were found to be single phase at 1100°C and unstable at lower temperatures. They first decompose into 1-7 and Fe and then transform to Fe<sub>2</sub>Ti, 2-17 and Fe. The substitution of Co for Fe lowers the phase transformation temperatures and stabilizes this phase in a larger temperature range. At high concentrations, the 2-17 and (Fe,Co, Ti) phases were found to coexist with the 1-1-11 phase in the as-cast samples.

# 28538 MODIFIED CHEMICAL VAPOR DEPOSITION FOR THE FABRICATION OF GRADIENT INDEX LENSES AND THE STUDY OF PHOTOREFRACTIVITY IN SOFT GLASSES

#### T.F. Morse Brown University

The objective of this work is to develop modified chemical vapor deposition techniques for the fabrication of gradient index of refraction lenses, rare-earth doped fiber lasers and photorefractive glasses. The approach entails the formation of a fine aerosol of glass-forming liquid organometallic reactants and dopants which are introduced into the flame of a CVD burner. As the burner passes along a rotating substrate tube the reaction products are thermophoretically deposited as sub-micron oxide particles onto the outer surface of the substrate and then sintered into a vitreous, pore-free layer. The composition of the glass can easily be varied by controlling the ratio of the reactant flows. Using this technique the P.I. will explore the feasibility of fabricating: (a) GRIN lenses by preparing glasses with smoothly varying composition gradients, and (b) uniformly doped fibers with a variety of novel ions for laser and laser-induced photorefractive devices.

## 28553 MISFIT DISLOCATIONS AND MAGNETIC ANISOTROPY IN EPITAXIAL FILMS

Carl V. Thompson

R.C. O'Handley Massachusetts Institute of Technology

SC: AROE, BRL, MTL

The objective of the research is to advance the state-of-the-art in controlling misfit dislocation distributions in magnetic epitaxial films and quantify the consequences of the resulting localized stress fields that develop around the dislocation arrays for exploitation in future magnetic thin film materials and devices.

# 28612 NEW SOURCES FOR CHEMICAL BEAM EPITAXY

L.P. Sadwick G.B. Stringfellow University of Utah SL: NVEOC SC: AROE, ETDL, HDL

The objective of this research is to investigate chemical beam epitaxy to identify growth mechanisms and

## E. High Strain Rate Behavior of Materials

develop new gas sources for the production of As, P and Sb-based ternary and quaternary III/V semiconductor materials for device applications. Investigations on the growth of III–V semiconductor materials by chemical beam epitaxy will be conducted using new gas sources. The research will concentrate on developing CBEI techniques and identifying processing conditions for high quality semiconductor materials. An informal collaboration with a commercial organization will fabricate high electron-mobility transistors and heterojunction bipolar transistors using the best materials grown under the program.

## E. High Strain Rate Behavior of Materials

## 24102 PENETRATION MECHANICS OF FIBER LAMINATE COMPOSITES

Stephan Bless University of Dayton

SL: MTL

SC: AROE, BRL, BWL, TACOM

Experimental techniques were developed to measure the deceleration of projectiles as they penetrate composite targets. Experiments were conducted with flat, hemispherical, and conical nose penetrators striking S2-glass GRP. Ballistic limits were measured. Four penetration regimes were identified: shock, cratering, cavity expansion, and membrane. The energy absorbed by the target during these various stages was determined. The shock stage was only important for blunt projectiles. Cratering and membrane stages were important for round and blunt projectiles. Cavity expansion was the dominant penetration mode for cone projectiles.

Reports:

No. 1 in previous edition.

2. Penetration Through Glass-Reinforced Phenolic, by Stephan J. Bless et al., MS.

# 26169 DETERMINATION OF THE DYNAMIC UNLOAD/RELOAD CHARACTERISTICS OF CERAMICS

Stephan Bless	
University of Dayton	
SL: BRL, MTL	SC: AROE

Techniques were developed for measuring the unloading behavior of ceramics, both the principal and trans-

## F. Miscellaneous

verse stresses. Experiments were conducted on TiB<sub>2</sub> and AlN. TiB<sub>2</sub> was found to exhibit remarkable pressure hardening, almost a doubling of the stress deviator as the stress was increased from  $1 \times to 2 \times$ the HEL. AlN has a constant stress deviator, but higher than the HEL value. Measurement of the transverse stress allowed researchers to compute the dynamic hydrostat of AlN. It was substantially softer than the extrapolated hydrostat using finite strain theory. This seems to indicate a phase change in this material. Examination of failure waves in plate impact experiments showed strong evidence for slow failure waves propagating behind the "plastic" wave front in glass.

#### Reports:

No. 1-3 in previous editions.

- 4. Applying Steinberg's Model to the Hugoniot Elastic Limit of Porous Boron Carbide Specimens, by N.S. Brar et al., *J Appl Phys* 69,7890(1991).
- Dynamic High-Pressure Properties of AlN Ceramic as Determined by Flyer Plate Impact, by Z. Rosenberg et al., J Appl Phys 70,167(1991).
- 6. Failure Waves in Glass, by Stephan J. Bless et al., MS, J Am Ceram Soc.

## 26173 TESTS FOR DETERMINING FAILURE CRITERIA OF CERAMICS UNDER BALLISTIC IMPACT

D.A. Shockey R.W. Klopp

D.R. Curran

**SRI International** 

SL: BRL, MTL SC: BRL

Symmetric pressure/shear experiments were performed on Coors AD-85 and AD-995 aluminas. A laser Doppler velocimeter system was used to monitor the transverse velocity at the free surface of the anvils. A model combining rate dependence, Mohr-Coulomb frictional behavior, and dilatancy will be used to analyze the velocity records and determine values for the material properties controlling ballistic performance. Experiments are planned for AD-85, AD-995, TiB<sub>2</sub>AIN, and B<sub>4</sub>C. Experiments have been designed to investigate how ceramics erode long rod penetrators. In these experiments,  $\frac{1}{4}$ -scale tungsten-and uraniumalloy rods will be shot into highly confined ceramic targets.

#### Reports:

No. 1 in previous edition.

#### **VI Metallurgy and Materials Science**

# 28272 LOCALIZATION IN TUNGSTEN HEAVY ALLOYS SUBJECTED TO SHEARING DEFORMATIONS UNDER SUPERIMPOSED HIGH PRESSURES

K.T. Ramesh

The Johns Hopkins University

SL: ARDEC, BRL SC: AROE

An investigation will be made of the mechanical behavior of tungsten heavy alloys subjected to extremely high rates of shear and very high pressures to assess the effect of superimposed hydrostatic pressure on the shear localization in alloys of interest to the design of kinetic energy penetrators.

## 28575 DYNAMIC MATERIAL RESPONSE FOR MODEL DEVELOPMENT

R.J. Clifton Brown University

SL: BRL SC: BRL

The research objective is to investigate the mechanisms of damage nucleation and evolution in brittle and ductile materials of potential importance in impact and/or energy absorption applications with emphasis placed on the issues of dynamic shearing resistance of ceramics, high rate response and stability of shearing deformation of tungsten heavy alloys, and mechanisms of dynamic rupture of ductile materials.

# F. Miscellaneous

## 26246 CRYSTAL CHEMISTRY OF CERAMIC/MINERAL SYSTEMS

Robert R. Reeber University of North Carolina at C

University of North Carolina at Chapel Hill

Thermal expansion is an important property of ceramics and industrial minerals. As more complex composite materials systems evolve the interpretation and understanding of the influence of thermal and residual stresses in these materials on their mechanical properties makes it critical to have accurate values of thermal expansion of each component. In earlier work with germanium, silicon, and a variety of sphalerite-structure type II–VI and II–V compounds it has been shown that thermal expansion can be quantitatively represented in terms of a multi-Einstein frequency lattice vibration distribution with appropriate least-squares determined coefficients. In

Analysis of Tilt in the High-Strain-Rate Pressure-Shear Plate Impact Experiment, by Richard W. Klopp and Rodney J. Clifton, J Appl Phys 67,7171(1990). AD A228 060

this work a broad selection of divergent silicon carbide thermal expansion data is fitted and assessed within the constraints of a semiempirical equation of state.

#### Reports:

No. 1 in previous edition.

2. Tribological Properties of Nitrogen Implanted Boron Carbide, by Robert R. Reeber et al., MS.

## 26647 POSITRON ANNIHILATION STUDIES OF INTERPENETRATING POLYMER NETWORKS

Andrew Crowson Phillip L. Jones Duke University

Experimentation includes the use of Positron Annihilation Lifetime Spectroscopy (PALS) to obtain isothermal positron data on thermotropic liquid crystal polymer composites (TLCP's). PALS is currently being used in conjunction with various other characterization tools (FTIR spectroscopy and thermal analysis) to evaluate free volume behavior and molecular structure as they relate to mechanical properties in thermoplastic composites. Injection molded samples of the thermoplastic composites ULTEM (polyetherimide)/VECTRA (copolyester of hydroxybenzoic acid and hydroxynaphthoic acid) and ULTEM/HX4000 (liquid crystal polymer (LCP) based on terephthalic acid, hydroquinone, and phenylhydroquinone) were obtained from D.G. Baird at VPI. The sample group included: 100 percent thermoplastic ULTEM, 100 percent LCP VECTRA, 100 percent LCP HX4000, and 30, 50, 70, and 90 percent composites of each system. PALS data was obtained on each of the above sample groups. This procedure yielded an increasing intensity of orthopositronium (I<sub>3</sub>) with increasing concentration of LCP for both systems. D.G. Baird has reported a partial miscibility of the ULTEM/HX4000 system based on dynamic torsion analysis and DSC data. This miscibility may be the factor causing the different trends in the positron data. Baird also indicated that the moduli of the ULTEM/VECTRA systems experience a negative deviation from the rule of mixtures while the ULTEM/ HX4000 systems show a positive deviation. This discrepancy in trends again may be connected to the discrepancy in positron results. A sample of the 90 percent HX4000 composite was obtained and analyzed. The positron data did not reveal the trend shown in previous mechanical data, where the modulus of this composite is actually grater than the pure TLCP. Currently, a study of the different flow regions experienced in an injection molded sample is being made.

## 27364 SHOCK WAVE INTERACTIONS WITH EXOTHERMIC MIXTURES

K.R. lyer

North Carolina State University

SL: MTL

This study has seen progress in the time resolved measurement of pressure during the shock wave's passage and the use of ideal alloy Hugoniots to explain and correct these measurements. Originally the manganin gauges used to measure pressure were epoxied to aluminum 6061 backing disks with their lead wires run from the side of the recovery fixture. This arrangement frequently failed before the shock wave should have reached the gauge so the gauges were mounted to Lexan disks with the lead wires run straight through the back of the disks and the momentum trap. This arrangement enabled the gauge to survive through the duration of the shock wave but the Lexan changed phase under the extreme pressure and temperature rises common of these conditions resulting in an erroneous pressure reading. So once again the aluminum was used as a backing material except the leads were run straight back through the backing disk as in the Lexan. With this arrangement many shots have been performed successfully with complete gauge readings throughout the duration of the shock wave's passage. Next samples of Ti and Al powder were mixed stoichiometrically for a Ti + 3Al -> TiAl3 reaction. These samples were prepared in retainer rings by green compaction to 55 percent of the solid density and backed by two aluminum 6061 disks with a manganin gauge sandwiched between them. A steel cover disk was placed over the front of each sample and a trigger was attached to this to start the Wheatstone bridge when an impact occurred. This arrangement was then placed inside the previously described recovery fixture and impacted with a steel flyer plate traveling at a known velocity. The gauges allowed pressure measurements during the passage of the shock wave.

## 27810 CHARACTERIZATION OF DIAMOND FILM GROWTH IN A COMBUSTION FLAME

John T. Prater Jeffrey T. Glass North Carolina State University

SL: MTL SC: ETDL, MICOM

## F. Miscellaneous

### VI Metallurgy and Materials Science

The combustion synthesis apparatus is in full operation. It is possible to reproduce the baseline growth conditions established by the Nippon group. The optimum parameters for depositing high quality diamond are: substrate temperature 500-750°C, O<sub>2</sub>C<sub>2</sub>H<sub>2</sub> ratio of 0.95-0.98, and a growth rate of about 30  $\mu$ m/h. While the growth apparatus was being assembled researchers were able to begin detailed characterization of the defect structures of baseline films with TEM. A strong substrate temperature dependence was observed. At substrate temperatures below 500°C a high density of microtwinning was observed. Above 600°C the microtwinning was no longer observed and the overall defect density was drastically reduced. Stacking faults and dislocations were present, but in much lower concentrations. These findings upset the conventional wisdom on the growth of defect-free diamond films. Prior to these studies it had been felt that highly defective films would result under growth conditions which favor growth on (111) surfaces. Under these conditions simple stacking sequence errors produce twin boundaries. Deposition parameters that favored preferred growth on (100) surfaces were generally believed to be the only workable approach for preparing in-situ defect-free layers. However, these studies demonstrated that defect-free films could be prepared on (111) surfaces by depositing at higher temperatures where surface diffusion is sufficient to permit annealing of the microtwin defects.

# 28620 SCIENTIFIC ASSESSMENT OF SELF-ASSEMBLING AND BIOMOLECULAR MATERIALS

Ronald D. Taylor National Academy of Sciences SL: ARO SC: AM

SC: AMBRDL, CRDEC, NRDEC

Findings and recommendations of the Panel on Biomolecular Materials will be presented in a published NRC report following the completion of the study.

# **VII GEOSCIENCES**

## A. Geomorphology/Hydrology

# 26902 DIGITAL ELEVATION MAPS AND WEATHER RADAR IN FLOOD FORECASTING: THE ARNO RIVER BASIN AS A CASE STUDY

Rafael L. Bras

Massachusetts Institute of Technology

SL: WES SC: CRREL

Efforts were directed towards testing and calibration of the Arno River distributed rainfall model and generating a computer animation of river basin evolution. Additional work was done in modifying the basin evolution model to include a "saturation-frombelow" runoff production mechanism. The distributed rainfall-runoff model of the Arno was tested extensively with data from the Sieve sub-basin. Calibration and overall results are quite satisfactory. A report was written and published detailing the development of the concept and result up-to-date. The computer animation of a basin evolution model was completed. Additional work was performed with the basin evolution model. The efforts were directed at studying the impact of a different runoff production mechanism. In particular, it was found that a saturation from below runoff production mechanism resulted in river networks and landscapes similar to those resulting from Hortonian schemes. Finally, a small exercise on the simulation of river networks was carried out to test the reasonableness of an energy expenditure hypothesis of channel development.

#### Reports:

- A Channel Network Evolution Model with Subsurface Saturation Mechanism and Analysis of the Chaotic Behavior of the Model, by Ede J. Ijjasz-Vasquez and Rafael L. Bras, TR, Sep 90, 135 pp. AD A231 608
- A Distributed, Physically-Based, Rainfall-Runoff Model Incorporating Topography for Real-Time Flood Forecasting, by Mariza C. Cabral et al., TR, Oct 90, 220 pp. AD A231 630
- The Relationship Between Catchment and Hillslope Scales: Implications of a Catchment Evolution Model, by Garry Willgoose et al., MS, J Geomorphology.

# 26972 MULTIPERIODIC WAVES IN SHALLOW WATER

Joseph Hammack University of Florida

SL: WES

Experimental measurements were compared with a symmetric subset of the KP solutions of genus 2, and found in excellent agreement. Procedures are being developed for comparing experimental measurements with asymmetric solutions of genus 2. When symmetric genus 2 waves are normally incident on a wide planar beach, they quickly generate a periodic array of rip currents - narrow, intense, seaward flows that have a profound effect on the distribution of coastal sediments, pollutants, and other materials. KP theory allows one to predict the long-shore spacing of the rip currents and, for the first time, to predict a bound on the width of the currents. When two-dimensional waves are obliquely incident onto a reflecting barrier, nonlinear interactions between the incident and reflected waves can produce a phenomenon of Mach reflections. Mach reflections of periodic water waves are modeled well by symmetric KP solutions of genus 2. This allows one to predict many features of the flow in the vicinity of the reflecting barrier that differ radically from models that assume linear reflection.

#### Reports:

 A Note on the Generation and Narrowness of Periodic Rip Currents, by Joe Hammack et al., J Geophys Res 96,4909(1991). AD A238 816

# 27401 COMPUTER SIMULATION OF SUB-AQUEOUS SEDIMENT TRANSPORT

Peter K. Haff

Duke University

SL: CRREL, WES

A microscopic two-dimensional bedload transport model was developed. It displays many of the characteristics of natural sub-aqueous sediment systems.

## A. Geomorphology/Hydrology

By solving the Newtonian equations of motion for each particle in the system, the dynamics of small bed patches involving from one to several hundred particles can be followed in detail. The fluid is treated at present simply as a rigid "slab" of material at the bed surface. A fixed shear stress applied to the "top" of the slab sets it in motion, and the relative motion of slab and "embedded" particles causes a drag force to be exerted on the particles. A counter-drag force in turn acts on the fluid slab. This system of fluid plus bed particles develops into a time-averaged equilibrium state, although over any short period of time the forces are unbalanced as particles come to rest or are accelerated from rest. Threshold shear-stresses, particle hop-height and particle hop-lengths are of the same order of magnitude as those observed experimentally. Mean mass fluxes computed numerically share a dependence on shear stress similar to that found in many semi-empirical formulas. Sensitivity studies have been performed as a function of particle elasticity, friction coefficient, fluid slab placement, integration time steps and coefficient of restitution, showing that the average behavior of the bed is relatively insensitive to these quantities over a large range of values. Techniques for quantifying the unsheared bed surface topography has been developed.

# 27471 SEMI-AFFINE TOPOGRAPHY AS A FRAMEWORK FOR SUBSURFACE FLOW AND SOIL MOISTURE MODELING IN RUGGED TERRAIN

Christopher J. Duffy The Pennsylvania State University

## SC: ETL

The very first effort in this research involved implementing tools for spatial analysis of digital elevation models, and time series analysis of hydrologic signals. The numerical analysis package known as MATLAB was used to develop software for estimating the spectrum of 2D and 1D series, and to estimate the fractal dimension of the data. The spectrum of power law processes has a characteristic slag. from which the fractal dimension may be estimated. The spectral approach is one way to compare the texture of the terrain of the Colorado Plateau of eastern Utah, and the Appalachian Plateau of western Pennsylvania. FEMWATER, a 2D and 3D finite element solver by G. Yeh, has been implemented for saturated-unsaturated flow. Much effort has gone into grid design for minimizing numerical errors and the computation time associated with this strongly nonlinear problem. A

### **VII Geosciences**

color graphics package is being used to create high resolution color images, and animate these images for the case of dynamic processes. In previous work at Reynolds Creek, it was found that the storage of water on steep, permeable hillslopes in volcanic terrain indicated a nonlinear relation between storage and baseflow, and furthermore that the process was hysteretic or that baseflow is not a unique function of storage. Preliminary analysis indicates that nonlinear behavior is also occurring in the Mahontango watershed of east-central Pennsylvania, which is in the Ridge and Valley Physiographic province.

#### Reports:

1. Spectral Analysis of Annual Time Series of Mountain Precipitation, by Christopher J. Duffy et al., *Hydraulics/Hydrology* of Arid Lands, 1990, 573. AD A232 130

## 27772 FUNDAMENTAL STUDIES ON HYDROLOGY, HYDRAULICS AND GEOMETRY OF RIVER NETWORKS

V.K. Gupta

University of Colorado

SC: WES

Recent discoveries regarding the presence of scaling invariance properties, the spatial structures of river flows, e.g., peak flows, and altitudinal geometry of river networks are requiring major new efforts on both theoretical and empirical sides to solve the problem of prediction from ungaged basins.

Reports:

- No. 1-4 in previous editions.
- 5. On Network Structure Function Computations, by Edward C. Waymire, MS.
- Spatial Uniformity of Power and the Altitudinal Geometry of River Networks, by Vivek Kapoor, Water Resources Res 26,2303(1990).

## 28504 SCALE AND HETEROGENEITY EFFECTS ON FLOW AND TRANSPORT IN MULTIPHASE SYSTEMS

Cass T. Miller

University of North Carolina at Chapel Hill

SL: CRREL, WES SC: ATHAMA

The objective of this research is to examine those systems, such as aqueous-solid and vapor-aqueous phase couples, where rates of interphase mass transfer may be slow enough to preclude the local equilibrium assumption, including phenomena that are effects of system dimensionality, measurement scale, and media heterogeneity on fluid flow and contaminant transport in multiphase systems.

## 28717 INTERACTION OF AEROSOLS AND DROPLETS WITH ELECTROMAGNETIC RADIATION

Petr Chylek State University of New York at Albany

SL: ASL, CRDEC

The research objective is to determine the effects of "dirty" aerosols on the absorption and propagation of optical wavelengths. The effects on aerosols containing small amounts of absorbing materials will be determined from experiments (some already performed) and from numerical solutions (Mie Theory). These data will be analyzed in terms of the suppression of resonance and, in the absence of such suppression, the potential for significantly increased absorption due to the internal field resonances of the particles.

## **B.** Snow, Ice and Frozen Ground

## 26031 FATIGUE CRACK PROPAGATION IN FRESHWATER ICE

Wilfred A. Nixon University of Iowa

SL: CRREL

Measurements of the light reflected from 1D dielectric surfaces (M261  $a,\sigma = 1.4 \mu m$ ,  $a = 8.0 \mu m$ ,  $\lambda =$ 0.6328 µm) with centers of symmetry have been accomplished. The experimental results have been compared with the Kirchhoff approximation. Following work on scattering from random symmetric surfaces, consideration was given to the problem of scattering two coherent beams from such surfaces. It was found analytically, numerically, and experimentally that for two angles of incidence, say  $\phi_1$  and  $\phi_2$ , there can be three peaks in the scattering curve at the angles of scattering  $\phi_s = \phi_2$  and  $(\phi_1 + \phi_2)/2$ . Consideration of enhanced backscattering can be critically important in developing laser radar signatures. This is illustrated by the comparison of the two signature models of the same missile -- one developed using measured bidirectional reflectance data at 1° away from the retrodirection, and the other developed from monostatic data in a true retrodirection. The problem of scattering from a surface nearly perpendicular to a mirror has been addressed both theoretically and experimentally. This problem is closely related to the previously considered one of scattering from symmetric surfaces, and due to its simplicity, can be of great help in elucidating the physical mechanisms giving rise to the enhancement in

the backscattering direction. It has been shown that the enhancement has a width of order  $\lambda = 0.53 \ \mu m$ was observed in the vicinity of the backscattering direction. So far, the results show no indication of any enhancement.

#### Reports:

 Crack Opening and Propagation in S2 Freshwater Ice, by L.J. Weber and W.A. Nixon, MS.

## 26260 STRENGTH-DEFORMATION BEHAVIOR OF FROZEN SOILS: PHYSICAL MECHANISMS

Charles C. Ladd

S. Shyam Sunder

John T. Germaine

Massachusetts Institute of Technology

SL: CRREL SC: WES

The research focus has been to complete the frozen Manchester Fine Sand (MFS) testing program and to continue with the testing of unfrozen MFS. Frozen Manchester Fine Sand Testing Program: Sixty seven triaxial compression tests on frozen MFS have been completed to date. Analysis of these results has lead to interesting correlations between confining pressure, relative density and strain rate. Unfrozen Manchester Fine Sand Testing Program: A total of 41 unfrozen MFS tests have been performed to date. The techniques for preparation and testing of unfrozen MFS have been continually evaluated and improved. Seventeen specimens are prepared by raining and vibration into a specially designed split-mold which rests directly on the triaxial cell base. Twentyfour specimens have been prepared using MSP. Thirtynine isotropically consolidated undrained compression tests and two isotropically consolidated drained compression tests have been performed.

# 26281 A FIELD INVESTIGATION OF WATER AND SALT MOVEMENT IN PERMAFROST AND THE ACTIVE LAYER

T.E. Osterkamp

J.P. Gosink

University of Alaska Geophysical Institute

SL: CRREL

Measurements of the profiles of temperature, total water content, unfrozen water content, bulk electrical conductivity, and electrical conductivity of the soil solution were continued in spring and into summer. The frequency of these measurements was increased since previous results seem to indicate that the flow processes were faster than believed. Sites were buried under more than four feet of snow and

## C. Other (Terrestrial)

would have been disturbed by digging them out. Access to the sites was also a problem. Since there is little movement of heat or water during winter it was decided to wait until spring to continue the measurements. One soil tube was left in the ground in the semi-controlled field freezing experiment. This tube was to be removed after it freezes in the winter of 1991–1992. A portable thermal conductivity probe for field measurements has been completed, tested, calibrated, and used to make field measurements.

## 27316 TOWARD A MOLECULAR-SCALE UNDERSTANDING OF FROST HEAVING: PHASE 1

John H. Cushman Purdue University

SC: CRREL

One publication has resulted from this project during this research period. This work describes a new efficient method for computing the chemical potential and free energy, state variables of significant importance to this project. The basic idea is to correct the underestimate obtained by the particle removal method. The new technique has been tested on a Lennard-Jones fluid at high density where standard methods have difficulties. Preliminary results are very encouraging. Current research efforts involve the study of dipolar fluids in slit pores using both microcanonical molecular dynamics and grandcanonical Monte Carlo methods. Dipolar fluids are being investigated as a possible elementary model for the more complex system. In many cases, simple models quite often provide qualitative estimates of the behavior of more complex systems.

Reports:

## 27482 THE DUCTILE TO BRITTLE TRANSITION IN POLYCRYSTALLINE ICE UNDER COMPRESSION

Erland M. Schulson Dartmouth College

SL: CRREL

Prior to initiating the work experiments had established that wing cracks develop in both columnar and granular ice. This result is significant because, when coupled with the effects of grain size, temperature and strain rate on strength, it supports the view that the classical frictional crack sliding-wing crack mechanism plays a major role in the brittle compres-

#### **VII Geosciences**

sive failure of ice. It could be argued, however, that the wings were artifacts, formed perhaps during unloading, for they were seen in specimens which had been either pulse loaded or loaded to failure. Observations were thus made using high-speed photography (1000 frames/s) of over a dozen coarsely grained (8 mm col. dia.) specimens of columnar ice compressed monotonically and uniaxially (orthogonal to the columns) at -10 and  $-20^{\circ}$ C at  $2 \times 10^{-2}$  $s^{-1}$ . To determine whether wing cracks form upon loading at lower strain rates, experiments were performed on specimens of the same kind of ice compressed at  $-10^{\circ}$ C at  $3 \times 10^{-5}$ s<sup>-1</sup>. The specimens were photographed at regular intervals during each test. In these cases most of the cracks formed just around the peak and none was seen to form along the plateau. Some wing cracks could be identified, but they formed a smaller fraction of the total number than in the brittle regime. The length of the axial extension was smaller and, unlike the case for brittle behavior, the cracks appeared to form independently of each other. The net impression, albeit tentative, is that within the ductile regime at a strain rate just below the ductile-to-brittle transition wing cracks form, but do not lengthen.

# 28599 A BOOK AND A SERIES OF MONOGRAPHS ON ICE PHYSICS

Victor E Petrenko Dartmouth College

SL: CRREL

The objective is to produce a series of monographs on Ice Physics, including all important topics which will then be unified as a textbook. Experimental facts, physical ideas and theories will be strongly organized and bound cohesively. Working at Dartmouth, Professor Petrenko will have the benefit of interacting with a substantial community of ice scientists, both at Dartmouth and at CRREL.

## C. Other (Terrestrial)

## 24381 HORIZONTAL STRESS IN SITU BY CONE PENETROMETER AND RELATED STUDIES

James K. Mitchell

University of California, Berkeley

SL: WES SC: CRREL

A New Computational Approach to the Chemical Potential, by K.-K. Han et al., J Chem Phys 93,5167(1990). AD A232 494

#### **VII Geosciences**

The primary objective of this research is to develop a reliable means for measurement or estimation of the in-situ geostatic lateral stress from the results of cone penetration and other in-situ test. The research has included laboratory chamber test, field tests, and analytical studies. In addition, two related studies that are concerned with aging of sand and its effect on properties, and the direct prediction of liquefaction resistance using cone penetration test measurements are a part of this project. Preparation of papers based on a previously completed Ph.D. dissertation has been in progress. In one, a new, simpler method for estimation of in-situ lateral pressure based on CPT sleeve friction is described and validated. In the other, the theory for prediction of cone penetration resistance using cavity expansion theory is developed and compared with measured values. Experimental research on aging phenomena in sands is now underway. Initially, small amplitude shear wave velocity measurements were used as a nondestructive indicator of aging of sand samples confined under constant pressure. No timedependent increases in stiffness with time were measured, indicating either that aging processes were not active in the sand being tested or the means for measurement were inadequate. A number of field CPT tests have been done at several sites where liquefaction was observed during the Loma Prieta earthquake of October 17, 1989. These data, as well as the results of a field sampling and testing program yet to be done at these sites, will be used to further evaluate the method for liquefaction potential assessment that was developed as a part of this project.

## Reports:

- 1. Testing with Lateral Stress Cone, Special Dilatometer and Stepped Blade at Three Sites in Drammen, by Tahir Masood et al., TR, Feb 90, 146 pp.
- Assessment of Eiguefaction Potential by Cone Penetration Resistance, by James K. Mitchell and Dar-Jen Tseng, Proc of the H. B. Seed Memorial Symposium, 1990, 335.
- Prediction of Cone Penetration Resistance and Its Application to Liquefaction Assessment, by Dar-Jen Tseng, PhD Thesis, 1989, 325 pp.
- 4. Determination of Lateral Earth Pressure in Soils by In-Situ Measurement, by Tahir Masood, PhD Thesis, 1990, 471 pp.
- Lateral Stresses on Displacement Penetrometers, by Richard Craig Sisson, PhD Thesis, 1990, 342 pp.

## 24713 WAVE PROPAGATION AND SCATTERING IN DENSE GEOPHYSICAL MEDIA

Akira Ishimaru Rubens Sigelmann University of Washington

SL: CECOM

SC: ASL, CRDEC, WES

Millimeter Wave Experiment: In the past, the transmitter and receiver were placed in two different planes which were slightly displaced so that the receiver and transmitter were not overlapped in the backscattering direction. This setup was changed so that the transmitter and receiver were in the same plane, even though data cannot be taken within 8 degrees of the back direction. The new experimental data are taken and the results show closer agreement between the experimental data and the numerical calculations. The discrepancies observed previously for TM waves are now eliminated. Additional data are taken on the scattered intensity correlations and their relationship with the surface correlation distance is being investigated. Work is in progress to construct two-dimensional rough surfaces and to conduct experiments which include the polarization effects. Optical Experiment: Experiments on optical scattering from leaves are being extended to scattering by soils and sand. Sand and clay with different size distributions were obtained. The experimental results will then be compared with radiative transfer calculations. The backscattering enhancement will be studied by using a recently reported focusing arrangement. The vector radiative transfer solutions with rough interfaces were obtained and computer codes are now being tested. Theoretical Studies: A theory developed previously using the second-order Kirchhoff approximations with shadowing functions is now being extended to two-dimensional surfaces with complete polarization characteristics. Also being studied is the modified smoothing method for twodimensional surfaces. Efforts are being made to unify the above two theories.

#### Reports:

No. 1-8 in previous editions.

- 9. Effect of a Random Medium on Microwave Imaging, by Michael J. Sierman et al., *IEEE Trans on Ant and Prop* 38,763(1990). AD A226 569
- Scattering and Depolarization of Waves Incident Upon a Slab of Random Medium with Refractive Index Different From That of the Surrounding Media, by Qinglin Ma et al., *Radio* Sci 25,419(1990). AD A232 533
- Scattering From Very Rough Surfaces Based on the Modified Second-Order Kirchhoff Approximation with Angular and Propagation Shadowing, by Akira Ishimaru and Jei S. Chen, J Acoust Soc Am 88,1877(1990). AD A232 534
- Numerical Simulation of the Second-Order Kirchhoff Approximation From Very Rough Surfaces and a Study of Backscattering Enhancement, by Jei S. Chen and Akira Ishimaru, J Acoust Soc Am 88,1846(1990). AD A232 164
- Transmission, Reflection, and Depolarization of an Optical Wave For a Single Leaf, by Qinglin Ma et al., *IEEE Trans on Geosci and Remote Sensing* 28,865(1990). AD A232 166

## D. Propagation

- Particle-Size Distribution Determination Using Optical Sensing and Neural Networks, by Akira Ishimaru et al., Opt Let 15,1221(1990). AD A238 515
- Scattering From Very Rough Metallic and Dielectric Surfaces: A Theory Based on the Modified Kirchhoff Approximation, by Akira Ishimaru and Jei Shuan Chen, Waves in Random Media 1,21(1991). AD A238 539

## **D.** Propagation

## 25730 NORMALIZED RADAR CROSS SECTION OF NATURAL SURFACES AT MILLIMETER WAVELENGTHS

Robert E. McIntosh

University of Massachusetts

SL: ASL, CECOM, SC: BRL, HDL, WES PM SMOKE

A new multipolarization antenna was installed in the 225 GHz transmitter allowing more accurate calibration of the radar. Polarimetric measurements of snow began with incident angles ranging from 25° to 80°. Polarimetric measurements of trees, in conjunction with the 95 GHz polarimeter, were to commence in April, 1991. The 95 GHz polarimeter was extensively modified during the latter half of 1990, and polarimetric measurements of snow have recently begun with that radar. It also was to be refurbished with a multiple polarization transmitter antenna at the end of the snow season.

# 26224 MILLIMETER-WAVE MEASUREMENT AND MODELING OF THE SCATTERING PHASE FUNCTION OF INHOMOGENEOUS MEDIA

Fawwaz T. Ulaby University of Michigan

> SL: BRL, CECOM, MTL, SC: ASL, CRREL, HDL, PM SMOKE PM SMOKE

Two different kinds of trees were measured with a newly developed polarimetric radar at 35 and 94 GHz. The system is based on the COR technique and is capable of measuring the Mueller matrix directly. The degree of polarization phase statistics, and polarization signatures are presented in this paper. The results show that the degree of polarization is sensitive to the radar frequencies and tree types. An extensive radar clutter database was generated by the University of Michigan's millimeter-wave mobile polarimetric system during the past few years. The

## **VII Geosciences**

data base includes millimeter-wave observations of snow, trees, vegetation, and soil and road surfaces at 35, 94, and 140 GHz. The radar measurements were often augmented with close-up observations of the targets including such measurement as water contents and surface roughness, where appropriate. For each data set, a summary of these observations and photographs of the target scene are provided. The millimeter-wave system consists of truck-mounted radars capable of making observations from a 20m high platform at incidence angles between 0 and 70 degrees. The receiver which is based on the vector network analyzer has 1 to 2 GHz bandwidth. The radar center frequencies are 35, 94, 140, and 215 GHz.

#### Reports:

No. 1 in previous edition.

- Millimeter-Wave Radar Scattering from Terrain: Data Handbook Version 2, by Fawwaz T. Ulaby and Thomas F. Haddock, TR, Sep 90, 206 pp. AD A228 392
- 3. Clutter Measurements by Millimeter-Wave Radars, by Yasuo Kuga et al., MS.

## 26384 PROPAGATION AND SCATTERING OF MICROWAVES AND MILLIMETER WAVES IN SNOW BASED ON DENSE RANDOM MEDIA THEORY

Leung Tsang

University of Washington

SC: CECOM, CRREL, MICOM, PM SMOKE

Complete polarimetric signatures of a canopy of dielectric cylinders overlying a homogeneous half space are studied with the first and second order solutions of the vector radiative transfer theory. The vector radiative transfer equations contain a general nondiagonal extinction matrix and a phase matrix. The energy conservation issue is addressed by calculating the elements of the extinction matrix and the elements of the phase matrix in a manner that is consistent with energy conservation. Two methods are used. In the first method, the surface fields and ti e internal fields of the dielectric cylinder are calculated by using the fields of that of an infinite cylinder. The phase matrix is calculated and the extinction matrix is calculated by summing the absorption and scattering to ensure energy conservation. In the second method, the method of moments is used to calculate the elements of the the extinction and phase matrices. The Mueller matrix based on the first order and second order multiple scattering solutions of the

#### **VII Geosciences**

vector radiative transfer equation are calculated. Results from the two methods are compared. The polarimetric signatures, copolarized and depolarized return, degree of polarization, and phase differences are studied as a function of the orientation, sizes and dielectric properties of the cylinders.

#### Reports:

- 1. Dense Medium Radiative Transfer Theory: Comparison With Experiment and Application to Microwave Remote Sensing and Polarimetry, by Boheng Wen et al., *IEEE Trans on Geosci and Remote Sensing* 28,46(1990). AD A227 960
- Copolarized and Depolarized Backscattering Enhancement of Random Discrete Scatterers of Large Size Based on Second-Order Ladder and Cyclical Theory, by Charles E. Mandt et al., J Opt Soc Am 7,585(1990). AD A227 954
- 3. Monte Carlo Simulations of Scattering of Waves by a Random Rough Surface with the Finite Element Method and the Finite Difference Method, by S. H. Lou et al., *Microwave* and Opt Tech Let 3,150(1990).
- 4. Polarimetric Signatures of a Layer of Random Nonspherical Discrete Scatterers Overlying a Homogeneous Half-Space Based on First- and Second-Order Vector Radiative Transfer Theory, by Leung Tsang and Kung-Hau Ding, *IEEE Trans on Geosci and Remote Sensing* 29.242(1991). AD A238 331
- Polarimetric Passive Microwave Remote Sensing of Random Discrete Scatterers and Rough Surfaces, by L. Tsang, J Electromagnetic Waves and Appl 5,41(1991). AD A238 330

## 26480 IMPROVED PROPAGATION MODELS FOR IRREGULAR MEDIA

Charles L. Rino

Vista Research, Inc.

SL: ASL, CECOM

A major objective of the research has been achieved, namely to develop a consistent multiple-phase-screen like formalism that is rigorously correct for both discrete and continuous random media. In a series of papers culminating in, "On propagation in Continuous Random Media," which was recently accepted for publication, it was shown that the widely used Markov approximation implicitly includes two distinct approximations. The first approximation requires small local perturbations and is a sufficient condition for applying the Novikov-Furutsu (NF) theorem, which can be viewed as a closure hypothesis. That is, by applying the NF theorem, one can derive a hierarchy of first-order differential equations for the signal moments. The second approximation requires that over a short distance, the spectral components propagate like plane waves. Neither narrowangle scatter nor neglect of backscatter is strictly necessary, but these auxiliary conditions greatly simplify any ensuing computations. So far, the method developed here has been applied only to media where first-order perturbation theory is adequate to determine the incremental scattering characteristics of the medium. It appears that this is qualitatively equivalent to be the first approximation for continuous media; however, there is no straightforward extension of the NF theorem to accommodate discrete random media. Nonetheless, by assuming that any correlation between the total random fields at the bounding planes and the scatter within the planes is negligible, one can reproduce and even extend wellknown results for sparse media.

## 26988 A NEW COMPOSITE ROUGH SURFACE SCATTERING THEORY

Gary S. Brown

Virginia Polytechnic Institute and State University

A normalization was developed for the scattered field to be used in conjunction with the first order smoothing method. The purpose of this normalization was to extend the range of the first order smoothing method. That is, the normalization is first applied to be integral equation and then the smoothing is applied to the normalized equation. The normalization amplifies the Born term in the first order smoothing approximation and extends the range of this technique. Now it has been possible to determine just how this new approach fits into the hierarchy of existing approximations. The normalized first order smoothing (NFOS) approximation breaks down to the following ranges. For small height compared to a wavelength and small slope, the method yields the Rice approximation. This is called a localized low frequency approximation because the current at a point on the surface depends only on the incident field and the surface at the point in question. If the surface slopes become moderate to large but the height stays small, NFOS still works but does not obtain as simple a result as the Rice approximation. In this limit one gets a nonlocalized low frequency approximation. The low frequency restriction results from the small height condition while the nonlocalization comes from the need to integrate over the entire surface to account for the nonzero slopes. Finally, the normalization effectively accounts for any low frequency features on the surface; e.g., it is exact if the small scale surface structure is modulated by a randomly undulated planar surface.

## 27031 BACKSCATTERING FROM ROUGH SURFACES

Zu-Han Gu Surface Optics Corp.

SL: CECOM, CRDEC

The research has been characterized primarily by development of methods to measure the fatigue crack length within a sample electronically. This has two benefits. First, an electronic measurement method will give a measure of crack length which is averaged over the whole sample. This contrasts with visual crack measurement methods, in which, because of the transparent nature of ice, the maximum crack length is always measured. The drawback of the visual method can be seen if a hypothetical situation is imagined. Suppose one portion of the crack front (along a grain perhaps, remembering that in ice grain sizes are of order 1-10 mm) jumps forward to become the longest section of crack. Then, because the rest of the crack is now behind this jumped section, further growth there is minimal, until the rest of the crack front "catches" up. Nonetheless, significant crack lengthening is happening during this period of no visually observed growth. By measuring the crack growth electronically an "averaged" crack length is obtained, which gives a clearer indication of the progress of damage through the specimen than the visually obtained length. The second benefit of the electronic measuring method is to provide a signal which can be related to crack length and which can then be used to control the testing machine so that, for example, the load on the specimen could be slowly reduced over time to allow a constant  $\Delta K$  fatigue test to be performed. It will be some time before the method can be used this way on ice, but the potential is there. The method involves measuring two displacements on the sample, using two gauges. One gauge is placed at the mouth of the crack and measures the crack mouth opening displacement. The other gauge is placed close to the crack tip and measures the near crack tip opening displacement. By the method of similar triangles, it is relatively simple to find from these two readings the position of the center of rotation of the beam specimen during loading.

#### Reports:

No. 1-2 in previous editions.

- Photofabrication of One-Dimensional Rough Surfaces for Light Scattering Experiments, by E.R. Mendez et al., MS, Appl Opt.
- 4 Enhanced Transmission Through Rough Metal Surfaces, by Zu-Han Gu et al., MS. Appl Opt.

- Coherent Effects in the Scattering of Light From Random Surfaces with Symmetries, by E.R. Mendez et al., Opt Let 16,123(1991). AD A238 625
- 6. Waves on Corrugated Surfaces: K-Gaps and Enhanced Backscattering, by V. Celli et al., MS.
- 7. Experimental Study of Enhanced Transmission Through Rough Metal Surfaces, by Zu-Han Gu et al., MS.
- 8. Light Sc.,  $r \in \mathfrak{L}$  From One-Dimensional Surfaces with an Even Problem E.R. Mendez et al., MS.
- Experiment and add of the Opposition Effect in the Scattering of Light From a Randomly Rough Metal Surface, by Zu-Han Gu et al., Appl Opt 28,537(1989). AD A228 242
- 10. Enhanced Transmission Through Randomly Rough Surfaces, by Zu-Han Gu et al., MS.
- 11. Interaction of Two Optical Beams at a Symmetric Random Surface, by Zu-han Gu et al., MS, Appl Opt.

## 27485 ELECTROMAGNETIC WAVE SCATTERING FROM CHARACTERIZED RGUGH SURFACES

Kevin O'Donnell

Georgia Institute of Technology

SL: CECOM, WES

The scattering of light by a one-dimensionally rough surface was investigated in terms of the Stokes scattering matrix. It was shown that only four unique quantities appear in this matrix. Two of these are simply related to the s and p polarized scattering cross-sections, although the other two quantities contain cross-correlations of the electric field amplitudes scattered by s and p incident states. Through experimental measurements with a well-characterized rough surface fabricated in photoresist, it was shown that all four unique Stokes matrix elements are significant for a surface that produces backscattering enhancement.

Reports:

# 27911 COMPARATIVE EVALUATION OF KIRCHHOFF, PERTURBATION. AND FULL WAVE SOLUTIONS FOR ROUGH SURFACE SCATTERING

R.E. Collin

Case-Western Reserve University

## SL: CECOM

In the paper, "Depolarization and Scattering of Electromagnetic Waves by Irregular Boundaries for Arbitrary Incident and Scatter Angles, Full-Wave Solutions,"

Anomalous Light Scattering From a Perturbed Grating, by M.E. Knotts and K.A. O'Donnell, *Opt Let* 15,1485(1990). AD A232 213

## **VII Geosciences**

Bahar and Rajan derive scattering coefficients for a rough surface with roughness along the z direction only i.e., v = h(x). The scattering coefficients are restricted by the condition  $\sin\theta_s \sin\phi_s = \sin\theta_i \sin\phi_i$ ; i.e., the wave number along the z direction must match that of the incident wave. In the 1981 paper, "Full-Wave Solutions for the Depolarization of the Scattered Radiation Fields by Rough Surfaces of Arbitrary Slope," Bahar assumes that these scattering coefficients can be used for surfaces with two dimensional roughness with the only necessary change being the replacement of h(x) by h(x,z) in the phase integral. Since no mathematical proof is given one has to question the validity of the assumption. Bahar's derivations make use of the telegraphist's equations which are not applicable to surfaces with two dimensional roughness. The use of the telegraphist's equations places an unnecessary restriction on the problem. A new full wave method has been developed that does not use the telegraphist';s equations. This method is simpler and more direct and makes it easier to understand the nature of the approximations involved. It takes into account the two dimensional roughness of the surface from the beginning.

## 27919 POLARIMETRIC MEASUREMENTS OF NATURAL SURFACES AT 95 GHz

Robert E. McIntosh

SL: BRL

University of Massachuseus

SC: ASL, HDL, LABCOM, MICOM

The phase noise level is now acceptable for accurate measurements. Other work consists of an intensive effort of polarimetric snow measurements with the 95 GHz polarimeter. These will occur both in Amherst and in Laramie, Wyoming, in conjunction with other polarimeters operating at 5,10, and 225 GHz. A new, multiple polarization transmitter antenna will be installed afterwards, allowing the radar to perform coherent and noncoherent polarimetric measurements of trees will begin when this modification is complete.

# 28219 A FULL WAVE STUDY OF RADAR CROSS SECTIONS OF ROUGH TERRAIN AND FOLIAGE COVERED TERRAIN

E. Bahar University of Nebraska

SL: CECOM

SC CRREL. HDL, MICOM

#### E. Atmospheric Remote Sensing

The objective of the research is to present a theory in a form understandable to the random media community. The effects of all approximations are to be carefully studied and physically justified. The theory will be exercised on one dimensional rough random surfaces in both the backscatter and forward scatter modes, on surfaces ranging from smooth, slightly rough, surfaces to very rough, large sloped, surfaces to very rough but low-slope surfaces.

# 29288 NUMERICAL SIMULATIONS OF LIGHT SCATTERING FROM ROUGH ONE-DIMENSIONAL GOLD SURFACES

Eric I. Thorsos

University of Washington

The research objective is to develop and exercise codes solving for the EM scattering from rough one dimensional gold surfaces. The P.I. will modify his procedure for solving the 1D integral equation for scattering from random rough metallic surfaces with complex refractive indices. Monte Carlo simulations will be used to compare this technique with experimental results.

## E. Atmospheric Remote Sensing

## 26404 FURTHER ANALYSIS OF ECOM-721 DATA

Supriy Chakrabarti University of California, Berkeley

Previous U.S. Army contracts funded the analysis of airglow and auroral data obtained by the ECOM-721 experiment. Recent modeling efforts have focused on the analysis of the ECOM-721 and rocket spectrometer measurements of the OI EUV dayglow. Under this contract the ECOM-721 database is being used to examine more complicated geophysical situations: a self-consistent analysis of the OII 834 Å dayglow and other OII emissions using realistic models of nospheric electron densities, a statistical study c the influence of solar and geophysical variations on the EUV dayglow and aurora, an analysis of the EUV spectrum of photo- and auroral electron-excited emissions in the sunlit dayside cleft aurora, an analysis of EUV emissions in the nightside and polar cap aurora, a study of the excitation mechanisms of NI and NII atomic nitrogen emissions in the dayglow and aurora. In order to proceed with the analysis in a more rational and efficient manner, work is in p.ocess archiving all unfiltered data accumulated by

ECOM-721, and for the first time, have plots of the entire database readily available, with background subtraction performed and with orbital parameters indicated on a sensible time scale. The visual archive will greatly facilitate the identification of geophysical events which merit study. The visual archive will also aid in assessing the quality of data selected for statistical and morphological studies of the dayglow and aurora.

# 26982 MULTIPARAMETER RADAR MEASUREMENTS OF PRECIPITATION IN COMPLEX TERRAIN METEOROLOGICAL AND HYDROLOGICAL APPLICATIONS

Kultegin Aydin

The Pennsylvania State University

SC: CRREL, WES

A major concern in estimating rainfall rate from radar measurements is knowing whether the radar returns are from rain alone or a mixture of rain and ice, or totally from ice phase hydrometeors. To form a basis for tackling this problem at C-band, the P.I. has initiated a simulation study based on disdrometer measurements of rainfall for deriving polarization radar signatures of rainfall in terms of the pairs  $(Z_{H}, Z_{DR}), (Z_{H}, K_{DP}), (Z_{H}, Z_{DP}) \text{ and } (\rho_{HV}(0),$  $Z_{DR}$ ), where  $Z_{H}$  is the effective reflectivity factor at H-polarization,  $Z_{DR}$  is the differential reflectivity. K<sub>DP</sub> is the specific propagation differential phase shift,  $Z_{DP}$  is the difference reflectivity and  $\rho_{HV}(0)$ is the zero-lag cross correlation. Rainfall tends to be clustered in certain regions on these polarization parameter planes which provide useful signatures for differentiating rain from mixed phase precipitation. Another study is focused on determining the polarizatio, radar signatures of melting hail at C-band. A number of radar observables including those mentioned above and linear depolarization ratio are being evaluated for this purpose. Hydrological modeling studies using radar measurements as input are continuing. The focus is on the Greve River watershed which is a major tributary of the Arno River. The sensitivity of the simulated watershed response to the spatial and temporal distributions and resolutions of rainfall is under investigation. Another study is focused on the vertical reflectivity gradient problem in rainfall measurements at extended range from the radar. This problem is being investigated by examining the behavior of reflectivity factor measurements with range and elevation angle for a variety of melting laver models.

Reports:

No. 1-2 in previous editions.

- Polarimetric Radar Remote Sensing of Rainfall and Liquid Water in Clouds, by Yuan-Ming Lure, PhD Thesis, 1990, 170 pp.
- A Differential Reflectivity Radar Hail Measurement Technique: Observations During the Denver Hailstorm of 13 June 1984, by K. Aydin et al., J Atmos Sci and Oceanic Tech 7,104(1990). AD A228 591
- 5. Polarimetric Radar Measurements of Rainfall Compared with Ground-Based Rain Gauges During MAYPOLE '84, by Kultegin Aydin et al., *IEEE Trans on Geosci and Remote Sensing* 28,443(1990). AD A230 947
- A Computational Study of Polarimetric Radar Observables in Hail, by Kultegin Aydin and Yang Zhao. AD A231 201

## 27870 MEASUREMENT OF THE ATMOSPHERIC TURBULENCE SPECTRUM USING LASER SCINTILLATIONS

Rod Frehlich

University of Colorado SL: ASL, CRDEC SC: MICOM

The following tasks were accomplished: (a) All raw data were processed and 30 percent of the data set was rejected due to poor weather conditions. (b) The universal form of the atmospheric turbulence spectrum for locally stationary conditions was estimated by a best fit to all the data conditioned by an accurate estimate of the inner scale of turbulence every four seconds. The preliminary spectrum agrees with the form proposed by Hill. This is the first estimate of the turbulence spectrum for locally stationary conditions. (c) The accuracy of the inner scale estimates were verified by a simulation of the data for known conditions. These simulations indicate the feasibility of 4 percent accuracy for inner scale estimates and 8 percent accuracy for estimates of the level of turbulence  $C_n^2$  using one second of data and probing 20 meters of the atmospheric boundary layer. The accuracy of the estimates is related to the number of independent samples which can also be determined from the fluctuations of the best fit parameters. (d) The variations in inner scale and level of turbulence have been estimated and often display large variations (a factor of 10 for level of turbulence and a factor of 4 for inner scale during a few minutes). These variations may have pronounced effects on imaging systems and boundary layer mechanisms.

Reports

Measurements of the Atmospheric Turbulence Spectrum and Intermittency Using Luse: Scintifiation, by Rod Frehlich, MS, SPII, Proc.

 Laser Scintillation Measurements of the Temperature Spectrum in the Atmospheric Surface Layer, by Rod Frehlich, MS, J Atmos Sci.

## 28094 HIGH-RESOLUTION PROBING OF BOUNDARY LAYER WIND AND MOISTURE FIELDS

Madison J. Post Robert M. Banta R. Michael Hardesty National Oceanic and Atmospheric Administration

Most of the research effort was spent investigating the technological tradeoffs associated with 1 and 2 µm coherent laser radars, and the effects of technology choices on measurement capabilities. At NOAA's Table Mountain Test Range one week was spent comparing NOAA's 10.6 µm lidar with CTI's 1 and 2 µm lidars. 2 µm was decided as the best wavelength. because of laser beam quality, low atmospheric absorption, lower degradation due to refractive turbulence, less expensive optical components, and better eye safety. The choice of transmitter is then for either a higher powered (50 mJ/pulse), lower PRF (10 Hz) system, or a lower powered (15 mJ/pulse), higher PRF (200 Hz) system. The former is flashlamp pumped, while the latter is cw diode pumped. The diode pump, high PRF system was chosen because of the higher spatial resolution attainable when scanning a given volume of the boundary layer in a fixed amount of time. Another issue is the possibility of doing DIAL work, and/or choosing the most transparent atmospheric window for the operating wavelength.

## 28102 PATH RESOLVED OPTICAL REMOTE SENSING OF ATMOSPHERIC WINDS

J. Fred Holmes

Oregon Graduate Institute of Science and Technology

SC. CRDEC. TECOM

The progress is summarized as follows: Coherent System: (a) Analyzed the system in more detail to predict signal-to-noise ratio as a function of back-scatter coefficient. (b) Determined a method of separating the effects of the aerosol speckle and turbulence in the time delayed statistics and simulated the method to confirm that it works. (c) Determined a method of signal processing that works in the presence of an unknown doppler shift in the heterodyne frequency and simulated the method to confirm that it works. (d) Cleaned, realigned and reactivated the CW. CO<sub>2</sub>

coherent lidar. (e) Made some progress in selecting the parts needed to modify the system for diphase modulation. Incoherent System: (a) Started analyzing the system in detail to determine the signal-tonoise ratio as a function of backscatter coefficient. (b) Determined a method of processing and simulated the method to confirm that it works.

# F. Small-Scale Atmospheric Processes

## 24881 SPATIAL INHOMOGENEITIES IN SMOKE PLUMES

E.L. Ludwig

SRI International

SC: CRDEC

In a paper submitted to the International Journal of Remote Sensing in 1991, Jones, Thomas, and Earwicker proposed a new technique for analyzing remotely sensed images. They applied the technique to analyze the fractal geometry of LANDSAT images. The method successively degrades image resolution by half, applies a "feature-detecting filter" to the degraded images, and examines the changes in the number of features whose "intensity" exceeds different thresholds. They used statistical relationships among features at different scales to estimate scaling parameters and fractal dimensions associated with satellite imagery. A paper has been prepared which describes how their approach can be extended to atmospheric vector fields. Features can be selected for physical significance; e.g., the distribution of eddies at different scales can be examined for spatial relationships using image display techniques. In the case of atmospheric motions, applications of this type may provide insight into the nature of the turbulent cascade which could be used to reconstruct statistically accurate realizations of subgrid motions and provide a basis for parameterization.

#### Reports

No. 1 in previous edition.

Using Multiresolution Feature Analysis to Interpret Atmospheric Observations, by FL, Ludwig, MS

## **26491** TURBULENT MICROFRONTS

Larry Mahrt Oregon State University

SE ASE SC (RDEC, DPG

#### E Small-Scale Atmospheric Processes

Additional work has been carried out on the LAMEX data, using specialization of the wavelet analysis theory/techniques developed by this group during the past year. In addition special software for data analysis and storage has been written and tested. The low frequency "modulation" feature found in the 50 h turbulent winds from the LAMEX sonic data has been investigated. The almost periodic signature found in the 95 percent flatness width of wavelet variance is found to be correlated with the momentum flux transport. The net momentum flux computed over half-hour periods seem to be large when the flatness width is small. This further strengthens the hypothesis that the small flatness width corresponds to more organized coherent structures responsible for the bulk of the transport. A separate study of gust events associated with microfronts has been carried out. Theoretical work on the definition of the sharp transitions as well as methods of detecting such transition zones have been developed. Sharp turbulent microfronts associated with a well-defined structure, such as an edge of an eddy or wind gust, contain a characteristic signature that can be detected by studying the change of the wavelet coefficient with dilation. The deviation of the coefficient from unity is a measure of the lack of sharpness of the transition zone. This criteria has been applied to the data to extract events and evaluate the contribution to the net momentum transport by such events.

#### Reports:

 Estimation of Eddy Characteristics From Time Series Using Localized Transforms, by L. Mahrt and J.H. Howell, MS.

# 27019 ATMOSPHERIC TURBULENCE STRUCTURE AT THREE VEGETATED SITES

Roger H. Shaw University of California, Davis

Activities have centered on the analysis of data collected during the campaigns in the two orchards and at the agricultural crop site. Statistical evaluations of atmospheric turbulence from within and immediately above these canopies have been compared with those from the deciduous forest experiment at Camp Borden, Canada in 1986/87. Specifically, data have been examined for the features of turbulence characteristic of such atmospheric layers. In addition, an objective technique has been applied to the data sets for the multilevel detection of temperature ramps. Such scalar ramps are signatures of coherent motions consisting of ejections and sweeps. This work is aimed at determining whether differences in canopy height and structure create fundamental differences in patterns of atmospheric turbulence.

# 27995 LAGRANGIAN STOCHASTIC MODELING OF DISPERSION IN THE PLANETARY BOUNDARY LAYER

Jeffrey C. Weil University of Colorado

SL: ASL SC: CRDEC, DPG, MICOM

The flux footprint is the contribution, per unit emission, of each element of a surface area source to the vertical scalar flux measured at height  $z_{m}$ ; it is equal to the vertical flux from a unit surface point source. The dependence of the flux footprint on crosswind location is shown to be identical to the crosswind concentration distribution for a unit surface point source; an analytic dispersion model is used to estimate the crosswind-integrated flux footprint. Based on the analytic dispersion model, a normalized crosswind-integrated footprint is proposed that principally depends on the single variable  $z/z_m$ , where z is a measure of vertical dispersion from a surface source. The explicit dependence of the crosswindintegrated flux footprint on downwind distance, thermal stability and surface roughness is contained in the dependence of z on these variables. By also calculating the flux footprint with a Lagrangian stochastic dispersion model, it is shown that the normalized flux footprint is insensitive to the analytic model assumption of a self-similar vertical concentration profile.

#### Reports:

- Footprint Estimation for Scalar Flux Measurements in the Atmospheric Surface Layer, by T.W. Horst and J.C. Weil, MS.
- Footprint Estimates for Atmospheric Flux Measurements in the Convective Boundary Layer, by J.C. Weil and T.W. Horst, MS.

#### 28344 PHYSICAL PROCESSES IN SNOWPACK DURING RAIN OR MELT EVENTS

Charles F Raymond University of Washington

SL: CRREL

The research objective is to develop further understanding of the mechanical response of snowpacks to rain or melt events and to determine the coupling between thermal and mechanical parameters. A field

#### **VII Geosciences**

program on natural snowpacks will measure evolving distributions of temperature and deformation during rain and melt events; map changes in texture and structure of the snowpack in relation to water penetration and deformation; and determine macroscale mechanical response to the evolution of local conditions. Laboratory experiments on prepared snow samples will examine the coupling between volumetric compression and grain coarsening processes in saturated snow. This information will be used to explain interactions between densification and grain growth of microstructural models, relate changes in the spatial pattern of deformation to changing distributions of temperature and liquid water and to define relative rates of weakening and strengthening in the snowpack in relation to wetting history and rate wetting.

#### 28664 WAVES AND STABILITY IN THE PLANETARY BOUNDARY LAYER

Carmen J. Nappo Richard M. Eckman National Oceanic and Atmospheric Administration

SL: ASL SC: CRREL, DPG

The research objective is to determine the role of atmospheric gravity waves inducing breakdown of the stable planetary boundary layer. The occurrence and characteristics of breakdown events in the boundary layer will be determined from data taken in a network of micrometeorological towers in eastern Tennessee. The occurrence of gravity waves and their characteristics will be analyzed from data taken by a microbarograph array incorporating the tower network and another array around one tower. The singular and joint probability density distributions of occurrence will be determined. Case studies of the three possible events will be conducted to clarify the role of the gravity wave in the breakdown events.

# 28954 TURBULENCE IN THE ATMOSPHERIC SURFACE LAYER: ANALYSIS OF THE FLAT DATA SET

Steven P. Oncley National Center for Atmospheric Research

SL: CRREL SC: DPG

The first two months of this project were spent preparing for a first analysis pass through the FLAT (Full Look at Turbulent Kinetic Energy) data set. This pass will consist of the computation of first.

#### G. Aerosol Research

second, and third-order moments on all of the data taken during the FLAT experiment, with the exception of the high-frequency hot-wire anemometer data. The results from this pass will be used to perform a data-quality study in which various instruments will be compared. Also, some of the corrections to be used on the final data set require information from the data set itself.

## 29188 TRAPPING OF INTERNAL GRAVITY WAVES IN AN INVERSION

H.J.S. Fernando

Arizona State University

SC: ASL

The research objective is to measure the mass exchange that occurs as a result of a buildup of turbulence-induced gravity wave energy within stratified stable layers and extend the results to atmospheric conditions. Experiments will be performed using various stably-stratified alcohol-salt mixtures. Grid turbulence will induce gravity waves in an interior layer of high stability. A unique Richardson number probe will be used to measure the local velocity and density gradients on both sides of the interface as the stable layer becomes saturated with gravity waves and mass is exchanged between the stability regimes. Measurements of this nonlinear process will be compared to linear theory.

# G. Aerosol Research

26962 COMPUTATION OF NONLINEAR OPTICAL SCATTERING BY DROPLETS

Steven C. Hill		
Peter Barber		
David Kaup		
Clarkson University		
SL: CRDEC	SC: ASL	

Large internal fields are particularly important in determining which nonlinear optical effects occur in droplets. To better understand where the large intensities occur in droplets a comparison was made with the Mie theory results and those obtained using ray tracing. The similarities are remarkable. The cone of high intensity near the forward surface is caused by rays that were bent once at the first droplet surface. The highest intensity region along the center axis is caused by rays that have reflected once internally. In a ray tracing model this highest intensity region is

#### G. Aerosol Research

infinitely thin. In the Mie model the width about the axis of this cylindrical region is about one internal wavelength. In a water droplet, the rays that cause the other "hot spots" on the axis are ones that have undergone three internal reflections. Efforts are being made to try to determine the effects of the internal intensity distribution on the shape of the droplets and the consequent increased rate of light emission. The T-matrix method for layered structures is being modified so it can model the increase in the refractive index near the high intensity region of an illuminated droplet. This may limit the Q's of droplets and cause the resonance frequencies to shift. It is usually assumed that when the frequency is two or three linewidths from an MDR then the lifetime is short enough to be negligible and the internal fields are not dominated by that resonant mode. The internal fields have been computed 200 linewidths away from a high Q  $(10^9)$ MDR and found them to be dominated by the MDR. This finding is relevant to discussions about the density of modes which are important in supporting nonlinear optics.

#### Reports:

- 1. Morphology-Dependent Resonances in Radially-Inhomogeneous Spheres, by D.Q. Chowdhury et al., MS, J Opt Soc Am.
- Fine Structures in the Angular Distribution of Stimulated Raman Scattering from Single Droplets, by Gang Chen et al., MS, Opt Let.
- 3. Frequency Splitting of Degenerate Spherical Cavity Modes: Stimulated Raman Scattering Spectrum of Deformed Droplets, by Gang Chen et al., MS. *Opt Let.*
- 4. Resonances and Internal Electric Energy Density in Droplets, by Steven C. Hill et al., MS.
- 5. Nonlinear Optical Processes in Droplets with Single-Mode Laser Excitation, by Richard K. Chang et al., MS.

#### 28052 LASER BEAM-AEROSOL INTERACTIONS

Robert L. Armstrong

New Mexico State University

SL: ASL. CRDEC SC: CRDEC

Researchers completed work on two droplet superheating projects, and obtained new findings in stimulated Raman scattering (SRS) and lasing from microdroplets and microjets. The superheating find-

#### VII Geosciences

ings included the discovery of evaporative instability in absorbing microdroplets irradiated by a highirradiance laser. This phenomenon is also related to previous superheating findings. New SRS results are concerned with the understanding of a unique ringlike region of SRS emission encircling the incident laser beam axis (the "Descartes" ring). Studies have been made of the properties of SRS emission from this ring, and possible causes of the emission have been identified.

# 28359 ORIENTATION AND PAIR CORRELATION AT HIGH DENSITY BY SUPERRESOLUTION HOLOGRAPHY

Peter Scott

State University of New York at Buffalo

SC: ASL, CRDEC

The research objective is to determine the pair correlation and the orientation distribution of nonspherical particles in a dense (1–5 percent) suspension of particles. Holographic techniques and equipment developed under a previous ARO contract will be used to measure the positions and orientation of dense (1–5 percent by volume) suspensions of large (100–500 micrometers) particles. These measurements will be processed with a super-resolution algorithm and the necessary statistic will be derived.

#### 28489 HIGH–INTENSITY AND HIGH–ENERGY LASER INTERACTIONS

Richard K. Chang Yale University

SL: CRDEC, MICOM SC: ASL, CRDEC

The experimental study of two-photon excited fluorescence and two-photon pumped lasing in single droplet has been completed. The standard nonlinear wave equation has been modified to account for the growth and coupling of nonlinear waves in droplets. Lastly, the experimental study of the laser-induced emergence of coherent radiation lasing and stimulated Raman scattering from one- and two-Descartes rings on the droplet surface has been completed.

# **VIII ELECTRONICS**

# **A.** Physical Electronics

#### 23206 TOPOLOGICAL TRANSFORMATIONS IN CHALCOGENIDE GLASSES

Laurie E. McNeil Wei-Kan Chu University of North Carolina at Chapel Hill

The diffusion of silver into germanium diselenide amorphous thin films is greatly enhanced by illumination with near or above bandgap light. Both bulk amorphous GeSe<sub>2</sub> and thin films have been prepared and illuminated over a range of photon energies, and the resulting silver depth profiles examined using Rutherford backscattering spectroscopy. The profiles resemble a gaussian distribution more closely than the step function that has been previously reported. Also, the thin films are much more sensitive to light than the melt quenched glass. Finally, the sensitivity of the films increases with above bandgap illumination, but not as rapidly as the absorbance increases. These results are being considered in light of possible models for the diffusion mechanism. An examination was made of the structure of amorphous  $Ge_{1-r}Sn_rSe_2$  at liquid nitrogen temperatures (atmospheric pressure) and at high pressure (room temperature) using Mössbauer spectroscopy. The low temperature study shows that the fraction of Sn atoms occurring in a tetrahedrally bonded site does not change with concentration, remaining at 0.85 for  $0.20 \le x \le 0.60$ . The high pressure study focuses on Ge0.5Sn0.5Se2 and provides new evidence that the glasses are made up of distinct structural clusters. This study also shows two different regions of response to pressure, which were interpreted as a low pressure region in which the intercluster interactions were changed and a high pressure region in which the intracluster interactions were affected.

#### Reports:

No. 1-12 in previous editions.

13. Cluster-Cluster Interactions in  $\alpha$ -Ge<sub>1</sub>, sn<sub>3</sub>Se<sub>2</sub>, by Marian J. Peters, PhD Thesis, 1990, 97 pp.

# 26147 CONTACTLESS OPTOELECTRONIC INTEGRATED CIRCUITS FOR REMOTE FIBER OPTIC COMMUNICATION AND SENSING APPLICATIONS

Stephen R. Forrest University of Southern California

SL: CECOM. HDL SC: MICOM

Work has continued on the optically powered optical logic circuits as the vehicle to demonstrate the advantages and disadvantages of the optical powering concept. The circuits fabricated consist of a bias resistor, two HPT structures discussed in previous reports, an HBT and two phototransistors. In addition, these are integrated with a 4 quadrant photovoltaic cell. The materials used for this integrated circuit are from the InGaAs/InP system. The photovoltaic cells have exhibited an open circuit voltage of 0.95 V per quadrant, resulting in a total array open circuit voltage of 3.8 V. This value is more than adequate to power the entire optical logic pixel. The short circuit current of the PV cells is still somewhat small due to excessive series resistance of the InP p-type contact. The optical logic OEIC was fabricated, and demonstrated optical latching when feedback was applied from the output laser to the feedback HPT. In addition, by eliminating optical feedback, the circuit performed as an amplifier according to its design criteria. The HBT used for laser pre-bias is different from the HPTs in that base contact is made. Here, Zn diffusion through the top collector layer is made to the p-type base. Current gains of from 100-200 are measured in these InGaAs/InP HPTs. Furthermore, the photoconductors used in controlling, by optical means, the transistor "bias" had response time <400 ps and gain-efficiency products of >11.

#### Reports.

- 1. Optically Powered Arrays for Optoelectronic Interconnection, by M. Govindarajan and S.R. Forrest, MS.
- 2. A High Sensitivity, High Bandwidth  $In_0 c_3Ga_{0.47}/As/InP$ Heterojunction Phototransistor, by L.Y. Leu et al., MS.

# 26188 MEASUREMENT OF OPTICAL PROPERTIES OF INFRARED BANDGAP SUPERLATTICES

Donald F. Nelson Worcester Polytechnic Institute

SL: HDL

The observation of Raman scattering from LO phonons in the InP substrate of a multiple quantum well sample has been used to compare predicted and observed scattering efficiencies. This led to several experimental improvements which brought the two into approximate agreement. A study has been completed and concerns an unusual Raman scattering resonance of this same multiple quantum well sample. It is a resonance involving a free-to-bound transition. Lastly, the improved embodiment of the TMM that has been implemented on the computer and used in the above calculations is also being written up for publication. It can be termed a diagonal representation of the TMM and is particularly useful for calculating single quantum well states and arbitrary profile well states.

#### Reports:

No. 1 in previous edition.

- 2. The Diagonal Representation for the Transfer Matrix Method for Obtaining Electronic Energy Levels in Layered Semiconductor Heterostructures, by B. Chen et al., MS, *Phys Rev.*
- 3. Raman Scattering of Slab-Mode Phonons in InGaAsP/InP Multiple Quantum Wells, by M. Lazzouni et al., MS, Appl Phys Let.

# 26434 III-V SEMICONDUCTOR QUANTUM WELL LASERS AND RELATED OPTOELECTRONIC DEVICES ON SILICON

N. Holonyak, Jr.

G. Stillman

K. Hsieh

University of Illinois

SL: HDL

#### SC: ETDL, MICOM

Studies are being made of problems specific to HI–V quantum well heterostructures (QWHs) and their application in lasers. With greater or lesser emphasis these studies include: (a) Al<sub>3</sub>Ga<sub>1</sub>, As-GaAs lasers on Si; (b) impurity induced layer disordering (IILD), which has now become important commercially; (c) phonon effects and the effects of high or low cavity Q (three dimensions) on photopumped QWH laser operation; (d) laser operation of high gap In<sub>3</sub>As(Al<sub>3</sub>Ga<sub>1</sub>, ),P:and, most importantly, (e) hydrolyzation-oxidation of  $NI_3$ Ga<sub>1</sub>, As-GaAs QWHs and superlattices.

# 26444 SHORT-PERIOD SUPERLATTICE MATERIALS FOR HETEROJUNCTION BIPOLAR TRANSISTORS

David L. Miller The Pennsylvania State University SC: ETDL

The goal of this project is to investigate the usefulness of short-period superlattices of InAs/GaAs and InAs/ AlAs for heterojunction bipolar transistors. The mode of growth which was employed is migration-enhanced epitaxy (MEE), also known as alternate-layer MBE. The first low-temperature (substrate temperature = 300°C) Be-doped MBE GaAs material grown by MEE which is conducting without post-growth anneal can be reported. This material has reduced mobility compared with Be-doped material grown at normal substrate temperatures. These results suggest that growth of short-period superlattice materials using MEE must be undertaken with care in the choice of substrate temperature. InAs/GaAs short-period superlattices have been grown on InP by MEE at 350°C. Superlattice x-ray diffraction peaks have been observed at the expected angles, for samples approximately 3000Å thick. Above that thickness, RHEED indicates considerable surface disorder and roughness during growth.

# **26708** MODIFICATION AND CHARACTERIZATION OF II–VI III–V AND HIGH $T_{\rm C}$ SUPERCONDUCTORS USING ION BEAMS

Robert G. Wilson Hughes Research Laboratories

SL: NVEOC

The research objective is to improve the fundamental understanding of the modification of III–V, II–VI and high-critical-temperature (HTC) superconductors due to ion implantation. The characterization of ion-beamimplanted III–V, II–VI and HTC superconductors is proposed as a means of understanding a number of critical issues including: ion ranges in a variety of electronics-related materials; role of substrate temperature in ion implantation; and synthesis of new and special materials or buried layers, using high fluence ion implantation; ion-beam fabrication of III–V waveguides.

#### 26761 SEMICONDUCTOR HETEROJUNCTION ENGINEERING

A. Franciosi

University of Minnesota, Minneapolis

SL: MICOM

Thin Si epitaxial layers (1-14 monolayers) were fabricated by molecular beam epitaxy on GaAs(001) and AlAs(001) substrates also obtained by molecular beam epitaxy on GaAs(001) wafers. In situ studies by monochromatic x-ray photoemission show initial layer-by-layer Si growth on both substrates with only minor Si in-diffusion. Reflection high energy electron diffraction analysis shows good epitaxy with some indication of three-dimensional growth at Si coverages higher than 4-8 monolavers. Comparison of the results with recent heterojunction theories suggest that the best predictions for the band offsets are obtained with the model solid approach using deformation potentials to describe the effect of strain. The Si epitaxial layers are found to remain stable upon growth of AlAs or GaAs layers on top of the Si layers.

#### Reports:

- 1. In-Situ Studies of Semimagnetic Heterojection Paraters, by Xiaohua Yu et al., Mat Res Soc Symp Proc 161,459(1990).
- 2. Low-Temperature Photoemission Measurements s of Valence-Band Discontinuities at Buried Heterojections, by Xiaohua Yu et al., *Phys Rev* B1872(1990). AD A233 017
- 3. In Situ High Resolution XPS Analysis of AlAs-GaAs Heterostructures with Tunable Band Offset, by G. Bratina et al., MS.
- 4. Tuning AlAs-GaAs Band Discontinuities and the Role of Si-Induced Local Interface Dipoles, by L. Sorba et al., MS, *Phys Rev Rapid Commun.* AD A240 367
- 5. Tuning AlAs-GaAs Heterostructure Properties by Means of MBE-Grown Si Interface Layers, by G. Ceccone et al. MS, *Surface Sci.*
- In Situ Studies of CdTe-GaAs(110) Heterojunction Parameters by Low Temperature Photoemission, by X. Yu et al., MS.
- 7. Epitaxial Growth and Interface Parameters of Si Layers on GaAs(001) and AlAs(001) Substrates, by G. Brantina et al., J Vac Sci Tech B9,2225(1991).
- 8. Band Offsets in Heterovalent Heterostructures: CdTe(111)-GaAs(001) and CdTe(001)-GaAs(001), by G. Bratina et al., MS, Appl Phys Let.

# 26896 QUANTUM DEVICES USING Si-BASED SUPERLATTICES AND SUPERSTRUCTURES

K.L. Wang

University of California. Los / ageles

SL: HDL

Infrared absorption of doped SiGe/Si multiple quantum wells has been demonstrated for the first time using Fourier transform infrared spectroscopy. A waveguide geometry is employed in the measurement in order to enhance the absorption by multiple

#### A. Physical Electronics

reflections. The calculated peak position for the transition between the ground and first heavy hole states agrees well with the experimentally observed value. In this calculation splitting of energy bands due to strain in the SiGe layer has also been taken into account. The observation of the inter-subband transition in multiple quantum wells suggests that high sensitivity infrared detectors (operating near 10 µm wavelength region) may be fabricated using a boundto-extended state transition. The use of Si-based material can be combined with Si VLSI technology for revolutionary focal plan technology. The p-type  $\delta$ -doping in MBEs has been demonstrated using a thermal boron source. The preliminary data indicate that extremely high doping densities with sharp profiles can be obtained. The quantum effect due to the sharp potential profile associated with the  $\delta$ -doping is also investigated. Quantum well structures using  $\delta$ -doped layers have also been grown.

#### Reports:

- 1. Quantum Devices Using SiGe/Si Heterostructures, by R.P.G. Karunasiri and K.L. Wang, MS, J Vac Sci Tech.
- Hole Intersubband Absorption in Δ-Doped Multiple Si Layers, by J.S. Park et al., Appl Phys Let 58,1083(1990).
- Intersubband Absorption in Si1., Ge, Si Multiple Quantum Wells, by R.P.G. Karunasiri et al., Appl Phys Let 57,2585(1990). AD A234 122
- 4. Selective Etching of SiGe on SiGe/Si Heterostructures, by G.K. Chang et al., J Electrochem Soc 138,202(1991). AD A234 401

## 27298 OPTICAL STUDIES OF LATERALLY CONFINED QUANTUM WELL STRUCTURES GROWN ON EX-SITU AND IN-SITU PATTERNED SUBSTRATES

Anupam Madhukar

University of Southern California

SL: ETDL, NVEOC

The research objective is to advance the understanding of compound-semiconductor structures suited for ultrafast electronics and optoelectronics. Attempts will be made to perform real-time diagnostics on electronic and optoelectronic materials as they are grown by molecular beam epitaxy (MBE) and to characterize these MBE-grown materials both electrically and optically.

#### 28335 DOUBLE SUPERLATTICE GaAs IR TRANSISTORS

D.C. Tsui Princeton University SL: ETDL

#### A. Physical Electronics

This research seeks to enhance the basic understanding of electron transport in compound semiconductors with miniband transitions in the infrared region of the electromagnetic spectrum. Carrier transport properties will be measured in gallium arsenide superlattices with miniband transitions in the infrared. Measurements will be made in the presence of external electric and magnetic fields. Superlattices will be engineered to reduce ground state tunneling effects contributing to the unwanted dark current in infrared devices.

#### 28347 MONTE CARLO SIMULATION OF MERCURY CADMIUM TELLURIDE

Michael Shur University of Virginia

SL: NVEOC SC: SDC

The research objective is to improve the understanding of charge transport in II–VI semiconductors. Monte Carlo simulations of charge transport in II–VI semiconductors will be accomplished with and without band structure. Monte Carlo simulations of electron scattering and impact ionization will be performed in HgCdTe. Velocity-field characteristics for holes and electrons will be determined for HgCdTe structures. Monte Carlo simulations will be used to describe charge transport in p-n diodes.

# 28351 MATERIALS AND DEVICE RESEARCH FOR HIGH-SPEED INTEGRATED OPTOELECTRONIC TRANSMITTERS USING VERTICAL-CAVITY SURFACE EMITTING LASER

Russell D. Dupuis University of Texas at Austin

SL: ETDL SC: NVEOC

This research objective is to conduct a series of experimental investigations concerning the design and materials growth of integrated optoelectronic structures. This research includes the design, growth, fabrication, and testing of optimized lasers and transistors with the objective of subsequent integration into optoelectronic circuits. In particular, the research will emphasize the realization of In-based, vertical-cavity lasers capable of room-temperature operation along with the development of high speed heterojunction bipolar transistors. Eventually, the research will be directed towards the monolithic integration of lasers and transistors into optical transmitters. The research will attempt to establish a rigorous foundation for such optoelectronic integration.

# 28392 FUSIBLE LINK TECHNOLOGY FOR POWER SEMICONDUCTOR DEVICES

B. Jayant Baliga

North Carolina State University

SC: ARO, ETDL

A thermal analysis for the fusible links was carried out to determine the dimensions of the links. From the analysis, it was found that to minimize the current required for fusing, the thickness and width of the fuses must be reduced as much as possible, while the thickness of the silicon substrate and the oxide layer must be increased. Calculations showed that for fuses fabricated on a 1  $\mu$  oxide layer, 1000Å thick fuses required a width of 1  $\mu$  to fuse at currents below 20 mA. However, for 100 Å; thick fuses, the width could be increased to 3  $\mu$ . The analysis also showed that the current required for fusing was independent of the fuse length. The mask design for the fusible links was completed. Four masks were designed. The first mask was used to pattern the polysilicon layer, the second was used to open contact windows through the oxide, the third to pattern the thick metal layer and the fourth to pattern the thin metal layer. The fourth mask had fuses of widths ranging from 1  $\mu$  to 6  $\mu$ . The masks also included some test elements to measure the resistivity of the polysilicon and metal layers and the contact resistance between the polysilicon and the metal. Two fabrication runs were carried out. For both the runs, the thickness of the thermally grown oxide was 1  $\mu$ . In the first run, fuses of thickness 1000 Å and 100 Å were fabricated.

# 28674 SCATTERING AND GUIDING OF WAVES BY METAL-STRIP GRATINGS

Song-Tsuen Peng New York Institute of Technology

SL: ARDEC, CECOM

The research objective is to conduct an investigation on the scattering and guiding of electromagnetic waves by metal-strip gratings embedded in multilayer dielectric structures. A series of theoretical investigations will be performed concerning the scattering and guiding of electromagnetic waves by metalstrip gratings. This analysis will include metal-strip gratings that are characterized by a finite conductiv-

ity and a nonzero thickness. The proposed research will attempt to establish a rigorous theoretical foundation for such analysis, to develop a clear physical understanding, and to accurately evaluate the effects of finite conductivity and finite thickness on the scattering and guiding characteristics of the class of grating waveguides.

# **B. Electron Devices**

#### 25015 QUANTUM TRANSPORT IN SEMICONDUCTOR DEVICES

David K. Ferry Arizona State University SL: ETDL SC: HDL, ONR

An ultra-short gate MESFET model has been developed for studies of devices with gate lengths in the 25-100 nm range. Studies have utilized a full transient momentmethod transport simulation. The full hydrodynamic equations are being implemented within this model, so that studies of quantization effects in density, momentum, and energy can be investigated. The self-consistent potential is filtered by a statistical potential averaging technique developed earlier for the inclusion of quantum potentials in near semiclassical transport studies. The simulated MESFET device has a 24 nm gate length. Doping in the channel is  $1.5 \times 10^{18}$  cm<sup>-3</sup>, and a semi-insulating substrate is included. The transient simulation starts from an initial steady state. The simulation time step is 0.5 fs.

#### 26051 FOCUSED ION BEAM IMPLANTATION

John Melngailis D.A. Antoniadis

Massachusetts Institute of Technology

SL: DARPA

SC: ETDL, HDL, NVEOC

Further measurements of the RF performance of the tunable Gunn diodes have been carried out. Compact voltage controlled oscillators, injection locked oscillators, and dielectric oscillators were built using the tunable focused-ion-beam implanted Gunn diodes. The frequency could be tuned from 5 to 25 GHz by varying the bias across the Gunn diode. This is the widest bandwidth achieved with a single oscillator. These devices represent a family of fixed and swept frequency sources which are extremely simple. They are of interest to a broad user community for military

#### **B**. Electron Devices

and commercial low cost RF functions. Further studies have been carried out on the light emission from the tunable Gunn diodes. The light emission comes only from the area where the Gunn domain is propagating, and can be seen in an optical microscope to change in size as the bias and frequency are changed. Focused ion beam implants of As into long channel CCD structures have been carried out in collaboration with A.L. Lattes and S.C. Munroe of Lincoln Laboratory. In long-channel CCD's which are used in imaging and signal processing, the speed is limited by the ability of charge to diffuse out of the long potential wells. A gradient of doping, which can be implanted with a focused ion beam, produces a built in drift field and speeds up the charge transfer. Thus CCD's with 26 µm channels built with a gradient of doping were found to have a maximum clocking frequency of 41 MHz compared to 2.5 MHz for conventional uniformly doped devices.

#### Reports:

No. 1 in previous edition.

- Research Laboratory of Electronics Progress Report No. 132, by Jonathan Allen and Daniel Kleppner, TR, Jun 90, 7 pp. AD A224 306
- 3. Merging Focused Ion Beam Patterning and Optical Lithography in Device and Circuit Fabrication, by James E. Murguia et al., MS, J Vac Sci Tech.

# 26151 STUDY OF ULTRA SHORT HFET DEVICES WITH INP SUBSTRATES

Lester E Eastman Cornell University

SL: ETDL SC: HDL

Means of reducing gate leakage current due to low Schottky barrier heights has been emphasized. Modest improvements have been achieved in other laboratories using: (a) high aluminum pseudomorphic InAlAs barriers just under the gate metal ( $\sim$ 3:1 less leakage current at GE), and (b) the use of platinum rather than titanium as the Schottky barrier metal  $(\sim 20:1$  less leakage current at Plessey) to raise the barrier by .090 V. In order to take advantage of the latter, future experiments will use Pt rather than Ti Schottky metal barriers. The use of a buried acceptor layer under Ti Schottky metal gates was pursued to sharply lower the gate leakage current. Be was used as the acceptor, and sheet density values of 4 and  $6 \times 10^{12}$ , 100Å below the gate, were investigated. At first, atomic planar doping was used, but anomalous, fast Be diffusion reduced the effect. Later a thin (50A) layer, uniformly-doped with Be, yielded sub-

#### **B**. Electron Devices

stantial results with 10–100:1 less gate leakage current. Diodes of Schottky metal on N on N  $^{+}$  InAlAs, lattice-matched to InP, were used to show the advantage of this buried acceptor layer, placed 100Å under the gate metal. MODFET wafers with increased donor sheet density near the channel, to offset the acceptor sheet density near the gate, were grown. Electron sheet density values near  $2 \times 10^{12}$ /cm<sup>2</sup> were achieved. Such structures, with Ti and Pt Schottky metal gates, are being processed into MODFET's. These MODFET's are being kept planar, following a successful study of bombardment isolation, to be sure that the gate pad, and its connection to the gate, will all have low leakage, enhanced Schottky barriers.

#### Reports:

No. 1-6 in previous editions.

- Submicrometer-Gate Indium Phosphide-Based Field-Effect Transistors for High-Frequency Applications, by Jente Benedict Kuang, PhD Thesis, 1990, 160 pp.
- Cryogenic Noise Performance of OMVPE-Grown InGaAs InP MODFET, by J.B. Kuang et al., SPIE Proc 1288,258(1990). AD A231-216
- High-Current Lattice-Strained In<sub>0.80</sub>Ga<sub>0.41</sub>A8 In<sub>0.85</sub>Al<sub>0.48</sub>A8 Modulation-Doped Field-Effect Transistors Grown by Molecular Beam Epitaxy, by J.B. Kuang et al., *Appl Phys Let* 57,1784(1990), AD A231-332
- Progress in High Frequency Heterojunction Field Effect Transistors, by Lester F. Eastman, Proc. of ESSDERC 90 Conference, 1990, 619. AD A231-064
- I.E. This number not used.
- Optimization of Modulation Doped FET Structures, by Paul J. Tasker et al., SPIE Proc 1288,212(1990) AD A231 169
- The In-Plane Effective Mass in Strained-Layer Quantum Wells, by B.K. Ridley, J Appl Phys 68,4667(1990). AD A231 140

# 26278 ELECTRON-PHONON INTERACTION, TRANSPORT AND ULTRAFAST PROCESSES IN SEMI-CONDUCTOR MICROSTRUCTURES

Sankar Das Sarma University of Maryland

SC: ETDL

Calculations were made of quasi-particle properties of a polar two-dimensional electron gas, taking into account both the Coulomb and the Frohlich interaction in the weak-coupling limit. The resultant manypolaron self-energy differs significantly from the one-polaron result, and shows interesting and observable many-body structure in the density of states. Electron-electron and electron-phonon interactions are found not to be multiplicative in such a coupled system. Dynamical electron-electron and electronphonon interaction corrections to the conductionand valence-band edges of photoexcited quasi-twodimensional quantum wells were calculated for arbitrary quantum-well widths and electron-hole densities. Band-gap renormalization, when expressed in Rydberg units, is shown to be an approximate universal function of the effective *rs* parameter and the well width.

## 26484 SELECTED AREA EPITAXIAL GROWTH FOR COMPLEMENTARY HBT APPLICATION

R.W. Grant

Rockwell International Corporation

SC: ETDL. HDL

The focus has been the fabrication of small npn and pnp heterojunction bipolar transistors processed in parallel which have acceptable high frequency performance. Additional material was grown by MBE to provide npn and pnp structures on the same wafer for processing. This involved the growth of pnps, material removal in alternate fields, the regrowth of npns, and the removal of the polycrystalline overgrowth, to produce npn and pnp layer structures on the same wafer. A basic limitation of the regrowth approach to produce complementary HBT circuits is the morphology of the epitaxy near the boundary between npn and pnp devices. This limits how close different type devices can be placed. There is a boundary region of about 5 microns outside of which smooth, high quality material is observed. Through the use of standard planarization techniques, metal connections can be reliably made over these boundaries. A suitable mask set was selected for co-processing. Key factors in the decision were the fabrication of a number of different size devices, as well as the realization of some simple circuits. npn and pnp devices were processed in separate fields in order to simplify fabrication: however, this approach also produced some complexities in retaining alignment marks. A number of process modifications were necessary to accommodate the concurrent processing of npn and pnp devices. At the base pedestal and light field emitter steps, etch processes were modified to cause the InAs/InGaAs contact layers of the npn devices to be etched at near the same rate as the GaAs contact layers in the pnp devices. In addition, the baseline digital process was modified in order to maximize the number of steps in which both devices could be processed simultaneously.

# 26666 GROUP II CUBIC FLUORIDES AS DIELECTRICS FOR 3-D INTEGRATION AND GaAs-BASED OPTOELECTRONIC STRUCTURES

Antoine Kahn Princeton University

\_\_\_\_\_

SL: ETDL

Several difficulties arise with the growth of GaAs on fluorides. The first is associated with the well known thermal mismatch between the two materials. This problem is dealt with by growing a Ca/Sr concentration ratio which gives lattice match at intermediate temperature  $\sim 300^{\circ}$ C. The second problem is more specific to the (100) orientation. The morphology of the (100) fluoride surface is not ideal on the microscopic scale, as (111) facets develop to reduce the large electrostatic dipole energy of the (100) surface. This faceting can induce anti-phase nucleation in the GaAs. Finally, adhesion of GaAs might not be sufficient on a "untreated" fluoride surface. A Japanese group has shown that electron beam irradiation prior to GaAs growth promotes stronger bonding and improves the quality of the layer. Electron beam irradiation is known to decompose the top fluoride atomic layers through an Auger-type relaxation, and to release E The remaining metal atoms, Ca and Sr, strongly bond to As and improve adhesion. A number of GaAs layers have been grown on Ca<sub>0.45</sub>Sr<sub>0.55</sub>F<sub>2</sub> at growth temperatures, ranging between 520°C and 610°C. During the growth of the top GaAs layer. RHEED consistently showed a  $(1 \times 1)$  structure with some evidence of three-dimensional growth. This could be due to the fact that the fluoride surface contains a high density of (111) facets. A faint  $(2 \times)$ structure was occasionally obtained. Scanning electron micrographs on a 2000Å GaAs film also showed roughness on the micron scale. The electron channeling patterns, indicative of near surface crystallinity. were sharp although inferior to those of the GaAs buffer layer. The best layers were obtained for a growth temperature of  $\sim 600^{\circ}$ C.

#### Reports:

No. 1-3 in previous editions.

- Ca<sub>0.5</sub>Sr<sub>0.5</sub>F<sub>2</sub> (100)GaAs by Molecular Beam Epitaxy, by S Horng et al., Proc. 2nd Intl Cont. on Elec. Mats, 1990, 229. AD A238 433
- Growth of GaAs/Ca<sub>0/4</sub>sSr<sub>0/55</sub>F<sub>2</sub> GaAs Structures by Molecular Beam Epitaxy, by S. Horng et al., MS.
- Growth of GaAs CaseSto Ey 100GaAs by Molecular Beam Epitaxy, by S. Horng et al., MS.
- Ca<sub>0.5</sub>Sr<sub>0.5</sub>F<sub>2</sub> (100)GaAs for Epitaxial Regrowth and Electron-Beam Patterning, by S. Horng et al., MS.

#### 26686 ISOLATION MECHANISMS IN III-V DEVICES

George N. Maracas Arizona State University	
SL: HDL	SC: ETDL

Work is continuing on a study of GaAs grown at low temperatures and the effects of its presence on devices. The growth of this material by gas source MBE has been optimized, and researchers are comparing the properties of the material grown with  $As_2$ and  $As_4$ . The study of deep levels created by excess As in the lattice is showing that As related defects diffuse into subsequently grown device structures rather quickly. This has implications in the feasibility of using this material for reliable devices.

#### Reports:

No. 1-5 in previous editions.

 Electrical and Optical Characterization of Gas Source and Solid Source MBE Low Temperature Buffers. by R.A. Puechner et al., MS.

# 26711 SIMULATION OF ELECTRONIC TRANSPORT IN SEMICONDUCTOR HETEROLAYER DEVICES

K. Hess

University of Illinois SL: ARO, ETDL

A manuscript has been prepared which is a summary of work on high energy-high field transport. The manuscript gives also an outlook on the current research. In the area of impact ionization it has been possible to derive the ionization rate including the intracollisional field effect, collision broadening and effects of the complex bandstructure for an energyrange of six electron volts. This is thought to be the most complete theory of the ionization rate to data and the only existing theory that includes all important quantum effects. The theory is being applied to transport in MOSFET's in the deep submicron regime and generally to impact ionization in silicon. Another manuscript presents a comprehensive theory of phonon scattering in mesoscopic systems. This theory permits applications to very complex structures and includes effects of quantum interference. Calculations are underway on the scattering rates for T-shaped nanostructures with various acoustic phonon models. Numerical tools and algorithms are being expanded to calculate wave functions. Green's functions and the energy spectra of complex nanostructures. Work on time dependence has been completed.

#### **B**. Electron Devices

#### **VIII Electronics**

#### Reports:

No 1-2 in previous editions.

- Field Assisted Impact Ionization in Semiconductors, by J. Bude et al., MS.
- 4. Monte Carlo Simulation of GaAs Al<sub>s</sub>Ga<sub>1</sub>, As Field-Effect Transistors, by Isik C. Kizilyalli and Karl Hess, MS.
- Transient Response in Mesoscopic Devices, by Leonard E Register et al., MS.
- Circular Bends in Electron Waveguides, by E Sols and M. Macucci, *Phys Rev* 41,887(1990), AD A226-426
- 7. Approaches to Quantum Transport in Semiconductor Nanostructures, by V. Pevzner et al., MS.
- Electronic Transport in Semiconductors at High Energy, by J.M. Higman et al., MS.
- 9. Scattering, Dissipation, and Transport in Mesoscopic Systems, by Fernando Sols, MS, *Phys Rev.*
- Numerical Simulation of Mesoscopic Systems with Open Boundaries Using the Multidimensional Time-Dependent Schrödinger Equation, by Leonard F Register et al., J Appl Phys 69,7153(1991). AD A238 202

#### 26755 SUPPRESSED ELECTRON-PHONON SCATTERING IN SUPERLATTICES

Lester E. Eastman Cornell University

#### SL: ARO, ETDL

The vexed question of describing confined optical phonons has and is being addressed. It is now generally accepted that both mechanical and electromagnetic boundary conditions have to be taken into account, so all the earlier treatments based on the featureless dielectric continuum concept can be discarded. Models based purely on mechanical boundary conditions are likely to be nearer the truth, but unease about potential discontinuities in these models persists. More recent attempts to many lattice dynamics to continuum models manage to overcome discontinuities by introducing short-range vibratory components in a somewhat ad hoc fashion, but they still reveal strong tendencies to emphasize EM over mechanical connector rules. This tendency is at its strongest in the treatment of Fuchs-Kliewer (FK) surface polaritons which derive their properties purely from EM boundary conditions, with mechanical considerations neglected entirely. Worse still, their interaction with electrons is still being treated as a Frohlich interaction instead of an EM interaction. FK modes, being transversely polarized, have a vector potential but not a scalar potential. One point of agreement is that guided LO modes interact with electrons more and more weakly the narrower the well, but if interface modes exist this phonon suppression is

likely to be canceled out. The main question is therefore, what structures do not support interface modes. The two interface modes which are important are (a) FK modes and (b) LO modes. The current thrust of the theoretical work is to resolve the boundary-condition problem and thereby to obtain conditions for inhibiting these modes.

# 26760 DEVELOPMENT OF A 500 GHz OPTOELECTRONIC MODULATOR USING SUPERCONDUCTING TRANSMISSION LINES

Gerard Mourou

University of Michigan

SL: HDL

The success of the 500-GHz GaAs-based travelingwave electro-optic phase modulator relies on one's ability to velocity-match the optical and electrical waveforms to within less than one picosecond. It was demonstrated that velocity mismatch as low as 0.5 picosecond is indeed possible by using a GaAs superstrate to encapsulate the electrical transmission line. This process slows the electrical signal to match the optical signal. The problem is further complicated by the need to use GaAs/AlGaAs structures to form the optical waveguide. Studies have indicated that the resulting increase in the speed of the optical signal amounts to no more than 1 picosecond in additional walkoff. Furthermore, the speed of the electrical signal can also be increased by introducing a submicrometer air gap between the substrate and superstrate. A new Ti:sapphire laser capable of delivering 100 mW of usable (750-950 nm) subpicosecond pulses has been developed for characterizing the device for its intended application as a modulator. A sister technology also under development is the fabrication of multihundred-gigahertz photodetectors. Tests are being made of both metalsemiconductor-metal photodiodes with submicrometer interdigitated electrodes and low temperature-grown GaAs (LT-GaAs)-based photoconductors, also with submicrometer interdigitated electrodes. The research into the area of LT-GaAs photodetectors is completely new and holds promise for single picosecond response times while maintaining high signal-to-noise. Another area of new interest, that also uses LT-GaAs, is the generation of high-voltage electrical pulses having 1 picosecond rise time and a full width at half maximum of 3 picoseconds. To date, researchers have switched 850 volts in a coplanar transmission line configuration having an electrode spacing of 60

micrometers. This corresponds to an electric field greater than  $10^4$  volts/cm. The high voltage pulse represents a 100-fold increase in a mplitude over conventional technology used to generate electrical pulses of comparable duration. With this new switching technology combined with electro-optic sampling all the required ingredients are in hand for performing nonlinear terahertz spectroscopy.

#### Reports:

- I.4 Picosecond-Risetime (Pigh-Voltage Photoconductive Switching, by T. Motet et al., MS, Appl Phys Let.
- Propagation of Picosecond Electrical Pulses in GaAs for Velocity-Matched Modulators, by Yi Chen et al., MS.

# 26923 NOVEL ENGINEERED COMPOUND SEMICONDUCTOR HETEROSTRUCTURES FOR ADVANCED OPTOELECTRONICS AND OPTOELECTRONIC INTEGRATED CIRCUIT APPLICATIONS

N. Holonyak, Jr.

University of Islanois

SU: HDL SC: NVEOC

The objective of the research is to advance the technology base required to realize high-performance phased array lasers, superlattice and quantum-well avalanche photodiodes, high-speed electronic amplifiers and laser or modulator drivers. An integrated research program will be conducted for the study of the crystal growth and characterization, as well as device design, fabrication and characterization of electronic and optoelectronic structures made of compound semiconductors.

#### 26941 MESOSCOPIC EFFECTS IN ELECTRONIC MICROSTRUCTURES

Rostislav Serota University of Cincinnati

SC: HDL

An investigation was made of orbital magnetic phenomena, such as the localization interaction corrections to the magnetic response and its mesoscopic fluctuations, in small disordered metallic systems. The Aharonov-Bohm response and the response to the flux penetrating the metal have been studied. Consequences of the absence of sample contact with electron reservoirs in a typical magnetic measurement have been worked out. Results indicate that (*a*) the atomic-like linear response of a clean metallic sample sets the scale of the maximal response for the flux smaller than the flux quantum; (b) for stronger fields, the scale of maximal response is set by the envelope of the de Haas - van Alphen oscillation; (c) the susceptibility fluctuation in a disordered metallic sample is shown to be larger than its mean value in the parameter  $(k_F l)$ , except for very weak fields whose flux through the sample is much smaller than the flux quantum; for such weak fields, the average susceptibility is shown to be paramagnetic in sign and of the magnitude larger than the Landau susceptibility, albeit smaller than the susceptibility fluctuation; and (d) the significance of the flux scale smaller than the flux quantum is attributed to the lack of phase and energy relaxation of a diffusing particlehole pair at the boundary of an isolated sample; for larger fluxes, the magnitude of the average susceptibility drops to the order of Landau value and eventually saturates to precisely the Landau diamagnetic susceptibility as the flux through the sample becomes larger than the flux quantum. A theory of orbital magnetism is being extended to the strong magnetic field regime which is possible to separate into two distinct regions: first, when the electron mean-freepath becomes longer than the flux length, leading to complicated quasi-ballistic scattering and, second, the quantum Hall regime when the cyclotron frequency becomes larger than the inverse elastic scattering time.

Reports:

No. 1-3 in previous editions.

 Orbital Magnetism of Mesoscopic Systems, by S. Oh et al., MS, *Phys Rev.*

# 27443 THEORETICAL AND EXPERIMENTAL STUDIES OF QUANTUM WELLS

Raphael Tsu

University of North Carolina at Charlotte

SL: ETDL

Resonant tunneling in 3-dimensionally quantum confined (3DQC) microcrystalline silicon ambedded in a SiO<sub>2</sub> barrier was experimentally observed. Amorphous silicon (*a*-Si) is evaporated on S<sup>4</sup> wafer of low *n*-doping. The 120A *a*-Si layer is subsequently annealed into *mc*-Si and thermally oxid red into a layer of *mc*-Si sandwiched between *a*-Si  $D_2$ . Aluminum contact on top of the oxide completes the diode structure for transport measurements in the vertical direction. The salient features of the experiment are summarized: (*a*) broad peaks give distribution of grain size; (*b*) sharp peaks, delta function like, give

#### **B**. Electron Devices

the density of states of the 3DQC of a cluster defined by wavefunction overlap of particles of nearly equal size; (c) steps give the density of states of onedimensionally quantum confined tunneling, 1DQC, due to the complete coupling of states forming a two-dimensional sheet, resulting in the usual quantum well configuration; (d) 3DQC gives rise to quantized charge accumulation of 2e per state, resulting in a potential rise of 2e/c with c being the capacitance. The results are extremely important to technology because silicon is involved, and to basic physics because transition from 3DQC to 1DQC in the same structure, and almost a "phase transition" from individual 3DQC to clustering resembling to Mott transition.

#### Reports:

- 1. Stark Quantization in Superlattices, by Raphael Tsu and L. Esaki, MS, Phys Rev Rapid Commun.
- 2. Resonant Tunneling in Microcrystalline Silicon Quantum Box Diode, by Raphael Tsu et al., MS
- 3. Some New Insights in the Physics of Quantum Well Devices, by Raphael Tsu, MS
- 4. Resonant Tunneling via Microcrystalline Silicon Quantum Confinement, by Qiu-vi Ye et al., MS, Phys Rev Let

# 27578 DEVELOPMENT OF NANOSTRUCTURE FABRICATION TECHNOLOGY AND NEW ELECTRON-QUANTUM WAVE DEVICES

Stephen Y. Chou

University of Minnesota, Minneapolis

SC: ETDL, HDL, SDC

An ultra-high resolution electron beam lithography system (EBL) for nanolithography has been built by modifying a commercial high resolution scanning electron microscope and adding pattern generator electronics, that were designed and built. Special measures have been taken in modification, design of electronics, and reduction of noise from various sources to achieve a very high resolution that can be equaled by only three or four other U.S. universities. Using the EBL system and novel fabrication technologies, it has been possible to make nanostructures and nanodevices of sub-30-nm minimum feature sizes. Two highlights reported here are first, the fabrication of two transistor gates that are 15 nm wide and separated by 10 nm on GaAs for lateral quantum effect devices. The spacing is three times smaller than anyone else has been able to achieve on bulk semiconductors. The linewidth is the finest ever produced at a university. Second is the fabrication of ultrahigh-speed metal-semiconductor-metal photodetectors on GaAs with sub-30-nm finger-width, the smallest ever reported in literature.

# 27883 AlAs/InAs/InGaAs QUANTUM WELL BASE n-n-n TRANSISTORS

Clifton G. Fonstad Massachusetts Institute of Technology

SL: ETDL SC: HDL

The research objective is to improve the understanding of phenomena underlying the operation of threeterminal quantum-well-base transistors. The research approach will be to apply techniques recently discovered at the Massachusetts Institute of Technology for exposing and making electrical contact to quantumwell bases and to explore the use of interlayers and doping to control depletion and accumulation effects on a scale small relative to the de Broglie wavelength of the electron.

# 28004 MODELING FAILURE AND RELIABILITY IN NEW-GENERATION DEVICES

Jeffrey Frey	
University of Maryland	

SC: ETDL. SDC SL: HDL

Researchers have moved toward an understanding of why, and how much, silicon MOSFETs can be expected to become relatively more reliable as their gate lengths are shrunk below about 0.15  $\mu$ . The average electron energy at any point in a device is a measure of how many electrons are "hot" enough to cause such reliability problems as gate and substrate currents in MOSFETs, or real-space transfer in HEMTs. By calculating this quantity for sample MOSFETs designed to have equal peak electric fields but with channel lengths from  $0.5 \,\mu$  to  $0.20 \,\mu$ , the peak value of energy decreased as gate lengths decrease below about 0.15 µ. Therefore, for these MOSFET channel lengths, fewer troublesome hot electrons exist in the channel, as channel length decreases. This phenomenon is explained by a reduction in the number of thermalizing collisions that any electron can undergo, as the channel length is shortened. Studies of the reliability of compound semiconductor MESFET and HEMT devices continued, and additional progress was made on developing models for the simulation of quantum effects in the potential well created at the heterostructure, and the interaction of these effects with the distribution of electrons in both

momentum and real spaces. An effort to produce color plots of the two-dimensional distributions of such quantities as particle densities, energies, and current densities, has begun.

## 28325 HIGH PERFORMANCE GaAs MICROCOMPUTER SYSTEM

W.P. Birmingham R.B. Brown R.J. Lomax University of Michigan

> SL: ARO, ETDL, MICOM, SC: ARO, SDC NVEOC, SDC

The major objective of this work is a computer which implements the MIPS II instruction set architecture in VLSI GaAs direct-coupled FET logic. The performance goals are 4-ns instruction time and  $\leq 1.5$ cycles per instruction, which will result in 167 native MIPS. The time goal was to have a first prototype in 1991. The major blocks are a CPU, floating point accelerator, memory management unit, and a  $1k \times 32$ GaAs SRAM. These chips, mounted on a multichip module, together with silicon secondary-cache chips and a bus interface chip, will replace the CPU board in a MIPS MC6280 chassis. The resulting general purpose computer will run a conventional Unix environment and support standard programming languages and languages and networking protocols. Work has been lone in several areas: system design of the GaAs microcomputer, circuit design, IC testing, and development of design automation tools for architectural and timing simulation and for automatic compilation of GaAs circuits.

#### Reports:

No. 1-3 in previous editions.

4. Implementing a Cache for a High-Performance GaAs Microprocessor, by O.A. Olukotun et al., MS.

# 28329 RISC PROCESSOR FOR SUPERWORKSTATION AND TERA-OPS PARALLEL PROCESSING APPLICATIONS

John E. McDonald Rensselaer Polytechnic Institute

NVEOC. SDC

SL: ARO, ETDL. MICOM. SC: ARO, SDC

Work has been done toward producing a RISC engine which the P.I. calls F-RISC (the Fast Reduced Instruction Set Computer). The work has been di-

#### **B.** Electron Devices

vided into three categories. First has been the development of a standard cell library for the Rockwell GaAs HBT process. The second task has been conducting a GaAs review of the architecture of the Si based predecessor project which served as the basis of the proposed work. The third has been the development of the CAD tool interface for creation of the first two chips needed for the architecture. F-RISC was based on the Berkeley RISC II architecture, which obtains at least part of its high performance by extensive pipelining in the system. Most of the rest of the speed improvement comes from utilization of the fast Rockwell HBT devices, which offer 18 ps minimum gate delay. A large part of the research involves determining the optimum partition of the architecture and management of heat dissipated. Advanced forms of packaging are required, specifically a high thermal cooling rate thin film multichip module (MCM) capable of supporting four phase clock signals up to 8 GHz. The selected implementation involves use if a thin film MCM, and a bit-slice partition for the digital subsections of the processor. Pipelining has been introduced where possible in the architecture to hide many of the chip-to-chip delays normally associated with the multichip realization. Several other chip-to-chip connections which cannot be pipelined must be kept short to minimize the impact of these delays.

Reports:

- 1. A Fast Reduced Instruction Set Computer for Implementation with Advanced Bipolar and Hybrid Water Scale Technology, by Hans J. Greub, TR, Feb 91, 311 pp.
- High-Performance Standard Cell Library and Modeling Technique for Differential Advanced Bipolar Current Tree Logic, by Hans J. Greub et al., *IEEE J Sol St Circuits* 26,749(1991). AD A238 621

#### 28345 FOCUSED ION BEAM FABRICATION OF MICROELECTRONIC STRUCTURES

John Melngailis

Massachusetts Institute of Technology

SL: ETDL SC: SDC

Focused ion beam induced deposition is a new technique of film growth. Minimum dimension deposits of metal down to 0.1  $\mu$ m have been demonstrated by earlier research. This technique provides a new level of flexibility in obtaining patterned metal films which may be quite useful for in-situ processing, in combination with, for example, MBE or MOCVD growth. In addition, it has already been accepted in practice as the technique of choice for repair of integrated

#### C. Antennas and EM Detection

circuits (making local submicrometer dimension wiring) and for the repair of photomasks and x-ray lithography mask. Work has concentrated on understanding the fundamental mechanisms of the processes and on measuring and modeling deposition on nonplanar surfaces.

# 28406 TRANSPORT SIMULATION IN SPATIALLY MODULATED LOW-DIMENSIONALITY SYSTEMS

Jean Leburton University of Illinois

SC: SDC

The objective of the research is to improve the fundamental understanding of charge transport in spatially-modulated low-dimensionality systems. Monte Carlo simulation techniques and quantum mechanical models for electronic states in complex confining geometries will be applied to model charge transport in polar semiconductor structures including: onedimensional structures with fluctuating confinement parameters: cavities with confinement in two spatial dimensions; and periodically modulated quantum wires.

# 28461 QUANTUM TRANSPORT IN SEMICONDUCTOR DEVICES

David Ferry Arizona State University

SC: ETDL

The objective of the research is to improve the fundamental understanding of quantum transport in semiconductor structures. Quantum-transport effects will be investigated both experimentally and theoretically in semiconductor heterostructures appropriate to both metal-semiconductor field-effect transistors and modulation-doped field-effect transistors.

#### 28508 SCANNING TUNNELING MICROSCOPY OF III-V SEMICONDUCTORS

John D. Dow William E. Packard Arizona State University

SC: ETDL

The research objective is to improve the state-of-theart in fabricating and characterizing semiconductor surfaces with atomic-level precision. Scanning tunneling microscopy will be used to characterize cleaved

#### VIII Electronics

and stressed semiconductor surfaces and to fabricate atomic-scale features on semiconductor surfaces.

# 28594 TIME RESOLVED STUDIES OF IN-WELL AND VERTICAL CARRIER TRANSPORT IN MQW SEMICONDUCTOR STRUCTURES

Alan Miller University of Central Florida

SL: ETDL

The research objective is to improve the fundamental understanding for charge transport in multiple quantum well structures. Ultrafast laser techniques will be used to resolve in-well and cross-well carrier transport properties in multiple quantum well semiconductors.

# 28646 DENSITY MATRIX, SPACE CHARGE DEPENDENT, STUDIES OF CAPACITANCE VERSUS VOLTAGE OF QUANTUM WELL STRUCTURES

Harold L. Grubin Scientific Research Associates, Incorporated

SC: ETDL, HDL

The objective of the research is to advance the understanding of charge transport in semiconductor structures for ultrafast electronics. The density-matrix formulation of quantum transport theory will be used to model space charge effects in quantum-well structures and related ultra-high performance devices.

# C. Antennas and EM Detection

# 25045 GUIDED WAVE PHENOMENA IN MILLIMETER WAVE INTEGRATED CIRCUITS AND COMPONENTS

Tatsuo Itoh University of Texas at Austin

SL: CECOM

The full wave formulation for the microstrip discontinuities are being extended for the analysis of the in-line and offset microstrip gap discontinuities. Both the longitudinal and transverse currents are included in the formulation for the first time. Three FET amplifiers are connected in series to form a circular ring oscillator which has a radiating feature. In this

manner, a quasi-optical circularly polarized oscillator was constructed and tested. The measured results indicate an excellent axial ratio. A new quasi-planar transmission line was introduced and characterized. The line consists of a microstrip line with a dielectric overlay on which another strip is placed via an air layer. The upper strip is mechanically supported by stitch-like sections where the strip rests on the dielectric overlay. The line is suited for creating a high impedance section and naturally forms a broadside coupled line between the upper and lower strips. This line was analyzed by the spectral domain method including the loss. The experimental results measured at Hughes Aircraft and the computed results agree well up to 18 CHz. In order to increase the degree of integration in the active quasi-optical circuits, both surfaces of the substrate are utilized. One surface is a uniplanar configuration made of slot line resonator/antenna while a microstrip active circuit is placed on another surface. The negative resistance and electronically controlled reactance are generated by three-terminal devices and are coupled electromagnetically to the slot. Good results have been obtained which are useful for implementations of array functions. In the past, a number of periodic power combining oscillators have been developed. The present project is to provide theoretical foundations for the analysis and design of this type of configuration. Since the devices are strongly coupled, the conventional Adler's theory cannot be applied. Instead, the theory introduced by Kurokawa for radial combiners is modified. At the same time, a time-domain voltage-update method is being developed based on the large signal analysis.

#### Reports:

No. 1-43 in previous editions.

- Microwave and Millimeter-Wave Oscillators and Planar Power Combining Structures for QWITT and Gunn Diodes, by Amir Mortazawi et al., TR, Aug 90, 103 pp. AD A226 246
- 45. A Modified End-Coupled Filter Structure Designed to Broaden the Bandwidth of an Active Filter, by Chi-Yang Chang and Tatsuo Itoh, MS.
- 46. A Second Harmonic Power Combining Transceiver, by A. Mortazawi et al., MS.
- 47. Voltage-Frequency Update for Nonlinear Analysis of Free-Running and Injection-Locked Multiple-Device Oscillators, by H.D. Foltz et al., MS.
- 48. Analysis of Shielded Coplanar Waveguide Step Discontinuity Considering the Finite Metallization Thickness Effect, by Chih-Wen Kuo et al., MS.
- 49. Optical Control of Microwave Active Band-Pass Filter Using MESFETs, by Yukio Yamamoto et al., MS.
- A Circularly Polarized FET Oscillator Active Radiating Element, by J. Birkeland and T. Itoh, MS.

- 51. A Layered Negative Resistance Amplifier and Oscillator Using a FET and a Slot Antenna, by Shigeo Kawasaki and Tatsuo Itoh, MS.
- 52. A Slot Antenna with Electronically Tunable Length, by Snigeo Kawasaki and Tatsuo Itoh, MS.
- 53. Planar Transmission Lines with Finitely Thick Lossy Conductors and Lossy Substrates, by T. Kitazawa et al., MS.
- 54. Analysis of Stitch Line for Monolithic Microwave Integrated Circuits, by K. Kawasaki and T. Itoh, MS.
- 55. A MESFET Controlled X-Band Active Band-Pass Filter, by Yukio Yamamoto et al., *IEEE Microwave and Guided Wave* Let 1,110(1991). AD A239 699
- 56. Laser Tuning of a Planar Active Band-Pass Hitter Using MESFETs, by Yukio Yamamoto et al., MS.
- 57. Quasi-Optical Transmitter with Injection-Locked FET Amplifier, by Shigeo Kawasaki and Tatsuo Itoh, MS.

# 25339 MILLIMETER-WAVE APPLICATION OF SEMICONDUCTOR DIELECTRIC WAVEGUIDES WITH PLASMA LAYERS (SURFACE OR BURIED) GENERATED FROM SEMICONDUCTOR LASER

Jerome K. Butler

Southern Methodist University

SL: CECOM

Work has progressed along both theoretical and experimental development of dielectric surface emitting structures. Experimental work has been concerned with the design and fabrication of periodic waveguides fabricated with Al<sub>2</sub>O<sub>3</sub>. The waveguides were designed for first order Bragg radiation in the frequency range from 90 to 100 GHz. A number of waveguides have been designed and constructed including some with multiple sections of corrugations on them. The radiation pattern from these waveguides was measured by electronic scanning of the frequency. The experimental pattern was compared with that obtained from a simulation based on the Huyghen-Fresnel radiation theory (for the -1 order Floquet-Bloch wave). By frequency scanning the local millimeter wave sources, the far-field pattern scanned relative to the normal of the waveguide. For most of the waveguide structures, the far-field beam or major lobe scanned from 1.8 to 2.0 degrees per GHz. Thus, the beam could be frequency scanned about 20 degrees over a 10 GHz range or about 10 percent of the operating frequency. Experimental studies were also carried out on a two-section grating structure. Each grating section was about 25 teeth long or about 30 mm. The separation between the grating ends was about 20 to 25 mm. Each of the gratings was designed to radiate broadside at different frequencies. For example one was designed to radiate at about 98 GHz, the other at 102 GHz. The twosection waveguide was then excited with a 100 GHz source. The power was split so that the double grating section was excited with equal amounts of power from both directions. The experimental and theoretical radiation patterns had very close agreement. When the field at the input of each grating had identical phase, the far-field pattern produced a single broadside lobe.

Reports:

No. 1 in previous edition.

2. Experimental Verification of Grating Theory for Surface Emitting Structures, by Raj Ayekavadi et al., MS.

#### 25350 RESEARCH IN GROUND-TO-AIR MICROWAVE IMAGING

Bernard D. Steinborg University of Pennsylvania

SL: MICOM SC WSMR

Extensive data-taking at X-band of high resolution (1) meter range resolution, 150 MHz bandwidth) coherent radar echoes of aircraft were obtained. The objective is to build a database for high resolution 2D and 3D studies of detection and classification of targets in clutter. Data formatting, reduction and system self-calibration are partially completed. The system bandwidth is being increased from 150 MHz to 1 GHz in preparation for ultra-wideband studies. The 1 GHz modulator is completed. The system will be a 3-band radar (S, X and  $K_{\mu}$ ). It will have two polarizations (HH and VV). To achieve the required high sampling rate a digital sampling oscilloscope will be employed. Because it samples only a small number of range binds per pulse, target motion is precluded; as a consequence this equipment is designed for observing stationary targets in clutter. The upper field site at the Valley Forge Laboratory will be the test site. Previously, a new algorithm with fewer constraints for self-calibration and which appears to have superior sidelobe suppression properties was studied by computer simulation and reported. The algorithm was named the Energy Conservation Algorithm because it was based upon Parseval's theorem which equates energies on both sides of the Fourier transform. The computer simulation studies gave excellent results and led to considerable research enthusiasm. In particular, the sidelobes were more successfully lowered by this algorithm than by any of the other algorithms studied by the P.I. over the years. The algorithm has been applied to a variety of data sets of 150 MHz, wideband radar echoes of aircraft. The results were surprisingly poor. Efforts are being made to correct these poor results.

Reports:

No. 1 in previous edition.

- 2. Improved Adaptive-Beamforming Target for Self-Calibrating a Distorted Phased Array, by Bongsoon Kang et al., *IEEE Trans on Ant and Prop* 38,186(1990). AD A226 139
- 3. High Resolution Microwave Imaging Program, by Bernard D. Steinberg et al., MS.
- 4. Comparison of the Performance of the Energy Conservation Algorithm Using Simulated vs Experimental Microwave Data, by B.D. Steinberg and G.K. Borsari, MS.
- A Modification to the Energy Conservation Algorithm, by B.D. Steinberg and Geordi Borsari, MS.
- 6. Recursive Algorithm of OCWA for Microwave Imaging Systems, by Jinlong Zhang and B.D. Steinberg, MS.
- 7. Reduction of Sidelobes Using the "Clean" Technique, by Bernard Steinberg and I.H. Kim, MS.

# 25422 FULL-WAVE ANALYSIS OF MICROWAVE INTEGRATED CIRCUITS USING THE SURFACE INTEGRAL FORMULATION

Roger E. Harrington

Syracuse University

SL: CECOM

Work on the quasi-dynamic approach to arbitrarily oriented printed microstrip circuits has continued. The "quasi-dynamic" approach differs from the "quasistatic" solution in the sense that phase variation is included in the quasi-dynamic analysis. The region of validity of the quasi-dynamic approach has been investigated. Numerical results have been used to validate the applicability of this technique. Work has been done on the analysis of a shielded microstrip line of arbitrary cross section using a mixed potential electric field integral equation. It appears that the mixed potential approach, originally proposed by Mosig and Gardiol and used extensively by Michalski and Zheng is the most efficient one to use in the analysis of printed circuits. Due to the advantage of low cost, small size, light weight, and high reliability the microwave printed circuit (MPC) has become more and more popular during the past three decades. The theories of the MPC have been widely discussed in the literature.

Reports:

No. 1-7 in previous editions.

 Electromagnetic Scattering From and Transmission Through Arbitrary Apertures in Conducting Bodies, by Taoyun Wang et al., *IEEE Trans on Ant and Prop* 38,1805(1990). AD A232 267

#### **Vill Electronics**

- 9. On the Location of Leaky Wave Poles for a Grounded Dielectric Slab, by Chung-I G. Hsu et al., *IEEE Trans on Microwave Theory and Tech* 39,346(1991).
- 10. On the Modeling of Conductor and Substrate Losses in Multi-Conductor, Multi-Dielectric Transmission Line Systems, by Tawfik Rahal Arabi et al., MS, *IEEE Trans on Microwave Theory and Tech.*

# 25557 ELECTRO-OPTICS DISPLAY RESEARCH, TEST AND EVALUATION LABORATORY PROGRAM

#### Donald L. Moon

University of Dayton

SL: NVEOC

The following objectives were met: (a) completed background reading and search of binocular vision modeling as it pertains to rectangular displays; (b) organized and installed a test set-up for studying the human response in terms of the field of view overlap, time of exposure, and rectangular display dimensions; and (c) began taking test data in the system designed in item (b).

#### Reports:

No. 1-2 in previous editions.

- 3. Dynamic Modulation Transfer Function of Display System, by A.A. Awwal, MS.
- Development of the Modulation Transfer Function and Contrast Transfer Function for Discrete Systems, Particularly Charge-Coupled Devices, by John C. Feltz, Opt Eng 29,893(1990). AD A230 837
- Restoration of Dynamically Degraded Gray Level Images in Phosphor Based Display Devices, by M.L. Gao et al., Opt Eng 29,878(1990). AD A231 337
- Device Nonspecific Minimum Resolvable Temperature Difference for Infrared Imaging Systems Characterization, by M.L. Gao et al., Opt Eng 29,905(1990). AD A230 783
- Modulation Transfer Function of Charge-Coupled Devices, by John C. Feltz and Mohammad A. Karim, Appl Opt 29,717(1990). AD A230 777

## 26128 BASIC POLARIMETRIC SIGNAL/IMAGE PROCESSING STUDIES

Wolfgang-M. Boerner Hyo J. Eom University of Illinois at Chicago

#### SL: BRL, WES SC: AFGL, BRADEC

A report has been prepared in which basic principles of radar polarimetry are introduced. The target characteristic polarization state theory is developed first for the coherent case using the three stage, the basis transformation, and the power matrix optimization procedures. Kennaugh's and Huynen's theories of radar target polarimetry are verified for the monostatic reciprocal case. It is shown that there exist in total five unique pairs of characteristic polarization states for the symmetric scattering matrix of which the two pairs, the cross-polarization null and copolarization max pairs, are identical, whereas the cross-pol max and the cross-pol saddlepoint pairs are distinct. These three pairs of orthogonal characteristic states are also mutually orthogonal on the polarization sphere. The fifth pair, the co-pol max / cross-pol null and the cross-pol max pairs which determines the target characteristic circle on the polarization sphere reestablishing Huynen's "polarization fork" concept.

Reports:

- Optimal Polarization States Determination of the Stokes Reflection Matrices [Mp] for the Coherent Case, and of the Mueller Matrix [M] for the Partially Polarized Case, by Wei-Ling Yan and Wolfgang-Martin Boerner, MS.
- 2. Determination of the Characteristic Polarization States of the Target Scattering Matrix {S(AB)} for the Coherent, Monostatic and Reciprocal Propagation Space, by An-Qing Xi and Wolfgang-Martin Boerner, MS.
- 3. On the Basic Principles of Radar Polarimetry: The Target Characteristic Polarization State Theory of Kennaugh, Huynen's Polarization Fork Concept, and Its Extension to the Partially Polarized Case, by Wolfgang-Martin Boerner et al., MS.
- 4. Polarization Correction and Extension of the Kennaugh-Cosgriff Target-Ramp Response Equation to the Bistatic Case and Applications to Electromagnetic Inverse Scattering, by Bing-Yuen Foo et al., *IEEE Trans on Ant and Prop* 38,964(1990). AD A231 141
- The Characteristic Radar Target Polarization State Theory for the Coherent Monostatic and Reciprocal Case Using the Generalized Polarization Transformation Ratio Formulation, by Wolfgang-Martin Boerner and An-Qing Xi, AEU 44,273 (1990). AD A231 211
- 6. On the Basic Principles of Radar Polarimetry: The Target Characteristic Polarization State Theory of Kennaugh, Huynen's Polarization Fork Concept, and Its Extension to the Partially Polarized Case, by Wolfgang-Martin Boerner and Wei-Ling Yan, MS.

#### 26381 MILLIMETER-WAVE GRID OSCILLATORS

David B. Rutledge

California Institute of Technology

SL: CECOM

The focus has been in developing a new oscillatorgrid design. In previous designs, the gate and drain lead were vertical lines, parallel to the electric field, and the source leads were horizontal, parallel to the magnetic field. In the new design, the gate leads are horizontal, and the drain and source leads are vertical. In this case, the electric field does not couple directly to the gate lead, but rather by parasitic coupling to the other leads. This means that the signal fed back to the gate is weak at low frequencies, and stronger at higher frequencies. This is called a "gate-feedback grid." It is thought that the gate-feedback circuit will allow making grid oscillators at frequencies up to the maximum allowed by the individual device. The transistor packages are not convenient for this configuration, so researchers have used chips and made wire-bond connections. Initial results have given oscillations, but there seems to be some difficulty locking the transistors to a mode of the cavity. It is possible that the feedback to the gate from the cavity is too weak to lock the transistors.

#### Reports:

No. 1-6 in previous editions.

- Monolithic Millimeter-Wave Two-Dimensional Horn Imaging Arrays, by Gabriel M. Rebeiz et al., *IEEE Trans on Ant and Prop* 38,1473(1990). AD A232 168
- 8. S-Parameter Measurements of Quantum-Well Devices, by Olga Boric et al., MS.
- 9. Progress in Grid Oscillators, by Zoya Basta Popovic et al., MS.
- An X-Band MESFET Grid Oscillator with Gate Feedback, by Robert M. Weikle, II et al., MS, *IEEE Trans on Ant and Prop.*
- 11. Development of a Monolithic 94 GHz Quasi-Optical 360 Degree Phase Shifter, by L.B. Sjogren et al., MS.
- 12. A 100-Element Schottky Diode Grid Mixer, by Jonathan B. Hacker et al., MS. *IEEE Trans on Ant and Prop.*
- 13. Adjustable *RF* Tuning Elements for Planar Millimeter Wave and Submillimeter Wave Circuits, by W.R. McGrath et al., MS.
- 14. Technology for Millimeter-Wave Imaging, by David Rutledge, MS.

# 26599 INTERINJECTION-LOCKED QUASI-OPTICAL POWER COMBINERS AND PHASED ARRAYS

Karl D. Stephan

University of Massachusetts

SL: CECOM

A resonant-tunneling diode has oscillated at X-band frequencies in a microwave circuit consisting of a slot antenna coupled to a semi-confocal open resonator. Coupling between the open resonator and the slot oscillator decreased the noise-to-carrier ratio by about 36 dB relative to that of the slot oscillator alone in the 100–200 kHz range. A circuit operating

near 10 GHz has been designed as a scale model for millimeter and submillimeter-wave applications.

Reports:

No. 1 in previous edition.

- Noise Characterization and Modeling of a Resonant Tunneling Diode Self-Oscillating Mixer, by Chong Lap Woo, MS Thesis, 2990, 69 pp.
- A Technique for the Measurement of Mutual Impedance of Monolithic Solid State Quasi-Optical Oscillators, by William P. Shillue and Karl D. Stephan, *Microwave and Opt Tech Let* 3,414(1990). AD A232 220

#### 26620 MILLIMETER-WAVE QUASI-OPTICAL ARRAYS

Richard C. Compton

Cornell University

SL: CECOM

Research efforts have resulted in the following: (a) Optimizing the performance of an active patch design using MESFETs, and constructing a second 16-element array with high power and high efficiency; (b) developing a theory describing the mutual synchronization and stability of coupled oscillator elements in the arrays; (c) improving the patch and device modeling for planar active radiating/oscillating elements; and (d) initial processing and characterization for the monolithic fabrication of a 50 GHz, 16-element active patch array using GaAs Schottky-barrier IMPATT diodes.

Reports:

No. 1-4 in previous editions.

- Quasi-Optical Power-Combining Using Mutually Synchronized Oscillator Arrays, by R.A. York and R.C. Compton, *IEEE Trans on Microwave Theory and Tech* 39,1000(1991). AD A238 434
- Experimental Verification of the 2D Rooftop Approach for Modeling Microstrip Patch Antennas, by R.A. York et al., MS, IEEE Trans on Ant and Prop.
- 7. Optical Control of MESFET and HEMT Millimeter/Microwave Circuits, by C. Rehwinkle et al., MS.
- Accurate Full-Wave Approach for Modeling Patch Antennas, by B.J. Rubin et al., MS.

# 26651 MILLIMETER-WAVE QUASI-OPTICAL AND SPATIAL POWER COMBINING TECHNIQUES

Kai Chang

Texas A&M University

SL: CECOM

Coplanar waveguide filters. An electronically tunable coplanar waveguide filter with over 20 percent

tuning range has been developed. A patent application has been filed. Several industries are interested in using these filters for their systems. Active antenna elements using annular ring antenna. Integrated active antenna elements using annular ring antennas and Gunn diodes have been developed. The antennas demonstrated an output power of over 70 mW at 6.8 GHz. Three-probe microstrip circuit for scattering parameter measurements. The simple, compact, low cost three-probe microstrip circuit developed for the input impedance measurements has been modified and extended to the scattering parameter measurements. The results agree very well with those from HP 8510 automatic network analyzer. Low loss quasi-optical filter. An efficient coupling technique using a narrow slot in a waveguide opening has been developed to couple power into the Fabry-Perot open cavity resonator. A low loss filter was formed by this cavity with an insertion loss of less than 1 dB. The coupling technique should be useful for power combining.

#### Reports:

No. 1-9 in previous editions.

- 10. Integrated Active Antenna Using Annular Ring Microstrip Antenna and Gunn Diode, by Richard E. Miller and Kai Chang, *Microwave and Opt Tech Let* 4,72(1991). AD A234 120
- Analysis and Modeling of a High-Temperature Superconducting Floating Resonant Strip in Waveguide, by Michael K. Skrehot and Kai Chang. Intl J Infrared and Millimeter Waves 11,2355(1990). AD A234-341
- 12. Active Integrated Antenna Elements, by Julio A. Navarro et al., *Microwave J* Jan 91, p 115. AD A234 277

#### 26791 RESEARCH ON LEAD TITANATE FILMS FOR RADIATION DETECTION

Paul Kruse Barry Cole Honeywell Inc. SL: CECOM SC: CECOM, MICOM, MTL

PbTiO<sub>3</sub> films were deposited on Si<sub>3</sub>N<sub>4</sub>/Si and Pt/ Si<sub>3</sub>N<sub>4</sub>/Si substrates using a dual-target ion beam sputtering system. Deposition temperatures were varied between 450°C and 510°C, while the ratio of sputtering times of the titanium target to the lead target varied from 30:1 to 5:1. The best crystallinity was achieved at 480°C and a Ti/Pb sputtering time ratio of 7:1 when sputtering on a Pt/Si<sub>3</sub>N<sub>4</sub>/Si substrate. The only phase present was the pyroelectric perovskite phase, and the tetragonal splitting was clearly visible. The (110) and (101) orientations were preferred over other orientations, but the mixture between these two was approximately random. Films deposited under the same conditions on a Si<sub>3</sub>N<sub>4</sub>/Si substrate contained more grains with the (100) and (001) orientation with a shift from a random balance of these two to more of a (100) preferred orientation. In addition, a significant amount of the pyrochlore phase was present. This phase is slightly lead rich and is not pyroelectric. The presence of this phase suggests that the deposition temperature might still be slightly low or that the sputter time ratio might need to be increased slightly. The deposited film compositions were determined using three techniques, x-ray diffraction, Rutherford backscattering (RBS) and DC coupled plasma emission spectroscopy. The PbTiO<sub>3</sub> films are inert to most etchants that were tried, showing that these films should be very stable against environmental effects. A good correlation has been seen between the deposition time ratio and the Ti/Pb ratio in the film. Pt electrodes were deposited to make electrical measurements. All films had leaky capacitances. When silicon nitride was sputtered on top of the PbTiO<sub>3</sub> films capacitance measurements could be made. However the Si<sub>3</sub>N<sub>4</sub> film, having a much lower dielectric constant, dominated the capacitance behavior. The PbTiO<sub>3</sub> films were visually smooth but under high magnification in an electron microscope, small pinholes less than 0.1 microns in diameter were observed. Researchers believe these pinholes are caused by the very high deposition rate of lead and the resulting surface roughness. The Pb atoms do not have sufficient migration time to leave a smooth, pinhole free surface.

# 26949 IMPROVEMENTS IN OSCILLATORS FOR PLANAR MILLIMETER-WAVE CIRCUITS

Steven E. Schwarz University of California, Berkeley

SL: CECOM, ETDL

The principal emphasis of this project has been on a novel type of Gunn Oscillator microwave and millimeter source. The theory of this device was completed and published in early 1990, and researchers proceeded toward experimental verification. Several other projects are in progress. In one of these, theoretical work is being performed to promote understanding of "over and under" microstrip couplers, that is, of microstrip hybrids constructed in such a way that one conductor is deposited directly over the other. An experimental coupler of this type has been demonstrated elsewhere. Another project is

#### C. Antennas and EM Detection

intended to demonstrate experimentally the reduction of ohmic loss in coplanar waveguides through the use of two techniques originally invented by D.F. Williams. A new project, just begun, investigates the possibility of using liquid in microwave technology. The intended use is in phase-shifting devices, such as interferometer switches. Liquid crystal materials are expected to exhibit large changes of refractive index when static electric fields are applied. These changes are expected to be slow, but nonetheless adequate for many switching applications.

# 27304 MONOLITHIC MILLIMETER WAVE RADIATING SYSTEMS AND FEED NETWORKS

David R. Jackson University of Houston

SL: CECOM, HDL, MICOM

The research objective is to investigate two novel radiating systems for millimeter wave applications: first, a phased array of actively loaded microstrip patches; and second, a circular array of novel leaky wave antennas fabricated on multilayer substrate to improve directional characteristics of the array. Theoretical analysis, numerical implementations, and experimental verification is proposed for each system. The modeling will be based on a rigorous spectral-domain theory, and will account for all feednetwork interactions.

#### 27307 MILLIMETER-WAVE IMAGING TECHNOLOGY

Joseph Maserjian David B. Rutledge Jet Propulsion Laboratory California Institute of Technology

SL: ARO, CECOM, ETDI

The superconductor-insulator-superconductor tunnel junction can be used as an extremely sensitive detector in millimeter and submillimeter wave applications. The large inherent capacitance associated with this device results in a substantial impedance mismatch with typical antennas and, therefore, requires a tuning circuit for optimum results. At frequencies where waveguide dimensions are realizable, impedance matching can be accomplished by embedding the detector in a waveguide circuit with adjustable waveguide backshorts. At higher frequencies, where waveguide dimensions become prohibitively small, a

#### **VIII Electronics**

planar transmission line embedding circuit provides a reasonable alternative. Typically, such planar circuits offer no post-fabrication adjustability, resulting in demanding materials and design requirements. An adjustable planar embedding circuit based on coplanar transmission lines with movable noncontacting shorting elements has been developed. The shorting elements each consist of a thin metallic plate with an optimized arrangement of rectangular holes, placed along the insulated metallic transmission line to provide a periodic variation of the line impedance. Scale modeling has shown that large VSWR's can be achieved with these elements. A low frequency tuning circuit incorporating these shorting elements has been tested to demonstrate practical tuning ranges.

# 27873 ADVANCED ELECTROMAGNETIC METHODS FOR AEROSPACE VEHICLES

C.A. Balanis

Arizona State University

SL: AVRADA, CECOM

The main purpose of the equivalent surface impedance approach is to obtain the proper surface impedance representing a composite tructure so that the original complex problem can be implemented into the existing PEC based computer codes, such as NEC and ESP. To achieve this goal, the equivalent surface impedance was obtained for the PEC plate coated with composite material based on the following assumptions. The first one was that the plane wave is normally incident upon the interface between the air and dielectric. The second was that the plate structure is of infinite extent. Based on these two assumptions, the equivalent surface impedance representation of the structure was determined by enforcing the IBC at the interface of the air and dielectric material. The resulting surface impedance has been incorporated into the NEC (wire-grid) and ESP (surface patch) codes to calculate radiation patterns of a monopole mounted on a dielectriccoated PEC late and radar cross sections of a partially coated PEC plate and cube. However, there exist some discrepancies between measurements and predictions. The reason for these discrepancies is due to the fact that the finite size of the structure was neglected. In order to account for the effect of finite size, some modifications to the previous approach have been made. The preliminary results of the new approach showed some improvements over the old ones. Even though the new approach seems encouraging, extensive applications of the new technique to

various EM structures are necessary in the following period of this research.

Reports:

- 1. Automation of the Geometry Data for the NEC and the ESP Using the Super-3D, by J. Peng et al., MS
- 2. Progress: Development of an Interactive Graphics Programfor EM Codes, by J. Peng et al., MS
- 3. Evaluation of Input Impedance and Radar Cross Section of Probe-Fed Microstrip Patch Elements Using an Accurate Feed Model, by J.T. Aberle et al., MS. *IEEE Trans on Ant and Prop.*

# 27904 PRINTED CIRCUIT ELEMENTS WITH APPLICATIONS TO ANTENNAS, SCATTERING AND CIRCUITS

N.G. Alexopoulos

University of California, Los Angeles

#### SL: CECOM

The equiangular spiral slot antenna is well known as a broadband circularly polarized element. However, in its simplest form, it is a bidirectional antenna. Attempts to provide unidirectional patterns typically involve the construction of a lossy cavity or a ground plane on one side. A paper has been prepared which numerically investigates the characteristics of a planar, balanced center-fed, two-arm spiral slot antenna which is located on a conductor-backed dielectric substrate. Geometric complexity of both the antenna perimeter and feed area indicate that a numerical algorithm is the most tractable approach to predict antenna performance. The P.L. employs Galerkin's method to solve the aperture integral equation using planar triangular patch modeling. It is an extension of the method used by Rao, Wilton, and Glisson to solve EFIE problems. Other research concerned with numerically investigating the characteristics of a planar, balance, center-fed, two-arm, spiral slot antenna located on a semi-infinite dielectric halfspace. The aperture integral equation is solved using the method moments with triangular patches modeling the aperture electric field  $E_a$ . Since the aperture is finite. both feed and termination regions are modeled. Microstrip patch antennas have been investigated by a variety of methods, such as the cavity model, the transmission line model and moment method techniques. Among them, the spectral domain analysis, one of moment method techniques, could be considered as the most accurate method. However, most of these reports were confined to the study of the input impedance of microstrip patch antennas. Little of radiation properties have been revealed. In order to calculate the radiation patterns accurately, the high accuracy of the current distribution on both patch and feed line is required. A rectangular microstrip patch antenna with coplanar feed was analyzed by the spectral domain method. The radiation patterns calculated from the current distribution are compared with the measurement data and presented.

#### Reports

- A Generalized Method for Distinguishing Between Radiation and Surface-Wave Losses in Microstrip Discontinuities, by Tzyy-Sheng Horng et al., *IEEE Trans on Microwave Theory* and Tech 38,1800(1990). AD: A233-950
- 2 A Rigorous Dispersive Characterization of Microstrip Cross and T Junctions, by Shih-Chang Wu et al., IEEE Trans on Microwave Theory and Tech 38,1837(1990). AD A233-995.

# 28151 DEVELOPMENT OF THE MODIFIED DIAKOPTIC THEORY: ANALYSIS

Chalmers M. Butler Clemson University

SL CECOM

Work has continued on the development of the modified diakoptic theory and its applications to the analysis of microstrip and stripline array antennas. At present, preliminary analyses are being conducted on simple antennas made up of stripline, microstrip, and slot components in preparation for the more complex analysis of arrays. Of particular interest is the fact that the modified diakoptic theory has been adapted to the problem of radiation by narrow slots. A stationary expression for the short-circuit admittance between slot "ports" has been formulated to accommodate this slot problem: As is expected, one arrives at a short-circuit admittance (Y-parameter) matrix description for the *n*-port slot structure, in contrast to an open-circuit description in the case of a "metallic" antenna. The slotted stripline problem. which is a building block for the stripline-fed slotted array, entails the coupling of slots to strips between plates so a stationary expression for coupling between slot ports and strip ports has been developed. too. This expression may be interpreted as a generalization of h-parameters from 2-port theory to n-port theory. The diakoptic theory has been applied successfully to the case of a slot in ground plane, a bent wire coupled to a slot in a ground plane, and a slot in a parallel plate waveguide. In addition to the above work on slotted arrays, considerable effort has been devoted to analyses of the microstrip transmission system itself.

#### 28339 QUASI-OPTICAL MILLIMETER WAVE POWER COMBINING

James J. Gallagher Georgia Institute of Technology

SL: ARO, C.COM, SDC

The research objective is to investigate the use of quasi-optical power combining utilizing arrays of MESFETs and resonant tunneling devices in the millimeter to submillimeter spectral region. Attempts will be made to experimentally investigate the use of arrays of solid-state active elements placed in a transverse plane of an open resonator structure (Fabry-Perot). Emphasis will be placed upon the interface between point like solid state sources and the extended fields that exist within an open resonator. Also, the class of solid-state active elements investigated for use will be those with the potential for high conversion efficiency from the primary power source to millimeter wave power output. Devices under consideration are MESFETs or resonant tunneling junctions

# 28483 THEORETICAL AND EXPERIMENTAL STUDY OF LOW-LOSS, HIGH EFFICIENCY MONOLITHIC ANTENNA STRUCTURES AT 94 GHz

Linda P.B. Katehi Gabriel M. Rebeiz University of Michigan

> SL: ARDEC, CECOM, MICOM

The research objective is to investigate monolithic planar phased array antennas for electronically scanned millimeter wave systems and subharmonic millimeter wave monopulse receiving techniques. With conventional printed circuit arrays, feed network losses dominate as systems move to shorter millimeter wavelengths due to metallic transmission lines. This investigation will focus upon multilayer dielectric waveguide structures for the feed network with metallic structures only as the radiating element. Emphasis will be placed upon structures that can be fabricated with conventional IC technology and processing.

# 28516 PERFORMANCE CHARACTERISTICS OF PHASE-CORRELATING FRESNEL ZONE PLATES

James C. Wiltse Georgia Institute of Technology

SL: CECOM

#### **VIII Electronics**

The research objective is to investigate the phase reversal zone plate antennas for millimeter to submillimeter wavelength applications. Attempts will be made to establish fundamental operating principles of zone plate antennas through an investigation of; the theory of their operation based upon the Kirchhoff-Fresnel integral representation of the farfield radiation pattern: of zone late parameters which will result in minimum aberrations in the field of view: and finally to experimentally verify theoretical results.

# D. Circuits, Networks & Related Systems

# 28070 CARRIER COLLECTION AND SCATTERING IN QUANTUM WELL AND SUPERLATTICE DEVICES

Robert M. Kolbas North Carolina State University

Time resolved photoluminescence of phonon assisted stimulated emission can be reported for the first time. The temporal characteristics of the phonon assisted stimulated emission are distinct from the quantum states. The phonon assisted recombination is always delayed in time with respect to the confined particle transitions and has a larger full width at half maximum than the confined particle transitions. The dynamics of stimulated phonon emission along with the smaller transition probability for the phonon assisted process may account for the distinct temporal characteristics. Data are available on the emission intensity versus wavelength versus time from which the dependence of the delay on excitation intensity is extracted. A paper has been prepared to provide the reader with a detailed summary of the development of the density of states (DOS) function for two dimensional systems. Specifically, the DOS is derived for an infinite quantum well, a finite well. and a periodic array of finite wells (a superlattice). Many authors state that the DOS is "simply" without reference, yet many who are new to the subject of two dimensional systems may not see the "simplicity." for instance, for the derivation of the DOS for a superlattice. The paper shows the relationships between the expressions for each case when the appropriate limits are taken. This comparison shows the consistency that such a general derivation furnishes to each expression. Another paper presents two ways to reduce leakage currents in transverse junction

E. Signal Processing, Communications & Related Systems

stripe lasers: by reducing surface leakage currents and by reducing bulk leakage currents.

#### E. Signal Processing, Communications & Related Systems

## 25674 COMMUNICATION TECHNIQUES IN STRESSED ENVIRONMENTS

Robert A. Scholtz University of Southern California

SC BRL. CECOM.

- NSA CSS. SMO

A paper has been published in which consideration was given to the problem of determining which gateways to used interconnect existing data networks to minimize linear combination of the average internet and intranet packet delays subject to a cost constraint on the amount to be spent to establish the gateways. This problem is formulated as a nonlinear combinatorial optimization problem. When the gateway locations are fixed, the resulting routing problem is not a convex programming problem. This is unexpected since the routing problem in datagram networks is usually formulated as a convex program. Researchers have developed an algorithm to solve this problem and have reported computational experience.

#### Reports

No. 1.27 in previous editions

- An Optimum Filter Design for a Cross-Spectrum Symbol-Rate Detector, by Seok-Ho Kim, PhD Thesis, 1990, 121 pp.
- 2) Channel Load Sensing Protocol in Spread Spectrum Packet Radio Networks, by Ming Yin, PhD Thesis, 1990, 179 pp.
- Signal Classification Based on Spectral Correlations, by Youngky Kim, PhD Thesis, 1990, 142 pp.
- Design and Performance Analysis of Locking Algorithms for Distributed Databases, by Shiow-Chen Shyu, PhD Thesis, 1989, 140 pp.
- 32. Minimax Routing in ATM Networks, by Ming-Jeng Lee and James R. Yee, MS
- 33 An Optimum Generalized Cross-Spectrum Symbol-Rate Detector, by Scok Ho Kim and R.A. Scholtz, MS. IEEE Trans on Commun
- 34 On Determining the Transmission Range for Multi-Hop Slotted ALOHA Packet Radio Networks, by Feng-Min Shiao and James R. Yee, MS.
- 35 Three Algorithms for Routing and Flow Control in Virtual Circuit Networks, by Yeong-Sung Lin and James R. Yee, Proc IEEE GLOBECOM, 1990, 339 AD A232 010
- 36 A Routing Algorithm for Virtual Circuit Data Networks with Multiple Sessions, by James R. Yee and Yeong-Sung Lin, MS, Networks

- 37 Multiple Capture in a Centralized Packet Radio System with Common Direct-Sequence Spread-Spectrum Modulation, by Dong-In Kim and Robert A. Scholtz, MS
- 38. This number not used.
- Local Access Algorithms in Hierarchical Mobile Packet Radio Networks, by Rong-Feng Chang and Victor O.K. Li, MS.
- Optimal Distributed Routing Algorithms for Datagram Communication Networks, by James R. Yee, Proc of Allerton Conf on Commun. Control and Computing, 1989, 829. AD A225-963
- 41 Fair Channel Access Algorithms in Multihop Packet Radio Networks, by Arr Mien Chou, PhD Thesis, 1990, 107 pp.
- Coding Adaptivity Issues in Spread-Spectrum Random-Access Networks, by Thomas Ketseoglou, PhD Thesis, 1990, 137 pp.
- 43 Algorithms for Interconnecting Ethernets with Multi-Port Bridges, by Song Chyau Liang and J.R. Yee, MS. IEEE Trans on Comp.
- 44 A Random Spreading Code Assignment Scheme for Centralized Spread-Spectrum Packet Radio Networks, by Dong-In Kum and R A. Scholtz, MS.
- 45. A New Multipher Adjustment Procedure for the Distributed Computation of Routing Assignments in Virtual Circuit Data Networks, by Yeong-Sung Lin and J.R. Yee, MS.
- 46 An Algorithm to Find Global Optimal Routing Assignments for a Class of PRNs, by James R. Yee and Feng-Min Shiao, MS.
- 47 On the Performance of Common Spreading Code CDMA Packet Radio Systems with Multiple Capture Capability, by Dong-In Kim. PhD Thesis, 1990, 129 pp.
- A Second-Order Greedy Algorithm for Interconnecting Ethernets, by J.R. Yee and Song-Chyau Liang, MS.
- A Topology and Discrete Capacity Assignment Algorithm for Reconfigurable Networks, by Ming-Jeng Lee and J.R. Yee, MS, Operations Res.
- A Branch and Bound Design Algorithm for Reconfigurable Networks, by J.R. Yee and Ming-Jeng Lee, MS.
- 51. A Model and Algorithm for Interconnecting Two Wans, by Song-Chyau Liang and J.R. Yee, MS.
- 52. Optimal Minimax Routing in ATM Networks, by Ming-Jeng Lee and J.R. Yee, MS.
- Epoch Synchronization of Random FH Signals in Broadband Noise, by Char-Dir Chung and Andreas Polydoros, MS.
- Adaptive Channel Code Matching Using Hidden Markov Chains, by R.E. Peile and R.A. Scholtz, MS.

#### 26118 DIGITAL SIGNAL PROCESSING

K. Steightz Bede Liu

Princeton University

Achieving efficient and reliable synchronization is a critical problem in building long systolic arrays. A paper has been prepared which addresses this problem in the context of synchronous systems by introducing probabilistic models for two alternative clock distribution schemes: tree and straight-line clocking. Analytic bounds are presented for the probability of failure. The basic conclusion is that as the onedimensional systolic array gets very long, tree clocking becomes preferable to straight-line clocking.

# 26460 REDUCING DATA DIMENSION TO LOWER SIGNAL COMPUTATIONAL REQUIREMENTS AND MAXIMIZE PERFORMANCE

Barry Van Veen University of Wisconsin - Madison

SC: SMO

A paper has been prepared which describes a cascade decomposition of the generalized sidelobe canceller (GSC) implementation for linearly constrained minimum variance beamformers. The GSC is initially separated into an adaptive interference cancellation module followed by a nonadaptive beamformer. It is proved that the adaptive interference cancellation module can be decomposed into a cascade of first order adaptive interference cancellation modules, where the order corresponds to the number of adaptive degrees of freedom represented in the module. This distributes the computational burden associated with determining the adaptive weights over several lower order problems and facilitates simultaneous implementation of beamformers with differing numbers of adaptive degrees of freedom. In another paper, statistical analysis of the adaptive convergence behavior of linearly constrained beamformers is given assuming the sample covariance estimator is used to estimate the covariance matrix. The sensor data is assumed to be Gaussian distributed and independent from snapshot to snapshot. The mean squared error in the absence of the desired signal is shown to be a multiple of a  $\chi$ -squared random variable. The presence of the desired signal results in an excess mean squared error which is Beta distributed and depends only on the signal power, number of snapshots, and number of adaptive degrees of freedom. The average excess mean squared error is directly proportional to the signal power and number of adaptive degrees of freedom and inversely proportional to the number of snapshots. These results provide clear motivation for partially adaptive beamforming.

#### Reports.

No. 1 5 in previous editions.

 Adaptive Detection in Subspaces, by Barry D. Van Veen and Chong H. Lee, Proc IEEE, p. 163 (1990). AD A231 023.

- Multiple Window Based Minimum Variance Spectrum Estimation for Multidimensional Random Fields, by Tsung-Ching Liu and Barry Van Veen, MS. *IEEE Trans on Acoust*, *Speech, and Signal Proc.*
- MWMV Spectrum Estimation for Multidimensional Random Fields: Theory and Implementation, by Tsung-Ching Liu, PhD Thesis, 1990, 120 pp.
- 9. Minimum Variance Beamforming, by Barry Van Veen, MS.

# 26646 NEW TEMPORAL/SPECTRAL/ SPATIAL-COHERENCE-EXPLOITING ALGORITHMS FOR ISTA

William A. Gardner Statistical Signal Processing, Inc.

SC: AMSAA

Conventional high-resolution array-based direction finding (DF) methods typically require several conditions that can be difficult to satisfy. These conditions arise because the matrix of correlations between the received data on different sensors contains contributions from desired signals and from interference and noise. By using a matrix of cyclic correlations between the received data on different sensors, DF methods can exploit cyclostationarity to select all signals having a specified cycle frequency and to discriminate against interference and noise, thereby greatly increasing performance in some environments and extending applicability to other environments considered to be intractable for conventional methods. The continuing investigation of DF for cyclostationary signals has yielded some interesting advances recently including a method that estimates the cycle frequencies present in the data, a method that can detect the number of signals present that have the specified cycle frequency, and results on the Cramer-Rao Lower Bound (CRLB) for the directions of arrival and other parameters. The new capabilities of estimating the cycle frequencies present in the data and detecting the number of signals present that have a specified cycle frequency essentially eliminate the requirement that those parameters be known a priori. The results on the CRLB indicate that the CRLB for the directions of arrival of cyclostationary signals can be orders of magnitude less than the corresponding CRLB for stationary signals, even when all parameters of cyclostationarity must also be estimated. In addition, extensive Monte Carlo simulations of the various cyclostationarity-exploiting DF algorithms have been completed. These confirm the theoretically predicted performance advantages of these new methods.

#### Reports:

No. 1-2 in previous editions.

- 3. Progress on Signal-Selective Direction Finding, by Stephan V. Schell and William A. Gardner, *Proc of 5th ASSP Workshop on Spectrum Estimation and Modeling*, 1990, 144. AD A234 324
- 4. High-Resolution Direction-Finding, by Stephan V. Schell and William A. Gardner, MS.
- Signal-Selective Time-Difference-of-Arrival Estimation for Passive Location of Manmade Signal Sources in Highly Corruptive Environments. Part I: Theory and Method, by William A. Gardner and Chih-Kang Chen, MS, *IEEE Trans on Acoust*, *Speech, and Signal Proc.*
- Signal-Selective Time-Difference-of-Arrive Estimation for Passive Location of Manmade Signal Source in Highly Corruptive Environments. Part II: Algorithms and Performance, by Chih-Kang Chen and William A. Gardner, MS.
- Detection of the Number of Cyclostationary Signals in Unknown Interference and Noise, by Stephan V. Schell and William A. Gardner, MS.
- Higher Order Cyclostationarity, Cyclic Cumulants, and Cyclic Polyspectra, by William A. Gardner and Chad M. Spooner, *Proc of 1990 Intl Symp on Information Theory and Its Applications*, 1990, 355. AD A232 453
- The Cramer-Rao Lower Bound for Parameters of Gaussian Cyclostationary Signals, by Stephan V. Schell and William A. Gardner, Proc of 1990 Intl Symp on Information Theory and Its Applications, 2990, 255. AD A232 362
- Exploitation of Spectral Correlation for Signal-Selective Direction Finding, by Stephan V. Schell, PhD Thesis, 1990, 243 pp.

#### **26697 AUTOMATIC TARGET RECOGNITION**

A.C. Kak

**Purdue University** 

#### SC: WSMR

The objective of the research is to study an automatic target tracking system with a unique approach referred to as expectation driven processing. The work also will integrate into the system novel approaches to target and terrain modeling as well as sensor fusion. The initial phase of the research will compare silhouette based and geometric reasoning based approaches to LADAR target identification. The second phase will work in cooperation with NVEOC to investigate sensor fusion. Both FLIR and LADAR sensor data will be used to develop feature sets for the recognition task. The phase may employ experimentation using unclassified sensor data supplied by Army laboratories. The third phase will consider the application of new results from expectation driven processing to the ATR task. This approach has shown promise in other applications in which multiple sources of data must be reconciled.

#### 26735 THE GAUSS MACHINE

Fred J. Faylor University of Florida

SC: WSMR

oc. wome

The current research program draws upon a theory which makes explicit use of the unique properties of Galois fields and the residue number system (RNS). It states that there exists a primitive element " $\alpha$ " which generates all the non-zero elements of the field  $Z_p = 0, 1, \dots, p-1$ , using the rule  $\alpha^n \mod p = b$ . That is, there is a 1:1 correspondence between the index m and the integer b. By representing the nonzero integers in  $Z_p$  by their exponents, multiplication can be replaced with exponent addition. Once a product is produced in this manner, it can be mapped back into the quadratic RNS, or QRNS, using a table to look up the value of  $\alpha^n \mod p$ ; i.e., exponent to integer. The principal innovation of this new theory, which is referred to as the Galois enhanced QRNS (or GEQRNS), is that the GEQRNS is a complex arithmetic system which is multiplier-free. Having a theory for arithmetic which is constructed only of additions may have a significant impact on ALU design since the multiplier real estate budget for a typical DSP microprocessor chip can be 40 percent of the total area. Because of this feature, and its proven ability to support high-speed concurrent arithmetic, it becomes a very attractive medium in which to design high-performance defense signal processing systems using either off-the-shelf components, or application specific integrated circuitry or VLSI. The GEORNS multiplier section consists of an adder and logarithmic correction table lookup cell. There is an external zero multiplier detection control line that will set the output of the table lookup correction cell to zero if any of the multiplicands are detected to be zero. The adder section can be used as an accumulator or to add externally supplied data to a partial product.

# 26813 A HIERARCHICAL APPROACH TO TARGET RECOGNITION AND TRACKING

D. Andrisani

M. Tenorio

Purdue University

SL: ARDEC

The research objective is to study a hierarchical target extraction, identification and tracking system based on passive sensors. This work includes two major sub-goals, (a) the investigation of hierarchical

system descriptions for algorithms on multiple levels, and (b) the illustration of this description applied to cooperating algorithms for a robust, passive tracking system for both ground and air vehicles. The initial phase of the research will investigate a hierarchical description on four levels: a preprocessing level and low, medium and high processing levels. Each level has distinct system functions to perform and utilizes varying degrees of algorithm sophistication. For example, the highest level will likely employ concepts from artificial intelligence such as reasoning and maintenance of "world" knowledge. Unique research questions must be addressed at each of these levels of the hierarchy as well as issues of system integration at all levels. This phase of the work will be theoretical. The second phase will use this theory on the important application of target tracking. This phase may employ experimentation using unclassified sensor data supplied by Army laboratories.

# 26823 ROUTING FOR TACTICAL AND STRATEGIC COMMUNICATION IN RADIO NETWORKS

Imrich Chlamtac University of Massachusetts

SC: AIRMICS

Algorithms: Part of the research deals with routing solutions. Heuristics will be constructed after it has been proven that exact solutions are of prohibitive complexity to be used as the basis for an operational protocol. Network performance analysis: In this part of the research the purpose is to develop an analytic model that will enable one to investigate buffer requirements, the throughput and delay characteristics of a class of radio networks which operate under an arbitrary link activation protocol and a deterministic routing policy. The performance evaluation of multihop radio networks will consider a collision free (TDMA) channel access policy. The exact analysis of the above system becomes intractable for even a very small network since the number of states given by  $2^{N2}$  for an N node network explodes rapidly. So far an approximate analysis for a multihop network operating under a TDMA protocol was only carried out assuming infinite storage capacity at the nodes and a randomly distributed TDMA cycle. Protocol design: protocols are used to realize meaningful exchange of data between communicating systems. In this phase of research work is in progress to construct an integrated environment which allows protocol specification and performance simulation using a common language in a tool entitled Integrated Estelle Translator-Simulator, which allows a network protocol to be specified in ISO FDT Estelle and observe its performance using discrete event simulation automatically derived from the specification.

## 27028 COMMUNICATION IN THE PRESENCE OF UNKNOWN INTERFERENCE

Brian L. Hughes

The Johns Hopkins University

SL: BRL SC: SMO

Earlier work has shown that random codes can achieve a larger capacity and smaller error probability than deterministic codes for certain arbitrarily varying channels (AVCs). Indeed, for many AVCs of practical interest, random coding is necessary to obtain a positive capacity. Unfortunately, the random codes considered in this work were far too complicated to implement in a real communication system. The random coding results for AVCs were reconsidered with constraints for a simpler class of random codes. This class of codes consists of deterministic codes used with random modulation and demodulation. Random modulation and demodulation, means applying a relatively simple random mapping T to the symbols within a codeword prior to transmission, and applying the inverse mapping at the receiver prior to decoding. Work has shown that the capacity and best error probability of an AVC for random codes can be achieved by codes in this simpler class. For discrete AVCs T is a random interleaver; for the Gaussian AVC, T is a random orthogonal matrix. Moreover, it was shown that deterministic codes that are asymptotically good for the discrete-alphabet AVC are precisely those that are asymptotically good for a certain fixed channel. Deterministic codes that are asymptotically good for the Gaussian AVC are those that are good for a certain discrete-time Gaussian channel. Work is in progress on exploring new communication techniques to improve the performance of frequency-hopped, M-ary frequency-shift-keying systems in the presence of multitone jamming and multiple-access interference. In particular, researchers are exploring methods for successfully decoding a transmitted message even when the number of interfering tones present in the received signal exceeds the erasure-correcting capability of the transmitter's code.

Reports:

 On the Error Probability of Signals in Additive White Gaussian Noise, by Brian Hughes, *IEEE Trans on Info Theory* 37,151(1991). AD 233-951

- An Asymptotically Optimal Random Modem and Detector for Robust Communications, by Brian Hughes and Murad Hizlan, *IEEE Trans on Info Theory* 36,810(1990). AD A233 693
- 3. Exponential Error Bounds for Random Codes on Gaussian Arbitrarily Varying Channels, by Tony G. Thomas and Brian Hughes, MS, *IEEE Trans on Info Theory*.
- 4. On the Optimality of Direct-Sequence for Arbitrary Interference Rejection, by Murad Hizlan and Brian Hughes, MS, *IEEE Trans on Commun.*
- 5. Interleaving and the Arbitrarily Varying Channel, by Brian L. Hughes, *IEEE Trans on Info Theory* 37,413(1991). AD A234 026

## 27032 SIGNAL LOCATION USING GENERALIZED LINEAR CONSTRAINTS

Lloyd J. Griffiths University of Southern California

SC: AMSAA, SMO, VAL

By applying derivative constraints individually to each array element, a group of constraints can be used to inhibit the output SNR degradation of the desired signal in an adaptive array beamformer subject to phase errors. Using the traditional type of derivative constraints at each array element would use all the degrees of freedom available to the adaptive array processor. Hence, a new type of constraint was used that only uses approximately half of the existing degrees of freedom. Experimental results using actual RF array data show significant SNR improvement.

#### 27076 CONCURRENT ARCHITECTURES FOR VLSI SIGNAL AND IMAGE PROCESSING

Keshab K. Parhi

University of Minnesota, Minneapolis

SL: NVEOC	SC: SDC
-----------	---------

A thorough analysis of finite word effects in pipelined recursive filters was carried out for first and second order filters. A CAD program is being written to design recursive filters starting from filter spectrum specifications (as opposed to transforming nonconcurrent filters using look-ahead computation). A systematic approach was developed to unfold any arbitrary bit-serial architecture to obtain the functionally correct digit-serial architecture. The unfolding algorithm can unfold any arbitrary data-flow graph with switches, interpolators, and decimators. The digitserial technique is now being used to design a code for mobile radio system. Folding transformation of signal processing algorithms was addressed. Hardware synthesis of dedicated DSP systems was investigated for multiple implementation styles and is being incorporated in the MARS (Minnesota Architecture Synthesis) system. A register allocation algorithm was developed for synthesis of digital data format converter architectures; this can lead to more silicon area efficient converter designs.

Reports:

No. 1–11 in previous editions.

- 12. Register Allocation for Design of Data Format Converters, by K.K. Parhi and Joo-Sang Lee, MS.
- 13. Dedicated DSP Architecture Synthesis Using the MARS Design System, by Ching-Yi Wang and K.K. Parhi, MS.
- 14. Pipelining in Algorithms with Quantizer Loops, by K.K. Parhi, *IEEE Trans on Circuits and Systs* 38,745(1991).
- 15. Synthesis of Control Circuits in Folded Pipelined DSP Architectures, by Deshab K. Parhi and Ching-Yi Wang, MS, *IEEE J Sol St Circuits*.

#### 27464 AUTOMATIC TARGET RECOGNITION

Avi C. Kak

Purdue University SL: ARDEC

SC: MICOM, SDC, VAL, WSMR

The objective of this research is to investigate machine vision algorithms and architectures for low resolution LADAR imagery with real-time performance requirements. Particularly of interest will be methods for target detection that do not require the acquisition of a full scene buffer, thus improving the system response time.

# 27493 SEQUENTIAL ACQUISITION SCHEMES FOR SSMA SYSTEMS WITH GENERALIZED SIGNATURE SEQUENCES

Sawasd Tantaratana University of Massachusetts

SL: BRL S

SC: SMO

A paper has been prepared which presents a unified performance analysis of direct-sequence spreadspectrum multiple-access communications with deterministic complex signature sequences. The probability density function of the multiple-user interference is determined. Using a round-down and round-up procedure on the p.d.f., arbitrarily tight lower and upper bounds on the probability of bit error are obtained. Results based on Gaussian approximation method are also presented. It is shown that complex sequences can yield better p.b.e. performance than binary sequences. Using complex sequences, the number of signature sequences that have good auto and cross correlation properties are greatly enlarged. New users that employ complex or binary signature sequences can be added into existing systems with graceful performance degradation.

Reports:

- Performance Bounds for DS/SSMA Communications with Complex Signature Sequences, by Alex W. Lam and E.M. Ozluturk, MS, *IEEE Trans on Commun.*
- 2. *M*-ary DS/SSMA Communications with Complex Signature Sequences, by Alex W. Lam et al., MS.
- 3. Notes on the Design of Truncated Sequential Tests with Non-i.i.d. Samples, by Sawasd Tantaratana, MS, *IEEE Trans on Commun.*

# 27751 STUDY OF VIDEO TRANSMISSION TECHNIQUES IN TACTICAL SWITCHED NETWORK SYSTEMS

Donald L. Schilling Tuvia Apelewicz SCS Telecom, Inc.

SL: CECOM SC: CECOM

The needs of the Army for a capability to utilize the "common user" switched network to interconnect data terminals and to process video intelligence data in the forward combat zones is the primary focus of this study. The study to date has been restricted to describing the physical, operational and transmission problems most likely to be encountered in introducing data terminals into the tactical 16 kBit voice switched network of MSE and TRITAC equipments. Attempts are being made to define the problems associated with transmission problems caused by "least favorable" circuit usage, failed circuits, pre-emption and the ability of the VPAD to shut down disconnected lines with automatic adjustment of the adaptive time compression (ATC) as a function of the number of available usable interconnections. The ATC buffer size indicates that a maximum of 40 mBit of storage is required for the transmission factors considered to date. At this phase of the study, the findings are very promising and the transmission of low speed and mid speed data under the control of a VPAD is both feasible and practical. The signaling, buffering (ATC), protocol requirements, signaling sequence requirements, data device control requirements, or any of the suspected transmission problems which would require additional black boxes to compensate for the unique characteristics necessary are to be considered for variable speed data transmission over voice dial-up tactical switched networks.

# 27754 IMPROVED INTERCEPTION CAPABILITY THROUGH THE USE OF TRANSFORM DOMAIN PROCESSING

L.B. Milstein

University of California, San Diego

#### SC: SMO

Work has begun on extending the research on the use of compressive receivers for signal interception of phase-shift keyed (PSK) waveforms to the interception of frequency-shift-keyed waveforms. In particular, up until recently, the research was focused on demonstrating the advantage that a compressive receiver could offer over a wideband radiometer in intercepting a binary PSK signal. This class of waveforms includes direct sequence spread spectrum signals using BPSK modulation, and it was shown that one can often achieve enhanced detectability relative to a radiometer. In addition, one always ends up with a more accurate estimate of *rf* frequency.

# 27834 CONGESTION/FLOW CONTROL AND ROUTING IN DATA NETWORKS: A CONTROL-THEORETIC APPROACH

Semyon M. Meerkov University of Michigan

SL: CECOM SC: AMSAA

The goal of the project is the development of a new and efficient architecture for congestion control in backbone, store-and-forward packet switched networks based on control-theoretic ideas. The following results have been obtained: (a) Stochastic and fluid approximation models have been developed that describe the dynamics (including congestions) in backbone datagram networks with a loop structure. (b) The problem of congestion control has been shown to be a feedback control problem where the goal of the feedback control is to match the admitted traffic to the network resources (buffers and links capacities, switch node processors utilization). (c) A new architecture for congestion control, utilizing the rate-based approach has been suggested. (d) Using the mathematical model developed, it has been shown that the proportional feedback with respect to buffer occupancy cannot solve effectively the congestion control problem (due to persistent oscillations that take place in the network with proportional source quenching control). (e) It has been shown that the introduction of the state space control stabilizes the network and, if the control gains are chosen appropriately, results in a robustly stable congestion con-

trol system. (f) The results of the analytical investigation have been confirmed using numerical simulation of 9-node network with a loop structure. In addition, using the simulation, it has been demonstrated that when the feedback gains are chosen in compliance with the theory developed, the control prevents the congestion for any type of input traffic and, if the network starts its operation in a congested regime, results in a rapid recovery from the congestion.

## 27886 HIGH-FREQUENCY SIGNAL-PROCESSING INTEGRATED CIRCUITS

Robert G. Meyer Donald O. Pederson University of California, Berkeley

SC: HDL

The research objective is to investigate high performance, high frequency monolithic signal-processing integrated circuits. The research focuses on performance in the gigahertz frequency range of wideband low-noise amplifiers, oscillators, switches, and mixers. The work is theoretical but is also concerned with computer simulation of designs, and fabrications and test of packages. The work addresses a range of fundamental concerns in the design, implementation and evaluation of high frequency circuits. The work will aim at synthesis of new circuit topologies and investigations of the interaction between device characteristics, process technology, and circuit design. Specific areas of research will be wideband low-noise amplifiers, oscillators, switches, and mixers. In addition, the research will consider the problems and opportunities involved in combining these functions to form complete, highly integrated monolithic systems.

#### 27899 ADVANCED ARRAY PROCESSING FOR COMMUNICATION SYSTEMS

Benjamin Friedlander Signal Processing Technology, Ltd.

SL: SWC

The objective of the research is to investigate advanced techniques for array processing in communications with application to signal direction finding and copy (interception). A wide range of tasks divides into two categories, (a) blind channel equalization, and (b) topics in direction finding (DF). The latter comprises various aspects of the DF problems in cochannel interference in the narrowband case and two broadband topics in DE namely, DF of frequency hoppers and a study of techniques for communicators using low-probability-of-intercept signals to defeat interceptor attempts at DE

# 27917 CYCLIC FEATURE ANALYSIS, DESIGN AND EXPLOITATION

William A. Gardner Statistical Signal Processing, Inc.

SC: HDL

The research objective is to investigate nth order cyclostationarity properties of general types of lowprobability-of-intercept signals and to investigate methods for their use in both secure communications and interception. Initially nth order cyclostationarity properties will be investigated from both the point of view of the communicator and the interceptor. These characterizations will be used in signal design as a means for reduction of the strength of, and elimination of, cyclic features that can be exploited by an interceptor. In addition, for interception, these characterizations will be used to propose feature sets and discrimination rules for signal classification and identification. The characterization of nth order cyclostationarity will provide a theoretic extension of the 2nd order results that now exist.

#### 27994 SPREAD-SPECTRUM RADIO SYSTEMS AND NETWORKS

Michael B. Pursley D.V. Sarwate University of Illinois

SC: BRL

The research objective is to investigate spread spectrum radio systems and networks. This includes a theoretical understanding of spread spectrum lowprobability-of-intercept (LPI) signaling methods for secure communications. Research in communication systems relevant to the Army must deal with the reality of mobile units with complex signaling requirements. The need for LPI signaling has led to spread spectrum signaling techniques. This project will consider the two major spread spectrum signaling strategies, frequency hop and direct sequence. This effort has four major thrusts that attempt to extend the understanding of mobile, military communications with a solid theory: (a) Investigate improved coding techniques for slow-frequency-hop radio. (b) extend the theory for continuous phase modulation for direct-sequence spread-spectrum communications, (c) investigate the effects of linear distortion on the performance of direct-sequence systems, and (d) investigate models for transmission and reception in frequency-hop multiple-access radio networks.

# 28297 MEGA-SCALE SIMULATION OF MULTILAYER DEVICES—FORMULATION, KINETICS AND VISUALIZATION

Robert W. Dutton Stanford University

SC: AMSAA, NRL

The research objective is to investigate modeling of devices in high performance circuits. This includes the visualization of device behavior in three dimensions and incorporation of IC geometry, materials, and process parameters in the modeling process. The research addresses a range of fundamental concerns in the design tools environment. The desired outcome is the optimization of device designs in a VLSI environment where the details of the design process are automatically coupled with the essential parameters of the manufacturing process and the underlying materials technology. In addition, due to the complexity of 3D modeling, it is essential to address the issues of data presentation, numerical methods for computation, modeling of kinetic transport, appropriate execution hardware, and finite element methods. The research is embedded in design tools concepts and an "open system" strategy will be employed so that the results can be transferred and influence the maximum number of organizations. The four major components of research are device modeling, algorithms, solution approaches, and presentation and visualization of results.

#### 28387 VLSI CIRCUITS FOR HIGH-SPEED DATA CONVERSION

Bruce A. Wooley Stanford University

A program of research has been completed into the essential circuit functions needed for digitizing signals at conversion rates above 100 MHz in CMOS and BiCMOS technologies and further progress was made in the study of analog-to-digital conversion at rates above 1 MHz with a precision of at least 12 bits. Results of the research into circuits for analog-to-digital conversion at rates above 100 MHz are

summarized in a doctoral dissertation. The principal accomplishments of this work include the design of a novel BiCMOS charge-steering comparator that performs 8-bit comparisons at 200 MHz while dissipating only 1.6 mW, the design of an 8-bit, 200-MHz CMOS sample-and-hold circuit where in Miller feedback is used to compensate for charge-injection errors, and the study of nonlinearities that accompany the practical implementation of analog switches. A novel self-calibrating comparator comprising one stage of preamplification followed by two stages of regeneration has been successfully designed and integrated in a 2- $\mu$ m BiCMOS technology. In this comparator low-offset bipolar circuits are combined with CMOS

in a 2- $\mu$ m BiCMOS technology. In this comparator low-offset bipolar circuits are combined with CMOS offset-cancellation techniques to achieve a resolution of 200  $\mu$ V at a comparison rate of 10 MHz. The comparator is a fully-differential circuit that operates from a single 5-V supply and dissipates only 1.7 mW. Offsets are canceled on every cycle during overdrive recovery. Work is also in progress on exploring the design of a 12-bit, 5-MHz comparator in CMOS technology.

Reports:

1. A Self-Calibrating BiCMOS Comparator, by Behzad Razavi and Bruce A. Wooley, MS.

# 28467 PROTOCOL ENGINEERING FOR BROADBAND NETWORKS

Ming-Tsan Liu Ohio State University

SL: CECOM SC: AIRMICS

The research objective is to investigate the design and specification of protocols in a broadband computer communication network environment. The study is dominantly design and analysis oriented with some experimental elements.

# 28506 FORMAL DESIGN OF COMMUNICATION PROTOCOLS BASED ON THE ESTELLE ISD FORMAL DESCRIPTION TECHNIQUE

Paul D. Amer

SL: AIRMICS, CECOM

University of Delaware

The research objective is to investigate computer communication protocols in a tactical context and, further, to conceive of tools for the very difficult tasks of both protocol design and verification. The work is organized into three major efforts. The first is to investigate the ways that the tactical environ-

#### **VIII Electronics**

ment envisioned in BIS 2015 impacts traditional protocols and the approaches to protocol design and verification. The second portion of the proposed work addresses the conceptualization of a visualization tool that can aid in this process of design and verification. Finally, the automatic generation of test sequences for protocol verification will be addressed.

#### 28985 RECONSTRUCTION OF REMOTELY SENSED ACOUSTIC SIGNALS

Stephen D. Casey American University

SL: LABCOM SC: HDL

The research objective is to investigate reconstruction techniques for remotely sensed acoustic signals. The work is a short term study but addresses a range of fundamental concerns in the area of signal reconstruction. The objective involves solving two illposed inverse problems. The study will (a) develop models of currently deployed passive remote acoustic sensors as convolution equations. Then apply the Berenstein theory to choose multiple sensors which will allow signal reconstruction from band limited sensors, (b) develop methods for choosing sets of strongly coprime emitted signals and construct deconvolution pulses, (c) modify the theory to account for atmospheric effects. (d) Identify the equations that most accurately model acoustic waves propagating through these atmospheric conditions. (e) develop a method of solution for these equations, (f) develop techniques for recovering the desired signal.

#### F. External Program

#### 24793 INTELLIGENT PROCESSING INITIATIVE OF GALLIUM ARSENIDE

Ralph T. Wood General Electric Company R&D Center

This program represents a strategy for integrating sensor technology, process modeling, adaptive control concepts and advanced microcomputer hardware with an expert knowledge base to form an intelligent processing system for GaAs crystal growth. The goal of this system is to maximize yield and minimize human interaction in the economic production of large diameter GaAs crystals by the high pressure liquid encapsulated Czochralski process. The application of such expert systems can stimulate the next generation of equipment for GaAs crystal growth and provide the U.S. a competitive edge in future high speed digital and analog integrated circuit technology.

# 26898 OPTOELECTRONIC INTEGRATED CIRCUITS FABRICATED USING ATOMIC LAYER EPITAXY

P. Daniel Dapkus University of Southern California

SL: HDL

The research objective is to explore and understand the integration of a wide variety of compoundsemiconductor heterojunction devices fabricated by atomic layer epitaxy. Atomic layer epitaxy will be used to fabricate monolithically integrated structures consisting of a variety of heterojunction devices with layer dimensions and doping levels that vary greatly from device to device.

#### 27865 INTELLIGENT PROCESSING OF GaAs FOR LARGE SINGLE CRYSTAL GROWTH

H.S. Goldberg

General Electric Company R&D Center

SL: NVEOC SC: ETDL

Research seeks to develop the scientific and technological base for processing of high quality bulk gallium arsenide single crystal material. This work is based on the concept of intelligent processing of materials. This concept employs physical models and heuristic information combined with artificial intelligence and high-speed real time computer control systems integrated physically and intellectually for the purpose of producing materials whose properties can be predicted and controlled within high degrees of accuracy and reproducibility.

# 28099 FUSION OF RANGE AND LUMINANCE DATA FROM LASER RADAR SYSTEMS

Wesley E. Snyder James W. Gault North Carolina State University

In a recent paper a unifying view was given of the relationship of MFA and Graduated Non-Convexity, another image-based optimization technique. The mathematics of MFA provides a powerful and general tool for both understanding and deriving optimization algorithms. The most recent effort has been directed

#### G. Joint Services Electronics Program

toward signals obtainable from the Tri-Services Laser Radar. There are five sensor modalities, course and fine range, intensity, doppler, and passive IR. Initial efforts have considered the intensity signal as an additional information source for the restoration of the range signal. Signals suitable for analysis and experimentation are essential to this work. There are three primary sources of such signals; the synthetic digital terrain board, the physical terrain and field data. The most recent efforts have been to derive meaningful digital terrain board scenes which can then be sampled using a software version of a sensor of interest. Recently, thoughts have turned to the restoration approach in a more general framework. This point of view considers a collection of sensors from which one would wish to deduce an uncorrupted view of a limited world. Each sensor contributes a particular perception which must be considered in the context of the perceptions of the other sensors. In addition to the sensors contribution to this model from which one would expect to derive a new reality, one would provide the model with; (a) a perception of what one believes the world to be, (b) models of sensor misconceptions (noise models), and (c) models of sensor interrelationships. The goal is to derive an improved view of this limited world by optimally aggregating the information from the sensors and researchers' a priori perceptions.

#### 28187 SOLID-STATE DYNAMICS IN NOVEL SEMICONDUCTOR NANOSTRUCTURES

M.A. Stroscio K.-W. Kim North Carolina State University

A full theory for single-particle LO- and SO-phonon interactions in quantum wires was developed. A principal finding of the research was that electron-SO-phonon scattering dominates over electron-LOphonon scattering in quantum wires with lateral dimensions less than about 60 Å.

# 28729 LIMITED REACTION PROCESSING: HETEROSTRUCTURE AND NOVEL DEVICE FABRICATION

James E. Gibbons Stanford University

SL: ARO, DARPA, ETDL SC: ETDL, HDL

This research is directed toward obtaining a more fundamental and exact understanding of rapid ther-

#### **VIII Electronics**

mal processing and limited reaction processing (LRP). Also, this research will investigate promising new device applications based on novel use of LRP, leading to the development of the next generation of semiconductor processing equipment. This work is based on the principle of minimizing the temperaturetime product in semiconductor processing in order to achieve abrupt interfaces and stable doping and impurity profiles. This affects the ability to achieve ultra-thin layers and heterointerfaces required for ultra-large-scale-integration of devices with feature sizes less than 0.2 microns.

# 28922 IN SITU GROWN QUANTUM-WIRE LASERS

Larry Coldren

University of California, Santa Barbara

The objective of this program is to develop an integrated process for the fabrication of quantum wire lasers, and to develop the theory and materials capabilities required to achieve arrays of surface emitting lasers. Molecular beam epitaxy will be used as the basis for the in-situ fabrication of quantum wire lasers. The laser devices will utilize lateral superlattices, fabricated in an in-situ processing chamber integrated with the MBE process. To achieve ultra-sensitive control of critical layer thicknesses, the lateral superlattices will be formed on off-axis substrates using fractional monolayer growth control.

# G. Joint Services Electronics Program

# 26213 BASIC AND APPLIED RESEARCH IN ELECTRONICS AND OPTICS

Jonathan Allen

Massachusetts Institute of Technology

SC: OASA (RDA)

Recent research is reflected in the report titles below.

Reports:

No. 1-65 in previous editions.

- Femtosecond Thermomodulation Study of High-T, Superconductors, by S.D. Brorson et al., Sol St Commun 74,2305 (1990). AD A226-341
- Quantum Theory of Self-Induced Transparency Solitons a Linearization Approach, by Y. Lai and H.A. Haus, *Phys Rev* 42,2925(1990). AD A234-133
- Ultrashort Pulse Generation with Additive Pulse Modelocking in Solid State Lasers: Ti:Al<sub>2</sub>O<sub>3</sub>, Diode Pumped Nd:YAG and

Nd:YLF, by J. Goodberlet et al., Ultrafast Phenomena VII, Volume 53, 1990, 11. AD A232 367

- Research Laboratory of Electronics Progress Report No. 132, by Jonathan Allen and Daniel Kleppner, TR, Jun 90, 87 pp. AD A226 438
- 70. Absence of Temperature-Driven First-Order Phase Transitions in Systems with Random Bonds, by A. Nihat Berker and Kenneth Hui, MS.
- Impulsive Excitation of Coherent Phonons Observed in Reflection in Bismuth and Antimony, by T.K. Cheng et al., Appl Phys Let 57, 1004(1990). AD A228 081
- 72. Short Pulse Gain Saturation in InGaAsP Diode Laser Amplifiers, by Y. Lai et al., *IEEE Photonics Tech Let* 2,710(1990). AD A232 461
- Fabrication and Testing of 0.1 
  µm-Linewidth Microgap X-Ray Masks, by M.L. Schattenburg et al., J Vac Sci Tech B8,1604(1990). AD A232 381
- 74. Transient Analysis of Frequency-Dependent Systems with Nonlinear Terminations, by Qizheng Gu et al., MS, IEEE Trans on Microwave Theory and Tech.
- A Compact, Low-Cost System for Sub-100 nm X-Ray Lithography. by A. Moel et al., J Vac Sci Tech B8, 1648(1990). AD A232 472
- 76. In<sub>0 53</sub>Ga<sub>0 47</sub>As/AIAs Resonant Tunneling Diodes with Peak Current Densities in Excess of 450 kA/cm<sup>2</sup>, by Tom P.E. Broekaert and Clifton G. Fonstad, *J Appl Phys* 68,4310(1990).
   AD A231 103
- 77. Phase Transitions on Misoriented Si(100) Surfaces, by O.L. Alerhand et al., MS.
- Spontaneous Emission Rate Alteration in Optical Waveguide Structures, by S.D. Brorson et al., *IEEE J Quant Electron* 26,1492(1990). AD A234 296
- 79. Starting Dynamics of Additive Pulse Mode Locking in the Ti:Al<sub>2</sub>O<sub>3</sub> Laser, by J. Goodberlet et al.. Opt Let Opt Let. AD A232 322
- 80. Monte Carlo Mean-Field Theory and Frustrated Systems in Two and Three Dimensions, by Roland R. Netz and A.N. Berker, MS, *Phys Rev Let*.
- Enhanced Spontaneous Emission From GaAs Quantum Wells in Monolithic Microcavities, by H. Yokoyama et al., Appl Phys Let 57,2814(1990). AD A232 679
- Femtosecond Relaxation Dynamics of Image-Potential States, by R.W. Schoenlein and J.G. Fujimoto, *Phys Rev* B43,4688 (1991). AD A233 967
- Demonstration of Optical Switching via Solitary Wave Collisions in a Fiber Ring Reflector, by J.D. Moores et al., Opt Let 16,138(1991). AD A234 337
- Optical Switching Using Fiber Ring Reflectors, by J.D. Moores et al., J Opt Soc Am B8,594(1991). AD A238 116
- Femtosecond Gain Dynamics and Saturation Behavior in InGaAsP Multiple Quantum Well Optical Amplifiers, by K.L. Hall et al., Appl Phys Let 57,2888(1990), AD A234 399
- Exchange Interaction in a Quantum Wire in a Strong Magnetic Field, by Jari M. Kinaret and Patrick A. Lee, *Phys Rev* B42,768(1990). AD A232-321
- Femtosecond Thermomodulation Study of Conventional and High-T<sub>e</sub> Superconductors, by S.D. Brorson et al., Ultrafast Phenomena VII, Vol 53, 1990, 354. AD A232 320

- 88. Quantum Noise in Soliton-Like Repeater System, by H.A. Haus, MS, J Opt Soc Am.
- 89. Patterning and Characterization of Large-Area Quantum-Wire Arrays, by K. Ismail et al., MS, Appl Phys Let.
- Atom Optics, by David W. Keith and David E. Pritchard, New Frontiers in Quantum Electrodynamics and Quantum Optics, 1990, 467. AD A233 960
- Frustration in Magnetic, Liquid Crystal, and Surface Systems: Monte Carlo Mean-Field Theory, by Roland Rudiger Netz, MS Thesis, 1991, 164 pp.
- 92. Squeezing in Fibers with Optical Pulses, by K. Bergman and H.A. Haus, *Opt Let* 16,663(1991).
- 93. A Theory of Coupled Cavity Modelocking with a Resonant Nonlinearity, by H.A. Haus, MS, J Opt Soc Am.
- Conductance of a Disordered Narrow Wire in a Strong Magnetic Field, by Jari M. Kinaret and Patrick A. Lee, *Phys Rev* B43,3847(1991). AD A238 610
- Patterning and Characterization of Large-Area Quantum Wire Arrays, by K. Ismail et al., *Appl Phys Let* 58,2539(1991). AD A238 537

# 27554 TWO-DIMENSIONAL SIGNAL PROCESSING, OPTICAL INFORMATION STORAGE AND PROCESSING AND ELECTROMAGNETIC MEASUREMENTS

Ronald W. Schafer

Demetrius Paris Georgia Institute of Technology

Recent research is reflected in the report titles below.

#### Reports:

- Mathematics as an Educational Tool for Signal Processing, by B.L. Evans et al., MS.
- 2. Estimating 2-D Angles of Arrival Using Overlapping Volume Arrays, by F.A. Sakarya and M.H. Hayes, MS.
- 3. FIR Filtering of Images on a Lattice with Periodically Deleted Samples, by T.R. Gardos and R.M. Mersereau, MS.
- Displacement Estimation Along Contours in Image Sequence Analysis, by Jianzhong Huang and R.M. Mersereau, MS.
- 5. Wavelet Representations and Coding of Self-Affine Signals, by EJ. Malassenet and R.M. Mersereau, MS.
- New Search Algorithm for Minimum Redundancy Linear Arrays, by K.A. Blanton and J.H. McClellan, MS.
- 7. The Design of Perfect Reconstruction Nonuniform Band Filter Banks, by Kambiz Nayebi et al., MS.
- Compilation for Interprocessor Communication in Clock-Skewed Parallel Processing System, by C.P. Hong and T.P. Barnwell III. MS.
- Eigenstructure Approach for Array Processing and Calibration with General Phase and Gain Perturbations, by G.C. Brown et al., MS.
- Multilayer Kohonen Image Codebooks with a Logarithmic Search Complexity, by K.K. Truong, MS.
- A Millimeter-Wave Integrated-Circuit Antenna Based on the Fresnel Zone Plate, by Mark A. Gouker and Glenn S. Smith, MS.

# 28326 JOINT SERVICES ELECTRONICS PROGRAM

J.A. Harris, Jr. Stanford University

Research is being conducted to improve the basic understanding of areas of modern electronics, including solid-state electronics, quantum electronics, and information electronics. Experimental and theoretical research will focus on efforts to understand the role of DX centers in contributing to noise in indium-based transistors; define and apply novel electron sources to the fabrication of novel ultrasmall devices; formulate techniques and define simulators for quantum-effect devices; fabricate and characterize novel semiconductor laser structures for optical interconnects; understand and apply new low-temperature in-situ cleaning for epitaxial growth of Si and Si-Ge; understand and apply low-temperature electroncyclotron-resonance cleaning and etching of Si and GaAs; determine microscopic properties of in-situgrown high-temperature superconducting thin films

#### **VIII Electronics**

by novel techniques of synchrotron radiation; formulate new digital signal processing techniques for future wideband digital portable communications systems; formulate new models and techniques for image compression, data compression and network information flow; and explore the use of neural nets for fast arithmetic computing.

## 28453 THE ELECTROMAGNETIC SPECTRUM

George Flynn

R. Osgood, Jr.

Columbia University

The research objective is to improve the understanding in areas of modern electronics including: solidstate electronics and quantum electronics.

#### Reports:

- 1. Photoemission From Thick Overlying Epitaxial Layers of CaF<sub>2</sub> on Si(111), by B. Quinious et al., MS.
- 2. Raman Study of Strain and Confinement Effects in Si/Ge Strained Layer Superlattices Under Hydrostatic Pressure, by Zhifeng Sui et al., MS, *Mat Res Soc Symp Proc.*

# IX EUROPEAN RESEARCH PROGRAM

# **A.** Physics and Mathematics

#### 5265 NUMERICAL OPTIMIZATION

F. Zirilli Universita di Roma "La Sapienzall" Rome, Italy

SL: TACOM, MICOM

A class of algorithms derived from the ones used on the package DAFNE and based on the numerical integration of a Cauchy problem for a system of ordinary differential equations has been developed. This work was motivated by classical mechanics. These algorithms require the solution of an  $N \times N$ linear system of equations at each step. The cost of solving this linear system when a large number of unknowns N is involved is the most important part of the computation. The linear system is solved by an interactive procedure (i.e., conjugate gradients) and only an approximate solution is computed (i.e., the conjugate gradient procedure is stopped after a number m of steps depending on the norm of the residual, 0 < m < N + 1). For the algorithms, local convergence and Q-superlinear rate of convergence has been proved. The algorithms have been used very successfully to solve three complementary problems derived from variational inequalities of mathematical physics. The complementary problems considered had up to 900 variables. The P.I. also worked on the idea of attempting to adapt the existing SIGMA algorithm, developed by the P.I., to work on complementary problems with many independent variables. In particular, the P.L and his colleagues tried to exploit the following special features of the complementary problem: (a) the objective function is a piecewise quadratic, and (b)the objective function value to be found is zero. The modified version of the SIGMA algorithm is much more efficient on complementary problems than the original one.

#### 5653 CHAOTIC BEHAVIOR IN QUANTUM MECHANICS

G. Casati Centro di Cultura Scientific "A. Volta" Como, Italy

SL: ARO, MICOM, CRDEC, ETDL, HDL, NVEOC

This research project is generally devoted to the investigation of the relevance of classical chaos to quantum mechanics, with special emphasis on quantum systems subjected to perturbations periodic in time. The problem of the excitation of a hydrogen atom under a monochromatic, linearly polarized, microwave field has attracted much interest in the past few years in connection with the possibility of experimental investigation on the relevance of classical chaos in quantum mechanics. The researchers have developed a reasonably clear general picture of the quantum excitation process. In particular, they found that the chaotic diffusion which takes place in the classical case and which leads to strong ionization can be suppressed by a localization phenomenon somewhat analogous to the one occurring in one dimensional lattice problems of solid state physics. More exactly, the P.I. has shown that one can distinguish between two regimes which are defined by the ratio, w\*, of the microwave frequency to the frequency of the unperturbed motion corresponding to the initially excited state. These regimes are determined by the cases  $w^* < 1$  and  $w^* > 1$ . For  $w^* < 1$  the excitation process is satisfactorily described by classical dynamics, whereas for  $w^* > 1$  quantum inhibitory effects produced by quantum interference are at work and a stronger field than predicted by the classical chaos border is required for ionization. The P.I. goes on to show how the localization effects that limit the diffusive classical-like excitation of a hydrogen atom in a microwave field can be destroyed by the introduction of a second incommensurate external frequency. His results have been confirmed by numerical computations and by an experiment at Stony Brook

#### **A.** *Physics and Mathematics*

with  $w^* < 1.364$ . Researchers have studied the different borders in the problem of excitation and ionization of hydrogen atoms in microwave fields. As confirmed by numerical and laboratory experiments, a main role is played by the localization phenomenon which leads to the quantum suppression of classically chaotic excitation and to strong fluctuation in ionization probability.

## 5933 MULTIGRID OPTIMIZATION AND ARTIFICIAL INTELLIGENCE

A. Brandt The Weizmann Institute of Science

SL. BRL. MICOM

Rehovot, Israel

During the initial period of this research, the P.L. Professor Achi Brandt, and his colleagues, Drs. Shlomo Talasan and Tamar Flash, and a student. Inna Ben-Zvi, considered a problem in robotic optimal control. They have conducted a preliminary study of multigrid algorithms for optimal trajectory planning for robotic manipulators. As a first task, they solved the unconstrained optimization of a twolink planar manipulator, where the cost is a weighted sum of torques and jerks (time derivative of torque). To do this, since the problem is severely nonlinear. they devised a continuation process on the coarsest grid which gradually introduces the nonlinear terms. using quadratic extrapolations from previous solutions to obtain the first approximation to each new solution. Having thus obtained a solution on a very coarse grid, increasingly finer solutions were then inexpensively calculated by a standard 1-FMG algorithm. Fast asymptotic convergence was observed. More recently, a constrained optimization was considered, where an obstacle is added to the above manipulator. Basically the same FMG algorithm was found to solve the problem with the same efficiency. Next, reaearchers plan to extend this same algorithm to the case where the trajectory total time is not fixed but appears as an extra term in the objective function. This yields a free boundary problem, and multigrid methods for dealing with such problems. are being developed. Other problems that have recently been considered include Image Processing. Image Restoration and Fiber Restoration (computerized microscopy). For example, in an image restoration problem a method was designed to separate away the question of how to relax edge directions. They applied mixed-state multilevel optimization to this problem. Successful results were obtained. Although the solver obtained was much more efficient than a single-level one, however, it was quite costly. They therefore decided to approach the problem from an

#### IX European Research Program

additional point of view with the idea of combining the two approaches in the future. The new approach was first to simplify the problem by considering the case where no blurring occurs and giving up the demand for strict "optimization" of any kind (although optimization criteria still serves as a general background for the method). This problem then reduces to the general and important mathematical problem of finding good approximations for noisy piecewise smooth functions, including the localization of their discontinuities. In the past year, the research has developed toward multiscale methods not anticipated in the original research proposal. Researchers believe these methods to be much more promising. As necessary parts of the program, the current research embarked on several specialized studies, of which two main ones are described: One has dealt with a special aspect of the surface approximation problem, that of reconstructing a (piecewise continuous) surface given sparse data using fast multigrid algorithms. As with dense data, the problem is transformed to minimization of a two term energy function, with one term forcing the solution towards the given data, the other enforcing smoothness throughout the image (except at designated surface discontinuities). Future research in this direction will, of course, include detection of discontinuities (depth and orientation) and their incorporation in the energy system. One approach to discontinuity detection may use the dummy variable v, since v is the Laplacian of the (interpolated) surface, each depth discontinuity in *u* generates a zero-crossing in *v*. Orientation discontinuities in u will produce extrema in v. Refining algorithms will be necessary to filter out false detections (not all zero-crossings are edges) and to determine as best as possible the true discontinuities' locations. The energy system will be modified to account for detected discontinuities, and the multigrid solver will likewise be adapted as has already been done for dense data. The study of fiber detection is part of developing a general approach to a fast multilevel detection of statistically significant features. It is a preliminary exercise for edge detection. because it has a simpler structure. The general concept has been checked and found to be valid. The problem is to detect fibers in high noise, where the fibers are very thin, and belong to a given family of curves. Statistical detection is possible due to the limited number of curves in the family, which enables (data dependent) construction of filters that will respond with high probability when evaluated on a true fiber, and with near-zero probability otherwise.

## 6271 NONLINEAR FILTERING AND APPROXIMATION TECHNIQUES

E. Pardoux INRIA Sophia Antipolis, France

SL: NVEOC, ARDEC

This research deals with theoretical and numerical aspects of stochastic differential systems with noisy measurements, applicable to the modeling of nonlinear filters. Filtering techniques are critical for obtaining state space information of nonlinear systems from measurements with errors, hence they are important in signal processing and nonlinear control. The research group has recently made advances in stochastic differential equations on several fronts. For one-dimensional systems with piecewise linear coefficients and which satisfy certain detectability hypotheses, an efficient approximate filter can be constructed from Kalman filters associated with the linear differential systems corresponding to the individual linear components of the coefficients. They have also shown the consistency of the maximum likelihood estimator (MLE) for unknown parameters in a stochastic differential system with asymptotically small noise. Using the theory of large deviations, they prove that the limiting points of the MLE sequence are minimizers of a least-squares type functional for the estimation of the parameters in the deterministic system obtained by zeroing the noise terms. Finally, they are currently investigating a numerical time discretization technique for solving the Zakai diffusion noise. The equation arises in computing likelihood functions in parameter estimation. The technique they are studying is a predictor-corrector (well known in deterministic differential equations) scheme on semigroups. They show the convergence order of the method to be  $V_2$ (in powers of the time step) which is optimal for this equation. Researchers have written a preliminary version of ZPB using the computer algebra language Maple. The general purpose of this software is to help perform easily numerical experiments for various problems (state estimation, detection, parameter estimation) concerning partially observed diffusion processes. The generated Fortran programs use routines from the scientific library NAG. For the visualization of the numerical results, they are developing Fortran programs using the Graphical Kernel System standard GKS.

## 6280 ELECTRONIC AND ATOMIC STRUCTURE OF SEMICONDUCTORS AND HIGH T<sub>c</sub> SUPERCONDUCTORS

R. Car E. Tosatti

Instituti di Fisica dell'Universita di Trieste Trieste, Italy

SL: ETDL, HDL, MTL, NVEOC, BRL, ARO

The research consists of investigations in the electronic and atomic properties of semiconductors and superconductors using computer simulations and ab initio quantum mechanical methods. Four main problems in condensed matter physics central to the research are as follows: (a) Microscopic simulation of the amorphous and liquid phase of elemental and compound semiconductors using the Car-Parrinello methods. (b) Simulation studies of the diffusion of hydrogen and other defects in crystalline silicon. (c) Theory of the electronic and vibrational properties of semiconductors, semiconductor interfaces, and of GaAs based superlattices. (d) Quantum simulations of highly correlated electron systems as models for high- $T_{\rm c}$  superconductors. The computer simulations involving Monte Carlo techniques and the "Car-Parrinello" method will be used to study these topics; results of these calculations will be compared to experimental data and published in the open literature. Recent research includes the following: (a) First-principle simulations of hydrogenated amorphous silicop (a-Si:H) have been carried out, and a short review of the main results have been published. Also n-dopants in diamond have been studied, in collaboration with an American group. (b)New results on structure and bonding of solid and liquid gallium have been obtained, using Car-Parrinello techniques similar to those used for Si and GaAs. (c) New simulations have been started for semiconductor surfaces, with strong progress mostly for clean Si(111)  $2 \times 1$ , for vacancies on Si(111)  $2 \times 1$ . A study of Si adatom binding and diffusion on Si(100) has also been conducted in collaboration with an outside group. (d) Vacancy induced self-diffusion in silicon at high temperature has been studied with ab initio molecular dynamics techniques. These results have been submitted for publication. Work is continuing on the vibrational properties of GaAlAs superlattices, focusing mainly on the effect of interface disorder on the Raman spectra.

## 6466 DETERMINISTIC METHODS IN STOCHASTIC CONTROL RESEARCH

M.H.A. Davis Imperial College London, UK SL: ARDEC

SC: NVEOC, ARO, BRL

The goal of the research is to show that a stochastic control problem can be reduced to a parameterized family of deterministic control problems to which the methods of deterministic control theory can be applied. It is conjectured that this can be accomplished by showing that the fundamental nonanticipative requirement on the control in a stochastic problem can be satisfied by reformulating the problem as an equality constraint and introducing an appropriate Lagrange multiplier. The partially observed stochastic optimal control problem is reduced to a family of infinite dimensional deterministic optimal control problems (control of the pathwise filtering random PDE). Nonanticipativity is introduced as in the complete observations case by a Lagrange multiplier process and optimization is carried over the class of anticipating controls. The Lagrange multiplier is defined in terms of the adjoint processes of the deterministic and stochastic infinite dimensional maximum principles.

## **B.** Chemistry and Biological Sciences

## 5973 STRUCTURAL AND BIOPHYSICAL CHARACTERIZATION OF A GLUTAMATE RECEPTOR

P.N.R. Usherwood University of Nottingham Nottingham, UK E.A. Barnard University of Cambridge

University of Cambridge Cambridge, UK SL: CRDEC, ARO SC: NRDEC

Molecular genetic techniques are being used to obtain a preparation of glutamate receptor (GluR) protein complex sufficient to enable further study of its structure and biophysical properties. The experimental app — h taken by Professor Usherwood's group, in collaboration with Professor Barnard's group at Cambridge, is to include purification of GluR from locust muscle; identification and enrichment of the GluR messenger RNA via expression in *Xenopus* oocytes; cloning the complementary DNA encoding the GluR; incorporation of GluR in lipid bilayers;

#### IX European Research Program

electrophysiological studies, and biophysical and structural characterization of reconstituted GluR complexes. They have succeeded in isolating and purifying the kainic acid (KA) GluR using the brain of Xenopus where it is exceptionally abundant. All the evidence obtained from the pure receptor indicated that surprisingly it consists of a single protein (containing several subunits) which possesses both the KA and the AMPA (a-amino-3-hydroxy-5-methylisoxazolepropionate) receptor binding sites. The largest subunit (42K) appears to have high homology with a 48K polypeptide that was isolated from the amphibian Rana by Wada. Reconstitution into asolectin/cholesterol bilayers has been successful, and channel openings were observed. The peptide sequences obtained for the Xenopus GluR were used to construct DNA primers, which in polymerase chain reaction yielded an 850-base fragment which has now been fully sequenced. This will be used as a probe to screen cDNA libraries from larval locust. The main objective is now to obtain full length cDNAs encoding subunits of the insect non-NMDA receptors of the nervous system. Work is continuing to characterize the full length CDNA which has been obtained in recent work. Additional molecular biology and full pharmacological studies will be undertaken. Also additional work with artificial bilayers containing membrane-spanning peptides will be completed.

## 6089 MOLECULAR IONIZATION AND DISSOCIATIVE IONIZATION AT HYPERTHERMAL SURFACE SCATTERING

A. Amirav Tel Aviv University Tel Aviv, Israel

SL: BRL

SC: CRDEC

This research project proposes to study molecular ionization and dissociative ionization induced by a collision with a surface at hyperthermal energies (1-20 eV). The P.I. has discovered that stable molecules such as anthracene, aniline, propyliodide, and fluorocarbons undergo collision-induced ionization from surfaces such as single crystal diamond. Molecules with low ionization potentials are ionized to give positive molecular ions. Those containing electronegative groups or atoms such as Cl, I, Br, and CN undergo dissociative ionization to give negative halogen or NO<sub>2</sub> ions and positive ions of the rest of the molecule. Recent experiments have shown that rhenium oxide appears to be a universal ionizer for all the organic molecules (and a large portion of

## IX European Research Program

inorganics) that have been tested. Ionization yield of close to 10 percent was achieved in a favorable molecule such as piperidine, while the yield in cyclohexanes and octane isomers was 0.001-0.0001 percent. This value is comparable to that of electron impact ionization, but with considerably smaller background. A similar enhancement of the molecular ion was seen with cholesterol. Ionization of clusters of carbon tetrachloride and other organic clusters is planned for future experiments. The main focus of the latest research was on the completion of the new and optimized apparatus, which included a new surface holder and manipulator, optimization of technical rhenium foil as the best practical surface for positive ion HSI, and instillation of an electron impact ion source to help calibrate the HSI. HSI of cholesterol has been obtained with good efficiency. The degree of ion fragmentation is fully tunable, and one can obtain HSI-MS dominated by the undissociated molecular ion at low incident kinetic energy. Studies have begun on isomer effects on the mass spectra of 1,2 and 3-bromopentanes.

## 6249 STEREOCONTROLLED CATALYSIS OF REACTIONS OF NITROALKANES

A.P. Davis University of Dublin Trinity College Dublin, Ireland

SL: ARO

## SC: ARDEC, BRL, EOARD

The objective of this project is to investigate the possibility of enantioselective catalysis of the conjugate addition of nitroalkanes to electron-deficient alkenes using chiral bicyclic amidine or guanidine bases as catalysts. Because of the interest of the Air Force in this area, the project is co-funded with EOARD. Professor Davis has used molecular modeling extensively to guide his synthetic efforts, which are proceeding at a good pace. At this stage of the project, they are at the stage of closure of the key intermediate to generate the desired guanidine compound which is expected to show catalytic activity.

## 6294 MECHANISMS OF LASER INDUCED REACTIONS IN OPAQUE HETEROGENEOUS ENVIRONMENTS

E Wilkinson Loughborough University of Technology Leicestershire, UK

SL: ARO

SC: CRDEC, NRDEC, ARDEC

#### **B.** Chemistry and Biological Sciences

This research effort will further develop the technique of diffuse reflectance laser flash photolysis that was pioneered by Professor Wilkinson. Studies will include the determination of absorption and emission spectra with decay kinetics of photoproduced transient intermediates at interfaces within zeolite cavities, in polymers, and on dyed fabrics. Elementary reaction rate constants of various excited states and of free radicals will be obtained in these heterogeneous environments. The materials to be studied include organic ketones, aza-aromatics, nitro-compounds, and dyes. Electron transfer from triplet anthracene to methylviologen has been studied in methanol solution prior to studying this same reaction on a silica surface. A germanium based detector for time resolved studies of near infrared luminescence from the singlet delta excited state of oxygen has been successfully assembled and tested. In addition, various microcrystalline samples and dyes adsorbed on cotton fabric have been studied using diffuse reflectance laser flash photolysis, the results of which form part of a recent publication in the Journal of the Indian Academy of Sciences.

## 6305 CATALYTIC AGENT DEGRADATION ON OXIDE FILMS AND IN MICROHETEROGENEOUS SOLUTION SYSTEMS

M. Gratzel Swiss Federal Polytechnic Institute Lausanne, Switzerland

SL: CRDEC

SC: ARO, CRDEC, NRDEC

This research is a continuation of Professor Gratzel's earlier catalytic photo-oxidation project. Here he proposes to investigate the destruction of simulants of toxic chemicals on the surfaces of oxide semiconductors, particles, or colloids, in particular oxides of Ti, Fe, Zn, Ni, and V. The principal pathways that have been found are oxidative mineralization and nucleophilic cleavage reactions. In recent experiments, both photocatalytic and dark decompositions of organophosphate compounds diethylbenzylphosphonate and diethylethylphosphonate were investigated in the presence of hydrogen peroxide as oxidant. It was found that ferric sulfate greatly accelerates the complete mineralization of both these phosphonates as well as the substituted aromatic compound nitro-o-xylene.

## 6307 SYNTHESIS AND APPLICATIONS OF LARGE HETEROMETALLIC CLUSTER SYSTEMS

D. Cardin W. Blau University of Dublin **Trinity** College Dublin, Ireland SL: NRDEC

SC: ETDL, ARO, EOARD

This project is on the synthesis and applications of large heterometallic cluster systems which show promising nonlinear optical (NLO) properties. This is an excellent collaboration between chemists and physicists; the chemistry group of Cardin prepares a wide array of materials for analysis by Blau's physics group for their NLO properties. The types of clusters being made are those derived from addition of dialkyltin groups to the metal-metal bonds of various metal carbonyl clusters such as  $Ir_4(CO)_{12}$ . The NLO properties, as determined by Chi-3 measurements, are then measured as a function of the cluster volume and composition. Other materials being prepared and studied include metal containing conjugated polymers. It has been shown that incorporation of a group 10 metal into the backbone of a polyacetylene polymer leads to enhancement of Chi-3 over the unsubstituted polymer. Other materials under study are gold colloids, metalloporphyrins, and the Fullerenes. Surprisingly  $C_{60}$  was found to have strong NLO properties.

## 6308 CATALYTIC MONOCLONAL ANTIBODIES FOR DECONTAMINATION OF SULFUR MUSTARD

B. Green The Hebrew University Jerusalem, Israel SL: CRDEC

SC: ARO, NRDEC, EOARD

This project is jointly funded by CRDEC and ARO. The goal of this work is to design and synthesize a series of at least five haptens which will be characterized by physical organic chemistry techniques. conjugated to two protein carriers, and used to raise monoclonal antibodies which will be purified, characterized, and submitted for testing to demonstrate binding and neutralization of sulfur mustard. The project is a multidisciplinary one and involves both chemistry and immunological work. The synthetic work was progressing well.

## C. Aeronautics and Mechanics

## 5824 RADIAL INFLOW TURBINE STUDY

R.L. Elder Cranfield Institute of Technology Cranfield, UK

SC: TACOM, PROP DIR, ARO

This research investigation has technical objectives of (a) obtaining an improved basic understanding of the flow processes in high speed radial inflow turbines and (b) obtaining needed experimental data to validate computational codes being developed by the Army and others. The objectives are being achieved by an experimental study of two comparative turbine rotors. The two test rotors, provided by Turbomach, are a metal rotor already in use, and a second rotor, also manufactured in metal, but to the design of a ceramic rotor. These rotors are incorporated into an existing experimental rig at Cranfield which is modified to accept the turbine unit. The rig includes conventional instrumentation to define turbine overall performance and laser anemometry to probe the detailed flow within the turbine. The laser anemometer is nonintrusive, has a spatial resolution small enough to measure flows within the passages of interest, and can be used in rotating blade rows (where strobing the data collection electronics with the blade passing frequency will allow the blade to blade variation of the flow velocity to be measured). Throughout the study, the major objective is to relate the detailed flow conditions with overall performance parameters obtained from turbine calibration. Such overall parameters are mass flow and enthalpy, and particular attention is being given to ensuring that the point measurements of the laser anemometer provide "bulk mean" parameters which agree with overall performance values.

## 6541 STUDY OF EXPLOSIVES

LE Field University of Cambridge Cambridge, UK

SL: ARDEC, BRL SC: ARO, BRL

This research has a primary objective of investigating liquid propellant (1846) ignition when subjected to impact. The Cavendish Laboratory's two dropweight facilities are being used to provide a range of impact loadings to obtain propellant sensitivity data. The transparent anvil drop-weight apparatus is being used to obtain direct visual information, recorded at

#### IX European Research Program

microsecond time intervals, of the liquid propellant deformation and the location of ignition sites. The temperature of the deforming layer and of any "hot spots" is being determined by using a heat sensitive film technique. Potential ignition mechanisms being investigated include (a) adiabatic compression of cavities, (b) boundary layer heating, and (c) viscous flow heating. These mechanisms are being studied both experimentally and theoretically.

#### 6571 COMPOSITE BEAM ANALYSIS

M. Borri Politecnico di Milano Milan, Italy SL: ARO SC: AVSCOM

This investigation is to develop the mathematical formulation for a composite material beam slice. taking into account the effects of constant pretwist and prebending. The results of the analysis will provide the solution of the cross section in terms of the displacement and the stress distribution due to six independent and equilibrated load conditions corresponding to the components of the cross section force and moment resultants. The research consists of the following tasks: (a) Theoretical developments of the principle of virtual work for a pretwisted and prebent beam with a constant curvature and twist; the possibility of the cross section tilted with respect to the axis will be investigated. (b) Discretization of the cross section via finite element method using the displacement formulation of the cross section problem. Description of the organization of the computer code. (c) Formulation of different elements like isoparametric plane element, lamina element, line element in anisotropic material. (d) Eigensolution analysis of the cross section problem. (e) Modification of a pre-existing computer code for straight beams to include the curved and titled geometry. (f)Development of two numerical test cases with NASTRAN comparison.

## **D.** Materials Science

## 5548 THE SOL-GEL-XEROGEL TRANSITION IN SILICA GLASS AND NOVEL ORGANIC DYE/INORGANIC GLASS PHOTOACTIVE MATERIALS

David Avnir The Hebrew University of Jerusalem Jerusalem, Israel

SL: MTL, NVEOC

#### **D.** Materials Science

Photophysical probes will be used to characterize the structural changes during monomer-sol-gel-xerogel transitions and to develop room temperature processes for preparing novel organic dye/inorganic glass photoactive materials. The phenomenon of room temperature phosphorescence (RTP) of trapped organic molecules, such as Rhodamine 6A/B in silica glass made by sol gel process, the RTP lifetimes and RTP intensities will be determined as a function of gelation time, changing parameters like pH, water/ silane ratio, alkoxy groups and the metal atom. Organic photochromic dye/inorganic oxide glass will be tested for photophysical performance, stability and rate of color changes. The development of photophysical probes for the study of the sol-gel process will continue employing new probes, both of the pyrene family and of other well tested molecules. Small angle x-ray and neutron scatterings will be used for materials characterization, with special emphasis on the application of recent theories of scattering from fractal objects. The role of water in determining the structural properties of the final product as well as the details of the kinetic behavior will be investigated. And, finally, the possibilities of using monolithic blocks or thin films in which organic laser dyes are trapped will be explored as possible substitutes for dye solutions in dye lasers. One of the major aims of this project has come to completion, namely, the preparation of photoactive sol-gel glasses exhibiting room-temperature phosphorescence. A remarkable manifestation of the special properties of the silica sol-gel cage is the observation that many trapped organic molecules exhibit efficient phosphorescence at room temperature even when exposed to air, and in many instances even without the aid of a heavy atom, and in several cases, even in the wet gel. It is noted that phosphorescence is a delicate process which is usually quenched at temperatures which are not cryogenic and by exposure to oxygen. The generality of the phenomenon was demonstrated with the following molecules: phenanthrene, naphthalene, quinine, 4-biphenyl carboxylic acid, 1-naphthoic acid, eosin-v and pyrene. It was observed that under various gelation conditions, most dyes exhibited not only phosphorescence but also delayed fluorescence. Specific glasses were needed to observe phosphorescence from the various glasses. For example, neutral conditions were sufficient to observe phosphorescence from phenanthrene, naphthalene and quinine, but basic conditions were needed for the carboxylic acids and for eosin. A heavy atom (Br) was needed in order to observe phosphorescence from pyrene,

#### **D.** Materials Science

and an SiO<sub>2</sub> glass doped with NaBr was therefore prepared. Very long emission lifetimes were observed. For instance, when bi-phenylcarboxylic acid was trapped in an SiO<sub>2</sub> glass prepared under basic conditions, the lifetime reached the order of several seconds. Lifetimes of the order of milliseconds were obtained even from the wet gels. A detailed mechanistic study of the sol-gel transition was carried out with that carboxylic acid, including an Arrhenius type analysis of the transition between the delayed fluorescence mode and the phosphorescence mode. An obvious potential application of these findings would be an attempt to obtain a phosphorescent laser.

## 5686 ELECTRODEPOSITION OF DENSE CHROMIUM COATINGS FROM MOLTEN SALT ELECTROLYTES

G. Lorthior

F. Lantelme Centre d'Etudes de Chimie Metallurgique, CNRS and University Pierre et Marie Curie Vitry-Sur Seine Paris, France

SL: BWL, ARO, MTL, ARDEC

This is a jointly supported program (MTL, AROE, ARO) with the objective to study the mechanism of electrodeposition of chromium from fused halide electrolytes, optimize parameters to obtain dense, adherent coatings and to characterize their physical properties. Chloride and chloride-fluoride mixtures are used in the temperature range of 400-500°C with pulse and reverse pulsed power to optimize the process to obtain dense and adherent coatings (120-200 microns thick) on flat and interior cylindrical steel substrates. The physical properties including hardness, density and microstructure of the coatings will be determined and related to the composition, temperature and current density used in the deposition runs. Research has shown the feasibility of pulsed current of chromium plating on nickel, iron, 4340 alloy. All the samples had a flat surface. The morphology of the deposits were examined by electronic microscopy. All the observations confirm: a the compacity of the coatings with a uniformity in size of crystals, b the good continuity between the deposit and the matrix, and c the grain size and the preferential orientation in the growth after etching of a cross section.

## 5884 A NEW APPROACH TO TUNABLE LASER MATERIALS

R. Reisfeld The Hebrew University of Jerusalem Jerusalem, Israel

SL: NVEOC, ETDL, HDL SC: MICOM, ETDL, HDL, MTL, ARO

The solid state tunable dye laser has shown good photostability when operated in the range of a few hundreds µj/pulse and with slope efficiency of about 7.5 percent. This is due to a stable perylene dye embedded in a composite glass, which is a sol-gel glass impregnated by a polymethyl methacrylate polymer. Professor Reisfeld's group is currently improving both slope efficiency and optical quality of the laser material. One of the purposes of this project is the investigation of thin film dye laser, namely waveguide light confined in a thin transparent film doped by a dye. Investigations will follow three directions: (a) photostable dyes and suitable solid hosts for them, (b) controlled refractive index of the film for the purpose of matching the thickness and refractive index to obtain a single mode waveguide, and (c) possibility of nonlinear optical effects in the waveguide. Malachite Green introduced into glasses exhibits a characteristic spectral behavior depending on the mode of preparation of the glass and its environment. Neutral monocation and di-cation forms can be prepared. Exceptionally high quantum efficiency is obtained with ammonia treatment. An analogy is found in the structure with electron or proton transfer. Very high affinity of this dye to sol-gel glass makes easy the preparation of the doped glasses at various optical densities. This can find application as saturable absorber for fmsec lasers and also a nonlinear optical waveguide for high laser powers.

## 6011 HIERARCHICAL STRUCTURE IN ADVANCED POLYMERS: PHASE BEHAVIOR, ORIENTATION, PROPERTIES

A. Keiler J.A. Odell University of Bristol Bristol, UK

SL: ARO, MTL

*Phase Relations:* The class in which the liquid crystal phase is metastable (monotropic) was chosen for in depth examination as regards the influence of the first formed (but metastable) liquid crystal (LC) phase on the subsequent formation of crystals (C). The two aspects examined were rate of crystallization and morphology. It was found that the overall

#### **IX European Research Program**

rate of crystallization was greatly enhanced by the pre-existing LC phase in cases where LC formed first. This was found to be due to enhanced nucleation rate rather than growth rate. The enhancement of nucleation rate is at least in qualitative agreement with expectations yet leaving some open ended question on the nature of the crystallization-promoting nuclei. Three distinct morphologies were identified on the level of the optical microscope: (a) Without the pre-existence of LC phase the morphology is the usual spherulites. (b) On transformation from the LC phase at low supercooling, the characteristic LC texture reorganizes into large scale "spherulite type" textures of two distinct classes: one which is highly birefringent, grows fast, yet nucleates sparsely, and another which is less birefringent, more slowly growing, but which nucleates abundantly, remnants of the original LC texture, (fine mottle) being incorporated into both. (c) On transformation from the LC phase at high supercooling, the characteristic LC texture (mottle) is preserved without change. The above has many implications on the structure hierarchy and the underlying mechanism of LC-C transformation. Large Scale Textures: This effect, discovered in the course of the previous contract, has been pursued. Significant new information was obtained on the origin and structure of large scale textures. Thus, the significance of the orientation effect of elongational flow became apparent, resulting from concentric contraction while in the isotropic phase. This has important implications for processing and handling (even accidental) of melts of intrinsically LC polymers. Further, a fine banded structure arising while passing through the nematic state connects this subject with another major area of LCP studies concerned with the initial relaxation from the oriented state. In this case, the banded structure appearing in combination with the large scale structures offers definitive opportunities for optical analysis of the underlying orientation relations, and of their dependence on flow conditions and sample type (molecular weight). A new successful start with electron microscopy has opened a window into the finer scale aspects of the structure hierarchy underlying these texture features and mechanisms. In situ shear-flow study: The first experimental work on orientation-disorientation by x-ray diffraction using a synchrotron source was exceptionally productive. Evaluation is awaiting data retrieval.

## 6148 ADIABATIC SHEAR BANDING AT DIFFERENT IMPACT VELOCITIES

J.R. Klepaczko University of Metz Metz, France

SL: MTL SC: BRL

A new experimental technique to study adiabatic shear bands at different displacement velocities has been pursued. The technique is in its early stage of development; i.e., the mechanical parts have been machined and the experimental setup has been assembled. The measuring techniques are in preparation.

#### 6579 SENSORY SYSTEMS FROM NATURE

J.F.V. Vincent University of Reading Reading, UK

SL: NRDEC

SC: ARO, AROE, CRDEC

The object of this short project was to produce a catalogue of sensory systems from nature; i.e., covering all animals and plants from single-celled to very complex organisms. The catalogue actually includes information from a rather more closely defined set of references. The main idea of putting the information onto a computerized database is to allow for its expansion as new sources of information are published or uncovered. Also included are some more general books in the database which will give some background on the biology and general working of sense organs. It was decided early on that the purpose was to provide information for the development of sensory systems where technology seems to be lagging behind nature or has not yet incorporated it. This means that the whole area of "biosensors" has been ignored. Similarly, the well-worked area of light-sensing has not been catalogued. The measurement of time seems to be better engineered by technology than biology so circadian and other behavioral rhythms have largely been omitted. The remaining criteria for the inclusion of papers and reviews are a some idea of a mechanism for sensing is presented, or b data included on sensitivity of the sense organ, or c a mechanism for transduction is presented. In effect this has allowed the inclusion of publications in the general areas of mechanotransduction (hearing, touch, perception of gravity), electromagnetic transduction (electric sensing, geomagnetic sensing) and thermal radiation; e.g., infrared receptors in snakes.

## **E. Environmental Sciences**

## 6185 PARTICLE DYNAMICS AND GRAVEL STREAM-BED ADJUSTMENTS

P.A. Carling Windermere Laboratory Ambleside, Cumbria, UK

A considerable snow-pack and high air temperatures caused high run-off rates in 1991. Long continuous multiday records of pebble transport were obtained using the detector log. Preliminary observation indicated that transport was in waves approximately every 30 seconds. These records were supplemented by detailed hydraulic data collected during two large hydrographs over 24-hour periods. Data include depth, velocity, and shear stress distributions, as well as fluctuations in bed level which can be correlated with the bedload records. The traversing echo-sounder failed to work due to cavitation problems around the head, but it is hoped that these problems will be solved for the 1992 season.

## 6296 IMPROVING THE CHARACTERIZATION OF ROCK STRUCTURE GEOMETRY

J.A. Hudson

Rock Engineering Consultants Welwyn Garden City, Herts, UK

In any rock engineering problem, there are a multitude of rock properties that could be measured. Similarly, there are a multitude of proposed rock mechanics mechanisms that can be invoked, and the structure can be designed to defend against many types of potential collapse mechanisms. Furthermore, all these properties and mechanisms influence one another to a greater or lesser extent. One is faced, therefore, with making a decision in an increasingly complex world on how to proceed from the original "top of the flowchart" rock engineering requirement. In order to identify and present the interactions between rock mechanics and rock engineering factors in these conditions, the P.I. previously proposed the use of rock mechanics interaction matrices. It has recently been realized that this approach is in fact a sub-set of a far wider set of procedural and analysis techniques based on information technology. The purpose of the present research is to develop a procedure to enable a client, engineer, contractor, or researcher to decide for any project the relevant rock properties and their priority, relevant boundary conditions, rock mechanics mechanisms that should be studied, the interaction between these,

and hence the overall type and sequence of site investigation, analysis, design, construction and monitoring that should be conducted for optimal use

## F. Electronics and Computer Sciences

## 5830 ENHANCED BACKSCATTERING FROM ROUGH SURFACES

J.C. Dainty Imperial College of Science and Technology London, UK

of the resources available.

SL: ARDEC SC: CECOM

Measurements of the angular scattering by identical gold and dielectric surfaces have continued at wavelengths of 0.63  $\mu$ m, 1.15  $\mu$ m and 10.6  $\mu$ m. Those at 3.39  $\mu$ m are being completed.

## 5940 PHYSICS RELATED TO FUTURE ELECTRONIC DEVICES

M. Pepper Cambridge University Cambridge, UK SL: ETDL

SL: ETDL SC: NVEOC

This research can be divided into three main areas: (a) physical processes in semiconductors, (b) electronic transport in small silicon devices, and (c)electronic properties of small GaAs structures fabricated by a combination of molecular beam epitaxy and high resolution electron beam lithography. In topic *a* the direct measurement of electron heating in (3D) InSb by the application of a pulsed electric field was investigated. When the resistance, R, is a function of the electron temperature,  $T_e$ , a measurement of the time dependence of R allows extraction of the electronic specific heat. Measurement of this quantity has shown that the density of states at the bottom of the conduction band is reduced by a significant factor below the value expected on the basis of free electron theory. This reduction is attributed to the formation of an impurity band. Electron transport in small silicon MOS devices has been investigated at low temperatures with particular reference to strain at the Si-SiO<sub>2</sub> interface (topic b). In a large device, this is not significant, but as the size decreases the entire channel can be affected by interfacial stress. The result can be a reduction in the energy separation of the valleys and an increase in the electron effective mass, leading to a reduction in

#### **IX European Research Program**

#### IX European Research Program

mobility. The rate of electron-electron scattering was investigated in devices sufficiently narrow for this process to be effectively one dimensional at low temperatures. It was found that disorder played a significant role and increased the scattering rate above the theoretical value calculated by assuming an absence of impurity scattering. The greatest body of the work under the program was on electron transport in reduced geometry samples prepared from GaAs-AlGaAs heterojunctions (topic c). The high electron mobility in these structures (in excess of 10<sup>6</sup>  $cm^2volt^{-1}s^{-1}$ ) corresponds to values of mean free path for scattering in excess of  $10^{-4}$  cms. This can be considerably greater than the size of a sample defined by high resolution electron beam lithography. Formation of two Schottky gates on the AlGaAs in a GaAs-AlGaAs heterojunction (split gates) allows the 2D electron gas to be narrowed until a transition to 1D behavior occurs. As the device length is short, the conductance is in the 1D ballistic regime (due to the absence of scattering). Consequently split gate devices, and allied systems, can be used to explore diffraction and interference effects in small, mesoscopic structures. For example, a superlattice of 1D channels was fabricated and investigated. In this respect, the present work has explored, among other topics, interference effects and the change in quantization in the presence of a strong electric field. A modification of the I-V relation in small structures in the presence of a defect in the channel was also found. This was attributed to the role of capacitive charging.

## 6170 ION BEAM MIXING IN MULTIPLE QUANTUM WELL STRUCTURES

B.L. Weiss University of Surrey Guildford, England SL: ARDEC SC: ETDL

The aim of this research is to investigate the use of ion implantation to induce mixing of multiple quantum well (MQW) structures and to study its application to the fabrication of optical waveguide devices in III–V semiconductor materials. These experiments are designed to clarify the physical mechanisms involved in the mixing of MQW layers and to determine the optical changes produced by this mixing. Several different III–V semiconductor materials are being studied in this effort along with various implanted ions and annealing techniques. The research also involves development of computer codes to model various optical waveguides including bur-

#### F. Electronics and Computer Sciences

ied, stripe geometry, MOW structures. Waveguide experiments are being carried out at several different infrared wavelengths to establish the optical properties of MQW structures before and after implantation. Comparison with diffusion techniques for achieving MOW layer mixing will be made and practical structures, such as non-square wells, will be analyzed. Ellipsometric measurements are to be performed and changes in the refractive indices are to be correlated with material properties and implantation procedures. This research should yield valuable information relating to the processing of MQW layers for laser fabrication and for optical computing devices required in future Army systems. Considerable progress has been made with regard to the implantation induced disordering of AlGaAs/GaAs quantum well structures and the modeling of the optical properties (absorption coefficient and refractive index) of quantum well structures. Several papers covering this work have been written and submitted for publication.

## 6291 NOVEL OPTOELECTRONIC DEVICES BASED ON COMBINING GaAs AND InP ON Si

P. Demeester University of Gent Gent, Belgium

SL: ARDEC, ARO

This research project addresses some of the basic technological procedures necessary in the fabrication of optoelectronic devices for optical interconnects and for optical computing. There are four main areas that are included in this research. The first is optimization of the heteroepitaxial growth of GaAs on InP and on Si for the development of high quality optical waveguide and laser structures. The second involves investigation of nonplanar growth techniques for the integration of lasers and optical waveguides in a single-step growth process. The third is based upon advances in the growth techniques and includes efforts to fabricate an optical modulator based on InP multiple quantum wells grown on a Si substrate. The final topic includes a study of the use of an epi-liftoff technique for the quasi-monolithic integration of III-V devices. This technique is an alternative to heteroepitaxy and may alleviate some the more serious difficulties encountered in such growth. Finally, the results of these investigations are to be combined to develop optical interconnect schemes for use in large volume, high density optoelectronic systems.

Such systems are required in massive electronic computers and in optical signal processors for Army target tracking applications. Recent work has concentrated on different topics: optimization of the heteroepitaxial growth of InP on GaAs (use of selective growth and shadow masked growth), further development of nonplanar growth for laser-waveguide coupling (and application to broad spectrum LEDs), optimization of In(AI)GaAs/AI/GaAs growth on GaAs (and application to lasers and modulators), and fabrication of a GaAs/InP OEIC for optical switching.

## 6458 LASER PROPAGATION THROUGH TURBULENCE

A. Consortini University of Florence Florence, Italy

SL: ASL, ARO

This research involves the analysis of experimental data concerning the intensity fluctuations of laser radiation propagating through a turbulent atmosphere. The data consist of highly-sampled intensity measurements, taken in collaboration with NOAA, over a very well monitored optical range. Atmospheric conditions varied from weak scintillation to the most saturated scintillation ever observed. The data base can be expected to yield the moments of the intensity, including the scintillation index, as well as the full probability density functions. The evolution of the probability distributions with changing propagation conditions will be investigated along with the effect of the inner scale of turbulence on the laser scintillation index. A deconvolution procedure to remove noise effects from actual intensity fluctuations will be studied. Results of this research will help to verify the applicability of current theoretical models concerning laser propagation through the turbulent boundary layer. From the large data table previously produced in the computer, plots of all quantities were made versus the cycle number for all measurements in order to check the regularity of the data. Scintillation index was analyzed versus wind. Separate files of histograms of intensity scintillation, one for each cycle, and new "filtered" histograms were produced. A deconvolution procedure was applied to data from multiple aperture measurements with good results. Two communications were submitted for a future Scientific Congress.

## 6563 INVESTIGATION OF (HgZn)Te FOR IR DETECTION, EMISSION AND PHOTONICS

R. Triboulet

Centre National de la Recherche Scientifique Meudon, France

SL: NVEOC. ARO SC: ETDL, HDL, MICOM, ARO, NVEOC

Annealing of  $Hg_{1,-1}Zn_{1}Te$  with x = 0.15 (MZT-0.15) under Hg overpressure has been performed at relatively high temperature (4000-5000°C) because of the low diffusion of mercury. The crystals are *p*-type with acceptor concentrations governed by Hg vacancies which are about five times higher than in MCT-0.22 with the same annealing conditions. These higher concentrations are related to the higher Hg content in MZT. Low temperature stoichiometric annealings lead to ntype conductivity. The corresponding diffusion is low compared to its value in MCT. It has not been possible to reach homogeneous n type samples because unknown residual acceptors are present in the material. Indium diffuses very slowly in MZT. It has a poor activity in the lattice and strongly weakens the electron mobility. Copper presents a high diffusion coefficient in MZT and can dope above p = 1019 cm<sup>-3</sup> with a weak mobility decrease. Precipitation experiments reveal a lower vacancy precipitation of Hg vacancies in MZT than in MCT. However, experimental results are scattered and depend on sample history. Results of interdiffusion between HgTe and ZnTe have been reported. They allow one to model the interdiffusion process. According to this process graded composition layers on ZnTe substrates have been grown and used as planar optical waveguides. Values of the refractive index so probed were given versus x. The interdiffusion coefficient is not a monotonous function of x. A study to relate its values to microscopic parameters was undertaken. Characteristic phonon frequencies of zero wave factor give valuable information on bonding parameters in solid solutions. A very simple analysis allows one to separate force constants and effective charge for each type of near neighbors dipoles in the lattice (Hg-Te and Zn-Te in MZT). The corresponding evaluation has been performed in MZT, MCT and  $Cd_1$ ,  $Zn_1Te$  (CZT). It shows very clearly the destabilization of the Hg-Te bond when Cd is substituted to Hg and its increase of force constant with Zn substitution. A refinement of this crude model was undertaken to obtain an evaluation of elastic constants in solid solution as a function of their composition. The apparatus to measure the linear thermal expansion coefficient from 4 K to 300 K is now in operation. Results now obtained on ZnTe and HgTe

#### **IX European Research Program**

are the same as those already given by an Australian group. Measurements of CdTe, MCT and MZT will be performed. A study of the low temperature electrical behavior of  $Hg_{1-x}Zn_xTe$  (MZT xsamples with x = 0.15 reveals the presence of an acceptor level whose energy varies like in  $Hg_{1-x}Cd_{x}Te(MCT x)$ with acceptor concentration. This level appears more of deep type although it is near the valence band (13 meV at low acceptor concentration). The regults also show that the material is highly compensated with a residual net acceptor concentration lying between 1015 and 1017 cm<sup>-3</sup> at 0 K. It seems that samples have a too-high acceptor density and an effort in the "purification" before growth is being undertaken. Results on the linear thermal expansion coefficient for several xin MCT and MZT have been obtained between 4 K and 300 K. From the measurements, it appears that the already published results are completely wrong and the (T) of MCT 0.22 is very near that of HgTe at low temperatures expressing a weak destabilization of the Hg-Te bond when Cd is substituted to Hg. This result is consistent with the rough estimation of force constants deduced from infrared results. The (T) of MZT 0.15 and MZT 0.25 expresses an

#### F. Electronics and Computer Sciences

increase of the HgTe bond strength with Zn substitution. A phenomenological model gives a quantitative expression of the (T) in MCT and MZT. A link with microscopic parameters is now undertaken. In order to improve the crystal growth of MZT crystals, a thermodynamic analysis of the Zn-Te, Hg-Te and Zn-Hg-Te systems has been performed. The thermodynamic analysis of all data in Zn-Te and Hg-Te binary systems yields up to the corresponding liquid properties by using Redlich-Kister polynomial forms for mixing functions in an associated model: constraints, at the melting point of the II-VI sphalerite and at the eutectic point in the Hg-Te system, allowing reduction of the independent parameter set to 8 for Zn-Te and 6 for Hg-Te. The association character decreases from Zn-Te to Hg-Te melts. By using all the limiting binary functions and taking into account ternary interactions, the Zn-Hg-Te ternary liquid is described before generating the quasi-binary section of the Zn-Hg-Te phase diagram: large repulsive interactions in the  $Zn_xHg_{1-x}$ Te alloys are found with a quasi-regular approximation and a miscibility gap is predicted below 3300°C. PHg partial pressures along pseudobinary melts appear to be nearly independent of the Hg-melt composition.

# **Proposal Numbers**

*Note:* The Roman numeral refers to the scientific division, and the alphabetic character refers to the division subsection. Proposal numbers are in ascending sequence within the subsections.

Proposal Number		Proposal Number		Proposal Number		Proposal Number	
5265-ER	IX-A	25181-CH	H-B	25697-PH	I-D	26260-GS	VII-B
5548-ER	IX-D	25190-EG	V-C	25702-1.8	101-D	26264-PH	I-E
5653-ER	iX-A	25193-MS	VI-B	25706-MA	IV-C	26272-MA	IV-A
5686-ER	IX-D	25199-MS	VI-A	25730-GS	VII-D	26278-EL	VIII-B
5824-ER	IX-C	25202-MS	VI-C	25731-1.8	111-C	26281-GS	VII-B
5830-ER	IX F	25222-CH	II-C	25739-CH	11-B	26284-CH	II-B
5884-ER	IX-D	25229-CH	tf-E	25752-LS	III-D	26287-MS	VI-D
5933-ER	IX-A	25245-EG	V-C	25760-MS	VI-A	26296-CH	11-C
5940-ER	IX F	25251-MS	VI-D	25761-CH	11-B	26381-EL	VIII-C
5973-ER	IX-B	25264-MA	IV-D	25771-EG	V-D	26383-PH	I-E
6011-ER	IX-Ð	25286-CH	11-E	25782-MA	IV-A	26384-GS	VII-D
6089-ER	IX-B	25290-CH	II-B	25794-EG	V-C	26385-LS	III-F
6148-LR	1X-D	25324-MA	IV-E	25819-MA	IV-C	26391-MA	IV-B
6170-ER	IX-F	25327-EG	V-D	25833-MS	VI-A	26.392-MS	VI-C
6185-ER	IX F	25339-EL	V10-C	25836-MA	IV-C	26.394-MA	IV-C
6249-ER	IX-B	25345-EG	V·A	25859-MA	IV-D	26400-MS	VI-A
6271-ER	IX-A	25347-MA	IV-C	25874-MA	IV-A	26403-EG	V·C
6280-ER	IX A	25349 PH	I-E	25906-PH	1-D	26404-GS	VII-E
6291-ER	IX-F	25350-EL	V111-C	26015-PH	I-D	26426-CH	II-A
6294-ER	1X-B	25373-MS	VI-C	26021-MS	VI-C	26427-MS	VIA
6296-ER	JX-E	25374-PH	I-D	26031-GS	VII-B	26434-EL	VIII-A
6305-ER	łX-Β	25390-MS	VI-B	26049-CH	II-D	26438-MA	IV-E
6307-ER	1X-B	25396-MA	IV-A	26051-EL	VIII-B	264.39-MS	VI-C
6308-ER	IX-B	25397-MS	VI-B	26057-EG	V-A	26441-CH	II-E
6458-ER	IX-F	25400-EG	V A	26061-EG	V-D	26442-PH	I-D
6466-ER	JX A	25408-PH	1-E	26063-MA	IV-F	26443-EG	V-A
6541-ER	IX-C	25409-EG	V-D	26068-MS	V1-C	26444-EL	VIII-A
6563-ER	IX F	25411-CH	II-B	26072-CH	U-E	26449-MS	VI-A
6571-ER	IX-C	25422-EL	VIII-C	26088-PH	T-E	26456-EG	V-C
6579-ER	IX-D	25424-MS	VI-B	26099-1.8	111-1-	26460-EL	VIII-E
21545-MS	VLA	25428-MA	IV-A	26106 CH	II-D	26462-PH	I-B
22459-MS	VED	25435-CH	II-A	26108-MA	IV-C	26463-MA	IV-A
23206-EL	VIIEA	25459-EG	V-A	26113-MA	IV-A	26480-GS	VII-D
23306 MA	1V-1-	25461-EG	V B	26145-CH	11-B	26484-EL	VIII-B
23577-MS	NI-D	25462-EG	V-D	26118-EL	VIII-E	26485-MS	VI-C
23908-MA 24102-MS	IV-E VI-E	25464 PH	1/D V-B	26123-MS 26126-CH	VI-C 11-C	26487-MA 26491-GS	IV-E VII-F
24102-MS 24166-MA	VI-D IV A	25467-EG	HI-D	26128-EL	VIII-C		VII-P I-B
24362-EG	N-D	25476-LS 25482-PH	LEE	26144-MA	IV-C	26566-PH 26571-MS	VI-C
24381 GS	VIEC	25487-PH	ьт. I-D	26145-CH	II-A	26576-1.5	III-B
24411-CH	11-A	25493-1.8	ni-B	26147-EL	VIII-A	26579-MS	VI-C
24413 CH	11 C	25500-CH	II-A	26151-1-1	VIII-B	26582-LS	III-D
24435-LS		25514-MA	1V-E	26160-PH	1-E	26591-MS	VI-C
24487-EG	V-C	25521-LS	III-E	26164-MS	VI-B	26595-EG	V-B
24557 MA	IV-C	25523-CH	H D	26167-MS	VI-B	26599-EL	VIII-C
24583-MS	VEB	25526-MS	VI-C	26169-MS	VI-E	26601-MS	VED.
24713-GS	VILD	25546-PH	I-E	26173-MS	VI-E	26616-MA	IV-B
24749 PH	14	25557-F1	VIII C	26188-EL	VIII-A	26617-MS	VI-C
24793-EL	VIII-F	255K6 ( H	II A	26191 CH	11-C	26620-EL	VIII-C
24845-MS	VLA	25594-EG	V A	26145-PH	1-D	26631-EG	V-B
24881-GS	VII F	25605-CH	пс	26211 PH	1-D	26636-CH	П·А
24931-1.5	III C	25617-CH	II A	26213-81.	VIII-G	26644-PH	1-D
24981-MS	VI-B	25623-11G	V-B	26218 MA	IV-A	26646-EL	VIII E
25015-EL	VIII B	25630 FG	V D	26223-PH	1-8	26647-MS	VLF
25045-EL	VIII C	25631 PH	t-E	26224 GS	VIED	26649-MA	IV-C
25069-MA	IV A	25653 PH	1 B	26232 1.8	III D	26651-EL	VIII-C
25104-CH	11-F	25662 MA	IN F	26238-CH	11 C	26656-MA	IV-D
25114 PH	₽-D	25663-1.5	111-D	26246 MS	VEE	26666 EL	V111-B
25126-1.5	III C	25669 (11	ΗВ	26256-CH	11 Đ	26667-MS	VI A
25167 PH	1-D	25674-1-1	VIII E	26257 PH	1.8	26673-MS	VI-B

## X indexes

## Proposal Numbers

Proposal Number		Proposal Number		Proposal Number		Proposal Numb- r	
				27620-MA	IV-F	28141-MS	VED
26674-MA	IV-D	27032-EL 27037-MS	VIII-E VI-A	27620-515 27625-EG	V-B	28143-MA	IV B
26676-PH	I-E VI-A	27044-MA	IV-D	27627-EG	V B	28146-MS	VED
26678-MS 26682-PH	1-D	27054-CH	n-E	27634-1.8	\{\-}·	28151-EL	V10+C 
26686-EL	VIII-B	27062-EG	V-B	27641-MA	IV A	28153-CH 28155-EG	V D
26695-PH	1-E	27075-EG	V-D	27646-PH 27690-MA	I-B IV-B	28159/EG	V-B
26697-EL	VIR-E	27076-EL	V111-E V1-B	27751-EL	VIII-E	28187-EL	VIII-F
26708-EL	VIII-A I-B	27163-MS 27273-PH	1-E	27752 EG	V-B	28192-MA	1¥-B
26709-PH 26711-EL	VIII-B	27282-MA	IV-F	27754-F.L	VIII-E	28215-EG	V-B VII D
26720-EG	V-C	27298-EL	VIII-A	27759-CH	If-C	28214/GS	VII D V-A
26728-MS	VI-C	27300-EG	V-D	27764-MS	VI D 1-B	28222-EG 28249-EG	V-B
26729-MS	VI-D	27,304-EL	VIII-C	27766-PH 27770-CH	11-C	28250 EG	V C
26735-EL	VIII-E	27.307-EL	V111-С 111-В	27772-GS	VILA	28252-EG	V-B
26736-MA	1V-D 1V-C	273144LS 27315-EG	V-A	27775-CH	11-C	28253-EG	VA
26746-MA 26747-MS	VI-B	27316-GS	V11-B	27780-PH	1-D	28258-PH	1-E 1-E
26748-CH	II-A	27364-MS	VI F	27786-MA	IV-B	28271-PH	a r: Vi-E
26750-LS	111-B	27365 MA	IV-D	27790-MA	1V-C VI-D	28272-MS 28283-EG	V.A
26751-MS	VI-C	27366-PH	1-E	27794-MS 27808-CH	11-E	28293-EG	V-B
26755-EL	VIII-B	27373-MS	V1-C IV-C	27810-MS	N1-F	28297-EL	VIII-E
26760-EL	V111-B	27381-MA 27392-MA	EV-F	27817-MA	IV-F	28298-CH	11-C
26761-EL 26767-LS	VIII-A III-F	27401-GS	VII-A	27834-EL	VIII-E	28307-EG	V-A
26769-EG	V-C	27403-MA	IV-A	278.38-PH	ЬE	28309-MA	IV-C V-C
26779-MA	IV-E	27407-MS	V1-B	27846-MS	N1-D	28310-EG 28373-PH	
26791-EL	VIII-C	27409-EG	V-A	27862-MA	IV-C - V-C	28314-CH	11-1:
26792-MA	1V-F	27417-EG	V-C	27864-EG 27865-EL	VIII-F	28316-EG	V-C
26797-EG	V-C	27418-PH 27425-PH	l-E 1-E	27868-MA	IV-C	28317-EG	V-A
26802-MA	IV-F VI-A	27431-PH	I-B	27869-MA	IV-A	28319-CH	ff-C
26806-MS 26811-MA	JV-F	27433-MA	IV-A	27870-GS	VIEE	28320 MA	1V-B V111-B
26813-EL	VIII-E	27440-CH	11-E	27873-EL	VIII C	28325-EL 28326-EL	VIII-G
26821-PH	I-B	27443-EL	VIII-B	27882-PH	1-E VIII-8	28328-MA	1V-E
26822-CH	n-c	27445-CH	II-E V-C	27883 EL 27886-EL	VIII-E	28329-EL	VIII-B
2682.3-EL	VIII-E	27455-EG 27458-PH	1-D	27887-CH	U-D	28335-EL	VIII-A
26825-MS	VI-B 1-D	27464-EL	VIII-E	27888-PH	1-8	28336-PH	1-D
26827-PH 26839-CH	ll-E	27468-1.5	m D	27890-LS	W-C	28339-EL	VIII-C VII-F
26863-EG	V-B	27469-EG	V-C	27892-MA	IV-E N-B	28344-GS 28345-EL	VIII-B
26871-MA	IV-B	27471-GS	VII-A	27894-EG 27899-EL	Vill-E	28347-EL	VIII A
26882-MS	VI-C	27472-MS	V1-C V-C	279814-151	VIII-C	28348-PH	I-E
26883-MS	VI-D 11-C	27480-EG 27482-GS	VII-B	27911 GS	VII-D	28350-EG	V-D
26887-CH 26891-MS	VI-C	27485-GS	VII-D	27916-1.8	HI-D	28351-EL	VIII-A
26896-EL	VIII-A	27488-LS	III-C	27917-EL	V111-E	28353-CH	II-A 1-i:
26898-EL	V10-F	27493-EL	VIII-E	27919-GS	VID III-C	28350-PH 28359-GS	VIEG
26899-PH	1-8	27494-1.5	111-A - 11-A	27956-1 S 27993-MA	IV-C	28361-US	fff-C
26902-GS	VII-A V-A	27502-CH 27505-CH	IED	27994 E1	V10-F	28362 PH	1-D
26908-EG 26909-MA	1V-A	27508-PH	I-B	27995-GS	VIEF	28368-MS	VI-C
26914-CH	II-B	27510-EG	V-D	28002-EG	V-B	28369-MS	VI-A 31-D
26923-EL	VIII-B	27515-EG	V B	28004-EL	V111-B	28371-CH 28373-CH	II-F
26930-MA	IV-F	27524-MA	IV-F	28005-MS 28007-MA	VI-C IV-B	28377-MA	1V B
26932 MA	iV-F	27532-PH	(-B (1-B	28011-DUX	III-C	28.387 EE	VIIE
26934-EG	V-D VIIEB	27534-CH 27538-EG	V-A	28013-CH	11-B	28392-EU	VIII-A
26941-EL 26945-MA	IV-F	27548-MS	VI-D	2802241.8	III A	28 196-PH	T-B V D
26949-EL	VIII-C	27552-MS	VI-A	28025-MA	IV-B	28399-EG 28402-CH	U-A
26959-PH	I-B	27554 EL	V10-G	28034-MA 28043-LS	IV-B III-C	28406 EI	VIII-B
26962-GS	VII-G	27556-PH	1/E IV-A	28052-G5	VII-G	28408-MA	IV F
26971-PH	1-E	27557-MA 27558-EG	V-8	28053-CH	D-E	28409-MS	V1-C
26972-GS 26974-PH	VII-A 1-E	27565-EG	N-C	28060-MA	IV-F	28416-PH	11
26982-GS	VII-E	27567 MA	IV-F	280% 7 MS	¥1-C	28427-EG	V-C VIII-G
26988-GS	VB-D	27568 CH	11-B	28070 EL	VIII-D	28453-EI 28457 f.S	All C
26993-MA	IV C	27574.MA	IV C	28071-MA 28080-1.S	IV B III C	28461-FL	VIII B
26995-EG	V-D	27578-EL	VIII B NEC	28094-65	NIL F	28467-11	VIII E
26996-PH	I-D IV-C	27579-MS 27580-MA	VI-C IV-A	28099-EL	VIII-F	28468 PH	1-D
26997-MA 27018-EC	3V-C 	27586-PH	1-E	28102-GS	VII-E	28469-CH	11 A
27018-EG 27014-GS	AR-F	27591 PH	1-E	28103-CH	H-D	28470 PH	11) 1 B
27025-CH	II-D	27600-CH	11-A	28109-MS	VI-D	28472-PH 28476-MA	1 B   N F
27028-EL	V10 F	27603-018	11.0	28123 LG 28131 815	N D IV E	284-19-384 28479-1.5	III D
27031-GS	VII D	27605 MS	AT D	28131 MA	••• (	2	

## **Proposal Numbers**

## X Indexes

Proposal Number		Proposal Number		Proposal Number		Proposal Number	
28480-MS	VI B	28565 CH	nъ	28700 CH	81.12	28908 MA	IV B
28483 EL	VIII C	28569 PH	1.8	28701 MA	IV B	28912 EG	V C
28486-CH	11 A	28575 MS	MH	28702 MA	13-4	28916-MA	н в
28489-GS	VII G	28591 PH	1.D	28711 CH	11 F	28922-11	VIILI
28499-PH	1 B	28594 EL	VIII B	28715 MA	IV C	28950 MA	1V-1
28502 PH	LE	28599-GS	VII B	28716 MA	IV-B	28954 GS	VII F
28504-GS	VH-A	28606-MA	IV A	28717 GS	VII A	28957 MA	IV A
28506-E1	VIIIE	28608-MS	VI B	28718 MA	IV C	28969 MA	IV A
28508-EL	VIII B	28612 MS	V1 D	28722 MA	IV C	28980 MA	IV A
28509-MS	VI A	28620 MS	VI E	28729-11	VILE		
28511 MA	IV D	28631 CH	ЧE	28735 MA	IV-B	28982 MA	IV C
28514 MA	IV A	28639-MS	VI C	28743 MA	IV C	28985 FT	VIII-E
28516-E1	VIII C	28646-11	VIII B	28764-MS	VI B	28986 MA	IV A
28531-PH	I B	28651 I G	A D	28767 CH	n c	28994 MA	IV F
28535-MA	IV-B	28652 PH	1.D	28797 MA	IV A	29016 MA	IV C
28538 MS	VED	28655 CH	II A	28799 MA	IV B	29031 MA	IV F
28548 MA	IV A	28664 GS	VILE	28803-MA	IV A	29053 MA	IV F
28549-MS	VI-8	28669-1.5	III C	28809 MA	IVF	29188 GS	VILE
28553-MS	VED	28674 EL	A III A	28835 MA	IV-D	29190-MA	IV F
28555 CH	H D	28679 MA	IV C	28883-MS	VEC	29288-GE	VII D
28561 PH	I B	28691-1-5	10 A	28900-MS	VI C	29310 CH	11-C

## Scientific Liaison and Scientific Cognizance Representatives

*Note:* The Roman numeral refers to the scientific division, and the alphabetic character refers to the division subsection. Proposal numbers are in ascending sequence within the subsections.

Aeroflightdynamics Directorate AVSCOM IV-8-28377 IV-D-28835 (SL) V-A-26908 V-B-25461 (SL) V-B-25467 (SL) V-B-25623 (SL) V-8-26595 (SE) N B-26631 V-B-26631 (SL) V-B-27752 (SL) V-B-27894 V-B-27894 (SL) V-B-18001 (SL) V-B-28159 V-B-28159 (SL) V-D-25462 (SE) V-D-25630 V-D-26061 (SL) V-D-26934 (SL) V-D-28123 (SL) V-D-28651 V D-28651 (SL) Aerostructures Directorate AVSCOM V-A-25594 V-A-16908 V-A-28222 (SL) V-A-28307 V-B-25461 (SE) V-B-25467 (SL) V B-26631 (SL) V-B-27752 (SL) V-B-28002 V-D-25462 (SL) V-D-26061 (SL) V D-26914 V-D-28651 VI-A-25760 (SL) VI.R. 15414 VI-B. 27407 VI-C-26571 VI-C-28900 Air Force Astronautics Laboratory (AFSC) 11-C-24413 (SL) II-D 27603 Air Force Engineering and Service Center 4ED-28371 (SL) Air Force Geophysics Laboratory VIII-C 26128 Air Force Office of Scientific Research T-E-28356 (SL) III-E 25521

V-B-26631

Management Information and Computer Sciences IV E-25514 11-1-16487 VIII E-26823 VHLF 18461 VIII E 28506 (SL) Aviation Applied Technology Directorate: AVSCOM V A-26908 (SL) V B-25461 (SE) V B 25467 (SL) V-D.25462 (SU) V D-25630 (SL) V-D 26061 V D-28123 VI-C-26439 Ballistic Research Laboratory 1-D 27780 I-D-28362 1.0.18651 II-A-25500 (SL) II-A-26145 11-B-25761 (SL) II-B-27534 IEC-24413 II-C-24413 (SL) 11-C-2688" II-D-25523 II-D-26106 (SL) 11-0-27025 IED-27603 (SE) 11-D-28103 (SL) 11-12-28565 11-D-28700 (SE) 11-E-27808 (SL) IV:A-25396 (SL) IV-A-25428 (SL) IV-A-25782 IV-A 25874 IV:A 26112 (SL) IV A 28980 (SL) IV A 28986 (SL) IV R. 26391 (SL) IV-B 26616 (SL) IV-B. 26871 (SL) IV B 27690 (SL) IV-B-28025 IV-B-28320 (SL) IV B 28377 IV-B-28535 JV-8-28716 IV-B-28735 (SL) IV-C 25347 IV:C 25836 IV C-26108 (SE) IV C 26394 IV C 26746 IV-C 26993 (SE) IV C 26997 IV C 27574

Army Institute for Relearch in

IV C 28679 IV C 28722 (SL) IV C 28743 IV F 25324 IV E 26438 (SL) VA 25445 V A 25400 (SL) X: A 25159 V A-25459 (SL) V A 26443 (SL) V 4-26908 VA 27409 VA 17538 VA 28283 (SL) VA 28307 VA-28317 V-B 26863 (SL) V-B-27062 V-B-27558 (SL) V B 28249 V B-28252 V B-28293 V-C 26403 X-C-26720 V C 26797 V C-27455 (SL) V C-28250 V-C 28310 (SL) N-D-24362 V-D-28399 VI-B-24583 (SL) VEB-26164 (SL) VI-B-26167 (SL) VER-26673 VI-B-28761 VI.C. 25526 VLC-26021 VEC-26021 (SL) VI-C-26068 VI-C-26068 (SL) VI C-26392 VEC-26392 (SL) VI C-26485 VI-C-26485 (SL) VLC 26617 (SL) VI-C-27579 VLC 28368 VEC-28368 (SL) VI-D 28553 VI-E-24102 VEE-26169 (SL) VI-E-26173 VI-E-26173 (SL) VEE-28272 (SE) VI-F-28575 VI-E 28575 (SL) VII-D-25730 VILD: 26224 (SL) VIED-27919 (SE) VIII-C 26128 (SL) VIII-E 25674 VIII F 27028 (SL) VIII-E 27493 (SL) VIII F 27994

13 4 5933 (51) IX A 6230 (SL) IX A 6466 IX B-6089 (SL) 18.38.6349 IX C 6541 IX C 6541 (SL) IX D 6148 Benet Weapons Laboratories. CCAC: ARDEC IV:A 25396 IV A-25782 IV: 4-28969 (SL) IV-B-26616 IV-B-28025 IV-B-28535 V-A-25400 VA-27409 (SE) V-A-28222 (SL) V A-28253 V A-28283 V-A-28307 (SL) V:A-28317 V:D 24362 (SE) V-D-27075 (SL) VI-A-28509 VI-B-26747 VI-B-26825 VI-B-27163 (SL) VI-B 27407 (SL) VI-C-26617 V1 C 28639 V14-24102 1X-D-5686 (SU) Construction Engineering Research Laboratory VEA 21545 (SL) VI-A-24845 (SL) VI-A 25199 (SU) VI-B 28480 VI-C-25373 VI-C-26728 Corpus Christi Army Depot AVSCOM DERSO VI-A-25833 Detense Advanced Research Projects Agency 1-E-26264 (SE) 115-27882 (SL) 14:28271 (SL) LE 28348 (SE) IEE-26072 (SL) VIIEB-26051 (SL) VIII-1: 28729 (SL) European Office of Aerospace R&D IX-B-6249 IX B 6367 IX-B-6308

#### Scientific Liaison and Scientific Cognizance Representatives

#### X Indexes

HODA. Office of the Assistant Secretary of the Army LE.15482 IV-F-23306 V-B-25461 V-B-25467 V-B-25623 V-D-25462 VIII-G-26212 Letterman Army Institute of Research II-B-25411 II-B-25669 National Security Agency Central Security Service VIII-E-25674 Naval Air Wartare Center II-B-25761 Naval Research Laboratory 1-B-28396 III-B-27314 VIII-E-28297 Navai Surface Weapons Center II-B-25761 (SL) Office of Naval Research VIII-B 25015 Office of Project Manager Smoke Obscurants VILD. 25730 (SL) VII-D-26224 VII-D-26224 (SL) VII-D-26384 Propulsion Directorate: AVSCOM V-B-26631 V-B-27627 V-B-28249 (SL) V-C-25245 (SL) V-C-26456 (SL) V-C-27018 V-C-27417 (SL) V-C-28250 V-C-28316 VI-A-26449 VI-A-26667 VI-A 27037 VI-B-26673 (SL) VI-C-25202 VI-C-25526 VI-C-26123 VI-C-26751 VI-C-27472 VI-C-28005 VI-C-28067 VI-C-28639 IX-C-5824 Rock Island Arsenal. ARRCOM VI-A-26667 Strategic Defense Command IV-B-28192 (SL) VIII-A-28347 VIII-B-27578 VIII-B-28004 VIII-B-28325 VIII-B-28325 (SL) VIII-B-28329 VIII-B-28329 (SL) VIII-B-28345 VIII-B-28406 VIII-C-28339 (SL) VIII-E-27076 YMLE-27464

Strategic Defense Initiative Organization. Innovative Science and Technology V.C.24487 (SL) V-C 28912 U.S. Army Armament Research. Development and Engineering Center II-A-25500 II-B-25761 II-B-25761 (SL) II-C-24413 (SL) II-C-28767 (SL) II-D-25523 II-D-26106 (SL) II-D-27603 (SL) 11-D-2788\* (SL) II-D-28565 (SL) H-D-28700 (SL) II-E-26441 II-E-28631 11-E-28711 (SL) IV-D-25264 IV-D-26736 (SL) IV-D-27044 (SL) IV-D-27365 (SL) 1V-D-28511 (SL) IV-D-28835 (SL) V-A-25345 V-A-25400 V-A-25459 V-A-26443 V. 4. 27315 V-A-27409 V-C-26403 (SL) V-C-26720 (SL) V-C-27455 V-D-24362 (SL) V-D-26995 (SL) V-D-27075 VI-A-25760 VI-A-26400 VI-A-26449 VI-A-26667 VI-A-26806 VI-A-27037 VI-A-27552 VI-B-25390 (SL) VI-B-26825 (SL) VI-B-28480 VI-B-28549 VI-8-28761 VI-C-26439 VI-C-26571 VI-C-26579 VI-C-26591 VLC-26617 VI-C-26728 VEC-27472 VI-C-27472 (SL) VI-C-28005 (SL) VI-C-28639 (SL) VI-E-28272 (SL) VII-D-27911 VIII-A-28674 (SL) VIII-C-28483 (SL) VIII-E-26813 (SL) VIII-E-27464 (SL) IX-A-6271 (SL) IX-A-6466 (SL) IX-B-6249 IX-B-6294 1X-C-6541 (SL) 1X-D-5686 (SL) IX-F-5830 (SL) IX F-6170 (SL) 1X-F-6291 (SL)

U.S. Army Armament, Munitions
and Chemical Command
II-D-26106
V-C-28310
U.S. Army Atmospheric Sciences
Laboratory
L-B-28499
IV-B-28716 (SL)
IV-B-28735 (SL)
VII-A-28717 (SL) VII-D-24713
VII-D-25730 (SL)
VII-D-26224
VII-D-26480 (SL)
VII-D-27919
VII-E-27870 (SL) VII-F-26491
VII-F-26491 (SL)
VII-F-27995 (SL)
V1f-F-28664 (SL)
VII-F-29188
VII-G-26962
VII-G-28052 (SL) VII-G-28359
VII-G-28489
IX-F-6458 (SL)
U.S. Army Aviation Systems
Command
IV-B-26391 IV-B-28025
IV-D-25859
V-B-25461 (SL)
V-B-25467 (SL)
V-D-25462 (SL)
IX-C-6571
U.S. Army Avionics Research
and Development Activity
VIII-C-27873 (SL)
U.S. Army Belvoir Research.
Development and Engineering Center
1[-A-24411
II-A-28655 (SL)
H-C-27775
II-D-26106
H-E-25286 (SL) H-E-26441
H-E-28153
IE-E-28631
11-E-28711
V-A-27315 (SL)
V-C-25190 V-C-27417
V-C-27565
V-C-28316
V-C-28427
V1-A-2576() (SL)
VI-A-26427
VI-A-26449 VI-A-26667
VI-A-26678
V1-A-28369
VI-B-24583
VI-C-25202
V1-C-26439 V1-C-26571
VI-C-26591
VI-C-26617
V1-C-26728
VLC-26751
V1-C-26882
VI-C-26891 VI-C-27373
VI-C-28883 (SL)
VIII-C-26128

U.S. Army Chemical Research. Development and Engineering Center I-B-25653 II-A-24411 II-A-25435 II-A-25435 (SL) II-A-25500 II-A-25586 H-A-27600 II-A-28469 II-A-28486 II-A-28655 11-8-25181 H.B. 25411 H-B-25411 (SL) II-B-25669 II-B-25669 (SL) II-B-25739 (SL) II-B-26115 11-B-26115 (SL) II-B-26284 II-B-26284 (SL) II-B-26914 II-B-26914 (SL) IL-B-27568 ILB-28013 II-C-24413 II-C-25605 II-C-26126 II-C-26238 II-C-26238 (SL) 11-C-26296 II-C-26296 (SL) II-C-26822 II-C-27770 II-C-27775 II-C-27775 (SL) 11-C-28298 II-C-28319 II-C-28767 11-D-26256 II-D-27505 II-D-27887 II-D-28103 II-D-28371 II-D-28700 II-E-25104 ILE-25104 (SL) II-E-25229 II-F-25286 II-E-26072 II-E-26441 II-E-268.39 II-E-27445 II-E-28053 II-E-28153 U-E-28314 II-E-28631 III-B-25493 III-B-26750 III-C-24435 III-C-24931 III-C-25731 111-C-27890 HI-C-28011 HI-C-28043 III-C-28043 (SL) HI-C-28361 111-C-28457 III-D-25476 HI-D-25476 (SL) III-D-25663 III-D-25663 (SL) 1H-D-25702 III-D-25702 (SL) III-D-25752 III-D-26232 1II-D-27468

## Scientific Liaison and Scientific Cognizance Representatives

H-C-25222

III-D-27916 III-D-27916 (SL) III-D-28479 III-D-28479 (SL) III-F-26767 IU-F-27634 IV-A-24166 (SL) IV-A-26113 (SL) IV-A-27403 (SL) IV-A-27433 (SL) 1V-A-28797 (SL) IV-E-25662 V-C-25190 V-C-26769 V-C-28250 (SL) VI-C-26591 VI-C-26591 (SL) VI-C-28409 VI-C-28409 (SL) VI-F-28620 VII-A-28717 (SL) VII-D-24713 VII-D-27031 (SL) VII-E-27870 (SL) VII-E-28102 VII-F-24881 VIE-F-26491 VII-F-27995 VII-G-26962 (SL) VII-G-28052 VII-G-28052 (SL) VII-G-28359 VII-G-28489 VII-G-28489 (SL) EX-A-5653 (SL) IX-B-5973 (SL) IX-B-6089 IX-B-6294 IX-B-6305 IX-B-6305 (SL) IX-B-6308 (SL) IX-D-6579 U.S. Army Cold Regions Research \* Engineering Laboratory -B-26750 III-B-27314 VII-A-26902 VII-A-27401 (SL) VII-A-28504 (SL) VII-B-26031 (SL) VIE-B-26260 (SL) VII-8-26281 (SL) VII-B-27316 VII-B-27482 (SL) VII-B-28599 (SL) VII-C-24381 VII-D-26224 VII-D-26384 VII-D-28219 VII-E-26982 VII-F-28344 (SL) VII-F-28664 VII-F-28954 (SL) U.S. Army Communications-Electronics Command 1-E-25631 II-B-27534 (SL) II-B-27568 (SL) TV-E-26438 IV-E-28328 (SL) VI-D-28109 (SL) VE-D-24713 (SL) VII-D-25730 (SL) VII-D-26224 (SL) VII-D-26384

VII-D-26480 (SL) VII-D-27031 (SL) VII-D-27485 (SL) VII-D-27911 (SL) VII-D-28219 (SL) VIII-A-26147 (SL) VIU-A-28674 (SL) VIII-C-25045 (SL) VIII-C-25339 (SL) VIII-C-25422 (SL) VIII-C-26381 (SL) VIII-C-26599 (SL) VIII-C-26620 (SL) VIII-C-26651 (SL) VIII-C-26791 (SL) VIII-C-26949 (SL) VIII-C-27304 (SL) VIII-C-27307 (SL) VIII-C-27873 (SL) VIII-C-27904 (SL) VIII-C-28151 (SL) VIII-C-28339 (SL) VIII-C-28483 (SL) VIII-C-28516 (SL) VIII-E-25674 VIII-E-27751 VIII-E-27751 (SL) VIII-E-27834 (SL) VIII-E-28467 (SL) VIII-E-28506 (SL) IX-F-5830 U.S. Army Concepts Analysis Agency IV-B-28143 IV-C-26997 U.S. Army Dugway Proving Ground VII-F-26491 VII-F-27995 VII-F-28664 VII-F-28954 U.S. Army Electronics Technology and Devices Laboratory 1-B-26821 (SL) 1-B-27532 I-B-28396 (SL) 1-B-28561 I-B-28569 (SL) 1-D-25167 (SL) I-D-25374 1-D-25487 I-D-25697 (SL) 1-D-27780 I-D-28591 (SL) 1-E-27838 J-F-18313 H-A-25586 H-A-266.36 II-A-26636 (SL) 11-4-25748 II-A-27502 11 - 25222 H C-27770 II-D-26256 H-E-27054 II-E-27054 (SL) ILE 27808 (SE) IV-A 26909 (SL) IV B 28192 1V-E-13908 IV E-25324 (SL) IV E 25662 (SL) V(D) 28155 (SL) VI A 21545 (SL). VI-A 24845 (SL) VI-A-26667 (SL) VI-B-24981

VI-B-26747 VI-C-28067 VI-D-22459 (SL) VI-D-25251 (SL) VI-D-26287 VI-D-26287 (SL) VI-D-26729 VI-D-27548 (SL) VI-D-27605 VI-D-27764 (SL) VI-D-27794 V1-D-28109 V1-D-28141 VI-D-28146 (SL) VI-D-28612 VI-F-27810 VIII-A-26434 VIII-A-26444 VIII-A-27298 (SL) VIII-A-28335 (SL) VIII-A-28351 (SL) VIII-A-28392 VIII-B-25015 (SL) VIII-B-26051 VIII-B-26151 (SL) VIII-B-26278 VIII-B-26484 VIII-B-26666 (SL) VIII-B-26686 VHI-B-26711 (SL) VIII-B-26755 (SL) VIII-B-27443 (SL) VIII-B-27578 VIII-B-27883 (SL) VIII-B-28004 VIII-B-28325 (SL) V101-B-28329 (SL) VIII-B-28345 (SL) V[[1-B-28461 VIII-B-28508 VIII-B-28594 (SL) VIII-B-28646 VIII-C-26949 (SL) VIII-C-27307 (SL) VIII F-27865 VIII-F-28729 VIII-F-28729 (SL) IX-A-5653 (SL) IX-A-6280 (SL) IX-B-6307 IX-D-5884 IX-D-5884 (SL) IX-F-5940 (SL) IX-F-6170 IX-F-6563 U.S. Army Engineer Topographic Laboratories IV-A-25874 IV-C-26108 IV-C-26394 VII-A-27471 U.S. Army Harry Diamond Laboratories 1-8-28531 I-B-28569 1-D-25167 I-D-25374 LD-26442 1-D-26996 I-D-28336 1.10.28652 1-E 27273 1-E-27418 TE-27418 (SL) 1 E-27586 145-28416 (SE)

1I-C-26191 VI-C-26891 VI-D-26287 VI-D-26729 VI-D-27764 VI-D-28612 VII-D-25730 VII-D-26224 VII-D-27919 VII-D-28219 VIII A-26147 (SL) VIII-A-26188 (SL) VIII-A-26434 (SL) VIII-A-26896 (SL) VIII-B-25015 VIII-B-26051 VIII-B-26151 VIII-B-26484 VIII-B-26686 (SL) VIII-B-26760 (SL) VIII-B-26923 (SL) VIII-B-26941 VIII-B-27578 VIII-B-27883 VIII-B-28004 (SL) VIII-B-28646 VIII-C-27304 (SL) VIII-E-27886 VIII-E-27917 VIII-E-28985 VIII-F-26898 (SL) VIII-F-28729 IX-A-5653 (SL) 1X-A-6280 (SL) IX-D-5884 IX-D-5884 (SL) IX-F-6563 U.S. Army Human Engineering Laboratory HI-E-25521 1V-E-28131 (SL) U.S. Army Infantry School IV-C-24557 (SL) IV-C-28679 (SL) U.S. Army Laboratory Command VII-D-27919 VIII-E-28985 (SL) U.S. Army Materials Technology Laboratories I-B-28561 I-E-28313 II-A-25586 II-A-26145 II-A-26426 II-A-26636 (SL) II-A-26748 H-A-27600 II-A-28402 II-A-28469 II-B-25181 II-B-25669 II-B-26115 II-B-26914 II-C-26126 IFC-26191 II-C-28298 II-C-28319 (SL) II-D 26256 11-1-25229 11-E-25229 (SL) II-E 26072 11-1-26441 II-F-26839 fFE 27054

#### Scientific Liaison and Scientific Cognizance Representatives

II-E-27808 11-E-28053 8FE-28153 (SL) TI-E-28314 (SL) II-E-28631 (SL) IV-A-25396 IV-A-25428 IV-A-25782 IV-A-27433 IV-A-28514 IV-C-24557 IV-C-25836 V.A.75345 (SL) V-A-25400 V-A-25459 (SL) V-A-25594 (SL) V-A-27315 (SL) V-A-27409 (SL) V-A-27538 V-A-28253 V-A-28317 V-D-24362 VI-A-25199 VI-A-25760 (SL) VI-A-25833 (SL) VI-A-26449 (SL) VI-A-26678 (SL) VI-A-26806 VI-A-26806 (SL) VI-A-27037 VI-A-27037 (SL) VI-A-27552 (SL) VI A-28369 (SL) VI-A-28509 VI-B-25193 (SL) VI-B-25397 VI-B-25424 (SL) VI-B-26164 (SL) VI-B-26167 (SL) VI-B-26673 VI-B-26747 VI-B-27163 VI-B-27163 (SL) VI-B-27407 (SL) VI-C-25373 (SL) VI-C-25526 VI-C-25526 (SL) VI-C-26021 VI-C-26021 (SL) VI-C-26068 (SL) VI-C-26123 VI-C-26123 (SL) VI-C-26392 VI-C-26392 (SL) VI-C-26439 (SL) VI-C-26485 (SE) VI-C-26571 (SE) VI-C-26617 VEC 26728 (SL) VI-C-26882 VI-C-26891 VI-C-27373 VI-C-27472 (SL) VI-C 27579 (SL) VEC 28005 (SL) VI-C 28067 (SL) VI-C-78368 VI C 28409 VI-C-28409 (SL) VEC-28639 (SE) VI-C-28883 VI-C-28883 (SL) VI-C-28900 VI-D-23577 VED-26601 VED-27548 VED-28141 (SL) VI-D-28553

V1-F-24102 (SE) VI-E-26169 (SL) V14-26173 (SE) VI-F-27364 (SL) VII-D-26224 (SL) VIII-C-26791 IX-A-6280 (SL) IX-D-5548 (SL) IX-D-5686 (SL) IX-D-5884 1X-D-6011 (SL) 1X-D-6148 (SL) U.S. Army Materiel Systems Analysis Activity IV-C-24557 IV-C-25347 IV-C-26394 IV-C-28718 IV D-25859 IV-D-26674 11-12-27044 IV-D-27365 VIII-E-26646 VIII-E-27032 VIII-E-27834 VIII-E-28297 U.S. Army Medical Bioengineering Research and Development 1 aborators VI-F-28620 U.S. Army Medical Research Institute of Chemical Defense II-A-25435 II-B-25669 II-B-28013 (SL) III-D-25702 III-D-25702 (SL) HI-D-25752 III-F-27634 (SL) U.S. Army Missile Command 1-D-25487 1-E-24749 I-E-28502 (SL) II-A-26145 II-A-28655 II-A-28655 (SL) H P-26284 (SL) 11-B-27534 (SL) II B-27568 (SL) II-D-25523 ILD-26106 11-D 28565 IV-A-24166 IV-A 27403 IV A-27433 IV-C 29016 IV-E-25662 (SL) IV-E-26779 (SL) V/C+24487/(SL) V-C-26403 N.C. 26720 N-C-27455 V-C-27469 VI-8-25390 VI-B-25397 VI-C 25202 VED 26601 VED-26883 VEF 27810 VII D-26384 VII-D-27919 VII-D-28219 VILE.27870 VIEE 27995 VIEG 28489 (SL)

VIII-A-26147 VIII-A-26434 VIII-A-26761 (SL) VIII-B-28325 (SL) VIII-B-28329 (SL) VIII-C-25350 (SL) VIII-C-26791 VIII-C-27304 (SL) VIII-C-28483 (SL) VIII-E-27464 1X-A-5265 (SL) 1X-A-5653 (SL) IX-A-5933 (SL) IX-D-5884 IX-F-6563 U.S. Army Natick Research. Development and Engineering Center II-A-25435 (SL) II-A-25500 (SL) II-A-25586 (SL) II-A-27600 II-A-28469 (SL) H-A-28486 (SL) II-B-25181 II-B-25411 II-B-25669 (SL) II-B-26115 II-B-26914 ILB. 27534 1I-B-27568 II-B-28013 (SL) II-C-26238 II-C-26296 II-C-28298 II-C-28319 II-D-26256 II-D-28371 II-E-25286 II-E-25286 (SL) II-E-26072 II-E-26441 II-E-27054 II-E-27445 11-E-28314 (SL) II-E-28373 II-E-28631 (SL) II-E-28711 (SL) (II-A-27494 (SL) III-A-28691 (SL) 111-B-26576 (SL) III-B-27314 (SL) III-C-24931 III-C-27488 III-C-27956 (SL) III-C-28043 (SL) 111-C-28090 1II-C-28361 III-C-28457 (SL) III-D-25663 10-D-27468 (SL) III-D-27916 (SL) 111-E-26767 IV-A-25069 IV-E-28131 (SL) V B-27625 VEA-28369 (SL) VI-C 26579 VEC 26591 (SL) VI-C-26882 VI-C-27373 (SL) VI-C 28883 (SL) VI-C-28900 (SL) VI-F-28620 IX B-5973 IX-8-6294 IX-B-6305 IX-8-6307 (SL)

#### X Indexes

IX-B-6308 IX-D-6579 (SL) U.S. Army Night Vision and Electro-Optics Center I-B-25653 I-B-26899 (SL) I-B-27532 (SL) 1-E-25408 (SL) 1-E-27425 (SL) 1-E-28258 (SL) 1-E-28502 (SL) 11-A-27502 (SL) II-C-25222 IV-A-25069 (SL) IV-C-27868 IV-C-28715 (SL) IV-C-29016 (SL) IV-E-25662 (SL) VI-A-26427 VI-D-26601 VI-D-26883 VI-D-27605 (SL) VI-D-27846 (SL) VI-D-28612 (SL) VI-F-27810 (SL) VIII-A-26434 VIII-A-26708 (SL) VIII-A-27298 (SL) VIII-A-28347 (SL) VIII-A-28351 VIII-B-26923 VIII.B. 28325 (SL) VIII-B-28329 (SL) VIII-C-25557 (SL) VIII-C-26791 (SL) VIII-E-27076 (SL) VIII-F-27865 (SL) IX-A-5653 (SL) IX-A-6271 (SL) IX-A-6280 (SL) IX-A-6466 IX-D-5548 (SL) IX-D-5884 (SL) IX-F-5940 IX-F-6563 IX-F-6563 (SL) U.S. Army Research Institute for the Behavioral and Social Sciences IV-E-26487 (SL) U.S. Army Research Office 1-B-26959 (SL) I-B-27646 (SL) I-D-25464 11-A-26748 (SL) II-C-24413 II-C-25222 IV-A-26113 IV-A-28957 (SL) IV-B-28025 IV-B-28025 (SL) IV-B-28799 (SL) IV-E-23908 V-C-27469 VI-A-26427 VI-F-28620 (SL) VIII-A-28392 VIII-B-26711 (SL) VIII-B-26755 (SL) VIII-B-28325 VIII-B-28325 (SL) VIII-B-28329 VIII-B-28329 (SL) VIII-C-27307 (SL) VIII-C 28339 (SL)

Scientific	Liaison a	and	Scientifi	c Co	gnizance	Re	presentatives

VIII-F-28729 (SL)	11-C-26238
IX-A-5653 (SL)	II-C-26296
IX-A-6280 (SL)	11-C-26822
IX-A-6466	II-C-26887
IX-B-5973 (SL)	11-C-27770
IX-B-6249 (SL)	II-C-27775
IX-B-6294 (SL)	II-C-28298
IX-B-6305	II-C-28319
IX-B-6307	II-C-28767
IX-B-6308	II-D-25523
IX-C-5824	II-D-26049
IX-C-6541	II-D-26106
IX-C-6571 (SL)	II-D-26256
IX-D-5686 (SL)	II-D-27505
IX-D-5884	II-D-27603
1X-D-6011 (SL)	II-D-27887
IX-D-6579	11-D-28103
IX-F-6291 (SL)	II-D-28371
IX-F-6458 (SL)	II-D-28555
IX-F-6563	H-D-28565
IX-F-6563 (SL)	11-D-28700
	II-E-25104
U.S. Army Research, Development	II-E-25229
and Standardization Group	II-E-25286
(United Kingdom)	II-E-26441
[1-A-24411	II-E-26839
II-A-25435	H-E-27054
II-A-25500	II-E-27445
II-A-25586	H-E-27808
II-A-25580 II-A-25617	
	11-E-28053
II-A-26145	11-E-28153
II-A-26426	11-E-28314
II-A-26636	II-E-28373
II-A-26748	II-E-28631
II-A-27502	II-E-28711
II-A-28353	III-C-28043
II-A-28402	IX-D-6579
II-A-28469	
II-A-28486	U.S. Army Sign
II-A-28655	Center CECOM
II-B-25181	IV-E-25514 (S
II-B-25290	IV-E-26487
11-B-25411	IV-E-27892
II-B-25669	IV-E-27892 (S
II-B-25739	IV-F-26802
II-B-25761	IV-F-26930
II-B-26115	IV-F-26945
II-B-26284	IV-F-27524
II-B-26914	IV-F-27817
II-B-27534	IV-F-28060
II-B-27568	V111-E-27899
11-B-28013	
II-C-24413	U.S. Army Surv
II-C-25222	Office
II-C-25605	1-E-278.38
II-C-26126	VIII-E-25674
II-C-26191	VIII-E-26460
II-C-26191	VIII-E-2646

I-C-26238
I-C-26296
I-C-26822
I-C-26887
I-C-27770
I-C-27775
1-C-28298
1-C-28319
1-C-28767
I-D-25523
I-D-26049
1-D-26106
I-D-26256
I-D-27505
I-D-27603
1-D-27887
I-D-28103
I-D-28371
1-D-28555
I-D-28565
I-D-28700
I-E-25104
I-E-25229
I-E-25286
I-E-26441
I-E-26839
I-E-27054
I-E-27445
I-E-27808
I-E-28053
1-E-28153
I-E-28314
I-E-28373
I-E-28631
1-E-28711
II-C-28043
X-D-6579
5. Army Signals Warfare
tter CECOM
V-E-25514 (SL)
V-E-26487
V-E-27892
V-E-27892 (SL)
V-F-26802
V-F-26930
V-F-26945
V-F-27524
V-F-27817
V-F-28060
/111-E-27899 (SL)
. Army Survivability Management
ice
-E-278.38
/III-E-25674

VIII-E-27028 VIII-E-27032 VIII-E-27493 VIII-E-27754 U.S. Army Tank-Automotive Command I-E-28356 1-E-28416 IV-B-27786 (SL) IV-B-28007 IV-B-28071 IV-B-28908 IV-C-28718 IV-D-25264 IV-D-25859 V-B-27515 V-B-27627 V-C-25190 V-C-25190 (SL) V-C-25245 (SL) V-C-26769 (SL) V-C-26797 V-C-27018 V-C-27417 V-C-27565 V-C-28250 V-C-28316 (SL) V-C-28427 (SL) V-D-25630 V-D-26934 (SL) V-D-26995 (SL) V-D-27075 (SL) VI-A-25199 VI-A-15833 VI-A-26400 VI-A-26427 VI-A-26667 (SL) VI-A-27552 VI-A-28369 VI-B-24583 VI-B-24981 (SL) VI-B-25424 VI-B-26673 VI-C-25373 (SL) VI-C-25526 VI-C-26123 VI-C-26617 VI-C-26728 (SL) VI-C-28005 VI-C-28409 VI-D-26601 VI-E-24102 IX-A-5265 (SL)

1X-C-5824

U.S. Army Test and Evaluation Command VII-E-28102 U.S. Army Toxic and Hazardous Materials Agency II-D-27505 H-D-28371 VII-A-28504 U.S. Army Training and Doctrine Command IV-C-28982 IV-E-27892 (SL) U.S. Army Vulnerability Assessment . Laboratory I-E-27838 (SL) VIII-E-27032 VIII-E-27464 Walter Reed Army Institute of Research III-B-26576 III-C-24435 III-C-28090 III-D-25476 (SL) III-D-28479 (SL) IV-C-27574 IV-C-28679 Waterways Experiment Station IV-B-28025 (SL) IV-B-28716 IV-B-28735 VII-A-26902 (SL) VII-A-26972 (SL) VII-A-27401 (SL) VII-A-27772 VII-A-28504 (SL) VII-B-26260 VII-C-24381 (SL) VII-D-24713 VII-D-25730 VII-D-27485 (SL) VII-E-26982 VIII-C-26128 (SL) White Sands Missile Range I-E-28258 (SL) IV-C-25347 IV-C-25819 IV-C-26394 IV-C-26997 VIII-C-25350 VIII-E-26697 VIII-E-26735 VIII-E-27464

## **Contractors and Grantees**

*Note:* The Roman numeral refers to the scientific division, and the alphabetic character refers to the division subsection. Proposal numbers are in ascending sequence within the subsections.

AT&T Technology Systems Greensboro, North Carolina I-E-28271

Aerodyne Research, Inc. Billerica, Massachusetts II-D-28103

University of Alabama-Tuscaloosa Tuscaloosa, Alabama V-A-28317

University of Alabama-Huntsville Huntsville, Alabama II-B-26284

University of Alaska Geophysical Institute Fairbanks, Alaska VII-B-26281

Alfred University Alfred, New York VI-D-27548

American University Washington, District of Columbia VIII-E-28985

Analytica, Inc. Branford, Connecticut II-A-25617

Arizona State University Tempe: Arizona I.D-26827 V-A-28222 V-B-28002 VJ-A-24845 VII-F-29188 VIII-B-2686 VIII-B-26686 VIII-B-28508 VIII-B-28508 VIII-C-27873

University of Arizona Tucson, Arizona I-E-26974 I-E-28356 II-E-27440 VI-C-28900

Arnold Engineering and Development Center Arnold Air Force Station, Tennessee V-C-28912

Auburn University Auburn, Alabama III-F-27634 V-D-26061

BDM Corp. McLean, Virginia VI-B-28608

Boston College Chestnut Hill. Massachusetts I-D-26682 I-D-28652 Boston University Boston, Massachusetts I-E-25631 II-B-27534 II-D-26256 IV-E-25662

Brandeis University Waltham, Massachusetts III-A-28691 III-C-25731

Bristol, University of Bristol, UK IX-D-6011

Brookhaven National Laboratory Upton, New York VI-A-26667

Brown University Providence. Rhode Island 1-D-25167 IV-A-27403 IV-B-28071 IV-B. 28716 IV-F.26811 V-D-24362 VI-D-28538 VI-E-28575 California Institute of Technology Pasadena. California I-E-26676 I-E-27273 II-A-24411 IV-A-25874 IV-E-26487 V-C-24487 VI-D-26287 VIII-C-26381 University of California, Berkeley Berkeley. California IV-A-26272 IV-C-26144 IV-C-27993 IV-D-28835 IV-E-27892 V-C-25245 VII-C-24381 VII-E-26404 VIII-C-26949 VIII-E-27886 University of California, Davis Davis California III-D-27916 V-D-27075 VII-F-27019 University of California, Irvine Irvine, California I-D-25464 I-D-26211 VI-C-26439

University of California, Los Angeles Los Angeles. California I-B-28396 III-D-26232 IV-B-28735 IV-B-28916 IV-E-25324 VI-C-26891 VIII-A-26896 VIII-C-27904 University of California, San Diego La Jolla, California IV-F-26802 V-C-25794 V-C-27455 VI-C-26392 VI-C-28368 VIII-E-27754 University of California, Santa Barbara Santa Barbara, California 1-B-28569 II-B-25411 II-C-25605 IV-A-27869 VIII-E-28922 Cambridge. University of Cambridge, UK IX-B-5973 IX-C-6541 IX-F-5940 Carnegie-Mellon University Pittsburgh. Pennsylvania II-E-28631 IV-A-27557 IV-A-28514 IV-F-28994 VI-B-27407 VI-D-28146 Case-Western Reserve University Cleveland, Ohio VI-A-27037 VI-B-25193 VI-B-25390 VII-D-27911 University of Central Florida Orlando, Florida I-E-27838 VIII-B-28594 Centre National de la Recherche Scientifique Meudon, France IX-F-6563 Centro di Cultura Scientific "A. Volta" Como, Italy IX-A-5653 University of Cincinnati Cincinnati, Ohio IV-B-28535 V-B-27515 VI-C-26579 VI-C-27373 VIII-B-26941

**Clarkson University** Potsdam, New York V-C-26797 VII-G-26962 Clemson University Clemson, South Carolina VI-C-26591 VIII-C-28151 Colorado School of Mines Golden. Colorado VI-C-26728 Colorado State University Fort Collins, Colorado 11-D-28565 IV-B-28034 University of Colorado Boulder, Colorado I-B-28561 I-E-26971 IV-B-28701 IV-E-28950 VII-A-27772 VII-E-27870 VII-F-27995 University of Colorado at Colorado Springs Colorado Springs. Colorado 1-D-25374 University of Colorado at Denver Denver, Colorado III-C-27488 Columbia University New York, New York I-B-2622. I-B-26462 IV-A-28803 IV-C-28715 V-D-26995 VIII-G-28-+53 Connecticut University Health Center Farmington, Connecticut III-C-27956 University of Connecticut Storrs, Connecticut 1-D-26442 II-C-27759 1V-C-28743 VI-A-25760 VI-C-26571 Cornell University Ithaca, New York 1-D-26996 I-E-26383 II-A-27502 II-D-25523 II-D-28700 III-B-26750 IV-F-23306 IV-F-26930 IV-F-26945 IV-F-29031 V1-A-26806 VI-B-26747 VIII-B-26151 VIII-B-26755 VIII-C-26620 Cranfield Institute of Technology Cranfield, UK IX-C-5824

DCW Industries. Inc. La Canada, California V-B-26863 Dartmouth College Hanover, New Hampshire I-B 28531 VI-B-28480 VII-B-27482 VII-B-28599 University of Dayton Dayton, Ohio VI-E-24102 VI-E-26169 VIII-C-25557 University of Delaware Newark. Delaware II-C-26887 HI-E-25521 VI-C-28409 VI-D-27794 VIII-E-28506 The Dow Chemical Co. Midland, Michigan VI-C-26068 Drexel University Philadelphia. Pennsylvania V-C-27417 Dublin, University of Dublin, Ireland 1X-B-6249 IX-B-6307 Duke University Durham. North Carolina {-B-2743} I-B-27766 I-B-27888 I-D-28468 I-E-25349 I-E-27556 II-E-25104 IV-A-28969 IV-B-28799 V-D-25409 VI-D-26729 VI-E-26647 VII-A-27401 Duke University Medical Center Durham, North Carolina III-F-26767 East Carolina University Greenville, North Carolina III-D-25752 Emory University Atlanta, Georgia II-A-28469 11-B-25739 Failure Analysis Associates Palo Alto. California VI-B-26164 Florence, University of Florence. Italy 1X-E-6458 Florida Atlantic University Boca Raton, Florida V-D-28123

## Contractors and Grantees

Florida State University Tallahassee, Florida IV-C-27868

University of Florida Gainesville, Florida 1-D-28362 II-B-26914 II-E-26441 IV-D-25859 VII-A-26972 VIII-E-26735

Flow Analysis Incoproprated Tullahoma, New York V-B-25623

Fluorochem, Inc. Azusa, California II-B-25761

General Electric Company R&D Center Schenectady, New York VIII-F-24793 VIII-F-27865

Gent, University of Gent, Belgium IX-F-6291

George Mason University Fairfax, Virginia IV-C-28309

George Washington University Washington, District of Columbia IV-C-24557

Georgia Institute of Technology Atlanta. Georgia 1-E-26264 1-E-27366 V-A-25400 V-B-25461 V-D-25327 V1-C-26021 V11-D-27485 V111-C-28339 V111-C-28339 V111-C-28516 V111-G-27554

Georgia State University Atlanta, Georgia I-B-26709

University of Georgia Athens, Georgia IV-A-24166 IV-A-27580

Grumman Aerospace Corporation Bethpage. New York V-B-28252

Hahnemann University Philadelphia, Pennsylvania III-D-28479

Harvard University Cambridge, Massachusetts 1-B-25653 1-E-27425 IV-C-26993 IV-F-29190

The Hebrew University of Jerusalem Jerusalem, Israel IX-B-6308 IX-D-5548 IX-D-5588

## **Contractors and Grantees**

Honeywell Inc. Bloomington, Minnesota VIII-C-26791 University of Houston Houston, Texas III-C-24435 IV-D-28511 VI-B-25397 VIII-C-27304 Hughes Research Laboratories Malibu. California VIII-A-26708 IBM Research Center Yorktown Heights, New York I-B-27508 I-D-27458 Illinois Institute of Technology Chicago, Illinois V-B-28215 University of Illinois Urbana, Illinois II-C-28319 11.0.27025 IV-C-28718 IV-F-26063 IV-F-28476 V-B-27558 VI-C-25526 VI-C-26617 VIII-A-26434 VIII-B-26711 VIII-B-26923 VIII-B-28406 VIII-E-27994 University of Illinois at Chicago Chicago. Illinois I-B-28499 IV-A-28606 IV-D-26674 V-D-26934 VIII-C-26128 Imperial College of Science and Technology London, UK IX-A-6466 IX-F-5830 INRIA Sophia Antipolis, France IX-A-6271 Integrated Systems Inc Santa Clara. California V-D-28350 Iowa State University of Science and Technology Ames, Iowa IV-C-25836 V-B-27062 University of Iowa Iowa City, Iowa I-E-27591 HI-B-26576 V-C-28310 VII-B-26031 JAI Associates Mountain View, California V-B-27752

The Johns Hopkins University Baltimore, Maryland II-C-28767 VI-E-28272 VIII-E-27028 Kansas State University Manhattan, Kansas 11.0.27775 University of Kansas Lawrence, Kansas HI-C-28669 III-D-25702 Kent State University Kent, Ohio IV-B-28908 University of Kentucky Lexington, Kentucky IV-E-26438 Lawrence Berkeley Laboratory Berkeley, California VI-A-25833 Lehigh University Bethlehem, Pennsylvania I-B-26899 VI-B-28549 VI-D-22459 Lockheed Missiles & Space Co., Inc. Palo Alto, California VI-C-26751 Loughborough University of Technology Leicestershire, UK IX-B-6294 University of Lowell Lowell, Massachusetts III-B-27314 Massachusetts Institute of Technology Cambridge. Massachusetts I-B-26566 I-R. 77537 II-D-28371 III-C-25126 III-C-28361 V-A-27538 V-B-27627 VI-A-28369 VI-C-25202 VI-D-25251 VI-D-28553 VII-A-26902 VII-B-26260 ViiI-B-26051 VIII-B-27883 VIII-B-28345 VIII-G-26213 MIT Lincoln Laboratory Lexington, Massachusetts T-D-25487 University of Maryland College Park. Maryland IV-B-26391 V-B-25467 VIII B-26278 VIII-B-28004 233

Jet Propulsion Laboratory

Pasadena, California

V-C-27018

VIII-C-27307

California Institute of Technology

#### X Indexes

University of Massachusetts Amherst, Massachusetts II-A-25435 II-C-26126 II-E-28314 VII-D-25730 VII-D-27919 VIII-C-26599 VIII-E-26823 VIII-E-27493 McGill University Montreal, Canada II-B-28013 Metz, University of Metz, France IX-D-6148 Michigan State University East Lansing, Michigan III-A-28022 Michigan Technological University Houghton, Michigan V-A-27409 University of Michigan Ann Arbor, Michigan I-D-26195 I-D-26644 II-A-25500 IV-C-25819 IV-D-27044 V-D-27510 VI-A-28509 VII-D-26224 VIII-B-26760 VIII-B-28325 VIII-C-28483 VIII-E-27834 Milano, Polytecnico di Milan. Italy IX-C-6571 University of Minnesota, Minneapolis Minneapolis, Minnesota II-C-26296 IV-A-25428 IV-A-25782 IV-A-28986 IV-D-27365 IV-F-28408 VIII-A-26761 VIII-B-27578 VIII-E-27076 University of Minnesota, St. Paul St. Paul, Minnesota IV-A-28797 University of Missouri at Columbia Columbia, Missouri II-A-28486 VI-A-26400 University of Missouri at Rolla Rolla. Missouri IV-A-25396 V-A-26443 V-A-28283 NASA Ames Research Center Moffett Field, California V-C-27469 National Institute of Standards and Technology

Gathersburg, Maryland VI-C-26123

National Academy of Sciences Washington, District of Columbia VI-F-28620 National Center for Atmospheric Research Bouider, Colorado VII-F-28954 National Oceanic and Atmospheric Administration Boulder, Colorado VII-E-28094 VII-F-28664 Naval Postgraduate School Monterey, California IV-E-28328 V-B-27894 University of Nebraska Lincoln, Nebraska 1-D-27780 VII-D-28219 University of New Hampshire Durham. New Hampshire VI-A-26449 University of Medicine & Dentistry of New Jersey Piscataway, New Jersey III-C-24931 New Mexico State University Las Cruces. New Mexico VII-G-28052 University of New Mexico Albuquerque, New Mexico IV-A-28980 New York Institute of Technology Old Westbury, New York VIII-A-28674 New York University Courant Institute of Mathematics New York, New York IV-A-25069 IV-A-26463 IV-C-26649 State University of New York at Albany Albany, New York II-E-26072 VII-A-28717 State University of New York at Binghamton Binghamton, New York IV-C-25347 State University of New York at Buffalo Buffato, New York III-D-26582 III-F-26099 VII-G-28359 State University of New York at Stony Brook Stony Brook, New York II-E-28153 IV-A-27433 IV-B-26616 V-A-25594 North Carolina State University Raleigh, North Carolina 1-D-28336 I-E-27586 T-E-28313

II-E-28373 IV-A-28702 IV-B-27786 IV-B-28192 IV-E-27567 VI-B-26673 VI-B-26825 الاشتلا VI-F-27364 VI-F-27810 VIII-A-28392 VIII-D-28070 VIII-F-28099 VIII-F-28187 University of North Carolina at Chapel Hill Chapel Hill, North Carolina II-A-25586 IV-C-29016 VI-D-27846 VI-F-26246 VII-A-28504 VIII-A-23206 Unit ensity of North Carolina at Charlotte Charlotte, North Carolina I-E-28416 VIII-B-27443 Northeastern University Boston, Massachusetts IV-C-27790 Northwestern University Evanston: Illinois II-E-27054 IV-B-28320 V-A-26057 VI-A-21545 VI-B-27163 Northwestern University, Chicago Chicago, Illinois III-F-26385 Nottingham, University of Nottingham, UK IX-B-5973 Ohio State University Columbus, Ohio H-A-26145 V-B-26595 V B-28249 VI C-25373 VI-D-28141 VIII-E-28467 Oklahoma State University Stillwater, Oklahoma I-B-28472 H-D-26106 11-1-26839 Old Dominion University Norfolk, Virginia 1-8-26821 IV-F-29053 Oregon Graduate Institute of Science and Technology Beaverton, Oregon VII-E-28102 Oregon State University Corvallis Oregon VILE 26491

#### **Contractors and Grantees**

University of Oregon Eugene, Oregon 1-E-25546 II-C-26191 The Pennsylvania State University University Park, Pennsylvania 1 F-28502 11-C-27770 11-E-28711 IV-E-23908 IV-F-26792 V-C-28427 VII-A-27471 VII-F-26982 VIII-A-26444 University of Pennsylvania Philadelphia. Pennsylvania IV-C 28982 IV-F-26779 IV-E-28131 VIII-C-25350 Pierre et Marie Curie, University Paris, France IX-D-5686 University of Pittsburgh Pattsburgh, Pennsylvania II-C-26238 III-C-28011 III-C-28043 Polytechnic Institute of New York, Farmingdale Farmingdale, New York II-A-26636 Princeton Combustion Research Laboratory. Inc Monmouth Junction, New Jersey V-C-26403 Princeton University Princeton, New Jersey 1-D-26015 11-D-28555 IV-A-26113 IV A-26909 IV-C-26997 IV-D-25264 V-C-27565 VIII-A-28335 V111-B-26666 VIII-F-26118 Purdue University Latavette: Indiana II-B-25290 IV-D-26656 IV-F-27392 V-A-28307 V-D-27300 VII-B-27316 VIII-E-26697 VIII E-26813 VIII-E 27464 Reading, University of Reading, UK IX D 6579 Rensselaer Polytechnic Institute Troy, New York 1.D.25697 LD-28591 IVE 27282

VA 25450

## **Contractors and Grantees**

V.D.25462 V-D-25771 VI-C-27579 VI-D-27605 VIII-B-28329 University of Rhode Island Kingston, Rhode Island III-D-25476 IV-F-27620 **Rice University** Houston, Texas II-C-25222 IV-C-26108 IV-F-26932 University of Rochester Rochester, New York 1-D-28470 I-E-24749 LE.25482 **Rock Engineering Consultants** Welwyn Garden City, Herts, UK IX-E-6296 Rockwell International Corporation Thousand Oaks, California I-D-25114 II-A-28655 VIII-B-26484 Rome, University of Rome. Italy IX-A-5265 Rutgers. The State University of New Jersey New Brunswick, New Jersey II-B-25669 III-A-27494 IV-C-27862 V-D-28651 Rutgers, The State University of New Jersey Piscataway, New Jersey 11-B-27568 V-C-28316 V-D-28155 VI-B-25424 SCS Telecom. Inc Port Washington, New York VIII-E-27751 SRI International Mento Park, California 1-B-26959 V-C-27864 VI-E-26173 VII-F-24881 Statistical Signal Processing, Inc Yountville. California VHI-E-26646 VIII-E-27917 Sandia National Laboratories Livermore, California II-D-27887 Scientific Research Associates, Incorporated Glastonbury, Connecticut VIII-B-28646 Signal Processing Technology, Ltd Pale Alto California VIII-E-27899

Columbia, South Carolina III-D-25663 University of South Florida Tampa, Florida VI-D-27764 University of Southern California Los Angeles, California I-B-26257 II-C-29310 VIII-A-26147 VIII-A-27298 VIII-E-25674 VIII-E-27032 VIII-F-26898 Southern Illinois University at Carbondale Carbondale Illinois II-E-27445 Southern Methodist Universus Dallas, Texas 11-F-75786 VIII-C-25339 Southwest Research Institute San Antonio, Texas VI-B-26167 Stanford University Stanford, California I-E-25408 I-E-26088 1-E-26160 I-E-26695 I-E-27418 1-F-28348 IE-A-28353 IV-A-28548 IV-A-28957 IV-B-28143 IV-B-28377 IV-C-26394 IV-D-26736 IV-E-25514 IV-F-27817 IV-F-28060 IV-F-28809 V-A-28253 V-B-27625 V-C-27480 VI-B-28761 VI-C-26882 VI-D-23577 VI-D-26883 VHI-E-28297 VIII-E-28387 VIII-F-28729 VIII-G-28326 Stevens Institute of Technology Hoboken, New Jersey IV-C-25706 Surface Onlics Corp. San Diego, California VII-D 27631 Surrey. University of Guildford, UK TX-F-6170 Swiss Federal Polytechnic Institute Lausanne, Switzerland 1X-B-6305

University of South Carolina

#### X Indexes

VIII-C-25422 Tel Aviv University Tel Aviv Israel 1X R 6089 University of Tennessee, Knoxville Knoxville. Tennessee VI-A-26678 Texas A&M University College Station. Texas III-D-27468 IV-C-27574 IV-F-27524 VIII-C-26651 Texas Tech University Lubbock, Texas IV-C-26746 University of Texas at Arlington Arlington, Texas II-E-27808 University of Texas at Austin Austin, Texas I-E-28258 II-A-26748 II-C-26822 II-C-28298 II-E-25229 II-E-28053 IV-B-26871 V-A-27315 V-B-28293 VIII-A-28351 VIII-C-25045 University of Texas at Dallas Richardson, Texas V-C-28250 Trieste, University of Trieste, Italy IX-A-6280 Tufts University Medford, Massachusetts I-E-27882 V-A-25345 Uniformed Services of the Health Sciences Bethesda, Maryland III-C-27890 United Technologies Research Center East Hartford, Connecticut 11-C-24413 V-B-26631 V-C-26456 University of Utah Salt Lake City. Utah II-D-27603 VI-B-24583 VI-D-28612 Virginia Polytechnic Institute and State University Blacksburg, Virginia V-A-26908 V-D 25630 VEC 28883 VII-D-26988

Syracuse University

Syracuse, New York

VI-A-25199

Vanderbilt University Nashville, Tennessee II-A-28402 V-C-26720 VI-D-28109

Virginia Commonwealth University Richmond, Virginia 1-D-25906

University of Virginia Charlottesville, Virginia II-A-26426 V-D-28399 VI-C-28067 VI-C-28639 VII-A-28347

Vista Research. Inc. Mountain View, California VII-D-26480

Washington State University Pullman, Washington V-B-28159

University of Washington Seattle, Washington VII-D-24713 VII-D-26384 VII-D-29288 VII-F-28344 Wayne State University Detroit: Michigan 11-B-26115 V-C-25190 V-C-26769 V1-B-24981

The Weizmann Institute of Science Rehovot, Israel 1X-A-5933

Wesleyan University Middletown, Connecticut III-C-28090

Western Michigan University Kalamazoo, Michigan II-D-27505

Windermere Laboratory Ambleside, Cumbria, UK IX-E-6185

University of Wisconsin Mathematics Research Center Madison, Wisconsin IV-B-28025

University of Wisconsin Madison Madison, Wisconsin I-B-27646 II-A-27600 II-D-26049

## Contractors and Grantees

IV-A-26218 IV-A-27641 IV-B-27690 IV-C-27381 IV-C-28679 IV-C-28722 VI-A-2752 VI-A-2752 VI-4-27472 VI-C-28005 VIII-E-26460

University of Wisconsin-Milwaukee Milwaukee, Wisconsin VI-A-26427

Worcester Polytechnic Institute Worcester, Massachusetts VIII-A-26188

University of Wyoming Laramie, Wyoming II-B-25181 III-C-28457

Yale University New Haven, Connecticut III-B-25493 IV-B-28007 VII-G-28489

Zernow Technical Services. Inc. San Dimas, California VI-C-26485

## **Principal Investigators**

Note: The Roman numeral refers to the scientific division, and the alphabetic character refers to the division subsection. Proposal numbers are in ascending sequence within the subsections.

Abeyaraine. Rohan V-A-27538

Abruna, Hector D II-A-27502

Acharya. Mukand V-B-28215

Addy, A.L. V-B-27558

Adler, L VI-C-25373

Aggarwal, J.K 1-E-28258

Agrawal, Dharma P. IV-B-28192

Aifantis, Elias C. V-A-27409

Aita, Carolyn R VI-A-26427

Albrecht-Buchle, Guenter III-F-26385

Alexander. Martin III-B-26750

Alexander, Millard H. II-C-28767

Alexopeulos, N.G VIII-C-27904

Allara, David L. II-C-27770

Allcock, Harry R II-E-28711

Allen, Jonathan VIII-G-26213

Amarakoon, Vasaniha VI-D-27548

Amer, Paul D. VIII-E-28506

Amirav, A IX-B-6089

Anderson, Charles E VI-B-26167

Anderson, L.W. 1-B-27646

Anderson, Robert L IV-A-24166

Anderson, Theodore IV-C-26194

Andrisani, D. VIII-E-26813

Anholt, Robert R.H. III-F-26767

Anson Fred C II-A-24411

Antoniadis, D.A. VIII-B-26051 Apelewicz, Tuvia

VIII-E-27751 Armstrong, Robert L

VII-G-28052

Ashok, S. II-C-27770

Auerbach. Anthony HLF-26099

Avellaneda, Marco IV A 26463

Averback, Robert S. VI-C-25526 Avnir, David

IX-D-5548 Avdin, Kultegin

VII-E-26982 Badler, Norman L IV-E-26779

IV-E-28131 Baer. Eric VI-B-25193

Baeslack, III, WA. VI-C-25373 Bahar, E

VII-D-28219

Bajaj, A. V-D-27300

Bakshi. Pradip I-D-26682 1-D-28652

Balanis, C.A. VIII-C-27873

Baliga, B. Javant VIII-A-28392 Banta, Robert M

VII-E-28094 Barber. Peter VII-G-26962

Barkey. Dale P VI-A-26449

Barlow, Richard E. IV-C-27993

IX-B-5973

I-D-26442

IV-A-25396 V.A-26443 V-A-28283

II-D-25523

Baum, Kurt

Bausch. Mark A.

V C-28912

III-C-28043

II-D-27887

V-C-27018

IV-B-28320

HI-D-26582

IV-C-26649

11-D-28565

IV-E-28328

1-D-28468

VI-A-28509

H-B-27568 Birmingham, W.P

Blau, W

Bless, Garry H. Abfalt VEE-26169

Bloom, David

Barnard, E.A

Bartram, Ralph H. Batra, Romesh C

Bauer, Simon H.

II-B-25761

II-E-27445

Beale, K.S.

Beekman, Eric J.

Behrens, Richard

Bellan, J.

Belvtschko, Ted

Berman, Harvey A

Berman, Simeon

Bernstein, Elliot R

Berzins, Valdis

Biedenharn, L.C.

Bilello, John C

Bird George R

VIII-B-28325

IX-B-6307

FF 26088

237

Bodonyi, Richard J. V-B-28249

Boemer, Wolfgang-M. VIII-C-26128

Bojanczyk. Adam W. IV-F-26945

Borri, M. IX-C-6571

Bradley, Michael S. II-C-27759

Bradshaw, Peter V-B-27625

Brandt, A IX-A-5933

Bras, Rafael L. VII-A-26902

Brill, Thomas B. H-C-26887

Bron, W.E. I-D-26211

Brown, Gary S

VII-D-26988

Brown. Herbert C.

II-B-25290

Brown, Ian G.

Brown, R.B

VI-A-25833

VIII-B-28325

VI-A-26678

Bunton, Clifford A

II-B-25411

Burns, Patrick J.

IV-B-28034

Butler, Chalmers M.

VIII-C-28151

Butler, Jerome K.

VIII-C-25339

Butler, P. Barry

V-C-28310

Byer, Robert L

1-E-25408

1-E-27418

I-E-28348

IV-B-28916

Caligiuri, Robert D

VI-B-26164

Caffisch R

Buchanan, Raymond A.

Calvert, Paul VI-C-28900

Cambanis, Stamatis IV-C-29016

Camlev. R E I-D-25374

Campbell, Stephen L. IV-B-27786

Car. R. IX-A-6280

Cardin, D. 1X-B-6307

Carling, P.A. IX-E-6185

Carta, Franklin O. V-B-26631

Casati, G. IX-A-5653

Casey, H. Craig 1-E-27556

Casey, Stephen D VIII-E-28985

Cebe, Peggy VI-A-28369

Cernansky, Nicholas P V-C-27417

Chaganty, N.R. IV-F-29053

Chakrabarti, Supriya VII-E-26404

Chan, Tony FC IV-B-28735

Chandrasekhara, M.S. V-B-27894

Chang, Fu-Kuo V-A-28253

Chang, Kai VIII-C-26651

Chang. Leroy L I-D-27458

Chang. Richard K VII-G-28489

Chapman, D.R. V-C-27480

Chern, Rey T II-E-28373

Chiang, Fu-Pen V-A-25594

Chiang, Yet-Ming VI-C-25202

Chin, Jik II-B-28013

Chlamtac, Imrich VIII-E-26823 Chou: Stephen Y VIII-B-27578

Chou, Y.T. VI-B-28549 Christe, Kull O

II A-28655 Chu Benjamin

II-E-28153 Chu, Wei-Kan VIII-A-23206

Chui, Charles K IV-F-27524

Chylek Petr

VII-A-28717 Ciftan, Mikael J-D-28468

Clark, Kenneth D IV-B-27786

Clark, Noel A. 1-E-26971

Clarke, Richard H I-E-25631

Clifton: R J VI-E-28575

Coldren, Larry VIII-F-28922

Cole, Barry VIII-C-26791

Colella, Phillip

1V-A-26272 Collin: R E VII-D-27911

Compton: Richard C VIII-C-26620

Condrate, Robert VI-D-27548

Conlisk, A.T. V-B-26595 Conover, WJ

IV-C 26746

Conrad, Hans VI-B 26825 Conrad, John R

VI-A-27552 Consortini: A 1X-F-6458

Cooper, David M V-C-27469

Cooper, Greg IV E 25514

Courtney Thomas H VI C 28639

Crandall, Michael G IV A 27869 Crim, F. Fleming 11 D-26049

Cronin-Golomb. Mark 1-h-27882

Crosicy, D R V(C-27864

Crowson: Andrew VI-F-26647

Crumbliss: Alvin L 11-E-25104

Curl: Robert F II-C-25222

Cusanovich, Michael A 1-E-28356

Cushman, John H. VII-B-27316

Dafermos, C.M. IV-A-27403

Dagdigian, Paul J II-C-28767

Dainty, J.C. 1X-F-5830

Dapkus, P. Daniel VIII-F-26898

David, Herbert A IV-C-25836

Davies, P V D-27300

Davis: A P 1X-B-6249

Davis, M.H.A IX-A-6466

De Boor, Carl IV-B-27690 De Lucia, Frank C

1-B-27431 DeWames, Roger I-

T-D-25114 Detwert, George S

V C 27469

Demain: Arnold 1 111-C 25126 111-C 28361

Demeester, P IX-F-6291

Dempster Arthur P IV C 26993 Dennis, John F

IV F 26932

Dev. Sandwip K TD-26827

Dietendort: Russell J V D 25462

238

#### Diott. Dana D 11-D-27025

Dodd. Richard A VI-A-27552

**Principal Investigators** 

Dolling: David S V-B-28293

Dow, John D VIII-B-28508

Drago, Russell S II-B-26914

Drews, Michael J VEC 26591

Duerksen, Gary L I-E-28271

Duffy, Christopher J VII-A-27471

Dupuis: Russell D VIII-A-28351

Dutton, J. Craig V-B-27558

Dutton: Robert W VIII-E-28297

Eastman, Lester F VIII-B-26151 VIII-B-26755

Eckman, Richard M VII-F-28664

Eisenstat, Stanley C IV-B-28007

Ekerdt, John G II-A-26748

Elder, R.L. IX-C-5824

Elman: Howard C IV B-26391

Embid: Pedro IV-A-28980

Eom. Hyo J VIII C-26128

Erickson, Jerald L IV-A 25428

Esaki, 190 I-D 27458

Evans, D. Fennell II-C 26296 Fasman, Gerald D

III C-25731

Fauchet, Philippe

Favro. Lawrence D

VEB 24981

Feigelson, R.S.

1 E 25408

VED 23577

1 D 28410

## **Principal Investigators**

Feldman, Michael R 1-E-28416

Fenn, John B. 11-A-25617

Fernando, H.J.S. VII-F-29188

Ferry, David VIII-B-25015 VIII-B-28461

Field, J.E IX-C-6541

Firshein, William III-C-28090

Flaherty, Joseph E. IV-F-27282

Flynn, George VIII-G-28453

Fonstad, Clifton G VIII-B-27883

Ford, Warren T 11-E-26839

Forrest, Stephen R. VIII-A-26147

Fosdick: Roger IV-A-28986

Fox: Alvin III-D-25663

Fox, Marye Anne II-C-28298

Franciosi, A VIII-A-26761

Frank: Curtis W VI-C-26882

Frehlich, Rod VII-E-27870

French, Donald A IV-B-28535

Freudenstein, E V-D-26995

Frey, Jeffrey VIII-B-28004

Friedlander, Benjamin VIII-E-27899

Friedman: Avner IV-A 25782

Frisch, Harry L. H-E-26072

Frost, Robert H VI C-25728

Fuller: Gerald VI D 26883

Gaonkar, G.H. V D-28123 Gardner, Carl L JV-B-28799

Gardner, William A VIII-E-26646 VIII-E-27917

Garg, Devandra P V-D-25409

Garrison, Jr., Warren M. VI-B-27407

Garton, Andrew VI-A-25760

Gault, James W VIII-F-28099 Gelbart, W.M

VI-C-26891 George: Nicholas I-E 24749

Gerhardt, Philipp III-A-28022

German, Randall M VI-C-27579

Gessow, Altred V-B-25467

Ghosh, S V:A-28317

Gibbons, James E VIII-F-28729

Gibson, Walter II-E-26072 Gidas, Basilis

IV-F-26811 Gillespie, David III-D-28479

Glass, Jeffrey T VEF-27810

Glimm, James IV-B 26616

Gilynn, Peter W IV F-28809 Goldberg, H S

VIII-E 27865 Gole, James I 1 E-27366

Gislub, Gene H IV B 28377 IV F-27817

Goodman, Joseph W 1 F 20695 Goodman, Rodney M

Ginele Flrich M VED 26729

IV E 2648

Gosink J.P. VIEB-26281 Gramann, Richard V-B-28293

Grant: R W VIII B-26484

Gratzei. M

IX-B-6305 Green: B IX-B-6308

Greazer, Edward M V-B-27627

Griffiths, Eloyd J VHLE-27032

Grimes, Russell N II-A-26426

Gross, Richard A III-B-27314

Grossberg, Stephen IV-E-25662

Gruban, Harold L. VIII B 28546

Gu, Zu-Han VII-D-27031

Guenther, Bob D. 1-E-27556

Gundersen, Cameron B 111-D-26232

Gundersen Martin A 1-B-26257

Gupta, NK VII-A-27772

Gupta: Vijay V1-B-28480

Gurtin: Morton E IV: A-27557 IV: A-28514 IV: F-28994

Hadiipanayis, George C VI-D-27794

Haff, Peter K VII A-27401

Hagan, D-1 1 E 27838

Haggerty, John S VI-C+25202

Hall Jr., Henry K IEE 27440

Hamed Awater V B 27515

Hammack Joseph VII A 26972

Hanusa Timothy P II A 28402

Hara Masanori VI B 25424

239

Hardt, Robert IV-A-25428

> Hardy, John R 1-D-27780

Harmer M.P. VI-B-28549

Harrington, Roger F VIII-C-25422 X Indexes

Harris, J. Milton II-B-26284

Harris, S.E. 1-E-26160

Harris, Jr., J.A. VIII-G-28326

Hartmann, Sven R 1-B-26462

Harwood, Caroline S III-B-26576

Hecht, Ralph M III-C-24435

Henein, N.A. V-C-25190 V-C-26769

Henshaw, John VI-C-28409

Herrmann, George IV-A-28957

Hess, K VIII-B-26711

Heuring, Vincent P. IV-E-28950

Hill, Craig U. II-A-28469

Hill, Steven C. VII-G 26962

Hindman, Richard G. V-B-27062

Histop, David W IV-E-27567

Ho, Yu-Chi IV F-29190

Hodges: D H V D-25327

Holmes, J. Fred VII-F-28102

Holmes, Mark H. IV-F-27282

Holmes, Philip J IV F-23306

Holmes, Robert R II-A-25435

Holonyak, Jr. N VIII-A 26434 VIII-B-26923

Horgan, C.O. V-D-28399

Houser. Thomas II-D-27505

Houston, Paul L II-D-28700

Hudson, J.A IX-E-6296

Huennekens, John P 1-B-26899

Hughes, Brian L. VIII-E-27028

Husk, G. Ronald II-E-28373

lglehart, Donald L. IV-F-28809

Irwin, M.J IV-E-23908

Ishimaru, Akira VII-D-24713

Itoh. Tatsuo VIII-C-25045

lyer. K R VI-F-27364

Jaccodine: Ralph J VI-D-22459

Jackson, David R VIII-C-27304

Jaeger, David A II-B-25181

Jeffries, Jay B L-B-26959

Jena, P J-D-25906

Jones, II. Guilford II-B-27534

Jones: Phillip L VI-F-26647

Jones, Richard A II-A-26748

Joseph, Daniel D IV-A-28797

Joshi, Aravind K. IV-E-26779

Kabamaba, Pierre T. V-D-27510

Kachanov, Mark V A-25345

Kahn, Antoine VIII-B 26666

Kailath: Thomas IV-D-26736 IV F-28060 Kak. A.C. VIII-E 26697 VIII-E-27464

Kallianpur, G IV-C 29016

Kalman, R.E. IV-D-25859 Kapania, R.K

V-A-26908

Karalamangala, A.S IV-F 28476

Karatzas, Ioannis 1V-C-28715

Kashyap, Rangasami U IV-D-26656 Katehi, Linda P.B

VIII-C-28483 Keller: A IX-D-6011

Keller, H B IV-A-25874

Kempa, K 1-D-26682 1-D-28652

Kevan, Stephen D 11-C-26191 Khanna, Shiv N

1 D-25906 Khargonekar, Pramod P

IV-D-27044 Kim, K. W

VIII-E 28187 Kinderlehrer, David

IV F-28994 Kingon: Angus I VI-B-26673

Klahunde, Kenneth J H-C 27775

Kłepaczko, J R IX-D 6148

Klopp: R W VI F 26173

Knight, Doyle V D 28651

Koc. C K IV D 28511 Koch, Stephan

TE 26974 Kohn: Robert V

IV-A 26463 Kokim Jozef L flf A 27494

Kolb Charles J II D 28103 Kolbas, Robert M VIII-D-28070

Kolsky, Herbert V D-24362 Korpel, Adrian

1-E-27591 Kosut, Robert L.

V-D-28350 Krajeinovie, D

V A-28222 Krempl. Erchard

V-A-25459 Krishnaswamy, J

VI D 26601

Kruse, Paul VIII-C-26791

Kumar. P.R IV-C-28718 IV-F-26063

Kumar, Vipin IV F 28408

Kuo, Kenneth K 11-C-24413

Kustin, Kenneth III-A-28691

Ladd: Charles C VII-B-26260

Lagowski, Jacek VI-D-27764

Lakdawala, VK I-B-26821

Langer, Stanley H II-A-27600

Lankford, Jr., James VI-B-26167

Lantelme, F IX-D-5686

Lavernia, F.J. VI/C 26439

Law, Chung K V C 27568

Law. K H IV B-28377

Lawler, J.E. I-B 27646

Leburton: Jean VIII-B 28406

Lee, Erastus H V A 25459

Lee. Peter C Y

4V A 26900

240

Leibowitz, Michael J

HI-C-2493] Lempicki, Alex LH: 7753]

Leone, Stephen R

I-B-28561 Lewandowski, John J

**Principal Investigators** 

VI-B-2539() Lewis, Randolph V.

III-C-28457

Lieberman, Edward M III-D-25752

Liechti, Kenneth M. V-A-27315

Lin, S P V-C-26797

Liu, Bede VIII-E-26118

Liu, Ming-Tsan VIII-E-28467

Liu, Tai-Ping IV-A-28548

Loewy, Robert G. V-D-25462

Logan, Kathryn V. VI-C-26021

Loh. Wei-Yin JV-C-28679

Long, G G VI-C-26123

Lorber, Peter F V(B)26631

Lorthior, G IX-D-5686

Lu. Toh-Ming VI-D-27605

Eubman, David M. II-A-25500

Ludwig: F1, VII-F-24881

Luhmann Jr., N.C. 1-B-28396

Luk. Franklin T IV-E-26930

Luo, Ren C IV-E 27567

MacCormack, Robert W V C-27480

MacKnight, William J

IFE 28314

Madey, John M J

Madhukar Anupam VIII A 27298

11-25349

#### **Principal Investigators**

Magruder, III, Robert H. VI-D-28109

Mahrt, Larry VII-F-26491

Majda, Andrew J. IV-A-26113

Manson, Steven T I-B-26709

Maracas, George N VIII-B-26686

Maradudin, Alexei I-D-25464

Marconi, Frank V-B-28252

Marek, Wiktor IV-E-26438

Mark, James E. VI-C-27373

Marquis, Robert E III-A-28022

Maserjian, Joseph VIII-C-27307

Matyjaszewski, Krzysztof II-E-28631

Mayer, James W. VI-A-26806

Mazur, Eric I-B-25653

McDermott, D B 1-B-28396

McDonald, John F VIII-B-28329

McElwee-White: Lisa II-A-28353

McGervey, John D VI-A-27037

McGrath, James E VI-C-28883

McIntosh, Robert E VII-D-25730 VII-D-27919

McKoy, Vincent V-C-24487

McManus: Samuel P II-B-26284

McNeil, Laurie E VIII-A-23206

McVey, John V-C-26456

Meerkov, Semyon M V-D-27510 VIII-E-27834

Mellor, A.M. V-C-26720 Meingailis, John VIII-B-26051 VIII-B-28345

Melton, Lynn A. V-C-28250

Menger, Fredric M II-B-25739

Merlin, Roberto D 1-D-26195

Messina, Neale V-C-26403

Metiu, Horia II-C-25605

VIII-E-27886 Meyer, Thomas J II-A-25586

Meyer, Robert G.

Meyer, Walter VI-A-25199

Meyers, Marc A VI-C-26392 VI-C 28368

Michaelis, Elias K III-C-28669 III-D-25702

Michaelis, Mary III-C-28669 III-D-25702

Mignolet, M.P V-A-28222 Miller, Alan VIII-B-28594

Miller, Alan K VI-C-26882

Miller, Cass T VII-A-28504

Miller, David L V-C-27417 VIII-A-26444

Miller, Jr., Willard IV:A-25782

Miller, William H VI-A-25199

Mills, Doug L 1-D-25374

Milstein, L.B. VIII-E 27754

Mishra, Umesh K I B-28569

Mitchell, James K VII C 24381

Mohamed: F.A VI C 26439

Moon: Donald L VIII C 25557 Morgan, Stephen L III-D-25663 Morosoff, Nicholas

II-E-25104 Morse, T.F VI-D-28538

Moss, Robert A. II-B-25669

Mossberg, T. omas W. I-E-25546

Mourou. Gerard VIII-B-26760

Mueller, Gregory P III-C-27890

Munk, Petr II-E-28053

Mura, Toshio V-A-26057

Nagib. H V-B-28215

Nappo, Carmen J VII-F-28664

Narayan, J VI-D-26601

Nayfeh, Ali H V-D-25630 Neilson, Robert H

II-E-25286 Nelson Donald F

VIII-A-26188

Nelson, Wilfred H III-D-25476

Nerode: Anil IV-F-23306 IV-F-29031

Nicolet, Marc-A VI-D-26287 Nieh, T.G.

VI-C-26751 Nirenberg, Louis

IV-A-25069

Nixon, Wilfred A VII-B-26031

O'Donnell, Kevin VII-D-27485 O'Handley, R C

VI-D-25251 VI-D-28553 Odell, J A

IX-D-6011 Oden, J. Tinsley

IV-B-26871

Olson: David E VI-C-26728

241

Olson, Gregory B VI-B-27163 X Indexes

Oncley, Steven P. VII-F-28954

Oppenheim, A.K. V-C-25245

Ornston, L. Nicholas III-B-25493

Osgood, Richard M. I-B-26223

Osgood, Jr., R. VIII-G-28453

Osterkamp, T.E VII-B-26281

Owens, R.M. IV-E-23908

Packard. Andrew IV-D-28835

Packard, William E. VIII-B-28508

Padmanabhan, Karur R. V-C-26769

Paesler, Michael A. I-F-28313

Pardoux, E. IX-A-6271

Parhi, Keshab K. VIII-E-27076

Paris, Demetrius VIII-G-27554

Parrish, Phillip VI-B-28608

Parthasarathy, T.A. VI-C-25526

Parzen, Emanuel IV-C-27574

Paul. Donald R. II-E-25229

Pederson, Donald O VIII-E-27886

Peng. Song-Tsuen VIII-A-28674

Pepper, M. IX-F-5940

Perepezko, John H. VI-C-27472 VI-C-28005

Petrenko, Victor E VII-B-28599

Petrucci, Sergio II-A-26636 Petuskey, William

VI-A-24845

I-E 26974

Peyghambarian, Nasser

Platzer. M.F. V-B-27894

Plotkin, Serge A. IV-B-28143

Poon, S. Joseph VI-C-28067

Post. Madison J. VII-E-28094

Potasek. M.J. IV-A-28803

Powell, Richard C. I-B-28472

Prager, Stephs 1 II-C-26296

Prater. John T. VI-F-27810

Pritchard, David E. I-B-26566

Psaltis, Demetri I-E-26676

Pursley, Michael B. VIII-E-27994

Quin. Louis D. II-C-26126

Quinn, John J. I-D-25167

Rabinowitz, Paul H. IV-A-27641

Rabitz, Herschel II-D-28555

Rafaniello, William VI-C-26068

Raj. Rishi VI-B-26747

Rajendran, A.M. VI-E-24102

Ramaprian. B.R. V-B-28159

Ramesh, K.T. VI-E-28272

Rao, Bhaskar D. IV-F-26802

Rao, C.R. IV-F-26792

Ratner, Mark A. II-E-27054

Raushel, Frank M III-D-27468

Ravani, Bahram V-D-27075

Ravishanker, Nalini IV-C 28743

Raymer, hael G 1-E-255% Raymond, Charles E VII-F-28344

Rebeiz, Gabriel M. VIII-C-28483

Reddy, J.N.

V-A-26908

Redner, Sidney II-D-26256

Reeber, Robert R. VI-F-26246

Rehfield, L.W. V-D-25327 Reisfeld R

IX-D-5884 Reisler, Hanna II-C-29310

Reiss, H. VI-C-26891

Reynolds, John R. II-E-27808

Rhee. Kyung Tai V-C-28316

Rhodes, Charles 1-B-28499

Rice, John R. IV-F-27392 Richmond, Geraldine L.

11-C-26191 Rino. Charles L VII-D-26480

Robbins, Herbert IV-C-27862

Robinson, Stephen M. IV-C-27381

Rodin: Gregory J. V-A-27315

Roe, R.J VI-C-26579

Ron, Amos IV-B-27690

Roth, J. Reece VI-A-26678

Russell, Alan J III-C-28011 III-C-28043

Rutledge, David B. VIII-C-26381 VIII-C-27307

Sabin, John R. 1-D-28362

Sachs, Frederick III-F-26099

Sadwick, I, P VI-D-28612 Salama, Kamel VI-B-25397

Santavicea, D.A. V-C-28427

Sarma, Sankar Das VIII-B-26278

Sarwate, D.V. VIII-E-27994

Sastry, Shankar IV-D-28835

Satyanarayana. A. IV-C-25706

Sauer, John A. VI-B-25424

Sawyer, R.F. V-C-25245

Schaap, A. Paul II-B-26115

Schafer, Ronald W. VIII-G-27554

Schetzina, J.F. 1-D-28336

Schilling, Donald L. VIII-E-27751

Schnabel, Robert B. IV-B-28701

Schoenbach, Karl H. 1-B-26821

Scholtz, Robert A. VIII-E-25674

Schrage, Daniel P. V-B-25461

Schulson, Erland M. VII-B-27482

Schuster, Gary B. II-C-28319

Schwarz, Steven E. VIII-C-26949

Schwer, Leonard E. VI-B-26164

Scott, James I-E-26971

Scott. Peter VII-G-28359

Serota: Rostislav VIII-B-26941

Seshadri, K. V-C 27455

Sethuraman, Jayaram IV-C-27868

Setiow. Peter III-C-27956

242

Shabana, A.A V-D-26934

## Principal Investigators

Shah, Jayant IV-C-27790

Shannon, Robert R. I-E-28356

Shaw, Roger H. VII-F-27019

Shayegan, M. I-D-26015

Shearer, Michael IV-A-28702

Sherby, Oleg D. VI-B-28761

Shetty, Dinesh K. VI-B-24583

Shieh, L.S. IV-D-28511

Shiflet, Gary J. VI C-28067

Shockey, D.A. VI-E-26173

Shore, Sheldon G. II-A-26145

Shortliffe, Edward H. IV-E-25514

Shriver, Duward E II-E-27054

Shu, Chi-Wang IV-B-28716

Shur. Michael VIII-A-28347

Siegel, Jerome III-E-25521

Sievers, A.J. I-E-26383 I-D-26996

Sigelmann, Rubens VII-D-24713

Simmonds, J.G. V-D-28399

Singel, David J. I-E-27425

Singpurwalla, N.D. IV-C-24557 Sinha, Subhash C.

V-D-26061

I-B-27888

Skrzypek, Josef

IV-E-25324

1I-C-25222

V-C-27864

Smith, G.P.

Smalley, Richard E.

Skatrud, David D.

#### **Principal Investigators**

Snyder, Wesley E. VIII-F-28099

Solberg, Myron 111-A-27494

Sollner, T.C.L.G. 1-D-25487

Sorokin, Peter P. I-B-27508

Srinivasan, G.R. V-B-27752

Srivastav, Ram P. IV-A-27433

Stalder, Kenneth R. I-B-26959

Steel, Duncan G. I-D-26644

Steele, J. Michael IV-C-28982

Steiglitz, K VIII-E-26118

Steinberg, Bernard D VIII-C-25350

Steinhardt, Allan O. IV-F-26945

Steinhoff, John V-B-25623

Stengel, Robert F IV-D-25264

Stephan, Karl D. VIII-C-26599

Stewart, John M. III-C-27488

Stillman, G. VIII-A-26434

Stonebraker. Michael IV-E-27892

Strikwerda, John C IV-B-28025

Stringfellow, G.B VI-D-28612

Stroscio, M.A. VIII-F-28187

Stroud, C R I-E-25482

Stufflebeum, John H II-C-24413

Sugama: Toshifumi VI-A-26667

Summers: Christopher J VIII-C-28339

Sun. C.T. V-A-28307

Sunder, S. Shyam VII-B-26260 Sung. C.S.P. VI-C-26571

Swanson, M.L.L. VI-D-27846 Symonds, P.S.

V-D-24362 Syvanen, Michael

III-D-27916 Tabakoff, Widen

V-B-27515

Tadjbakhsh, Iradj V-D-25771 Tan, Teh Y.

VI-D-26729

Tannenbaum. Allen JV-D-27365

Tantaratana, Sawasd VIII-E-27493

Taylor, Fred J. VIII-E-26735

Taylor, Ronald D. VI-F-28620

Tenorio, M. VIII-E-26813

Tester, Jefferson W. II-D-28371 Thies, Mark C.

VI-C-26591

Thomas, John E. I-B-27766

Thomas, Robert L. VI-B-24981

Thompson, Carl V. VI-D-28553

II-D-26106

Thompson, James R IV-C-26108

Thompson, Donald L.

Thompson: Richard C II-A-28486

Thorsos: Eric 1 VII-D-29288

Tiersten, Harry F 1-D-25697 1-D-28591

Ting, T.C.T. IV-A-28606 Tirrell, Matthew

IV A 28797 Tosath, E IX:A:6280

Triboulet, R IX-E-6563 Tsang, Leung VII-D-26384

Tsong, 1 S.T. V1-A-24845

Tsu, Raphael

VIII-B-27443 Tsui, D.C. 1-D-26015

VIII-A-28335 Tufts, Donald W. IV-F-27620

Tukey, J.W. IV-C-26997

Tzavaras, A.E.

IV-A-26218 Ulaby, Fawwaz T

VII-D-26224 Ullman, Frank G 1-D-27780

Usherwood, P.N.R IX-B-5973

Van Siryland, E.W. I-E-27838

Van Veen, Barry VIII-E-26460

VanderLugt, Anthony I-E-27586

Venakides, S. IV-A-28969

Verber, C.M. 1-E-26264

Vincent, J.E.V. IX-D-6579

Virkar, Anil V. VI-B-24583

Vitter, Jeffrey

IV-B-28071 Vlannes, Nickolas P.

VI-D-27605 Vodvanoy, Vitah

111-F-27634

Vranos, A. V-C-26456

Waber, James T VI-A-21545 Wagener, Ken B

ff-E-26441 Wallace, W.E. VI-D-28146

Wallis: Richard 1-D-25464

243

Walrand: Jean IV:C 26144 Walsh, John E. I-B-28531

> Wang, K.L. VIII-A-26896

X Indexes

Wang, Paul IV-B-28908

Wayman, C.M. VI-C-26617

Weaver, James C. III-C-28361

Webber, Stephen E II-E-28053

Wegman, Edward J. IV-C-28309

Weil, Jeffrey C. VII-F-27995

Weiss, B.L. IX-F-6170

Wells, Valana L. V-B-28002

Wempner, Gerald A. V-A-25400

West, Lawrence C. I-E-28271

White, Henry W. VI-A-26400

White, John M. JJ-C-26822

Whitehouse, Craig M. II-A-25617

Wigen, Philip E. VI-D-28141

Wight, Charles A. II-D-27603

Wilcox, David C. V-B-26863

Wild, James R. III-D-27468

Wilkins, Dick VI-C-28409

Wilkinson E IX-B-6294

Williams, Forman A. V-C-25794

Williams, William O IV-A-27557

Wilson, Robert G VIII-A-26708

Wiltse, James VIII-C-28339 VIII-C-28516

Wisian-Neilson, Putty II-E-25286

Wittig. Curt II-C-29310

Wong. Ngai Chuen I-B-27532

Wong. Shan S. III-B-27314

Wood, Ralph T. VIII-F-24793

Woodroofe, Michael B. IV-C-25819 Wooley, Bruce A VIII-E-28387 Yalisove, Steven M VI-A-28509 Yariv, Amnon I-E-27273

Yates, John T II-C-26238 Yau, Stephen IV-D-26674 Ym, Wan-Lee V-A-25400

Yong, Yook-Kong V-D-28155

Young, Donald VI-D-22459

Young, J.F. 1-E-26160 Yu, Bin 1V-C-28722

## Principal Investigators

Yu. Francis T.S. 1-E-28502

Zacks: Shelemyahu 1V-C-25347

Zernow, Louis VI-C-26485

Zinilii, E IX-A-5265

## **Subject Index**

*Note:* The Roman numeral refers to the scientific division, and the alphabetic character refers to the division subsection. Proposal numbers are in ascending sequence within the subsections.

VIII-E-26646, VIII-E-26813, VIII-E-26823,

Absorption Coefficients I-E-27838, I-E-28271 Absorption Spectra I-B-27508, 1X-B-6294 Acceleration Sensitivity 1-D-25697, 1-D-28591 Acetic Acid II-B-26914 Acetone II-B-26284 Acetonitriles II-A-26636 Acetyl Compounds II-A-26426 Acetvicholinesterase II-B-26115, III-D-26582 Acidities II-E-27445 Acinetobacter calcoaceticus III-B-25493 Acoustic Impedance IV-B-26616 Acoustic Resonators I-D-28591 Acoustic Signals VIII-E-28985 Acoustic Waves 1-D-25697, VIII-E-28985 Acoustics IV-A-26113 Acoustoelastic Constants VI-B-25397 Acoustooptic Systems I-E-27586 Acrylates III-C-28043 Acrylonuriles II-E-25229. II-E-27808 Adaptive Arrays VIII-E-27032 Adaptive Control IV-D-25264, IV-D-28835, IV-F-26063, V-D-25409, V-D-28350 Adaptive Information Processing IV-F-26063 Adhesion II-E-25229, VI-A-26667, VI-C-26579, VIII-B-26666 Adhesive Bonds V-A-27315, VI-B-24981 Adhesives V-A-27315, VI-A-25760 Adiabatic Processes IV-A-26218 Adiabatic Shear Bands IV-A-25396, V-A-28283, IX-D-6148 Adsorbates II-C-25605, II-C-26822, II-E-28053 Adsorption II-C-26822, II-C-27775 Advection IV-A-26463 Aerial Images I-E-28258 Aerodynamics V-B-25461, V-B-25467, V-B-26631 V-B-28002, V-D-28123 Aeroelastic Stability V-D-28123 Aeroelasticity V-B-25461 Aeromechanical Stability V-B-25467 Aerosols IV-A-25428, VII-A-28717, VII-G-28052 Aerospace Vehicles VIII-C-27873 Aging VI-A-27037, VI-B-26825 Agricultural Crops VII-F-27019 AIDS IV-A-25782 Air Purification II-C-27775 Aircraft Control IV D-25264, IV-D-27365 Aircraft Detection VIII-C-25350 Airtoils V-B-26631, V-B-27752, V-B-27894, V-B-28002, V-B-28159, V-B-28249, V-D-28651 Airglow VIEE-26404 Aldehydes 11-F- 27340 Algebra IV F-29031 Algebraic Computation IV-B-28007 Algebraic Equations IV-B-27786 Algebraic Functions IV-F-23306 Algebraic Methods IV-D-26674 Algorithms 1/E-24749, 1/E-28416, 111-F 26099, IV-A-24166, IV-B-28071, IV-B-28143, IV-B-28320, IV-C-25347, IV-C-25706 IV-C 26108, IV C-26144, IV-C-26993, IV C-27790, IV-C-28718, IV-C 28982, IV-D 26656, IV D-26736, IV-D-27044, IV-D-28835, IV E-23908, IV-E-26438, IV-E 26487, IV E-27892, IV E 23306. IV F 26063, IV F-26792, IV F-26814 IV F-26930, IV F-26945, IV-F-27282 IV F 27392, IV F 27524, IV F 27620, TV F-27817, TV F-28060 - EV F-28408 IV F-29031, VIII-C 25350, VIII E 25674,

VIII-E-27076, VIII-E-27464, VIII-E-28297. VIII-F-28099, VIII-G-27554, IX-A-5265, IX-A-5933 Aliphatic Alkenes II-E-26839 Alkali Diatomic Molecules I-B-26899 Alkaline Earth Compounds II-A-28402 Alkaline Earth Fluorides 1-D-26442 Alkaline Earth Molecules I-B-26899 Alkaline Phosphatase II-B-26115 Alkanes II-B-26914, IX-B-6249 Alkenes II-E-26839, 1X-B-6249 Alloying VI-C-27579, VI-C-28639 Alloys Annealing VI-C-28067 Corrosion Protection VI-A-26678 Deformation VI-E-28272, VI-E-28575 Fracture Properties VI-C-28067 Fracture Toughness VI 25390 Friction VI-A-26806 Hardness VI-A-26806 Impact Tests VI-C-26439 Martensitic Transformations VI-C-26617 Mechanical Properties IV-A-28986, VI-C-26439, VI-C-27579, VI-C-28005, VI-C-28067, VI-E-28272 Microstructure VI-B-26167, VI-C-26439, VI-C-26751, VI-C-27472, VI-C-27579, VI-C-28005, VI-C-28067 Processing VI-B-26825 Sintering VI-C-27579 Solidification VI-C-26439 Spray Atomization VI-C-26439 Structure VI-A-26806 Superplastic Properties VI-C-26751 Tensile Tests VI-B-26167 Aluminum Cavitation VI-B-26825 Corrosion VI-A-26678 Corrosion Protection VI-A-26400, VI-A-26667. VI-A-26678 Etching 1-B-28561 Shock Loading VI-F-27364 Weldability VI-C-26728 Aluminum Alloys VI-A-26628, VI-B-25390. VI-C-25373, VI-C-26439, VI-C-27472, VEC 28005 - VEC 28067 Aluminum Antimonides I-D 25167, 1-D-25487, II-A-26748 Aluminum Arsenides 1-D 27458, II-A-26748, VIII-A-26444, VIII-A-26761, VIII-B-27883, VIII-G-26213 Aluminum Gallium Arsenides I-B-26257, 1-B-28569, 1 D-25487, 1-D 26015, 1 D 26644, 1-E-26974, VIII-A-26434, VIII-B-26714, 1X-F-6170 Aluminum Glasses VI-C 28067 Aluminum Matrix Composites VI-A-26400, VI-B-25390, VI-C-26439 Aluminum Metallizing VI D 26287 Aluminum Nitrides VI B-26673, VI-C 26068. VI-E 26169, VI E 26173 Aluminum Oxide II-C-26126, VI-B 28549 VEC 26024, VEC 26123, VEC 26751, VI-D-26601, VI-E-26173 Aluminum Oxide Membranes II-F 25304 Aluminum Phosphides II A 26748 Amines II B 26914 - II C 28298 Amino: Acids II A 25500, 11I-C 24435 Ammonia II C 25222, II C 26822

Ammonium Nitrate II-C-26887 Ammonium Surfactants II-B-25181 Amorphous Materials VIII-A-23206 Amplifiers 1-D-28652, 1-E-25546, VIII-B-26923, VIII-C-25045, VIII-E-27886, VIII-G-26213 Amplitude Modulators 1-E-28271 Anaerobic Aromatic Biodegradation III-B-26576 Aniline IX-B-6089 Animals IX-D-6579 Anionic Polymerization II-E-28631 Anisotropy V-A-25459, V-A-27409 Annealing VI-C-28067, IX-F-6563 Annihilation Reactions II-D-26256 Antenna Feed Networks VIII-C-27304 Antennas VIII-C-25045, VIII-C-26599, VIII-C-26620. VIII-C-26651, VIII-C-27304, VIII-C-27307, VIII-C-27904, VIII-C-28151, VIII-C-28483, VIII-C-28516, VIII-E-27032, VIII-G-27554 Authracene 1X-B-6089 Anti-Armor VI-B-26164 Antibodies 1X-B-6308 Antimonides I-D-25167, I-D-25487, I-E-26383, II-A-26748, IX-F-5940 Antimony VI-D-28612, VIII-G-26213 Antimony Alloys VI-C-27472 Aperture Effects 1-E-26264 Apopinenes II-B-25290 Applied Logic IV-F-29031 Applied Mathematics IV-A-25782, IV-A-26113, IV-B-28535 Approximation IX-A-6271 Arc Jet Plasmas I-B-26959 Arc Welding VI-C-26728 Armor VI-B-26164, VI-C-26485 Armor Materials VI-C-26021, VI-C-26068 Aromatic Aldehydes II-E-27440 Aromatic Biodegradation III-B-26576 Aromatic Compounds II-E-28053, III-B-26750, IX-B-6294 Array Processing IV-D-26736, VIII-E-27899 Arsenic I-D-25114, VI-D-26287, VI-D-28612, VIII-B-26666 Arsenides Annealing VI-D-26287 Chemical Reactions VI-D-26287 Cleaning VIII-G-28326 Clusters II-C-25222 Contact Layers VIII-B-26484 Cryogenic Noise Performance VIII-B-26151 Crystal Defects VI-D-27764 Crystal Growth I-D-26015, VIII-A-26434, VIII-F-24793, VIII-F-27865 Diffusion Mechanisms VI-D-26729 Electrical Contacts VIII-B-27883 Electrical Properties I-B-26821, VIII-B-26760 Electron Emission I-B-28569 Electronic Properties IX-A-6280, IX-F-5940 Epitaxial Growth VI-D-26287, VIII-A-26444. VIII-B-26666, VIII-B-26686, IX-F-6291 Epitaxial Layers VIII-A-26761 Etching 1 B-28561, VIII-G-28326 Excitation 1-D-26644 Heterojunctions J-B-26257, TX-F 5940 Interfaces II-C-25222 Ion Implantation 1X-F-6170 Ontical Properties 1-D-28470 Optical Stark Elect I-E 26974 Optoelectronic Properties VIII-B-26666 Processing VIII-F 24793, VIII F 27865

Properties II-A-26748 Quasi-Optical Properties I-D-25487 Simulation VIII-B-26711 Superlattices I-D-27458, VIII-A-26444 Surface Properties II-C-27770 Switching Properties 1-B-26821 Transport Properties 1-D-25167, VIII-A-28335 Vibrational Properties IX-A-6280 Arthrobacter III-B-26750 Artificial Intelligence IV-E-26779, IX-A-5933 Asymptotic Properties IV-F-26792 Atmospheric Effects VIII-E-28985 Atmospheric Gravity Waves VII-F-28664 Atmospheric Surface Layer VII-F-28954 Atmospheric Turbulence VII-E-27870, VII-F-27019, IX-F-6458 Atom Interferometry I-B-26566 Atomic Adsorption I-B-26223 Atomic Collisions IJ-D-26106 Atomic Interferometry I-E-28356 Atomic lons I-B-26709 Atomic Layer Epitaxy VIII-F-26898 Atomic Optics 1-B-26566 Atomic Position Measurement 1-B-27766 Atomic Properties 1-B-26566, 1-B-26709 Atomic Structure IX-A-6280 Atomization V-C-26797 Attitude Control IV-D-28511 Auroras VII-E-26404 Austenite VI-C-26617, VI-C-26728 Autoignition V-C-25190 Automatic Target Recognition VIII-E-26697. VIII-E-27464 Automatic Teller Machine Networks IV-C-26144, VIII-E-25674 Axons []]-D-25752 Aza-aromatic Compounds IX-B-6294 Azabutadienes II-E-27440 Azaethylenes II-E-27440 Azides II-A-28655 Azomethane [I-C-26822 Bacillus subtilis III-C-25126, III-C-27956, III-C-28090 Backscattering 1-D-25464, II-D-27025, VII-B-26031, VII-D-24713, VII-D-27031, VII-D-27485, VII-D-28219, VII-E-28102, IX-F-5830 Bacteria III-B-25493. III-C-28361 Bacteria Detection III-D-25476 Bacterial Degradation III-B-26750 Bacterial Polyesters III-B-27314 Bacterial Spores III-C-27956, III-D-25476 Bacteriorhodopsin 111-C-25731 Ballistic Compressors V-C-26403 Ballistic Electrons 1-D-26682 Ballistic Properties VI-C-26021, VI-C-26068 Ballistic Tests V-A-28307 Ballistics V-A-27409, VI-B-26164 Band Structure I-D-26015, II-C-26191 Barium Borates VI-D-23577 Barium Ions II-A-28402 Barium Magnesium Germanates 1-E-27425 Barium Sodium Niobates I-E-26971 Barium Titanates 1-E-27882 Battle Management Systems IV-F-29190 Battlefield Simulation IV-B-28034 Bayerite VI-C-26123 Bayesian Sampling IV-F-23306 Beam Coupling I-E-25482 Beamformers VIII-E-26460 Beams (Structural Forms) IV-E-23306, V-B-25467, V-D-24362, V-D-25327, V-D-25630, V-D-25771, IX-C-6571 Bearing Steels VI-A-27552 Bearingless Rotors V-B-25467 Belief Functions IV-C-26993 Belief Networks IV-E-25514 Benzoates III-B-26576 Benzonitriles II-A-26636

Beryllium VI-D-26729, VIII-B-26151 Bifurcation IV-F-23306 Bifurcation Theory IV-A-25874 Binocular Vision Modeling VIII-C-25557 Biocatalytic Reactions III-C-28043 Biochemistry III-D-27468, IV-A-25874 Biodegradation III-B-25493, III-B-26576, III-B-26750, III-B-27314 Biological Agent Analysis II-A-25617 Biological Membranes IV-F-23306, VI-C-28900 Biology III-B-26576 Biomolecular Materials VI-F-28620 Biophysical Properties JX-B-5973 Biosynthesis III-D-26582 Biotechnology VI-C-28900 Biphenyls III-B-26750 Bismuth 1-B-27508, VIII-G-26213 Bismuth Fluorides 1-E-27366 Bismuth Germanates 1-E-25631 Bismuth Ions VI-D-28109 Bistable States 1-D-28468 Blade Tip Aerodynamics V-B-25461 Blade Tip Vortices V-B-26595 Blade Vortex Interactions V-D-25462 Block Design IV-C-26746 Boehmite VI-C-26123 Boost Phase V-C-27469 Bootstrap Methods IV-C-28679 Boranes II-A-26145, II-B-25290, II-D-25523 Borates 1-D-26195, VI-D-23577 Borides II-A-26145, VI-C-26021, VI-C-26392, VI-C-28368, VI-D-25251, VI-E-26169. VI-E-26173 Borohydrides II-A-26145 Boron VI-C-26728 Boron Alloys VI-D-27794 Boron Carbides VI-E-26169, VI-E-26173, VI-F-26246 Boron Nitrides II-A-26145 Borosilicates VI-D-27548 Boundary Layers V-B-26595, V-B-26863, V-B-27558, V-B-27625, V-B-27894, V-B-28293, V-D-28399, VII-E-28094, VII-F-27995, VII-F-28664 Boundary Value Problems IV-F-23306 Box Beams V-B-25467 Box Splines IV-B-27690 Brain III-D-25702, III-D-26232, III-E-25521 Brittle Fracture V-A-25345, VI-B-25193 Broadband Networks VIII-E-28467 Bromides II-B-25181 Bromine II-A-26426 Buckling IV-A-25874, V-D-25630, V-D-25771 Buckminsterfullerene II-C-25222 Buffer Overflow IV-C-26144 Butadienes II-E-27440 Butyl Phosphates II-E-26072 Cadmium Manganese Tellurides 1-D-25167. I-D-27458, VI-D-27846 Cadmium Tellurides 1-D-27458, VIII-A-26761, III-A-28347 Cadmium Zinc Tellurides VI-D-27846 Calcium III-B-26750, III-D-26232, HI-F-26099, VIII-B-26666 Calcium Fluorides J-B-26223, VIII-G-28453 Calcium Ions II-A-28402, III-D-26232, III-F-27634 Calcium Strontium Fluorides VIII-B-26666 Calcium Tungstates 1-E-25631 Calculus of Variation IV-F-28994 Capacitance VIII-B-28646 Capacitors 1-D-26827 Carbide Reinforced Composites VI-C-25202, I-C-26439, VI-C-26751 Carbides II-A-28353, VI-A-24845, VI-B-25390, VI-B-25397, VI-B-26673, VI-B-28761, VI-C-26392, VI-C-28368, VI-D-26601,

#### Subject Index

Carbodrinudes II-E-27440 Carbon II-E-28711, VI-D-27794 Carbon Dioxide III-C-28043 Carbon Fibers VI-C-26591 Carbon Films VI-D-26601 Carbon Monoxide II-C-26238 Carbon Sulfides II-D-27025 Carbon Tetrachloride IX-B-6089 Carbonyl Clusters 1X-B-6307 Carboranes II-A-26426 Carboxylic Acids IX-D-5548 Cascade Superfluorescence 1-B-26462 Catalysis II-A-27600, H-A-28469, II-B-25739, II-C-26126, II-D-26256, III-D-26582, IX-B-6249 Catalysts II-A-28469, II-B-26914, II-C-26238, I-E-26839. IX-B-6305 Catalytic Antibodies IX-B-6308 Cathodes 1-B-26257 Cauchy Singular Integral Equations IV-A-27433 Cavitation VI-B-26825 Cells (Biology) III-C-27890, III-C-28361, III-D-25752, III-F-26099, III-F-26385, III-F-27634 Cellular Automata IV-F-23306 Cellulose II-C-26126 Centrifugal Compressors V-B-27627 Ceramic Armor VI-C-26021, VI-C-26068 Ceramic Fibers VI-B-26747 Ceramic Matrix Composites VI-C-25202, VI-C-26751 Ceramic Precursors VI-C-27373 Ceramic Reinforced Composites VI-B-25390. I-B-25397 Ceramic Reinforcements VI-C-26439 Ceramics Ballistic Properties VI-C-26068 Combustion Synthesis VI-C-26392, VI-C-28368 Compacting VI-C-26392 Compaction VI-C-28368 Compressive Strength VI-C-26068 Cracking VI-B-28549 Crystal Chemistry VI-F-26246 Deformation VI-B-28761 Densification VI-C-26392 Dynamic Loading VI-E-26169, VI-E-28575 Elastic Properties VI-B-26747, VI-B-28761 Failure Criteria VI-E-26173 Flaw Testing VI-B-28549 Fracture Properties VI-B-24583 Grain Boundary Engineering VI-D-27548 Hardness VJ-A-26806 Impact Tests VI-E-26173 Interfaces VI-B-28480 Ion Beam Modification VI-A-26806 Mechanical Properties V1-A-26806 Microstructure VI-A-26806, VI-B-28761, I-C-25526, VI-C-26123, VI-C-26392, VI-D-27548 Processing VI-B-26747, VI-C-26123, VI-C-26392 Shear Resistance VI-E-28575 Sintering VI-C-25526, VI-C-26123 Strength VI-B-24583 Superplastic Properties VI-B-26747, VI-B-28761, VI-C-25526, VI-C-26392, VI-C-26751 Surface Properties VI-A-24845 Tensile Tests VI-B-28761 Thermal Expansion VI-F-26246 Tribological Properties VI-F-26246 Cerenkov Lasers 1-B-28531 Cerium Coatings VI-A-26400 Cessum Vapor I-B-26462 Cesium Zinc Iodides 1-D-27780 Chalcogenide Glasses VIII-A-23206 Channels (Waterways) VII-A-26902 Chaos 1X-A-5653 Charge Carriers 1-D-26015, 1-D-26682 Charge Coupled Devices VIII-C-25557 Charge Transfer II-A-25586, II-C 25222, VIII-B-26051 Charge Transport VIII-B-28406, VIII-B-28594,

III-B-28646

VI-D-27794, VI-E-26169, VI-E-26173,

VI-F-26246

Chelates II-E-25104 Chemical Agent Analysis II-A-25617 Chemical Agents II-C-26238, II-C-27775 Chemical Beam Epitaxy VI-D-28612 Chemical Bonds II-C-26238 Chemical Detection II-A-25500 Chemical Kinetics V-C-27455 Chemical Lasers I-E-27366 Chemical Markers III-A-28691. III-D-25663 Chemical Reactions II-A-27600, II-B-25411, I-C-24413, II-C-26822, II-D-26106, II-D-27505, II-D-28700, V-C-27455, [X-B-6249 Chemical Reactivity II-B-25181, II-B-25739 Chemical Reactors V-D-27510 Chemical Vapor Deposition VI-D-28538 Chemiluminescence II-B-26115. II-D-25523 Chemisorption II-C-25222, II-C-26238 Chloride Induced Corrosion VI-A-26678 Chlorides [-D-27780, []-B-25761, []-D-28371. 11-A-26400 Chlorine II-A-26426 Chlorine Compounds II-C-26822 Chloro Aluminum Phthalocyanine I-E-27838 Chloroboranes II-B-25290 Chlorodinitromethane II-B-25761 Chloroethylenes II-B-25761 Chlorohexane 11-D-27505 Cholesterol IX-B-6089 Choline Transporters III-D-26232 Chromatographic Silicon Dioxide II-A-27600 Chromium VI-A-21545, VI-D-26729 Chromium Alloys VI-C-28005 Chromium Coatlags IX-D-5686 Chromium Emission Spectra 1-D-26442 Chromium Ions I-B-28472, I-E-27425, VI-A-26678 Chymohelizymes III-C-27488 Circuit Complexity IV-F-28060 Circuit Design VIII-E-27886 Circuit Fabrication VIII-B-26051 Clays II-C-28298 Cloning III-C-27956, III-C-28457, III-C-28669, III-D-26232. III-D-27916 Clostridium botulinum III-A-28691 Clostridium perfringens III-C-27956 Clostridium thermocellum III-C-25126 Clouds (Meteorology) VII-E-26982 Clutter VIII-C-25350 Clutter Databases VII-D-26224 Coastal Sediments VII-A-26972 Coatings 1-B-27646, II-A-24411, II-C-27759, V-A-27409, VI-A-21545, VI-A-26400, VI-A-26667, VI-A-27552, VI-A-28509, VI-B-24981, VI-B-28480, VI-D-26601 Cobaloximes II-E-26072 Cobalt II-E-28373 Cobalt Alloys VI-C-28067, VI-D-28146 Cobalt Complexes II-B-28013, II-E-26072 Cobalt Compounds II-A-26426 Cobalt Ions VI-A-26667 Code Theory IV-F-26811 Coding Techniques VIII-E-27994 Coding Theory IV-C-28722 Cold Starting V-C-25190 Colloidal Catalysts II-E-26839 Colloids II-B-25411, VI-D-28109, 1X-B-6305, 1X-B-6307 Color Centers 1-E-27425 Color Matching 1-E-24749 Combinatorial Optimization IV-B-28143 Combustion II-C-24413, II-C-28767, II-C-29310, II-D-28103, IV-A-25069, IV-A-25782, IV-A-26113, V-C-25190, V-C-25245, V-C-25794, V-C-26456, V-C-26769, V-C-26797, V-C-27018, V-C-27565, V-C-28316 Combustion Synthesis VI-C-26392, VI-C-28368, VI-F-27810 Communication Devices VIII-A-26147

Communication Networks VIII-E-26823, VIII-E-27834, VIII-E-28467 Communication Protocols VIII-E-28506 Communication Signals IV-D-26736 Communication Systems VIII-E-27028, VIII-E-27493, VIII-E-27899, VIII-E-27917, VIII-E-27994 Communication Techniques VIII-E-25674 Communication Theory IV-E-26487 Compacting VI-C-26392 Complexity IV-E-26438 Composite Beams V-B-25467, V-D-25327, V-D-25630. IX-C-6571 Composite Fuselage Frames V-D-25462 Composite Materials Acoustoelastic Constants VI-B-25397 Buckling V-D-25771 Corrosion Protection VI-A-26400 Cracking VI-C-26891 Cure Monitoring VI-C-26571 Deformation V-A-25400, V-A-28317, VI-B-25390. VI-C-26751 Design VI-C-28409 Dynamic Loading VI-B-26164 Elastic Properties IV-A-28606, VI-C-26751 Fracture Properties V-A-25345, VI-B-24583, VI-B-25390, VI-C-26891 Impact Tests V-A-28253, V-A-28307 Interfaces II-E-25229, IV-A-28606, VI-B-25390. VI-B-28480 Manufacturing VI-C-26882 Mechanical Properties VI-A-28509, VI-B-25397, VI-C-25202, VI-C-26439, VI-C-26751. VI-C-26882, VI-C-26891, VI-C-27373. VI-F-26246, VI F-26647 Microstructure VI-C-26751 Nondestructive Testing VI-B-25397 Penetration Mechanics VI-E-24102 Physical Properties IV-A-26463 Process Defects V-A-28222 Processing VI-C-25202 Superplastic Properties VI-C-26751 Thermal Wave Studies VI-B-24981 Composite Structures V-B-25467, V-D-28399 Compressibility V-B-26863 Compressible Turbulence IV-B-28716 Compression IV-A-25396 Compressive Deformation VI-B-28761 Compressive Loading V-C-26403 Compressive Strength VI-B-25390, VI-C-26068 Compressive Tests VII-B-27482 Compressors V-B-27627 Computation IV-C-27381 Computational Algebra IV-F-29031 Computer Aided Design IV-D-25264 Computer Architecture IV-B-28735, IV-E-23908. VIII-B-28325, VIII-B-28329 Computer Communication Protocols VIII-E-28506 Computer Generated Holograms 1-E-28416 Computer Networks VIII-E-27834, VIII-E-28467 Computer Programming IV-B-28034, IV-E-26779 Co-sputer Programs IV-E-28328, IV-E-28950 Computer Systems IV-E-27817 Computer Vision IV-C-27790 Computer Work Stations VIII-B-28329 Computerized Animation IV-E-26779, VII-A-26902 Computerized Microscopy IX-A-5933 Computenzed Modeling I-E-26264 Computerized Simulation I-B-28472, IV-B-28034. IV-C-26746, IV-E-25324, IV-E-28131, IV-F-23306, IV-F-28809, IV-F-29190, VII-A-26972, VII-A-27401 Computers IV-B-28192, IV-B-28320, IV-B-28377 Concentration IV-A-26272 Concrete VI-C-26891 Cones V.B. 25467 Connectionism IV-E-26779 Conservation Laws IV-A-28957 Contaminant Transport VII-A 28504

### X Indexes

Continuum Mechanics IV-A-28514, IV-F-28994, V-A-27538 Continuum Physics IV-A-28986 Control IV-C-28718 Control Systems IV-D-25264, IV-D-28511, IV-F-26930, V-D-25409, VIII-F-27865 Control Theory IV-D-27044, IV-D-27365, V-B-25467, V-D-27510, IX-A-6466 Controller Designs IV-D-28835 Convection IV-F-27817 Convergence (Mathematics) IV-F-26063, IV-F-26792, IX-A-5765 Convergence Theory IV-F-26932 Conversion Coatings VI-A-26400, VI-A-26667 Copolymers II-E-27808, II-E-28053, II-E-28373 Copper 1-B-26821, 11-A-27502, 1-B-26223 Copper Alloys VI-C-26439, VI-C-28067 Copper Colloids VI-D-28109 Copper Complexes II-B-28013, II-E-26072 Copper Ions VI-D-28109 Copper Metallizing VI-D-26287 Copper Substrates VI-D-26601, VI-D-27605 Corrosion VI-D-27794 Corrosion Inhibition VI-A-26449, VI-A-26678 Corrosion Protection VI-A-26400, VI-A-26667 Corrosion Resistance VI-A-25833 Corrugated Surfaces VII-D-27031 Corundum VI-C-26123 Cosine Transforms IV-F-27620 Couman'i Dyes II-B-27534 Crack Propagation VI-B-24583, VI-B-28549, VII-B-26031, VII-B-27482, VII-D-27031 Cracking (Fracturing) IV-B-28320, V-A-25345, V-A-26057, V-D-25462, VI-B-28549, VI-C-26891, VI-C-28368, VII-B-27482. VII-D-27031 Crash Worthiness V-D-25462 Cravfish III-D-25752 Creep Tests V-A-27315 Cryogeme Noise VIII-B-26151 Crystal Chemistry VI-F-26246 Crystal Defects I-D-25114, I-D-25906, IV-A-25428, V-A-26057, V-A-28222, VI-D-23577, VI-D-25251, VI-D-26729, VI-D-27764, IX-A-6280 Crystal Growth 1-B-27646, 1-D-26015, II-D-28371, IV-A-27557, VI-D-23577, VI-D-26287, VI-F-27810, VIII-A-26434, VIII-B-26923, VIII-F-24793, VIII-F-27865, VIII-G-28326 Crystal Structure fl-A-26748, IJ-E-26072, VI-D-27794 Crystallinity II-D-27603, VI-A-28369, VIII-C-26791 Crystallization VI-C-27373, VI-C-27472, IX-D-6011 Cubanes II-A-26748 Cure Monitoring VI-C-26571 Cvanates III-D-28479 Cyclic Phosphorus Compounds II-A-25435 Cyclocarboranes II-A-26426 Cylinders IV-A-25069, V-A-28283 Cytoskeletal Reagents III-F-26099 Damping V-A-26908, V-D-24362, V-D-28123 Data Analysis IV-C-26997, IV-C-27574, IV-C-27993 Data Communication 1-E-26088 Data Compression VIII-G-28326 Data Conversion VIII-E-28387 Data Dimension Reduction VIII-E-26460 Data Format Converters VIII-E-27076 Data Fusion I-E-28258, VIII-F-28099 Data Network Gateways VIII-E-25674

Data Networks VIII-E-27834 Data Processing VIII-E-27751 Data Structures IV-B-28071, IV-F-28408 Data Transter I-E-26264 Database Management Systems IV-E-27892 Databases VIII-C-25350, VIII-E-25674 Datagram Networks VIII-E-25674 Datagram Networks VIII-E-25674 Datagram Networks VIII-E-25674 Deciduous Forests VII-E-27019 Decision Theory IV-E-25662

Decision Trees IV-E-26487 Decomposition Reactions II-C-26238, II-C-26887. II-C-28298, II-C-29310, II-D-25523. II-D-26049, 1I-D-27887, II-D-28565. II-D-28700 Decontamination II-A-28469, II-B-25739, II-B-26284, HI-D-27916, IX-B-6308 Defect Complexes I-D-25906 Defect Engineering VI-D-27764 Defect Modes 1-D-26996 Deflagration V-C-25794 Deformation II-E-28314, IV-A-25396, IV-A-26218, V-A-25400, V-A-26057, V-A 26443. V-A-26908, V-A-28307, V-A-28317. V-D-25327, V-D-26934, VI-A-21545. VI-A-27037, VI-B-25390, VI-B-25424. VI-B-26164, VI-B-26167, VI-B-28761, VI-C-25373, VI-C-25526, VI-C-26439. VI-C-26751, VI-E-28272, VII-B-26260, VII-F-28344, 1X-C-6541 Degradation II-C-26887 Dehydrogenase III-C-24435 Delamination V-A-25400, V-A-28307, V-B-25467, VI-B-25193 Density Estimation IV-C-26108, IV-C-28309 IV-C-28722 Density Functions IV-C-26649 Deoxyribonucleic Acids III-B-25493, III-B 26576. III-C-25126, III-C-27890, III-C-27956. III-C-28011, III-C-28090, III-C-28457. HI-C-28669, HI-D-25702, HI-D-26232. III-D-27916, III-D-28479 Dephosphorylation II-B-25411 Depleted Uranium VI-B-26164 Depth Perception IV-E-25662 Deterministic Methods IX-A-6466 Detonations IV-A-26113, IV-A-28980, V-C-28310 Deuterium VI-A-21545 Diakoptic Theory VIII-C-28151 Diamond IX-A-6280, IX-B-6089 Diamond Films ( B-26959, I-B-27646, I-E-28356, VI-B-24981, VI-D-26601, VI-F-27810 Dielectric Cylinders VII-D-26384 Dielectric Materials II-A-26636, IV-A-25428, VIII-B-26666, 1X-F-5830 Dielectric Properties II-A-26636, II-E-27808. VII-D-26384, VIII-A-28674 Dielectric Resonators IV-A-26909 Dielectric Surfaces I-D-25464, VII-D-24713 Dielectric Waveguides VIII-C-25339, VIII-C-28483 Diesel Engines V-C-25190, V-C-25245, V-C-26769. V-C-28316, V-C-28427 Differential Algebraic Equations IV-B-27786 Differential Equations IV-A-24166, IV-A-25069. IV-A-25782, IV-A-25874, IV-A-26218. IV-A-27403, IV-A-27869, IV-A-28548. IV-A-28702, IV-A-28803, IV-B-26391. EV-B-26616, IV-B-28535, IV-B-28716. IV-C-29016, IV-D-26674, IV-F-27282. IV-F-27392, IV-F-28994, IV-F-29031. V-A-26443, 1X-A-5265 Differential Geometrical Methods 1V-C-28743 Differential Systems IX-A-6271 Diffraction 1-D-25464 Diffraction Gratings IV-A-25428 Diffusers V-B-27627 Diffusion II-D-26256, II-E-26072, III-B-26750, IV-A-25874, IV-A-26113, IV-A-26463. IV-A-27580, IV-F-27817, V-A-27315. VI-A-21545, VI-B-24981, VI-D-26729 VIII-A-23206, VIII-A-26147, VIII-A-26761. 1X-A-5653, IX-A-6280 Diffusion Barrier Coatings VI-B-28480 Diffusion Barriers VI-D-26287 Diffusion Flames V-C-26456, V-C-27455 Digital Elevation Maps VII-A-26902 Digital Elevation Models VII-A-27471 Digital Imaging V-C-28316 Digital Radio 1-E-27586

Digital Scanners 1-E-26695 Digital Signal Processing IV-F-27524, IV-F-27817, VIII-E-26118, VIII-G-27554, VIII-G-28326 Digital Systems IV-D-26736 Diode Laser Pumping I-B-28472 Diodes VIII-A-28347, VIII-C-26599, VIII-G-26213 Dioxetanes II-B-26115 Direction Finding VIII-E-26646, VIII-E-27899 Dislocations (Crystal Defects) V-A-26057, V-A-27409, VI-B-27163, VI-D-28553 Dispersions II-C-26296 Display Systems VIII-C-25557 Dissociative Ionization IX-B-6089 Distributed Databases VIII-E-25674 Distributed Memory Systems IV-B-28007 Distributed Systems IV-D-27365 Domain Decomposition IV-F-23306 Domain Wall - Defect Interactions VI-D-25251 Doping VIII-B-26051, VIII-B-27883, VIII-F-28729 Doppler Radar Imaging 1-E-26676 Dosimetry II-E-26072 Drag V-D-28123 Drive Shafts V-D-25462 Drops (Liquids) V-C-27018, V-C-28250, VII-A-28717, VII-G-26962, VII-G-28052, VII-G-28489 Drosophila melanogaster III-D-27468 Ductile Brittle Transformation VII-B-27482 Ductile Materials V-A-25459 Ductility II-E-25229, VI-C-27579 Durability V-A-27315 Dye Lasers I-B-26462, 1X-D-5884 Dyed Fabrics IX-B-6294 Dyes 1-B-28472, II-B-27534, II-B-27568, IX-B-6294, IX-D-5548 Dynamic Allocation IV-C-28715 Dynamic Loading V-A-25594, V-A-26908, V-C-26403, V-D-25771, VI-B-26164, VI-E-26169, VI-E-28575 Dynamic Logic IV-F-23306 Dynamic Response V-A-26908 Dynamic Scheduling IV-F-26063 Dynam , Simulation V-D-27075 Dynamic Stability V-D-25771 Dynamic Stall V-B-25461, V-B-25467, V-B-27752, V-B-27894, V-B-28159, V-D-28123 Dynamic Systems 1V-A-25782, IV-A-27403, IV-A-27580, IV-F-29031, IV-F-29190. V-D-25630, V-D-27510 Eddies IV-A-26113, V-C-27048, VII-F-26491 Edge Detection IV-D-26656 Edge Effects V-D-28399 Eigenvalues IV-A-25069, IV-B-28007, IV-B-28377 Elastic Brams IV-F-23306 Elastic Limits VI-E-26169 Elastic Properties IV-A-25428, IV-A-28606, IV-F-23306, V-A-25345, V-A-25459. V-A-27409, V-D-25327, V-D-28399, VI-B-26747, VI-B-26825 Elastic Stress Analysis V-A-25345 Elastic Systems IV-A-28957 Elastic Waves V-C-26720 Elastodynamics IV-B-28535 Elastomers II-E-25229, VI-C-27373 Elastoplastic Materials IV-A-28702 Electric Circuits VIII-B-26051, VIII-E-28297 Electric Contacts VI-D-26287 Electric Currents VI-B-26825 Electric Field Effects II-A-24411 Electric Fields 1-D-27458, 111-C-28361, VI-B-26825 Electric Switches 1-B-26257, 1-B-26821, VIII-E-27886 Electrical Contacts VIII-B-27883 Electrical Devices 1-D-25114 Electrical Impedance Tomography IV-A-26463 Electrical Properties 1-B-26821, 1-D-26827, 1-D-28336, H-C-27770, IV-A-25428, VI-D-26287, VI-D-26601, VI-D-27846, VI-D-28141. VII-B-26281, VIII-B-26686, VIII-B-26941 Electrical Pulse Propagation VIII-B-26760

Electrochemical Corrosion VI-A-26678 Electrochemistry II-A-24411, II-A-26426, II-C-26191, II-E-27054, VI-A-26449, VI-C-26728 Electrode Coatings 11-A-24411 Electrode Processes II-A-24411 Electrodeposition II-A-27502, IX-D-5686 Electrodes I-B-26257, II-C-26191 Electroless Plating VI-C-27579 Electroluminescence 1-D-28336 Electrolytes II-A-24411, VI-C-26728, IX-D-5686 Electromagnetic Measurements VIII-G-27554 Electromagnetic Radiation I-D-25374, VII-A-28717 Electromagnetic Scattering VII-D-26224, VII-D-26384. VII-D-26988, VII-D-27485, VII-D-27911, VII-D-29288, VIII-A-28674, VIII-C-25422, VIII-C-26128. VIII-C-27904. VIII-D-28070 Electromagnetic Spectrum VIII-G-28453 Electromagnetic Waves I-B-28499, IV-A-26909. VIII-A-28674 Electromechanical Systems IV-D-28835 Electron Beam Lithography IX-F-5940 Electron Beams 1-B-26257, 1-B-26821, 1-B-28396. I-E-27556, VIII-B-26666 Electron Bombardment I-B-26709 Electron Emission I-B-26223, I-B-26709, I-B-28569 Electron Gas VIII-B-26278 Electron Heating IX-F-5940 Electron Impact Ionization IX-B-6089 Electron Molecule Collisions V-C-24487 Electron Phonon Interactions 1-D-26682, 1-E-25349, VIII-B-26278, VIII-B-26755 Electron Scattering II-C-25605, VIII-A-28347 Electron Spectrum 1-B-26709 Electron Transfer IX-B-6294 Electron Transport VIII-A-28335, IX-F-5940 Electron Tunneling 1-D-25167 Electronic Ceramics VI-D-27548 Electronic Defects VI-D-27764 Electronic Devices I-B-28569, VIII-E-28297 Electronic Energy Levels VIII-A-26188 Electronic Imaging 1-E-24749 Electronic Materials I-B-28561 Electronic Properties 11-C-26191, 1X-F-5940 Electronic States II-D-28565, VIII-B-28406 Electronic Structure 1-D-25906. II-C-25222. II-C-26191, IX-A-6280 Electronic Transport 1-D-26015 Electrons 1-D-26682 Electrooptic Displays VIII-C-25557 Electrooptic Polymers 1-E-26088 Electrooptics VI D-26883, VI-D-27605 Electrophilic Imines II-E-27440 Electroplasticity VI-B-26825 Electropolymerization VI-A-26449 Electroporation III-C-28361 Electrospray Ion Sources II-A-25617 Elevation Maps VII-A-26902 Elliptic Control Problems IV-B-28535 Elliptic Equations IV-F-23306, IV-F-27392 Embrittlement VI-C-26617 Emission Spectra I-D-26442. IX-B-6294 Emulsions II-B-25411, II-B-25739, II-B-26914. 11-C-26296 Endoglucanase JII-C-25126 Energetic Materials II-A-28655, II-C-26887, 11-C-28767, 11-C-29310, 11-D-26106. H-D-27025, H-D-27887, H-D-28565, II-D-28700, V-C-26720, V-C-28310 Energetic Neutral Species 1-B-28561 Energy Conservation Algorithms VIII-C-25350 Energy Transfer I-B-27431, I-D-26211, I-E-27366, II-C-28767, II-D-26106, II-D-27025, V-C-27864 Engineering Design V-D-28350 Entropy IV-C-27574 Enzymatic Reactions II-A-25435 Enzymes III-B-26576, III-B-27314, III-C-24435, III-C-27488, III-C-28011, III-C-28043, III-D-26582, III-D-27468, III-D-27916

Eosin IX-D-5548 Epidemiology IV-A-25782 Epitaxial Films V1-D-28553 Epitaxial Growth 1-D-26015, 1-D-27458, VI-D-26287, VI-D-26601, VI-D-28612, VIII-A-26444, VIII-A-26761, VIII-A-27298, VIII-B-26484, VIII-B-26666, VIII-B-26686, VIII-F-26898. VIII-G-28326, IX-F-5940, IX-F-6291 Epoxidation II-E-26839 Epoxy Adhesives VI-A-25760 Epoxy Matrix Resins VI-C-26571 Epoxy Resins VI-A-25760 Equations of Motion IV-D-28511, V-D-25630 Escherichia coli III-B-25493, III-C-24435, III-C-25126, III-C-27956. III-D-27916 Esters II-B-25290, II-B-25411, II-B-28013, II-E-26839, IU-B-27314 Estimating IV-C-26394, IV-C-27862, IV-F-26792, JV-F-26813 Estimation Algebra IV-D-26674 Estimation Theory IV-D-26736 Etching I-B-28561 Ethanol II-C-26238 Ethernets VIII-E-25674 Ethers II-B-26914 Ethylenes I-B-25653, II-E-27440 Evaporation V-C-27018 Excimer Emission 1-B-26899 Excimers II-B-27568 Excitation I-B-25653, I-B-26223, I-B-26821, I-B-27508, I-D-25167, I-D-25374, I-D-26195, I-D-26442, I-D-26644, I-D-27458, I-E-26383. I-E-26974 I-E-27838. II-A-25586. II-C-25605, II-C-26238, II-C-29310, II-D-26106, II-D-27025, II-D-28565, HI-D-25476, V-C-24487, V-C-27864, V-D-25630, VII-E-26404, VII-G-26962, VIII-G-26213, IX-A-5653, IX-B-6294 Excitons 1-D-26644, 1-D-27458, 1-E-26974 Exhaust Plumes V-C-24487, V-C-27469, V-C-28912 Exoenzymes III-B-27314 Exothermic Mixtures VI-F-27364 Experimental Design IV-C-25819 Expert Systems IV-D-25264, IV-E-25514, IV-E-26487, VI-C-26882 Explosives II-A-25500, II-D-27025, V-C-28310, IX-C-6541 Extrusion III-A-27494 Fabrics IX-B-6294 Failure IV-C-27868, IV-C-27993, V-A-25400, VI-B-26164, VI-E-26169, VI-E-26173. VIII-B-28004 Far Infrared Lasers 1-B-27431, 1-B-27888 Far Infrared Radiation 1-D-26996 Fatigue (Mechanics) V-A-25594, VI-B-24583, VII-B-26031, V(I-D-27031 Fatty Acids III-F-27634 Fault Tolerance IV-D-25264, IV-E-27817 Feed Networks VIII-C-27304 Feedback VIII-C-26381 Feedback Control VIII-E-27834 Feedback Systems IV-D-27044 Fernites VI-C-26728, VI-D-27548 Ferritin Proteins 1-E-28313 Ferroelectric Crystals 1-E-26695, 1-E-26971 Ferroelectric Memories 1-D-26827, 1-E-26971 Ferromagnetic Materials I-D-28468 Ferromagnetic Resonance Spectra 1-D-25374 Ferromagnetism 1-D-25906 Feynman Integrals 1V-F-23306 Fiber Laminate Composites VI-E-24102 Fiber Ontics VIII-A-26147 Fiber Reinforced Composites Buckling V-D-25771 Impact Tests V-A-28253 Interfaces VI-B-28480 Fibers II-E-28314, VI-B-25193 Field Effect Transistors VIII-B-25015, VIII-B-26151,

VIII-B-26711, VIII-B-28004, VIII-B-28461, VIII-C-25045 Filament Wound Structures V-A-25400 Film Growth VIII-B-28345 Films II-C-27759 Filtering 1-E-27586, IV-C-28718, IV-D-26674, IV-F-26063, VIII-G-27554 Filters VIII-C-25045, VIII-E-25674, VIII-E-27076, IX-A-6271 Fine Structure VII-G-26962 Finite Difference Technique IV-B-28025 Finite Element Technique IV-B-26391, IV-B-26871, IV-B-28320, IV-B-28535, IV-B-28716, IV-B-28908, IV-F-23306, V-A-26443, V-A-28317, VIII-E-28297 Flame Propagation V-C-26456 Flame Structure V-C-27455 Flames V-C-25245, V-C-27864 Flash Photolysis IX-B-6294 Flaw Testing VI-B-28549 Flexible Gun Tubes V-D-25771 Flexible Systems V-D-28350 Flight Control Systems IV-D-25264 Flight Dynamics V-B-25467 Flood Forecasting VII-A-26902 Flow Fields V-B-25461, V-B-25623, V-B-27515, V-B-27558, V-B-27752, V-C-24487, V-C-27480 Flow Kinetics V-C-27864 Flow Separation V-B-26863, V-B-27558, V-B-27752, V-B-28252, V-B-28293, V-D-28651 Flow Velocities V-B-27894 Flow Visualization V-B-28215 Fluid Dynamics IV-A-28797, IV-B-26616, IV-B-28735, V-B-26631, V-B-27062, V-B-27558 V-B-27627, V-B-27752, V-B-28252 Fluid Flow IV-A-26113, V-C-27864, VII-A-28504 Fluid Mechanics IV-A-26113 Fluid Mixing IV-B-26616 horescence I-B-27508, II-E-28053, V-C-27864. VII-G-28487. IN D-5548 Fluorides Anharmonic Local Modes 1-E-26383 Bond Dissociation Energies 1-E-27366 Electrical Properties VIII-B-26666 Epitaxial Growth VIII-B-26666 Enitaxial Layers VIII-G-28453 Excitation 1-B-25653 Lasing Properties 1-B-28472 Optical Properties I-D-26442 Photoemission I-B-26223 Thin Films I-B-28561 Fluorine II-D-26106, VI-D-22459 Fluorobenzenes II-D-26106 Fluorocarbons IX-B-6089 Flux Measurements VII-F-27995 Foams 11-E-26072 Fohage VII-D-28219 Food III-A-27494 Food Processing III-A-27494, III-A-28691 Force Fields II-D-28555 Forests VII-F 27019 Form Perception IV-E-25662 Forsterite 1-E-27425 Forward Flight V-B-25467, V-B-25623, V-B-26631, V-B-27752, V-B-28002, V-D-26061, V-D-28123 Fourier Analysis IV-F-27620 Fractal Geometry VII-F-24881 Fractals V-A-25594 Fracture VI-C-26439 Fracture Properties IV-B-28320, V-A-25345, V-A-25400, VI-B-24583, VI-B-25193, VI-B-25390, VI-B-25424, VI-B-26167, VI-B-28549, VI-C-25373, VI-C-26891, VI-C-28067, VII-B-26260 Fracture Toughness V-A-26057, VI-B-24583 VI-B-25390, VI B 25424, VI-B-27163 VI-B-27407, VI-B-28480, VI-C-25202, VI-C-25526

## X Indexes

Free Boundary Problems IV-A-25069 Free Edge Effects V-A-25400 Free Electron Gas IV-A-24166 Free Electrons 1-D-25167 Free Energy VII-B-27316 Free Radicals II-C-28767, 11-E-27808, IX-B-6294 Freezing VII-B-27316 Frequency Conversion I-E-27418, I-E-28348 Frequency Division 1-B-27532 Frequency Shifts 1-B-27431, 1-B-27888 Freshwater Ice VII-B-26031 Fresnel Transforms 1-E-27586 Fresnel Zone Plates VIII-C-28516 Friction VI-A-26806 Friction Welding VI-C-25373 Frictional Torque V-C-26769 Frost Heaving VII-B-27316 Frozen Soils VII-B-26260 Fructose III-A-28691 Fruit Orchards VII-F-27019 Fuel Blends V-C-27417 Fuel Injection V-C-26797 Fuel Sprays V-C-26797, V-C-27018, V-C-28250, V-C-28427 Fullcrenes II-C-25222, 1X-B-6307 Fullerne VI-A-26400 Functional Analysis IV-D-27365 Functions (Mathematics) IV-F-28060 Fuselage Frames V-D-25462 Fuselages V-D-27300 Fusible Links VIII-A-28392 Gadolinium Alloys VI-C-28067 Gadolinium Iron Intermetallics VI-D-28146 Gallium Aluminum Arsenides I-D-27458, 1X-A-6280 Gallium Antimonides 1-D-25167 Gallium Arsenide Lasers VIII-A-26434 Gallium Arsenide Microcomputer Systems VIII-B-28325 Gallium Arsenide Substrates 1-D-25114 Gallium Arsenides Annealing VI-D-26287 Chemical Reactions VI-D-26287 Cleaning VIII-G-28326 Clusters If-C-25222 Crystal Defects VI-D-27764 Crystal Growth VIII-A-26434, VIII-F-24793, VIII-F-27865 Diffusion Mechanisms VI-D-26729 Electrical Properties I-B-26821, VIII-B-26760 Electron Emission 1-B-28569 Electronic Properties IX-A-6280, IX-F-5940 Epitaxial Growth VI-D-26287, VIII-A-26444, VIII-B-26666, VIII-B-26686, IX-F-6291 Epitaxial Lavers VIII-A-26761 Etching I-B-28561, VIII-G-28326 Excitation 1-D-26644 Heterojunctions I-B-26257. IX-F-5940 Interfaces II-C-25222 Ion Implantation IX-F-6170 Optical Properties I-D-28470 Optical Stark Efect I-E-26974 Optoelectronic Properties VIII-B-26666 Processing VIII-F-24793, VIII-F-27865 Properties II-A-26748 Quasi-Optical Properties 1-D-25487 Simulation VIII-B-26711 Superlattices 1-D-27458, VIII-A-26444 Surface Properties II-C-27770 Switching Properties 1-B-26821 Transport Properties VIII-A-28335 Gallium Nitrides II-A-26748 Gallium Phosphides 1 D-26211, II-A-26748 Games 1V-F-23306 Gamets 1-F-27425 VED-28141 Gas Dynamics IV A-26463, IV-A-28548 Gas Propelled Guns V-D-25771

Gas Turbines V/C-26456

Gate Feedback VIII-C-26381 Gate Leakage Currents VIII-B-26151 Gate Structures I-B-28569 Gateways VIII-E-25674 Gauss Machine VIII-E-26735 Gaussian Processes IV-C-26649 Gelation V-A-28222, VI-C-27373 Genes III-B-25493, III-B-26576, III-C-24931. III-C-25126, III-C-27890, III-D-27916 Genetics III-A-28691, III-D-27468, IV-C-27868 Geometric Methods IV-C-28743, IV-D-26674 Geometric Reasoning IV-D-26656 Geometry V-F-29031 Geophysical Events VII-E-26404 Geostatic Lateral Stresses VII-C-24381 Germanates J-E-25631, 1-E-27425 Germanides VIII-A-26896 Germanium VI-F-26246 Germanium Alloys VI-C-26439 Germanium Arsenide Selenides 1-D-26996, 1-E-26383 Germanium Oxides 1-E-27366 Germanium Selenides VIII-A-23206 Gibbsite VI-C-26123 Glass Substrates VI-D-27605 Glass Surfaces II-A-25586 Glasses Failure VI-E-26169 Internal Stresses 1-E-28313 Lasing Properties 1-B-28472 Mechanical Properties VI-C-28067 Microstructure VI-C-28067 Photorefractivity VI-D-28538 Relaxation 1-D-26996, 1-E-26383 Structural Changes IX-D-5548 Topological Transformations VIII A-23206 Glassy Polymers VI-B-25424 Glial Cells III-D-25752 Global Optimizing IV-F-26063 Glutamate Receptors III-C-28669, III-D-25702. IX-B-5973 Glyceraldehyde-3-Phosphate Dehydrogenase III-C-24435 Glycerols V-A-27315 Glycoproteins III-F-26767 Gold VI-D-26287 Gold Colloids IX-B-6307 Gold Ions VI-A-25833 Gold Oxides VI-A-26427 Gold Surfaces VII-D-29288, IX-F-5830 Gradient Flows IV-A-25782 Grain Boundaries VI-D-27794 Grain Boundary Engineering VI-D-27548 Grain Growth VI-C-25526 Granular Flow 1V-F-23306 Graph Algorithms IV-B-28143 Graphics VIII-C-27873 Gratings I-E-27882, VII-D-27485, VIII-A-28674 Gravel Streambeds 1X-E 6185 Gravity Waves VII-F-28664, VII-F-29188 Grid Oscillators VIII-C-26381 Ground to Air Imaging VIII-C-25350 Growth Models IV-F-23306 Guanidine Thiocyanate III-D-28479 Guided Waves VIII-C-25045 Gun Propellants V-C-26403 Gun Tubes V-D-25771 Gunn Diodes VIII-B-26051, VIII C-26651. VIII-C-26949 Gyroscopes 1-B-26566 Gyrotropy I-D-27780

Hail VII-E-26982 Halides 1-B-27431 Hall Effect VI-D-27764 Halobatterium halobium III-C-25731 Halogen Oxidizers II-A-28655 Hamiltonian Systems IV A-27641 Haptens IX-B-6308 Hardening V-A-28283, VI-B-26825 Hardness V1-A-26806, V1-A-27552 Harmonic Overtones V-D-28155 Hazardous Chemicals Destruction II-D-28371 Heart Cells III F-26099 Heat Generation III-A-28691 Heat Pulses II D-27025 Heat Release V-C-26769 Heat Resistance III-A-28022 Heat Transfer VI-C-26439 Heating V-A-25594, VII-G-28052 Helicopter Rotors V-D-28123 Helicopters V-B-25467, V-B-25623, V-B-26595, V-B-26631, V-B-27752, V-D-26061, V-D-27510 Helizymes III-C-27488 Hessenberg Systems IV-B-27786 Heterojunction Transistors VIII-A-26147 Heterojancijons J-B-26257, 1-D-25114, 1-D-26015, VIII-A-26444, VIII-A-26761, VIII-B-26484, VIII-F-26898, IX-F-5940 Heterometallic Clusters IX-B-6307 Heterostructures 1-D-26015, 1-D-26195, 1-D-26044, 1-D-26682, 1-E-28313, 1-E-28356, VIII-A-26188, VIII-A-26434, VIII-A-26896, VIII-B-26923. VIII-B-28461, VIII-F-28729 High Energy Lasers VII-G-28489 High Explosives II-D-27025 High Power Devices 1-B-26257 High Power Lasers 1-E-28348 High Power Switching I-B-26821 High Pressure V-C-27417, VI-A-24845, VI-E-28272 High Strength Steels VI-A-25199 High Temperature V A-25594, VI-A-24845 High Temperature Coatings VI-A-28509 High Temperature Superconductors 1-D-26195 High Temperature Water II-C-26887 Highway Driving 1V-D-25264 Hilbert Functions IV-F-23306 HIV-Latency Time IV-C-26649 Holograms 1-E-26264, 1-E-28416 Holographic Memories 1 F-36264 Holography VII-G-28359 Homeostasis III-D-25752 Housethes III-D-27916 Hover V-B-25467, V-B-27752, V-D-28123 Human Body Modeling IV-E-28131 Human Brain III-D-26232 Humidity V-A-27315 Hydraulies VII-A 27772, 1X E-6185 Hydrides II-B-25290 Hydroboration II-B-25290 Hydrocarbon Air Combustion V-C-27455, V-C-27565 Hydrocarbons III-B-26750, V-C-27417 Hydrodynamics IV-A-25069, IV-A-28797 IV-B 28799, IV-F-23306 Hydrogen 1-D-25906, 11-D-28700, VI-A-25199, IX-A-5653, IX-A-6280 Hydrogen Bonding II-A 25435, II-E-27445 Hydrogen Embrittlement VI-A-25833 Hydrogen Lasers J-E-26160 Hydrogen Pairing 1-D-25906 Hydrogen Trapping VI-A-21545 Hydrology VII-A-27471, VII-A-27772, VII-E-26982 Hydrolysis [1-B-28013, 11-E-26839, 111-D-27468, VI-A-26667, VI-C-27373 Hydrophobic Substances II-E 28053 Hydroquinone Oxidation II-A-27600 Hydrostatic Pressure VI-B-24583, VI-E 28272 Hydroxides VLA-26427 Hydroxyl 1-B-26959, 11-B-25411, 41-D-25523 Hydroxylammonium Nitrate V C-25794 Hygrothermal Environment V D-25462 Hyperbolic Equations IV-B-268"1 Hyperbolic Partial Differential Equations IV A-28702 Hypercubes IV A-24166 Hypersonic Flow V-B 26863, V/C-27469, V/C 27480 Hyperthermal Surface Scattering IX B-6089

Ice VII-B-26031, VII-B-27482, VII-B-28599, VII-D-27031

### Subject Index

Identification IV-C 28718 Ignition II-C-28767, II-D-28565, V-C 25190, V-C-26720, V-C-27018, V-C-27417, V-C-27565, V-C-28310, V-C-28316, 1X-C-6541 Image Compression VIII-G 28326 Image Formation IV-F-28476 Image Processing 1-E-24749, 1-E-26264, IV-E-25662, IV E-27567, IV-F-26811, IV-F-27620, V-C-28316, V-D-25409, V-D-27075, VII-D-24713, VIII-C-26128, VIII-E-26460, VIII-E-27076, VIII-E-27464, VIII-G-27554, VIII-G-28326, IX-A-5933 Image Restoration VIII-C-25557 Image Segmentation IV-C-27790 Imaging VI-B-24981, VIII-C-25350, VIII-C-27307 Imaging Arrays VIII C-26381 Imidization VI-C-26571 Immes II-E-26072, II-E-27440 Immunochemical Properties III-D-25702 Impact Ignition V-C-26720, IX-C-6541 Impact Ionization VIII-A-28347, VIII-B-26711 Impact Tests V-A-28253, V-A-28307, VI-B-26164, VI-C-26392, VI-C-26439, VI-C-26485, VI-E-26173. JX D-6148 Impedance IV-B-26616, VIII-C-26599, VIII-C-27307, VIII-C-27873 Impurities I-D-25167, 1-D-26195, VI-D-22459, VI-D-27846, VIII-E-28729, IX-A-6280 Indium J-D-25114, VIII-G-28326 Indium Aluminum Gallium Arsenides IX-F-6291 Indium Antimonides 1-E-26383, II-A-26748, IX-F-5940 Indium Ar. ...des 1 D-25167, 1-D-25487, 11-A-26748, VIII-A-26444, VIII-B-26484, VIII-B-27883 Indium Galhum Arsenide Phosphides VIII-A-26188. VIII-G-26213 Indium Galhum Arsenides VIII-A-26147. VIII-B-26151, VIII-B-26484, VIII-B-27883 Indium Phosphides I-D 28470, VIII-A-26147, VIII-A-26188, VIII-B-26151, IX-F-6291 Indium Vacancy Complexes VI-D-27846 Interens : IV-C-26993, IV-E-25514, IV-E-26487 Information Electronics VIII-G-28326 Information Processing IV-F-26063 Information Theory IV-E-26487 Intrared Absorption VIII-A 26896 Intrared Bandgap Superlattices VIII-A-26188 Intrared Cameras VI-B-24981 Infrared Detection IX-F-6563 Infrared Devices VIII-A-28335 Intrared Digital Imaging V-C 28316 Intrared Focal Plane Arrays 1-E-28356 Infrared Imaging Systems VIII-C-25557 Infrared Lasers 1-E-26383 Intrared Pulses I-E-25349 Infrared Radiation I-B-27888 Infrared Sources III F 26385 Infrared Spectroscopy II C 26238 Initial Value Problems IV-A-26463 Insecticides III-D-27468 Insulators T B-26223 Integral Equations IV A 27435 Integral Wavelet Transform IV-F-27524 Integrated Circuits J-E-26088, J-E-26676, VIII-A-26147, VIII-B-26923, VIII-B-28345, VIII-C-25045, VIII-C 25422, VIII-E-27886. VIII-E-28297, VIII-E-24793, VIII-E-26898, VIII-G-27554 Integrated Optics 1 E-28271 Integrated Optoelectronic Transmitters VIII-A-28351 Intelligent Control VIII F-24793, VIII F-27865 Intelligent Decision Strategies IV-D-26656 Inteiligent Polymers VI C 28900 Interactive Graphics VIII C 27873 Interfaces I-B-26223, I-D-25374, 1 D-26015, 1 D 26682, H C 25222, H-C-26191, H-C-27759, H-C 27770, H-F 25229. IV-A-25428, IV-A-27403, IV-A-28606. IV-A 28986, IV-B-26616, VI-A 25760.

VI-A-26667, VI-B-25390, VI-B-28480, VI-C-25373, VI-C-26579, VI-D-22459, VIII-A-26761, VIII-F-28729, 1X-A-6280, IX-B-6294 Interfacial Fracture V-A-25400 Interference I-E-25546. VIII-E-27028 Interferometry 1-B-26566 Intermetablics VI-C-26751, VI-C-28005 Internal Reflections 1-E-26971 Internal Stresses 1-E-28313 Interpolation Theory IV-D-27365 Interstitials VI-A-21545 Inverse Problems V-A-26057 lodide Ions II-B-26284 Jodides I-D-27780 Ion Beams VI-A-27552, VIII-A-26708, VIII-B-28345, 1X-F-6170 Ion Bombardment I-B-26257 Ion Channels III-D-25702, III-F-26099 Ion Clustering II-E-27054 Ion Conductance II-B-25739 Ion Implantation VI-A-25833, VI-A-26678, VI-A-27552, VIII-A-26708, VIII-B-26051, IX-F-6170 Ion Mobility Spectroscopy II-A-25500 Ion Pair Return II-B-26284 Ion Permeabilities III-D-25752 Ion Sources II-A-25617, II-A-28402, VI-A-25833 lor: Transport II-E-27054 Ionic Homeostasis 111-D-25752 Ionic Molecular Solids 1-D-27780 Ionization 1-B-26709, II-A-25500, II-D-28565, VIII-A-28347, VIII-B-26711, IX-A-5653, IX-8-6089 Ionized Beam Deposition VI-D-27605 Ionomers VI-B-25424 lons 1-B-26709, 1-E-25631, 11-A-27600, 11-B-26284 Iron III-B-26750, VI-A-21545 Iron Allovs VI-C-25373, VI-C-26617, VI-C-27579, VI-C-28067, VI-D-27794, VI-D-28146 Iron Borates J-D-26195 Iron Carbides VI-B-28761 Iron Chlorides II-A-27600 Iron Oxides IX-B-6305 Iteration IV-B-26391, IV-B-27786, IV-B-28735, IV-C-26394, IV-F-27817 Iterative Encoding Methods I-E-28416

Jacobi Matrices IV-F-27817 Joining VI-C-25373

Keto Esters II-B-25290 Ketones II-B-25290, IX-B-6294 Kinetic Energy Penetrators VI-E-28272 Kinetic Transport VIII-E-28297 Klystrons I-B-28569 Knowledge Acquisition IV-D-25264, IV-E-26487 Knowledge Based Systems IV-D-25264 Laminar Flames V-C-27455

Laminated Beams V-A-25400 Laminated Plates V-D-25630 Laminates V:A-25345, V-A-25400, V-A-26908, V-A-28253, V-A-28307, VI-A-28509, VI-B-25390, VI-B-28480, VI-C-26882, VI-E-24102, TX-C-6571 Lanthanides II-A-26145 Lanthanum Borides II-A-26145 Laser Beams V-C-28912, VII-G-28052 Laser Damage 1-D-26211 Laser Dves ILB-27534, ILB-27568, IX-D 5548 Liser Flash Photolysis IX-B-6294 Laser Frequency Shifts 1-B-27431 Laser Interactions VII-G-28489 Laser Materials 1 D-26442, 1 E-27425, 1X-D-5884 Laser Propagation LX F-6458 Laser Pumping I-B-28472 Laser Pyrolysis II-D-27603

Laser Radar I-E-28258, VII-B-26031, VII-E-28094, VIII-F-28099 Laser Radiation I-B-26223, I-E-27418, IX-F-6458 Laser Scintillation VII-E-27870 Laser Spallation VI-B-28480 Laser Speckle V-A-25594 Laser Spectroscopy 1-D-26644 Lasers 1-B-27431, 1-B-27888, 1-B-28472, 1-D-28336, I-E-25482, I-E-25546, I-E-25631, I-E-26160. I-E-26383, I-E-27366, I-E-27425, VIII-A-26434, VIII-A-28351, VIII-B-26923, VIII-F-28922, VIII-G-26213, IX-D-5884 Latex Particles II-E-26839 Latrotoxins III-D-26232 Lead Ions 1-D-26442, VI-D-28109 Lead Titanates VIII-C-26791 Leakage Current VIII-B-26151 Learning IV-E-26487 Least Squares Analysis IV-B-27786 Leaves (Vegetation) VII-D-24713 Lenses I-E-28356, VI-D-28538 Life Distribution IV-C-27993 Lift V-D-28123 Lifting Theory IV-D-27365 Ligands III-C-27890 Light (Visible Radiation) II-D-27025. IV-A-25428 Light Absorption 1-E-28271 Light Diffraction 1-D-25464 Light Emission VIII-B-26051 Light Scattering I-D-25464, I-D-26195, 1-E-25546, I-E-26971, VI-D-23577, VII-D-27031, VII-D-29288 Light Sources IV-A-28803 Light Transmission 1 D-25464, VII-A-28717 Limit Theorems IV-F-29053 Linear Programing IV-F-26932 Lipid Membranes II-B-25669, VI-C-28900 Lipid Monolayers II-B-25739 Lipids II-C-26296 Liposomes II-B-25669 Liquefaction VII-C-24381 Liquid Crystal Polymer Composites VI-F-26647 Liquid Crystal Polymers I-B-28472, VI-B-25193 Liquid Crystal Television I-E-28502 Liquid Crystals I-E-26695, I-E-26971, II-C-28319, VIII-G-26213, JX-D-6011 Liquid Jets V-C-26797 Liquid Propellants V-C-25794, IX-C-6541 Lithium Alloys VI-C-26439 Lithium Borates VI-D-23577 Lithium Fluorides I-E-26383 Lithium Niobates I-E-25408, I-E-27418 Lithium Zinc Ferrites VI-D-27548 Lithography VIII-B-26051, VIII-B-27578, VIII-G-26213, 1X-F-5940 Loam III-B-26750 Logic IV-E-26438, IV-F-23306, IV-F-29031 Logic Circuits VIII-A-26147 Logic Sampling IV-E-25324, IV-E-25514 Logistics IV-C-26993 Logistics Readiness IV-C-24557 Luminance VIII-F-28099 Luminescence 1-E-25631 Lung Surfactants III-F-27634 Machine Vision 1-E-28258, IV-C-27790, IV-E-26779, V-D-25409, VIII-E-27464 Machined Glasses J-E-28313 Magnesium II-B-25761 Magnesium Alloys VI-C-26439 Magnesium Ions HI-F-27634 Magnesium Oxide II-C-27775, VI-A-26806, VI-B-28549, VI-C-26123 Magnetic Anisotropy VI-D 28553 Magnetic Bonds II-D-28555 Magnetic Fields I-D-25374, I-D-26015, I-E-26383, VIII-G-26213 Magnetic Hardening VI-D 27794 Magnetic Materials VI D-28146

#### X Indexes

Magnetic Properties 1-D-25374, 1-D-25906. VI-D-25251, VI-D-27794, VI-D-28141. VIII-B-26941 Magnetic Resonance 1-E-27425 Magnetic Semiconductors VI-D-28141 Magnetic Thin Films VI-D-28553 Magnets VI-D-27794 Magnon Scattering 1-D-26195 Magnons 1-D-25167 Maleic Anhydrides II-E-25229 Mammalian Glial Cells III-D-25752 Manchester Fine Sand VII-B-26260 Manganese Alloys VI-C-26617 Manganese Ions 1-E-27425 Manufacturing JV-F-26063, VI-C-26882 Many Body Systems IV-A-27580 Mans VII-A-26902 Martensitic Steels VI-B-27163 Martensitic Transformations VI-C-26617 Mass Exchange VII-F-29188 Mass Spectroscopy II-A-25500, II-A-25617 Mass Transfer VII-A-28504 Mass Transport IX-E-6185 Materials Processing VIII-F-24793, VIII-F-27865 Mathematical Models I-B-26709, I-B-26821, 1-B-26959, 1-B-27508, 1-D-26211, 11-C-28767. II-D-26256, IV-A-25396, IV-A-25428, IV-A-25874, IV-A-26113, IV-A-26218. IV-A-27403, IV-B-28716, IV-B-28735, IV-B-28799 IV-C-26108 IV-C-26649 IV-C-26993, IV-C-27381, IV-C-27574, IV-C-27790, IV-C-28722, IV-C-28743, IV-D-26656, IV-E-25514, IV-F-23306, IV-F-26792, IV-F-29190. V-A-27409, V-A-28317, V-B-25467, V-B-27625, V-D-25771, VI-B-25193, VI-B-26164, VI-B-26167. VI-C-26591. VI-E-28575. VII-A-26902. VII-A-26972. VII-D-26224. VII-D-26480, VII-F-27995, VIII-C-26620, VIII-E-26697, VIII-E-27834 Matrices (Mathematics) IV-C-26394. IV-D-26736. IV-F-26945, IV-F-27817 Matrix Computations IV-F-23306 Maximum Likelihood IV-F-26792 Mechanical Alloying VI-C-28639 Mechanical Design V-D-26995 Mechanical Force Fields II-D-28555 Mechanical Properties II-E-28314, IV-A-28986. V-A-27538, V-C-26403, VI-A-26667, VI-A-26806, VI-A-28369, VI-A-28509, VI-B-25193, VI-B-25397, VI-B-25424, VI-B-26164, VI-B-26825, VI-B-28480, VI-C-25202, VI-C-26439, VI-C-26728, VI-C-26751, VI-C-26882, VI-C-26891, VI-C-27373, VI-C-27579, VI-C-28005. VI-C-28067, VI-C-28883, VI-D-26601, VI-E-28272, VI-F-26246, VI-F-26647, VII-F-28344 Mechanical Systems V-D-26934, V-D-26995, V-D-27075, V-D-27390 Mechanics IV-A-26463, IV-A-28548, IV-A-28986 Medical Reference Systems IV-E-25324, IV-E-25514 Melting VII-F-28344 Membrane Potential III-D-25752 Membrane Proteins III-C-25731 Membranes II-B-25669, II-E-25104, II-E-26072, HI-C-28090, HI-D-25702, HI-F-26099, IV-A-25874, IV-F-23306, VI-C-28900 Memories (Storage Devices) I-D-26827, I-E-26264. I-E-26971 Mercuric Ions III-D-26232 Mercury Cadmium Tellurides I-D-25114, VI-D-27846. VIII-A-28347 Mercury Zinc Tellurides IX-F-6563 Mesogens II-E-28314 Message Routing VIII-E-27834 Metabolism III-D-27468 Metal Activation II-B-28013 Metal Aikyis i B 20225

Metal Borides II-A-26145 Metal Carbonyl Clusters IX-B-6307 Metal Chelates 11-E-25104 Metal Films VIII-B-28345 Metal Ion Complexes II-A-28486 Metal Ion Implantation VI-A-25833 Metal Ions II-A-27600 Metal Laminates VI-A-28509 Metal Liquid Like Films II-C-27759 Metal Matrix Composites VI-A-26400, VI-B-25390, VI-B-25397 VI-C-26439, VI-C-26751 Metal Oxide Films VI-A-26427 Metal Oxide Particles II-C-27775 Metal Oxide Surfaces II-C-26238 Metal Surfaces I-B-26223, I-D-25464, II-C-26191, VII-D-24713, VII-D-27031, VII-D-29288 Metallacarboranes II-A-26426 Metallizing VI-D-26287 Metalloporphyrins 1X-B-6307 Metals VI-B-26825, VI-B-28480, VI-C-28639 Metaphosphoric Acid Derivatives II-C-26126 Meteorology VII-E-26982 Methacrylates III-C-28043, VI-C-28900 Methanococcus jannaschii III-C-28011 Methyl Halides I-B-27431 Methyl Radical NB-26959 Methylene Chloride II-D-28371 Micelles II-B-25411, II-B-25669, IEC-26296. ILE-28053 Microbial Cells III-C-28361 Microbial Degradation III-B-27314 Microbial Destruction III-A-28691 Microbial Spores III-A-28022 Microcomputer Systems VIII-B-28325 Microcracking V-D-25462 Microelectronic Devices 1-B-28569 Microelectronic Structures VIII-B-28345 Microelectronics VIII-G-28326 Microemulsions II-B-25411, II-B-25739, II-B-26914. 11-C-26296 Microlenses 1-E-28356 Micromechanics IV-A-26463 Microorganisms III-B-26750, III D-25476. HI-D-25663 Microphase Separation II-E-26441 Microscopes 1-E-28313 Microscopy 1-E-27594 Microstrip Antennas VIII-C-25045, VIII-C-26620, VIII-C-28151 Microstrip Circuits VIII-C-25422, VIII-C-26651 Microstrip Couplers VIII-C 26949 Microstrip Devices VIII-C-26651 Microstrip Patches VIII-C-26620, VIII-C-27304, VIII-C-27873, VIII-C-27904 Microstructure II-A-25586, IV-F-23306, V-A-28283, VI-A-26806, VI-A-28509, VI-B-25390, VI-B-26167, VI-B 26825, VI-B-27407 VI-B-28761, VI-C 25373, VI-C-25526, VI-C-26123, VI-C-26392, VI-C 26439, VI-C-26728, VI-C-26751, VI-C-2\*472, VEC-27579, VEC 28005, VEC-28900, V1-D-27548, V1-D-27794, V1-F-27810, VII-F-28344, VIII-B-26278, VIII-B-26941 Microwave Circuits VIII-C-26599 Microwave Devices VIII-C-26620 Microwave Generators I-B-26257 Microwave Imaging VII-D 24713, VIII-C 25350 Microwave Integrated Circuits VIII-C 25045. VIII-C-25422 Microwave Sources VIII-C 26949 Microwaves 1-D-28652, 1-E-28271, VII-D 26384. Millimeter Wave Antennas VIII C-27304. VIII-C 28483, VIII-G-27554 Millimeter Wave Circuits VIII-C 26949 Millimeter Wave Devices VIII-C-25045, VIII C 25339.

VIII-C-26381. VIII-C-26620. VIII-C-26651 Millimeter Wave Imaging VIII-C-26381. VIII-C-27307 Millimeter Wave Power Combining VIII-C-28339 Millimeter Wave Radar VII-D-25730. VII-D-26224

Millimeter Wave Sources VIII-C-26949 Millimeter Waves 1-B-27431, 1-B-28396, 1-D 28652, VIED-24713, VIED-25730, VIED-26224, VII-D-26384 Mineralization III-A-28022, IX-B-6305 Minerals VLE-26246 Mixers VIII-E-27886 Mixing V-C-28250 Mixtures V-C-27417, VI-F-27364 Mobile Radio Systems VIII-E-27076 Mobile Robots 1-E-28258 Modal Logics IV-F-23306 Modulation 1-E-25482, 1-E-27556 Modulation Transfer Functions VIII-C-25557 Modulators 1-E-26088, 1-E-28271, VIII-B-26760, IX-F-6291 Moisure Fields VILE-78094 Moisture Sensors III-A-27494 Molecular Adsorption I-B 26223 Molecular Beam Epitaxy 1-D-25114, VIII-A-27298. IX-F-5940 Molecular Biology III-B-26576, IX-B-5973 Molecular Bonds II-D-28555 Molecular Collisions I-B-27888 Molecular Crystals 1-E-25631 Molecular Decomposition II-D-26049 Molecular Dissociation I-B-27508 Molecular Dynamics II-D-26106, II-D-27025, II-D-28555, VI-A-27037 Molecular Excitation II-C-29310 Molecular Films II-C-27770 Molecular Free Radicals II-C-28767 Molecular Genetics 1X-B-5973 Molecular Hybridization III-D-28479 Molecular Ionization 1X-B-6089 Molecular Ions I-E-25631 Molecular Motion II-D-28555 Molecular Properties VI-A-25760 Molecular Solids 1-D-27780 Molecular Structure II-D-27887, II-E-26072. II-E-28314, II-E-28711, VI-C-28900, VI-F-26647 Molecular Surfaces II-A-25586 Molecular Transport III-C-28361 Molecular Vapor Synthesis II-C-27775 Molecular Vibration 1-B-25653 Molecular Weight II-E-28053, II-E-28631 Molecules I-B 25653, II-C-25605 Molybdates J-E-25631 Molybdenum VI-C-27579 Molybdenum Alloys VI-C 25373 Monte Carlo Simulations IV F 29053 Motion Perception IV-E-25662 Motion Planning IV-E-27567 Mountain Terrain VII-A-27471 Muck HLB: 26750 Multibody Systems V-D-26934 Multidimensional Signals IV-C 26144 Multigrid Optimization IX-A-5933 Multihop Radio Networks VIII-E 26823 Multiphase Flows IV A-28980 Multiphase Systems VII A 28504 Multiple Quantum Well Structures VIII-B-28594. IX-E-6170, EX-E-6291 Multiprocessors IV-B-26391, IV-B-28192, IV-F-27817. Multivariate Analysis IV-C-26394 Multivariate Density Estimation IV C 26108 Multivariate Spline Approximation IV-B-27690. Musca domestica III-D-27916 Muscle III D-26582 Mustard II B-25739, II-B-26284, II-B-26914, IX B-6308

Nanostructures 14: 28356, VIII B 27578 Naphthalenes II D-27025, TEE 28053, IX D 5548 Natural Language Processing IV E 26779 Nature IX D-6579 Neodymuum Alloys VI D-27794, VI D 28146 Nerve Agenty II B 25739

## Subject Index

Nerve Cells III-C-27890 Nervous Systems III-D 25752, IX-B-5973. Network Analyses IV-C-26993 Network Architecture IV-E-25324 Network Flow IV-B-28143 Network Performance VIII-E-26823 Network Reliability IV-C 25706 Network Topology 1-D-26996 Networks 1-E-26695, VIII-E-25674, VIII-E-27834. VIII-E-27994 Neural Networks J-E-26676, IV-D-25264, IV-E-25324, IV-E-25662, IV-E-26487, IV-F-28060, VII-D-24713, VIII-G-28326 Neuronal Receptor Systems III-C-28669 Neurons J.E. 26676, III-D-25702, III-D-26582 Neurotoxins III-D-27468 Neurotransmitters II-A-25500 Nickel II-C-26238, VI A-21545, VI-C-28368 Nickel Alloys VI-C 26617, VI-C-27579, VI-C-28639 Nickel Compounds II-A-26426 Nickel Ions VI-A-20667 Nickel Oxides J-D-26195, II-C-26238, IX-B-6305 Niobates 1-E-25408, 1-E-26971, 1-E-27273, 1-E-27418, L-E-27882 Niobium Alloys VI-C-28005 Niobium Hydrides 1-D-25906 Nitramines II-C-24413, II-C-28767, II-D-27603, II-D-28103, II-D-28565, V-C-25794 Nitrates 1-D-27780, IEC-26887, V-C-25794, VI-A-26400 Netration 11-B-25761 Nurene Complexes II-A-28353 Nume Oxide II-C-26238, V-C-27864 Nitrides II-A-26145, II-A 26748, II-A-28353, VI-A-24845, VI-A-26427, VI-A-27552, VI-B-26673, VI-C-26068, VI-D-27794, VI-D-28146, VI-E-26169, VI-E-26173. Nitro Compounds IX-B-6294 Nitroalkanes II-D-26049, IX B-6249 Nitroanilines VI-D-27605 Nitrobenzenes II-D-26049 Nitroed anes II-B-25761, II-D-26049 Nitroethylen, 5 II-B-25761 Nitrogen I-D-28362, V-C-27864, VI-C-26439, VED.27794 VILE-26404 Nitrogen Alloys VI-D-26287 Nitroven Compounds II-C-26822 Nitrogen Ions VI-A-26678 Nitrogenation VI-D-28146 Nitromethanes II-D-26049 Nitrotoluenes II-D-27505 Noble Gases 1-B-26899 Noise (Electronic) VIII-G-28326 Noise Properties VIII-C-26599 Noisy Systems IV-D-25859 Nondestructive Testing V-A-25345, VI-A-25199, VI-B-24981, VI-B-25397, VI-C-26891, VII-C-24381 Nonlinear Analysis IV-A-26113, IV-A-27641, IV-F-28994 Nonlinear Beam Coupling 1-E-25482 Nonlinear Beam Theory V-B-25461 Nonlinear Continuum Mechanics IV A 28514 Nonlinear Controller Designs IV-D-28835 Nonlinear Differential Equations IV-A-27869. IV A-28548 Nonlinear Equations IV-A-27869, IV-F 23306 Nonlinear Filtering IV D-26674, IX-A-6271 Nonlinear Elexible Systems V D-28350 Nonlinear Hyperbolic Equations IV-B-26871 Nonlinear Mechanical Force Fields II-D-28555 Nonlinear Moments IV F-23306 Nonlinear Numerical Methods IV B-28916 Nonlinear Optical Frequency Conversion 1/E-28348 Nonlinear Optical Materials 1 B 28472, 14:-25408, V1-D:23577 - V1 D:27605 Nonlinear Optical Properties 1-E-26383, 41 E-28314, IX B 6307 IX D 5884

Nonlinear Optical Scattering VII G-26962

Nonlinear Optics 1-D-26644, 1-E-25546, 1-E-27418, 1-E-28356, IV-A-28803, VII-G-26962 Nonlinear Optimization 1V-B-28701 Nonlinear Partial Differential Equations IV-A 25069. IV-A-26218, IV-A-27403, IV-A-28702. IV-A-28803, IV-B-28535, IV-B-28716, IV-F-27282, IV-F-27392, IV-F-28994, V-A-26443 Nonlinear Programing 1V-F-26932 Nonlinear Systems IV-D-27365, IV-E-25662, IX-A-6271 Nonlinear Vibration V-D-25630 Nonlinear Waves IV:A-25782, IV:A-28548, IV-B-26616, IV-B-28799, VII-G-28489 Nonparametric Statistics IV-C-25836 Nozzles V-B-27515 Nucleic Acids III-D-28479 Nucleophilic Decontamination Agents II-B-26284 Nucleophilic Displacement Reactions II A 25435 Nucleonde Sequence iII-C-27956 Numerical Analysis IV-A-25874 IV-B-28535 IV-B-28716, IV-B-28916, IV-F-29031, V.D. 78155 Numerical Iteration IV-B-27786 Numerical Methods IV-A-25874 Numerical Optimization 1X A-5265 Numerical Simulation IV-B-28799, VII-D-24713, VII-D-29288 Nylon 6 11-E-25229 Object Oriented Image Segmentation IV-C 27790 Object Recognition IV-D-26656, IV-E 25662 Odorant Recognition III-F-26767 Olfactomedin III-F-26767 Olfactory Reception III-F-26767, III-F-27634 Optical Amphifiers VIII-G-26213 Optical Beams I-E-25482, VII-D-27031 Optical Bistability 1-E-28356 Optical Computing 1-E-26676 Optical Disks 1-E-26676 Optical Fibers I-E 25482 Optical Fields 1-B-27766 Optical Frequency Conversion 1-E-28348 Optical Frequency Division 1-B-27532 Optical Gratings 1-E-27882 Optical Interconnects I-E-26695, I-E-28416. VIII-G-28326. IX-E-6291 Optical Interference T-E-25546 Optical Limiting I-E 27838 Optical Enhagesphy VIII B-26051 Optical Logic Circuits VIII-A-2614\* Optical Materials 1-B-28472, 1-E 25408, 1-E-28356, VI-D-23577. VI-D-27605 Optical Microscopy 1-E-27591 Optical Modulators I-E 26088, IX E-6291 Optical Parametric Oscillators I B-27532 Optical Phonons VIII-B-26755 Optical Processing 1-E-24749 Optical Properties I-B 28472 | 1 D 25167 | 1 D 26442 1-D-26644, 1-D-28336, 1-D-28470, 1-E-26383, T-E-28356. If-D-27603. II-E-28314. IV: A-25428 VI-D-28141, VII-A-28717, VIII A 26188 VIII-A-27298, VIII-B-26686, IX B-6307 IX-D-5884, 1X-F-6170 Optical Pulses T/D-28470, 1/E-25349 Optical Pumping 1-B-26462, 1-D-26996 Optical Readers 1-E 26676 Optical Remote Sensing VII E-28102 Optical Resonance 1-E-27425 Optical Scattering VII-D-24713, VII G-26962 Optical Second Harmonic Generation II C 26191 Optical Sensing VII-D-24713 Optical Signal Processing 1-E-27586 Optical Sources LE-25408 Optical Storage VIII-G-27554 Optical Switches 1/E-26695, 1/E 28356 Optical Switching IV-A 28803, VIII-G-26213 Optical Waveguides VIII-B 26760, VIII-G-26213 1X-F-6170, 1X-F-6291, 1X-F-6563

Optical to Electronic Data Transfer 1-E-26264 Onlics 1-B-26566 Optimal Coding IV/C 28722 Optimal Control IV-D-27044, IV-D-28511 Optimizing IV-B-28143, IV-B-28701, IV-C-28715, IV-D-27365, IV-F-26063, IV-F-26932, IV-F-28809, IV-F-29190 Optoelectronic Devices 1/D-26015, VIII-A-26434 VIII-A-28351, VIII-B-26666, VIII-B-26760, IX-F-6291 Optoelectronic Integrated Circuits VIII-A-26147, VIII-B-26923. VIII-F-26898 Optoelectronic Systems 1-E-25482 Optoelectronics 1-E-26676, 1-E-28271, VIII-A-27298, VIII-B-26923 Orchards VILF-27019 Order Statistics IV-C-25836 Organic Clusters IX-B-6089 Organic Compounds II-D-27505, III-B-26750 Organic Dyes 1-B-28472, 1X-D-5548 Organic Reagents II-B-25669 Organic Sulfides II-B-25411 Organic Waste II-D-28371 Organometallic Compounds II-A-28402 Organophosphates III-D-27468, III-D-27916. IX-B-6305 Organophosphonates II-C-26238 Organophosphorus Compounds JI A-25500, IEC-27775. III-D-27468 Oscillating Airfoils V-B-26631, V-B-27752, V-B-27894 V-B-28159 Oscillations IV-A-26272, IV-A-26463 Oscillators J-B-27532, 1-D-25487, 1-D-28362, VIII-B-26051, VIII-C-25045, VIII-C-26381, VIII-C-26599, VIII-C 26620, VIII-C-26949, VIII-E-27886 Oxidation 1-B-28561, II-A-27600, II-A-28655, II-B-25411, II-B-26914, II-C-26238, II-D-25523, II-D-27505, II-D-28371, II-E-26839, II-E-27445, V-C-27417, V-C-27455, V-C-28250, V1-D-22459, V1-D-26287 Ovidative Addition Reactions II A-25435 Oxide Coatings VI-A-21545 Oxide Films VI A-21545, VI-A-26427, IX-B-6305 Oxide Membranes II-E-25104 Oxide Particles II-C-27775 Oxide Reinforced Composites VI-C-26751 Oxide Substrates VI D-26601, VI-D-27605 Oxide Vapor Reagents II-C-27775 Oxides Ballistic Properties VI-C-26021 Doping VI-D-22459 Elastic Properties VI-B-20747 Etching 1-B-28561 Excitation 1-B-25653 Fracture Properties VI-B-24583, VI-B-28549, VI-C 25526 Hardness VI-C 25526 Lasing Properties 1-B-28472 Microstructure VI A 26806 Phase Stability VI-C-25526 Photoemassion 1-B-26223 Shock Tube Studies V-C 27864 Sintering VEC 25526 / VEC 26123 Strength VI-B-24583 Stress Relaxation VI-D-22459 Superplastic Flow VI-B-26747 Superplastic Properties VI C-25526 Surface Decontamination IX B-6305 Tensile Tesis VI-B-28549 Oxidizers II-A-28655 Oxygen 3 (126238, VI-C-26439, VI-D-27794, 1X-B-6294 Oxygen Consumption III-D-25752 Oxygen Permselective Membranes II-E-25104 Oxygenases III-B-25493 Oxynitride Films VI-A-26427 Oxyphosphoranes II-A-25435

#### X Indexes

Packet Radio Networks VIII-F-25674 Pair Correlation VII-G 28359 Palladium II-C-26238, II-C-26822, VI-D-26287 Palladium Hydrides 1-D-25906 Palladium Ions VI-A-25833 Palladium Plating VI-A-21545 Parabolic Equations IV-F-23306 Parallel Algorithms IV-F-26945, IV-F-28408 Parallel Processing 1V-E-26779, 1V-F-26932, IV-F-27282, IV-F-28060, VIII-B-28329, VIII-G-27554 Parallel Processors IV-B-26616, IV-B-28007, IV-B-28320, IV-B-28377, IV-B-28735, IV-F-27817 Parallel Programing IV-B-28908 Parallel Systems IV-F-27392 Parallelism Detection 1V-B-28192 Paralysis III-D-27468 Partial Differential Equations IV-A-25069, IV-A-26218, IV-A 27403, IV-A 28702, IV-A-28803, IV-B-26391, IV-B-26616, IV-B-28535, IV-B-28716, IV-C-29016, IV-D-26674, IV-F-27282, IV-F-27392, IV-F-28994, IV E 29031, V-A-26443 Particle Dynamics IX-E-6185 Particle Reinforced Composites VI-C-25202. VI-C-26439 VI-C-26751 Particle Sizing I-E-24749 Particle Suspensions VII-G-28359 Passivation Coatings 1-B-27646 Passive Advection IV-A-26463 Passive Films VI-A-26400 Passive Remote Sensing VIII-E-28985 Pathogen Detection III-D-28479 Pattern Analysis IV D-26656 Pattern Recognition 1-E-28502, IV-E-26487 Pebble Transport IX-E-6185 Pendulums V-D-27300 Penetration IV-B-28320 V1-B-26164 Penetration Mechanics V-A-26443, V-A-28307, VLF. 24102 Penetrometers VII-C-24381 Penicillium funiculosum III-B-27314 Pentane V-C-27417 Peptides II-A-25500 Pertoration V-A-28307 Periodic Systems V-D-26061 Periodic Waves VII-A-26972 Permatrost VII-B-26281 Permanent Magnet Materials VI-D-28146 Permittivity 1-E-26088, 11-A-26636, 11-E-278-98 Peroxo Metal Ion Complexes II-A-28486 Perturbation Theory IV-A-25874, IV-E-23306 IV-F-27620 Pervienes IX D-5884 Pesticides II-A-25500, III-D-27468 Petroleum Patch VI-C-265+1 Pharmacology IX-B-5973 Phase Modulation 1-E-28502 VIII-E-27994 Phase Reversal Zone Plate Antennas VIII-C-28516 Phase Shift Keyed Waveforms VIII-E-27754 Phase Shifters VIII-C-26381 Phase Transformations 1-D-25374, 1-D-27780, II-B-25181, II-D-28371, IV-A 27403, V-A-27538, VIII-G-26213 Phased Array Lasers VIII-B-26923 Phased Arrays VIII-C-25350 VIII-C-26599, VIII C-27304 Phenanthrenes III-B-26750, IX-D-5548 Phonon Assisted Sumulated Emission VIII-D-28970 Phonon Emission VIII-D-28070 Phonon Scattering VIII-B-26711, VIII-F-28187 Phonons 1-D-25167, 1-D-26195, 1-D-26211, II-D-27025, VIII-A-26188, VIII-G-26213 Phosgene II-C-26822 Phosphatases II-B-26115 Phosphate Esters II-B-28013 Phosphates II-B-25411. IEB-25669, IEE 26072.

II-E-26839, III-B-26750, III-D-27468 III-D-27916, VI-A-26400, VI-A-26667 Phosphazenes II-E-28631, II E-28714 Phosphides 1-D-26211, 1-D-28470, II-A-26748. VIII-A-26188. VIII-B-26151, VIII-G-26213. IX-E-6291 Phosphinates II-B-25411 Phosphoesterase II-B-28013 Phosphonates II-C-26238, IX-B-6305 Phosphoranes II-A-25435 Phosphoranimines II-E-28631 Phosphorescence 1X-D-5548 Phosphorescent Lasers IX-D-5548 Phosphorus II-A-25435, VI-D-28612 Phosphorus Chemistry II-C-26126 Phosphorus Compounds II-A-25435, II-C-26238, II-C-26822 Phosphorylation H-C-26126 Phosphotriesterases 111-D-27468 Photoabsorption 1-B-26709 \*--tonetive Materials 1X-D-5548 Photoactive Molecules II-A-25586 Photocatalysis II-C-28298 Photochemistry 1-B-26223, II-A-28469, II-B-27534. II-C-26238. III-C-27956 Photodecomposition II-C-29310 Photodegradation II-B-27534 Photodetectors VIII-B-26760 Photodiodes 1-D-25114 VHI-B-26923 Photodissociation 1-B-27508, 11-C-26238, 11-C-26822 Photoelasticity V-A-27409 Photoemission 1-B-26223, VIII-A-26761, VIII-G-28453 Photoionization 1-B-26709 Photoluminescence I-D-27458, I-D-28336, VI-D-27764. VIII-D-28070 Photolysis II-D-26049, TX-B-6294 Photon Absorption 11-D-28565 Photon Scanning Tunneling Microscope 1/E/28313 Photonic Materials VI-D-28109 Photonics IX-F-6563 Photooxidation TX-B-6305 Photophysics II-B-27534 Photoredox Chemistry II-A-28469 Photorefractive Crystals 1/E-27273 Photorefractive Materials I-E-27882 Photorefractivity VI-D-28538 Photostability IX-D-5884 Phototransistors VIII-A-26147 Physical Mathematics IV-A-24166 Physical Optics T-E-28356 Piezoelectromagnetism IV-A-26909 Pinball Algorithm IV-B-28320 Pipelined Recursive Filters VIII-E-27076 Piperidine 1X-B-6089 Pitching Airfoils V-D-28651 Pitting Corrosion VI-A-26678 Planar Networks IV-C-25706 Planetary Boundary Layer VII-F-27995, VII-F-28664 Planetary Surfaces 1-E-26676 Plant Foods 111-A-28691 Plants (Vegetation) IX-D-6579 Plasma Instabilities 1-D-28652 Plasma Ion Implantation VI-A-26678 Plasma Polymer Thin Films II-E-25104 Plasma Sprayed Coatings VI-B-24981 Plasmas (Physics) 1-D-26682 Plasmid Stabilization III-C-25126 Plasmons 1-D-25167, 1-D-26682 Plastic Deformation V-A-25400, V-A-25594. V-A-26057, V-A-27409, V-D-24362, VI-8-26164, VI C-25373 Plastic Shear IV-A-26218 Plating Stiffeners V-B-25461 Platinum II-C-26822 Platinum Electrodes II-A-27502 Platinum Ions VI-A-25833 Point Defects VI-D-26729 Polarimetric Measurements VII-D-27919 Polarization 1-E-26971, 11-C-26822

Polarization Reversal EE 26971 Polarons 1-D-2516 Pollutants VII-A-26972 Polyacetylenes (X-B-6307 Polyamic Acuts VI C 26571 Polyamides II-E-25229 Polyarylene Ethers VI C 28883 Polybenzoxazoles/VI-C/28883 Polybutadienes VI-C 26579 Polycarbonates VI-A-27037 Polyclectrolytes II A(244)11. If E(27054 Polyesters III-B-27314 Polyethylene Terephthalates VI B 25193 Polygermanosiloxane/Coatings/VI-A-26667 Polyimide Resins VI-A-25760, VI-A 26667 Polyimides VI-C-28883 Polylysines HI-C-27890 Polymer Addatives II-E-28153 Polymer Blends II-E-25229, II-E-27808, VI-C-26579 Polymer Fibers VI-B-25193 Polymer Films II-A-25586, II-E-27808, VI-A-26449. VI-D-26883 Polymer Gels VI-C-27373 Polymer Glasses VI-A-27037 Polymer Interfaces II-E-25229 Polymer Matrix Composites V-A-28253 Polymer Membranes II-E-25104 Polymer Networks VI-F-26647 Polymer Solutions II-E-28153 Polymer Surfaces I-E-26971 Polymer Synthesis II-E-28373, VI-C-28900 Polymeric Coatings VI-A-26667 Polymerization II-E-25286. II-E-26441, II-E 27440. II-E-27808, II-E-28631, V-A-28222 VI-A-26449, VI-C-28900, VI-D-27605 Polymers Aging VI-A-27037 Biocatalytic Processing III-C-28043 Crystallinity VI-A-28369 Crystallization IX-D-6011 Curing V A-28222 Deformation VI-A-27037 Dielectric Properties II-E-27808 Diffusion II-E-26072 Ductility II-E-25229 Effects on Laser Dyes II-B-27534 Electrical Properties VI-A-26449 Fracture Toughness VI-B-25424 Hierarchical Structure VI-B-25193, IX-D-6011 Mechanical Properties II-E-28314, VI-A-28369 Miscibilities II-E-25229 Molecular Dynamics VI-A-27037 Molecular Structure II-E-28314, B F 28711 Processing VI-A-28369 Spectra IX-B-6294 Synthesis II-E-25286, II-E-28711 Tensile Properties VI-A-27037 Thermal Properties II-E-28314 Polymethylthiophene Films V1-A-26449 Polynitroethanes II-B-25761 Polyoxometalates II-A-28469 Polypepudes VI-C 28900 Polyphenylene Sulfides VI-A-26667 Polyphosphazenes II-E-25286, II-E-27054, II-E-28631, H-E-28711 Polypivalolactones II-E-26441 Polysiloxanes II-A-24413, II-E-27054, VI-C-27373 Polystyrene Ionomers VI-B-25424 Polystyrenes II-B-25739, II-E-25229, II-E-26072, ILE-28053, VI-C-26579 Polytitanosiloxane Coatings VI-A-26667 Polytopes IV-F-23306 Polyurethanes II-E-28314 Porphyrins II-E-25104 Positron Annihilation VI-A-21545, VI-F-26647 Potassium Iodides 1-D-26996 Potassium Ions HI-D-25752 Potassium Niobates I-E 27882 Potassium Nitrates 1-D-27780

### Subject Index

Potassium Selenates 1-D-27780 Potassium Tantalum Niobates 1-E-27273 Potassium Vapor I-B-26899 Powder Metallurgy VI-C-25373, VI-C-27579, VLC 28639 Power Combining VIII-C-26599, VIII-C-26651, VIIEC-28339 Praseodymium Alloys VI-D-28146 Precipitation (Chemistry) II-D-28371 Precipitation (Meteorology) VII-A-27471, VII-E-26982 Predator Prey Systems IV-F-23306 Pressure Measurement V-B-28215 Pressure Regulation III-C-28011 Primers VI-A-25760 Printed Circuits VIII-C-27904 Printed Microstrip Circuits VIII-C-25422 Probability IV-C-26993, IV-C-27868, IV-C-28715, JV-C-28982, JV-E-25514, JV-E-26487, IV-F-28809 Projectile Impact VI-C-26485, VI-E-24102 Projectiles V-B-28252 V-D-25771 Propane V-C-27417 Propellant Compression V-C-26403 Propellants II-C-24413, II-D-27603, II-D-28103, II-D-28565, V-C-25794, V-C-26403, V-C-26720, V-C-28310, V-C-28912, IX-C-6541 Properties VI-C-26439 Propyliodide IX-B-6089 Protease III-C-28011 Protein Complexes 1X-B-5973 Proteins 1-E-28313, III-C-27956, III-C-28090, III-C-28457, III-C-28669, III-D-25702, III-F-26767 Protocol Design VIII-E-26823 Protocol Engineering VIII-E-28467 Prototyping IV-D-28835 Pseudomonas diminuta III-D-27468 Pseudomonas putida III-B-25493 Pulse Compression 1-E-25482 Pulse Generation VIII-G-26213 Pulse Loading V-D-24362 Pulsed Jet Combustion V-C-25245 Pulsed Power I-B-26257, I-B-26821 Pulsed Radiation 1-E-25349 Pyrene Excimers II-B-27568 Pyrenes IX-D-5548 Pyrogenic Coatings VI-A-26667 Pyrolysis II-A-26145, II-A-26748, II-D-27603, II-D-27887, III-D-25663 Pyrometallurgy VI-C-26728 Quadratic Programmy IV F 23306 Quadrature IV-B 28320 Quality Control IV-C-24557 Quantum Devices VIII-A-26896 Quantum Dots I-D-26682 Quantum Effects 1-D-27458 Quantum Electronics 1-D-25487, VIII-G-28326, VIII-G-28453 Quantum Hydrodynamics IV-B-28799 Quantum Mechanics 1-D-28468, 1-E-25482, 1X-A-5653 Quantum Mechanics Models VIII-B-28406 Quantum Optics 1-D-28468, 1-E-25546, 1-E-28356 Quantum Semiconductor Device Models IV-B-28799 Quantum Statistics I-E 25546 Quantum Transport VIII-B-25015, VIII-B-26711, VIII-B-28461 Quantum Wave Devices VIII-B-27578 Quantum Well Amplitude Modulators 1-E-28271 Quantum Well Base Transistors VIII-B-27883 Quantum Well Devices VIII-C-26381, VIII-D-28070 Quantum Well Heterostructures 1-E-28313 Quantum Well Lasers VIII-A-26434 Quantum Well Photodiodes VIII-B-26923 Quantum Well Structures VIII-A-26188, VIII-A-27298. VIII-B-28594, VIII-B-28646, IX-F-6170 Quantum Wells 1-D-25167, 1-D-25487, 1-D-26015,

1-D-26195, 1-D-26644, 1-D-27458, 1-D-28470, 1-E-26974, 1-E-28271, VIII-A-26896,

VIIEB 26151, VBEB 26278, VIIEB 27443, VIIEG 26213, IX F 6291 Quantum Wile Lasers VIII F 28922 Quantum Wares ED-25167 (ED-26682) VIIEE 28187 Quartz VED 26601 Quartz Resonators ED 25697 A D 28155 Quasi Optical Devices VIII C 26620, VIII C(2665) Quasi Optical Power Combining VIII C 28339 Quenching V C 27864 Quinines IX D 5548 Racemic Compounds II C 28319 Racemic Ketones II B (17290) Radar I E 28258, VII & 26902, VII B 26031 VIED 27919, VIEE 26982, VIEE 28099 Radar Clutter Databases VII D 26224 Radar Cross Sections VIED 25730, VIED 28219. VIII C 27873 Radar Data VIII C 25350 Radar Imaging 11: 26676 Radar Polarimetry VIII C 26128 Radial Inflow Turbines V B 27515, IX C 5824 Radiation Detection VIII C 26791 Radiation Interactions LB 26709 Radiation Patterns VIII C 27904 - VIII C 28516 Radiation Sources 1 D 26682 Radiative Intensity V C 27469 Radiative Transfer VII D 24713 Radical Beams I B 27646 R. ho Networks VIILE 15674, VHEE 26823 Radio Signal Distortion 1/E-27586 Radio Systems VIII E 27076, VIII E 27904 Raintall VIEA 26902 / VIEE 26982 / VIEE 28344 Raman Scattering 11D 26195 114, 25482, 11F 25546. VIEG 26962 VIEG 28052, VIII A 26188 Raman Spectroscopy I B 25653, III D 25476 Random Codes VHLE-22028 Random Texture IV D 26656 Random Walks IV E 23306 Rank Transformation Tests IV C 26745 Ranking IV C 25836 Rare Earth Compounds VI A 26400 Rare Earth Ions I B 28472 Rate Distortion Functions IV E 28060 Reaction Kinetics II A 27600 / II D 26256 / IFE 28631 Reaction Rates II-C 24413, V/C 27469, IX/B 6294 Reactive Armor VI C 26488 Reactive Multiphase Flows IV A 28980 Real Time 1.E. 28502, TV-E. 25662, TV-E. 26487 IV E-26930 EV-E-27524 IVEA 28369 Reasoning IV D 26656 IV E 26438 Recursive Filters IV D-26674 Recursive Partitioning Methods IV C 28679. Redox Catalysis II A 28469 Redox Chemistry II-A 28486 Reduced E struction Set Computers VIII B 28329 Reflectivity I-D 25374 Refractivity I B 28472 | I E 27838 | H A 26636 VED 28109, VED 28538, VIED 29288 VIEG 26962 IX D-5884 IX F-6170 IX F-6563 Refractory Metal Solicides I B 2856E Retractory Metals VI & 28509 Regression IV ( 1871 Regression Models IV C 28679, IV F 26792. Reliability IV C 24557 / IV C 25706 / IV C 26993 IV C 27868 IV E 27812 ALD 27548 VIII B. 2800s Remote Sensing IVE 26801 - VILD 26384 VILE 26982 VILL 28162 VILE 24881 VIII A 2614 - VIII E 28985 Residual Stresses VI & 28500 P sins VEE 28883 Resonance T.B. 26/09/11E-26/60/T.E. 27425 V D 25462 V D 25630 VH G 26062 Resonant Primping 1 F 16974 Resonant Surface Waves (V.J. 21306 Resonant Systems 1 () 26644 Resonant, Europeirne T.D. 26195

Resonant Tunneling Diodes I D 25487 IV B 28799. X111 C 26599 X111 G 26213 Resonant Tunneling Structures 1 D 26015, 1 D 27458 Resonators I B 28396 / I D 25697, 1 D 28591 IV A 26909, V D-28155, VIII C 26599 Retrospection IV-E 26438 Rhentum VI-C-27579 Rhemum Oxides IN B 6089 Rheology III A 27494 Rheometers II E 28153 Rhodamine Dves II-B 27534 Rhodopseudomonas paiustris III B 26576 Rip Currents VII A 26972 Risk Assessment IV C 26993 River Basins VII A 26902 River Networks VII A 2772 Road Surfaces VII D-26224 Robotic Manipulators V D 25409, V D 27075, V D. 27300 IX A 5933 Robotics 1 E 28258, 1V-E-26779 Rock Properties IN-E 6296 Rock Structure IX 1-6296 Rocket Exhaust V C 24487, V C 27469, V C 28912 Rocket Launch V C 27469 Rocket Propellants V C 26403 Rotary Wings V(B)25623, V(B)2691(4), V(B)27752. V-B 28002, V-D-25462, V-D-26061, V-D-27300, V-D-28123 Rotor Blades V(B) 25461, V(B) 25623, V(B) 26595, N-D 25327 Rotor Noise V B-28002 Rotor Shatts V-D-25462 Rotor Wake V(B)25467, V B 25623 Rotorcraft V-B-25461, V-B-25467, V-D-25462, X-D-27300 Rotors V(D)28123, 1X-C 5824 Rough Surfaces 1/D/25464, V/X 25594, VII/D/24713, VII-D-26384, VII-D 26988, VII D 27031 VH D 27485, VII D 27911, VII D 28219. VII-D-29288, IX 1:5830 Rough Terrain VII-D-28219 Roundoff Noise IV-F 26802 Roung VIII-E-26823 Routing Algorithms IV-C-26144, VIII E-25674 Rubber V/C-26403 Rubber Toughening II E 25229 Rubidium Ions 1-D 26996 Rubidium Manganese Chlorides 1 D/27780 Rule Management Systems IV E 27892 Ruthenium II-C-26822 Ruthenium Compounds II A 26426 Rydberg Atoms I-B 26709 Saccharomyces cerevisiae III C 24931 Salt Fog. Corrosion VI A 20578 Salt Movement VII B 26283 Samarium from Cobalt Intermetallics VI D-28146 Sampling IV C(28679) IV F 23306, IV F 29653 Sands VIEB-26260, VIEC 24381 VIED 24713 Satellite Imagery VII-F 24881 Scanning Junneling Microscops VIII-B-28508 Scene Analysis IV D 26056 Scheduling IV B 28192, IV F 26063 Schottky Barriers VED-26287, VIII B-26151. Schottky Diodes VI D 26287 Sciatic Nerve III D 25752 Sontillation VILE 27870, 18-E-6458 Scintillation Cameras IV E 26811

### X Indexes

Semiconductor Devices 1 E 26088, 4V-B 28716. IV B-28709, VIII A 28392, VIII B-25015. VIII R. 28461 Semiconductor Dielectric Waveguides VIII-C 25339 Semiconductor Frim Lasers I B 28531 Semiconductor Heterojunctions VIII-A 26761. VIII E 26898 Semiconductor Heterostructures 1-D 26195, 1 D 26682, 1 E 28356, VIII B 26923 Semiconductor Lasers 1 D 28336, 1 E 25482. 11. 25546. 11: 28356 Semiconductor Quantum Well Lasers VIII A 26434 Semiconductor Super'atrices I/D 25167, TD-27458 Semiconductor Surfaces I B 26223 Semiconductor Switches I-B 26257, I-B 26821 Semiconductors Atomic Structure 1X-A-6280 Chemical Vapor Deposition II A-26748 Deposition LB-2856 Electrical Properties II-C-27770, VI-D-28141 Electron Emission I-B-28569 Electronic Structure IX A 6280 Epitaxial Growth I/D/27458, VI/D/28612 Etching 1-B-28561 1-xectation 1-D-25167 Exciton Dynamics I-E 26974. Interfaces II-C-26191, II-C-27770, IX-A-6280 Ionization VIII B 26711 Magnetic Properties VI-D-28141 Microstructure VIII-B-26278 Optical Properties 1-D-28470, 1-E-26383, 4-E-28356. VED-28141 Physical Processes 1X-1-5940 Plasma Stabilities 1-1) 26682 Reliability VIII-B 28004 Scanning Tunneling Microscopy VIII-B-28508 Surface Decontamination IX-B-6305 Surface Properties I-B 28561, II-C-26191, H C-27770, VIII-B-28508, IX-A-6280 Transport Properties 1-D-26017, VIII-A-28335, VIII-A-28347, VIII-B-26278, VIII B-26711, VIII B-28461, VIII-B-28594, VIII-B-28646, VIE-F-2818 Sense Organs IX D-6579 Sensor Array Signal Processing IV-E-26945 Sensor Data Eusion 1-E-28258 Sensory Processing IV-E 27567 Sensory Systems IX-D-6579 Shudows IV Shallow Water VII-A-26972 Shared Memory Computers IV B-26391 Shear VII-B-26260 Shear Bands IV-A-25396, IV-B 28320, V-A 27409, V.A. 28283, V-A-28317, IX-D-6148 Shear Deformation V-A 26908, V-A 28307 Shear Flow IV-F-23306, V-C-28250 Shells (Structural Forms) IV(A)25874, V/A 28253 Shock Mechanics) IED 27025 Shock Loading VI C-26485 Shock Separated Flow V-B 26863 Shock Tube Studies V/C 27864 Shock Waves IV A 26113, IV A 28969, IV B 26616, VA 28307, VB-28293, V/C 27469, VI-F 27364. Signal Analysis IV-1: 27524 Signal Classification VIII-E 27917 Signal Computation VIII-E-26460 Signal Conversion VIII-E 28387 Signal Detection IV-F 26792 Signal Direction Finding VIIEE 27899 Sign J. Interception VIII E: 27754, VIII F: 27899. VIII E 27917 Signal Location VIII-E 27032 Signal Processing I D-25374, 14E-27586, IV-E-23908, IVE 26792, IVE 26802, IVE 26930, IV F 26945, IV F 27524, IV F 27620. IV-1 27817, IV E-28060, IV E-28476 VIEE 28102, VIEC 26128, VIII E 26118 VIII F 27076, VIII E 27886, VIII G-27554, VIII G 28326

Second Harmonic Generation 11,-25408. If C 26193

Secure Communications VIII F-27917 VIII F-27904

indiment Transport VII A 26972 - VII A 27491

Selenides 1 E 26383, VED 23477, VIII A 23206

Search Algorithms VIII G 27554

sediments III B 26750

Selenates 1 D 2778

Selemum 5 F 28711

Second Harmonic Radiation I B 26462

Semici iductor Contacts VLD 26287

Signal Reconstruction VIII-E-28985 Signal Sources VIII-E-26646 Silanes II-C-28298 Silica Glass IX-D-5548 Silicides I-B-28561 Silicor Cleaning VIII-G-28326 Contacts IX-F-6291 Crystal Defects VI-D-27764 Crystalline Nanoparticles VI-B-26673 Defects IX-A-6280 Donor Complexes 1-D-26996, 1-E-26383 Electron Emission 1-B-28569 Epitaxial Growth VIII-G-28326 Epitaxial Lavers VIII-A-26761 Etching 1-B-28561. VIII-G-28326 Heterostructure Properties VIII-A-26896 Ionization VIII-B-26711 Oxidation VI-D-22459 Resonant Tunneling VIII-B-27443 Surface Properties II-C-27770 Thermal Expansion VI-F-26246 Silicon Alloys VI-C-25373, VI-D-26287 Silicon Carbide Reinforced Composites VI-C-26439. VI-C-26751 Silicon Carbides VI-A-24845, VI-B-25390, VI-B-25397, VI-B-26673, VI-C-25202. VI-F-26246 Silicon Devices (X-F-5940 Silicon Dioxide I-B-26223, I-B-28561, II-A-27600, VI-D-22459, VI-D-27605, VI-D-28109 Silicon Germanides VIII-A-26896 Silicon Jons VI-A-26678 Silicon Metallizing VI-D-26287 Silicon Nitride Matrix Composites VI-C-25202 Silicon Nitrides VI-B-26673 Silicon Oxides 1-E-27366 Silicon Substrates VI-D-27605, VIII-A-26434, VIII-A-28392, 1X-F-6291 Silicon Surfaces I-B-26223, VIII-G-26213 Silk III-C-28457 Silt Loam III-B-26750 Silver I-D-26996. II-C-27759. VI-D-26287. VI-D-27605, VIII-A-23206 Silver Doped Films II-A-25586 Silver Gallium Scienides VI-D-23577 Silver Ions 1-D-26996, 11-A-27502 Silver Surfaces II-C-26822 Silvlphosphoramines II-E-25286 Silylphosphoranimines II-E-28631 Single Crystals 1-E-27425, II-C-26191, VI-A-21545, VI-B-28549, VIII-F-27865 Singular Value Decomposition 1V-F-26945, IV-F-27817 Singular Values IV-F-26930 Sintering VI-C-25526, VI-C-26123, VI-C-27579 Skin Friction V-B-27625 Slot Antennas Vill C-25045, VIII-C-26599. VIII-C-27904 Smart Materials VI-B-28608 Smoke Plumes VII-F-24881 Snow VII-D-25730, VII-D-26224, VII-D-26384. VII-D-27919 Snowpack VII-F-28344 Sodium I-E-27366, VI-D-23577 Sodium Chloride Solutions VI-A-26678 Soft X-Ray Lasers 1-E-26160 Softening V-A-28283 Soil Mechanics VII-B-26260 Soil Moisture VII-A-27471 Soil Properties III-B-26750, VII-B-26260, VII-B-26281, VII-B-27316, VII-C-24381, VII-D-24713, VII-D-26224 Solid Polyelectrolytes II-E-27054 Solid Propellants [I-C-24413, II-D-27603, II-D-28103, II-D-28565, V-C-28912 Solid State Lasers J-B-28472, J-B-28531, J-D-28336. I-E-25631, J-E-26383, I-E-27425, I-E-28348, VIII-G-26213 Solid State Plasmas I-D-26682

Solidification VI-C-27472 Solitons IV-A-28803, VIII-G-26213 Solubility VI-C-27579, VI-C-28639 Solutions IX-B-6305 Solvent Effects II-B-27534 Sonic Boom V-A-26908 Soot V1-A-26400 Sorting Algorithms IV-B-28071 Sound Transmission VIII-E-28985 Space Stations IV-D-28511 Spalling VI-B-28480 Spatial Smoothing IV-F-26802 Speckle Interferometry V-A-25594 Spectroscopy I-B-27508, 1-D-26644, 1-E-28313, II-A-25500, II-C-26238, VIII-B-26760 Speech Recognition IV-F-26811 Spider Silk III-C-28457 Spinning Viscous Fluids IV-A 28797 Spline Approximation IV-B-27690 Spline Interpolation IV-F-27524 Spore Germination III-C-27956 Spore Protease III-C-27956 Spores III-A-28022, III-C-27956, III-C-28090, 11-12-25476 Spray Heating V-C-28250 Spread Spectrum VIII-E-25674, VIII-E-27493. VIII-E-27754, VIII-E-27994 Springs (Mechanics) B-D-28555 Sputtering VI-A-26427, VI-A-27552 Stability IV-A-25874, IV-A-28514, V-D-25771, V-D-28123, VII-F-28664 Stainless Steels VI-A-26449, VI-D-26601 Stall V-B-25461, V-B-25467, V-B-27627, V-B-27752, V-B-27894, V-B-28159, V-D-28123 Stannanes II-C-28298 Statistical Data Analysis IV-C-27574 Statistical Decision Theory IV-E-25662 Statistical Estimation IV-C-27862 Statistical Inference IV-C-26993 Statistics IV-A-25782, IV-C-25836, IV-C-27868, IV-C-28679, IV-C-28982, IV-F-28809 Steel Matrix Composites VI-A-26400 Steels IV-A-25396, V-A-26057, VI-A-25199, VI-A-25833, VI-A-26449, VI-A-26667, VI-A-27552, VI-B-26825, VI-B-27163, VI-B-27407, VI-C-26728, VI-D-26601 Stochastic Analysis IV-F-29031 Stochastic Bilinear Systems IV-F-26792 Stochastic Control IV-C-28715, IV-F-26063, IX-A-6466 Stochastic Growth Models (V-F-23306 Stochastic Numerical Methods IV-B-28916 Stochastic Optimization IV-F-28809 Stochastic Partial Differential Equations IV-C-29016 Stochastic Processes IV-B-26616, IV-C-26649. IV-C-29016, VII-F-27995 Stochastic Systems IX-A-6271 Strain (Mechanics) II-B-28013 Strain Compression IV-A-25396 Strain Hardening V-A-28283 Strain Rate IV-A-26218, V-A-25594, V-A-27315, VI-B-26167 Strain Tests V-A-25459 Streambeds 1X-E-6185 Stress (Physiology) III-E-25521 Stress Analysis V-A-25345 Stress Corrosion Cracking V-A-26057 Stress Relaxation VI-D-22459 Stress Sensitivity IV-A-26909 Stressed Environments VIII-E-25674 Stresses VI-A-28509, VI-B-24583, VII-C-24381 Stretch Activated Ion Channels III-F-26099 Stripline Array Antennas VIII-C-28151 Stroh Formalism IV-A-28606 Strontium J-E-26160, VIII-B-26666 Strontium Ions 11-A-28402 Structured Programing IV-B-28034 Styrenes II-E-26839 Submillimeter Quantum Electronics 1-D-25487

### Subject Index

Submillimeter Waves 1-B-27431, 1-B-27888, I-B-28396, VIII-C-27307, VIII-C-28339, VIII-C-28516 Sulfides 1-D-28336. II-B-25411. II-D-27025. VI-A-26667 Sulfonated Polystyrene lonomers VI-B-25424 Sulfoxides II-E-27445 Sulfut II-E-28711, VI-C-26728 Sulfur Compounds II-A-25435, II-C-26822 Sulfur Dioxide 1-B-25653, 1-B-27888 Sulfur Hexafluoride I-B-25653 Sulfur Hydrogen Donor Complexes I-D-26996 Sulfur Mustard IX-B-6308 Super Hydrides II-B-25290 Supercapacitors II-A-26636 Superconducting Transmission Lines VIII-B-26760 Superconductivity 1-D-27780 Superconductors 1-D-26195, VIII-A-26708, VIII-G-26213, VIII-G-28326, IX-A-6280 Superconvergence IV-F-23306 Supercritical Fluids III-C-28043, VI-C-26591 Supercritical Water II-D-27505, II-D-28371 Superfluorescence I-B-26462 Superlattices 1-D-25114, 1-D-25167, 1-D-25374, . 1-D-26015 1-D-27458, 1-E-26974 1V-B-28799, VI-D-26729, VIII-A-26188, VIII-A-26444. VIII-A-26896, VIII-A-28335, VIII-B-26755, VIII-B-26923, VIII-B-27443, VIII-D-28070. VIII-F-28922, VIII-G-28453, IX-A-6280 Superplastic Ceramics VI-B-26747, VI-B-28761, VI-C-25526, VI-C-26392, VI-C-26751 Superplastic Deformation VI-C-25526 Superplasticity VI-C-26751 Superradiance 1-B-26462 Supersonic Flow V-B-27558 Surface Chemistry I-B-27646, II-B-25739, II-C-26191, II-C-26238, II-C-26822 Surface Impedance VIII-C-27873 Surface Mediated Photocatalysis II-C-28298 Surface Modifications II-C-26126, VI-A-25833 Surface Properties I-B-26223, I-E-28356, II-C-26191, II-C-27770, III-F-27634, V-A-25594. VI-A-24845, VII-D-24713, VII-D-27031, VII-D-29288, VIII-B-28508, IX-A-6280 Surface Scattering IX-B-6089 Surface Wave Resonators 1-D-25697, 1-D-28591 Surface Waves 1-D-25374, IV-F-23306 Surfactant Stabilized Systems II-C-26296 Surfactants II-B-25181, III-B-26750, III-F-27634 Suspensions VII-G-28359 Switched Networks VIII-E-27751 Switching J-E-26971 Switching Networks I-E-26695 Symbolic Computation IV-B-28908 Synapses I-E-26676 Synchrotron Radiation 1-E-26383 Synthesis (Chemistry) II-A-26145, II-E-25286. II-E-27440, II-E-28314, II-E-28711 System Failure IV-C-27868 Systolic Arrays VIII-E-26118 Tantalum VI-C-27579 Tantalum Alloys VI-D-26287 Target Detection VIII-C-25350 Target Recognition VIII-E-26697, VIII-E-26813. VIII-E-27464 Target Survivability IV-C-25347 Target Tracking VIII-E-26697, VIII-E-26813 Technology Transfer IV-E-28950 Tellundes Annealung 1X-F-6563 Crystal Defects 1-D-25114 Epitaxial Growth I-D-25114 Heterojunction Properties VIII-A-26761 Monte Carlo Simulation VIII-A-28347

Optical Properties I-D-28336

Transport Properties VIII-A-28347

Vacancy Complexes VI-D-27846

Quantum Wells I-D-27458

Temperature VII-F-28344 Tensile Properties VI-A-27037 Tensile Tests VI-B-25193, VI 9-25390, VI-B-25424. VI-B-26164, VI-B-26167, VI-B-26747, VI-B-28549, VI-B-28761 Terrain VII-A-27471, VII-D-26224, VII-D-28219, VII-E-26982 Terrain Analysis I-E-28258 Terrain Modeling VIII-E-26697 Tetanus Toxins III-C-27890 Textures IV-D-26656, IV-E-26487 Thallium Lasers 1-E-27366 Thermal Adaptation III-A-28022 Thermal Chemistry II-C-26822 Thermal Conductivity IV-A-25396 Thermal Decomposition II-D-27887, VI-C-26485 Thermal Expansion VI-F-26246, 1X-F-6563 Thermal Images 1-E-28258 Thermal Imidization VI-C-26571 Thermal Processing VIII-F-28729 Thermal Properties II-D-27025, III-A-27494. IV-A-28514 Thermal Softening V-A-28283 Thermal Stability VI-D-26287, VI-D-26601 Thermal Stresses V-A-25400 Thermal Wave Imaging VI-B-24981 Thermionic Emission 1-D-25487 Thermochemical Transport Models V-C-28310 Thermochemistry VI-A-24845 Thermodynamic Models VI-C-26591 Thermodynamic Properties II-E-28314, IV-A-28514, IX-F-6563 Thermolysis II-B-25761 Thermomechanics IV-A-26218, V-A-26443, V-A-27538 Thermomodulation VIII-G-26213 Thermoplastics VI-A-28369, VI-C-28883 Thermotropic Liquid Crystal Polymers VI-F-26647 Thermoviscoplastic Materials V-A-26443 Thermus aquaticus III-C-24435 Thin Films I-B-26959, I-B-27646, I-B-28561, 1-D-25374 1-D-25464 1-D-26827 1-D-28362 I-D-28470, I-E-26088, I-E-26971, I-E-28313, II-A-25586. II-A-26145 II-B-26914 II-D-27603, II-E-25104, II-E-26072, II-E-28314, VI-A-26400, VI-A-26427, VI-A-28509, VI-B-24981, VI-B-25424, VI-B-26747. VI-D-26287, VI-D-26601, VI-D-26883. VI-D-27605, VI-D-28141, VI-D-28553. VI-F-27810, VIII-A-23206, VIII-A-27298 VIII-B-28329, VIII-B-28345, VIII-C-26791. VIII-G-28326. VIII-G-28453, IX-D-5548. 1X-D-5884 Thiocyanates III-D-28479 Thioethers II-B-26914 Thiophosphinates II-B-25411 Thyratrons J-B-26257 Time Evolution IV-A-27580 Time Series Analysis IV-A-25782, IV-C-26108, IV-C-26394, IV-C-27574, IV-C-28743. IV-F-26811 Tin VI-D-26287, VIII-A-23206 Tin Alloys VI-C-27472 Tin Dioxide II-A-25586 Titanates I-E-27882. VIII-C-26791 Titanium VI-C-26728, VI-F-27364 Titanium Allovs VI-A-26806, VI-C-28005, VI-D-28146 Titanium Borides VI C 26021, VI C 26392, VI-C-28368, VI-E-26169, VI-E-26173 Titanium Carbides VI-C-26392, VI-C-28368 Titanium Ions VI-A-25833, VI-A-26678 Titanium Monoxide II-C-27775 Titanium Nitride Coatings VI-A-27552 Titanium Oxides VI-C-25526, 1X-B-6305 Titanium Silicon Carbides VI-A-24845 Titanium Silicon Nitrides VI-A-24845 Tobacco Mosaic Virus III-C-24931 Toluenes II-D-27505, VI-C-26591 Tomography III-F-26099, IV-A-26463, IV-F-26811 Tool Steels VI-D-26601

Topography VII-A-27471 Torque V-C-26769 Total Internal Reflections 1-E-26971 Toughening Mechanisms VI-B-27163 Toxic Chemicals IX-B-6305 Toxic Paralysis III-D-27468 Toxins and Antitoxins III-C 27890, III-D-27916 Tradeoff Modeling IV-C-27381 Transceivers VIII-C-25045 Transistors J-B-26257, J-B-28569, IV-B-28799, VIII-A-26444, VIII-A-28335, VIII-A-28351, VIII-B-25015, VIII-B-26151, VIII-B-26484, VIII-B-26711, VIII-B-27883, VIII-B-28004, VIII-B-28461, VIII-C-25045, VIII-C-26381, VHEG-28326 Transition Metal Atoms I-D-25906 Transition Metal Catalysts II-C-26238 Transition Metal Nitride Coatings VI-A-27552 Transition Metals 1-B-26223, II-E-25104, II-E-28711 Transmission Lines VIII-B-26760, VIII-C-25045, VIII-C-27904, VIII-C-28483 Transonic Flow V-B-25461, V-B-27062 Transparency 1-E-26160, VIII-G-26213 Transport Properties 1-D-25167, 1-D-26015, IV-A-26463, V-C-27469, VIII-A-28335, VIII-A-28347, VIII-B-25015, VIII-B-26278, VIII-B-26711, VIII-B-28406, VIII-B-28594, VIII-B-28646, VIII-F-28187, IX-F-5940 Trees VII-D-27919 Trees (Vegetation) VII-D-25730, VII-D-26224 Tribology VI-F-26246 Tubular Beams V-D-25327 Tunable Laser Materials IX-D-5884 Tunable Lasers I-D-26442, I-E-25631, I-E-27425 Tunable Optical Pulses 1-E-25349 Tunable Optical Sources 1-E-25408 Tungstates 1-E-25631, II-A-28469 Tungsten VI-C-27579 Tungsten Alloys VI-B-26167, VI-C-27579. VI-C-28639, VI-D-26287, VI-E-28272, VI-E-28575 Tungsten Arc Welding VI-C-26728 Tungsten Carbides II-A-28353, VI-D-26601 Tungsten Nitrene Complexes II-A-28353 Tungsten Nitrides II-A-28353 Tungsten Penetrators VI-B-26164 Tunneling Diodes IV-B-28799, VIII-C-26599 Turbines V-B-27515, 1X-C-5824 Turbulence IV-A-25874, IV-A-26113, IV-B-28716, V-B-27515, V-B-27558, V-B-27625, V-B-27752, V-B-28293, V-C-25245, V-C-28250, V-C-28427, VII-E-27870, VII-F-27019, VII-F-28954. VII-E-29188, 1X-E-6458 Turbulent Boundary Lavers V-B-28293 Turbulent Eddies V-C-27018 Turbulent Microfronts VII-F-26491 Turbulent Mixing V-B-26863

Ultraviolet Laser Radiation 1-B-26223 Ultraviolet Lasers 1-E-26160 Ultraviolet Radiation II-C-26822 Ultraviolet Radiation Resistance III-C-27956 Ultraviolet Spectra 1-B-28499 Uncertainty IV-E-26487 Universal Coding IV-C-28722 Universal Coding IV-C-28722 Universal Flave V-B-27627 Uranium V-B-26164 Urazoles II-E-27445

Vacuum Microelectronic Devices I-B-28569 Vanadates I-B-28472 Vanadium I-D-25906 Vanadium Alloys VI-C-25373 Vanadium Monoxide II-C-27775 Vanadium Oxides IX-B-6305 Vaporization V-C-28250, V-C-28427 Variational Analysis IV-C-26997 Vegetation VII-D-26224, VII-D-28219, VII-F-27019 Vesicles II-B-25669

#### V-D-25771, V-D-27300, V-D-27510, V-D-28155 Vibrational Energy I-B-25653 Vibrational Relaxation II-D-27025 Video Transmission Techniques VIII-E-27751 Vinylidene Chlorides II-B-25761 Virtual Circuits IV-C-26144, VIII-E-25674 Viruses III-C-24931 Viscoelastic Materials IV-A-28957 Viscoelastic Properties IV-A-26218, V-A-27315 Viscoplastic Cylinders V-A-28283 Viscoplastic Flow V-A-26443 Viscoplastic Materials IV-A-25396 Viscosity II-B-27534, H-E-28153, IV-A-25782 Viscous Aerodynamics V-B-25461 Viscous Flow IV-A-25874, IV-B-28025, V-B-27752 Viscous Fluids 1V-A-28797 Viscous Liquid Jets V-C-26797 Visibility IV-C-25347 Vision V-D-25409 Vision Modeling VIII-C-25557 Visual Stimuli IV-E-25324 Visualization Methods IV-C-28309 Voltage VIII-B-28646 Volterra Equations IV-F-23306 Vortex Loops V-B-26595 Vortices IV-A-26113, V-B-25461, V-B-27752, V-B-28159, V-B-28215, V-B-28252, V-C-26456, V-C-27018, V-D-25462 Voter Models IV-F-23306 Wake V-B-25461, V-B-25467, V-B-25623, V-B-28159, V-D-28123 Water II-D-27505, II-D-28371, IX-D-5548 Water Activated Heat Generation III-A-28691 Water Movement VII-B-26281 Water Penetration VII-F-28344 Water Storage VII-A-27471 Watersheds VII-E-26982 Wave Coupling VII-G-28489 Wave Equations IV-A-25782 Wave Fronts IV-B-26616 Wave Interactions IV-B-26616 Wave Packets I-E-25482 Wave Propagation 1-B-28499, 1-D-25374, IV-A-28969, V-A-26908, V-A-28307, V-C-26720, VII-D-24713, VII-D-26384, VII-D-26480 Waveguide Filters VIII-C-26651 Waveguides 1-D-28470, VIII-A-26708, VIII-A-28674, VIII-B-26711, VIII-B-26760, VIII-C-25045, VIII-C-25339, VIII-C-26949, VIII-C-27307, VIII-C-28483, VIII-G-26213, IX-D-5884, IX-F-6170, IX-F-6291, IX-F-6563 Waves VII-A-26972 Weather Fronts VII-F-26491 Weather Radar VIJ-A-26902 Welding VI-C-25373, VI-C-26728 Weldments VI-C-25373, VI-C-26728 Whisker Reinforced Composites VI-C-25202.

Vibration V-B-25461, V-B-25467, V-D-25630,

 Wind (Meteorology) VII-E-28094, VII-E-28102, VII-C-2675;
 Wind (Meteorology) VII-E-28094, VII-E-28102, VII-F-26491, VII-F-27019, VII-E-27995
 Wind Tunnel Tests V-B-26631, V-B-28159, V-B-28215, V-B-28293
 Wing - Body Juncture Flow V-B-28249
 Wing Tip Vortices V-B-28159

X-Ray Lasers 1-E-26160 X-Ray Optical Elements 1-E-28356 X-Ray Scattering V1-A-28369 Xenon V1-A-26806 Xenopus III-D-26232

Yeasty III-C-24931, III-C-28361, III-D-26232 Yield Stress VI-B-24583 Ytterbium 1-B-26709 Yttrum Alloys VI-C-27472 Yitrum Iron Gamets VI-D-28141

### X Indexes

Yttrium Iron Intermetallics VI-D-28146 Yttrium Oxides VI-B-26747, VI-C-26751

Zeolites 1X-B-6294 Zinc 1-E-26160, 11-B-25761, VI-D-26729, VIII-A-26147 Zine Cadmuum Sulfides 1-D-28336 Zine Oxides 1X-B-6305 Zine Phosphates VI-A-26400, VI-A-26667 Zine Selenides 1-D-28336 Zine Tellurides 1X-F-6563 Subject Index

Zirconium VI-C-26728 Zirconium Alloys VI-C-26439 Zirconium Oxide Matrix Composites VI-C-26751 Zirconium Oxides VI-A-26806, VI-B-24583, VI-B-26747, VI-B-28549, VI-C-25526